HIP JOINT FORCES IN HIP REPLACEMENT PATIENTS AND NORMAL SUBJECTS DURING ACTIVITIES OF DAILY LIVING

by

Anna Fitzsimmons

This thesis and computer disk are submitted in partial fulfillment of the requirements for the degree of Ph.D in the Bioengineering Unit, the University of Strathclyde

University of Strathclyde
Glasgow
December 1995

ABSTRACT

A high number of revision hip replacement operations are currently performed due to loosening of the primary implant. The loading imposed on the prosthetic joint and its fixation mechanisms may be one of the many factors contributing to the loosening process. Previous work to determine hip joint loading has concentrated on gait, stair negotiation and rising from a chair. However, since patients often comment on the difficulty of getting into and out of a car and bath, these activities are also included in the current project.

The 3 orthogonal components of hip joint force have been calculated for 16 post-operative hip replacement patients between one and two years after surgery and also for 10 age-matched normals.

A biomechanical model of the lower limb was developed including 37 muscle elements. Algorithms were incorporated to correct for curved muscle paths, providing realistic muscle moment arms with changing joint angle configuration. An optimization routine which minimizes the overall maximum muscle stress was incorporated to determine muscle forces which were then used in the calculation of joint force. The model utilizes anatomical muscle and bone data, kinematics measured using a 6 camera Vicon motion analysis system and ground reaction forces measured using force platforms.

In validity tests, the predicted muscle activity patterns for normal subjects were found to be consistent with published EMG data for most muscles. The mean peak resultant hip joint force of 3.8 times body weight calculated for the patients during gait at 1.01m/s was consistent with the results published for patients with instrumented hip prostheses at a measurement time of more than 12 months after surgery.

The maximum mean peak resultant hip joint force determined for patients was 5 times body weight, calculated at the left hip when getting out of the passenger side of a right hand drive car. A simple calculation of torsional moment about the stem of the femoral component during this and other activities showed it to be close to or to exceed the experimentally determined limits of torsional strength of implant fixations, reported in the literature.

The maximum mean peak resultant hip joint force calculated for normals was 6.3 times body weight, determined at the left hip on getting into the passenger side of a right hand drive car.

It is suggested that car entry and exit and other activities should be performed in safer styles and that the results of this thesis should be incorporated into the design and testing of hip prostheses.

ACKNOWLEDGEMENTS

There are many people that I would like to acknowledge for their help and encouragement throughout this project.

Firstly, I would like to thank Professor J.P Paul for giving me the opportunity to study in the Bioengineering Unit and for his advice and constructive criticism throughout the project.

Dr A.C. Nicol, my supervisor, has played an invaluable role in advising and guiding me throughout the work. He always made time to help me at any hour of the day and for this and his encouragement, I am extremely grateful.

Mr I.J. Kelly, the co-supervisor of the project has made vital contributions, helping me to recruit patients, answering any questions regarding the patients and giving general advice.

I also wish to thank Dr Shaw Dunn at the University of Glasgow for teaching me the basics for anatomy so enthusiastically and Professor R.A. Brand for providing me with data for use in the muscle model.

The help of Judith Lane in laboratory testing and data analysis has been invaluable. That of John Runciman with the muscle wrapping calculations was also much appreciated.

I could not have carried out the work without the subjects and I would like to express my gratitude to the 26 volunteers who gave a considerable amount of their time to the project. I am also grateful to my friends, especially Caroline and Nucky who participated in some of the early experimental sessions, assisting in the development of the experimental protocol. My thanks also go to Caroline for her enthusiasm to discuss ideas and her general help and support throughout the project.

I also wish to mention some other individuals, notably Sheila Nicol for her help with computer work and the technical staff in the machine shop and electrical workshop for constructing the equipment. My special thanks also go to my dad for the long hours spent in his workshop helping to make various pieces of equipment for the project including the musculoskeletal model.

I would also like to thank the Medical Research Council and the Arthritis and Rheumatism Council for Research for their generous funding of the project.

Finally, although many people have been involved in the project, the ones that I want to thank most for their endless encouragement are Duncan, Caroline and my family. Thankyou Kate, mum and dad for your constant support in everything that I do.

CONTENTS

ABBREVIATIONS AND SUBSCRIPTS

Unless otherwise stated, notation used is as follows:

Abbreviations

X, Y, Z	Right hand cartesian coordinate system axes
[B]	Direction cosine matrix
m	Mass
L	Length
bwt	Body weight
Mx	Moment about X axis
My	Moment about Y axis
Mz	Moment about Z axis
F	Force
Fx	Force in the direction of the X axis
Fy	Force in the direction of the Y axis
Fz	Force in the direction of the Z axis
Fr	Resultant hip joint force acting on the femoral head
θ_{XY}	The direction of the peak resultant hip joint force vector projected onto the sagittal plane of the femur and measured relative to the femoral longitudinal axis.
θ_{YZ}	The direction of the peak resultant hip joint force vector projected onto the frontal plane of the femur and measured relative to the femoral longitudinal axis.
θ_{XZ}	The direction of the peak resultant hip joint force vector projected onto the coronal plane of the femur and measured relative to the femoral medio-lateral axis.
g	Acceleration due to gravity
σ	Muscle stress
PCSA	Muscle physiological cross sectional area
A-P	Anterior-posterior
M-L	Medio-lateral
S-I	Superior-inferior
pk	Peak

ASIS	Anterior superior iliac spine
RASIS	Right anterior superior iliac spine
LASIS	Left anterior superior iliac spine
inter ASIS distance	Distance between the right and left anterior superior iliac spines
midPSIS	Midpoint between the right and left posterior superior iliac spines
GTR	Greater trochanter
FRIL	Anterior of the right iliac crest
FLIL	Anterior of the left iliac crest
MEP	Medial epicondyle
LEP	Lateral epicondyle
FTH	Front of the thigh
LTH	Lateral side of the thigh
FIB	Fibula head
TIB	Tibial tuberosity
LMA	Lateral malleolus
MMA	Medial malleolus
SHA	Front of the shank

turn Walk with a 90° change in the direction of progression

asc Stair ascent

des Stair descent

rise Rising from a chair

con Car entry. The outside hip (i.e the left hip) is tested as the subject enters the car.

cox Car exit. The outside hip (i.e the left hip) is tested as the subject exits from the car.

cin Car entry. The inside hip (i.e. the right hip) is tested as the subject enters the car.

cix Car exit. The inside hip (i.e the right hip) is tested as the subject exits from the car.

bon Bath entry. The outside hip (i.e. that corresponding to the last foot to leave the ground) is tested as the subject enters the bath.

box Bath exit. The outside hip (i.e. that corresponding to the first foot to make contact with the ground) is tested as the subject exits from the bath.

bin Bath entry. The inside hip (i.e. that corresponding to the first foot to make contact with the bath floor) is tested as the subject enters the bath.

bix Bath exit. The inside hip (i.e. that corresponding to the last foot to leave the bath floor) is tested as the subject exits from the bath.

ASIS	Anterior superior iliac spine
RASIS	Right anterior superior iliac spine
LASIS	Left anterior superior iliac spine
inter ASIS distance	Distance between the right and left anterior superior iliac spines
midPSIS	Midpoint between the right and left posterior superior iliac spines
GTR	Greater trochanter
FRIL	Anterior of the right iliac crest
FLIL	Anterior of the left iliac crest
MEP	Medial epicondyle
LEP	Lateral epicondyle
FTH	Front of the thigh
LTH	Lateral side of the thigh
FIB	Fibula head
TIB	Tibial tuberosity
LMA	Lateral malleolus
MMA	Medial malleolus
SHA	Front of the shank

turn Walk with a 90° change in the direction of progression

asc Stair ascent

des Stair descent

rise Rising from a chair

con Car entry. The outside hip (i.e the left hip) is tested as the subject enters the car.

cox Car exit. The outside hip (i.e the left hip) is tested as the subject exits from the car.

cin Car entry. The inside hip (i.e. the right hip) is tested as the subject enters the car.

cix Car exit. The inside hip (i.e the right hip) is tested as the subject exits from the car.

bon Bath entry. The outside hip (i.e. that corresponding to the last foot to leave the ground) is tested as the subject enters the bath.

box Bath exit. The outside hip (i.e. that corresponding to the first foot to make contact with the ground) is tested as the subject exits from the bath.

bin Bath entry. The inside hip (i.e. that corresponding to the first foot to make contact with the bath floor) is tested as the subject enters the bath.

bix Bath exit. The inside hip (i.e. that corresponding to the last foot to leave the bath floor) is tested as the subject exits from the bath.

Subscripts

'-'	'with respect to'
LAB	Laboratory
F	Femur
P	Pelvis
S	Shank
T	Tibia
SF	Shank and foot
CM	Centre of mass (followed by subscript denoting segment concerned)
O	Origin of a coordinate system (followed by subscript denoting coordinate system concerned)
FPO	Force platform origin
MUS	Muscle
HC	Hip joint centre
KC	Knee joint centre
AC	Ankle joint centre

CHAPTER 1. INTRODUCTION

With recent advances in material characteristics and surgical procedures, the long term success rate of total hip replacement prostheses should have continued to improve at a rapid pace. However, this is not the case and in 1994 over 5000 revision procedures were carried out in the United Kingdom (Scottish office statistics). The loading imposed on the prosthetic joint and its fixation mechanisms may be one of the many factors contributing to the loosening of the primary implant.

Early work to determine the three dimensional configuration of hip joint force during gait was carried out by Rydell (1966) and Paul (1967). Rydell measured forces directly in subjects with strain gauged prostheses and recorded mean peak joint forces of between 1.59 and 3.27 times body weight. Paul determined forces by the method of calculation. A musculoskeletal model was developed to determine muscle and then joint forces using data including external kinematics and kinetics along with anatomical muscle data and subject anthropometric data. Paul calculated mean values of 3.27 for female subjects and 5.55 times body weight for male subjects who walked at a greater speed.

Since this early work, researchers have developed the methods used to determine joint forces and examined common daily activities including stair negotiation and rising from a chair in addition to gait. However, post-operative hip replacement patients often comment on how difficult they find it to get into and out of a car and bath. Hence the aims of this project are to determine and analyze the three dimensional configuration of hip joint force developed when getting into and out of a car and a bath in addition to those produced during gait, stair negotiation and rising from a chair. The activity of changing the direction of progression when walking is also investigated since, like the car and bath activities, this involves a significant amount of twisting. Joint forces are calculated for 16 post-operative hip replacement patients and a control group of 10 age-matched non-arthritic subjects.

The results should contribute to the understanding of the cause of loosening and be useful in the design and testing of prostheses. They should also provide information to aid clinicians in training patients to perform the activities in a safe and secure style.

This thesis presents and discusses these results and the calculation method used to determine them. The method used to calculate the joint forces requires knowledge of the musculoskeletal anatomy of the lower limb and the first section of the thesis gives an overview of this information (chapter 2). There have been a variety of approaches taken to calculate joint forces and it was important to investigate these methods before developing the one used in the current study. The second part of the thesis therefore discusses the methods

used by other authors (chapter 3) and then describes that developed in the current study (chapter 4). Details of the subjects taking part in the study and details of the activity tests performed are then presented (chapter 5).

The data obtained from the activity tests were then used in the calculation of joint force. The methodology used to calculate joint force involves the intermediate stages of joint moment, joint angle and muscle force calculation. It was important to assess the results of these intermediate stages before going on to use them in the final calculation of joint force and the results of this assessment are the next topic for discussion (chapter 6). Incorporated into this discussion is an assessment of the validity of the results. As with any theoretical model used to calculate muscle and joint forces, the model developed in this project involved many theoretical assumptions and it was important to check that it gave valid results.

Having examined the results of the intermediate stages of calculation, the final joint forces were calculated for all of the activities and are presented (chapter 7) and discussed (chapter 8). The overall conclusions drawn from the results and discussion form the topic for the final section of the thesis (chapter 9).

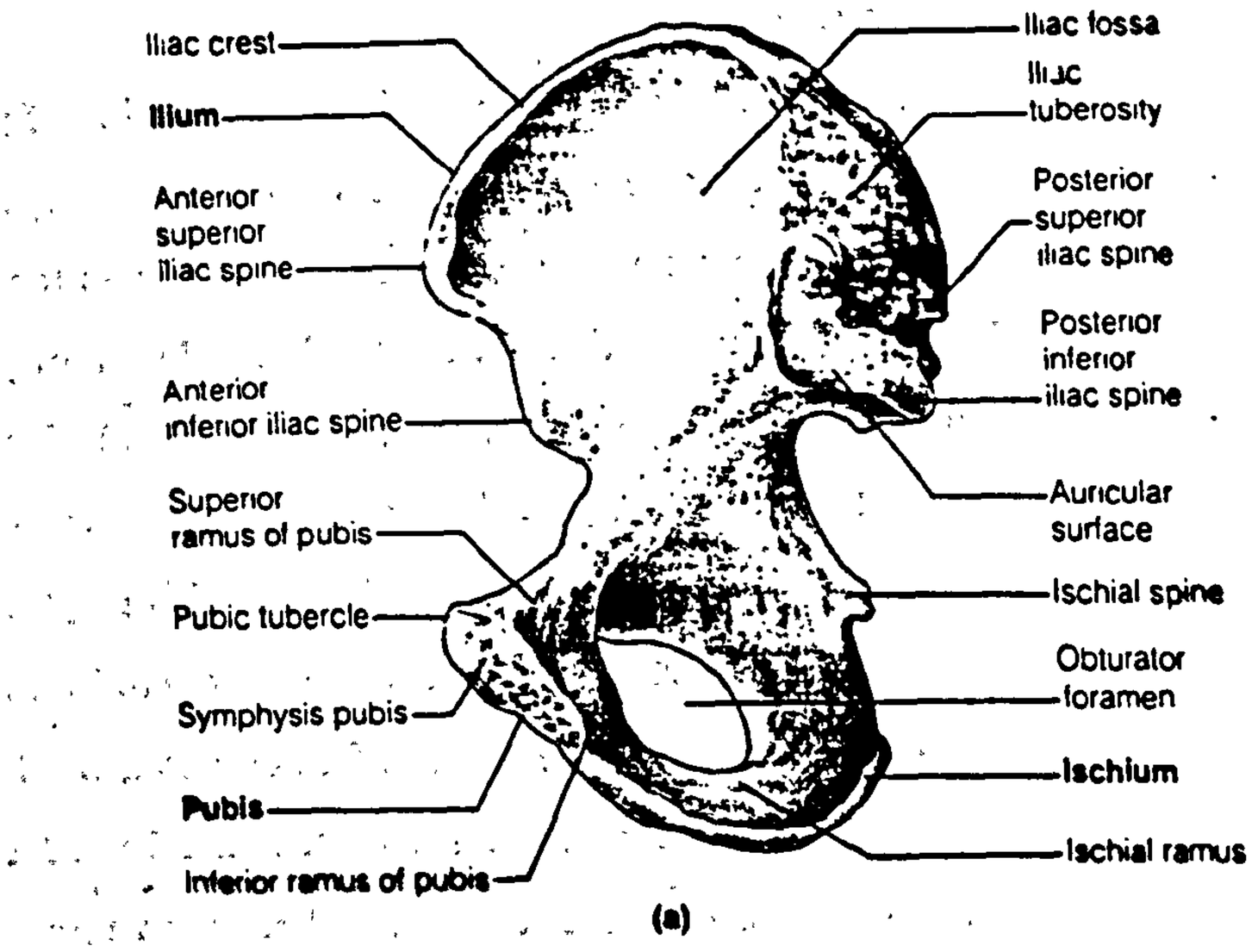

Figure 2.1 Right coxal bone. (a) Medial and (b) lateral views (from Gaudin and Jones, 1989).

CHAPTER 2. FUNCTIONAL ANATOMY OF THE LOWER LIMB

The anatomy of the lower extremity is described in this chapter to the extent necessary for understanding of the model of the lower extremity developed in this project. Although the hip joint is of primary concern, the anatomy in the region of the knee and ankle joints has been included to a limited extent since these joints are also included in the model in a simplified manner. If any more detail is required, reference may be made to standard texts (Gaudin and Jones, 1989, Nordin and Frankel, 1989, Palastanga et al, 1994).

2.1 SKELETAL STRUCTURE

The structure of the main bones of the lower limb is described such that the positions of the origins and insertions of the muscles included in the mathematical model may be identified and the bony landmarks referred to later in the thesis may be located.

2.1.1 Pelvis

The pelvic girdle supports the upper body and is made up of two coxal bones, commonly known as hipbones or pelvic bones. These are illustrated in figures 2.1 and 2.2. Each of these is described by three areas.

The ilium is the largest of these and forms the superior area. It is bordered superiorly by the iliac crest, the ends of which are marked by the anterior and posterior superior iliac spines. Below these are the corresponding inferior iliac spines. The lateral surface of the ilium is marked by the anterior, posterior and inferior gluteal lines which form muscle attachment areas. The ilium articulates with the sacrum and this supports the vertebral column.

The ischium is the area in the posterior corner of each coxal bone. The ischial spine forms the outer border to this area and the ischial tuberosity projects inferiorly from this area. The ischial tuberosity is separated from the ischial spine by the lesser sciatic notch. The lowest part is the ramus.

The pubis forms the anterior inferior corner and is made up of the superior and inferior ramus. The pubic bones articulate with each other at the pubic symphysis. Together, the pubis and ischium border the large opening called the obturator foramen.

The acetabulum, a large depression in the lateral surface of each coxal bone is located at the junction of the three areas. The articular surface of the acetabulum is covered with hyaline cartilage which articulates with the femoral head.

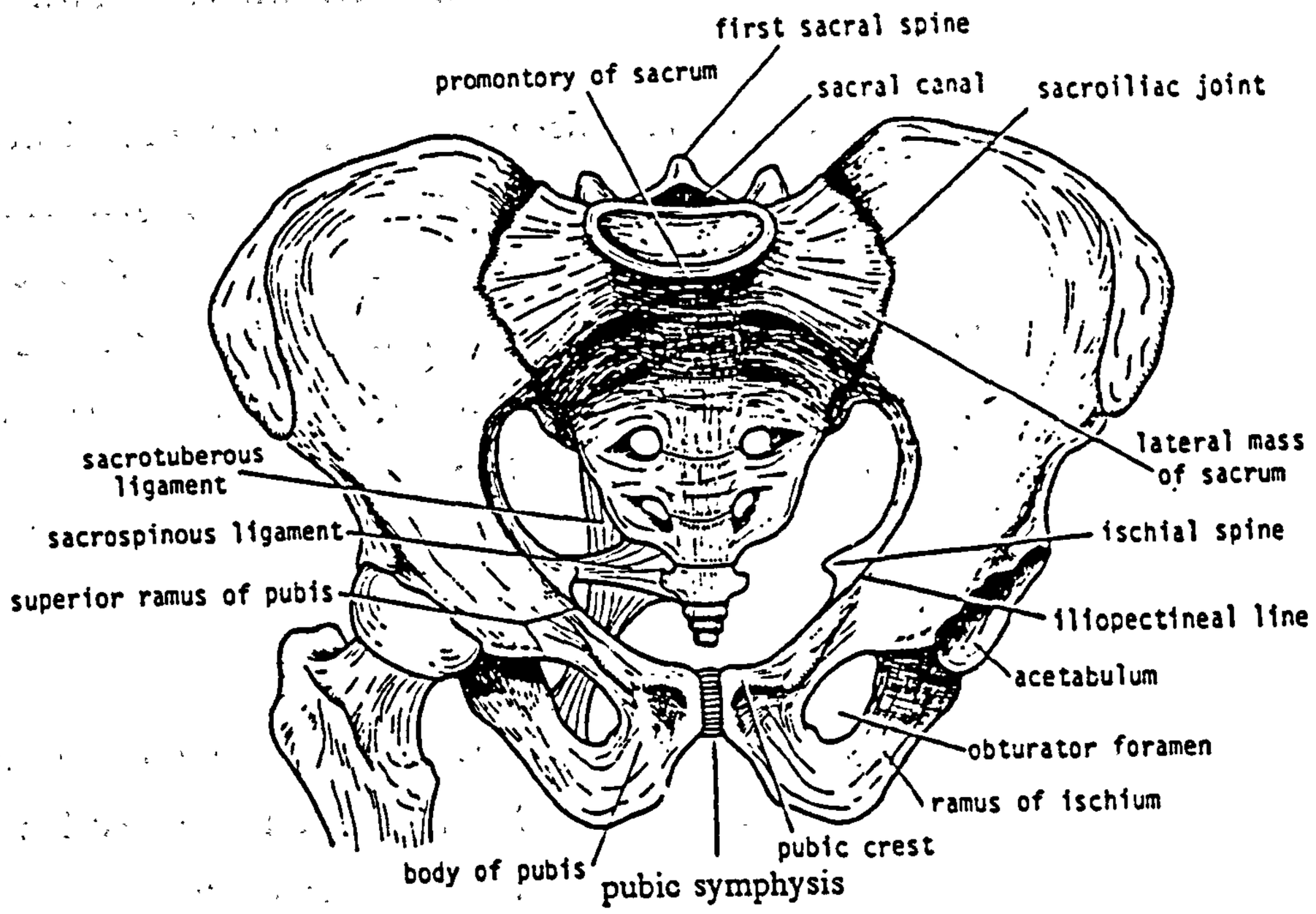

Figure 2.2 Anterior view of the male pelvis (from Snell, 1981).

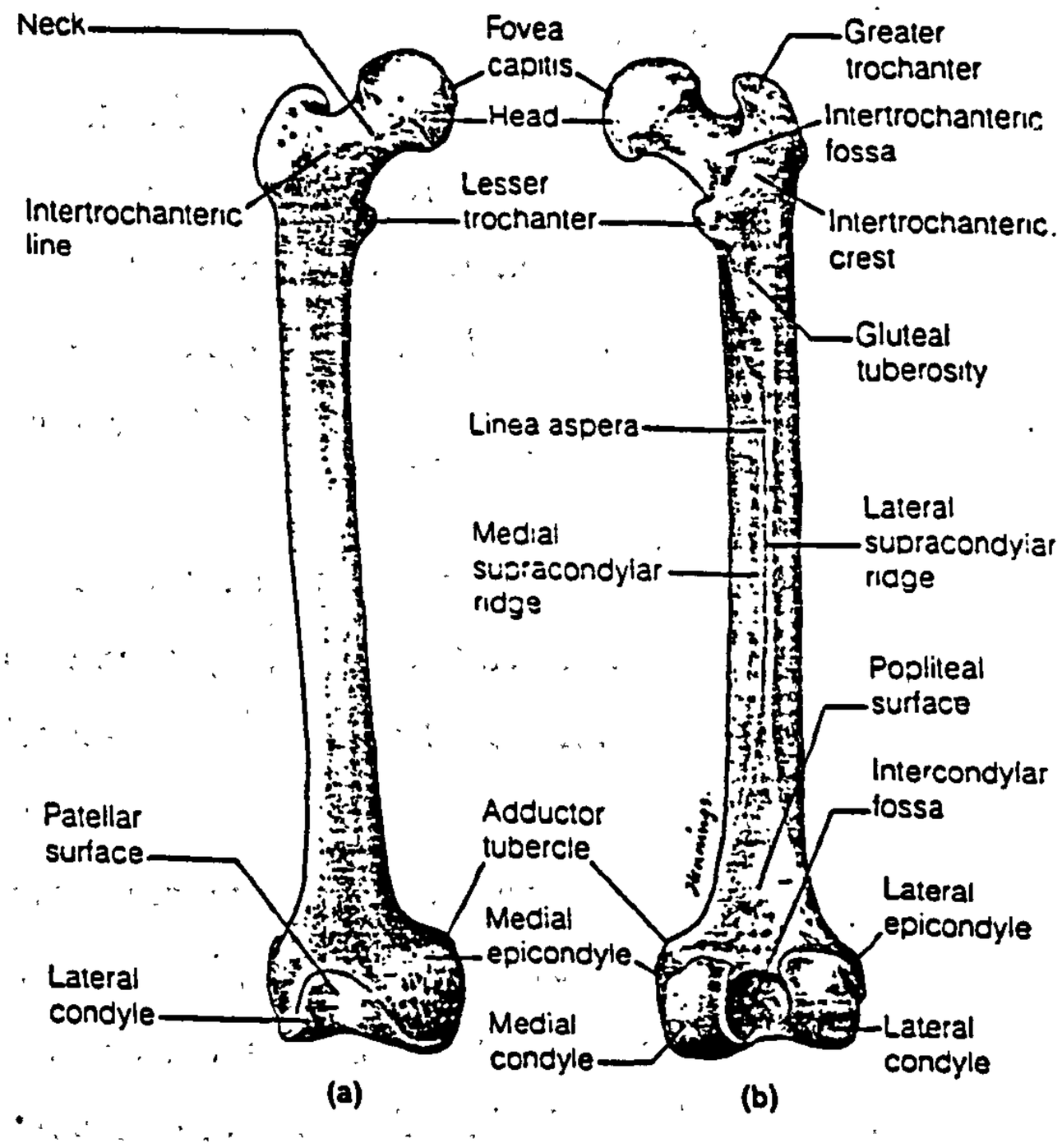

Figure 2.3 Right femur. (a) Anterior and (b) posterior views (from Gaudin and Jones, 1989).

2.1.2 Femur

The femur is the longest bone in the body. This is illustrated in figure 2.3. The head of the femur articulates with the acetabulum at the hip joint. The femoral head is connected to the shaft by the neck, the orientation of which is usually described by two angles as shown in figure 2.4. The inclination of the neck to the shaft in the frontal plane, the neck-to shaft-angle, is usually approximately 125° in adults, but it can vary between 90° and 135° (Nordin and Frankel, 1989). In the transverse plane, the angle of anteversion is formed between a line parallel to that between the posterior femoral condyles and a line through the head and neck of the femur. This angle is normally around 15° in adults but it can vary from approximately 8° to 30° (Norkin and Levangie, 1992).

Two bony prominences occur just distal to the neck. These are the greater and lesser trochanters which form attachment sites for muscles. A ridge called the linea aspera is situated on the posterior surface of the shaft and at its superior end, it expands into the gluteal tuberosity. Both the linea aspera and gluteal tuberosity form sites for the attachment of muscles.

At its distal end, the femur enlarges to form medial and lateral condyles which articulate with the tibia. The anterior surface between the condyles forms a wide shallow depression called the patellar surface. Epicondyles on the medial and lateral surfaces of the distal end form muscle attachment sites.

2.1.3 Patella

The patella or knee cap is a small triangular floating sesamoid bone, embedded in the quadriceps tendon. Articular facets for the femoral condyles are situated on the posterior surface. The patella protects the knee joint. It aids knee extension by producing anterior displacement of the quadriceps tendon, thereby lengthening the lever arm of the quadriceps muscle.

2.1.4 Tibia and Fibula

The tibia and fibula illustrated in figure 2.5 make up the bones of the lower leg. The tibia or shin bone is the larger of the two and lies medial to the fibula. The proximal end of the tibia expands into the medial and lateral condyles which articulate with the femur. Just below the condyles there is a roughened tibial tuberosity on the anterior surface of the shaft. The distal end of the tibia forms a concave surface which makes up part of the ankle joint. The medial malleolus is located on the medial side of the distal end.

At the proximal end, the fibula head articulates with the tibia and at the distal end, the fibula enlarges into the lateral malleolus which forms part of the ankle joint.

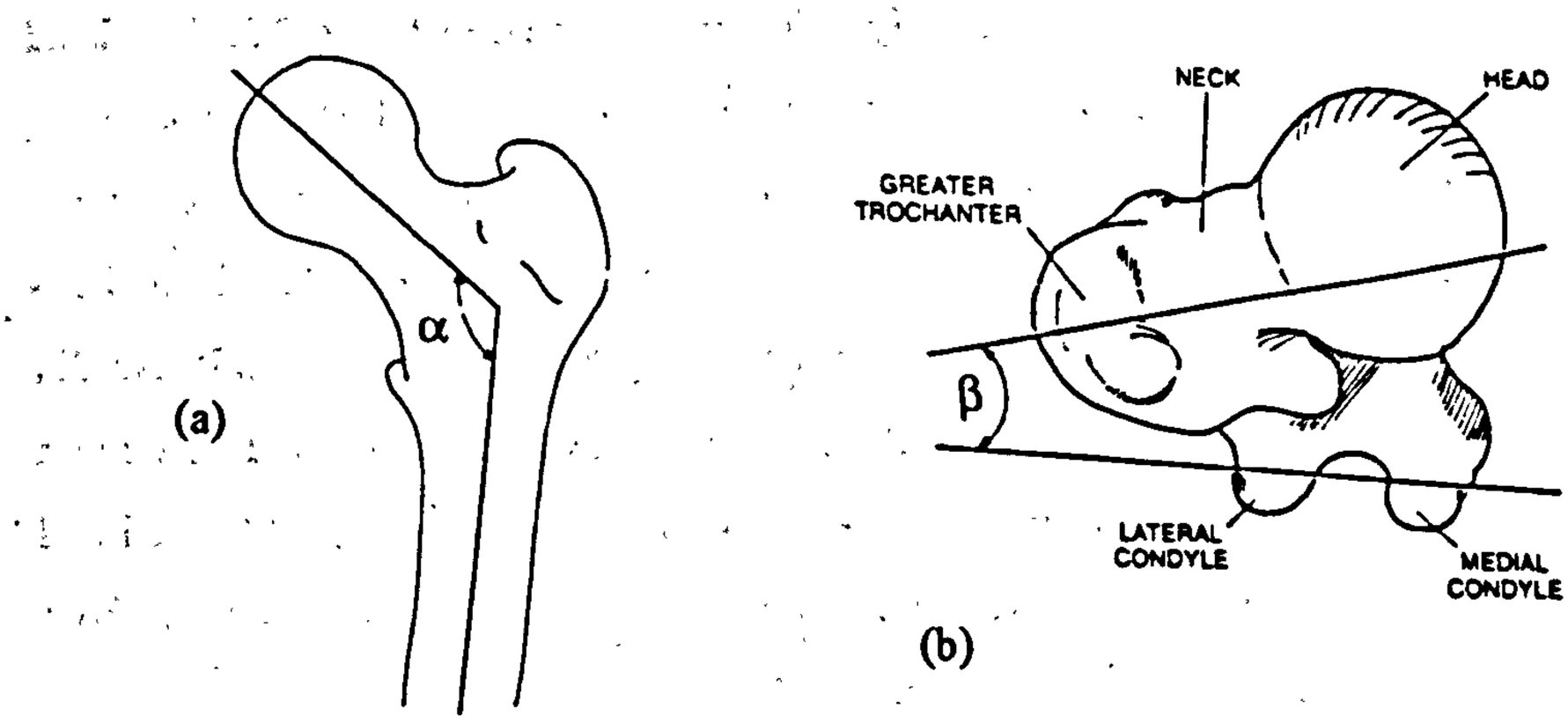

Figure 2.4 (a) Femoral neck to shaft angle, α and (b) top view of the proximal end of the left femur showing the angle of anteversion, β (from Nordin and Frankel, 1989).

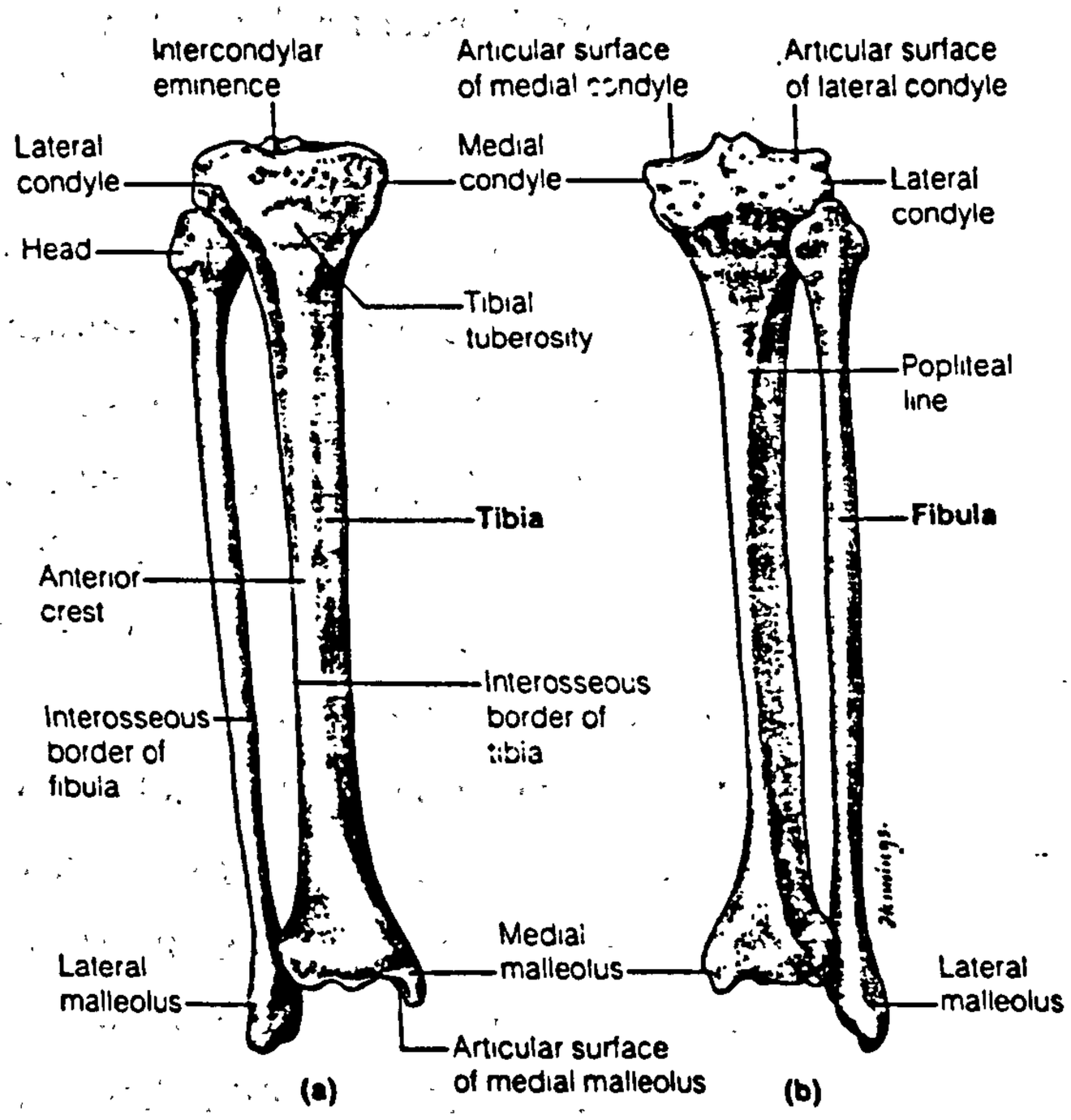

Figure 2.5 Right tibia and fibula. (a) Anterior and (b) posterior views (from Gaudin and Jones, 1989).

2.1.5 Pes

The pes or foot is shown in figure 2.6 and consists of the tarsus, metatarsus and phalanges. The tarsus is formed by 7 tarsal bones of different shapes and sizes. These lie distal to the tibia and fibula and between the two malleoli. The metatarsus comprises 5 metatarsal bones which articulate with the tarsals. The phalanges make up the digits of the foot.

2.2 STRUCTURE AND FUNCTION OF THE JOINTS

2.2.1 The Hip Joint

The head of the femur articulates with the cup shaped acetabulum at the hip joint. It is one of the largest and most stable joints in the body and allows a wide range of motion as is required in many daily activities. The range of motion is greatest in the sagittal plane, with flexion up to approximately 140° and extension to 15°. Abduction up to 30° may occur and adduction to 25°. External rotation may be up to 90° and internal rotation to 70° when the hip joint is flexed (Nordin and Frankel, 1989). It should be noted here that rotation at the hip joint takes place about the mechanical axis of the femur and not about the long axis of the shaft of the femur. The mechanical axis is that which runs between the knee and hip joint centres.

The hip joint is a synovial ball and socket type joint as shown in figure 2.7. The acetabular cavity is thickened by a fibrocartilaginous rim, the acetabular labrum. The capsule encloses the joint and is attached medially to the acetabular labrum. On the lateral side it is attached halfway along the posterior aspect of the neck and anteriorly to the intertrochanteric line which runs between the greater and lesser trochanters. The capsule is reinforced by the iliofemoral and pubofemoral ligaments which lie anteriorly to the hip joint and also the ischiofemoral ligament which lies posteriorly as shown in figure 2.8. These ligaments limit movements at the hip joint.

The iliofemoral ligament is the strongest of these and is shaped like an inverted Y. It runs from the anterior inferior iliac spine to the upper and lower parts of the intertrochanteric line of the femur. The ligament becomes taut in extension and external rotation of the femur relative to the pelvis. The superior band of the ligament also becomes taut in adduction.

The pubofemoral ligament is triangular in shape. The base is connected to the superior ramus of the pubis, and the apex to below the lower end of the intertrochanteric line. As was the case for the iliofemoral ligament, the pubofemoral ligament becomes taut in extension and external rotation. However, it slackens in adduction and becomes taut in abduction.

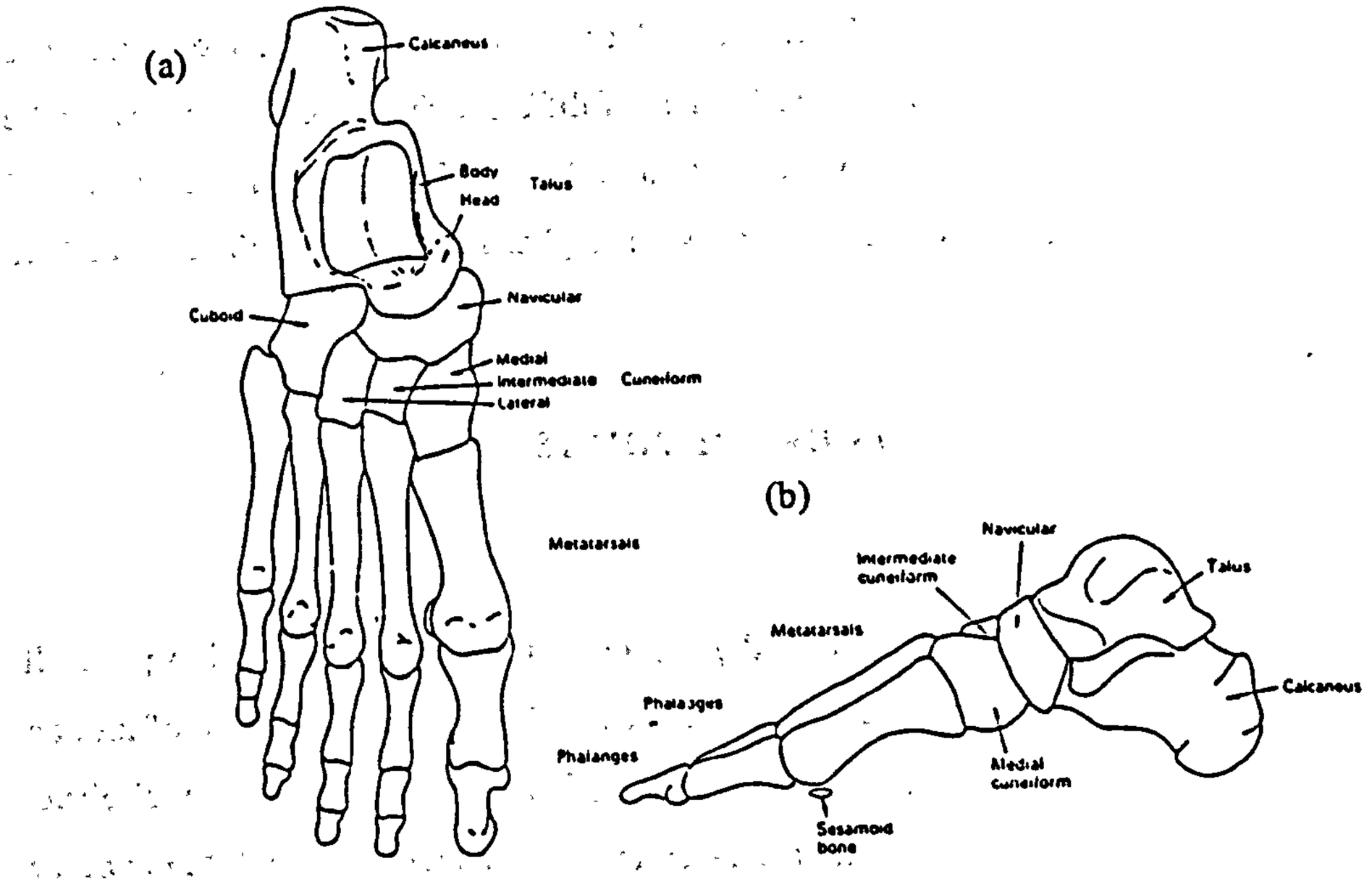

Figure 2.6 Right foot. (a) Superior and (b) medial views (from Palastanga et al, 1994).

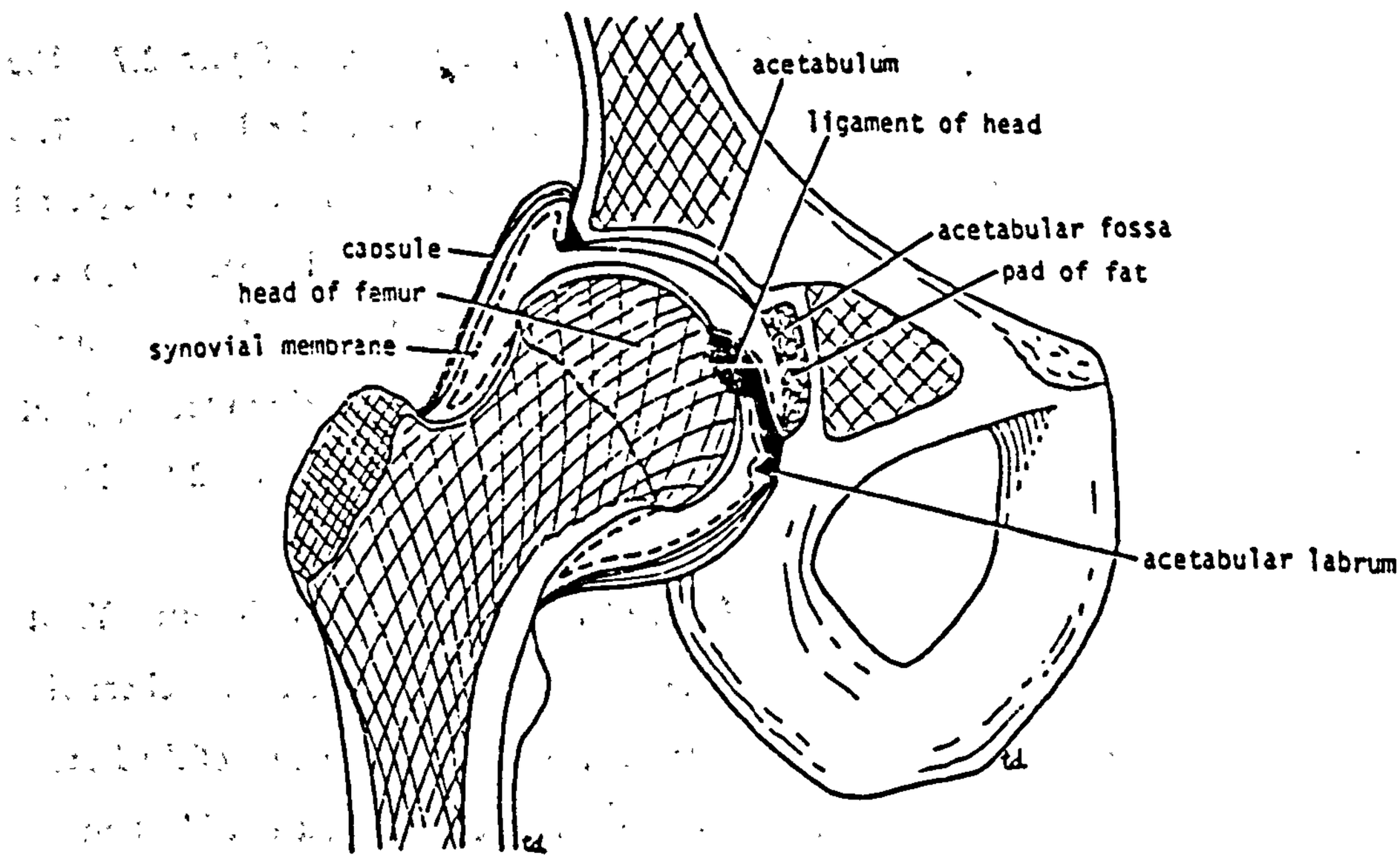

Figure 2.7 Coronal section of the right hip joint (from Snell, 1981).

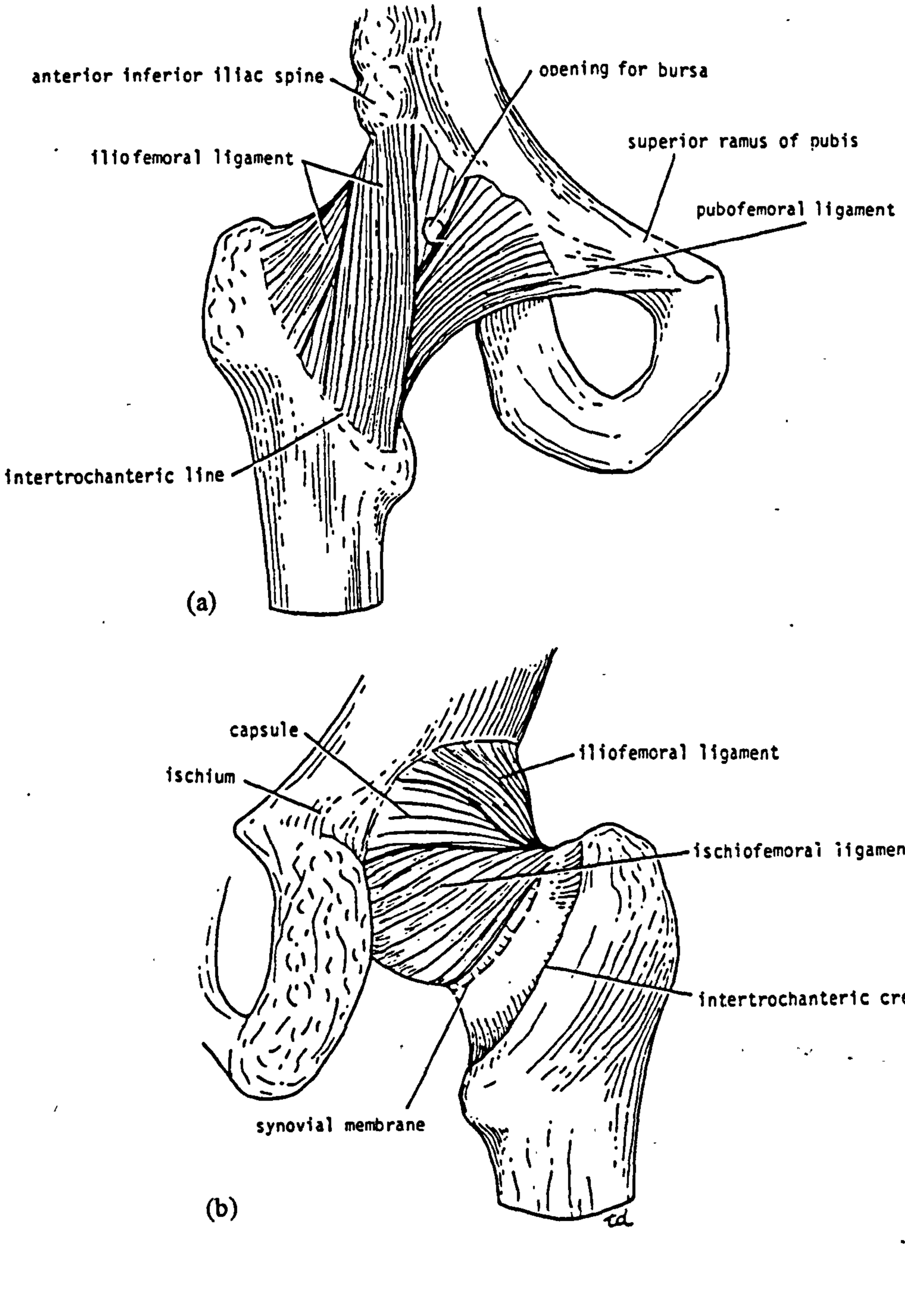

Figure 2.8 Right hip joint. (a) Anterior and (b) posterior views (from Snell, 1981).

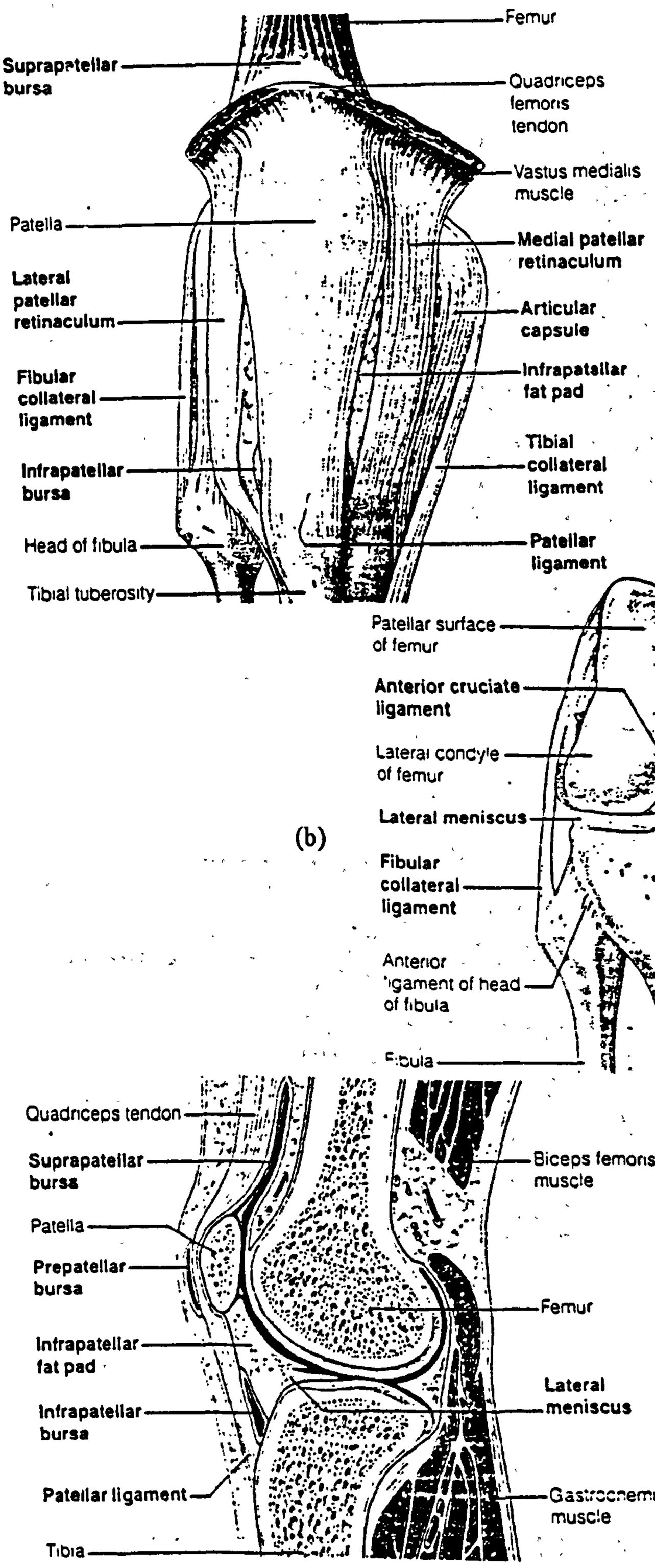

Figure 2.9 Right knee joint. (a) Anterior view, (b) anterior flexed view and (c) sagittal section (from Gaudin and Jones, 1989).

The ischiofemoral ligament is spiral in shape and runs from the body of the ischium, behind the hip joint to the greater trochanter. Like the others, it becomes taut in hip extension. It also limits abduction and internal rotation.

The ligament of the head of the femur lies within the joint as can be seen from figure 2.7. This has a small limiting action on adduction of the hip joint.

The capsule is lined with a synovial membrane. This membrane also covers the part of the femoral neck which is within the capsule and ensheaths the ligament of the head of the femur. It covers the acetabular fossa, the area of the floor of the acetabulum which is non-articular.

2.2.2 The Knee Joint

The knee joint is the largest and possibly the most complex joint in the body. It consists of two joints involving the tibia, femur and patella, the articulating surfaces of which are covered with hyaline cartilage. The tibiofemoral joint is that between the tibial and femoral condyles and is a synovial hinge type joint with some rotatory movement. A synovial gliding type joint called the patellofemoral joint is formed between the patella and the patellar surface of the femur. These are illustrated in figure 2.9.

The knee joint allows motion in three planes but motion is dominated by that in the sagittal plane where the range of flexion is from 0° to 140°. At full extension, knee rotation is limited but as the knee flexes, more rotation is possible. The maximum range of rotation is achieved when the knee is flexed at 90°. External rotation up to 45° and internal rotation up to 30° is then possible. As the knee is flexed beyond 90°, the range of rotation decreases again, mainly due to soft tissue restrictions. The range of abduction and adduction varies with knee flexion in a similar manner to rotation. At full extension almost no abduction or adduction is possible but as the knee flexes to 30°, a few degrees is possible. Beyond 30°, the range of adduction and abduction reduces, again due to soft tissue restrictions (Nordin and Frankel, 1989).

The knee joint is surrounded by a capsule on its medial, lateral and posterior sides. This is lined by a synovial membrane which pouches up on the anterior side to form a bursa in the area where there is no capsule. A number of ligaments are located outside and within the capsule.

The extracapsular ligaments include the patella ligament which lies in front of the joint. It is attached to the patella above and to the tubercle of the tibia below and is an extension of the central part of the quadriceps tendon. The lateral and medial collateral ligaments lie on the respective sides of the joint and help to prevent abduction and adduction of the knee joint. The oblique popliteal ligament lies on the posterior side and helps to strengthen the

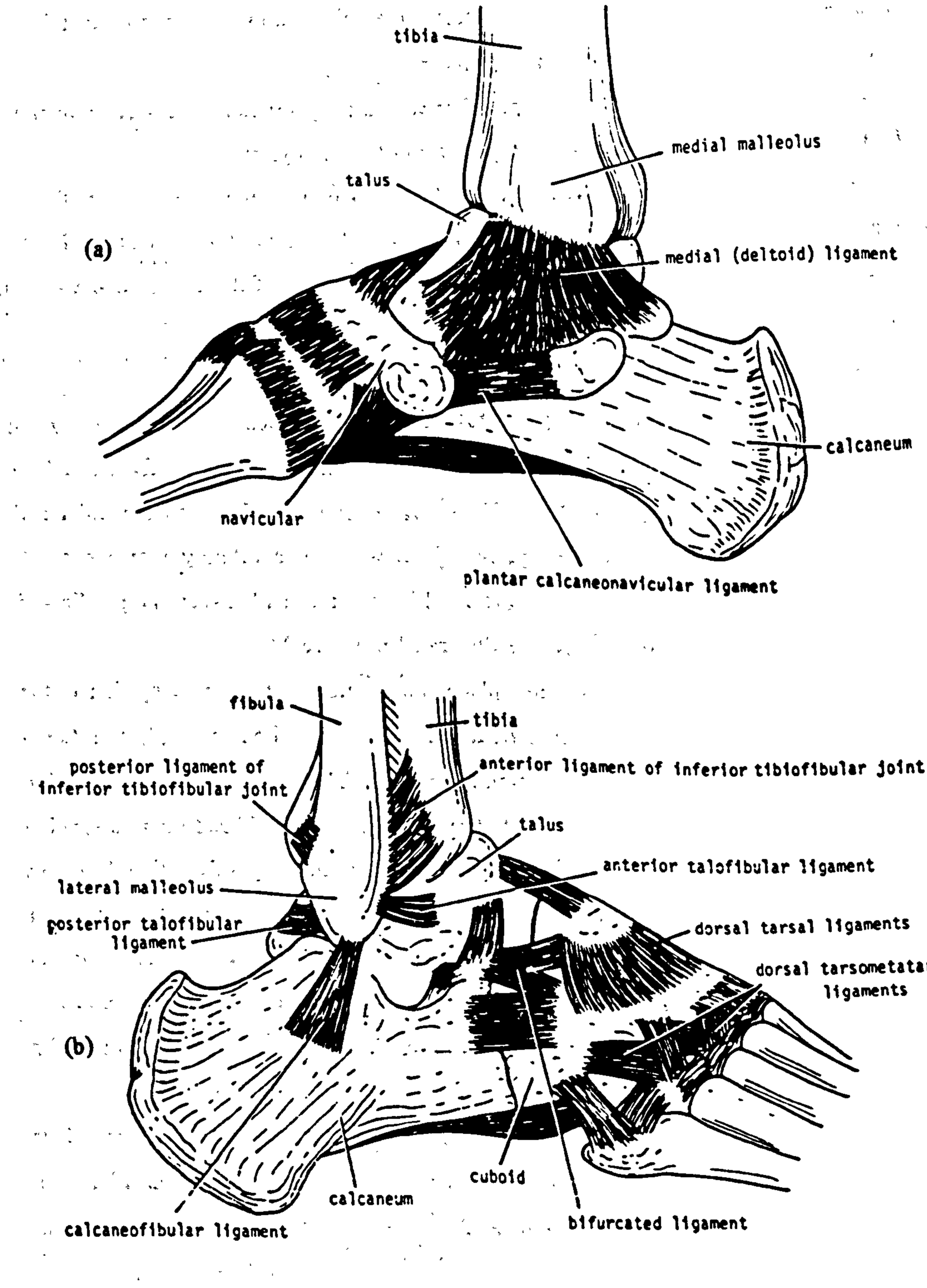

Figure 2.10 Right ankle joint. (a) Medial and (b) lateral views (from Snell, 1981).

lower posterior part of the joint. On each side of the patella, the capsule is strengthened by expansions of the tendons of the vastus lateralis and medialis.

The intracapsular ligaments include the anterior and posterior cruciate ligaments. They provide resistance to anterior and posterior displacements of the tibia with respect to the femur and give some medio-lateral stability.

2.2.3 The Ankle Joint

The ankle joint is a synovial hinge type joint formed by articulations of tibia, fibula and talus as shown in figure 2.10. It consists of the tibiotalar, fibulotalar and distal tibiofibula joints. In the sagittal plane maximum dorsiflexion is approximately 10-20° and maximum plantarflexion, 25-35° (Nordin and Frankel, 1989).

The ankle joint is maintained by the shape of the three joints as well as by the structures surrounding it. The joint is surrounded by a capsule which is lined with a synovial membrane. A strong medial or deltoid ligament lies on the medial side of the joint whilst a weaker lateral ligament system lies on the lateral side. These ligaments act to maintain joint stability and control movements.

2.3 MUSCLES OF THE LOWER LIMB

The location, structure and function of the muscles of the lower limb are described in this section. Those crossing the hip joint are discussed in detail whilst those crossing the knee and ankle joints are discussed to the extent to which they are included in the mathematical model developed in this project. It is common to describe the function of a muscle as would be the case with the limb segments in the anatomical position. However, when the limb segments are in other configurations, the function of a muscle at a particular joint may change as its line of action relative to the joint centre changes. These changes are highlighted in this section.

2.3.1. Muscles around the Hip Joint

The muscles around the hip joint can conveniently be divided into groups according to their main function. These are hip extensors, abductors, adductors, flexors and rotators. Some of the muscles will have other actions in addition to their main role and these will be discussed.

Hip extensors

The hip extensors include gluteus maximus and the hamstrings. Gluteus maximus is the largest of the gluteal muscles and is quadrilateral in shape. As can be seen from figure 2.11

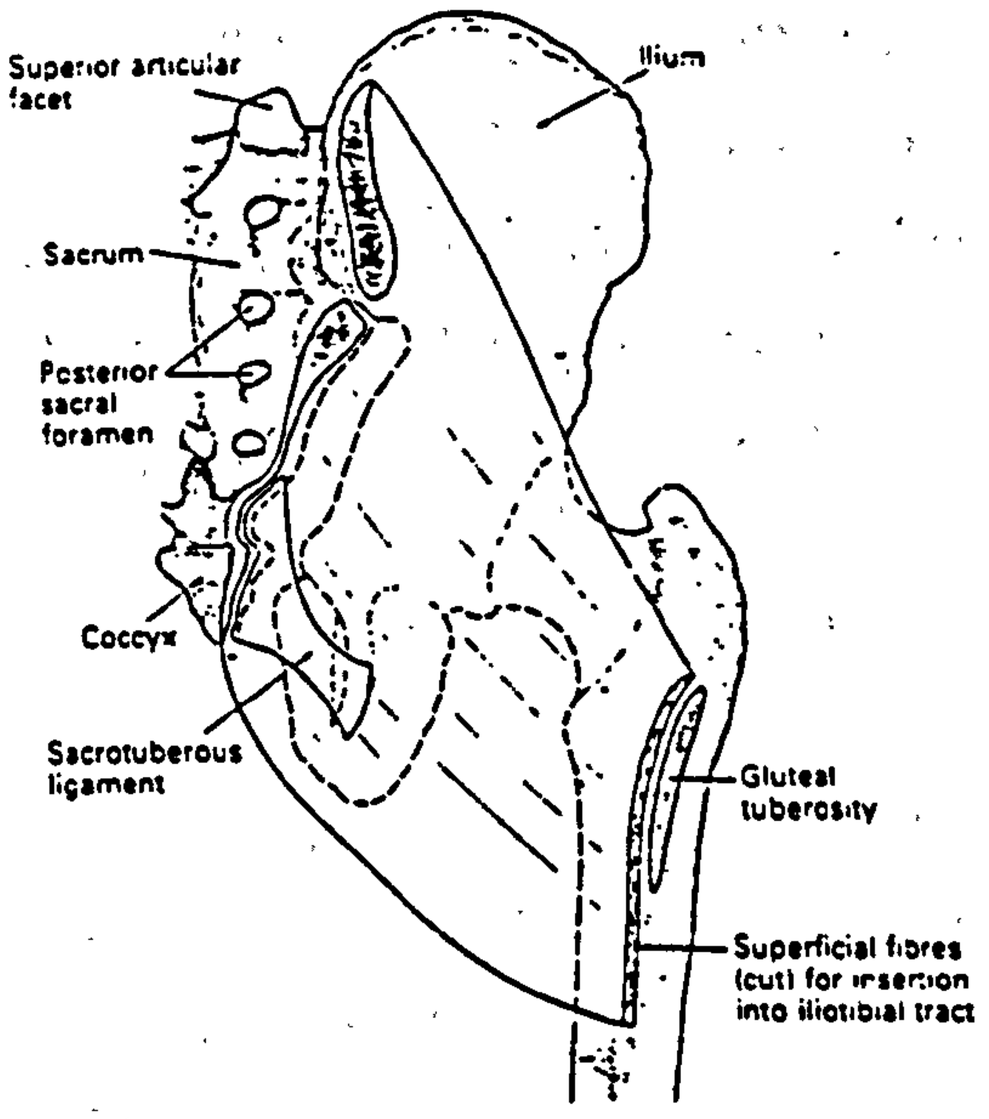

Figure 2.11 Right gluteus maximus. Posterior view with bony attachments shaded and the direction of the fibres in diagrammatic form (from Palastanga et al, 1994).

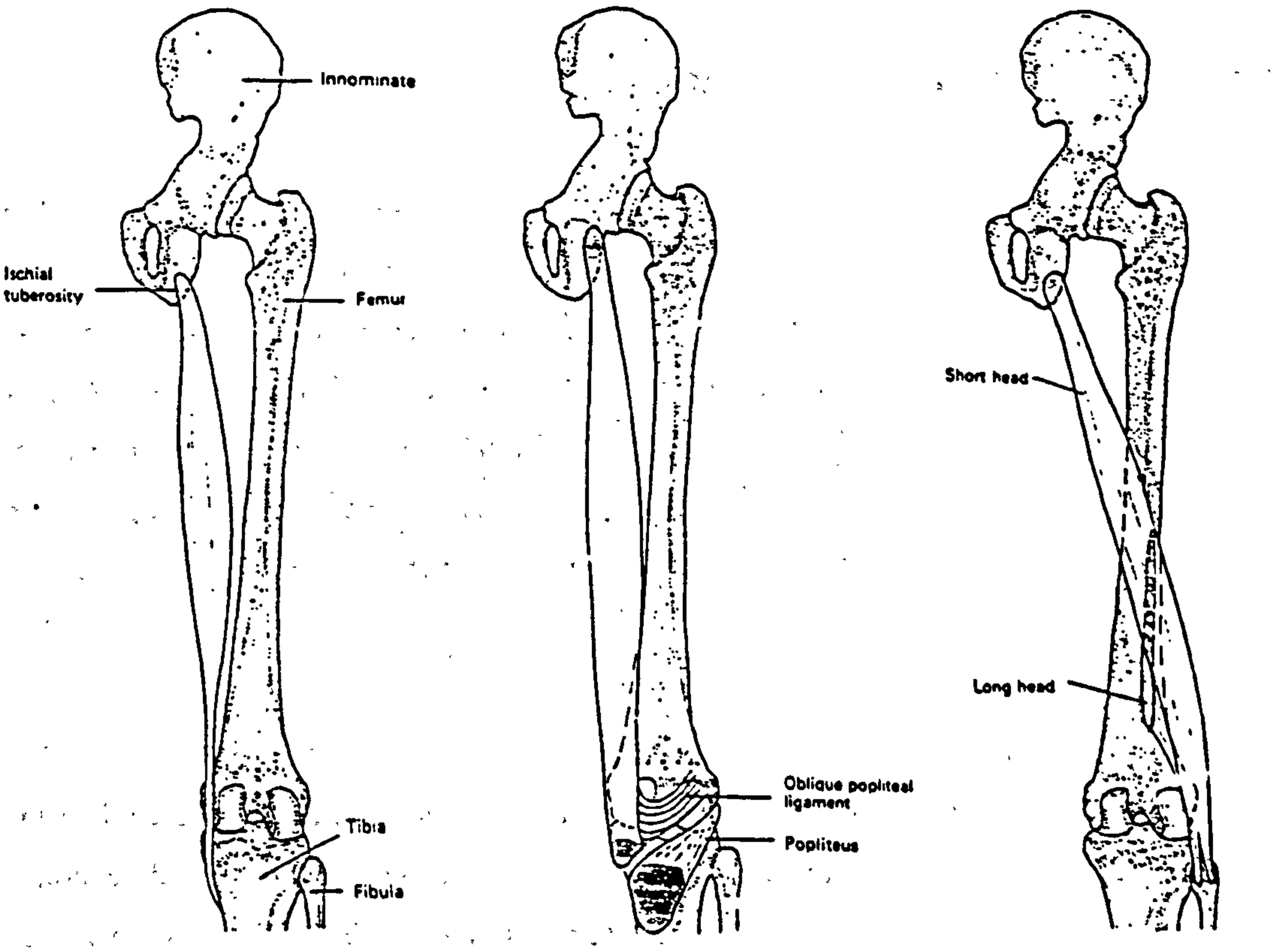

Figure 2.12 Posterior views of (a) semitendinosus, (b) semimembranosus and (c) biceps femoris. Right leg. (from Palastanga et al, 1994)

it originates from the outer surface of the ilium behind the posterior gluteal line, from the sacrum and coccyx and from the sacrotuberous ligament. It passes downwards and laterally and most fibres insert into the iliotibial tract whilst a few insert into the gluteal tuberosity of the femur. In addition to being an extensor, gluteus maximus is also an external rotator. The lower fibres are adductors and the upper ones, abductors. The fibres which insert into the iliotibial tract help to maintain the knee joint in extension and limit adduction at the knee joint through the action of the iliotibial tract. As a hip extensor, gluteus maximus will resist an external moment tending to flex the hip joint. It will either work concentrically, causing extension, or eccentrically, trying to resist flexion. Since it is very powerful, it is ideally suited to stepping up onto a stool, climbing and running. It will act with the hamstrings in raising the trunk from a flexed position as in rising from a sitting or stooping position.

The hamstring group consists of semitendinosus, semimembranosus and biceps femoris. Both semitendinosus and semimembranosus originate from the ischial tuberosity. Semitendinosus then inserts into the upper part of the medial surface of the tibia and semimembranosus into the postero-medial surface of the medial tibial condyle as shown in figures 2.12a and 2.12b. As was the case for gluteus maximus, these muscles will resist an external moment tending to flex the hip joint and work concentrically, causing extension, or eccentrically, trying to resist flexion. They are also knee flexors. When the knee joint is partly flexed, they act as knee internal rotators. The long head of biceps femoris also originates from the ischial tuberosity whilst the short head originates from the linea aspera and lateral supracondylar ridge on the posterior surface of the femur. These two heads unite and insert into the head of the fibula as shown in figure 2.12c. Biceps femoris acts with the other hamstrings as a hip extensor and knee flexor. It will also act as an external rotator in the semi-flexed knee.

Hip abductors

Hip abductors include gluteus maximus, gluteus medius, gluteus minimus and tensor fascia lata.

The action of gluteus maximus has already been described. As already stated, it is the upper fibres of this muscle which can act as abductors. Gluteus medius lies beneath gluteus maximus and is a fan shaped muscle with the broad part lying more superiorly as shown in figure 2.13. Gluteus medius originates from the ilium between the iliac crest above, the posterior gluteal line behind and middle gluteal line below. The fibres pass downwards and laterally to insert into the lateral surface of the greater trochanter of the femur. Gluteus medius is a powerful abductor of the hip joint and has a vital role in walking, running and weight bearing on one limb. When the opposite limb is off the ground, the pelvis on that side

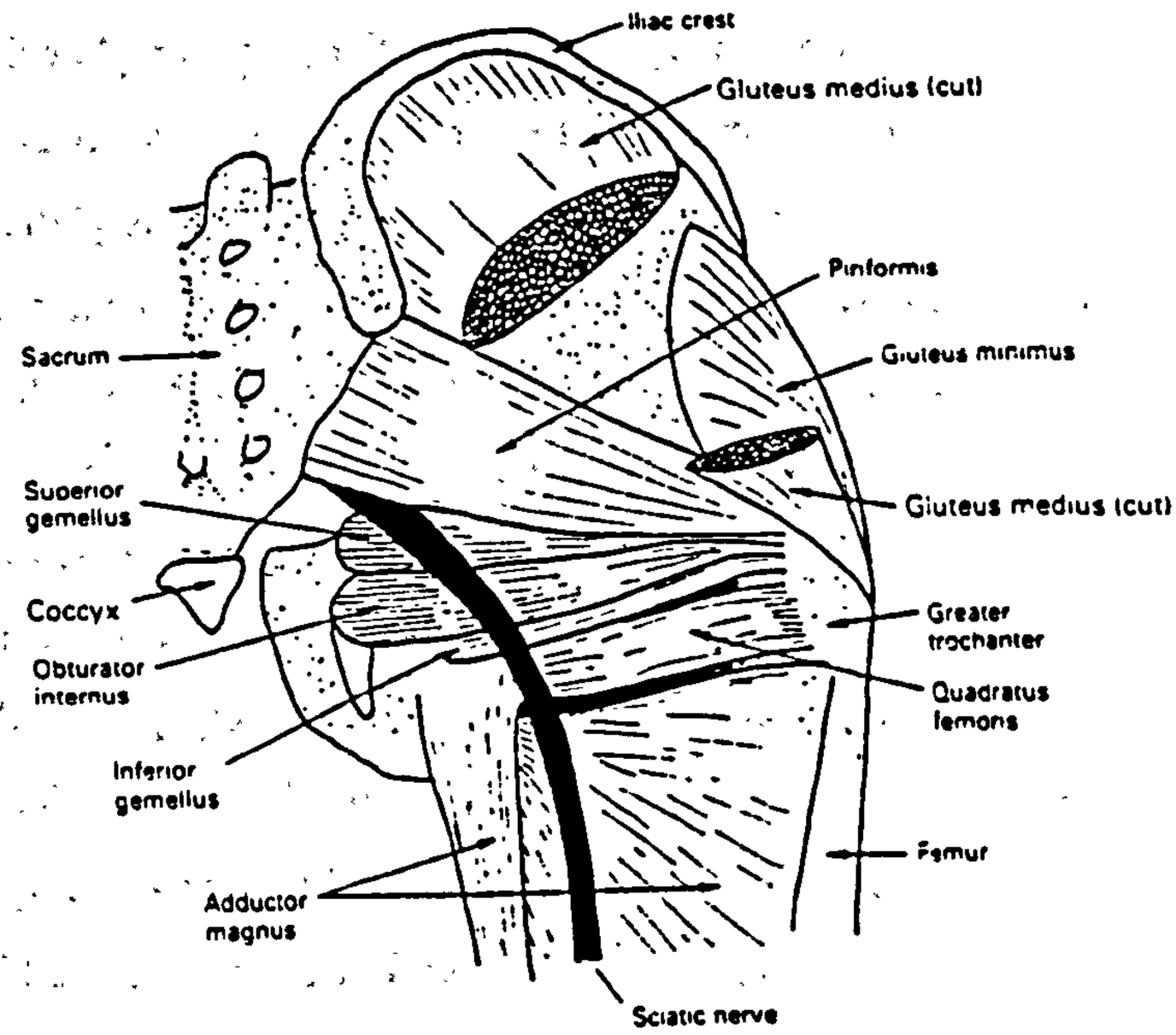

Figure 2.13 Right gluteal region. Posterior view with gluteus maximus removed (from Palastanga et al, 1994).

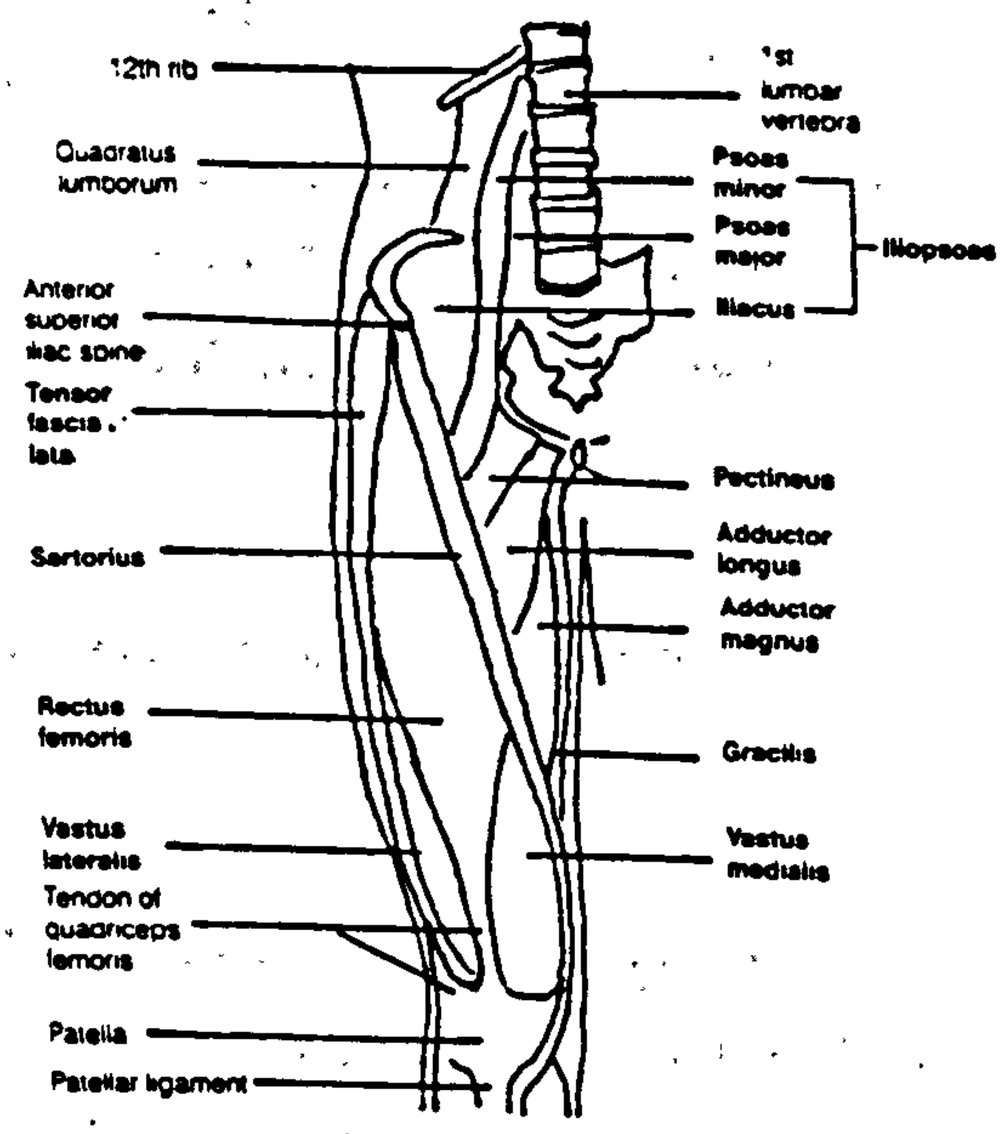

Figure 2.14 Muscles of the hip and thigh. Anterior view (from Gaudin and Jones, 1989).

tends to drop due to lack of support. Gluteus medius on the supporting side acts as an abductor at this time, counteracting the tendency to adduct and preventing the pelvis from dropping.

Gluteus minimus originates from the outer surface of the ilium between the middle and inferior gluteal lines and inserts into the anterior surface of the greater trochanter of the femur. It is a triangular shaped muscle being wide at the top and narrowing towards the insertion as shown in figure 2.13. Its action is the same as that of gluteus medius and it works with gluteus medius to support the pelvis during walking and running.

Tensor fascia lata overlies gluteus minimus. It originates from the outer edge of the iliac crest between the anterior superior iliac spine and the iliac tubercle and then runs downwards and slightly backwards to insert into the iliotibial tract. Figure 2.14 shows the position of this muscle in relation to other muscles of the hip and thigh. Tensor fascia lata helps gluteus medius and minimus as an abductor and is also a hip flexor. By exerting traction on the iliotibial tract, it also assists in maintaining the knee in an extended position. As long as the line of action of the iliotibial tract remains in front of the axis of flexion of the knee, it assists in maintaining knee extension.

Hip adductors

Hip adductors include adductor magnus, adductor longus, adductor brevis, gracilis and pectineus. Adductor magnus, adductor longus, adductor brevis and gracilis are illustrated in figure 2.15 and pectineus in figure 2.16.

Adductor magnus is the largest and most posterior of the adductor group. Semimembranosus and semitendinosus lie behind it whilst adductor brevis and longus lie in front. It forms a triangular sheet whose apex originates from the outer surface of the inferior ramus of the pubis, from the ramus of the ischium and from the ischial tuberosity. Those fibres arising from the ischial tuberosity insert into the adductor tubercle on the medial condyle of the femur. These are hip extensors. The rest insert along the length of the posterior surface of the femur and form the adductor portion. The muscle can also act as an internal or external rotator depending on its line of action with respect to the mechanical axis of rotation of the femur. This will change with the position of the thigh.

Adductor longus is a long slender triangular muscle which overlies the middle part of adductor magnus. It originates from the front of the body of the pubis and inserts into the medial lip of the linea aspera of the femur. It is an adductor but its rotational action will depend on the position of the thigh as did that of adductor magnus. Adductor longus can also act as a flexor on the extended thigh and as an extensor on the flexed thigh.

Adductor brevis, another triangular shaped adductor, originates from the outer surface

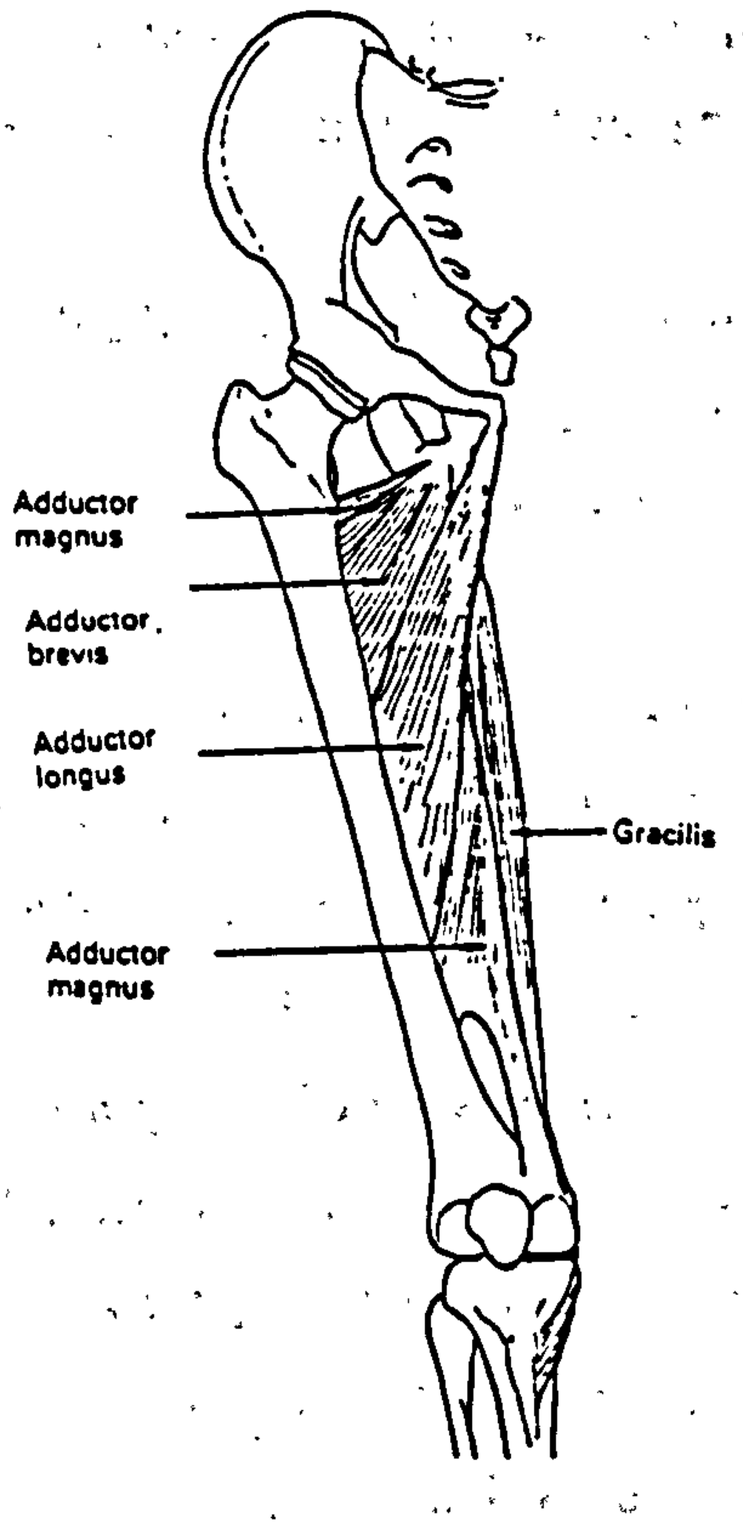

Figure 2.15 Adductor muscles of the right leg. Anterior view (from Palastanga et al, 1994).

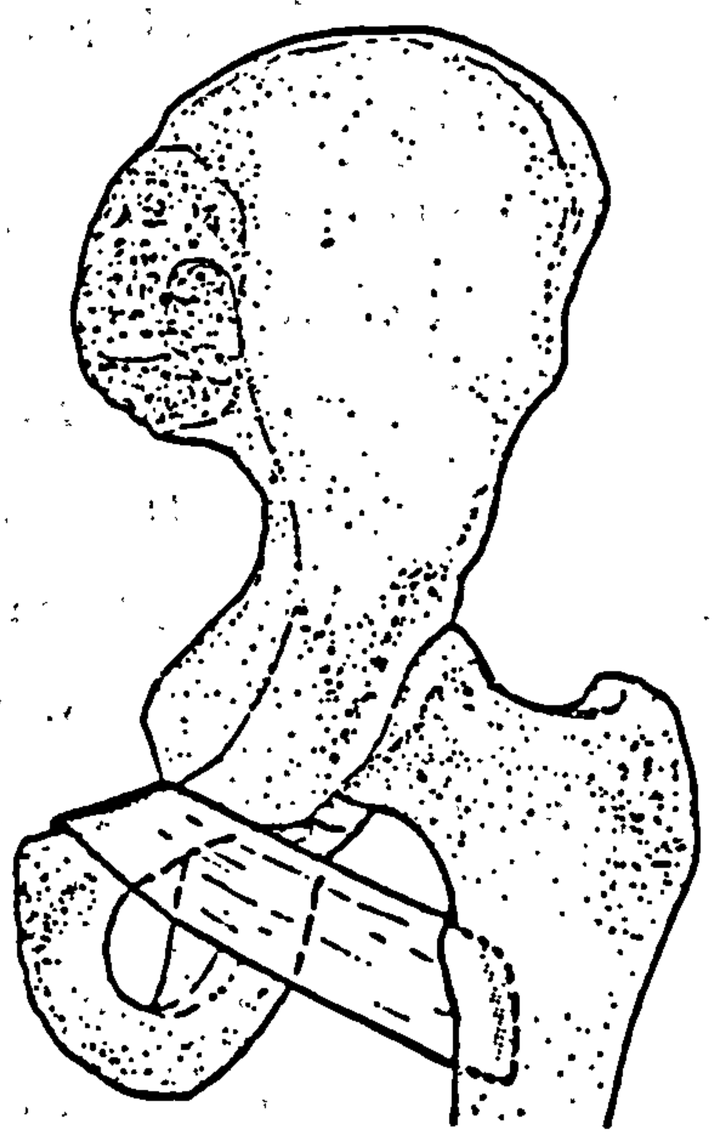

Figure 2.16 Left pectineus. Anterior view (from Palastanga et al, 1994).

of the inferior pubic ramus and runs downwards and laterally to insert into linea aspera of the femur.

Gracilis is a long thin muscle which originates from the outer surface of the inferior ischial ramus and passes downwards, medial to the other adductors to insert into the upper part of the medial surface of the tibia. In addition to being a hip adductor and flexor, it also has an important role as a knee flexor. It assists the knee in simple flexion activities such as at the beginning of the swing phase of gait. When the knee is in a semi-flexed position, it can act as an internal rotator at the knee.

The final adductor to be described is pectineus. The fibres originate from the superior ramus of the pubis and pass downwards, backwards and laterally to insert into the upper end of the linea aspera as shown in figure 2.16. It is a hip adductor and in the upright position, it will act as a flexor. However when the degree of hip flexion is high such as when rising from a very low chair or squat position, the line of action of the muscle relative to the axes of rotation of the femur will be altered such that it becomes a hip extensor.

Hip flexors

The hip flexors include psoas major, iliacus, rectus femoris, sartorius, pectineus and tensor fascia lata.

Psoas major, a large thick muscle is situated mainly in the abdominal cavity. It originates from the twelfth thoracic to the fifth lumbar vertebrae and passes downwards and forwards to join iliacus before passing over the pelvic brim. It passes in front of the hip joint and then behind to insert into the lesser trochanter of the femur as shown in figure 2.17. As a hip flexor, it will resist an external moment tending to extend the hip and work concentrically, causing hip flexion or eccentrically, trying to resist hip extension. It will act on the thigh in walking, running and jumping and pull the trunk forwards when rising from a lying or sitting position. Since it originates from the vertebrae, it will also act on the lumbar spine. There has been some debate over its rotational effects at the hip joint, but when considering its line of action relative to the mechanical axis of the femur it is likely that it will act as an internal rotator.

Iliacus is a large triangular muscle as illustrated in figure 2.17. It acts as a hip flexor with psoas. The fibres originate from the iliac fossa in the abdomen and then converge with psoas to insert into the lesser trochanter as described above. Controversy over its rotational effects exists as was the case for iliacus. Together, psoas and iliacus are usually referred to as iliopsoas.

Rectus femoris forms part of the quadriceps femoris muscle group which acts as a knee extensor. However, rectus femoris also passes in front of the hip joint and is therefore

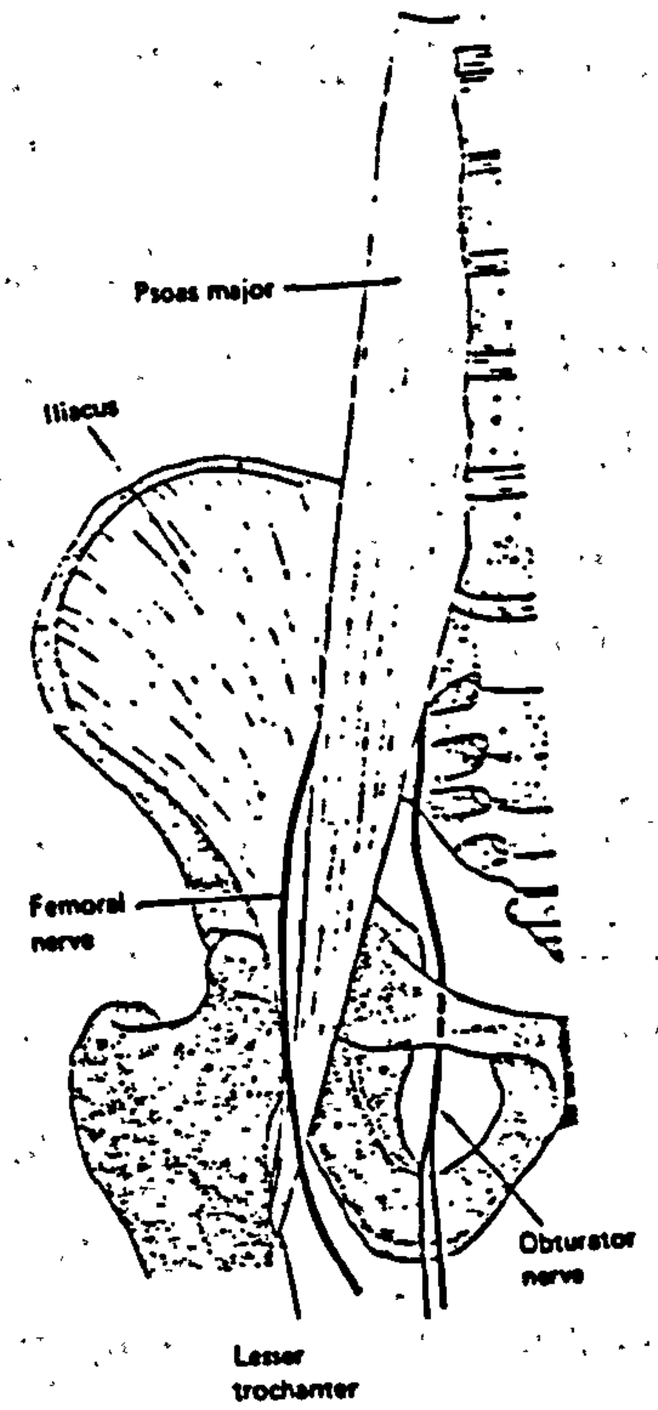

Figure 2.17 Right psoas major and iliacus. Anterior view (from Palastanga et al, 1994).

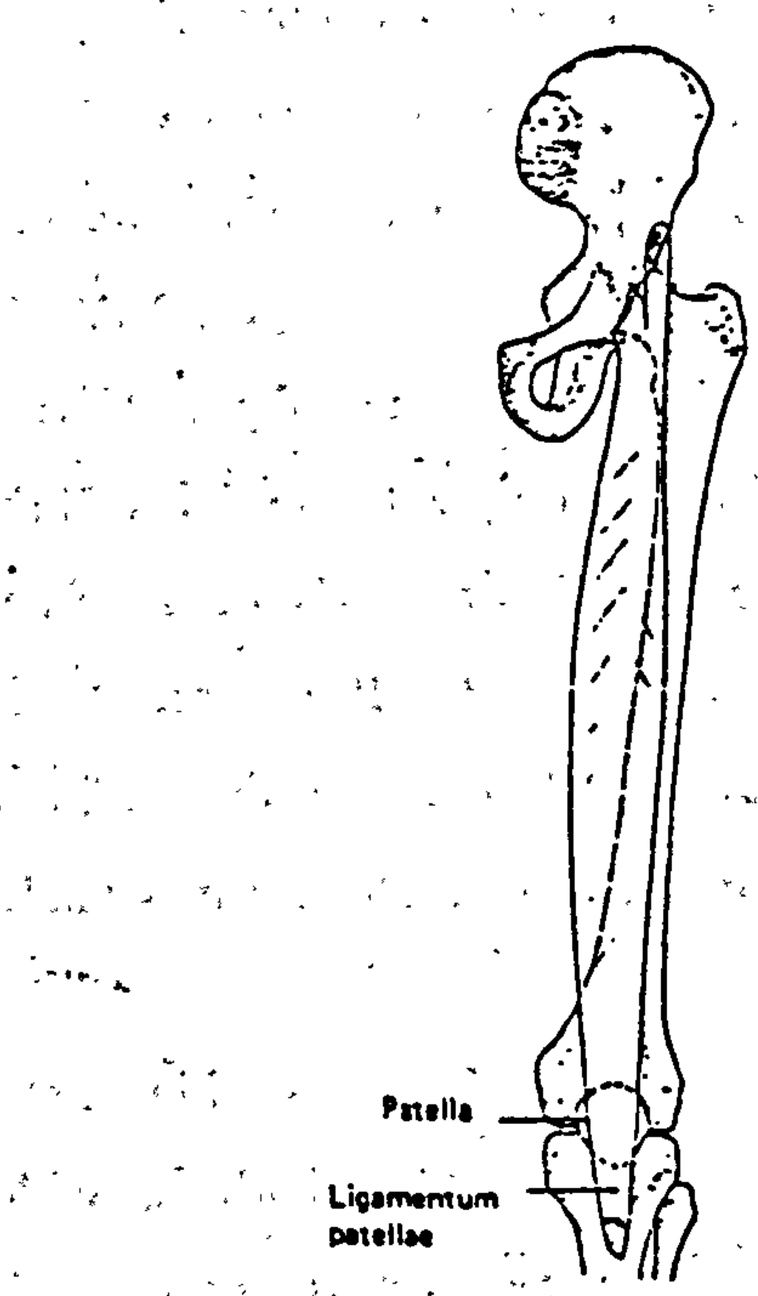

Figure 2.18 Left rectus femoris. Anterior view (from Palastanga et al, 1994).

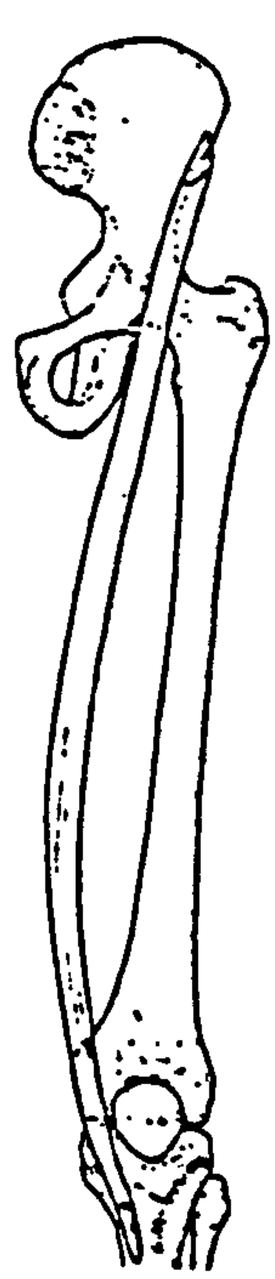

Figure 2.19 Left sartorius. Anterior view (from Palastanga et al, 1994).

included here as a hip flexor. It lies on the anterior thigh and has two heads. One is the straight head from the anterior inferior iliac spine, and the other, the reflected head from the ilium above the acetabulum. The two heads unite in front of the hip joint and insert into the quadriceps tendon and so into the patella as can be seen in figure 2.18. Rectus femoris works strongly when the external moment tends to extend the hip and flex the knee.

Sartorius is mainly a knee flexor but as it passes in front of the hip joint it is also a hip flexor. It is therefore particularly useful when both hip and knee flexion are required simultaneously as in the swing phase of running. Sartorius originates from the anterior superior iliac spine and passes downwards and medially across the front of the thigh as shown in figure 2.19 to insert into the upper part of the medial surface of the tibia. In addition to its role as a hip flexor and knee flexor, it also acts as a hip abductor and external rotator and a knee internal rotator.

The actions of pectineus and tensor fascia lata as hip flexors have already been considered in the sections on hip adductors and abductors respectively.

Hip rotators

Muscles which externally rotate the femur relative to the pelvis include piriformis, obturator internus, gemellus superior and inferior, quadratus femoris and obturator externus. Gluteus maximus is also an external rotator. The effects of this muscle have already been described in the section on hip extensors.

Piriformis is a triangular shaped muscle which lies in the same plane as gluteus medius. The base forms the origin which arises from the anterior surfaces of the second, third and fourth sacral vertebrae. The fibres pass downwards and laterally through the greater sciatic foramen to insert into the upper border of the greater trochanter as shown in figure 2.13. In the anatomical position, piriformis is an external rotator at the hip joint. However, in sitting, the line of action relative to the mechanical axis of the femur will change and piriformis becomes an abductor. An example of this situation is when moving the leg out of a car in preparation for standing up.

Obturator internus is another triangular muscle partly situated in the pelvis and partly in the gluteal region as shown in figure 2.13. It arises from the internal surface of the obturator membrane and the surrounding bones and passes out of the pelvis through the lesser sciatic foramen to insert into the upper border of the greater trochanter. As was the case for piriformis, obturator internus is an external rotator in the anatomical position but when the hip is flexed to right angles, it becomes an abductor. Hence its functional activity is similar to that of piriformis.

The gemelli aid obturator internus in its action. The gemellus superior arises from the

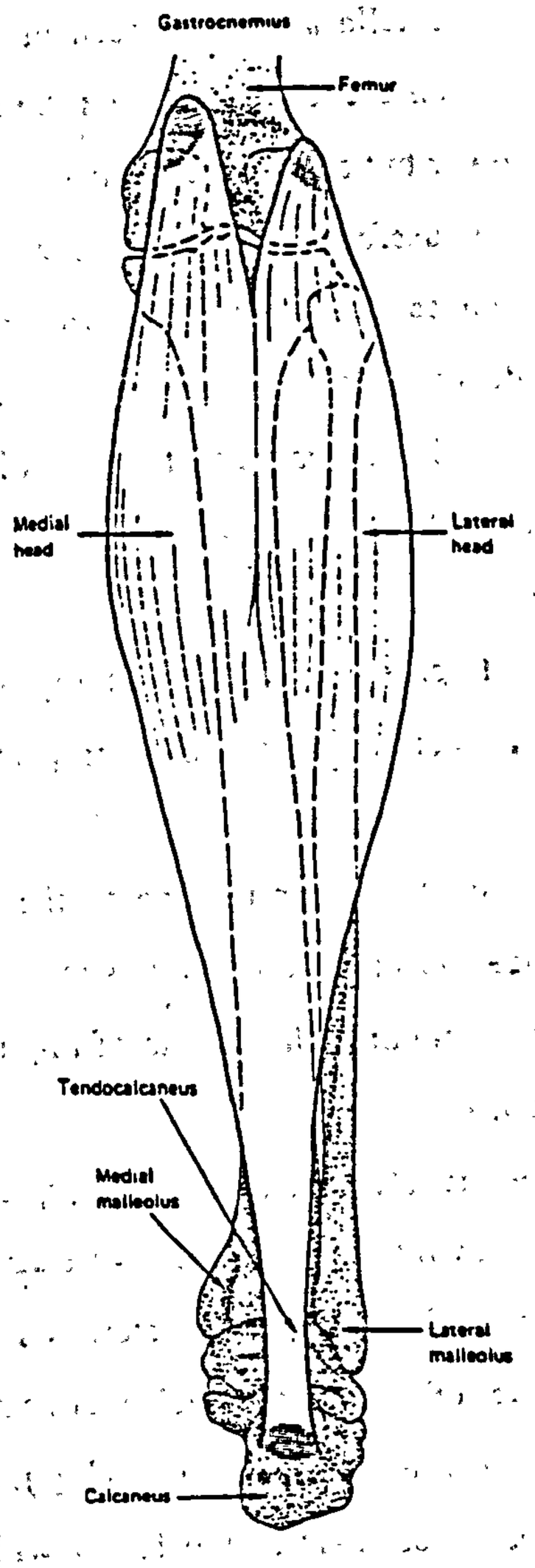

Figure 2.20 Right gastrocnemius. Posterior view (from Palastanga et al, 1994).

spine of the ischium and the gemellus inferior from the upper part of the ischial tuberosity. The gemelli join obturator internus as it passes out of the pelvis around the lesser sciatic notch to insert into the upper border of the greater trochanter as shown in figure 2.13.

Quadratus femoris is a flat quadrilateral muscle situated below gemellus inferior and above the upper part of adductor magnus as shown in figure 2.13. It originates from the lateral border of the ischial tuberosity and passes laterally to insert into the quadrate tubercle on the intertrochanteric crest of the femur. As is the case for the other muscles described in this section, quadratus femoris is an external rotator in the anatomical position and an abductor when the hip is flexed as in sitting.

Obturator externus is a triangular muscle deep to quadratus femoris. It arises from the outer surface of the obturator membrane and the adjacent margin of the pubic and ischial rami. It passes laterally below and then behind the hip joint to insert into the medial surface of the greater trochanter. Again, this muscle is an external rotator in the anatomical position and an abductor when the hip is flexed to right angles.

Having described the external rotators, a brief comment should be made here with regard to the internal rotators. It has already been observed in the previous sections describing hip abductors and flexors, that internal rotators include the anterior fibres of gluteus medius and minimus and possibly, psoas major and iliacus.

2.3.2 Muscles around the Knee Joint

Many of the knee joint muscles included in the mathematical model developed in this project have already been discussed in previous sections as they also cross the hip joint. However, there are some which cross the knee alone or both the knee and ankle and details of these are discussed in this section.

As the main movements of the knee are flexion, extension and some rotation when the knee is semi-flexed, the muscles crossing the knee joint may be considered in the functional groups of flexors, extensors, and rotators.

Knee flexors

The knee flexors include the hamstrings, gastrocnemius, gracilis and sartorius. The actions of the hamstrings, gracilis and sartorius have already been discussed as these are two joint muscles which cross the hip as well as the knee joint.

Gastrocnemius is also a two joint muscle, crossing both the knee and ankle joints. It has two heads, one arising from the lateral aspect of the lateral femoral condyle and the other from above the medial femoral condyle as shown in figure 2.20. The two heads unite and join the tendo calcaneus otherwise known as the Achilles' tendon. This inserts into the calcaneus, also known as the heel bone. The main function of gastrocnemius is as a strong

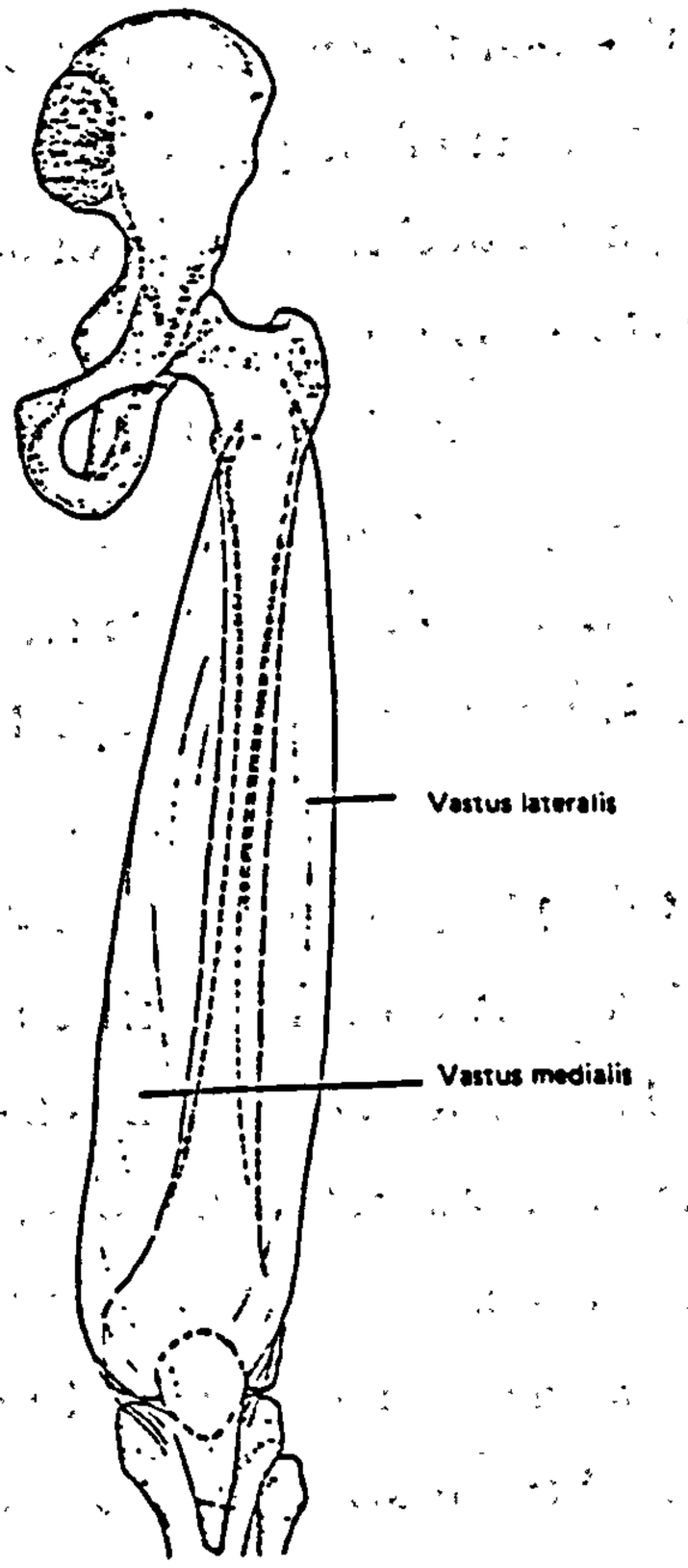

Figure 2.21 Left vastus lateralis and medialis. Anterior view (from Palastanga et al, 1994).

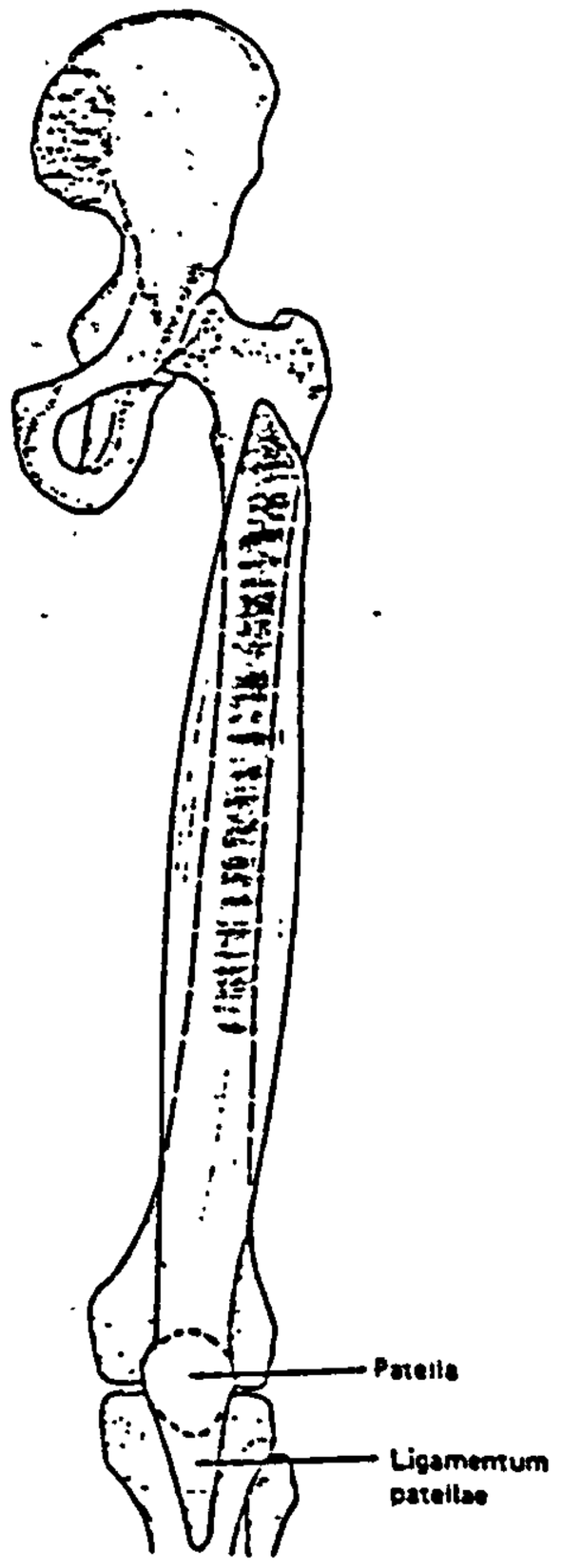

Figure 2.22 Left vastus intermedius. Anterior view (from Palastanga et al, 1994).

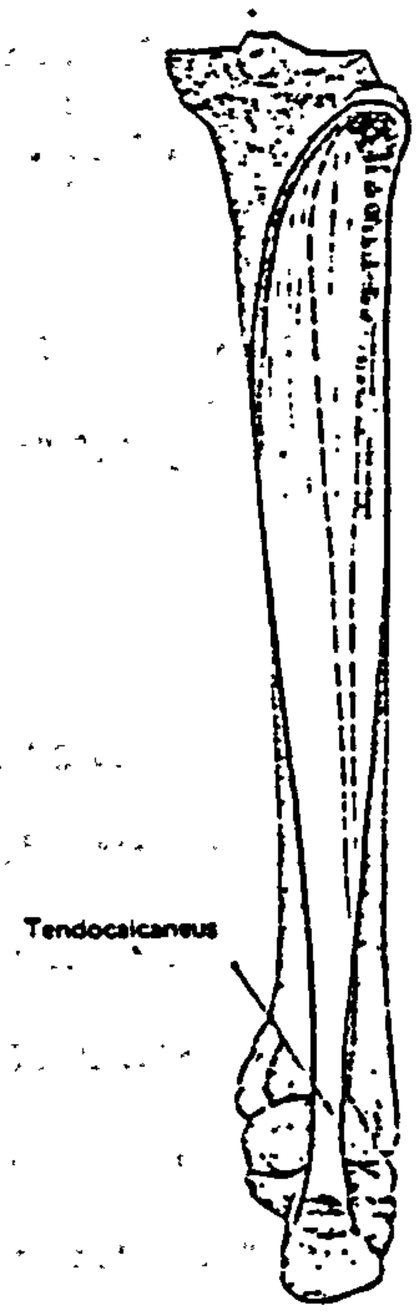

Figure 2.23 Right soleus. Posterior view (from Palastanga et al, 1994).

plantarflexor of the ankle providing the considerable amount of propulsive force required in walking, running and jumping. It is also a strong knee flexor.

Knee extensors

The quadriceps femoris group and tensor fascia lata are knee extensors. Tensor fascia lata has already been discussed in the section on hip abductors. The quadriceps femoris group is composed of four parts. These are vastus lateralis, vastus medialis, vastus intermedius and rectus femoris. The actions of rectus femoris have already been described in the section on hip flexors. This section will therefore concentrate on the vasti.

Vastus lateralis is located on the antero-lateral aspect of the thigh, originating from the intertrochanteric line, the base of the greater trochanter and the lateral lip of the linea aspera of the femur. It passes downwards and forwards to insert into the quadriceps tendon and so into the patella as shown in figure 2.21. Some fibres pass to the front of the lateral condyle of the tibia and blend with the iliotibial tract to form an expansion which attaches to a line running towards the tibial tuberosity. This part of the attachment largely replaces the knee joint capsule in this region.

Vastus medialis is situated in the antero-medial region of the thigh as can be seen in figure 2.21. It arises from the intertrochanteric line and the medial lip of the linea aspera of the femur and, like vastus lateralis, passes downwards and forwards to insert into the quadriceps tendon which attaches to the patella. Some fibres attach to the front of the medial condyle of the tibia and run to the tibial tuberosity, largely replacing the knee joint capsule in this region.

Vastus intermedius lies between vastus lateralis and medialis, beneath rectus femoris as illustrated in figure 2.22. It originates from the upper two thirds of the anterior and lateral surfaces of the femur and passes downwards to insert into the quadriceps tendon and so to the patella.

The main function of the quadriceps group is as a knee extensor although rectus femoris also acts at the hip as previously described. Each component of the group has a particular role which may come into action at different degrees of knee flexion. Vastus medialis is a good example of this as it is more active in the final stages of knee extension when it acts to resist lateral movement of the patella due to the angulation of the femur. The quadriceps group acts strongly in stepping activities such as when stair climbing.

Knee rotators

Biceps femoris acts as an external rotator at the semi-flexed knee. Its action has already been discussed as it crosses the hip as well as the knee joint.

Internal rotators of the knee joint include semitendinosus, semimembranosus, gracilis,

Muscle	Origin	Insertion	Action
Gastrocnemius	Lateral and medial condyles of femur	Calcaneus	Flexes leg, plantarflexes foot
Soleus	Proximal ends of tibia and fibula	Calcaneus	Plantarflexes foot
Plantaris	Distal posterior shaft of femur	Calcaneus	Flexes leg, plantarflexes foot
Popliteus	Lateral condyle of femur	Proximal, posterior shaft of tibia	Flexes and internally rotates leg
Tibialis posterior	Posterior shaft of tibia and fibula, interosseus membrane	Navicular, cuboid, cunieforms, metatarsals 2 to 4	Plantarflexes and inverts foot
Flexor hallucis longus	Distal shaft of fibula	Distal phalanx of great toe	Flexes great toe, plantarflexes and inverts foot
Flexor digitorum longus	Distal shaft of tibia	Phalanges of toes 2 to 5	Flexes toes, plantarflexes and inverts foot
Peroneus longus	Lateral shaft of fibula	First cunieform and metatarsal 1	Plantarflexes and everts foot
Peroneus brevis	Lateral shaft of fibula	Metatarsal 5	Plantarflexes and everts foot
Tibilalis anterior	Proximal lateral shaft of tibia, interosseous membrane	First cunieform and metatarsal 1	Dorsiflexes and inverts foot
Peroneus tertius	Distal anterior shaft of fibula, interosseous membrane	Metatarsal 5	Dorsiflexes and everts foot
Extensor hallucis longus	Anterior shaft of fibula, interosseous membrane	Distal phalanx of great toe	Extends great toe, dorsiflexes and inverts foot
Extensor digitorum longus	Anterior shaft of fibula, interosseous membrane	Phalanges of toes 2 to 5	Extends toes, dorsiflexes and everts foot

Table 2.1 Ankle joint muscles (from Gaudin and Jones, 1989)

and sartorius. All of these muscles cross the hip as well as the knee joint and their action has therefore already been discussed. Popliteus is also an internal rotator of the knee joint. It attaches above to the lateral surface of the lateral femoral condyle and below to the posterior surface of the tibia as shown in figure 2.12. At commencement of knee flexion, it rotates the femur externally relative to the tibia, slackening the knee ligaments thereby releasing the knee from the locked position. It will also come into action when strong knee flexion is required.

2.3.3 Muscles around the Ankle Joint

Only two ankle joint muscles are included in the model developed in this project and hence only these are included in this section. These are gastrocnemius and soleus which are the major plantarflexors of the ankle joint. Brief details of the remaining ankle joint muscles are given in table 2.1 but further details may be obtained from standard texts (Gaudin and Jones, 1989, Nordin and Frankel, 1989, Palastanga et al, 1994).

Gastrocnemius has already been discussed as it crosses the knee joint as well as the ankle. Soleus lies deep to gastrocnemius, arising from the posterior surface of the tibia and upper quarter of the posterior surface of the fibula. It joins the tendo calcaneus and inserts into the calcaneus as can be seen from figure 2.23. Whilst gastrocnemius produces the strong propelling force in walking, soleus is an important postural muscle.

CHAPTER 3. A REVIEW OF BIOMECHANICAL MODELLING METHODS

This chapter is concerned with the methodology used to determine hip joint forces. Hip joint forces can be determined by two methods. The first method involves calculation of joint force in which a musculoskeletal model is usually developed to determine muscle and then joint forces using data such as external kinematics and kinetics along with anatomical muscle data and subject anthropometric data. Secondly, there is the 'in vivo' method in which an instrumented hip prosthesis is implanted into a patient and hip joint forces are measured directly as the subject performs the required activities. Both methods have advantages and disadvantages.

The calculation method has the advantage that it is non-invasive and thus any subject with or without a hip prostheses can be analyzed. However, its accuracy is questionable due to the many assumptions that have to be made in the calculations and errors in the experimental methods used.

The 'in vivo' method has the advantage that measurement is direct avoiding the need for calculation and its inherent assumptions and errors. However, it is restricted to the few subjects with instrumented hip prostheses. Results obtained from this method should be applied to subjects with normal hips with caution. The fact that the subject has undergone surgery and has a prosthetic rather than a normal joint will alter the method and vigour with which an activity is performed. The surgical approach may influence function and differences in angles and dimensions between the prosthesis and parts replaced may influence the final results.

This chapter is primarily concerned with the calculation method as that is the one that is used in the current study. Generally, in order to calculate hip joint forces incurred whilst a subject performs an activity, the position and orientation of the lower limb segments must be recorded. Markers are placed at specific sites on the subjects' limbs and their changing positions recorded by a camera system as the subject performs an activity. The markers should be placed in such a way that coordinate systems may be set up to define the limb segments using the marked points. Joint kinematics may then be calculated using these coordinate systems and points including joint centres and centre of mass positions may be located.

The external loading on the limb segments is also measured using a load transducer such as a force platform. The position and load data are then combined to calculate the 3D intersegmental moments at the hip joint and possibly the knee and ankle joints depending on the complexity of the analysis required. Accurate determination of the joint moments

depends on accurate location of joint axes and joint centres. The moments calculated must be balanced by forces in load carrying structures surrounding the joint concerned. There is a greater number of load carrying structures available than moments equations and past researchers have taken various approaches to solve the statically indeterminant problem. The system may be simplified by categorising load carrying structures into functional groups and assuming certain groups to be active in certain situations. Alternatively, the combination of active structures may be chosen so that some function is optimized. Minimizing muscle force or energy is an example of such an approach.

This chapter aims to give an overview of the alternative strategies that can be used for the various stages in the calculation procedure and thereby introduce the model developed in the current study. Details of the methods used in the current study are then presented in chapter 4.

3.1 BODY SEGMENT KINEMATICS

The position and orientation of a segment within space is obtained by comparing the coordinate system set up in the segment with a stationary coordinate system. In the past, researchers have defined the limb segments using a variety of coordinate systems and applied a range of methods to locate joint centres. Many different marker systems have been used in order to set up the coordinate systems and joint centres.

Joint kinematics are analyzed by comparing the coordinate system of the moving distal segment with that of the stationary proximal segment. There are various methods available for use in determining joint kinematics.

The aim of this section is to evaluate the different methods of locating the joint centres of the lower limb, the different coordinate systems and marker systems and also the methods used in joint kinematic analysis.

3.1.1 Joint Centres

It is important to locate joint centres precisely in order that the calculated joint moments are as accurate as possible. The hip, knee and ankle joints are included in this section as these have all been included in the model developed in this project.

Hip joint centre

The deep location of the hip joint centre beneath soft tissues makes its exact determination difficult. Investigators in the past have attempted to locate the hip joint centre in a variety of ways. Some have used radiographs (Crowninshield et al, 1978a, Johnston et

al, 1979) but it is not always feasible to use radiographs and alternative approaches have been taken.

Ishai (1975) determined the hip joint centre in his subjects by a two stage method. He measured the anterior-posterior (A-P), medio-lateral (M-L), and superior-inferior (S-I) position of the hip joint centre relative to the anterior superior iliac spine (ASIS) on a skeleton and then divided each coordinate by the distance between the right and left ASIS (inter ASIS distance). He then obtained a first approximation for the hip joint centre of a subject by multiplying the values obtained by that subject's inter ASIS distance. This technique is known as an anthropometric scaling technique. The joint centre position was then refined when the gait cycle of the subject had been analyzed so that the distance between the hip and knee joint centres did not change by more than a specified amount.

Goh (1982) attempted to use the same method as Ishai (1975) but found it to be inaccurate. He tried to improve on the method by using measurements derived from Dostal and Andrews (1981) and found improvements in the M-L position. However, in the sagittal plane, he found the method still to be inaccurate and from tests using interrupted light photography, found the leg to swing about the tip of the greater trochanter. Hence he took the position of the tip of the greater trochanter in standing as the hip joint centre position in the A-P and S-I directions.

Andriacchi et al (1980,1982) and Andriacchi and Strickland (1983) predicted the hip joint centre to be 1.5 or 1.5-2cm distal to the midpoint of a line between the ASIS and pubic symphysis in the frontal plane and an unspecified distance medial to the greater trochanter.

By examining childrens' radiographs, Tylkowski et al (1982) predicted that the hip joint centre would be located 11% of the inter ASIS distance medial to, 12% distal to and 21% posterior to the ASIS.

Bell et al (1989) evaluated these two approaches, examining radiographs of 39 children and 31 adults. They tried to improve on them by producing a method which combines the most accurate parts of both. In this, the approach of Andriacchi et al was used for the frontal plane, and that of Tylkowski et al for the A-P location but using 22% instead of 21%. This method was found to locate the hip joint centre to within 2.6cm of the true location with 95% confidence.

Cappozzo (1984) obtained the hip joint centre by recording the trajectory of markers on the thigh as a subject performed abduction/adduction and then flexion/extension of the thigh and then deducing the centre of rotation on these movements.

Bell et al (1990) went on further to analyze the methods of Andriacchi et al, Tylkowski et al and Cappozzo. In their previously described study of 1989, Bell et al had evaluated the

methods of Tylkowski et al and Andriacchi et al by measuring the hip centre location relative to bony landmarks on radiographs. Hence they had not taken into account the effects of errors associated with marker placement on living subjects with varying amounts of underlying soft tissues. This study of 7 adult males included such effects and produced a new method which predicted the hip joint centre to be 14% of the inter ASIS distance medial to and 30% distal to the ASIS in the frontal plane. A marker placed over the greater trochanter was used to predict the A-P joint centre position. This method predicted the hip joint centre location to within 1.07cm of the true location.

Finally, a group from Newington children's hospital, Davis et al (1991) developed an algorithm to calculate hip joint centre location based on the radiographic examination of 25 hip studies. The equations which were used to locate the A-P, S-I and M-L coordinates of the hip joint centre relative to the ASIS involved measurements deduced from the radiographic examination as well as the inter ASIS distance and leg length measurements.

It was decided that the method of Bell et al (1990) was most suitable for the model developed in this project when applied to subjects with normal hips. This is because the method has been comprehensively analyzed and its accuracy has been determined when used with markers. Although pelvises do not grow in a regular manner, it seems logical that the location of the hip joint centre on the frontal plane should be expressed relative to the ASIS in terms of the inter ASIS distance. This is especially true for the M-L location since the inter ASIS distance is measured in the M-L direction. With regard to the A-P location, the degree of anteversion varies between subjects as was described in section 2.1.2. This will affect the accuracy with which the joint centre is located but as it is impossible to quantify this angle without orthogonal radiographs, the method of Bell et al (1990) was adopted. The same method was applied to both males and females.

It would have been ideal to have obtained the location of the hip joint centre in patients using post-operative orthogonal radiographs taken in a standardised manner so that some attempt at reducing scaling and parallax errors could be made. However, only frontal plane radiographs were available for some of the subjects and not all of these had been taken in a standardised way. It was therefore decided to use the method of Bell et al (1990) for the patients as well as normals. This assumes that the post-operative hip joint centre location is restored to that before the hip was diseased with arthritis.

Knee joint centre

The knee joint is not a simple hinge but exhibits complex joint motion due to rolling and sliding action during flexion and extension. Hence the axis of rotation does not remain fixed but moves along a path determined by the geometry of the articulating surfaces and

ligamentous attachments.

In many studies, the knee joint has been simplified so that a fixed point for the knee joint centre is used. Some researchers have defined the knee joint centre as a fixed point in a coordinate system based in the thigh whilst others have defined it relative to the shank. Cappozzo (1984), Kadaba et al (1990) and Davis et al (1991) all define the knee joint centre in a thigh based system. In general, when the knee joint centre is determined relative to the thigh, it is defined to be in the region of the midpoint between the femoral epicondyles.

Ishai (1975) defined the knee joint centre relative to a shank based coordinate system. They set up the axes of the shank relative to the tibial tuberosity, fibula head and lateral malleolus using equations based on the measurement of 8 tibiae. They then assumed the knee joint centre to lie on the longitudinal axis of the shank at a specified distance above the tibial plateau. Goh (1982) also used the method developed by Ishai (1975).

It was decided in this project to use the method developed by Ishai (1975), fixing the knee joint centre relative to the shank. It is difficult to say whether this or the midpoint between the femoral epicondyles reflects the true knee joint centre position most accurately. However, during gait and other activities there is generally less skin movement relative to underlying bone in the shank than the thigh and therefore defining the joint centre relative to the shank reduces errors due to skin movement.

Ankle joint centre

Like motion at the knee joint, that at the ankle is complex but many researchers have simplified the ankle joint centre to be fixed at a single point.

Ishai (1975) and Goh (1982) defined the ankle joint centre to be at the level of the lateral malleolus on the longitudinal shank axis. A similar approach was taken by Cappozzo (1984). It was decided to use the method developed by Ishai (1975) and used by Goh (1982). This is consistent with the method chosen to determine the location of the knee joint centre.

3.1.2 Coordinate Systems and Marker Systems

The anatomical coordinate system of a segment should accurately represent the segment since joint kinematics are calculated using segment coordinate systems. Also, previous literature has cited centre of mass position, principal axes of inertia and joint centres relative to segment coordinate systems.

The system of markers used must allow the segment coordinate systems to be set up. However, the markers must also be situated where there is likely to be low skin movement relative to the underlying bone as motion occurs. Skin movement errors are thereby reduced and the segment may be assumed to be a rigid body. The markers should also be placed at

a large enough distance apart so that error propagation through calculation is minimal. Markers must also be placed where they will not obstruct the subjects' movements.

The points which need to be used to set up the coordinate system in a segment may not coincide with these requirements. This may be overcome by setting up a technical coordinate system as well as the required anatomical coordinate system. Three points are necessary to set up a coordinate system in a segment. If three points are chosen which satisfy the afore mentioned requirements, then these can be marked and used to set up a technical coordinate system. The technical markers may be placed directly on the skin or mounted in clusters on plates. For one static test, extra markers are placed over the points required to define the anatomical coordinate system. These points can then be located in the technical marker system and only the technical markers are required in the dynamic tests.

Coordinate systems and marker systems used in defining the pelvis, thigh and shank are described in this section as these are the segments included in the model developed in this project.

Pelvis

The bony landmarks which have most frequently been used to locate the pelvic coordinate system are the anterior superior iliac spines (ASIS) and posterior superior iliac spines (PSIS) or sacrum. Ishai (1975), Goh (1982), Cappozzo (1984), Kadaba et al (1990) and Davis et al (1991) all use markers on the right and left ASIS and a tail marker consisting of a marker on the end of a wand with its base on the region of the midpoint between the PSIS or on the sacrum.

The anatomical coordinate system used in this project also uses the ASIS and the midpoint between the PSIS. The marker is placed directly on the midpoint between the PSIS via a short stem rather than a longer wand. Although a wand increases the distance between markers, thereby reducing errors in calculation, the use of a wand was infeasible in this project. This is because various activities in addition to gait were being studied and a wand would have obstructed the subjects from carrying out the activities in a normal manner. The coordinate system set up uses the same points as Bell et al (1990) and hence the hip joint centre could readily be located in this system.

As stated previously, the points used to set up the anatomical coordinate system may not necessarily correspond with the requirements of marker placement. This was found to be the case for the pelvic ASIS markers. Although the system is suitable for gait, the subjects' arms were found to obscure the ASIS markers as they performed other activities such as getting into and out of the car. Hence a technical coordinate system was set up in the pelvis using the midpoint between the PSIS with markers placed further back on the right

and left iliac crests. A static test performed with both technical and anatomical markers allowed the position of the ASIS to be located in the technical coordinate system. In dynamic tests, the ASIS markers could then be removed.

Thigh

The thigh is perhaps the most difficult segment to define accurately using markers since any marker placed on it is likely to be subjected to a high amount of skin movement relative to the underlying bone.

Goh (1982) avoided the use of thigh markers altogether. Having set up the knee joint centre in the shank based coordinate system and the hip joint centre in the pelvic based system, he defined the long axis of the thigh as passing from the knee joint centre to the hip joint centre. Assuming the knee to be a single axis hinge joint, he then set the thigh M-L axis to be parallel to that of the shank.

Unlike Goh, Cappozzo (1984) used markers on the thigh. He defined the coordinate system of the thigh using the medial and lateral femoral epicondyles and the hip joint centre. However, since the use of markers on the epicondyles did not satisfy the requirements of marker positioning, Cappozzo set up a technical marker system using the thigh markers.

In order to overcome the problem of defining the thigh coordinate system in accordance with marker placement requirements, Kadaba et al (1990) and Davis et al (1991) used thigh marker systems including markers on wands. The wands were aligned and markers placed in such a way that the thigh axes could be determined directly from the marker system without the need for extra markers and a technical coordinate system.

As it is possible for knee external rotation to be up to 45° and internal rotation to be up 30° when the knee is flexed to 90°, it was considered important to define the thigh independently of the shank and hence not use the method of Goh (1982). However, if the thigh is defined independently of the shank then thigh markers must be used. This may introduce errors due to skin movement relative to underlying bone.

It was decided to use the hip joint centre and medial and lateral epicondyles to define the thigh coordinate system as Cappozzo (1984) had done. Such a system should give an accurate representation of the thigh segment, allowing the centre of mass to be determined relatively accurately and realistic hip and knee angles obtained. However, a marker could not be used on the medial epicondyle in dynamic tests as it would obstruct the normal activity of the subject. The lateral epicondyle would be subjected to high skin movement relative to underlying bone. Indeed, Perry et al (1988) found the skin movement on the lateral epicondyle to be 4cm between 0° and 90° of knee flexion. In order to overcome these problems, one of two approaches could be taken. Either a system of wands could be used

or a system of thigh markers could be used and a technical coordinate system set up. It was decided to set up a technical coordinate system. Although this involved more calculation stages and therefore the possibility of error propagation, it did not rely on accurate positioning of wand systems.

In the model developed in the current study, two thigh markers were used with the hip joint centre to set up a technical coordinate system. The thigh markers were placed distally, one on the front and one on the lateral side of the thigh. A static test with markers on the thigh, femoral epicondyles and pelvis allowed the epicondyle markers to be located relative to the technical system. Dynamic tests could then be performed without the need for femoral epicondyle markers.

Shank

As has already been described, Ishai (1975) and Goh (1982) set up a shank coordinate system relative to the tibia, fibula head and lateral malleolus using equations based on the measurement of 8 tibiae.

Cappozzo (1984) used a marker on the front of the shank, fibula head and lateral and medial malleoli to define the shank axes. As in the thigh, not all of these positions corresponded with the requirements for marker placement. A technical system including three shank markers was therefore set up.

Kadaba et al (1990) and Davis et al (1991) used a shank system of markers including wands as they had done for the thigh. As for the thigh, the wands were aligned and markers placed in such a way that the shank coordinate system could be set up directly from these markers without the need for a technical coordinate system and a static test.

The coordinate system used by Ishai (1975) and Goh (1982) was considered to define the shank segment in such a way that the position of the centre of mass could be defined accurately and realistic knee and thigh angles could be obtained. This was also consistent with the decision to locate the knee and ankle joint centres using their method. However, Perry et al (1988) reported skin movement relative to underlying bone in the region of the fibula head to be 1.7cm between 0° and 90° of knee flexion. It was therefore decided to set up a technical marker system using markers on the tibial tuberosity, lateral malleolus and on the front of the shank. The position of the fibula head could be determined in the technical coordinate system in the static test and then in the dynamic test, only the tibial tuberosity, lateral malleolus and shank markers were required.

3.1.3 Joint Kinematics

In the analysis of joint kinematics, the coordinate system of the moving distal segment is compared with that of the stationary proximal segment.

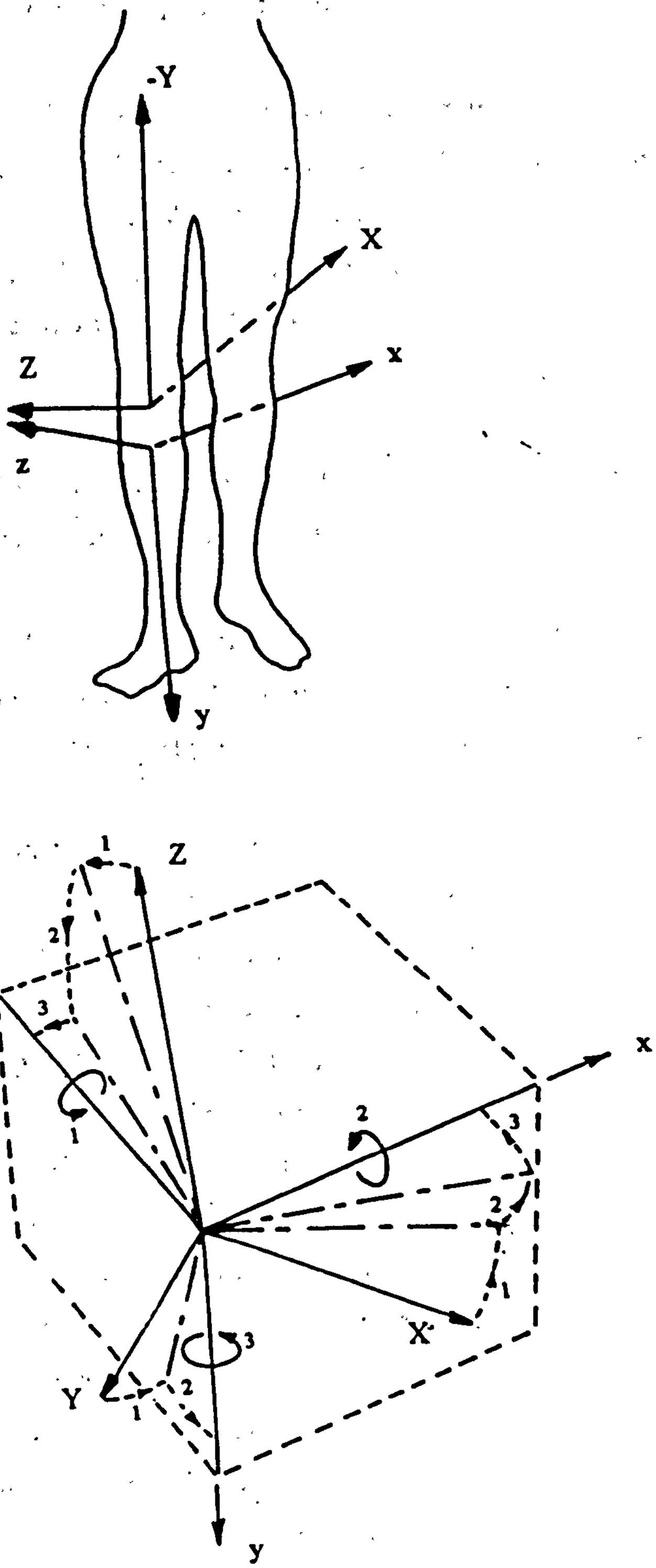

Figure 3.1 Euler angles. Rotation of femoral axes about tibial axes x, y and z.

The coordinate system in the proximal segment can be described by X, Y, Z with unit vectors I, J, K relative to the stationary ground coordinate system and origin, O. Similarly, the distal segment coordinate system can be defined by x, y, z with unit vectors i, j, k relative to the stationary ground coordinate system and origin, o. The position of o relative to O can be obtained by a translation vector in terms of X,Y,Z. The orientation of the distal coordinate system can be expressed with respect to the proximal system by the following direction cosine matrix:

$$\begin{bmatrix} iI & iJ & iK \\ jI & jJ & jK \\ kI & kJ & kK \end{bmatrix}$$

This direction cosine matrix is denoted by [B]. It is used in the analysis of joint kinematics which are usually described by one of three main methods. These are the Euler angle, floating axis and equivalent screw displacement axis techniques.

Euler angles

Euler angles are defined as a set of three rotations required to produce alignment of the coordinate systems embedded in the distal and proximal segments. The three rotations correspond to flexion-extension, abduction-adduction, and internal-external rotation. The product of the three independent direction cosine matrices describing the three rotations is equivalent to the direction cosine matrix [B] previously described. Hence by comparison of this product with [B], the angles of flexion-extension, abduction-adduction and internal-external rotation may be calculated.

The order in which rotations are made about the original and intermediate axes varies in the literature. Strictly speaking, for the angles to be termed 'Euler', the first and last axes of rotation should be the same. However, this definition is not always strictly adhered to in the literature.

A form of Euler angles was illustrated by Huntington et al (1979) in the calculation of knee joint angles as illustrated in figure 3.1. The femoral axes are firstly rotated about the medio-lateral tibial axis, z, to bring the longitudinal femoral axis, Y, into the frontal plane of the tibia. The magnitude of this rotation is taken as the angle of flexion or extension. This position of the femoral axes is used as the start point for the next rotation. The axes are rotated about the anterior-posterior tibial axis, x, until the longitudinal axes of the femur and tibia are aligned. The magnitude of this rotation is equivalent to the angle of abduction or adduction. Finally, axial rotation is given by the rotation required about the longitudinal axis of the tibia, y, to bring the medio-lateral axis of the femur, Z, in line with that of the

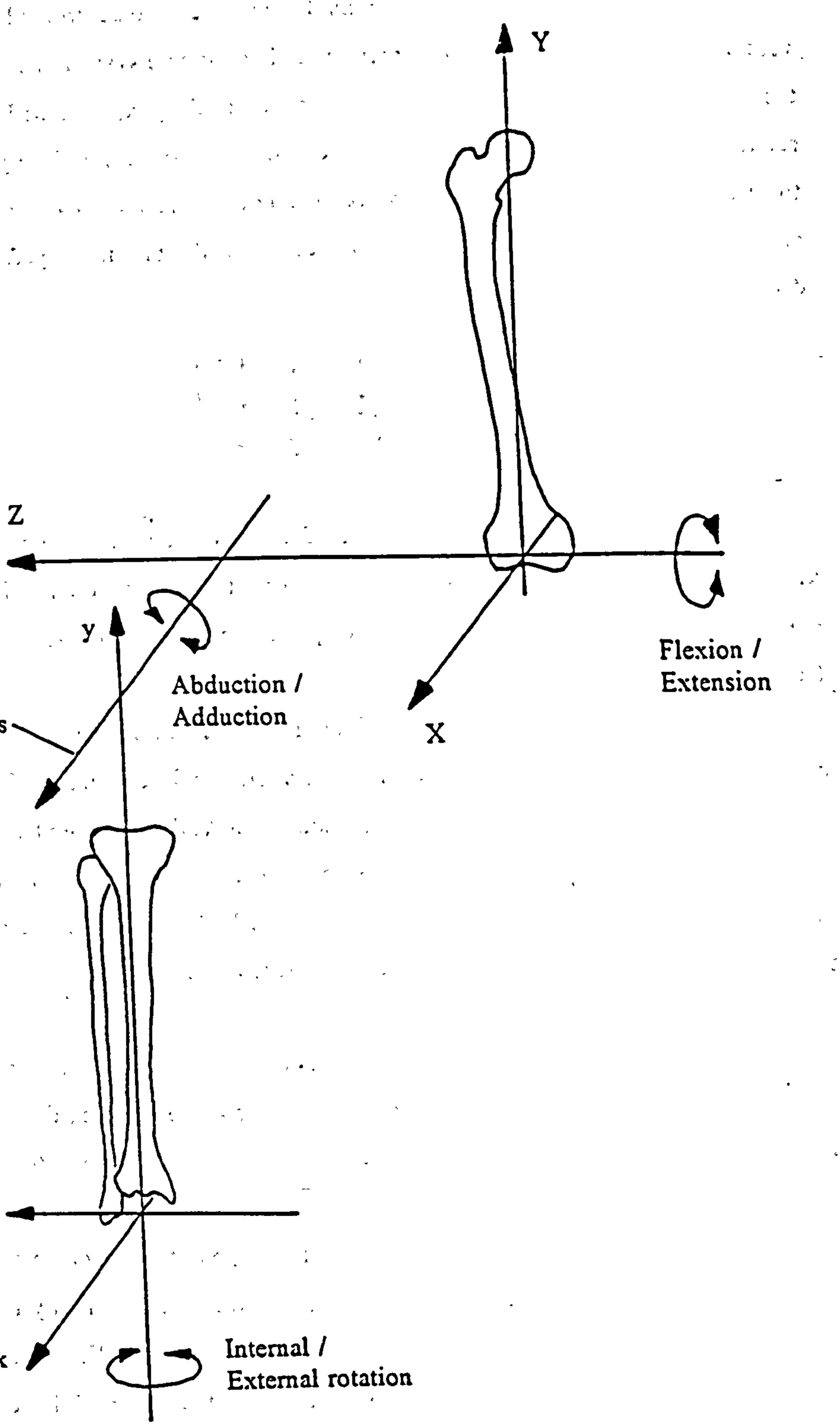

Figure 3.2 Floating axis technique to determine joint angles.

tibia. Although the first and last axes of rotation are not the same and the angles are therefore not Euler by the strict definition, this does illustrate the use of three rotations to calculate the joint angles. In this application, the angles should strictly be termed 'Cardan' or 'Bryant' angles.

The disadvantage of this technique is that the results depend on the order in which the rotations are performed and a lack of standardisation can make comparison between different studies difficult.

Floating axis

The floating axis technique has the advantage over analysis using the Euler angle approach in that it is not order dependent. The technique uses two body fixed axes, one embedded in each of the segments concerned, and a floating axis perpendicular to the two body fixed axes as shown in figure 3.2. Grood and Suntay (1983) illustrated the technique, applying it to the knee joint. The tibial body fixed axis was chosen so that rotations about it correspond to internal/external rotation. Hence the longitudinal tibial axis, y, was used. The femoral medio-lateral axis, Z, was chosen as the femoral body fixed axis since rotations about this axis correspond to flexion/extension. Abduction/adduction then occurs about the floating axis which was defined as being perpendicular to the two body fixed axes.

From mathematical analysis of the system, the individual components of the direction cosine matrix, [B], previously described may be written in terms of the angles of flexion/extension, abduction/adduction and internal/external rotation as follows:

$$\begin{bmatrix} \cos\alpha\cos\gamma - \sin\gamma\sin\alpha\cos\beta & -\cos\gamma\sin\alpha - \cos\alpha\cos\beta\sin\gamma & \sin\gamma\sin\beta \\ \sin\beta\sin\alpha & \cos\alpha\sin\beta & \cos\beta \\ -\cos\alpha\sin\gamma - \cos\gamma\sin\alpha\cos\beta & \sin\alpha\sin\gamma - \cos\gamma\cos\alpha\cos\beta & \cos\gamma\sin\beta \end{bmatrix}$$

where flexion is given by α and in a right knee, external rotation is given by γ and adduction is given by β-$\pi/2$. Hence by equating the two forms of the direction cosine matrix, the three joint angles can be obtained from the following:

$$\gamma = \tan^{-1}\frac{K.I}{K.k} \qquad 3.1a$$

$$\beta = \cos^{-1} K.j \qquad 3.1b$$

$$\alpha = \tan^{-1}\frac{I.j}{J.j} \qquad 3.1c$$

Equivalent screw displacement axis

In this method, the relative motion between two rigid bodies is expressed as a rotation about and a translation along some axis in space, the screw displacement or helical axis. The

disadvantage of this method as compared to the others is that it is difficult to compare the results obtained with clinical joint angles. Hence the method will not be discussed in detail here. More detail can be found in Small et al (1992).

In summary, the advantage of the floating axis analysis technique is that it is rotation order independent unlike the Euler approach. The results produced are readily related to clinical angles unlike the equivalent screw displacement axis technique. Hence the floating axis technique was chosen for use in the current study.

3.2 EXTERNAL LOADING

The external loading on a limb segment is that due to the interaction between the segment and the environment. The three types of external loading are contact loading, gravitational loading and inertial loading.

Contact loading on the lower limb is usually the ground reaction force. i.e. that between the foot and the ground. It is the reaction to the gravitational and inertial forces acting on the centre of mass of the whole body.

Gravitational loading on a limb segment is that due to the effect of the gravitational pull on the segment mass. It acts vertically and is considered to act at the centre of mass of the segment. The value of the load is given by

$$F_G = m_{SEG} * g \qquad 3.2$$

where F_G is the gravitational load, m_{SEG} is the segment mass and g is acceleration due to gravity.

A segment which is accelerating or decelerating will also be subjected to inertial loading. Where linear acceleration occurs, an inertial force will act to oppose this acceleration. The load is considered to act at the centre of mass of the limb segment and its value is given by

$$F_I = m_{SEG} * a \qquad 3.3$$

where F_I is the inertial force, m_{SEG} is the segment mass and a is the linear acceleration of the segment centre of mass.

Where angular acceleration occurs about a principal axis of inertia, it will be opposed by an inertial moment. This is considered to act at the centre of mass of the limb segment and the value is given by

$$T_I = I_{SEG} * \alpha$$
$$\text{where } I_{SEG} = m_{SEG} * K_{SEG}^2 \qquad 3.4$$

where T_I is the inertial moment about the principal axis, I_{SEG} is the segment moment of inertia about the principal axis, K is the radius of gyration about the same axis through the centre of mass and α is the angular acceleration about the axis.

The effect of these loads at a joint can be calculated by considering the limb segments distal to the joint and the loads applied to them as a free body diagram. This allows calculation of intersegmental joint moments and forces due to external loading.

Quantities including segment masses, centre of mass positions and radii of gyration are required in order to calculate the magnitude of the external loading. There have been many anthropometric studies performed on various groups of subjects to produce values for such quantities. Some have been made on cadavers (Dempster, 1955) whilst others used live subjects (Drillis and Contini, 1966). The disadvantage of cadaveric studies is that cadavers can never be entirely comparable with living subjects. The values used in this project are those of Drillis and Contini (1966). The subjects used were male adults aged between 20 and 40. However, in order that the results may be applied to other categories of subjects, the results were expressed as percentages of body height and mass.

3.3 INTERNAL LOADING

Having calculated the components of intersegmental joint moment due to external loading, the forces in load carrying structures crossing the joint must be calculated so that the moments are balanced and there is equilibrium.

The intersegmental joint moment can be considered to be caused entirely by muscles if two assumptions are made. The first is that the articular contact force acts through a single point which is the pre-selected joint centre, making its moment arm zero and therefore its contribution to the intersegmental moment zero. The second is that the moments due to ligament forces are insignificant compared with those caused by muscles. Whilst it would not be possible to make such assumptions in a full 3D analysis of the knee and ankle joints, it is possible to make both of these assumptions when considering the hip joint. The first can be made if friction at the joint surface is assumed to be zero. The second has been made in the past by researchers including Crowninshield et al (1978a).

Once these muscle forces have been calculated, the components of joint contact force can be calculated. These are the forces required to balance the external forces and forces in

the load carrying structures crossing the joint.

In order to perform the calculation, the lines of action of the load carrying structures relative to the joint must be determined. There is usually a greater number of potential load carrying structures than there are equilibrium equations. The system must either be simplified or the combination of active structures chosen so that some function is optimized. An example of this is minimization of total muscle force.

In the following sections, the methods used in determining the lines of action of muscles is discussed. The alternative approaches used to select and calculate forces in load carrying structures will then be assessed. In doing so, the methods used in the mathematical model developed in the current study will be introduced.

3.3.1 Lines of Action of Muscles

In the most simple analysis the line of action of a muscle is considered to be a straight line between the origin and insertion. There are two main areas of inaccuracy associated with this approach. Firstly, the inherent shape of the muscle may make it inaccurate to represent it as a straight line between origin and insertion. Secondly, the line of action may be altered from a straight line by the passage of the muscle over underlying structures.

Jensen and Davy (1975) compared the straight line approach with a method which they proposed to account for the curvature in a muscle's line of action. They proposed that the force transmitted by a muscle can be considered to act along a line defined by the locus of its transverse cross section. In a cadaveric study of sartorius, rectus femoris and gluteus medius, they found that in a position corresponding to standing erect, there was a relatively small difference between the two approaches in terms of total moment capability but often a substantial difference in component distribution.

Although this approach could give a more accurate representation of the line of action of a muscle, it would be infeasible for application to the mathematical model developed in the current study. This is because the model developed in the current study incorporates a high number of muscles and is applied to different subjects as they perform various activities involving highly changing joint angle configurations.

Most mathematical models developed to date have adopted the straight line approach but incorporated certain alterations to allow for significant changes in the path of a muscle as it crosses another structure or is retained by other soft tissue (Pierrynowski and Morrison, 1985a, Spoor et al, 1989, Delp et al, 1990, Runciman and Nicol, 1994).

In producing a model of the lower extremity muscular anatomy, Brand et al (1982) improved on the straight line approach by using effective origins and insertions for muscles

which cannot be assumed to work in a straight line. They marked the effective point as that at which the estimated centroid of the cross section of the muscle or tendon crossed the joint (with the limb in the anatomical position) and would give the most realistic moment arm. The muscle line of action could then be assumed to be a straight line between the effective origin and real insertion or effective insertion and real origin. This approach is more realistic but as the limb segment configuration changes, the muscle lines may still pass through underlying structures.

Delp et al (1990) found this to be the case. They compared the muscle paths of Brand et al (1982) with those of their own model and found that when the skeletal configuration was changed from the anatomical position, several of the muscle paths of Brand et al passed through bones or deeper muscles (e.g. iliacus, gluteus maximus, sartorius). Delp et al (1990) reduced the problem in their own model by considering a muscle to act in a straight line unless at some point the muscle was constrained by retinacula or wrapped over a bone. If this was the case, additional intermediate 'via' points were introduced so that the muscle line of action was represented by a series of line segments. The number of via points required depends on the joint positions and hence additional wrapping points were introduced at certain angles.

Runciman and Nicol (1994) developed a new technique to correct for muscle wrapping. They modelled the contours of the hard tissue of the shoulder as geometrical shapes including spheres and cylinders and applied a new 'dominant muscle plane' technique to calculate the effective origin or insertion as appropriate when wrapping occurred. The angles at which wrapping occurred and effective points obtained were not pre-determined. Hence, when the model was applied to different subjects with changed skeletal geometry and therefore altered origin and insertion positions, these alterations were input and then the method inherently calculated the joint angles at which wrapping occurred and the new effective points.

The mathematical model developed in the current study uses various methods to account for wrapping as is appropriate to each muscle. Among others, these include the method developed by Runciman and Nicol (1994). Chapter 4 gives details of these methods.

3.3.2 Muscle Forces

Following the calculation of intersegmental joint moments and the determination of the lines of action of the muscles, the forces in these structures can be calculated. There are usually more load carrying structures available than there are equilibrium equations. Various approaches have been taken in order to overcome the problem and produce a unique solution.

The first approach which may be termed the 'reduction method' involves reducing the number of unknown variables so that the problem becomes statically determinant. Paul

(1967) took this approach to assess the forces at the hip joint. He grouped the muscles crossing the hip joint on anatomical and functional grounds and then chose the combination of groups which would be active to balance the external joint moments. Morrison (1967) applied a similar technique to the knee as did Procter (1980) at the ankle.

The second approach is termed the 'optimization approach' which assumes that the movements of the human body are performed in such a way as to optimize (i.e maximize or minimize) certain criteria. Common examples of criteria minimized in the past include total muscle force, muscle energy and muscle stress (Seireg and Arvikar, 1973, 1975, Crowninshield et al, 1978a, Hardt, 1978).

Optimization is performed subject to imposed constraints which must be met. The intersegmental moments must be balanced by the moments due to the forces in the load carrying structures. Muscle forces must be non-negative since muscles do not sustain compressive forces. Other constraints may be imposed. For example, the maximum stress in any muscle can be constrained to be less than a certain value so that physiologically unreasonably large muscle forces are not predicted (Crowninshield et al, 1978a).

Optimization techniques were first applied to predict muscle forces in the early seventies (Seireg and Arvikar, 1973, Penrod et al, 1974). They were first applied to gait by Seireg and Arvikar (1975). The objective function minimized was the sum of the muscle forces plus four times the sum of the moments at all of the joints. Seireg and Arvikar reported that in general the theoretical results correlated well with reported patterns of EMG. However, simultaneous activity was only predicted in a few of the 31 muscle parts included in the model. The prediction of only a few active muscles results from the inherent limitation using linear optimization that the number of non zero solutions predicted must be constrained to be less than or equal to the number of equality plus inequality equations. The results of Seireg and Arvikar also illustrated that when no constraints are imposed on the maximum achievable muscle forces, linear optimization may produce unreasonably large muscle forces in the few most advantageously situated muscles. For example, a force of approximately 2100N was predicted in tibialis anterior during gait even though it is a relatively small muscle.

Following the early work of Seireg and Arvikar, Crowninshield (1978) proposed a method to predict more reasonable muscle activity. He too applied linear optimization but the objective function minimized was the sum of the individual muscle stresses i.e. the sum of the force in each muscle divided by its physiological cross sectional area. Hence, unlike the method of Seireg and Arvikar where the muscle with the longest moment arm would be predicted to be most advantageous, this method also takes into account the size of the

muscle. Thus activity in a small muscle can be reduced even though it may have a high moment arm. The method shows a preference for muscles with a high product of moment arm and physiological cross sectional area. Additional constraints were imposed on individual muscle stresses so that they were below critical values. Thus synergistic activity was predicted whilst maintaining physiologically reasonable muscle forces. When the method was applied to gait, Crowninshield et al (1978a) reported that they found reasonably good correlation between predicted muscle force and EMG patterns for most muscles.

Hardt (1978) also attempted to improve on the method of Seireg and Arvikar. In optimization of the sum of muscle forces with no constraints, the only properties of muscles included are the moment arms, the physiology of the system being ignored. Hardt proposed that the central nervous system must surely consider the dynamic and static properties of muscles when devising its control strategy. Hence he proposed a cost function to minimize, in a simplified form, the instantaneous energy requirements of the muscles. On comparison of the results of minimization of muscle force with minimization of energy during gait, Hardt found more muscles to be active when energy was minimized but the correlation between predicted muscle force patterns and EMG was still by no means perfect. He concluded that for the real system to be modelled accurately, there must be more input as to the physiology of the system and more complete modelling.

Like Hardt, Patriarco et al (1981) also compared minimization of muscle force and minimization of mechanico-chemical muscle power output. They too found the incorporation of physiologically based information to be crucial in improving the consistency of predicted muscle force patterns with EMG.

Kaufman et al (1991) proposed an optimization criterion of minimum muscular activation. He incorporated the physiological characteristics of muscles mathematically as constraints on muscle forces. These characteristics included geometrical, morphological and force-length-velocity-activation properties.

The optimization techniques adopted by Seireg and Arvikar (1973,1975), Crowninshield (1978), Crowninshield et al (1978a), Hardt (1978), Patriarco et al (1981) and Kaufman et al (1991) were all linear. Linear optimization is advantageous as well established algorithms exist for it, producing efficient and stable solutions. However, the underlying principle in applying optimization techniques is that the body performs activities in a manner which optimizes some variable, be it muscle force, stress, energy or perhaps something else. Whatever the variable may be, it should not be limited to be linear and hence some researchers have used non linear optimization techniques. Non linear optimization is also one way of increasing the number of non zero variables in the solution and predicting more

simultaneous activity.

Pedotti et al (1978) were the first to investigate the use of non-linear objective functions in the prediction of muscle forces during gait. They compared the use of several linear and non-linear optimization criteria involving minimization of muscle force. From comparison with EMG, Pedotti et al proposed the sum of the squares of actual muscle force divided by maximal force achievable at that instant as the most feasible criterion. The maximum force in a muscle was also constrained to be less than the maximum force achievable. Force-length-velocity relationships were used to calculate these maximum achievable forces.

Crowninshield and Brand (1981) also applied a non linear optimization technique to gait, proposing a cost function of maximization of endurance. This physiologically based optimization function may be reasonable in prolonged repetitive activities such as gait and Crowninshield and Brand reported that they found good temporal agreement between the muscle activity and EMG patterns during gait.

More recently there have been attempts to assist the optimization approach with EMG as an input rather than a validation technique. Cholewicki and McGill (1994) proposed an 'EMG assisted optimization' procedure in which individual muscle forces are estimated from EMG and then adjustments made to them so that joint moment equations are satisfied. The adjustments are minimized by a non-linear optimization routine. Problems with this method include the lack of non-invasive electrical access to deeper muscles.

Hence overall there have been a range of linear and non linear optimization approaches taken incorporating a variety of objective functions and constraints. Those mentioned are but a few of the studies reported in the literature using the optimization technique. The technique has been widely criticised. The comment which appears repeatedly is the importance of a sound physiological basis to the approach and the incorporation of sufficient physiological information to make the results as realistic as possible.

Finally, in addition to the 'reduction' and 'optimization' approaches, there have been alternative methods used. For example, Pierrynowski and Morrison (1985a) developed a physiological hierarchial model. The first level is concerned with the musculoskeletal system and includes muscle moment arms, lengths and velocities. The second includes the force-length-activation relationship of muscle. The third level is the control model and it selects active muscles to satisfy the moment balance within the constraints of the first two levels. It is based on a simple neurophysiological model of pattern generators. On application to gait, Pierrynowski and Morrison (1985b) found that the force profiles for most muscles compared well with EMG activity.

In summary, there have been a variety of approaches taken in solving the indeterminant

problem. From the examples discussed previously, it can be seen that a variety of cost functions have been used in the past including the minimization of muscle force; stress, energy and activation and maximization of endurance. It is important that in any approach taken, the validity of the model is assessed. The most common method of validation taken has been to compare the pattern of predicted muscle activity with EMG patterns measured in the subject or taken from the literature. The limitation of comparison with the literature is that it is assumed that the pattern of muscle activity is the same for each person performing a particular activity. Even if the correlation between predicted activity and EMG is acceptable, the magnitudes of the muscle forces calculated should also be checked to ensure that they are physiologically reasonable. If joint forces are calculated from the muscle forces and external loading then these can be used in the validation procedure. The joint forces calculated can be compared with those obtained by direct measurement in studies using instrumented prostheses. Brand et al (1994) took this approach. They calculated the hip joint forces in a patient with an instrumented prosthesis and compared the results with those obtained by direct measurement.

The method adopted in this project is one of linear optimization and is based on the approach taken by Bean et al (1988). It involves a double linear optimization method. In the first step, the maximum muscle stress is minimized and hence the lowest stress value which allows feasible solutions is deduced. In the second step, the muscle stresses are constrained to be below this value and the combination of muscle forces which minimizes the sum of the muscle forces is chosen. The first step maintains the stresses to be within physiologically reasonable limits but does not do this by the imposition of arbitrary upper limits. It also appears feasible that having obtained the lowest stress levels giving feasible solutions, the body will select the combination of muscles to minimize the total muscle force. Runciman and Nicol (1994) successfully applied this double linear optimization technique to a model of the shoulder joint. They compared the predicted muscle activity patterns with EMG measurements made in the same subjects during 5 activities and in general found predicted muscle activity to be consistent with measured EMG.

3.3.3 Joint Contact Forces

Having determined the external loading and forces in the load carrying structures, the three orthogonal components of joint force can be obtained since for equilibrium, the overall net force on the segment must be zero. These components can then be combined to give the magnitude and direction of the resultant joint force. The simplicity of the calculation depends on the joint under consideration. The method can be applied directly at the hip but calculation at more complex joints such as the knee may require additional assumptions.

CHAPTER 4. METHODOLOGY

Having introduced the methods in chapter 3, chapter 4 now describes these in more detail. Methods to determine body segment kinematics and external loading are discussed first followed by the mathematical muscle model developed to determine muscle and then hip joint forces.

4.1 BODY SEGMENT KINEMATICS

A Vicon motion analysis system (Oxford Metrics Ltd) was used to measure marker position within a laboratory frame of reference as the subject performed the required activities. The following subsections describe the measurement system used to obtain 3D positional data followed by the methods used to determine segment and joint kinematics from the 3D positional data.

4.1.1 Kinematic Measurement System

The Vicon measurement system consists of 6 cameras. Each camera emits pulses of infrared light and detects reflection of this light from any retroreflective marker within its field of view. If two or more cameras receive such reflections and the positions of the cameras with respect to the measurement space are known then the 3D coordinates of the marker centre can be calculated.

The positions of the cameras with respect to the measurement space are determined by calibration. Markers are placed in known 3D positions within the measurement space and using the images of these markers, the system calculates the 3D position of each camera. The calibration set of markers is then removed from the measurement space and the tests performed.

The 3D positional data obtained in the current study whilst the subjects performed the various activities were filtered using a 10Hz non-recursive low pass filter before being used to calculate segment and joint kinematics. Details of the filter are described by Stewart (1995).

4.1.2 Marker Positions, Technical and Anatomical Coordinate Systems

The markers used were spheres with a diameter of 25mm. As has already been described in section 3.1.2, the points used in setting up joint centre positions and anatomical coordinates systems did not always correspond with the requirements of marker placement. Hence there was a need for a technical coordinate system to be set up in each segment using

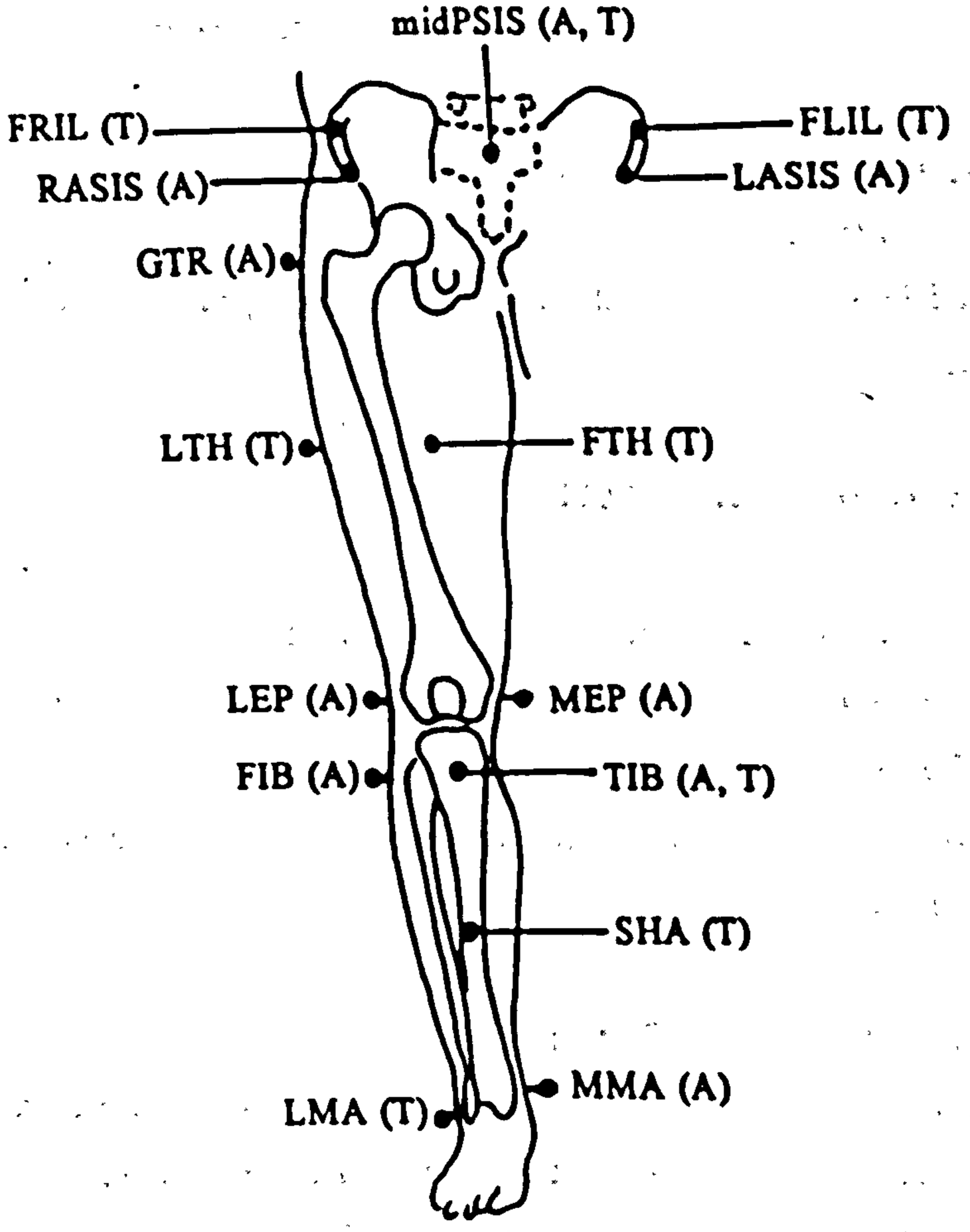

midPSIS	Midpoint between the posterior superior iliac spines.
RASIS, LASIS	Right and left anterior superior iliac spines.
FRIL, FLIL	Right and left iliac crests. Markers were placed towards the anterior of the crests, approximately 50mm from the ASIS.
GTR	Greater trochanter.
FTH	Front of the thigh.
LTH	Lateral side of the thigh.
MEP	Medial femoral epicondyle
LEP	Lateral femoral epicondyle
TIB	Tibial tuberosity.
FIB	Fibula head.
SHA	Front of the shank.
MMA	Medial malleolus.
LMA	Lateral malleolus.

Figure 4.1 Marker set up. 'T' denotes that a marker is technical and 'A' that it is anatomical.

marked points which satisfy the requirements of marker placement. For one static test, extra markers were placed over the points required to define the anatomical coordinate systems. These points could be located in the technical coordinate systems and only the technical markers were then required in the dynamic tests.

Figure 4.1 describes the location of the markers together with the abbreviated name for each marked point. Markers are denoted as anatomical or technical. Twenty-five markers were used for the static tests including 5 on the pelvis and 10 on each of the lower limbs. Thirteen were used in dynamic tests including 3 on the pelvis and 5 on each of the lower limbs. The method used for transformation between technical and anatomical coordinate systems is illustrated by the following general example.

Considering a segment as shown in figure 4.2, let C, D and E be markers placed on points required to set up the anatomical coordinate system with origin D. Let vectors 1 and 2 be set up using these points as illustrated. Using static test data, the anatomical coordinate system can be defined as follows:

Y_A : Vector 1

X_A : Cross product of vectors 1 and 2

Z_A : Cross product of X_A and Y_A

with corresponding unit vectors I_A, J_A and K_A relative to the laboratory coordinate system. From these unit vectors, a direction cosine matrix, $[B_{A\text{-}LAB}]$ relating the anatomical and laboratory coordinate systems can be set up. This direction cosine matrix is used in transforming points expressed in the laboratory coordinate system into the anatomical system. The inverse, $[B_{LAB\text{-}A}]$ is used in conversions from the anatomical to the laboratory system.

Similarly, let c, d and e be markers on the same segment but on points required to set up the technical coordinate system. A technical coordinate system can be defined using these points and a direction cosine matrix, $[B_{T\text{-}LAB}]$ relating the technical and laboratory coordinate systems can be set up. The direction cosine matrix relating the anatomical and technical systems can then be calculated as follows:

$$[B_{T\text{-}A}] = [B_{T\text{-}LAB}] * [B_{LAB\text{-}A}] \qquad (4.1a)$$

The origin of the anatomical coordinate system can also be calculated with respect to the technical system as follows:

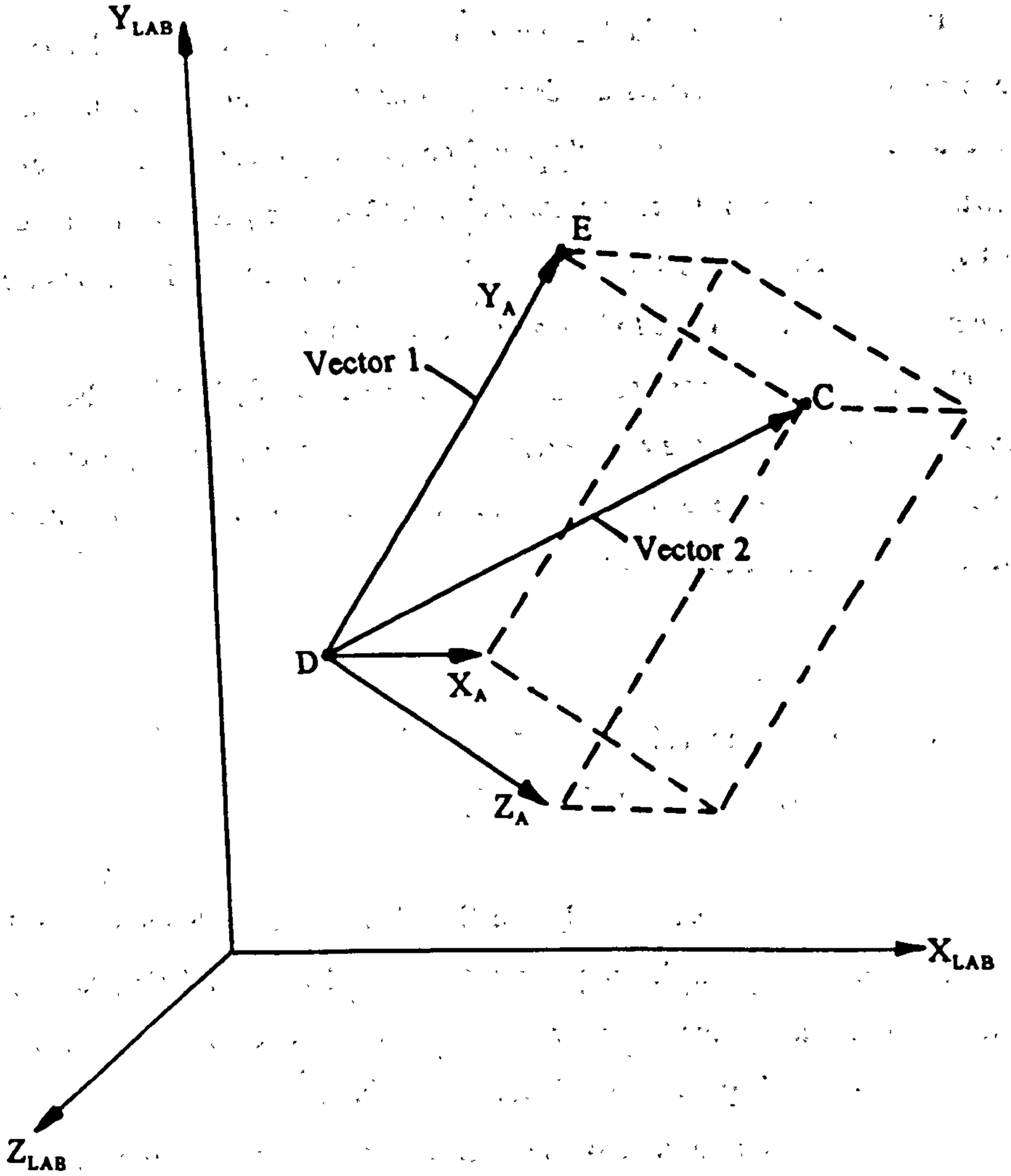

Figure 4.2 Setting up a segment coordinate system

$$(X,Y,Z)_{OA\text{-}T} = [B_{T\text{-}LAB}] * [(X,Y,Z)_{OA\text{-}LAB} - (X,Y,Z)_{OT\text{-}LAB}] \qquad (4.1b)$$

where $(X,Y,Z)_{OT\text{-}LAB}$ are the coordinates of the origin of the technical coordinate system with respect to the laboratory system.

Having obtained this information from the static test, the anatomical markers, C, D and E are removed in the dynamic tests leaving only the technical markers, c, d and e. Using the technical markers in dynamic tests, the direction cosine relating the technical and laboratory coordinate systems, $[B_{T\text{-}LAB}]$ can be set up. Using this and the direction cosine matrix, $[B_{T\text{-}A}]$ obtained from the static test, the direction cosine relating the anatomical and laboratory systems can be obtained as follows:

$$[B_{LAB\text{-}A}] = [B_{LAB\text{-}T}] * [B_{T\text{-}A}] \qquad (4.1c)$$

The origin of the anatomical coordinate system with respect to the laboratory coordinate system can be obtained from the following:

$$(X,Y,Z)_{OA\text{-}LAB} = [[B_{LAB\text{-}T}] * (X,Y,Z)_{OA\text{-}T}] + (X,Y,Z)_{OT\text{-}LAB} \qquad (4.1d)$$

Hence from the use of the technical and anatomical markers in the static test and then only technical markers in the dynamic test, the orientation of the anatomical coordinate system and its origin with respect to the laboratory system can be obtained for each segment in dynamic tests. The laboratory coordinate system is then used as a common reference system for all segments.

Pelvis and hip joint centre

As introduced in section 3.1.2 and listed in figure 4.1, the points used to set up the pelvic anatomical coordinate system were the right and left anterior superior iliac spines (RASIS and LASIS), and the midpoint between the posterior superior iliac spines (midPSIS). The system was defined as follows:

Z_p: Through RASIS and LASIS, pointing laterally in the right side and medially in the left

Y_p: Perpendicular to the plane defined by Z_p and midPSIS, pointing superiorly

X_p: Cross product of Y_p and Z_p, pointing anteriorly

The corresponding unit vectors relative to the laboratory coordinate system were, I_p, J_p, and K_p. These were used to set up the direction cosine matrix, $[B_{P\text{-}LAB}]$ relating the pelvic anatomical coordinate system and the laboratory system. The technical marker system used

markers placed towards the anterior of the right and left iliac crests, (FRIL and FLIL) and also the midPSIS. The method of Bell et al (1990) introduced in section 3.1.1 was used to set up the hip joint centre relative to the pelvic anatomical coordinate system. This predicts the location of the hip joint centre in the frontal plane to be 14% of the inter ASIS distance medial to the ASIS and 30% of the inter ASIS distance distal to the ASIS. A marker placed over the greater trochanter was used to predict the anterior-posterior location.

Femur

The anatomical femoral coordinate system was defined using markers on the medial and lateral epicondyles (MEP and LEP) along with the hip joint centre. The system was defined as follows:

Y_F: Through the hip joint centre and midpoint of MEP and LEP, pointing superiorly

X_F: Perpendicular to the plane containing Y_F and the line between MEP and LEP, pointing anteriorly

Z_F: Cross product of X_F and Y_F axes pointing laterally in the right leg and medially in the left leg

with corresponding unit vectors, I_F, J_F and K_F relative to the laboratory coordinate system. These unit vectors were used to set up the direction cosine matrix, $[B_{F\text{-}LAB}]$ relating the femoral anatomical coordinate system and the laboratory system. The hip joint centre was used with points on the front and lateral sides of the thigh (FTH and LTH) in setting up the technical coordinate system.

Shank, knee and ankle joint centres

As introduced in section 3.1.2, the method developed by Ishai (1975) and used by Goh (1982) was used to set up the shank coordinate system and obtain the ankle and knee joint centres with respect to this coordinate system. The method used markers on the fibula head (FIB), lateral malleolus (LMA) and tibial tuberosity (TIB) along with a set of equations derived from a study of 8 cadaveric tibiae. The external measurements used in the equations are illustrated in figure 4.3 and are as follows:

S_1 : M-L distance between tibial condyles (in mm)

S_2: M-L distance between medial tibial condyle and fibula head (in mm)

S_3: M-L distance between malleoli (in mm)

S_4: Distance between tibial plateau and tibial tuberosity (in mm)

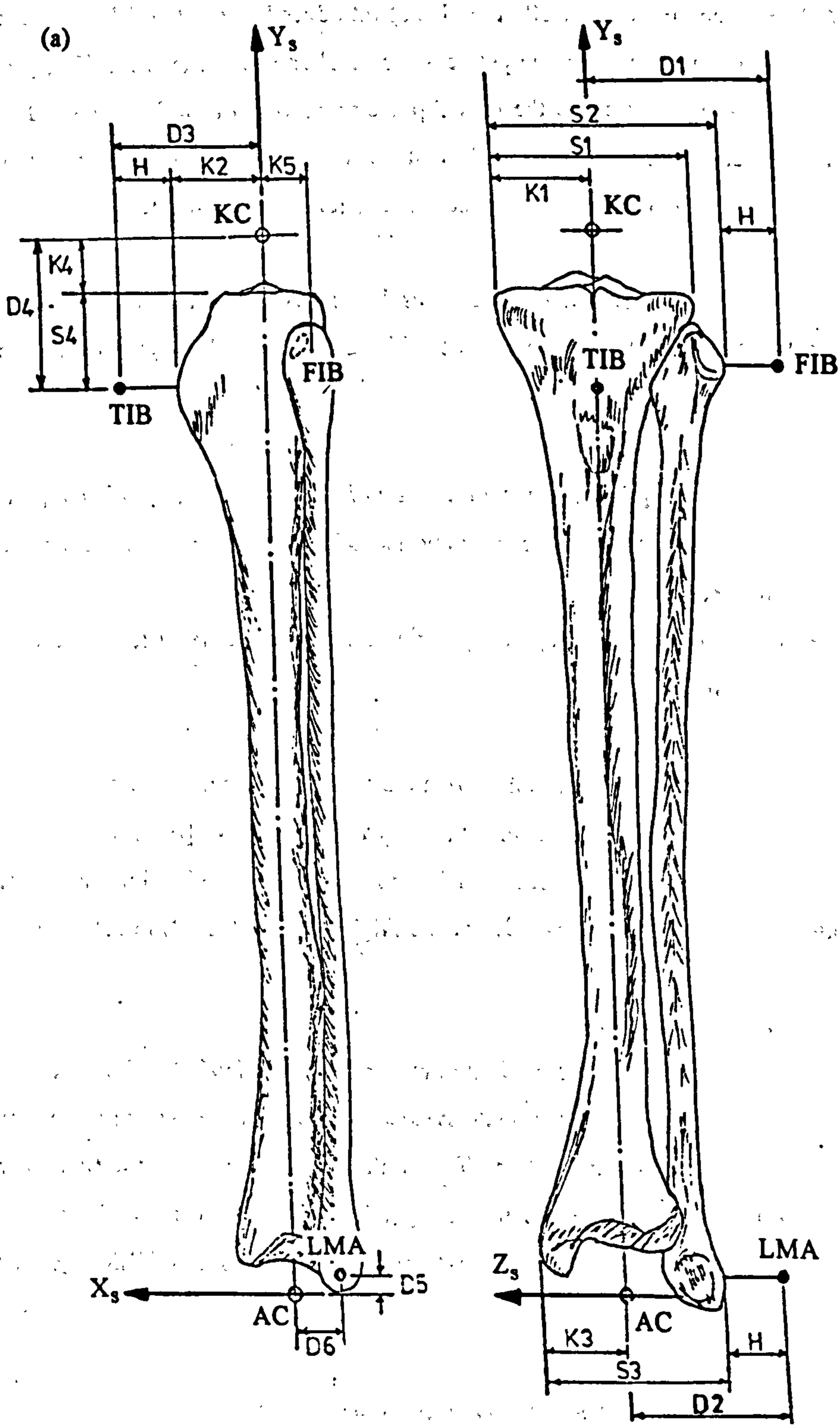

Figure 4.3 Anatomical coordinate system of the left shank.
(a) Lateral view and (b) frontal view (from Goh, 1982).

The equations were then:

$$K_1 = 0.37*S_1 + 14 \qquad K_2 = 0.75*S_1 - 21.6$$
$$K_3 = 0.32*S_1 + 4.4 \qquad K_4 = 25 \qquad \text{(4.2a-d)}$$

The dimensions required to set up the longitudinal shank axis and knee and ankle joint centres were then calculated as follows:

$$D_1 = S_2 - K_1 + H \qquad D_3 = K_2 + H$$
$$D_2 = S_3 - K_3 + H \qquad D_4 = S_4 + K_4 \qquad \text{(4.2e-h)}$$

D_5 and D_6 were assumed to be zero. Hence the ankle joint centre was assumed to lie on the longitudinal axis of the shank at the level of the lateral malleolus.

Figure 4.3 illustrates the way in which the shank coordinate system was set up using these dimensions. As with the pelvis and femur, Y_s points superiorly, X_s points anteriorly and Z_s points laterally in the right leg and medially in the left leg. The mathematics used to obtain the direction cosine matrix, $[B_{S\text{-}LAB}]$ relating the shank anatomical coordinate system and the laboratory system are not detailed here but are described by Goh (1982).

The points used to set up the technical coordinate system in the shank were the tibial tuberosity (TIB), lateral malleolus (LMA) and a point on the front of the shank (SHA).

4.1.3 Joint Kinematics

Hip and knee joint angles were calculated using the floating axis technique as described in section 3.1.3. Flexion-extension, abduction-adduction and internal-external rotation angles were calculated at the hip using equations 3.1a-c and considering the pelvis as the proximal segment and the femur as the distal segment. Flexion-extension, varus-valgus and internal-external rotation angles were calculated at the knee using the same method but this time considering the proximal segment as the femur and the distal one as the shank.

4.2 EXTERNAL LOADING

The three types of external loading, namely contact, gravitational and inertial loading have already been introduced in section 3.2. Only contact and gravitational loading are included in the current study. Inertial loading has been ignored as the periods of interest in all activities are those when the foot is in contact with the ground. Inertial loads will then be relatively small in comparison to contact loads, assuming the subject is not moving at high speed. The activities performed did not demand high speeds and hence the assumptions made were feasible. The vigour and speed with which the subjects performed the activities is also likely to be relatively low since the subject group consisted of hip replacement

patients with a mean age of 71 and non-arthritic subjects with a mean age of 63. However, this is debatable since some hip replacement patients and non-arthritic subjects of these ages are extremely active, sometimes more so than younger subjects. Other researchers including Wretenberg et al (1993), Ellis et al (1984) and Andriacchi et al (1980) have also ignored inertia.

This section is concerned with the determination of contact loads and gravitational loads and then the calculation of joint moments using these loads.

4.2.1 Contact Loading and Force Platforms

Contact loading between the ground and foot was measured using three Kistler force platforms mounted flush with the floor surface. One was model 9281B and the other two were 9261A. Each force platform consists of a top surface supported by 4 pillars instrumented with piezoelectric wafers. When a subject stands on the force platform, the piezoelectric material in each pillar generates a charge proportional to the force applied to it. The force in each pillar in each of the three coordinate directions can then be obtained. Knowing the coordinates of each pillar relative to the force platform origin, it is possible to calculate the three components of force and moment at the force platform origin due to the forces in the pillars. In order to perform stair negotiation and car and bath tests, it was necessary to bolt blocks onto force platform 9281B. The accuracy with which the horizontal and vertical ground reaction forces were measured was found not to be altered by doing this.

4.2.2 Gravitational Loading

As introduced in section 3.2, the method of Drillis and Contini (1966) was used to determine the masses of the thigh and combined shank and foot segments in relation to the body mass as follows:

$$m_F = 0.0946 * \text{body mass} \qquad (4.3a)$$

$$m_{SF} = 0.0555 * \text{body mass} \qquad (4.3b)$$

The distance of the centre of mass from the distal joint was expressed in terms of the segment length. For the thigh and combined shank and foot this was as follows:

$$L_{CMF} = 0.573 * \text{length of femur} \qquad (4.4a)$$

$$L_{CMSF} = 0.533 * \text{length of shank} \qquad (4.4b)$$

4.2.3 Joint Moments

Components of joint moment about each of the three anatomical coordinate axes were calculated at the hip, knee and ankle. The common reference coordinate system chosen to work with initially was the laboratory system. Moments calculated in this coordinate system could then be converted into the appropriate segment coordinate system.

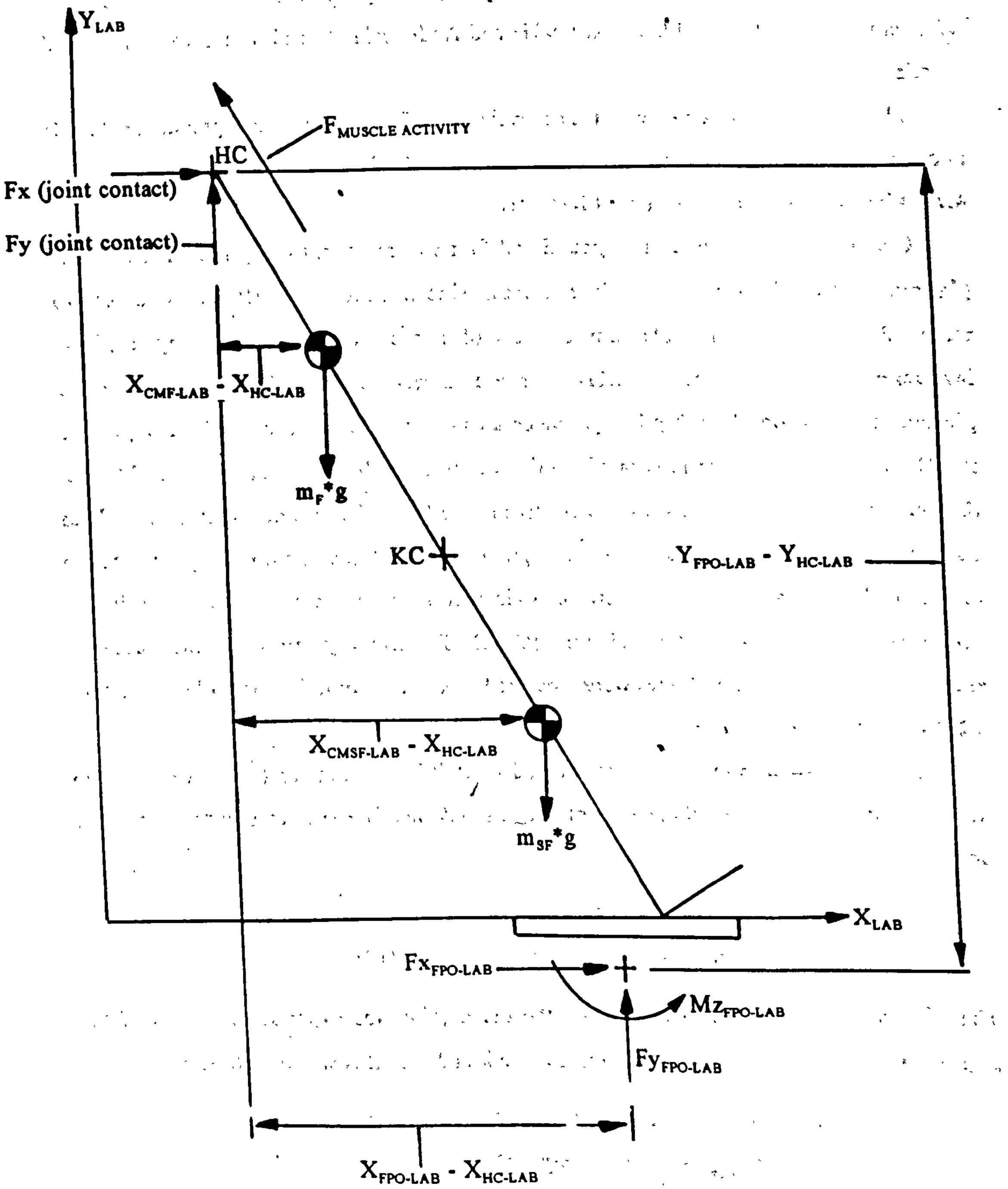

Figure 4.4 Free body diagram for the calculation of Mz_{HC-LAB}

The following example is for the calculation of the three components of moment at the hip. Forces and moments measured at the force platform origin were already expressed in the laboratory coordinate system. However, before moments could be calculated, the hip joint centre and segment centre of mass positions had to be calculated with respect to the laboratory coordinate system as follows:

$$(X,Y,Z)_{HC\text{-}LAB} = [[B_{LAB\text{-}F}] * (X,Y,Z)_{HC\text{-}F}] + (X,Y,Z)_{OF\text{-}LAB} \quad (4.5a)$$

$$(X,Y,Z)_{CMF\text{-}LAB} = [[B_{LAB\text{-}F}] * (0, L_{CMF}, 0)] + (X,Y,Z)_{OF\text{-}LAB} \quad (4.5b)$$

$$(X,Y,Z)_{CMSF\text{-}LAB} = [[B_{LAB\text{-}S}] * (0, L_{CMSF}, 0)] + (X,Y,Z)_{OS\text{-}LAB} \quad (4.5c)$$

The three components of moment at the hip joint relative to the laboratory coordinate system could then be calculated. Figure 4.4 shows the sagittal plane free body diagram used in the calculation of $Mz_{HC\text{-}LAB}$. Free body diagrams were also constructed for the other two planes and the three components of hip joint moment calculated as follows:

$$\begin{aligned} Mx_{HC\text{-}LAB} = {} & [(Y_{FPO\text{-}LAB} - Y_{HC\text{-}LAB}) * Fz_{FPO\text{-}LAB}] - \\ & [(Z_{FPO\text{-}LAB} - Z_{HC\text{-}LAB}) * Fy_{FPO\text{-}LAB}] + \\ & [(Z_{CMF\text{-}LAB} - Z_{HC\text{-}LAB}) * m_F * g] + \\ & [(Z_{CMSF\text{-}LAB} - Z_{HC\text{-}LAB}) * m_{SF} * g] + Mx_{FPO\text{-}LAB} \end{aligned} \quad (4.6a)$$

$$\begin{aligned} My_{HC\text{-}LAB} = {} & [(Z_{FPO\text{-}LAB} - Z_{HC\text{-}LAB}) * Fx_{FPO\text{-}LAB}] - \\ & [(X_{FPO\text{-}LAB} - X_{HC\text{-}LAB}) * Fz_{FPO\text{-}LAB}] + Mz_{FPO\text{-}LAB} \end{aligned} \quad (4.6b)$$

$$\begin{aligned} Mz_{HC\text{-}LAB} = {} & [(X_{FPO\text{-}LAB} - X_{HC\text{-}LAB}) * Fy_{FPO\text{-}LAB}] - \\ & [(Y_{FPO\text{-}LAB} - Y_{HC\text{-}LAB}) * Fx_{FPO\text{-}LAB}] - \\ & [(X_{CMF\text{-}LAB} - X_{HC\text{-}LAB}) * m_F * g] - \\ & [(X_{CMSF\text{-}LAB} - X_{HC\text{-}LAB}) * m_{SF} * g] + Mz_{FPO\text{-}LAB} \end{aligned} \quad (4.6c)$$

Similar equations were set up for the knee and ankle joint moments. In the calculation for the knee joint, the equations were the same as those for the hip joint except that the hip joint centre was replaced by the knee joint centre and the term including the mass of the femur was omitted. At the ankle joint, the equations were again the same except that the hip joint centre was replaced by the ankle joint centre and terms including the mass of each

Muscle	Lower limb joints crossed by the muscle A = Ankle K = Knee H = Hip	Muscle	Lower limb joints crossed by the muscle A = Ankle K = Knee H = Hip
1 Adductor brevis (S)	H	20 Obturator internus	H
2 Adductor brevis (I)	H	21 Pectineus	H
3 Adductor longus	H	22 Piriformis	H
4 Adductor magnus (1)	H	23 Quadratus femoris	H
5 Adductor magnus (2)	H	24 Gemellus superior	H
6 Adductor magnus (3)	H	25 Biceps femoris (L)	H K
7 Gluteus maximus (1)	H	26 Gracilis	H K
8 Gluteus maximus (2)	H	27 Rectus femoris	H K
9 Gluteus maximus (3)	H	28 Sartorius	H K
10 Gluteus medius (1)	H	29 Semimembranosus	H K
11 Gluteus medius (2)	H	30 Semitendinosus	H K
12 Gluteus medius (3)	H	31 Tensor fascia lata	H K
13 Gluteus minimus (1)	H	32 Biceps femoris (S)	K
14 Gluteus minimus (2)	H	33 Gastrocnemius (M)	K A
15 Gluteus minimus (3)	H	34 Gastrocnemius (L)	K A
16 Iliacus	H	35 Vastus intermedius	K
17 Psoas	H	36 Vastus lateralis	K
18 Gemellus inferior	H	37 Vastus medialis	K
19 Obturator externus	H		

Table 4.1 Muscles included in the model.

1 Adductor brevis (S) - S denotes superior part.
2 Adductor brevis (I) - I denotes inferior part.
25 Biceps femoris (L) - L denotes long head.
32 Biceps femoris (S) - S denotes short head.
33 Gastrocnemius (M) - M denotes medial head.
34 Gastrocnemius (L) - L denotes lateral head.

segment were omitted. The loading due to the gravitational pull on the foot segment mass was neglected in the calculation of ankle joint moment.

Having calculated the moments at the joints in terms of the laboratory coordinate system, the hip and knee joint moments were obtained with respect to the coordinate systems immediately distal to the joint concerned, i.e. in femoral and shank systems. The ankle joint moment was converted into the shank coordinate system in the absence of a foot coordinate system. The calculations were performed as follows:

$$(Mx, My, Mz)_{HC-F} = [B_{F-LAB}] * (Mx, My, Mz)_{HC-LAB} \quad (4.7a)$$

$$(Mx, My, Mz)_{KC-S} = [B_{S-LAB}] * (Mx, My, Mz)_{KC-LAB} \quad (4.7b)$$

$$(Mx, My, Mz)_{AC-S} = [B_{S-LAB}] * (Mx, My, Mz)_{AC-LAB} \quad (4.7c)$$

4.3 MUSCLE MODEL

In order to calculate hip joint forces, the forces in the load carrying structures crossing the joint must be calculated. These are required so that the moments due to external loading are balanced and the segment is in equilibrium. A mathematical model of the load carrying structures in the lower limb is therefore required and it is the aim of this section to describe the model developed in the current study. A general outline of the model will be given followed by details in the subsequent sections.

4.3.1 Model Outline

The model incorporates 37 muscle elements as listed in table 4.1. Several muscles of the lower limb are two joint muscles crossing both the knee and hip joints or both the knee and ankle joints. The forces in the muscles of the lower limb will therefore be dictated by the combined kinetics and kinematics of the hip, knee and ankle and the force in one muscle will affect the force in another. Hence the kinetics and kinematics of all three joints and the muscles crossing these joints should be included in the model.

Ideally to completely describe the actions of the structures in the lower limb, the hip, knee and the ankle should all be considered in three dimensions and all of the load carrying structures included. For the purposes of this project, the hip joint was of primary concern and it was considered in three dimensions. As described in section 3.3, hip ligaments only constrain joint moments near the limits of the range of motion. In the majority of the activities in the current study, the motion was within this range and hence hip ligaments were not included in the model. As can be seen from table 4.1, 31 muscle elements crossing the hip were included, 7 of which crossed both the hip and knee joints.

For simplification the knee joint was only considered in the sagittal plane. Moment balance was performed only about the flexion-extension axis and the 13 knee joint muscles included in the model were considered to contribute primarily to moment balance about this axis. The ligaments and articular surfaces were assumed to provide little if any resistance to flexion or extension at the knee and to be primarily involved in abduction/adduction and internal/external rotation balance. Other researchers including Crowninshield et al (1978a) have made similar assumptions.

Whilst most of the muscles crossing the knee joint were included in the model, the ankle joint muscles were included in far less detail, gastrocnemius being the only muscle crossing the ankle joint to be included. This makes up the majority of the two joint muscle bulk crossing both the knee and ankle joints and is a plantarflexor. No dorsiflexors cross the knee. Gastrocnemius was only included as a potential load carrying structure when the external moment tended to dorsiflex the ankle. If the external moment tended to plantarflex the ankle then the force in gastrocnemius was set to zero. This assumes that gastrocnemius does not act antagonistically at the ankle joint

Hence whilst three moment equations were included at the hip and one at the knee, there were no moment equations included for the ankle but its effect was included via the action of gastrocnemius. In the validation studies in sections 6.1.6, 6.2.6 and 6.3.6, the force output from gastrocnemius was generally found to be insufficient to balance the external moment tending to dorsiflex the ankle. It was assumed that soleus and other plantarflexors would make up the deficiency and this is shown to be feasible in sections 6.1.6, 6.2.6 and 6.3.6.

Having outlined the model, the following sections describe the model in more detail. These cover the setting up of the muscle origin and insertion data, muscle wrapping, determination of muscle moment arms and the calculation of muscle and then hip joint forces.

4.3.2 Muscle Data

Data on muscle origins and insertions were required for the model so that muscle lines of action could be determined. The data set used was that of Brand et al (1982) (see appendix I). The data were derived from cadaveric measurements performed on one female and two males. As can be seen from table 4.1, some muscles were split into two or three elements. This is because these muscles had broad origins or insertions whose location would significantly affect the moment arms. Hence origins (gluteus maximus, gluteus medius, gluteus minimus) or insertions (gluteus maximus, adductor brevis, adductor magnus) were set up as two or three different points to account for the different effects of each element.

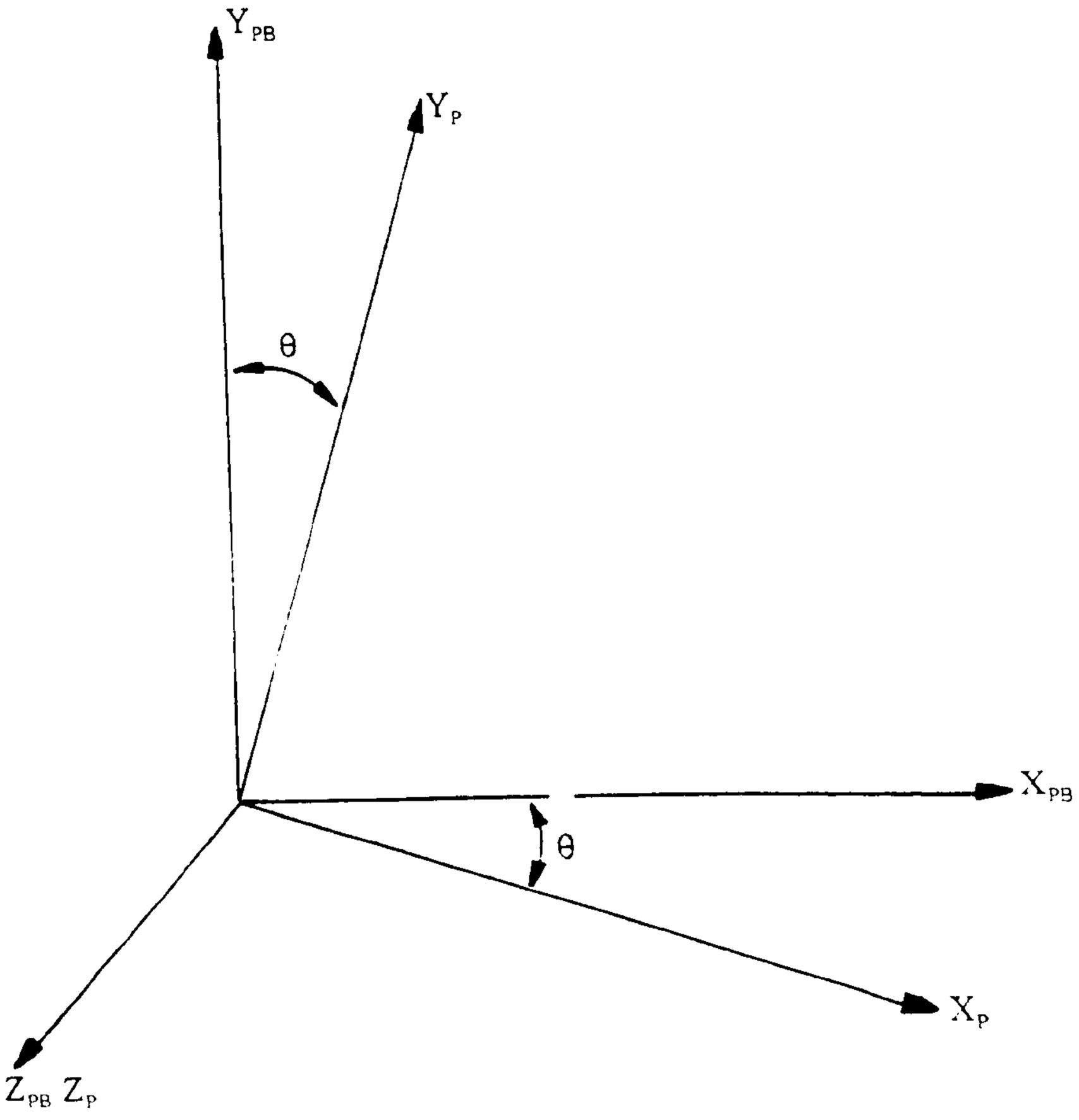

Figure 4.5 The anatomical pelvic coordinate system $(X,Y,Z)_P$ and the pelvic coordinate system of Brand et al (1982) $(X,Y,Z)_{PB}$. The two systems are equivalent if a rotation of θ is made about the medio-lateral axis.

For muscles which do not work in a straight line Brand et al used effective origins or insertions. In these cases, the origin (iliacus, psoas, obturator internus) or insertion (sartorius, gracilis, semitendinosus) was marked by a single point where the estimated centroid of the cross section of the muscle or tendon crossed the joint to give a more realistic prediction of moment arm.

Muscle data coordinate systems

The origins and insertions were located with respect to coordinate systems set up in the relevant limb segments.

The pelvic coordinate system of Brand et al (1982) was defined as follows, the origin being at the centre of the acetabulum.

Y_{PB} : Through the midpoint of RASIS and LASIS and the midpoint of the pubic tubercles pointing superiorly

X_{PB} : Perpendicular to the plane containing the midpoint of the pubic tubercles, RASIS, and the midpoint of RASIS and LASIS pointing anteriorly

Z_{PB} : Cross product of Y_{PB} and X_{PB} pointing laterally in the right side and medially in the left

Due to the practical difficulty of placing markers on the pubic tubercles, an alternative approach was taken in order to set up the pelvic coordinate system of Brand et al. As can be seen from figure 4.5, the anatomical pelvic coordinate system set up in section 4.1.2 is equivalent to that of Brand et al if a rotation of 0° is made about the medio-lateral axis. The angle was measured on 6 dry bone pelvises including three males and three females. The mean value was found to be 10°. A muscle origin, C, expressed in the coordinate system of Brand et al was then calculated with respect to the pelvic anatomical coordinate system as follows:

$$X_{C-P} = \left[X_{C-PB} * \cos(10^\circ) \right] - \left[Y_{C-PB} * \sin(10^\circ) \right]$$
$$Y_{C-P} = \left[X_{C-PB} * \sin(10^\circ) \right] + \left[Y_{C-PB} * \cos(10^\circ) \right] \qquad (4.8a-c)$$
$$Z_{C-P} = Z_{C-PB}$$

The same procedure was applied to all pelvic muscle origins. It is recognised that this angle will vary across different subjects. Indeed in the study of the 6 pelvises the value varied between 5° and 14°. However, the use of the mean value was thought to be the most accurate solution in the absence of the use of markers over the pubic tubercles.

The femoral coordinate system of Brand et al (1982) was coincident with the anatomical

coordinate system described in section 4.1.2. The origin of that of Brand et al was at the midpoint between the lateral and medial femoral epicondyles.

The tibial coordinate system of Brand et al (1982) was set up using markers on the medial and lateral malleoli and the tibial tuberosity. The coordinate axes were then defined as follows:

Y_T: Through TIB and the midpoint between LMA and MMA pointing superiorly

X_T: Perpendicular to the plane containing LMA, TIB and the midpoint between LMA and MMA, pointing anteriorly

Z_T: Cross product of X_T and Y_T, pointing laterally in the right leg and medially in the left

The corresponding unit vectors, I_T, J_T, K_T relative to the laboratory coordinate system were used to set up the direction cosine matrix, $[B_{T-LAB}]$ relating the tibial muscle data coordinate system and the laboratory coordinate system. The origin of this tibial system was at the midpoint between the medial and lateral malleoli. The lateral malleolus (LMA), tibial tuberosity (TIB) and a point on the front of the shank (SHA) were used to set up the technical coordinate system. Hence a common technical coordinate system was used for both the tibial muscle data coordinate system and anatomical shank coordinate system described in section 4.1.2.

Application of data to subjects

In order to predict an individual subject's muscular geometry based on coordinate measurements made on cadaveric specimens, Brand et al (1982) used a scaling scheme. Each origin and insertion coordinate was scaled as:

$$X' = \frac{X}{X_{SC}} \qquad Y' = \frac{Y}{Y_{SC}} \qquad Z' = \frac{Z}{Z_{SC}}$$

where X, Y and Z are measured coordinates, X_{SC}, Y_{SC} and Z_{SC} are anthropometric scaling factors and X', Y' and Z' are scaled coordinates. The published data included the averaged actual and averaged scaled origin and insertion coordinates. The scaling mechanism was devised so that the data could be applied to another subject by multiplying the scaled coordinates by the scaling factors as measured on that subject. The scaling factors proposed by Brand et al were:

Pelvic X : Anterior-posterior (A-P) distance from the pelvic frontal plane to the top of the sciatic notch.

Pelvic Y : Vertical height of the iliac crest (iliac crest - ischial tuberosity Y coordinate difference)

Pelvic +Z
(Right side) : ASIS - hip centre Z coordinate difference.

Pelvic -Z
(Right side) : Ischial tuberosity - hip centre Z coordinate difference.

Femoral X : Distance between the medial and lateral femoral epicondyes.

Femoral Y : Femoral head centre Y coordinate (distance between the midpoint between the femoral epicondyles and the hip joint centre).

Femoral Z : Distance between the medial and lateral femoral epicondyes. (for gastrocnemius).
Lateral distance from the femoral head centre to the top of the greater trochanter (for all other muscles).

Tibial X : Distance between the medial and lateral tibial condyles.

Tibial Y : Tibial tuberosity Y coordinate (distance between the midpoint between the malleoli and the tibial tuberosity).

Tibial Z : Distance between the medial and lateral tibial condyles.

Pelvic +Z (right side): As described in section 4.1.2, the hip joint centre was located in the M-L direction as 14% of the distance between the right and left anterior superior iliac spines (inter ASIS distance) medial to the ASIS. Hence the pelvic +Z factor was given directly as 14% of the inter ASIS distance.

Femoral X and Z (for gastrocnemius) and tibial X and Z: These factors could be obtained by palpation and the use of callipers. An estimation of the soft tissue thickness over the femoral epicondyles and tibial condyles was also made by palpation so that the true distance between the bony landmarks was obtained.

Femoral Y: This was determined using static test data. The position of the hip joint centre could be located with respect to the laboratory coordinate system using the equation 4.5a. The position of the midpoint between the femoral epicondyles was obtained directly in the laboratory coordinate system. The distance between these two points gave the femoral Y factor.

Tibial Y: Again, from the static test, the position of the tibial tuberosity was obtained relative to the shank coordinate system deduced in section 4.12. It could then be obtained

relative to the laboratory coordinate system using the following:

$$(X,Y,Z)_{TIB-LAB} = [[B_{LAB-S}] * (X,Y,Z)_{TIB-S}] + (X,Y,Z)_{OS-LAB} \qquad (4.9)$$

The position of the midpoint between the malleoli was obtained directly with respect to the laboratory coordinate system. The tibial Y factor was then calculated as the distance between the tibial tuberosity and midpoint between the malleoli.

Remaining factors and the practical musculoskeletal model: The pelvic X, Y and -Z (right side) and femoral Z (for all muscles except gastrocnemius) factors proved more difficult to determine than those previously described. They could not be determined directly from palpation and alternative approaches had to be taken. In order to aid the development of these approaches and to examine the application of the data of Brand et al (1982) in more detail, a practical musculoskeletal model of the lower extremity was made. This is shown in figure 4.6. The model included the pelvis, right femur, fibula and tibia and muscle elements as listed in table 4.1. The skeletal parts were made of plastic, the mould having been taken from a European male skeleton. The muscle elements were represented by elastic threads, the ends of which were attached to the points of origin and insertion using specially made pegs.

The origin and insertion coordinates were located in each segment of the model by scaling of the data of Brand et al. The femoral X and Z (for gastrocnemius), tibial X and Z, pelvic *+Z* (right side), femoral Y and tibial Y scaling factors were obtained directly by measurement of the skeletal parts. The methods used to obtain these for test subjects have already been discussed.

The pelvic Y factor, i.e. the vertical distance between the iliac crest and the most inferior point on the ischial tuberosity was also measured directly on the practical model and found to be 192mm. This could not be measured directly on the subjects. However, with the subject lying on his or her front, the distance between the iliac crest and the centre of the ischial tuberosity could be obtained by palpation and by the use of large callipers. The corresponding measurement on the musculoskeletal model was 172mm and hence in order to determine the scaling factor for the subject, the subject measurement was multiplied by 192/172 assuming this ratio to be the same for all subjects.

Similarly, the femoral Z factor for all muscles except gastrocnemius, (i.e the distance between the femoral head centre and the top of the greater trochanter) was measured directly on the practical model and found to be 50mm. Although this could not be measured on the subject, it was possible to obtain a measurement of the distance between the femoral head centre and the most lateral point on the greater trochanter. In order to do this, the distance

Figure 4.6 The Musculoskeletal Model

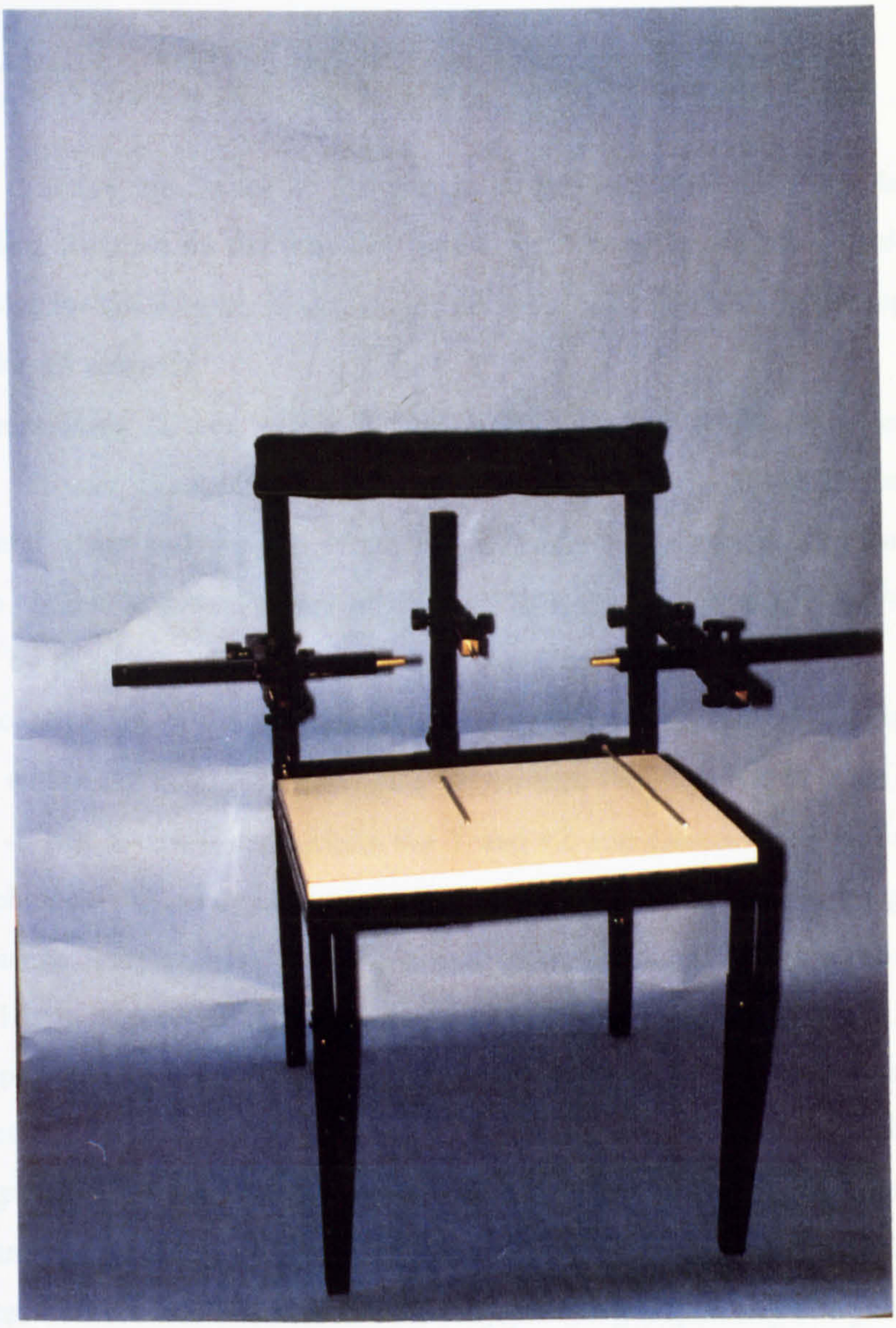

Figure 4.7 The Measurement Chair

between the greater trochanters, G, was measured with the subject standing in the anatomical position. The soft tissue thickness over the right and left greater trochanters was also obtained by palpation to give a total thickness of T. The distance between the most lateral point on the greater trochanter and the femoral head centre, D, was then obtained as follows:

$$D = \frac{G - T - \text{InterASIS distance} + (2 * 0.14 * \text{InterASIS distance})}{2} \qquad (4.10)$$

This assumes the factor to be the same for both the right and left sides. The corresponding distance on the practical model was 65mm and hence in order to obtain the scaling factor for the subject, D was multiplied by a ratio of 50/65, assuming the ratio to be the same for all subjects.

The remaining factors, pelvic X and pelvic -Z (right side) proved more difficult to determine. It was impossible to obtain the pelvic X factor, i.e the distance between the pelvic frontal plane and the top of the sciatic notch by palpation. It would also be very difficult to obtain the lateral distance between the hip joint centre and the ischial tuberosity accurately by palpation. Hence alternative approaches were taken.

On construction of the practical musculoskeletal model, the pelvic origins were found to lie well within the expected positions if the average values of Brand et al (1982) were used for pelvic -Z and X coordinates whilst the Y and +Z coordinates were obtained by the usual scaling technique. The only exceptions to this were obturator internus, the gemelli, the long head of biceps femoris, semitendinosus and semimembranosus but a movement of these points by 10mm laterally in the Z direction made their location acceptable. Using these facts, it was proposed to try to use alternative dimensions for scaling in the pelvic X and -Z (right side) directions, based on measurements made on the practical musculoskeletal model.

The proposed factor for the pelvic X direction was the A-P distance between the pelvic frontal plane and midPSIS. This was measured directly on the practical model. An estimate of this measurement was obtained for the subjects using a specially designed chair as shown in figure 4.7. Pointers were brought to rest against the RASIS, LASIS and midPSIS and the required factor determined from the positions of these pointers. Adjustments were made to allow for soft tissue thickness over the RASIS, LASIS and midPSIS. The average measured coordinates of Brand et al were divided by the new factor as measured on the musculoskeletal model. These newly scaled coordinates were then applied to the subjects by multiplication by their factors as estimated using the specially designed chair The validity of this approach was assessed by using the fact that the A-P distance between the origins of adductor longus and the middle part of gluteus maximus predicted using the new factor should be approximately the same as this factor. A study of the subjects with the greatest

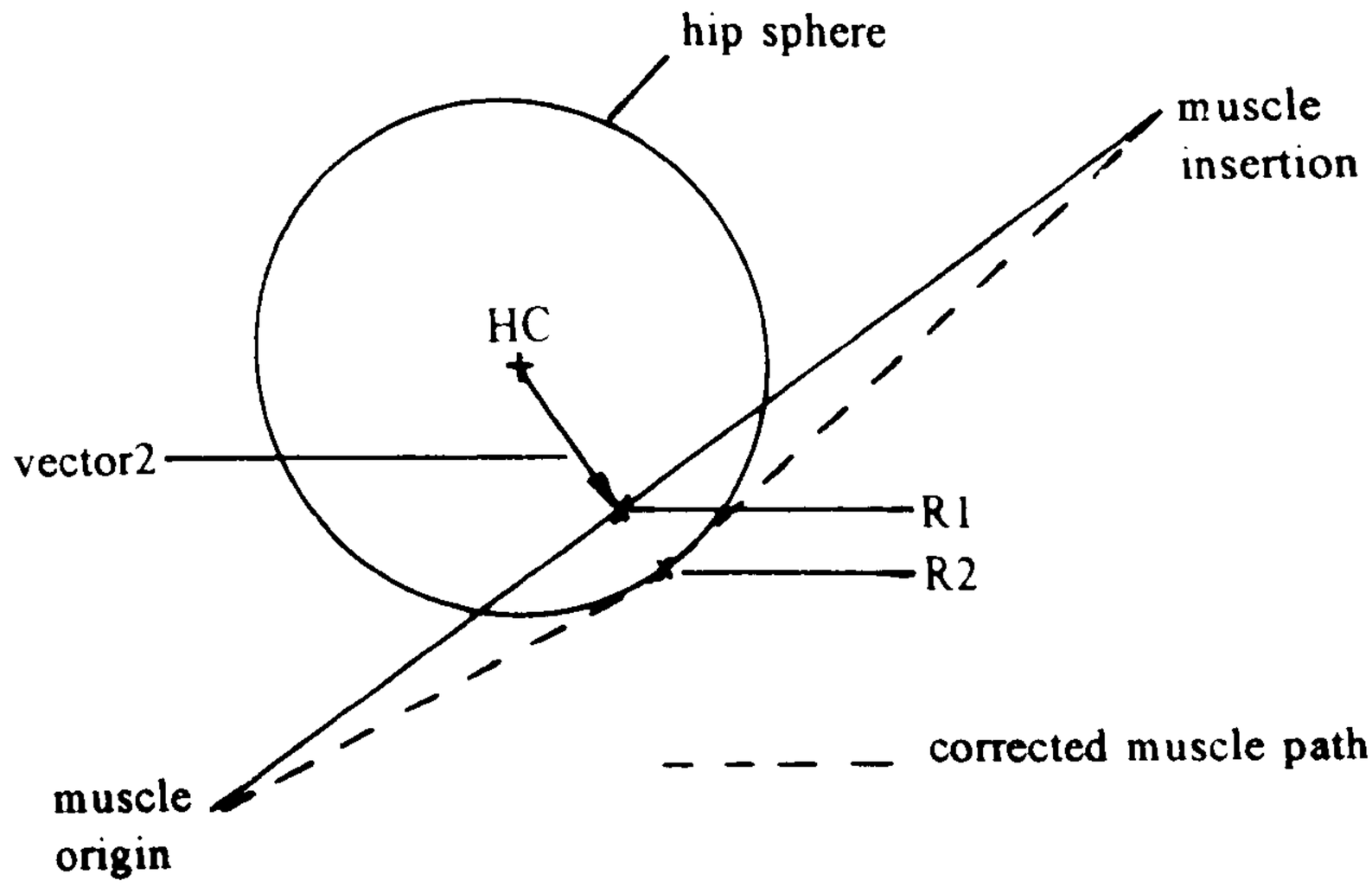

Figure 4.8 An illustration of the approach taken in making adjustments for the wrapping of muscles around the posterior surface of the hip joint. Point R2 is calculated and set up as an effective origin or insertion as appropriate.

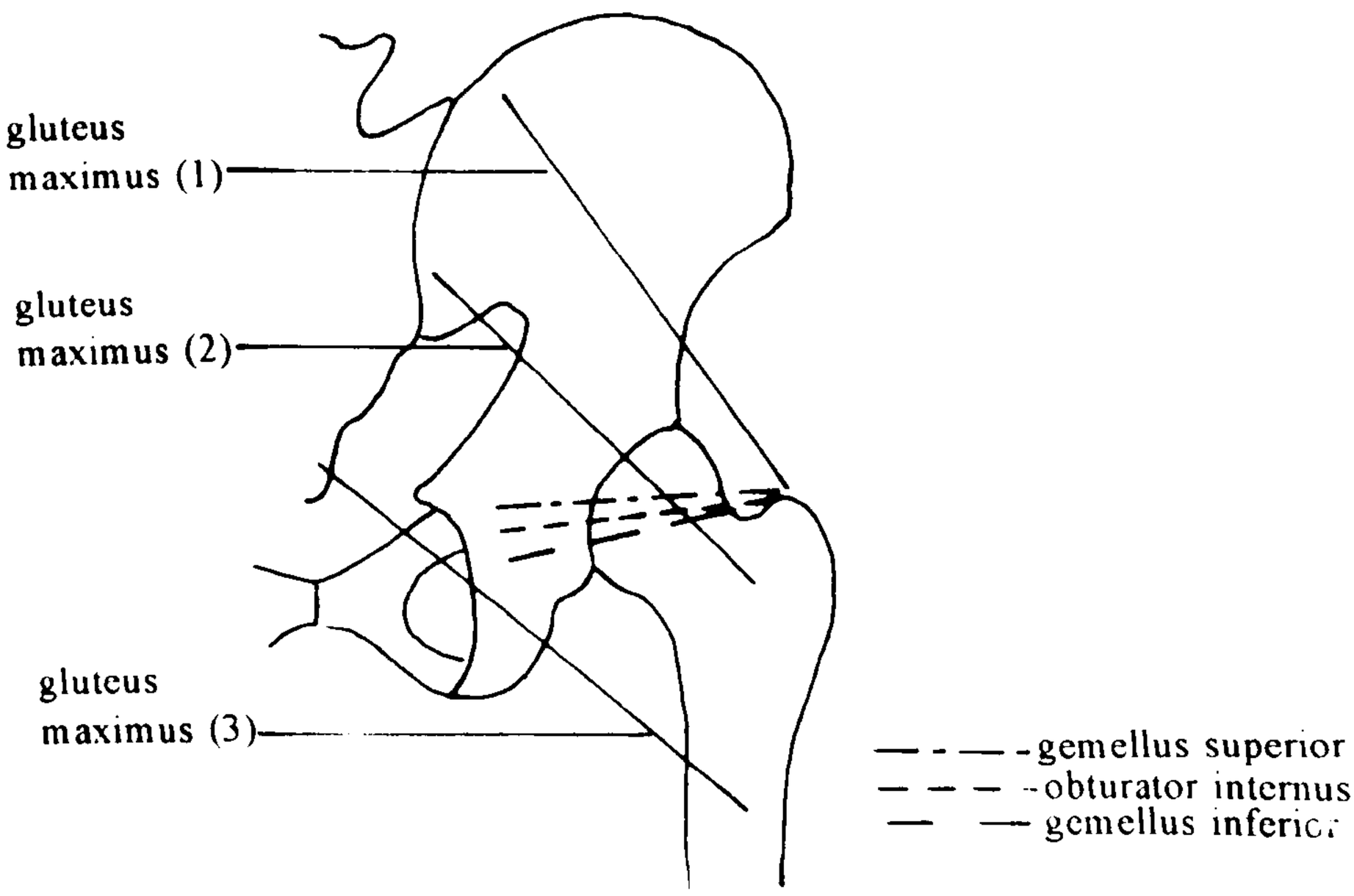

Figure 4.9 A posterior view of the practical musculoskeletal model showing the relative positions of the lines of action of the elements of gluteus maximus and the gemelli.

and smallest estimated factors showed that the percentage differences between the distance obtained from the measurement chair and that from the muscle origin positions was 2% in both subjects. Hence this indicated that the newly proposed scaling method was viable.

In developing a new approach to scaling in the -Z pelvic direction (right side), it was decided to avoid the use of the ischial tuberosities due to the difficulty in accurately locating them in the medio-lateral (M-L) direction by palpation. It was therefore proposed to use the distance between the RASIS and LASIS as the factor in this direction. Hence the average -Z coordinates (right side) of Brand et al were divided by the inter ASIS distance measured on the musculoskeletal model. The newly scaled values were then applied to each subject by multiplication by his or her inter ASIS distance. An indication of the validity of the approach was attained by examining the distance between the right and left origins of adductor longus predicted using the new scaling method. As described in section 2.3.1, adductor longus originates from the front of the body of the pubis, below and medial to the pubic tubercles. It is reasonable to accept that the distance between the points on the right and left sides of the pelvis should not vary excessively between subjects. The value obtained from the skeletal model was 44mm. That predicted for the subjects using the new scaling factor varied between 41 and 54mm with a mean value of 48mm. These values and the variation between them are reasonable and indicate that the proposed scaling method is acceptable.

4.3.3 Muscle Wrapping

As stated in section 3.3.1, muscles do not always lie in straight lines between origins and insertions but the line of action may be altered by the passage over underlying structures. The data of Brand et al (1982) includes some adjustments to allow for this. Indeed, iliacus, psoas and obturator internus were given effective origins and sartorius, gracilis and semitendinosus, effective insertions to give more realistic predictions of moment arm. From the construction of the practical musculoskeletal model using the data of Brand et al and also from the comments of other researchers (Delp et al (1990), Seireg and Arvikar (1973) and Dostal and Andrews (1981)), it was decided that more alterations were required to the data in order to model the lines of action of the muscles more accurately. The muscles to which adjustments were made are gluteus maximus, iliacus, psoas, rectus femoris, obturator internus, piriformis, the lower part of gluteus minimus and the gemelli. The wrapping of each of these muscles around underlying structures and the methods used to adjust for this wrapping are discussed in the following sections.

Obturator internus, piriformis, gemelli and the lower part of gluteus minimus

On manipulation of the practical musculoskeletal model it was observed that these

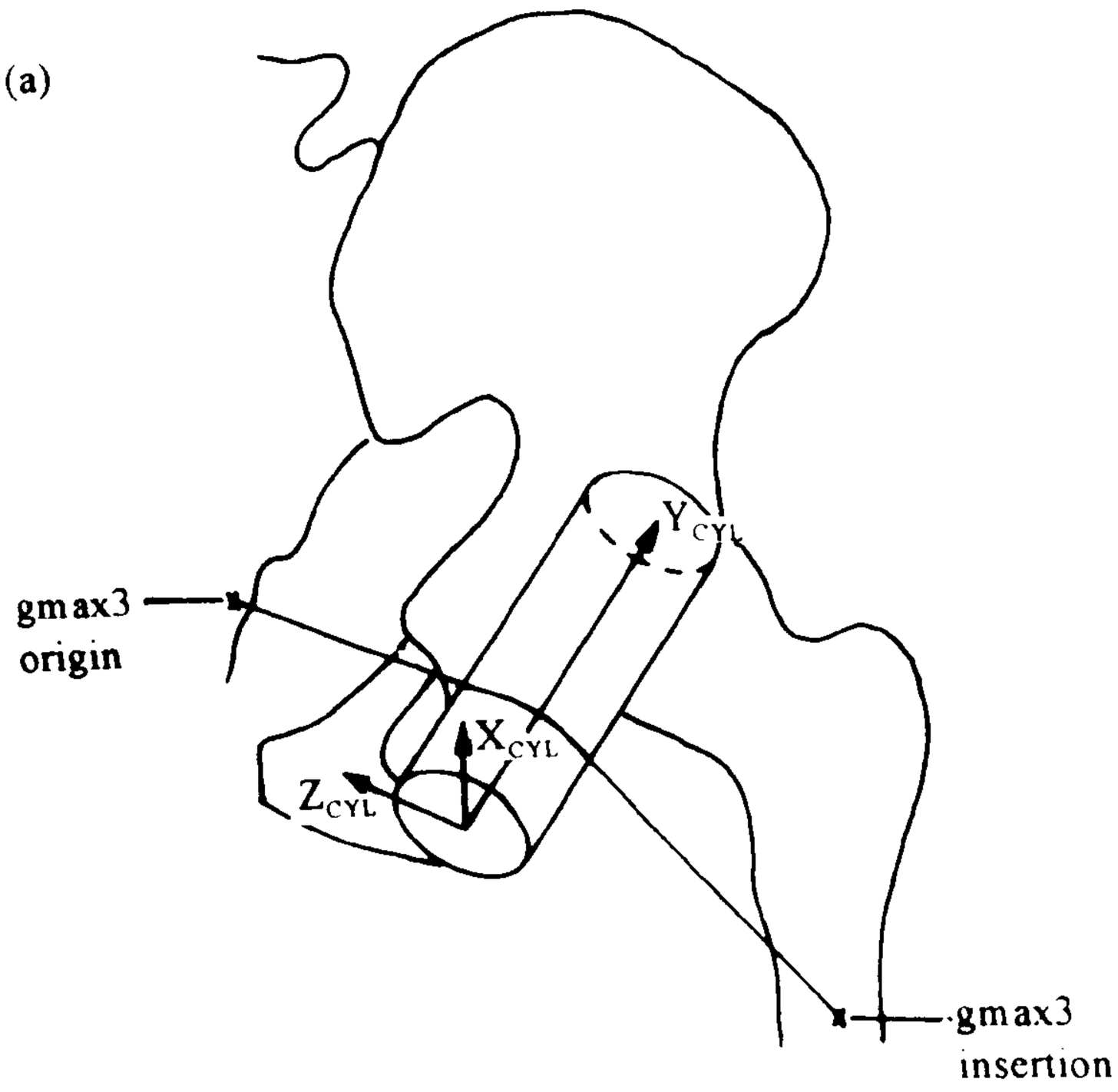

Figure 4.10 An illustration of the approach taken in making adjustments for the wrapping of the lower part of gluteus maximus, gmax3 around the pelvic region between the hip joint centre and the ischial tuberosity.
(a) Modelling of the pelvic region as a cylinder.
(b) An end view of the cylinder used in the calculation of the coordinates of the effective origin of gmax3.

muscles can interact with the posterior surface of the hip joint beyond approximately 20° of internal rotation. In order to check for such interaction, the posterior surface of the hip joint was assumed to be spherical. A straight line was constructed between the origin and insertion of the muscle concerned and the shortest distance between this and the hip joint centre calculated. This distance was equal to the magnitude of vector2, passing through the hip joint centre and crossing the line of the muscle perpendicularly at point R1 as shown in figure 4.8. If the distance was less than the radius of the hip sphere then an effective origin or insertion was located at a point R2. This point was located at a distance equal to the radius of the hip sphere from the hip centre in the direction of vector2. This is illustrated in figure 4.8. It was possible for R2 to lie on the acetabular or femoral region of the hip sphere and an effective origin or insertion point was set up accordingly. Details of the method are presented in appendix C.1.

Anatomical information required in the calculations were the hip sphere radius and also the angle of opening of the acetabulum. A hip sphere radius of 25mm was used as determined from measurements of cadaveric material and the practical musculoskeletal model. This lies within the range of diameters (35 to 58mm) quoted by Morrey (1991). The acetabulum was assumed to face 45° caudally and 15° anteriorly as quoted by Morrey (1991).

Gluteus maximus

The data of Brand et al (1982) used in the current study include gluteus maximus as three elements. On manipulation of the practical musculoskeletal model, it was observed that the underlying structures caused the path of the lower two elements to deviate from a straight line beyond a certain angle of hip flexion. Furthermore, as stated in section 3.3.1, Delp et al (1990) observed gluteus maximus to pass through underlying structures when comparing the muscle paths of Brand et al with their own and changing the skeletal configuration from the anatomical position. They also observed intersection with underlying structures on their own model. Seireg and Arvikar (1973) and Dostal and Andrews (1981) made similar observations.

Figure 4.9 is an illustration of the posterior view of the practical musculoskeletal model. It shows the positions of the three elements of gluteus maximus relative to some of the underlying structures. The methods used to adjust for wrapping of the elements are detailed in the following sections.

Lowest element - gluteus maximus 3 (gmax3) : From manipulation of the practical musculoskeletal model, it was found that the lowest element of gluteus maximus, gmax3, interacted with the ischial tuberosity or the pelvic region between the ischial tuberosity and the hip joint centre during hip flexion.

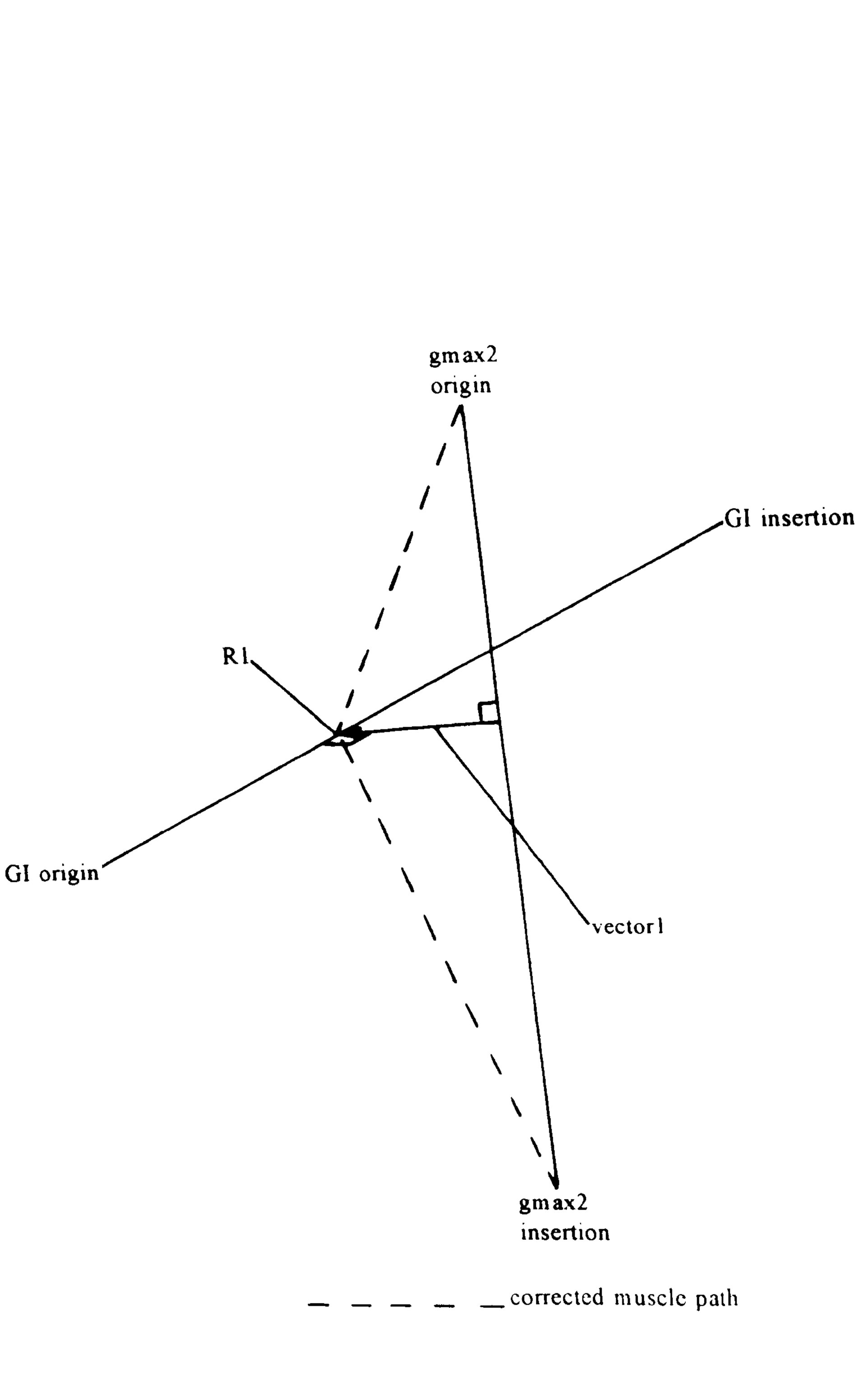

Figure 4.11 An illustration of the approach taken in making adjustments for the wrapping of the middle element of gluteus maximus, gmax2 around gemellus inferior, GI. Point R1 is calculated and set up as the effective origin.

The method used to adjust for this wrapping is based on that developed by Runciman and Nicol (1994). The pelvic region concerned was modelled as a cylinder, the long axis of the cylinder running between the region of the ischial tuberosity and the hip joint centre as illustrated in figure 4.10a. Viewing the cylinder end on as in figure 4.10b showed whether or not flexion was great enough to cause wrapping. If wrap did occur then this end view was used to calculate the coordinates of the effective origin in the XZ plane of the cylinder. The location of the effective origin in the direction of Y_{CYL} was calculated assuming the progression of the muscle in the direction of Y_{CYL} to be constant. The calculated coordinates were then transformed back into the pelvic coordinate system. Details of the calculation procedure are presented in appendix C.2.

Checks were required prior to these calculations in order to ensure that the origin and insertion of the muscle lay outside the cylinder. The program was set up so that if they were found to lie inside the cylinder then an error message was produced and the processing terminated. This situation was not found to occur during data processing for any of the subjects.

Middle element - gluteus maximus 2 (gmax2) : Manipulation of the practical musculoskeletal model revealed that the middle element of gluteus maximus, gmax2, interacted with the underlying lateral rotator muscles beyond approximately 45° of hip flexion. The primary cause of the change in the path of gmax2 was the interaction with gemellus inferior. The relative positions of the lines of action of gmax2 and gemellus inferior are shown in figure 4.9.

The method used to check for and adjust for any interaction is illustrated in figure 4.11. Both muscles were considered as straight line elements. If interaction occurs then gmax2 will be deflected in its path at a point somewhere along the length of the line of gemellus inferior. This point was assumed to be located at R1 in figure 4.11 where the distance between the two straight line elements representing the muscles is a minimum. The minimum distance is equal to the magnitude of vector1 which is perpendicular to both straight line elements. By making these assumptions the location of R1 was calculated and set up as the effective origin of gmax2. Thicknesses of the muscles were incorporated in the method such that the distance between the lines of action of the two muscles was always at least half the thickness of gemellus inferior plus half the thickness of gmax2 in the area of wrapping. A total thickness of 10mm was assumed from cadaveric measurement. If wrapping of gemellus inferior had occurred around the back of the hip joint as described previously, then extra checks were required at the start of the wrapping calculation of gmax2. Details of the method are presented in appendix C.3.

(a)

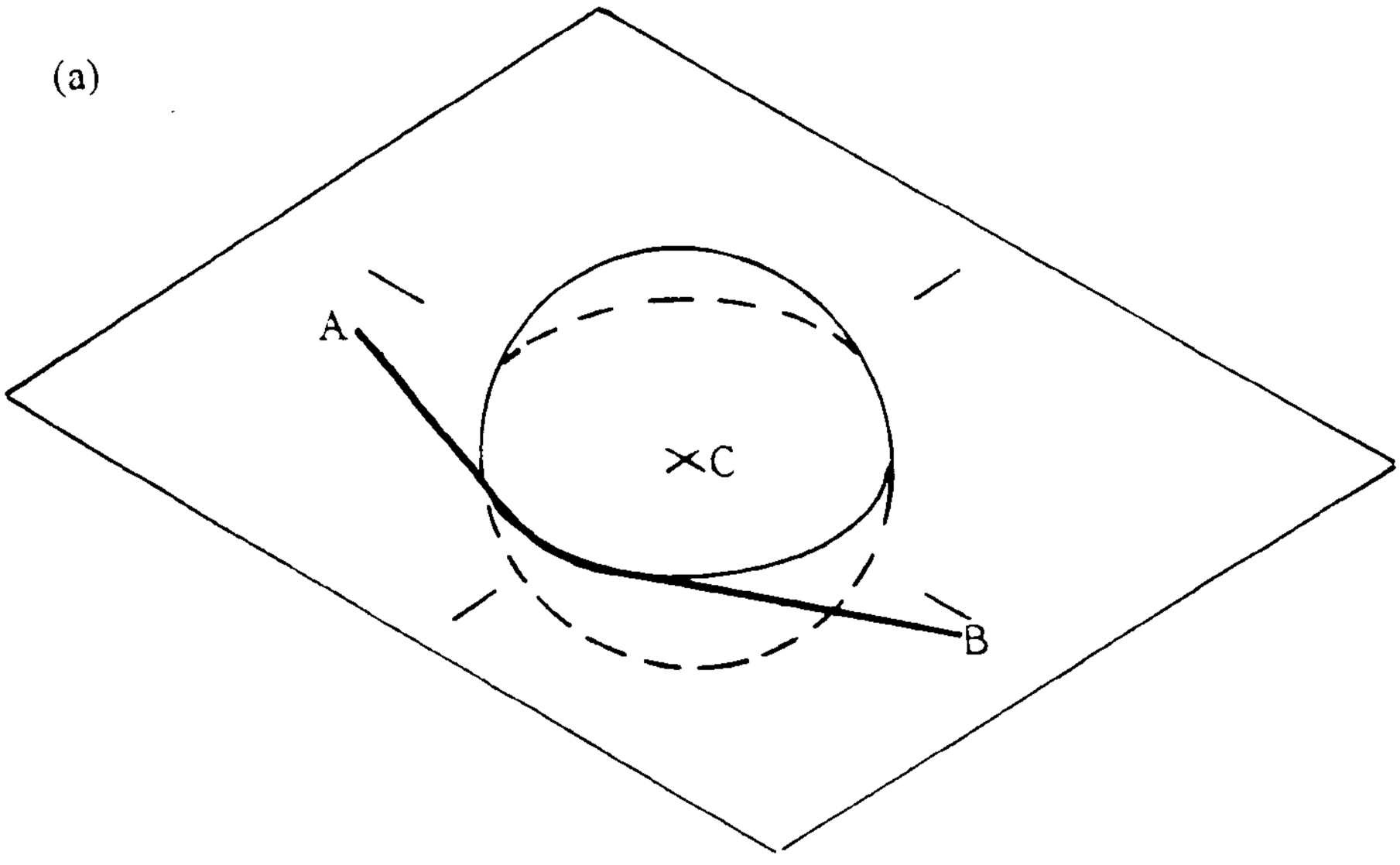

(b)

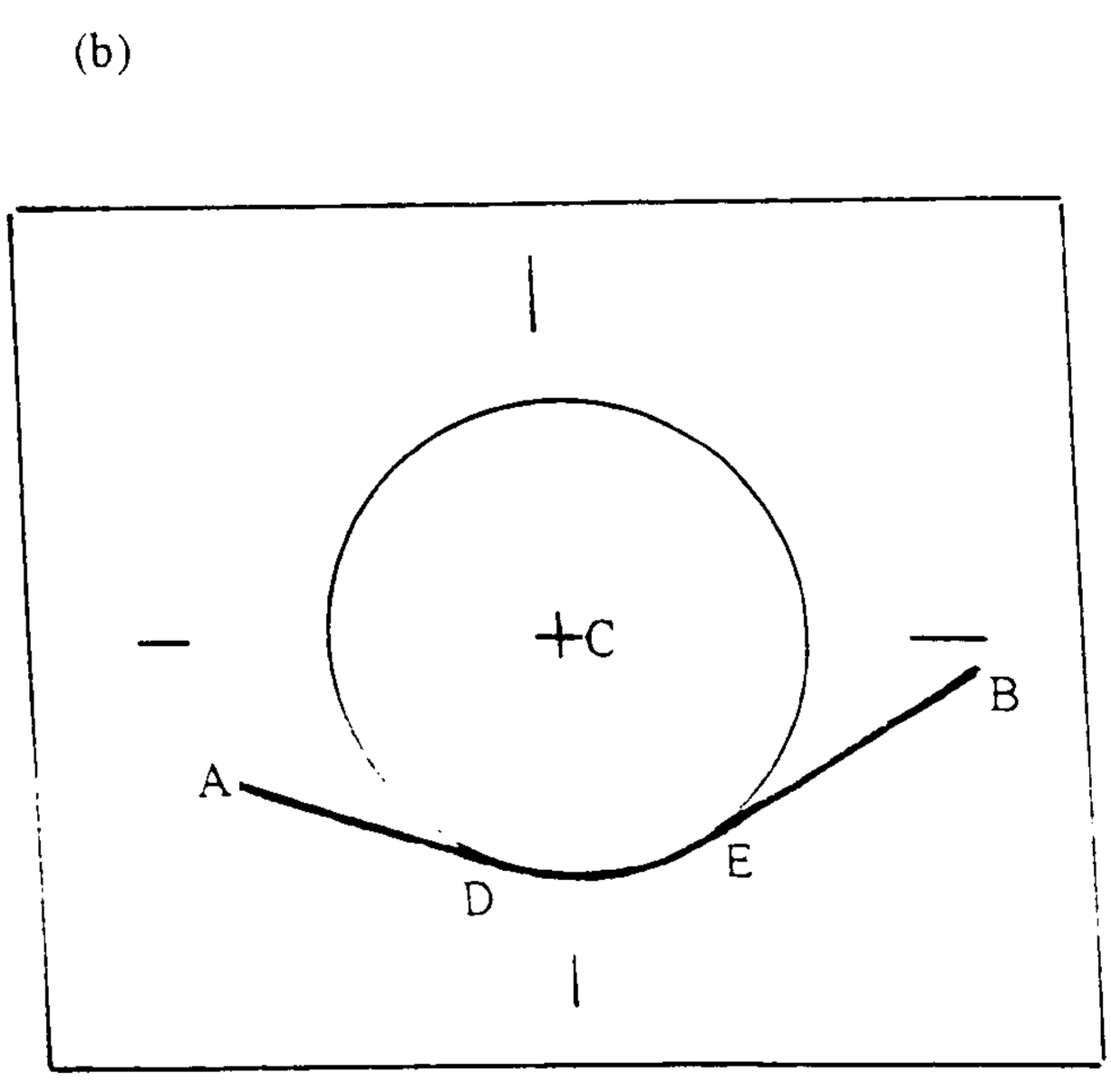

Figure 4.12 (a) Intersection of a string between 2 points A and B and a sphere. The string lies in the plane defined by the sphere centre, C and points A and B.
(b) A view on the plane defined by the sphere centre and the ends of the string. This view is used to calculate contact points D and E.

Highest element - gluteus maximus 1 (gmax1) : As detailed in section 2.3.1, the upper part of gluteus maximus inserts into the iliotibial tract whilst the lower part inserts into the femur. Hence, Brand et al (1982) were able to determine the coordinates of the insertion of the lowest part directly by measurement. However, the insertions of the upper two elements were established using the X and Z coordinates of the femoral insertion of the lowest part. The Y coordinates of these two elements were established from the Y coordinate differences of the origins.

On construction of the practical musculoskeletal model, it was found that the insertion of the highest element, gmax1, lay deep to gluteus medius and adjustments were required so that it would lie outside. In order to do this, a plane was set up to represent, in a simplified manner, gluteus medius. The plane contained the origins and common insertion of the highest and lowest elements of gluteus medius. The perpendicular distance between the insertion of gmax1 and this plane was then calculated. If it was less than a specified value then the origin was moved outwards, perpendicular to this plane so that the distance equalled the specified value. The value was equal to half of the thickness of gmax1 plus half of the thickness of gluteus medius in the area concerned. A total thickness of 9mm was assumed as determined from cadaveric measurement.

Iliacus and psoas

Manipulation of the practical musculoskeletal model revealed that iliacus and psoas interacted with the front of the hip joint during hip extension. Delp et al (1990) also found the lines of action of iliacus and psoas to pass through the hip when the data of Brand et al (1982) were applied to their own model and the skeletal configuration was changed from the anatomical position. Hence, although Brand et al had used effective origins for iliacus and psoas to account for the fact that they do not work in a straight line, further adjustments were required.

The method used for these adjustments is based on that of Runciman and Nicol (1994), the hip joint being modelled as a sphere. The principle of the method may be illustrated by considering the passage of a string over a sphere as in figure 4.12a. When the string is pulled taut, it lies in a plane defined by the ends of the string and the sphere centre. The plane may be uniquely defined provided that the ends of the string and the sphere centre are not collinear. The intersection of the sphere and the plane will form a circle with a radius equal to that of the sphere. This is illustrated by viewing the system in the 2D plane shown in figure 4.12b. The contact points, D and E, can then be calculated in the 2D environment and translated back to the original 3D environment.

An adaptation of the technique can be applied to solve the problem of iliacus and psoas

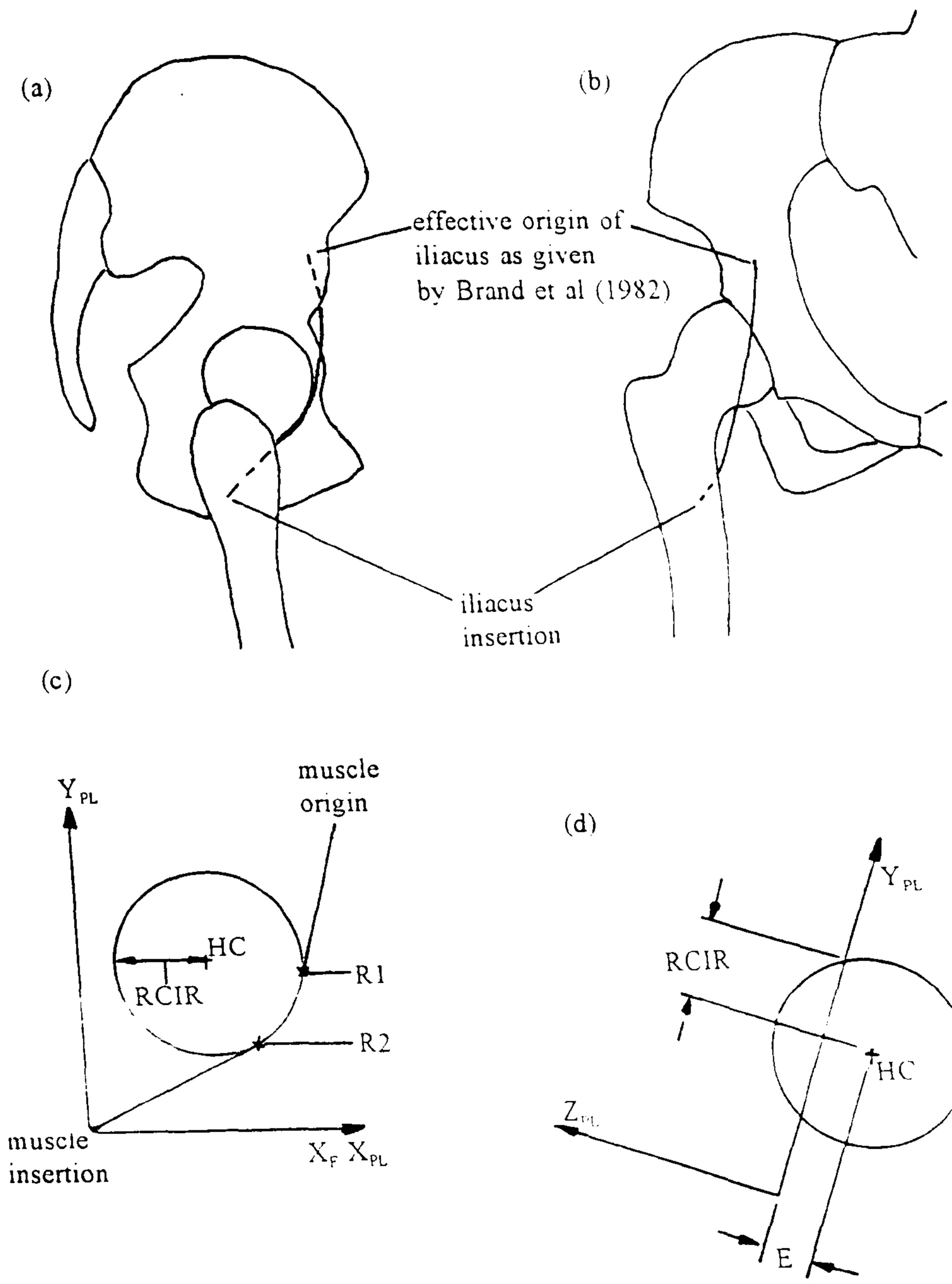

Figure 4.13 (a) Sagittal and (b) frontal views of the practical musculoskeletal muscle model showing the line of action of iliacus.
(c) The intersection of the muscle plane with the sphere forms a circle of radius RCIR.
(d) Calculation of distance E allows determination of RCIR.

wrapping around the front of the hip joint. Figures 4.13a and 4.13b illustrate the line of action of iliacus. That of psoas is similar. Due to constraints of hard and soft tissues muscles do not always follow the shortest line between origin and insertion and the plane will be altered form the theoretical one described in figure 4.12. The dominant plane of each muscle must therefore firstly be determined. In each case, the plane was assumed to contain the origin of the muscle and a line passing through the insertion parallel to the femoral X axis. A muscle plane coordinate system was set up as illustrated in figures 4.13c and 4.13d with X_{PL} parallel to the femoral X axis, X_F. Y_{PL} lies in the muscle plane and is perpendicular to X_{PL}. Z_{PL} is perpendicular to both X_{PL} and Y_{PL}. The intersection of the plane with the sphere will form a circle as shown in figure 4.13c. The radius of this circle will not be equal to that of the sphere since the muscle plane does not contain the sphere centre. However, the perpendicular distance between the sphere centre and the muscle plane can be determined as distance E in figure 4.13d, allowing calculation of this radius as RCIR. Contact points R1 and R2 in figure 4.13c were calculated with respect to the muscle plane coordinate system. These were then used to set up an effective origin or insertion depending on whether wrapping occurred on the femoral side of the sphere or on the acetabular side.

Implementation of the method required several checks to be made. Firstly, it was checked whether or not the plane did in fact cut the sphere by calculating the perpendicular distance between the plane and the sphere centre. If this was greater than the radius of the sphere then wrapping did not occur and there was no need for further calculation. However, if the plane did cut the sphere then a check was performed for intersection of the line between the origin and insertion with the circle formed by intersection of the plane with the sphere. If intersection did occur then there was wrapping and calculation proceeded as previously described. The origin and insertion were required to lie outside the circle formed by the intersection of the plane and the sphere. The program was set up so that if they did not, then an error message was produced and processing terminated. This did not occur.

Details of the method are presented in appendix C.4. The anthropometric dimensions required regarding hip sphere radius and angle of opening of the acetabulum were determined as described in the section on wrapping of muscles around the back of the hip joint.

Knee joint wrapping

As the knee flexes beyond a certain angle the quadriceps tendon may wrap around the distal end of the femur before inserting into the patella. Indeed, both Delp et al (1990) and Seireg and Arvikar (1973) included adjustments in their model to account for such wrapping. Delp et al (1990) included wrapping points for knee flexion angles greater than 90° so that the tendon wrapped around the bone rather than passing through it. Adjustments to the

RFEM : Radius at the most anterior point on the distal femur
TPAT : Patella thickness
RTOT : RFEM + TPAT
θ : Knee flexion angle
A : RTOT*cosθ

(a) If A>RFEM - no wrapping occurs.

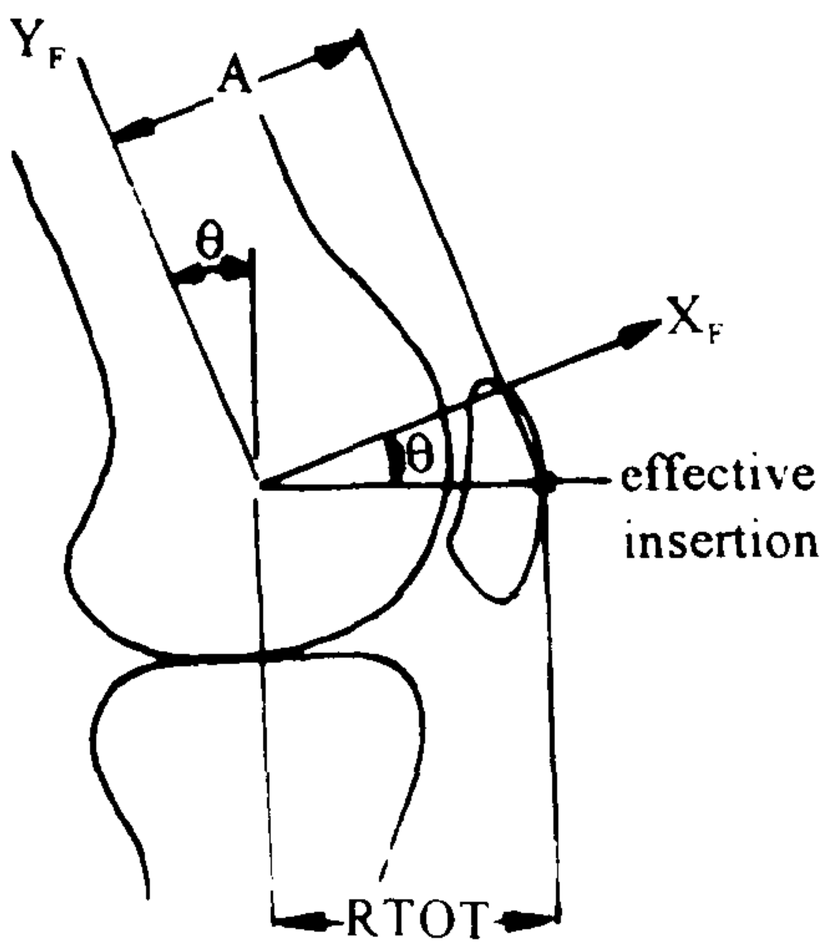

The coordinates of the effective insertion of rectus femoris are given relative to the femoral coordinate system by

$$X_{REIN-F} = A$$
$$Y_{REIN-F} = -(RTOT*\sin\theta)$$
$$Z_{REIN-F} = 0$$

(b) If A<RFEM - wrapping occurs.

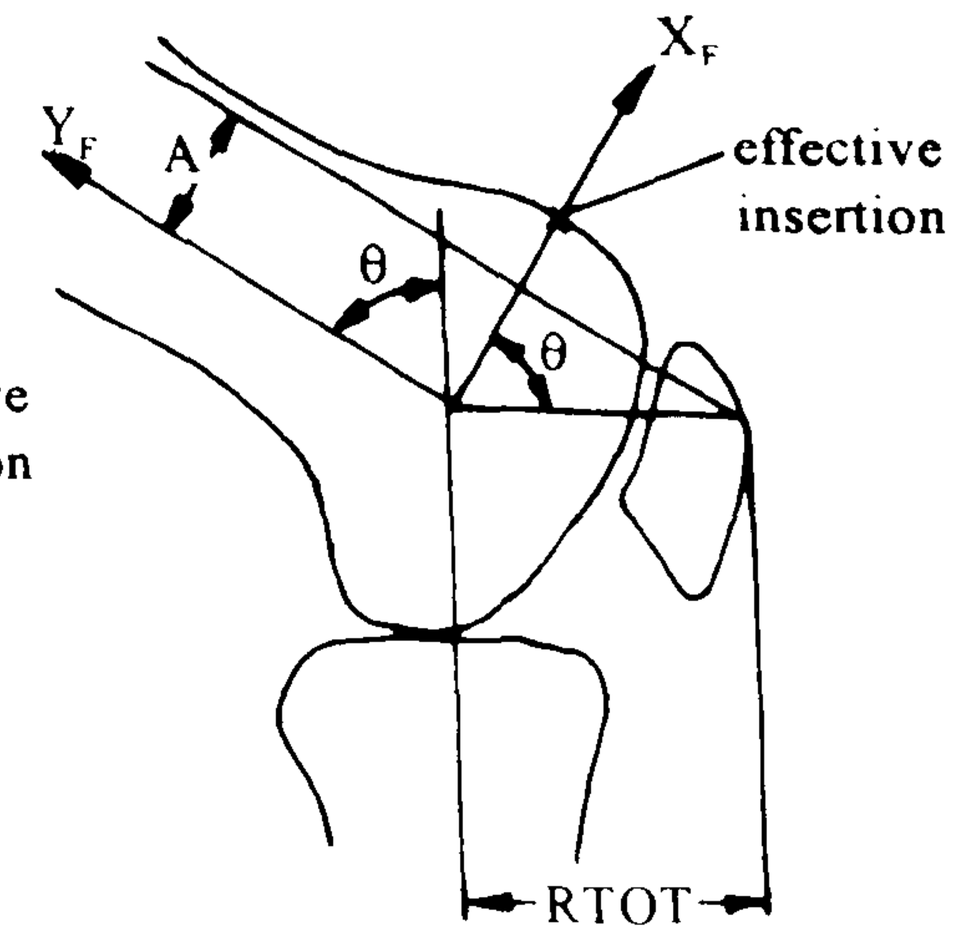

The coordinates of the effective insertion of rectus femoris are given relative to the femoral coordinate system by

$$X_{REIN-F} = RFEM$$
$$Y_{REIN-F} = 0$$
$$Z_{REIN-F} = 0$$

Figure 4.14 An illustration of the approach taken to calculate the coordinates of the effective insertion of rectus femoris.
(a) No wrapping occurs around the distal end of the femur.
(b) Wrapping occurs around the distal end of the femur.

insertion were required in the model in the current study so that a realistic moment arm would be obtained for rectus femoris at the hip. A simple approach was adopted for this purpose as illustrated in figure 4.14. Anthropometric measurements used in this method are the radius at the most anterior point between the condyles on the distal femur (RFEM) and the maximum patella thickness (TPAT). These were expressed as a percentage of the distance between the femoral epicondyles. This percentage was determined from measurement of the practical musculoskeletal model and assumed constant for all subjects.

In conclusion to this section on muscle wrapping, adjustments have been made to those muscles observed to have the most serious interaction with underlying structures. It has been necessary to make simplifying assumptions in order to determine effective origin and insertion points but the results obtained will be more accurate than those which do not include the effects of wrapping.

4.3.4 Moments due to Muscle Action

The model developed in the current study incorporates moment balance in 3D at the hip and balance in the sagittal plane at the knee. Moment arms at both the hip and knee joints therefore had to be determined and the methods used to do this are described in the following sections.

Hip joint moment arms

Having determined the origin and insertion coordinates of each muscle, effective or otherwise, the equations of the lines of action of those crossing the hip joint were calculated. The contribution of each muscle to external moment balance at the hip joint could then be obtained. Before any calculation of lines of action could be performed, all coordinates concerned were converted into the femoral based coordinate system.

A point, A, in the pelvic coordinate system was transformed into the femoral system via the common laboratory system as follows:

$$(X,Y,Z)_{A\text{-}LAB} = [[B_{LAB\text{-}P}] * (X,Y,Z)_{A\text{-}P}] + (X,Y,Z)_{OP\text{-}LAB} \qquad (4.11a)$$

$$(X,Y,Z)_{A\text{-}F} = [B_{F\text{-}LAB}] * [(X,Y,Z)_{A\text{-}LAB} - (X,Y,Z)_{OF\text{-}LAB}] \qquad (4.11b)$$

A point, B, in the tibial coordinate system of Brand et al (1982) was transformed into the femoral system, again via the common laboratory system as follows:

$$(X,Y,Z)_{B\text{-}LAB} = [[B_{LAB\text{-}T}] * (X,Y,Z)_{B\text{-}T}] + (X,Y,Z)_{OT\text{-}LAB} \qquad (4.12a)$$

$$(X,Y,Z)_{B\text{-}F} = [B_{F\text{-}LAB}] * [(X,Y,Z)_{B\text{-}LAB} - (X,Y,Z)_{OF\text{-}LAB}] \qquad (4.12b)$$

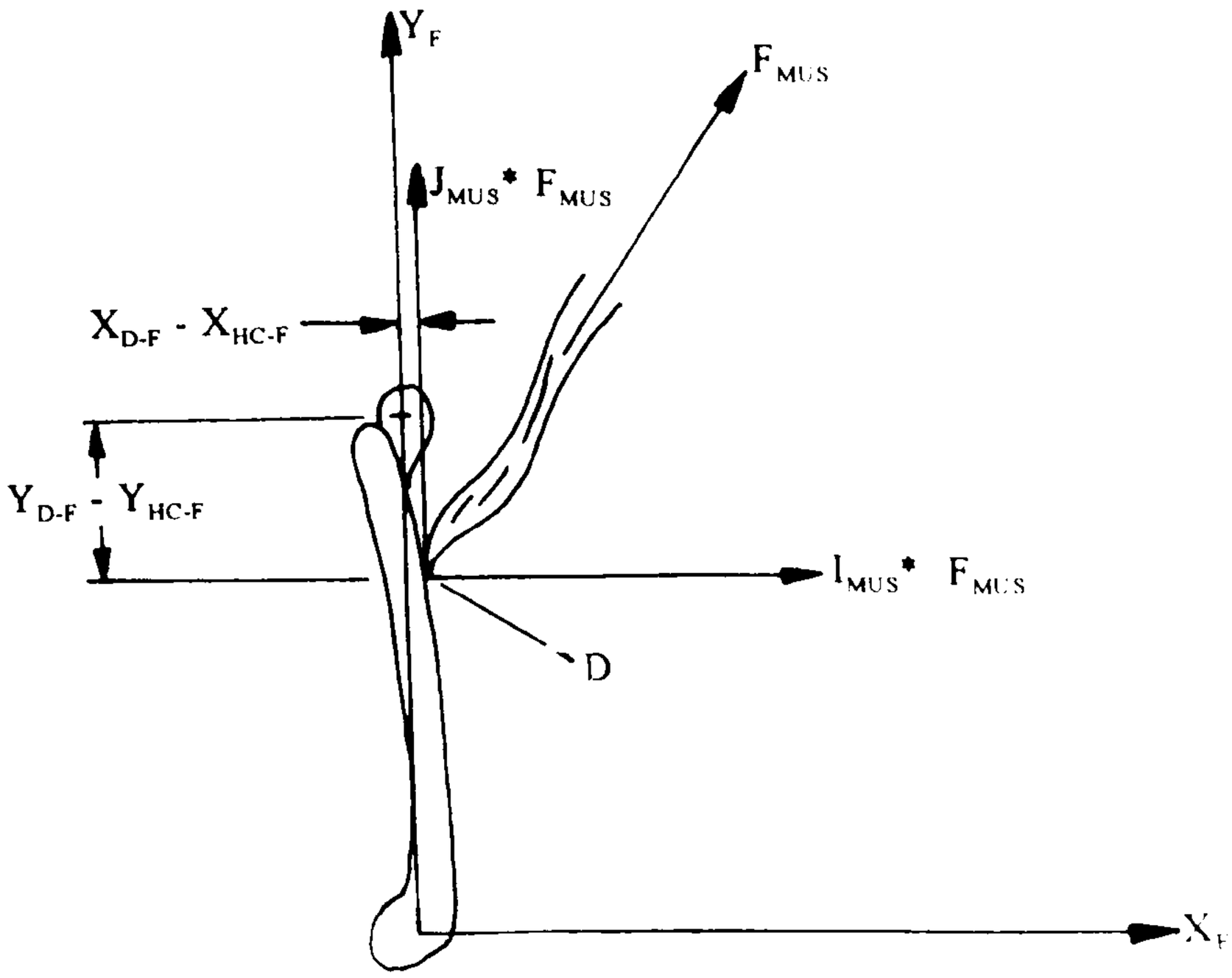

Figure 4.15 A muscle crossing the hip joint with insertion D will produce a moment $Mz_{HC\text{-}F\,(MUS)}$ when it is active.

The unit vector of each muscle crossing the hip joint, describing the line of action relative to the femoral coordinate system could then be calculated. The following calculation is an example for a muscle with its origin at C and insertion at D.

$$(I, J, K)_{MUS\text{-}F} = \left(\frac{(X_{C\text{-}F} - X_{D\text{-}F})}{E}, \frac{(Y_{C\text{-}F} - Y_{D\text{-}F})}{E}, \frac{(Z_{C\text{-}F} - Z_{D\text{-}F})}{E}, \right) \qquad (4.13)$$

$$\text{where } E = \left[(X_{C\text{-}F} - X_{D\text{-}F})^2 + (Y_{C\text{-}F} - Y_{D\text{-}F})^2 + (Z_{C\text{-}F} - Z_{D\text{-}F})^2 \right]^{1/2}$$

Using this unit vector the moment contribution of the muscle about the hip joint could be determined as a function of the force in that muscle. Figure 4.15 illustrates the approach used as applied to moment action about the Z axis in the following equation.

$$\begin{aligned} Mz_{HC\text{-}F\ (MUS)} &= \left[(X_{D\text{-}F} - X_{HC\text{-}F}) * (J_{MUS\text{-}F} * F_{MUS}) \right] \\ &- \left[(Y_{D\text{-}F} - Y_{HC\text{-}F}) * (I_{MUS\text{-}F} * F_{MUS}) \right] \end{aligned}$$

This may be rewritten as follows:

$$Mz_{HC\text{-}F\ (MUS)} = \left[(X_{D\text{-}F} - X_{HC\text{-}F}) * J_{MUS\text{-}F} - (Y_{D\text{-}F} - Y_{HC\text{-}F}) * I_{MUS\text{-}F} \right] * F_{MUS} \qquad (4.14a)$$

Similar equations can be set up for moments about the X and Y axes as follows:

$$Mx_{HC\text{-}F\ (MUS)} = \left[(Y_{D\text{-}F} - Y_{HC\text{-}F}) * K_{MUS\text{-}F} - (Z_{D\text{-}F} - Z_{HC\text{-}F}) * J_{MUS\text{-}F} \right] * F_{MUS} \qquad (4.14b)$$

$$My_{HC\text{-}F\ (MUS)} = \left[(Z_{D\text{-}F} - Z_{HC\text{-}F}) * I_{MUS\text{-}F} - (X_{D\text{-}F} - X_{HC\text{-}F}) * K_{MUS\text{-}F} \right] * F_{MUS} \qquad (4.14c)$$

The approach was applied to all of the 31 muscles which cross the hip joint. The moment contribution made by each muscle about each of the three femoral coordinate axes was thereby expressed in terms of the force in that muscle. The results were expressed in matrix form as follows:

$$\begin{bmatrix} Mx \\ My \\ Mz \end{bmatrix}_{H\text{-}F\ MUSCLE\ ACTIVITY} = \begin{bmatrix} n_{1,1} & \cdots & n_{1,31} \\ n_{2,1} & \cdots & n_{2,31} \\ n_{3,1} & \cdots & n_{3,31} \end{bmatrix} * \begin{bmatrix} F_{MUS\ 1} \\ \vdots \\ F_{MUS\ 31} \end{bmatrix} \qquad (4.15)$$

The numbering of the muscles, 1 to 31, corresponds to that given in table 4.1.

Knee joint moment arms

Thirteen muscles which cross the knee joint have been included in the model. Moment balance at the knee was only undertaken about the flexion-extension axis. Hence only flexion-extension moment arms were required for these muscles and these were input from

the published data of Spoor and Leeuwen (1992). These moment arms were obtained from measurements made on the cadaver of an 89 year old female. Spoor and Leeuwen compared the moment arms determined from magnetic resonance imaging (MRI) measurement with those from tendon travel over a range of knee flexion angles. They concluded that in general the method of tendon travel was more accurate than the use of MRI. Hence the values used in this study are the ones determined from tendon travel.

Spoor and Leeuwen reported that the moment arm of tensor fascia lata could not be derived from MRI because the unknown force distribution in fascia lata does not allow estimation of the line of pull. They also reported that the tendon travel method would not be expected to give reliable results. Hence tensor fascia lata was not included in the knee joint moment balance.

It is recognised that the use of the same moment arms in all subjects as derived from the one cadaver is not ideal. However, this appeared to be the most comprehensive study publishing moment arms and in the absence of more information this was the most feasible solution available. The moment arms (o_{25} ... o_{37}) were set up in matrix form as follows:

$$[\,Mz\,]_{\text{K-S MUSCLE ACTIVITY}} = [\,o_{25} \;\cdots\; o_{37}\,] * \begin{bmatrix} F_{\text{MUS 25}} \\ \vdots \\ F_{\text{MUS 37}} \end{bmatrix} \qquad (4.16)$$

The numbering of the muscles, 25 to 37 corresponds to that given in table 4.1.

4.3.5 Muscle Forces and Optimization

Having explained the methods used to determine intersegmental joint moments and muscle moment arms in sections 4.2.3 and 4.3.4, it is the aim of this section to describe how this information was used in the calculation of muscle forces. The technique used is that of optimization as introduced in section 3.3.2. The optimization technique assumes that the human body performs activities in such a way as to optimize certain criteria whilst satisfying imposed constraints.

The optimization procedure used in the current study is a double linear optimization. The Simplex algorithm as described by Press et al (1989) was used and details of the solution procedure can be obtained from this reference. In the first optimization the maximum muscle stress was minimized subject to constraints defined later in this section. In the second optimization, the maximum muscle stress was constrained to be less than that produced in the first optimization and total muscle force was minimized. Again, additional constraints were imposed as detailed later in this section.

The solution from the first optimization may or may not be unique. That is, there may

or may not be more than one possible combination of muscle forces which satisfy the constraints and produce the same maximum muscle stress. If the solution is unique then the solution to the second optimization procedure will be the same as that to the first. If not, then the second optimization chooses the solution from the first which results in minimum total muscle force.

Objective functions for optimization are usually written as a function of the variables. The variables in the first optimization included maximum muscle stress, σ, and 37 unknown muscle forces, $F_{MUS\ 1}$ - $F_{MUS\ 37}$. The objective function for the first optimization could then be written mathematically as follows:

$$\textbf{Minimize} \qquad 0*F_{MUS\ 1} + 0*F_{MUS\ 2} + \ldots + 0*F_{MUS\ 37} + 1*\sigma \qquad (4.17)$$

Constraint equations for each muscle incorporating muscle force, physiological cross sectional area, PCSA and σ were set up as follows:

$$\textbf{Muscle 1} \qquad 0 \le -1*F_{MUS\ 1} - 0*F_{MUS\ 2} - \ldots - 0*F_{MUS\ 37} + PCSA_1*\sigma \qquad (4.18a)$$

$$\textbf{Muscle 2} \qquad 0 \le -0*F_{MUS\ 1} - 1*F_{MUS\ 2} - \ldots - 0*F_{MUS\ 37} + PCSA_2*\sigma \qquad (4.18b)$$

$$\vdots$$

$$\textbf{Muscle 37} \qquad 0 \le -0*F_{MUS\ 1} - 0*F_{MUS\ 2} - \ldots - 1*F_{MUS\ 37} + PCSA_{37}*\sigma \qquad (4.18c)$$

Constraint equations were also imposed such that moments due to external loading were balanced by those due to muscle forces in 3D at the hip joint and in the sagittal plane at the knee joint. Constraint equations were thus set up as follows using values for $Mx_{HC\text{-}F}$, $My_{HC\text{-}F}$, $Mz_{HC\text{-}F}$ and $Mz_{KC\text{-}F}$ as described in section 4.2.3 and values for n and o as described in section 4.3.4.

$$0 = Mx_{HC\text{-}F} + n_{1,1}*F_{MUS\ 1} + n_{1,2}*F_{MUS\ 2} + \ldots + n_{1,31}*F_{MUS\ 31} + 0*\sigma \qquad (4.19a)$$

$$0 = My_{HC\text{-}F} + n_{2,1}*F_{MUS\ 1} + n_{2,2}*F_{MUS\ 2} + \ldots + n_{2,31}*F_{MUS\ 31} + 0*\sigma \qquad (4.19b)$$

$$0 = Mz_{HC\text{-}F} + n_{3,1}*F_{MUS\ 1} + n_{3,2}*F_{MUS\ 2} + \ldots + n_{3,31}*F_{MUS\ 31} + 0*\sigma \qquad (4.19c)$$

$$0 = Mz_{KC\text{-}S} + o_{25}*F_{MUS\ 25} + o_{26}*F_{MUS\ 26} + \ldots + o_{37}*F_{MUS\ 37} + 0*\sigma \qquad (4.19d)$$

Moment constraint equations were not included for the ankle but its effect was included via the action of gastrocnemius. The forces in the two heads of gastrocnemius were constrained to be zero if the external moment tended to plantarflex the ankle but were allowed as variables if there was a tendency to dorsiflex.

In the second optimization, maximum muscle stress, σ was set up as a constant value equal to that derived in the first optimization. It was not therefore an optimization variable. To maintain the number of variables constant in both optimizations, a redundant variable OV_{38} was introduced. The objective function for the second optimization was then written

in terms of the variables as:

$$\textbf{Minimize} \qquad 1*F_{MUS\ 1} + 1*F_{MUS\ 2} + \ldots + 1*F_{MUS\ 37} + 0*OV_{38} \qquad (4.20)$$

The stress in each muscle was constrained to be less than the maximum stress, σ, by imposing a constraint equation for each muscle as follows:

$$\textbf{Muscle 1} \quad 0 \le PCSA_1*\sigma - 1*F_{MUS\ 1} - 0*F_{MUS\ 2} - \ldots - 0*F_{MUS\ 37} - 0*OV_{38} \qquad (4.21a)$$

$$\textbf{Muscle 2} \quad 0 \le PCSA_2*\sigma - 0*F_{MUS\ 1} - 1*F_{MUS\ 2} - \ldots - 0*F_{MUS\ 37} - 0*OV_{38} \qquad (4.21b)$$

$$\vdots$$

$$\textbf{Muscle 37} \quad 0 \le PCSA_{37}*\sigma - 0*F_{MUS\ 1} - 0*F_{MUS\ 2} - \ldots - 1*F_{MUS\ 37} - 0*OV_{38} \qquad (4.21c)$$

Additional constraints identical to those in the first optimization procedure were imposed for the action of gastrocnemius. Replacing σ by OV_{38} in equations 4.19a-d gave the moment constraint equations for the second optimization.

The values of physiological cross sectional area, PCSA, used in the optimization procedures were obtained from Friederich and Brand (1990). Two sets of data were available. The first was measured on the cadaver of a 37 year old male and the second on that of a 63 year old female. The data taken from the 63 year old female were used in the optimization procedures as her age was more closely matched to that of the subjects involved in the current study. The data are presented in appendix B. However, data for quadratus femoris were not presented for the female cadaver. An estimate for the PCSA for this muscle was therefore made based on the values available for the other muscles in the female cadaver and on the value for quadratus femoris relative to that of the other muscles in the male cadaver.

4.3.6 Joint Force Calculation

The final stage of the calculations involved combining the contact forces, gravitational forces and forces in the muscles crossing the hip joint in order to calculate the three components of hip joint force. The forces were firstly converted into a common coordinate system. That chosen for the expression of hip joint forces was the femoral coordinate system.

The contact and gravitational forces were originally determined in the laboratory coordinate system and were converted into the femoral system as follows:

$$(Fx, Fy, Fz)_{PPO-F} = (Fx, Fy, Fz)_{PPO-LAB} * [B]_{F-LAB} \qquad (4.22a)$$

$$(Fx, Fx, Fy)_{F-F} = (0, -m_F*g, 0) * [B]_{F-LAB} \qquad (4.22b)$$

$$(Fx, Fy, Fz)_{SF-F} = (0, -m_{SF}*g, 0) * [B]_{F-LAB} \qquad (4.22c)$$

Each muscle force calculated in section 4.3.5 was that along the line of action of the muscle. The line of action was described relative to the femoral coordinate system by the unit vector of the muscle, $(I, J, K)_{MUS-F}$ given by equation 4.13 in section 4.3.4. The components of muscle force in the femoral coordinate directions were then given by

$$(Fx, Fy, Fz)_{MUS-F} = F_{MUS} * (I, J, K)_{MUS-F} \qquad (4.23)$$

The same calculation was performed for all 31 muscles crossing the hip joint. Components of hip joint force acting on the femoral head were then obtained in terms of the femoral coordinate system from the following:

$$Fx_{H-F} = -1 * [\sum_{i=1}^{31} Fx_{MUS\,i-F} + Fx_{HPO-F} + Fx_{F-F} + Fx_{SF-F}] \qquad (4.24a)$$

$$Fy_{H-F} = -1 * [\sum_{i=1}^{31} Fy_{MUS\,i-F} + Fy_{HPO-F} + Fy_{F-F} + Fy_{SF-F}] \qquad (4.24b)$$

$$Fz_{H-F} = -1 * [\sum_{i=1}^{31} Fz_{MUS\,i-F} + Fz_{HPO-F} + Fz_{F-F} + Fz_{SF-F}] \qquad (4.24c)$$

CHAPTER 5. LABORATORY SUBJECT TESTS AND DATA PROCESSING

Having described the model developed in order to calculate hip joint forces in chapter 4, this chapter is concerned with the acquisition of data for input into the model and use of the model in obtaining hip joint forces. The original objective of the project was to determine the forces at the hip joint in post-operative hip replacement patients and age-matched non-arthritic subjects. Hence this chapter will describe the criteria on which subjects were selected and then the tests performed, equipment used and data analysis carried out.

5.1 SUBJECT SELECTION

5.1.1 Patients

Sixteen patients were selected for the study including 7 males and 9 females. Their mean age was 71 years with a standard deviation, S.D. of ±6.5 years. The youngest patient was 58 and the oldest, 80. One patient had rheumatoid arthritis whilst all of the others had undergone hip surgery due to osteoarthritis. Ten patients had received Howse prostheses and six, Charnley prostheses. The patients were selected on the following criteria:

- They could be tested between approximately one and two years after their operation. It was assumed that by this time the subjects were completely recovered from the operation and their activity had reached a stable level (Rowe, 1990).
- They had very few or preferably no other musculoskeletal problems or joint replacements in addition to their hip prosthesis.
- They were not obese. Results from subjects with a high amount of soft tissue over the underlying bony points would not be reliable. They would be subject to errors due to difficulties in locating bony landmarks by palpation, difficulties in estimating the soft tissue thickness and also marker wobble.
- They were capable of performing at least the walking tests and were happy to come into the laboratory and take part in the study.

The process of patient selection involved studying the patients' hospital notes with the orthopaedic surgeon to select potential subjects. If the patient was willing to partake in the study, a visit was made to their home to give more details of what would be involved in the study and a questionnaire as shown in appendix D.1 was completed. This was designed to give an insight into the usual level of activity of the patient. It also encouraged the patients

to think about the way in which they normally performed the activities under study when in their usual home environment. It was decided to do this as although the test rigs constructed in the laboratory for these activities were as realistic as possible, it was helpful for the subjects to think about how they normally performed a manoeuvre in their natural environment before coming into the slightly artificial laboratory situation.

5.1.2 Normals

Ten non-arthritic subjects took part in the study and they will be referred to as 'normals' or 'normal subjects'. The mean age of these subjects was 63.3 years (S.D.±3.3). The youngest was 58 and the oldest, 68. The subject group included 4 males and 6 females. The criteria used for the selection of normal subjects were that they should be of a similar age to that of the patients and have no or very minor musculoskeletal problems. Normal subjects who were obese were avoided for the same reasons as given in the patient selection criteria.

The normal subjects were asked to complete a slightly different questionnaire to that of the patients and this is shown in appendix D.2. This includes questions regarding the normal level of activity of the subject and also the methods by which the subject normally performed the manoeuvres.

5.2 TESTS PERFORMED

Each subject visited the laboratory for one day of testing. As has already been described in sections 4.1.1 and 4.2.1, a Vicon motion analysis system and Kistler force platforms were used to obtain kinetic and kinematic data. In order that the marker set described in section 4.1.2 would be visible, the females were asked to wear shorts and a T shirt. The males wore shorts or swimming trunks and a T shirt. All subjects wore their own shoes.

The subjects were welcomed and made comfortable. Markers were then placed on the subject at sites given in figure 4.1 and a static test was performed. The anatomical markers were then removed, leaving only the technical ones and activity tests were carried out. At the start of each activity test, the subject performed a few practice runs to relax and perform the activity as naturally as possible. Data were then recorded for five runs of each activity with a view to producing three trials with complete data sets. However, if the subject was tiring then this number was reduced. All activities were performed at a natural speed selected by the subject. The activity tests carried out are described in the sections 5.2.1 to 5.2.6. Figures 5.1 to 5.5 presented at the end of this chapter illustrate the activities. The subject in the figures is a young male and hence not one of the subjects included in the

Measurement taken	Method of measurement
Height	Height scale
Weight	Clinical beam balance
Distance between fibula head and medial tibial condyle	Palpation and callipers
Distance between tibial condyles	Palpation and callipers
Vertical distance between tibial plateau and tibial tuberosity	Palpation and measurement tape
Distance between medial and lateral malleoli	Palpation and callipers
Distance between femoral epicondyles	Palpation and measurement tape
Distance between right and left anterior superior iliac spines (inter ASIS distance)	Palpation and callipers
Distance between right and left greater trochanters with the subject standing in the anatomical position	Palpation and callipers
Vertical distance between the iliac crest and ischial tuberosity	Palpation and callipers
Distance between the frontal plane of the pelvis and the midpoint between the posterior superior iliac spines (midPSIS)	Palpation and measurement chair described in section 4.3.2
Soft tissue thickness over the RASIS, LASIS, midPSIS, femoral epicondyles and tibial condyles	Palpation and callipers

Table 5.1 Anthropometric measurements

current study. The pelvic marker set up shown on this subject is also different to that used in the current study.

Anthropometric measurements were also taken as shown in table 5.1. The majority of these were for use in setting up the shank coordinate system and determining the scaling factors used in the mathematical model.

5.2.1 Level walking

Each subject walked in a straight line at their preferred speed and data were recorded for both right and left sides. The period analyzed was the stance phase.

5.2.2 Walking turn

Each subject walked in a straight line for approximately 6 steps and then made a sharp turn of approximately 90° and continued walking in the new direction. Figure 5.1 illustrates this activity. Both right and left sides were analyzed. In general the subjects performed a right turn by propulsion from the left foot and a left turn by propulsion from the right foot. In these cases, the left side was analyzed on turning right and the right side on turning left. However, it was observed that one subject turned right by twisting on the right foot and left by twisting on the left foot. In this case, the right side was analyzed on turning right and the left side on turning left. The period analyzed was the stance phase.

5.2.3 Rising from a chair

Data were collected for both the right and left sides as the subject stood up from and then sat down onto a purpose built chair with a seat height of 440mm. This height is within the range of heights of most kitchen and dining room chairs. Figure 5.2 illustrates how the chair was placed over the force platforms so that each side was tested simultaneously as the subject performed the manoeuvre. The subjects were asked to rest their hands on the edge of the seat as they performed the activity and to take as much weight through their arms as they required. A pressure pad switch was used to indicate the time at which the subject lost and then made contact with the seat. The period analyzed was that between the instant when the subject lost contact with the seat and that when the subject made contact with the seat again.

5.2.4 Stair negotiation

A purpose built 4 step staircase with an instrumented second step was used for stair negotiation tests. This is shown in figure 5.3. The right or left half of the second step could be instrumented as required. This was achieved by bolting an insert onto the force platform to form the required half of the second step and then assembling the rest of the staircase around this step. The riser height was 180mm and the tread depth, 280mm. A handrail of

height 900mm was fitted to each side of the staircase. The dimensions of the steps and handrails are in accordance with those found in the Scottish and English and Welsh building regulations and from measurements of several staircases, it was found that these represent a common situation.

Both right and left sides were tested during ascent and descent, the time period of interest being that when the foot was in contact with the instrumented step. The subjects were asked to rest their hands on the rails as they went up and down the stairs, taking as much weight through their arms as required. In general the subjects climbed and descended cyclically but one subject was more comfortable taking one step at a time.

5.2.5 Car tests

A mock car assembly representing the passenger side of a right hand drive car was used for car tests as shown in figure 5.4. In general 4 car tests were performed. The abbreviations used for these and descriptions of each are as follows:

con: Car entry. The outside hip (i.e the left hip) was tested as the subject entered the car.

cox: Car exit. The outside hip (i.e the left hip) was tested as the subject exited from the car.

cin: Car entry. The inside hip (i.e. the right hip) was tested as the subject entered the car.

cix: Car exit. The inside hip (i.e the right hip) was tested as the subject exited from the car.

In order to test the inside hip (i.e. the right hip), the car floor was instrumented by bolting an insert to the force platform and then arranging the rest of the car assembly around this insert. The insert was made flush with the surrounding car floor so that the floor appeared as normal as possible to the subject. When testing the outside hip (i.e. the left hip) this insert was removed and the car floor constructed as one solid piece. The assembly was then arranged so that a force platform outside the car assembly could be used to test the left hip.

A pressure pad switch was used to indicate whether or not the subject was in contact with the seat. The time period of interest during entry tests started when the subject's foot made contact with the relevant force platform or insert and finished when the subject made contact with the seat. On exit it started when the subject lost contact with the seat and finished when the relevant foot left the force platform or insert. Some subjects swung both

legs out onto the ground before standing up. If this was the case then the hip could not be tested on exit as the subject remained seated throughout the entire period when the right foot was in contact with the insert.

5.2.6 Bath tests

Bath tests were performed using a mock bath assembly as shown in figure 5.5. For the safety of the test subjects a bath stool was used inside the bath in all bath tests. The height of the bath stool was 145mm. In general 4 bath tests were performed The abbreviations used for these and descriptions for each are as follows:

bon: Bath entry. The outside hip (i.e. that corresponding to the last foot to leave the ground) was tested as the subject entered the bath.

box: Bath exit. The outside hip (i.e. that corresponding to the first foot to make contact with the ground) was tested as the subject exited from the bath.

bin: Bath entry. The inside hip (i.e. that corresponding to the first foot to make contact with the bath floor) was tested as the subject entered the bath.

bix: Bath exit. The inside hip (i.e. that corresponding to the last foot to leave the bath floor) was tested as the subject exited from the bath.

In order to test the inside hip, part of the bath floor was instrumented by bolting an insert onto the force platform and then arranging the rest of the bath assembly around it. The insert was made flush with the rest of the bath floor so that the floor did not appear irregular to the subject. On testing the outside hip, the insert was removed and the bath floor constructed as one solid piece. The assembly was arranged so that a force platform outside the bath could be used to test the outside hip.

The subjects got into and out of the bath from the side normally used at home. If they were able to and felt comfortable sitting down after getting into the bath then they did so. However, some usually only got into the bath to use the shower and did not normally sit down. The test periods of these subjects therefore only included getting in and out and not sitting down and standing up. The time periods of interest also varied as follows according to the style of the manoeuvre:

- **bin**: The time period of interest always started when the inside foot made contact with the insert over the force platform. If the subject sat down, then the period ended when the subject made contact with the seat as indicated by the pressure pad switch. If the subject remained standing, then the period ended when the outside foot

made contact with the bath floor.

- **bix**: If the subject sat down in the bath then the time period of interest started when the subject lost contact with the seat as indicated by the pressure pad switch. If the subject started from a standing position then the period started when the outside foot left the bath floor. The period always ended when the inside foot lost contact with the insert over the force platform.
- **bon**: Some subjects stepped towards the bath onto the outside foot and then lifted the inside foot into the bath, followed by the outside foot. In these cases, the time period of interest began when the outside foot hit the force platform and ended when it left the force platform. Others stepped towards the bath onto the outside foot and then brought the inside foot to be beside it. They then lifted the inside foot into the bath followed by the outside foot. In these cases, the period did not include the initial step forward but was started when the inside foot left the ground and ended when the outside foot left the force platform.
- **box**: Some subjects brought the outside foot out of the bath followed by the inside foot and remained standing beside the bath. The time period of interest was then that between the instant when the outside foot contacted the force platform and that when the inside foot contacted the floor outside the bath. As others got out they brought the outside foot out and then brought the inside foot out to such a position that it was natural to immediately follow this by a step with the outside foot. If this was the case then the time period of interest included this step with the outside foot. It started when the outside foot contacted the force platform and ended when the outside foot left the force platform.

Not all of the subjects were capable of performing all of the activities but each subject performed as many activities as their fitness allowed. The use of force platforms in the methodology also restricted the amount of testing possible. It was important that only the foot corresponding to the hip under test contacted the force platform during an activity. This requirement made the testing of some subjects during some of the activities impossible. For example, during the walking turn, the subjects' feet were sometimes so close together that they both touched the force platform simultaneously. In such cases tests were aborted as it would be impossible to acquire useful data whilst the subject performed the activity naturally. The bath and car assemblies were designed to provide as much adjustment in position relative to the force platform as possible in order to allow for a range of styles of activity performance. Data were only collected if it was possible to set up the assemblies so that

only the foot corresponding to the hip under test contacted the force platform whilst the subject performed the activity naturally. Sometimes this was not possible and tests were aborted.

5.3 DATA PROCESSING

The Vicon motion analysis system data and force platform data collected in the laboratory tests were processed in order to determine joint angles, joint moments, muscle forces and joint forces.

The Vicon system was operated at a frequency of 50Hz. Marker movement was thereby represented as a series of 50 static positions in each second. Each of these was referred to as a 'frame'. As long as a marker was viewed by two or more cameras in a frame then its position was set up as a discrete point. The points produced were manually identified as the marker locations listed in figure 4.1. If a marker could not be seen by at least two cameras due to obscuring by arm movement for example, then there was a gap in the output for that marker. Interpolation could be performed over gaps which were of a short time duration or in which there was only a small amount of movement of the missed marker. However, the trial had to be rejected if the gap was of a long time duration or movement of the missed marker was too great. In most cases, five trials of each activity were recorded in each subject. The three trials with the most complete marker data were chosen as the best ones for further analysis. Occasionally it was not possible to obtain three good trials and only one or two were acceptable. The identified Vicon data were further processed to give 3D positional data for each marker. These were then filtered using a 10Hz non-recursive low pass filter as described by Stewart (1995).

The force platform data, 3D marker positional data and anthropometric measurements were then the inputs to a computer program set up using methodology described in chapter 4 to calculate joint angles, joint moments, muscle forces and joint forces for each trial. The program was written in Turbo Pascal and run on a PC. The compiled version is presented on a floppy disk inside the back cover of this thesis. Details of how to run the program are given in appendix A.1.

The output values were normalized using a Lagrangian interpolation approach to make the time periods of interest in each activity 100%. Details of the normalization procedure are presented in appendix A.2. The compiled version of the program written in Turbo Pascal to perform the normalization is also presented on the floppy disk inside the back cover of this thesis and details of how to run it are given in appendix A.1.

Averaged outputs of joint angles, joint moments, muscle and joint forces were obtained for each activity in each subject from the three normalized trials. As stated previously, sometimes only two trials were acceptable and hence the outputs were then the average of these two.

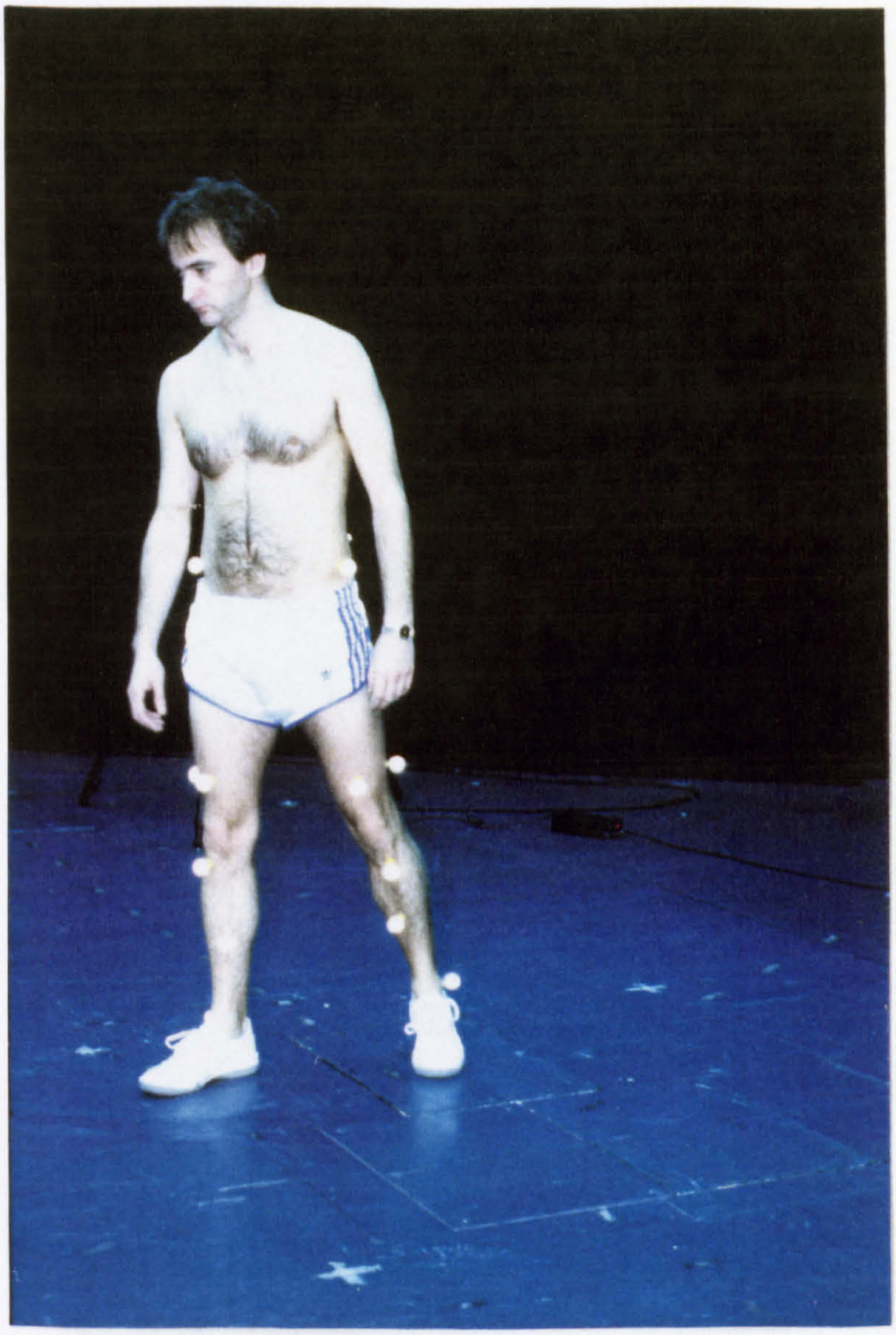

Figure 5.1 The Walking Turn

Figure 5.2 Rising from a chair

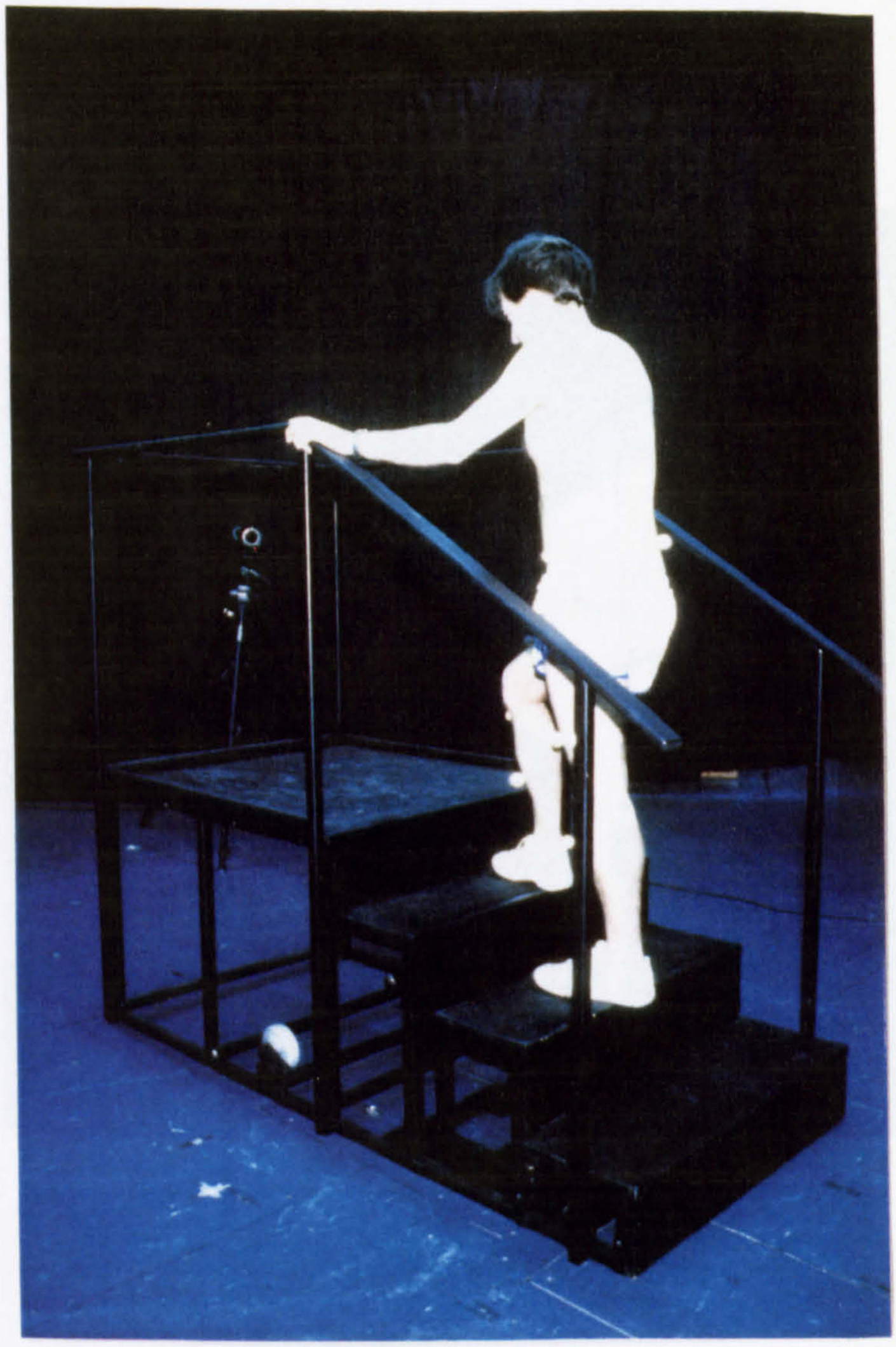

Figure 5.3 Stair Negotiation

Figure 5.4 The Car Test

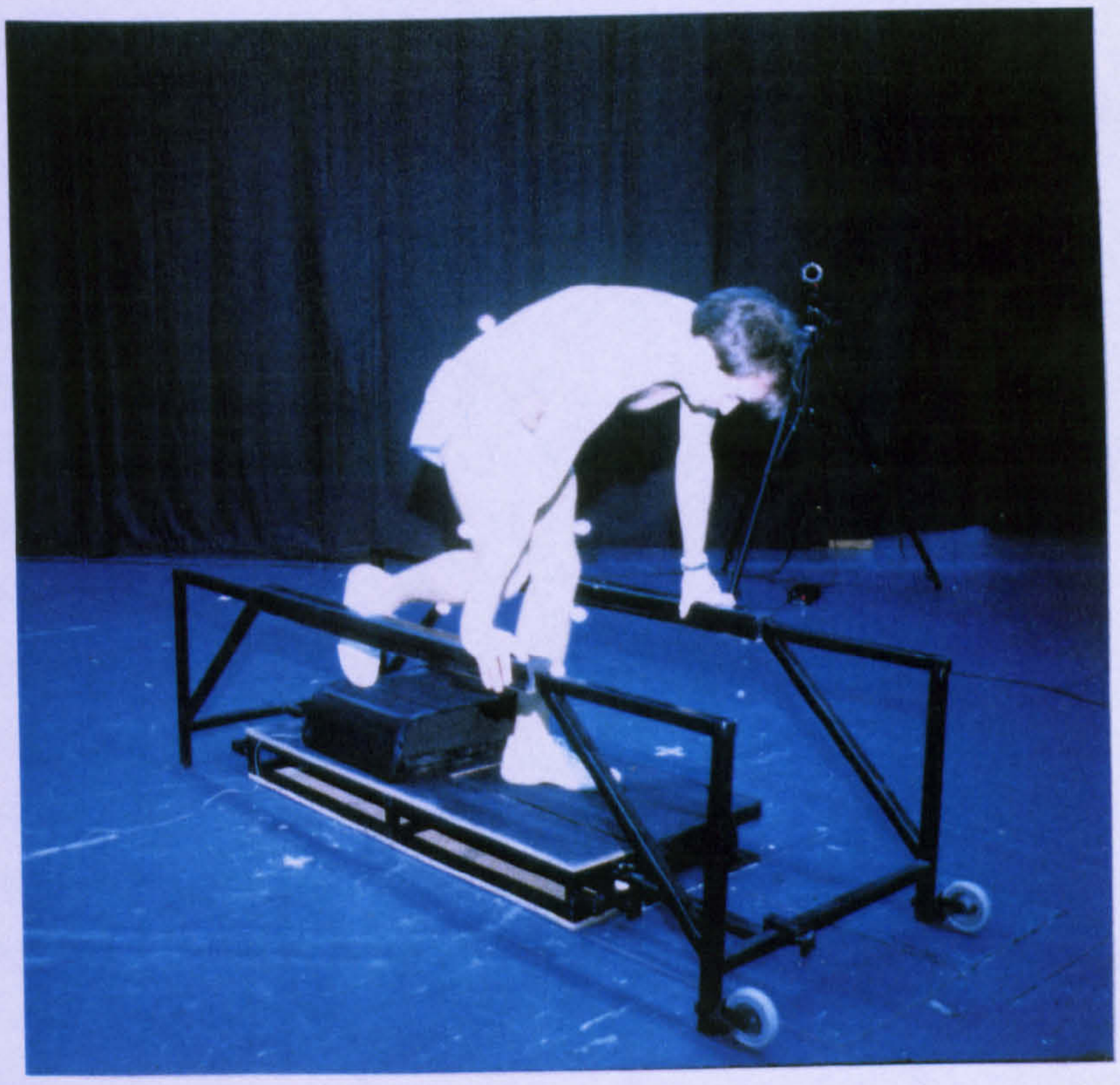

Figure 5.5 The Bath Test

CHAPTER 6. INTERMEDIATE RESULTS AND DISCUSSION

As described in chapter 4, the methodology used to calculate hip joint forces involved intermediate stages of joint moment, joint angle and muscle force calculation. It was considered important in developing the model to assess the results of these intermediate stages before using the results in the determination of hip joint forces. Hence the first aim of this chapter is to present and discuss a selection of the results of the intermediate steps prior to presentation of the final values of hip joint force in chapter 7.

The second aim of this chapter is to test the validity of the results. As with any theoretical model used to calculate muscle and joint forces, the model developed in this project includes many theoretical assumptions and it is important to check that it gives valid results.

There are various methods which can be used in validation. Ideally, the predicted muscle force values should be compared with measured muscle forces. However, as it is not currently possible to directly measure muscle forces in live human subjects, alternative approaches must be taken. None of these can ever fully validate the results of a model but may go part way to indicating whether or not the results are feasible.

A comparison of resulting force patterns with EMG results can indicate whether the predicted pattern of activity is realistic. However, this will give no information about the magnitude of the muscle forces. The validity of the magnitudes can be checked by examining the stresses in the muscles to determine whether or not they are physiologically acceptable. Most authors have taken one or both of these approaches in validation (Hardt (1978), Pedotti et al (1978), Crowninshield et al (1978a), Patriarco et al (1981), Crowninshield and Brand (1981)).

An alternative approach to analysing the predicted muscle forces is to analyze the joint forces calculated using these muscle forces. Brand et al (1994) took this approach, comparing the predicted joint forces with those measured in the same patient using a strain gauged hip implant.

The methods used in the current study have already been partially validated since the optimization procedure and objective functions used are the same as those applied by Runciman (1993) in a model of the shoulder joint. Runciman compared his predicted muscle activity patterns with EMG measurements made on the same subjects during 5 activities. He found the predicted muscle activation to be consistent with the muscle activation measured during the EMG study for the 3 activities of flexion, abduction and athletic push-up. Runciman reported discrepancies in some of the predicted results for the press-up and chin-

up activities which were related to limitations of the model. The joint detailed in Runciman's model was the glenohumeral joint but due to the complexity of the stabilisation of the shoulder complex some EMG results were obtained for muscles which crossed more structures than just this joint.

The approach taken to further validate the model developed in the current project is to compare the resulting predicted muscle force patterns with published EMG data and to check that the muscle stresses are within physiologically acceptable limits. In chapter 8, the hip joint forces calculated for the patients are compared with those measured in patients using strain gauged prostheses. The results used for comparison are those of Rydell (1966), Kotzar et al (1991) and Bergmann et al (1993,1995).

The activities included in this chapter are gait, stair negotiation and rising from a chair since published data are widely available for these activities. The other activities (walking turn and car and bath entry/exit) have not to the author's knowledge been studied before and no data are available for comparison. It was assumed that if the model gave valid results for gait, stair negotiation and rising from a chair then it could be applied to these new activities with confidence.

The results for the right limbs of three normal subjects denoted as 'G', 'I' and 'E' are discussed in this chapter. These include one male subject and two females. The male subject, 'G' was of height 1.61m and mass 67kg. One female, 'I' was of height 1.62m and mass 71.5kg and the other, 'E' was of height 1.65m and weight 58kg. Each activity is discussed in detail in sections 6.1 to 6.3. In examining the joint moments, joint angles and muscle forces calculated at the intermediate stages of joint force calculation, it was considered important to assess the results in relation to those reported by other authors. However, conclusions drawn from these assessments have to be made with caution since the different authors have used a variety of methods of calculation and made a range of assumptions. Also, the majority of the work presenting joint moments and angles and muscle forces has been performed on young adults whilst the ages of 'G', 'I' and 'E' were 62, 65 and 58 respectively. It may be expected that younger subjects will perform an activity with more vigour than older ones. Having said this, some older subjects are more active than some younger ones. Hence comparisons are made but there are likely to be some differences in results due to the variation in calculation methods, assumptions made and subjects studied.

(a) Sagittal plane hip joint moment ($Mz_{HC\ -\ F}$). A positive moment indicates an external moment tending to flex the hip joint and hip extensor muscle activity. A negative moment indicates an external moment tending to extend the hip joint and hip flexor muscle activity.

(a)

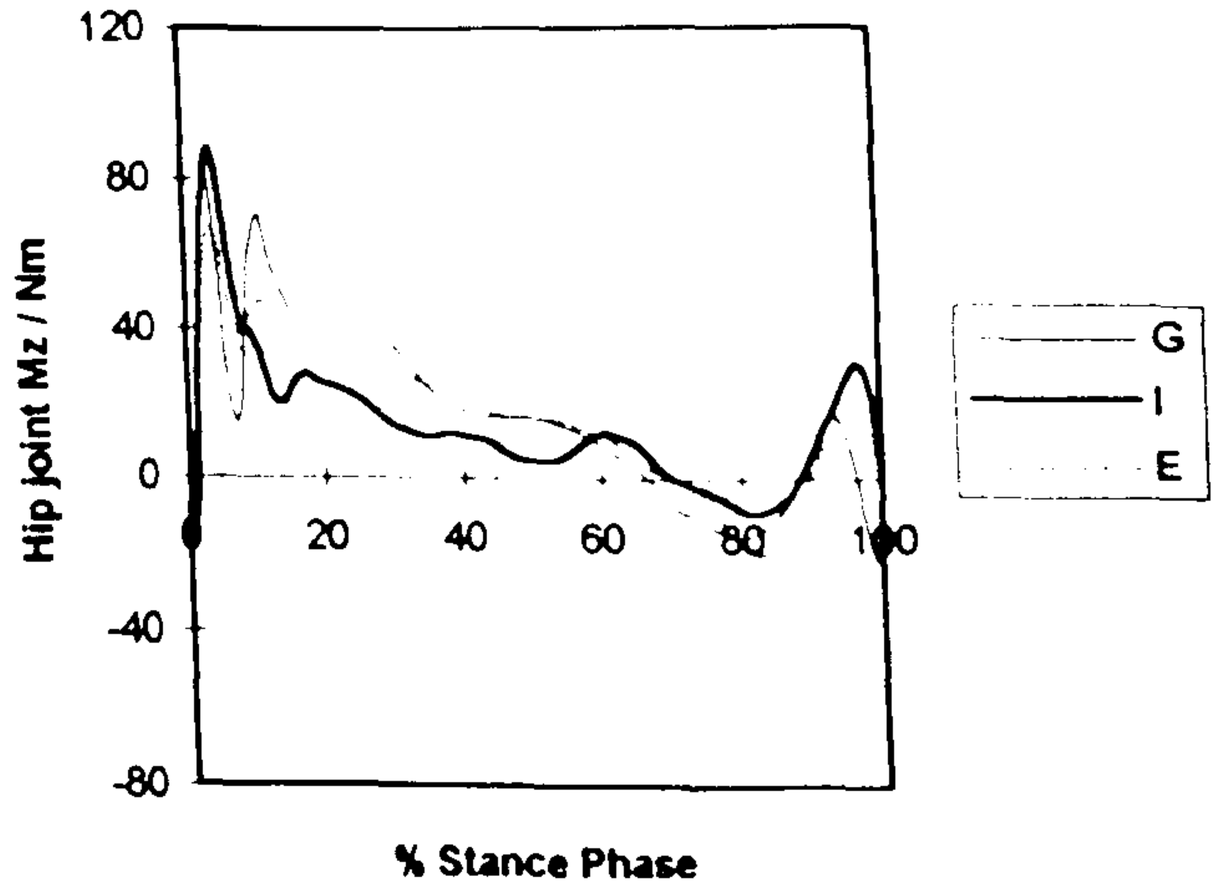

(b) Frontal plane hip joint moment ($Mx_{HC\ -\ F}$). A positive moment indicates an external moment tending to adduct the hip joint and hip abductor muscle activity. A negative moment indicates an external moment tending to abduct the hip joint and hip adductor muscle activity.

(b)

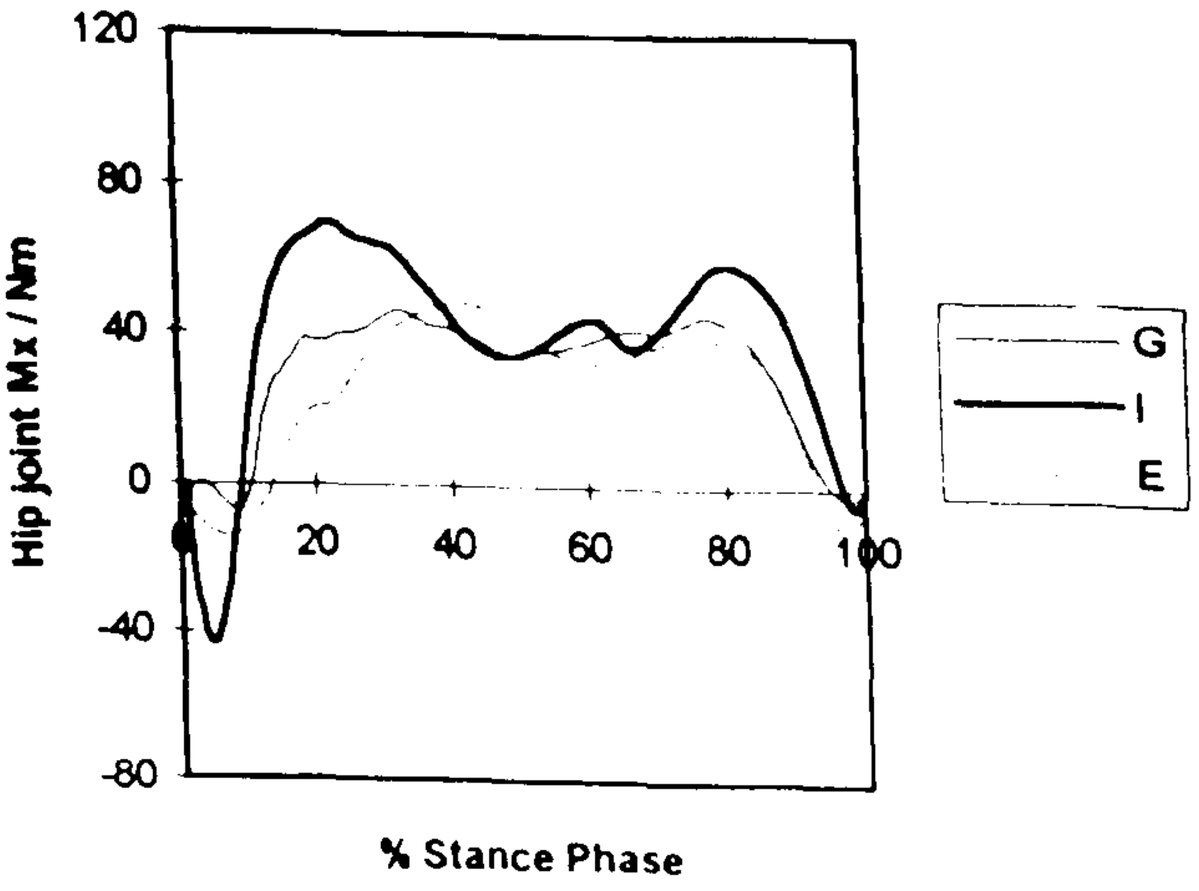

(c) Transverse plane hip joint moment ($My_{HC\ -\ F}$). A positive moment indicates an external moment tending to internally rotate the femur relative to the pelvis and hip external rotator muscle activity. A negative moment indicates an external moment tending to externally rotate the femur relative to the pelvis and hip internal rotator muscle activity.

(c)

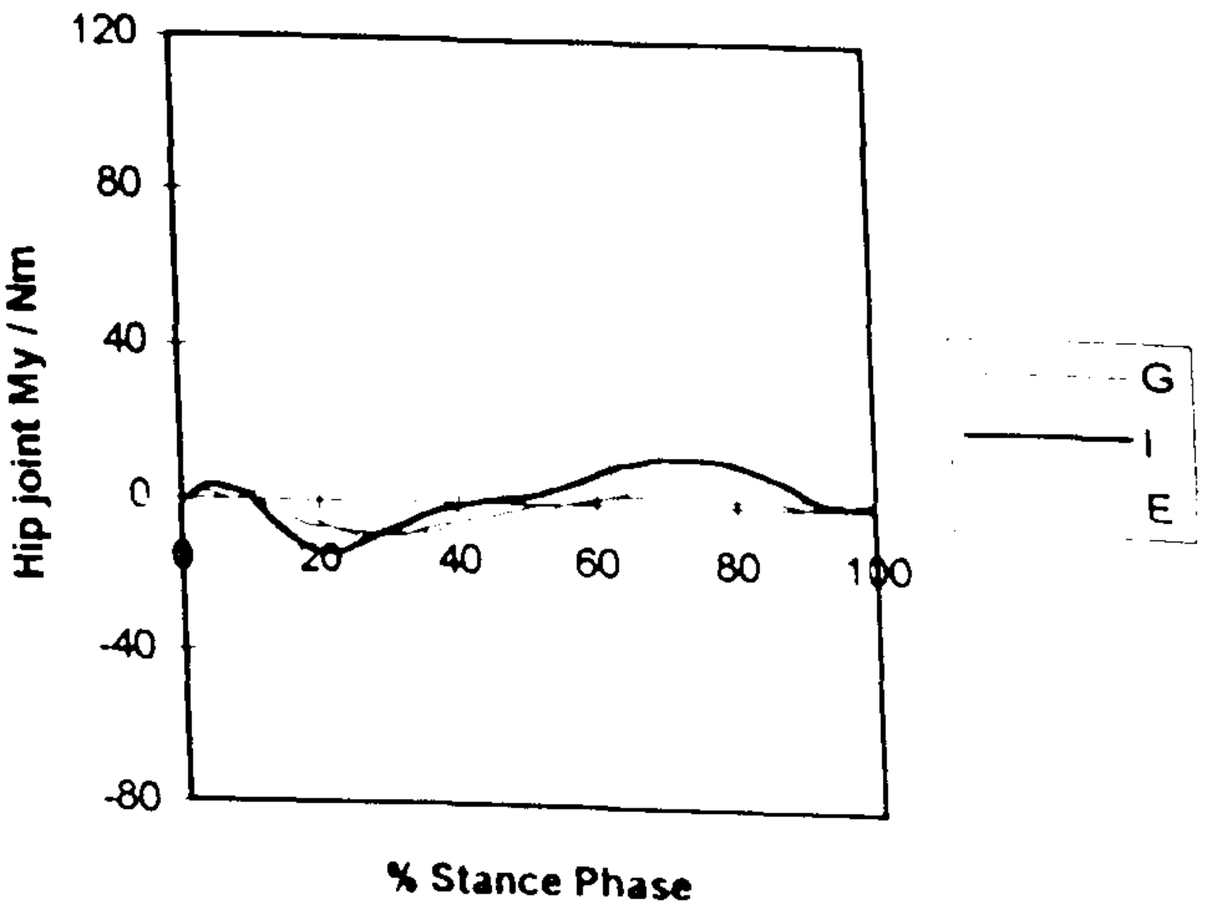

Figure 6.1 Hip joint moments measured in subjects 'G', 'I' and 'E' during the stance phase of gait.

6.1 GAIT

Each subject walked at their natural speed. 'G' walked at 1.14 m/s, 'I' at 1.32 m/s and 'E' at 1.25 m/s. The mean speed of the three subjects was 1.24m/s. The cadence of all three subjects was 111 steps per minute.

6.1.1 Joint Moments

It was considered important to examine the joint moments obtained and assess them in relation to those reported by other authors before proceeding to the stage of muscle force calculation. The works chosen for this assessment are Winter (1984) and Apkarian et al (1989).

Winter (1984) measured moments in the sagittal plane at the hip, knee and ankle joints at low, natural and high cadences. He presented curves of the mean joint moment in terms of body mass throughout the gait cycle with bands of the coefficient of variation (CV). The CV was presented to reflect the variability of the results. It was calculated as the root mean square of the standard deviation of the moment over the stride period divided by the mean of the absolute moment of force over the stride period. Winter studied 16 subjects with a mean natural cadence of 105 steps per minute and a standard deviation, S.D. of ±7.7 steps per minute. The mean age of these subjects was 25.6 years (S.D.±6.2). In order to compare the joint moments calculated for 'G', 'I' and 'E' with those of Winter, they were normalized to body mass giving values in Nm/kg.

Apkarian et al (1989) presented moments at the hip, knee and ankle joints for three subjects aged 21, 26 and 24 with gait speeds of 1.21m/s, 1.18m/s and 1.40m/s.

The values used for comparison from both Winter and Apkarian et al have been obtained by measuring the curves presented by these authors.

Hip joint

Figure 6.1a shows the variation in hip joint moment in the sagittal plane throughout the stance phase. There is an initial blip in the external moment tending to flex the hip joint due to heel strike effects. This moment then takes on a more settled value and hip muscle extensor activity is required throughout this time to resist hip flexion. The moment reduces as the centre of gravity passes over the supporting foot and in late stance the external moment tends to extend. Just prior to toe off there is an additional tendency for the external moment to flex the hip. The ground reaction force vector was therefore tilted to pass in front of the hip joint at this time. This was due to a high horizontal ground reaction force component in comparison to the vertical component as the subjects propelled themselves

Figure 6.2

Sagittal plane knee joint moment ($Mz_{KC\ .\ S}$) measured in subjects 'G', 'I' and 'E' during the stance phase of gait. A positive moment indicates an external moment tending to extend the knee joint and knee flexor muscle activity. A negative moment indicates an external moment tending to flex the knee joint and knee extensor muscle activity.

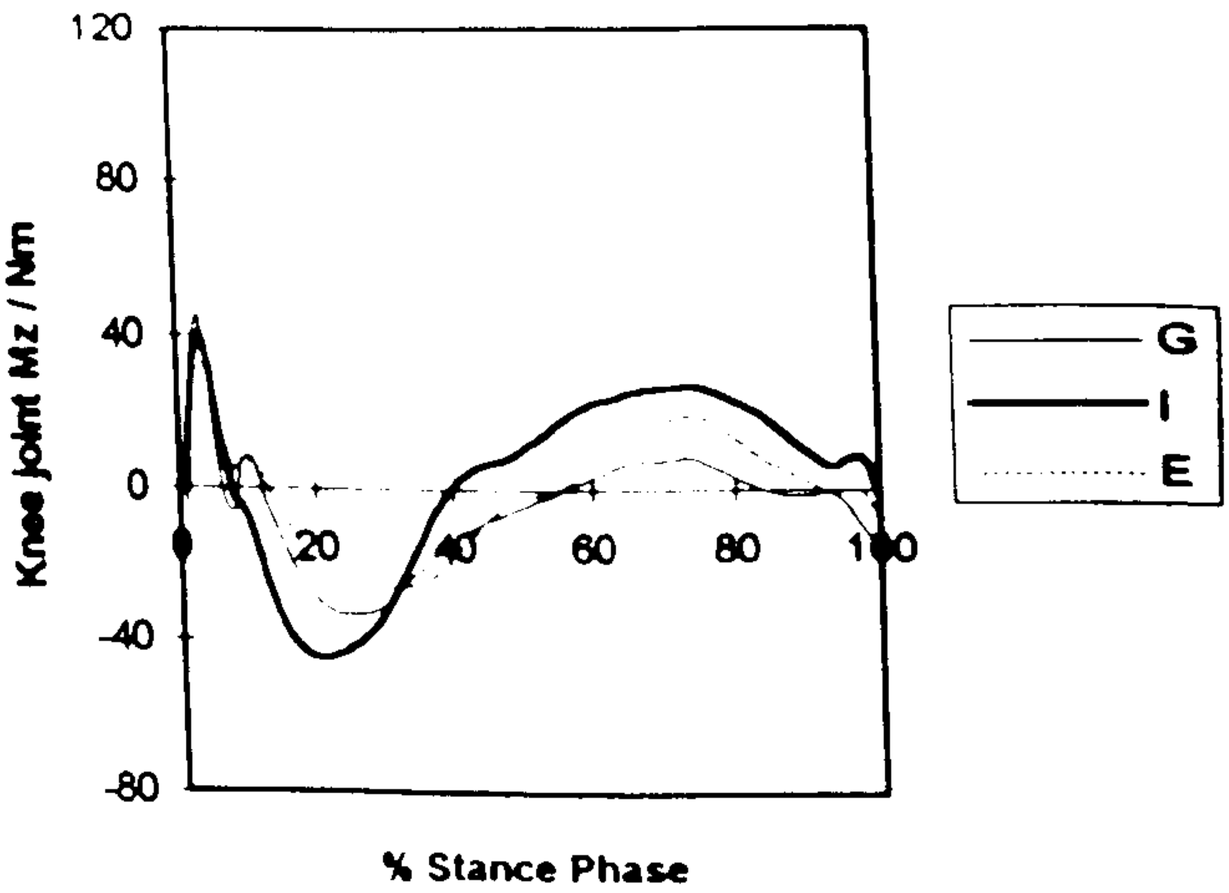

Figure 6.3

Sagittal plane ankle joint moment ($Mz_{AC\ .\ S}$) measured in subjects 'G', 'I' and 'E' during the stance phase of gait. A positive moment indicates an external moment tending to dorsiflex the ankle joint and ankle plantarflexor muscle activity. A negative moment indicates an external moment tending to plantarflex the ankle joint and ankle dorsiflexor muscle activity.

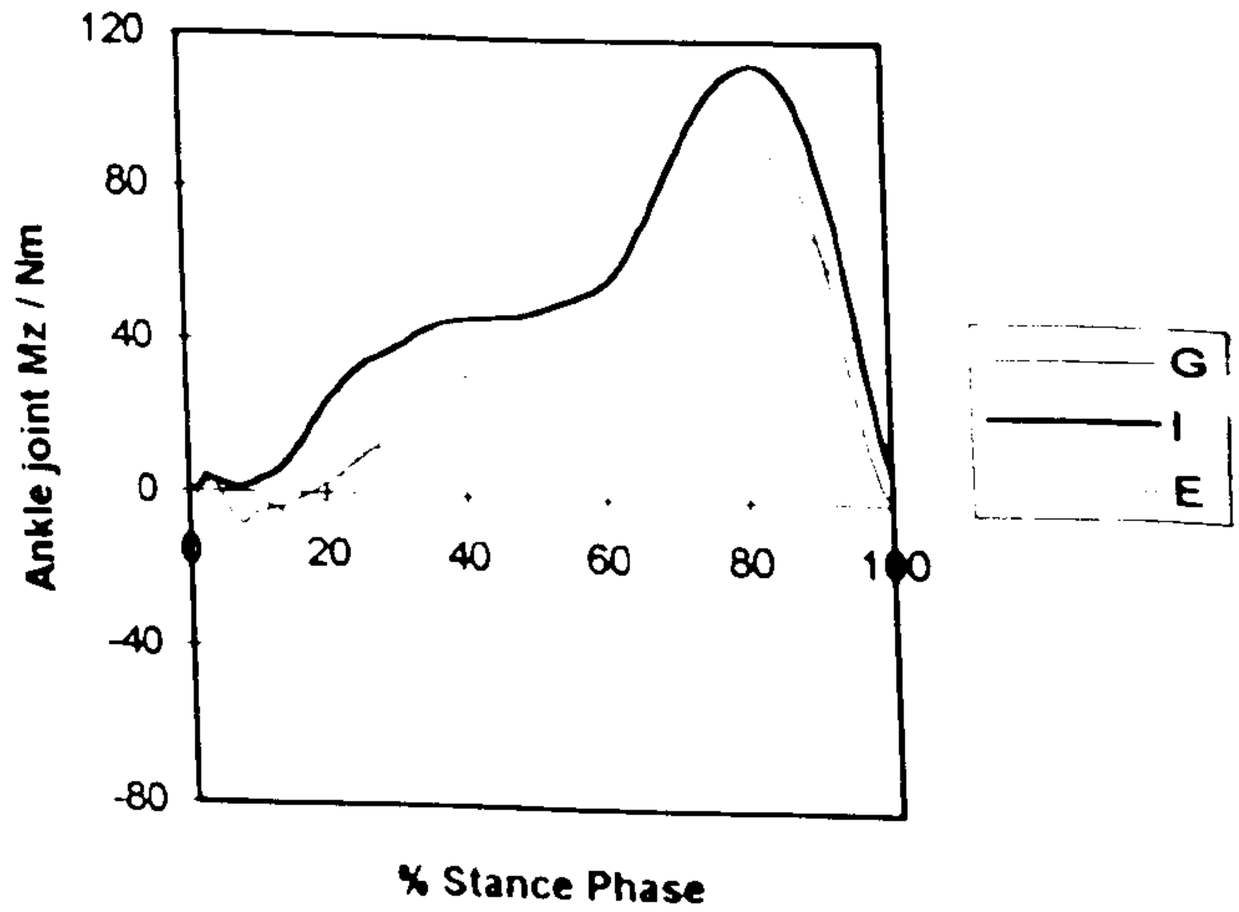

forwards at the very end of stance. Winter also reported sagittal plane hip joint moment curves with an initial external moment tending to flex the hip joint followed by a moment tending to extend the hip joint later in stance. However, they did not report an additional external moment tending to extend just prior to toe off.

In order to compare the values of hip joint moment measured in 'G', 'I', and 'E' with those reported by Winter, they were calculated in terms of body mass. Following heel strike, the mean peak moment tending to flex the hip joint in subjects 'G, 'I' and 'E' was 53Nm which is equivalent to 0.81Nm/kg. This is greater than the mean peak of 0.57Nm/kg presented by Winter but within the range of 0.29-0.95Nm/kg covered by the CV. The mean peak moment tending to extend the hip in subjects 'G', 'I' and 'E' was 15Nm which is equivalent to 0.23Nm/kg. This is less than the mean peak of 0.38Nm/kg reported by Winter but within the range of 0.19-0.76Nm/kg covered by the CV.

In the frontal plane, figure 6.1b illustrates a large hip abductor muscle moment to be active throughout the whole of the stance phase. The opposite limb is off the ground at this time and the pelvis on that side tends to drop due to lack of support. The abductors are therefore active, counteracting the tendency to adduct and preventing the pelvis from dropping. The mean peak value of this moment in subjects 'G', 'I' and 'E' was 54Nm. This lies at the bottom of the range of 54-104Nm presented by Apkarian et al.

As can be seen in figure 6.1c, the component of hip joint moment in the transverse plane is extremely small in comparison to the other two components. The mean peak external moment tending to externally rotate the femur relative to the pelvis in subjects 'G', 'I' and 'E' was 11Nm and that tending to internally rotate was 7Nm.

Knee joint

Figure 6.2 shows the sagittal plane component of knee joint moment. At heel strike there is a momentary tendency to extend the knee joint as the ground reaction force vector passes in front of the knee joint. This is quickly followed by an extensor muscle moment which controls knee flexion and then actively extends the knee up to mid-stance. The moment then becomes a knee flexor muscle moment. Following heel strike, the mean curve of sagittal plane knee joint moment presented by Winter also shows an extensor muscle moment followed by a flexor muscle moment.

The mean peak extensor muscle moment in subjects 'G', 'I' and 'E' was 35Nm which is equivalent to 0.53Nm/kg. Winter presented a mean peak extensor muscle moment of 0.52Nm/kg with a range of 0.10-1.00Nm/kg covered by the CV. The mean peak flexor muscle moment of subjects 'G', 'I' and 'E' was 18Nm which is equivalent to 0.28Nm/kg. Winter presented a mean peak flexor muscle moment of 0.24Nm/kg. The maximum value

(a)

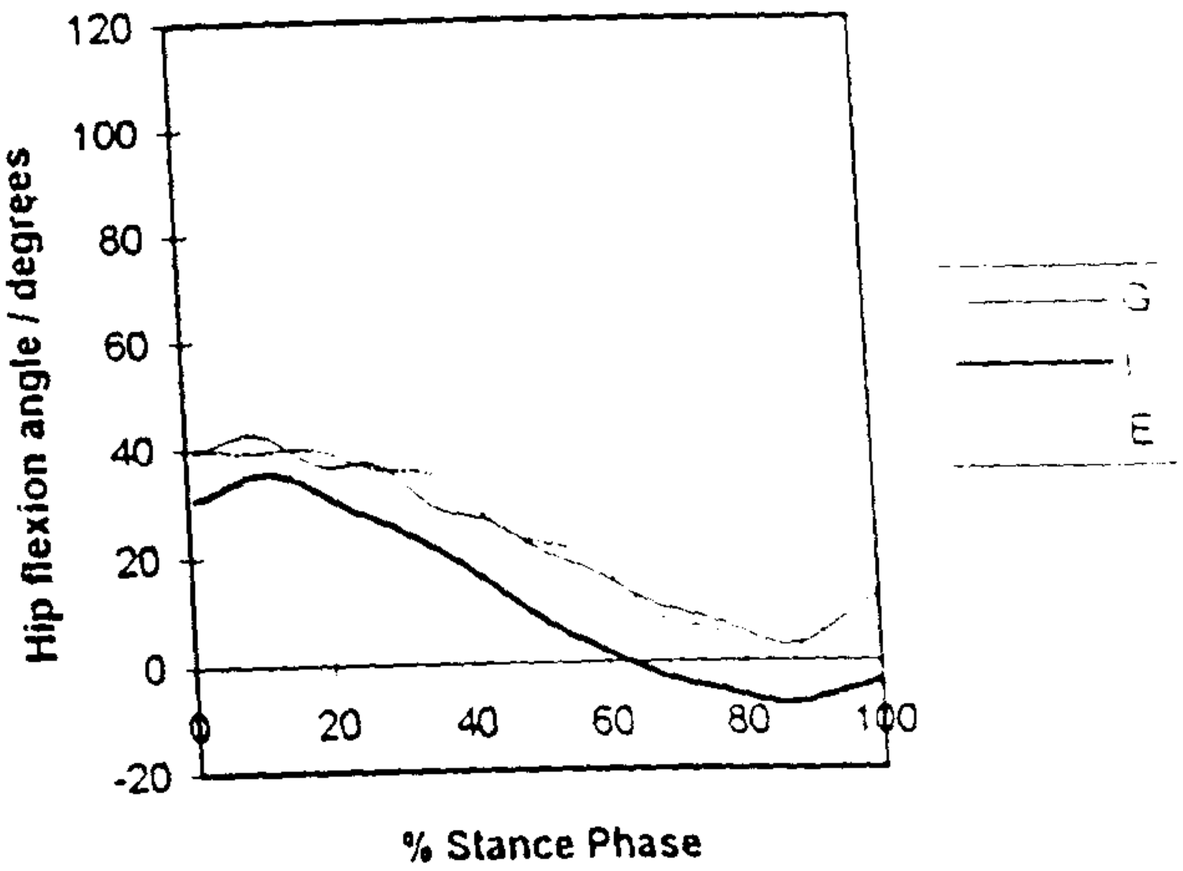

(b)

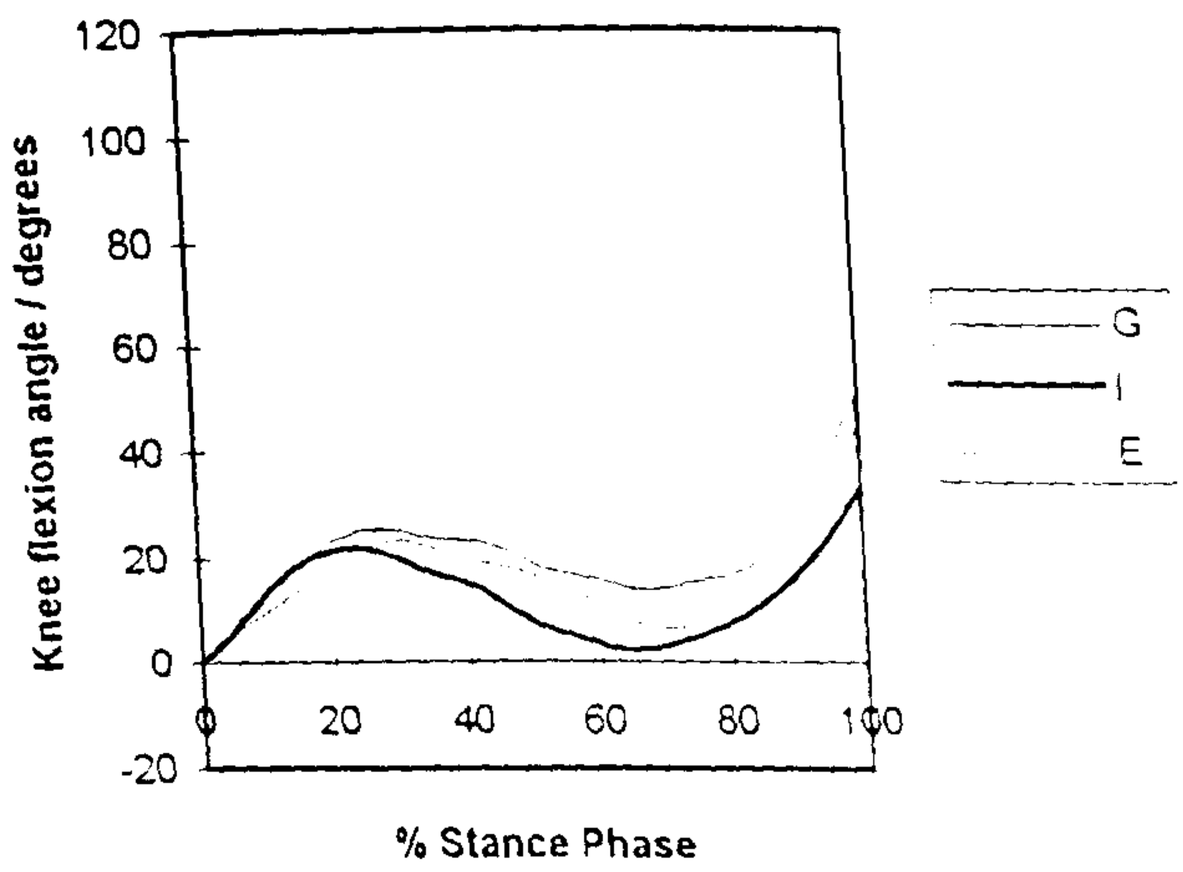

Figure 6.4 (a) Hip flexion and (b) knee flexion angles measured in subjects 'G', 'I' and 'E' during the stance phase of gait.

of knee flexor muscle moment covered by the CV of Winter was 0.62Nm/kg. The minimum value was zero since some of Winters' subjects did not exhibit a knee flexor muscle moment, the knee extensor muscle moment continuing into late stance.

Ankle joint

As can be seen from figure 6.3, the sagittal plane component of ankle joint moment is predominantly a plantarflexor muscle moment. This acts to control forward rotation of the tibia and then builds up significantly to reach a maximum value during push off. In subjects 'G' and 'E' there was also a small initial dorsiflexor muscle moment acting to control the lowering of the foot to the floor after heel strike. The mean sagittal plane ankle joint moment curves of Winter also show a predominantly plantarflexor muscle moment. The mean peak plantarflexor muscle moment of 'G', 'I' and 'E' was 93Nm which is equivalent to 1.42Nm/kg. This is less than the mean peak of 1.66Nm/kg presented by Winter but just within the range of 1.41-1.90Nm/kg covered by the CV.

6.1.2 Joint Angles

As was the case for joint moments, it was considered important to examine the joint angle patterns and values and assess them in relation to those presented by other authors. Kadaba et al (1990) was chosen as the source for comparison. Kadaba et al measured joint angles during gait in 40 subjects with an age range of 18-40 years. Twenty eight males and 12 females were included. The mean cadence of the males was 112 steps per minute (S.D.±9) and the mean speed was 1.34m/s (S.D.±0.32). The mean cadence of the females was 115 steps per minute (S.D.±9) and the mean speed was 1.27m/s (S.D.±0.16). Values used for comparison were measured from the curves of Kadaba et al.

Figure 6.4a shows the hip to be flexed at heel strike. The magnitude of hip flexion then reduces throughout the stance phase as the body moves forward. Subject 'I' exhibits some hip extension in late stance. The mean peak hip flexion angle of subjects 'G', 'I', and 'E' was 39°. That presented by Kadaba et al was 37° (S.D.±3). The mean of the minimum values from the curves of 'G', 'I' and 'E' was -1°. That presented by Kadaba et al was -3° (S.D.±3). Hence the mean hip flexion and extension angles calculated for subjects 'G', 'I' and 'E' fall within the ranges of values covered by the standard deviations of Kadaba et al.

Figure 6.4b shows knee flexion to be zero at heel strike and then increase to a maximum. The knee then extends towards mid-stance and flexes towards toe off in preparation for the swing phase. The mean value of maximum knee flexion in subjects 'G', 'I' and 'E' was 23°. That presented by Kadaba et al was 16° (S.D.±7). Hence the mean value for 'G', 'I' and 'E' is greater than that of Kadaba et al but just within the range covered by the standard deviation. The mean minimum value of knee flexion measured in subjects 'G', 'I'

and 'E' was 8°. That presented by Kadaba et al was 2° (S.D.±4). Hence the mean value for 'G', 'I' and 'E' is just above the range covered by the standard deviation of Kadaba et al. However, it is less than the value of 14° which was measured from the knee joint angle curve presented for one subject by Apkarian et al (1989).

6.1.3 Muscle Activity Patterns

Having determined joint moments and joint angles, the next stage in the calculation was to determine muscle forces. It was important to examine the patterns of muscle activity obtained and compare them to EMG measurements as part of the validation process.

EMG data from the University of California, Berkeley (1953) was chosen for comparison purposes. This study was a comprehensive investigation including 28 muscles in each of 6 subjects. Muscular electrical activity was measured by inserting fine wire electrodes into the muscles and recording the action potentials. Although the study was carried out 42 years ago the methods used were rigorous. Hence this study was considered to be appropriate for use in validation.

The muscle force curves for subjects 'G', 'I' and 'E' are presented with the EMG data reported by the University of California, Berkeley (1953) for the stance phase of gait in figures 6.7a-u at the end of section 6.1. In the following discussion, the patterns of muscle activity predicted in subjects 'G', 'I' and 'E' are initially analyzed alone and then compared with the EMG data.

Predicted muscle activity patterns

The predicted muscle activity shown in figures 6.7a-u follows a pattern which may be expected from the joint moment curves shown in figures 6.1 to 6.3. At heel strike the ground reaction force vector passes in front of both the hip and knee and there is a momentary requirement for hip extensor and knee flexor action. The hamstrings are ideally suited for this purpose as they are both hip extensors and knee flexors and there is activity in semitendinosus, semimembranosus, and the two heads of biceps femoris (fig 6.7a-d). There is some instantaneous activity in gastrocnemius as this acts as a knee flexor (fig 6.7p) and in gluteus maximus as this acts as a hip extensor (fig 6.7g). Adductor magnus is also active at this time (fig 6.7h). With the hip in the flexed position which occurs at heel strike, the line of action of adductor magnus will be such that it acts as a hip extensor.

Following heel strike, hip abductor activity was required throughout the whole of the stance phase. The model predicted gluteus minimus and medius to be active throughout this phase providing a significant component of abduction activity (fig 6.7e,f).

In addition to abduction activity, both hip and knee extensor activity were required in early stance after heel strike. Gluteus maximus was predicted to be most active in early

stance providing a significant amount of hip extensor activity (fig 6.7g). The predicted activity diminished throughout the stance phase as less extensor activity was required. Although it diminished, the activity did continue throughout most of the stance phase, the proximal fibres probably aiding gluteus medius and minimus in providing abductor activity. Adductor magnus was predicted to be active in early stance, acting as a hip extensor with the hip was in such a flexed position (fig 6.7h). Semimembranosus, semitendinosus and the long head of biceps femoris were also predicted to be active in early stance as hip extensors (fig 6.7a-c). These are two joint muscles acting as knee flexors as well as hip extensors. Hence their predicted activity in early stance was antagonistic at the knee as knee extensor activity was required at this time. This knee extensor activity was predicted to be primarily provided by the vasti and also somewhat by rectus femoris (fig 6.7k-n). Rectus femoris is a two joint muscle having flexor action at the hip. Hence its predicted activity at this time was antagonistic at the hip.

Later in stance, hip and knee flexor activity were required in addition to hip abductor activity. Activity was predicted in iliopsoas, providing a significant amount of hip flexor moment (fig 6.7q). Adductor longus was also predicted to be active (fig 6.7i). At this time, the hip flexion angle was either very small as in the cases of subjects 'G' and 'E' or the hip was in extension as in the case of 'I'. The line of action of adductor longus relative to the hip joint would then be such that it was aiding iliopsoas in producing hip flexor activity. Rectus femoris was also predicted to be active in late stance as a hip flexor but its extensor action at the knee joint was then antagonistic as knee flexor activity was required (6.7n). The knee flexor activity was provided by gastrocnemius (6.7p). The hamstrings, principally semimembranosus and the short head of biceps femoris were also predicted to be active, aiding gastrocnemius in providing knee flexor activity (fig 6.7c,d). The action of semimembranosus was antagonistic to the requirements at the hip joint at this time.

Just before toe off the external hip joint moment becomes one tending to flex again requiring hip extensor activity. Semimembranosus, semitendinosus and the long head of biceps femoris show activity at this time, providing the required hip extensor activity (fig 6.7a-c). However, zero moment is required at the knee joint at this time and hence vastus intermedius was active to counteract the effects of the hamstrings at the knee joint (fig 6.7m).

From the description of the predicted muscle activity it can be observed that the model predicted antagonistic activity. For example, in early stance both hip and knee extensor activity were required. Some hamstring activity was predicted providing hip extensor activity but also knee flexor activity which was antagonistic to the requirements at the knee joint at that time. Activity was also predicted in rectus femoris providing knee extensor action but

also hip flexor action which was antagonistic to the requirements at the hip at this time. Antagonistic activity was also predicted in late stance in the hamstrings and in rectus femoris.

Early calculations of muscle and hip joint forces performed by Paul (1967) did not predict antagonistic activity. Paul considered the hip joint alone and combined muscles into functional groups so that it would be possible to distribute the intersegmental moments between the muscles. Poulson (1973) extended the work of Paul, including both the hip and the knee joints in the model and predicted some antagonistic activity. However, the work of Poulson still involved combining the muscles into functional groups. Like Poulson, the current study includes moment balance at both hip and knee joints and predicts antagonistic activity. However, the use of the Simplex optimization procedure eliminates the need to combine muscles into functional groups allowing 37 separate muscle elements to be included. The optimization procedure involves two stages.

In the first optimization procedure the solution of muscle forces is chosen which minimizes the maximum muscle stress. The solution from the first optimization can either be unique or there can be more than one possible combination of muscle forces which produce the same maximum muscle stress. In the second optimization, the maximum muscle stress is constrained to be less than that produced in the first optimization and the solution is chosen which results in minimum total muscle force. Antagonistic activity was predicted in the current study in order to meet these optimization criteria. If the model were a simple one including only one moment equation then the muscles would all be either agonists or antagonists. Antagonistic activity could be set to zero without any loss of optimality since if any antagonistic activity occurred then an agonist would be forced to have a higher stress resulting in a solution with greater maximum muscle stress. However, this was not the case in the current study since four moment equations were included and a muscle working antagonistically in one moment balance may be an agonist in another moment balance.

Comparison of predicted muscle activity with EMG data

Having examined the patterns of muscle activity predicted in the current study it was important to compare these with measured EMG data as part of the validation process. Unless otherwise stated, the EMG data referred to in this section is that measured by the University of California, Berkeley (1953) for gait at normal speed.

As can be seen from figures 6.7a-u, consistency between muscle activity predicted in the current study and that measured in the Berkeley study was displayed in early and late stance. In early stance both hip and knee extensor activity were required. Activity was displayed in both studies in semitendinosus, the long head of biceps femoris, gluteus maximus, the vasti and rectus femoris (fig 6.7a,b,g,k,l,m,n). Adductor magnus activity was

also predicted in subjects 'G', 'I' and 'E' and measured in two subjects in the EMG study (fig 6.7h). In late stance both hip and knee flexor activity were required. Activity was shown in both studies in the short head of biceps femoris, adductor longus, rectus femoris, sartorius, gastrocnemius and iliopsoas (fig 6.7d,i,n,c,p,q) . Throughout the whole of the stance phase hip abductor activity was required and this was supplied in both studies by gluteus minimus and gluteus medius (fig 6.7e,f).

Some differences were observed between the two studies in the activity of semimembranosus, the gluteal muscles and tensor fascia lata (fig 6.7b,e,f,g,t). The activity of the gluteal muscles terminated later in subjects 'G', 'I' and 'E' than in the EMG study and intermittent activity was predicted in semimembranosus in subjects 'G', 'I' and 'E' whilst hardly any activity was shown in the EMG study. Tensor fascia lata was predicted to be active in mid and late stance in subjects 'G', 'I' and 'E' whilst activity was measured in this muscle in mid and early stance in the EMG study. There are two possible reasons for these differences. Firstly, it is possible that the subjects performed gait in such a way that the requirements of these muscles differed between the two studies. Secondly it is possible that the theoretical model does not exactly reflect the action of these muscles. The second explanation is most likely for tensor fascia lata since the model includes the action of this muscle at the hip joint but not at the knee joint.

There were also slight differences between the timing of muscle activity between the two studies at the very start and the very end of the stance phase. At the start of the stance phase the activity in semitendinosus, the long head of biceps femoris, gluteus maximus, adductor magnus, the vasti and rectus femoris started slightly later in subjects 'G', 'I' and 'E' than in the EMG study (fig 6.7a,b,g,h,k,l,m,n). These differences are likely to be due to the model not reflecting the true muscle activity which occurs immediately prior to heel strike in order to balance the inertial loading. At the very end of the stance phase, activity in adductor longus and iliopsoas terminated earlier in subjects 'G', 'I' and 'E' than in the EMG study (fig 6.7i,q). At this time, the external moment measured at the hip joint in subjects 'G', 'I' and 'E' changed from a tendency to extend the hip joint to a tendency to flex as explained in section 6.1.1 resulting in early termination of iliopsoas and adductor longus activity. Although slight differences in the timing of muscle activity were observed between the two studies at the start and end of the stance phase they were not of major concern since these were not the instants of peak hip joint force.

Overall, although there were some differences in muscle activity patterns between the current study and the EMG study, the majority of the muscles exhibited patterns which were consistent between the two studies.

6.1.4 Muscle Force Values

Having studied the patterns of muscle activity, it was considered an important step in the development of the model to examine values of muscle force and assess them in relation to those reported in a selection of past studies before going on to use them in the calculation of joint force. The works chosen for comparison are those of Paul (1967), Morrison (1967), Poulson (1973) and Crowninshield et al (1978a). These studies used a range of methods in muscle force calculation.

Paul (1967) performed a total of 18 laboratory tests on 12 subjects between the ages of 18.5 and 36.9 years. The study included 3 females and 9 males. The mean speed of gait was 1.46m/s with a minimum of 1.04m/s and a maximum of 2.08m/s. Paul considered the hip alone and combined the muscles into 6 functional groups so that it was possible to distribute the intersegmental joint moments among the muscles. Comparison with this work is of limited value since alternative solutions for the different muscle groups which could be active at one time were presented. The muscle values reported were those for one female subject with a stride length of 1.51m and stride time of 1.04 seconds giving a gait speed of 1.45m/s. This is 1.2 times the mean speed of 1.24m/s recorded for subjects 'G', 'I' and 'E'.

Morrison (1967) took a similar approach considering the knee alone and combining the muscles into functional groups. He conducted gait tests on a total of 12 subjects between the ages of 18 and 38. He presented a table of maximum muscle force values for the 12 subjects studied and presented the curves of muscle force for 3 subjects in detail, representing the range of results.

Poulson (1973) also grouped the muscles but considered the functions of the hip and knee together in his analysis. He combined the muscles into 9 major groups and then determined the combination of muscle groups which would be active to balance the external joint moments. His analysis produced a set of solutions from which he chose that giving the minimum value for the sum of all force actions. Poulson conducted tests on 8 subjects between the ages of 23 and 31. He presented the results for 6 subjects at three gait speeds. The mean slow speed was 1.07m/s, the mean normal speed, 1.49m/s and the mean fast speed, 2.06m/s. The mean value of 1.24m/s recorded in the current study for subjects 'G', 'I' and 'E' is between the slow and normal speeds of Poulson. Comparisons made to Poulson in this chapter are made to his results predicted at normal speed.

Crowninshield et al (1978a) took an optimization approach to solve the problem of distributing the intersegmental joint moments among muscles, including the hip, knee and ankle in the analysis. Twenty seven musculotendinous units were included and the knee and ankle anatomy were modelled as far as was necessary to include the major effects of the two

joint muscles. The cost function minimized was the sum of the individual values of muscle force divided by their cross sectional areas, i.e. the sum of the muscle stresses. Additional constraints were imposed on the solutions, limiting the stress in each muscle to be less than a critical value. Crowninshield et al presented muscle force curves for three gait cycles from each of four normal subjects.

In making comparisons to the works of Paul, Morrison, Poulson and Crowninshield et al, individual muscles and groups of muscles will be considered in turn. These are hamstrings, gluteus maximus, quadriceps femoris, iliopsoas, abductors, adductors and gastrocnemius. The results of Poulson, Paul and Morrison were expressed in pounds or in terms of body weight and had to be converted into Newtons for comparison purposes. Values quoted for Paul have been measured from the curves that he presented for one typical test subject. Those for Morrison have been measured from the curves of the three subjects that he presented as being representative of all of his test subjects. Similarly those for Crowninshield et al have been measured from the curves presented for the four test subjects. Those for Poulson are a combination of values which he quoted and measurements from the curves which he presented.

The comparisons start with the hamstring group. This consists of semitendinosus, semimembranosus and the two heads of biceps femoris. The mean peak magnitude of activity in subjects 'G', 'I' and 'E' was 781N at heel strike. This lies within the range of values presented at heel strike by Paul, Poulson and Morrison. Poulson presented a mean peak of 820N. Paul presented a value of 388N and Morrison, between 892N and 1257N. These researchers found the maximum hamstring activity to be at or just after heel strike whilst figures 6.7a-d show additional activity later on in stance in subjects 'G', 'I' and 'E'. This is most noticeable in semimembranosus and the two heads of biceps femoris.

The activity in the long head of biceps femoris continued until between 28 and 36% stance phase with a mean peak value during early stance of 162N. Crowninshield et al also reported prolonged activity of biceps femoris after heel strike although its value was higher, being approximately 300N.

Semimembranosus showed intermittent activity later in stance in subjects 'G', 'I' and 'E' with a mean peak value of 258N. Crowninshield et al reported activity in semimembranosus throughout most of stance phase with a magnitude ranging from approximately 300 to 500N.

The short head of biceps femoris also showed some activity in late stance in subjects 'G', 'I' and 'E'. This is not shown in the results of Paul, Poulson and Crowninshield et al but it is possible as it was shown by at least one subject in the EMG studies carried out at the University of California at Berkeley (1953) (fig 6.7d).

Gluteus maximus showed peak activity at heel strike in subjects 'G', 'I' and 'E' with a mean peak magnitude of 598N and then 550N in early stance. Poulson reported maximum activity in early stance with a mean peak value of 1328N and a range of 731-2978N. The value presented by Paul in early stance was 710N. That reported by Crowninshield et al was between approximately 750 and 1450N. The mean peak value calculated in early stance in the current study is just below the value of Paul and the lower ranges of Poulson and Crowninshield et al. It is equal to 77% of the value of Paul and 75% and 73% of the lowest values of Poulson and Crowninshield et al respectively. The relatively low values in comparison with those of Poulson may be partly explained by the fact that hamstring activity in subjects 'G', 'I' and 'E' continued after heel strike aiding gluteus maximus in providing hip extensor activity. The same argument may not be applied to the difference between the results of 'G', 'I' and 'E' and Crowninshield et al since the hamstring activity continued after heel strike in the subjects of Crowninshield et al. The differences between the results of the current study and those of Crowninshield et al could be due to variation in gait style between the subjects in the two studies requiring different muscle activity levels. Differences could also be due to differences in methodology used in the calculation of muscle force.

The quadriceps femoris group consists of the vasti and rectus femoris. The main activity of the vasti in subjects 'G', 'I' and 'E' was observed to be in early stance when the mean peak force was 943N. The mean peak value in rectus femoris at this time was 139N giving a total quadriceps force of 1082N. This is 1.5 times greater than the top value in the range of 476 to 714N presented by Morrison over three typical subjects. However, it is only 1.2 times greater than the mean peak value of 899N presented by Poulson. Higher activity was observed in rectus femoris in late stance, the mean peak value being 217N. This value is between that of 85N presented by Poulson and the peak value of approximately 450N reported by Crowninshield et al in late stance.

The peak activity in iliopsoas in 'G', 'I' and 'E' was in late stance, the mean peak magnitude of the force being 334N. This is only 15% of the mean peak of 2272N presented by Poulson and outwith his range of 1725-2708N. It is closer to the value of 510N reported by Paul and equal to 65% of Paul's value. It is also within the range of values of approximately 250 to 600N presented by Crowninshield et al. Some of the difference between the mean peak value reported by Poulson and that predicted in the current study could be due to differences in the methodology use in the calculation of muscle force. Differences in gait style could also result in different muscle activity levels. However, a mean peak force of 2272N as predicted by Poulson would not be reasonable for the subjects in the current study. This would lead to a muscle stress of 181N/cm^2 as calculated from the

physiological cross sectional area data used in the current study. There have been diverse opinions as to the maximum stress a muscle can sustain and Kaufman et al (1991) reported that estimates have ranged from 10 to 100N/cm^2. The value of 181N/cm^2 is well above the top end of this range and is physiologically unreasonable.

The abductors include gluteus medius, gluteus minimus and tensor fascia lata. The majority of activity was found to be in the gluteal muscles. The mean magnitudes of the two peaks in activity of the abductors of subjects 'G', 'I' and 'E' were 1067N in early stance and 1062N in late stance. The magnitudes of these peaks are between the values reported by Paul and Poulson. Paul presented an early stance peak of 433N whilst Poulson presented 1216N. In late stance Paul presented 383N whilst Poulson predicted 1454N. With regard to the individual muscle forces, the two mean peaks of 457N and 432N predicted for gluteus minimus are almost identical to the value of approximately 450N presented by Crowninshield et al. Crowninshield et al presented gluteus medius forces ranging from approximately 700 to 1400N. The two mean peaks of 610N and 564N in subjects 'G', 'I' and 'E' are equal to 87% and 81% of the values at the low end of this range.

The adductors include adductor magnus, adductor longus, adductor brevis, gracilis and pectineus. The majority of activity in 'G', 'I' and 'E' was in adductor magnus at heel strike and early stance and in adductor longus in late stance. At heel strike and early stance mean peak values of 468N and 282N respectively were predicted in adductor magnus. Crowninshield et al presented a value of approximately 400N. In late stance a mean peak force of 194N was predicted in adductor longus in subjects 'G', 'I' and 'E'. This is 65% of the value of approximately 300N presented by Crowninshield et al and lies between those of 124N and 195N presented by Poulson and Paul respectively for the adductors close to toe off.

The final muscle considered here is gastrocnemius. Following a heel strike peak, the main activity in subjects 'G', 'I' and 'E' was from mid to late stance, the mean peak value at this time being 671N. Morrison presented a range of 515-1715N over his three representative subjects and Crowninshield et al, between approximately 500 and 1250N. The value of 671N predicted in the current study lies within these ranges and is 87% of the mean peak value of 775N presented by Poulson.

6.1.5 Muscle Stress

Having examined the values of muscle force, the next important step was to assess the stresses developed in the muscles as the parameter of stress was the physiological input to the model. The first stage in the optimization procedure used in the model chooses the solution of muscle forces which minimizes the maximum stress in any one muscle. The

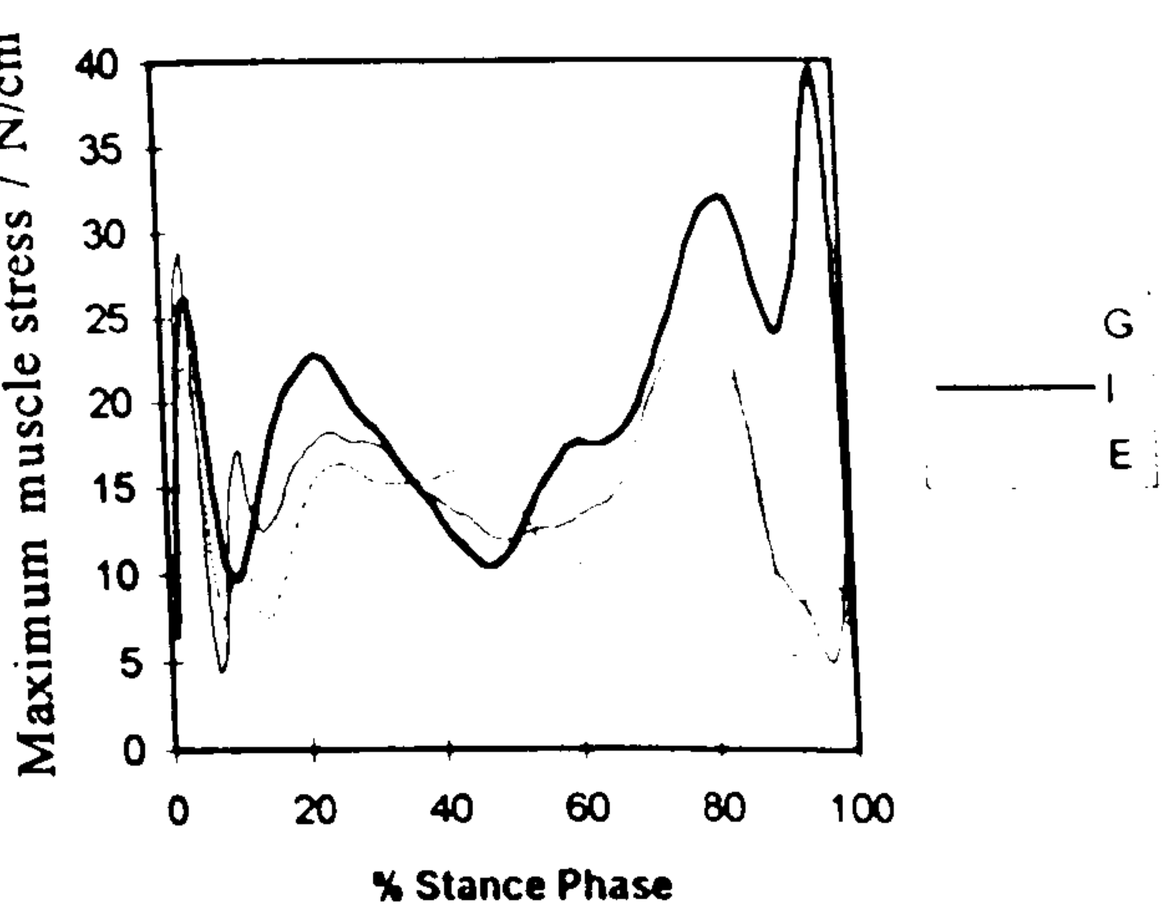

Figure 6.5 Maximum muscle stress calculated for subjects 'G', 'I' and 'E' during the stance phase of gait.

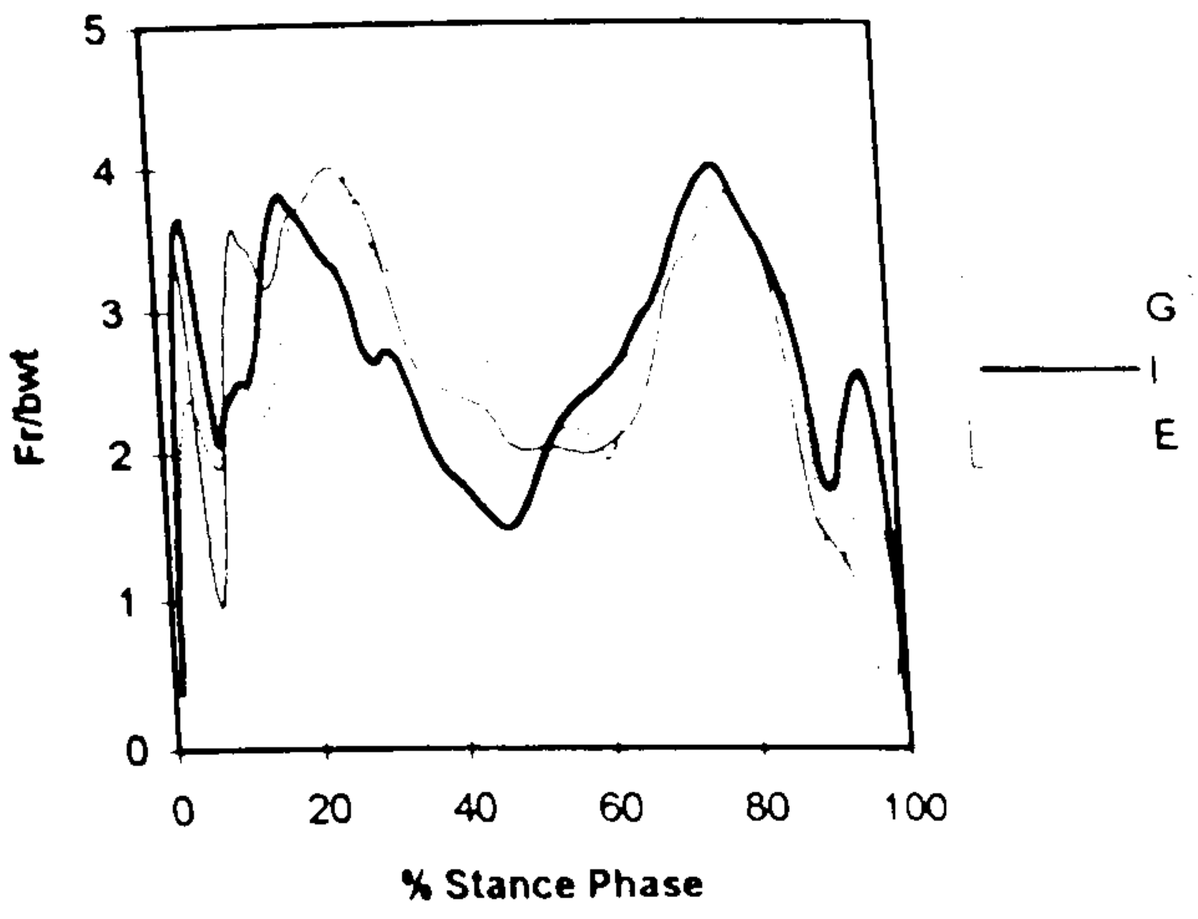

Figure 6.6 Resultant hip joint force, Fr, in terms of body weight calculated for subjects 'G', 'I' and 'E' during the stance phase of gait.

solution to the first optimization can be unique or there can be a number of combinations of muscle force solutions produced with the same maximum muscle stress. In the second optimization procedure the maximum muscle stress is constrained to be less than that obtained from the first optimization and the solution is chosen which results in the minimum value for the sum of the muscle forces. Assessing the stress is an important part of the validation process since muscle stresses must not be physiologically unreasonable.

Figure 6.5 shows the maximum muscle stress throughout the stance phase of gait in subjects 'G', 'I' and 'E'. The mean maximum value of muscle stress incurred during gait in subjects 'G', 'I' and 'E' was 30.3N/cm^2. The maximum value was 39.5N/cm^2 as observed in subject 'I'. Kaufman et al (1991) reported that there have been diverse opinions as to the maximum stress a muscle can withstand with estimates ranging between 10 and 100N/cm^2. The values for 'G', 'I' and 'E' were well below the upper limit of this range and hence the results are physiologically reasonable.

All muscles will have stress values less than or equal to the maximum value. This is illustrated in table 6.1 which shows the values of stress in the individual muscles or muscle elements of subject 'G' at the instants of the two peaks in resultant hip joint force in the stance phase of gait. The resultant hip joint force during the stance phase is shown in figure 6.6. If the model were a simple one including only one moment equation then the solution to the optimization procedure would only include activity in agonist muscles as described in section 6.1.3. The stress would be minimized when all of the agonists were of equal stress value. If the stresses were not equal in this simple model then it would be possible to redistribute some of the load from a muscle at a higher stress to one of a lower stress resulting in a lower maximum stress level. However, the model in the current study is not a simple single moment model but includes four moment equations. For the stresses in all of the muscles to be equal, there exists only one possible ratio between the moments. If this ratio changes then the muscle stresses cease to be equal.

6.1.6 Ankle Moment Balance

The final stage in the development of the model was to check that ankle joint moment balance could be achieved. The theoretical model does not include ankle joint moment balance. However, the ankle joint moment is taken into account in the model in determining the action of gastrocnemius. When the external moment tends to dorsiflex the ankle joint, gastrocnemius is included as a variable in the model but when the moment tends to plantarflex, gastrocnemius is not included. Hence it must be checked that any imbalance in ankle joint moment can be accommodated by the other ankle joint muscles.

During gait there was some imbalance at heel strike requiring dorsiflexor action but the

Muscle	Muscle stress / N/cm^2		Muscle	Muscle stress / N/cm^2	
	Peak 1	Peak 2		Peak 1	Peak 2
1 Adductor brevis (S)	0	0	20 Obturator internus	0	0
2 Adductor brevis (I)	0	0	21 Pectineus	0	25.8
3 Adductor longus	0	21.0	22 Piriformis	0	0
4 Adductor magnus (1)	0	0	23 Quadratus femoris	0	0
5 Adductor magnus (2)	18.7	0	24 Gemellus superior	0	0
6 Adductor magnus (3)	18.4	0	25 Biceps femoris (L)	18.3	0
7 Gluteus maximus (1)	18.3	13.8	26 Gracilis	0	0
8 Gluteus maximus (2)	18.3	0	27 Rectus femoris	14.7	25.3
9 Gluteus maximus (3)	15.2	0	28 Sartorius	0	25.8
10 Gluteus medius (1)	18.3	25.2	29 Semimembranosus	5.9	0
11 Gluteus medius (2)	18.3	20.6	30 Semitendinosus	18.6	0
12 Gluteus medius (3)	11.8	0	31 Tensor fascia lata	0	25.6
13 Gluteus minimus (1)	18.4	25.4	32 Biceps femoris (S)	0	25.4
14 Gluteus minimus (2)	18.4	25.3	33 Gastrocnemius (M)	0	17.1
15 Gluteus minimus (3)	18.3	0	34 Gastrocnemius (L)	0	25.4
16 Iliacus	0	25.3	35 Vastus intermedius	18.3	0
17 Psoas	0	25.4	36 Vastus lateralis	18.3	0
18 Gemellus inferior	0	0	37 Vastus medialis	18.3	0
19 Obturator externus	0	0			

Table 6.1 Stresses in the muscles of subject 'G' at the instants of the 2 peaks in resultant hip joint in the stance phase of gait.

1 Adductor brevis (S) - S denotes superior part.
2 Adductor brevis (I) - I denotes inferior part.
25 Biceps femoris (L) - L denotes long head.
32 Biceps femoris (S) - S denotes short head.
33 Gastrocnemius (M) - M denotes medial head.
34 Gastrocnemius (L) - L denotes lateral head

majority of imbalance occurred in late stance, requiring additional plantarflexor action. The maximum unbalanced ankle joint moment was 83Nm tending to dorsiflex the ankle joint in late stance in subject 'G'. The additional ankle joint plantarflexors available to balance this moment are soleus, tibialis posterior, peroneus longus, peroneus brevis, flexor hallucis longus and flexor digitorum longus. It is recognised that tibialis posterior, peroneus longus, peroneus brevis, flexor hallucis longus and flexor digitorum longus have additional roles to that of plantarflexing the ankle as shown in table 2.1. Hence these muscles may not be active simultaneously. However, in order to demonstrate by simple calculation that the residual ankle joint moment can be balanced, they were all assumed to be active with equal stress. Using ankle joint muscle moment arms from Spoor et al (1990) and physiological cross section areas from Friederich and Brand (1990), this muscle stress was found to be 22.7 N/cm^2. This is well below the upper limit of the range of estimations of maximum achievable muscle stress quoted as 10-100 N/cm^2 by Kaufman et al (1991). Hence the residual ankle joint moment can be balanced whilst maintaining the muscle stress within physiologically reasonable limits.

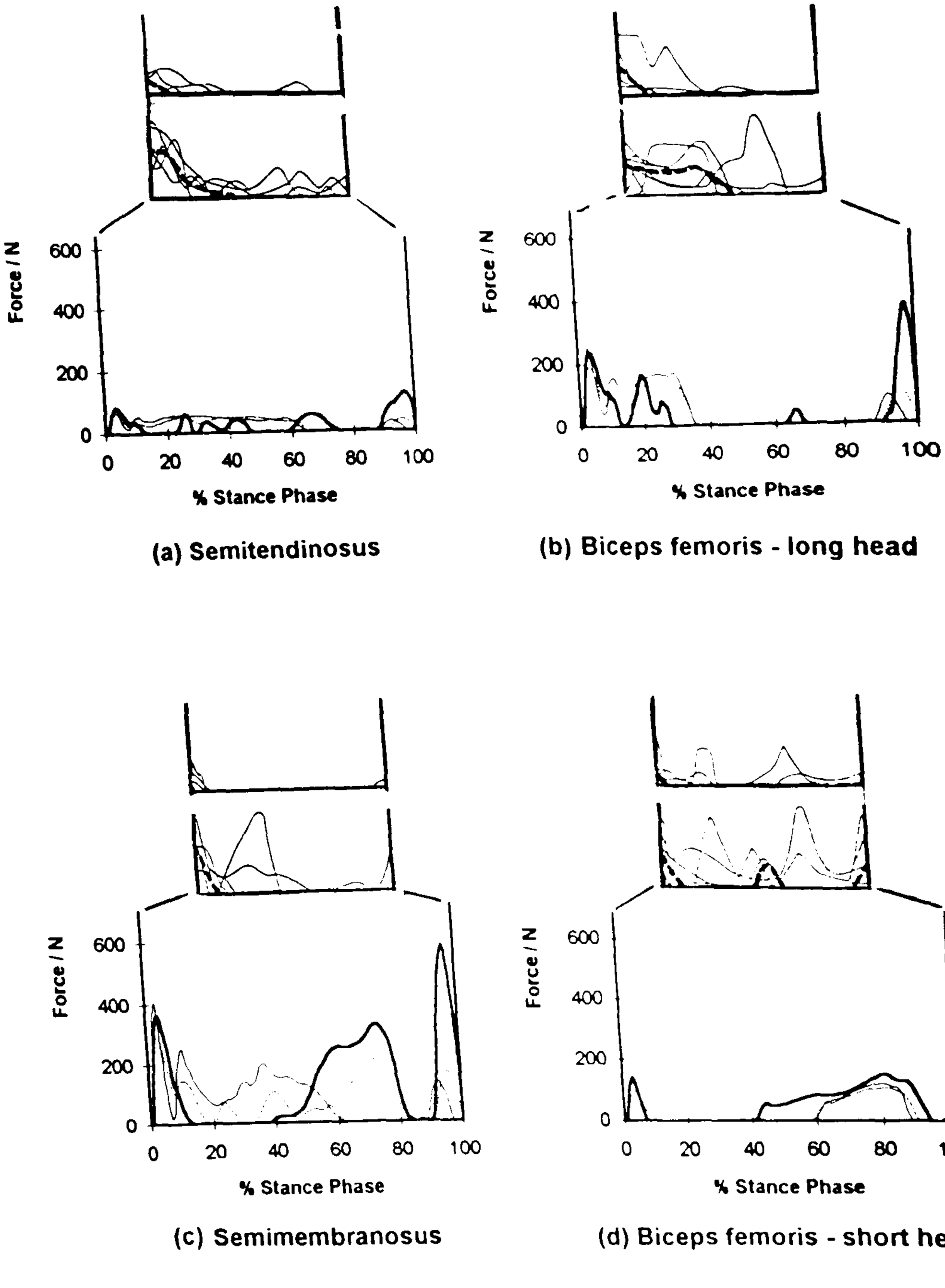

Figure 6.7 Muscle activity during the stance phase of gait.

For each muscle the top figure shows the EMG data of the University of California, Berkeley (1953) for normal speed gait and the middle one shows the EMG data for fast speed gait. The dotted line on the EMG curves represents the average curve for all subjects in the EMG study.

For each muscle the bottom figure shows the predicted muscle activity in the current study for subjects 'G', 'I' and 'E'.

G
I
E

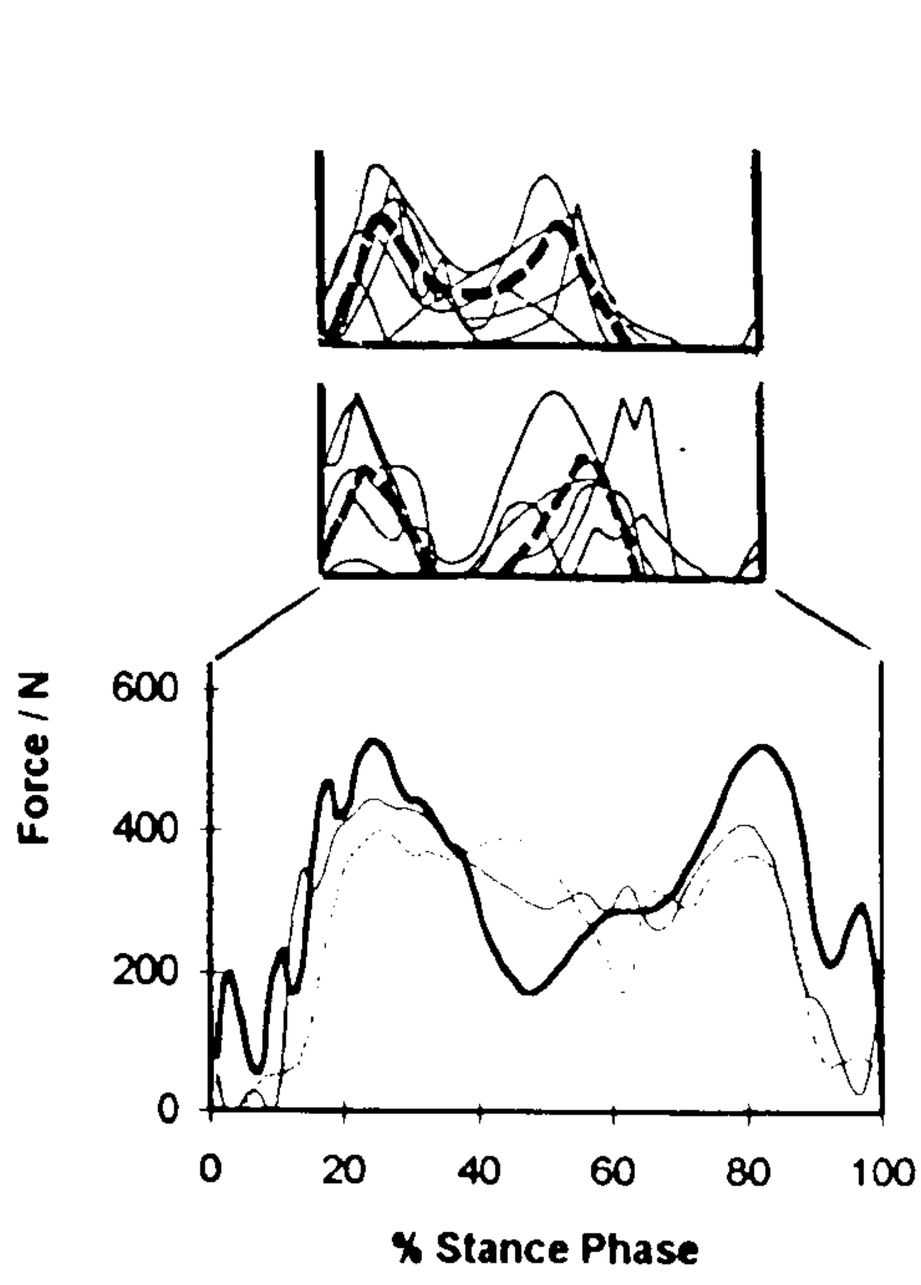

(e) Gluteus minimus

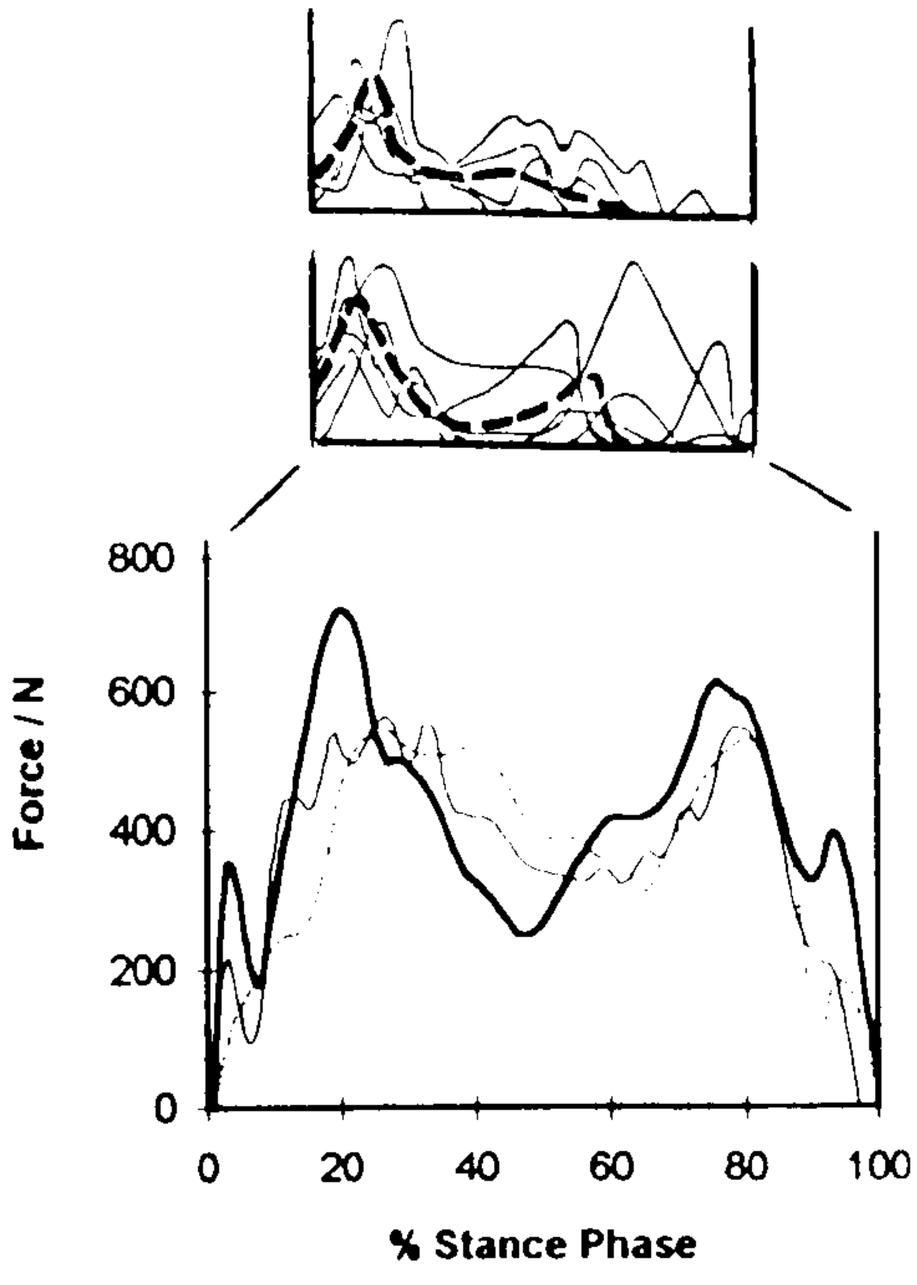

(f) Gluteus medius

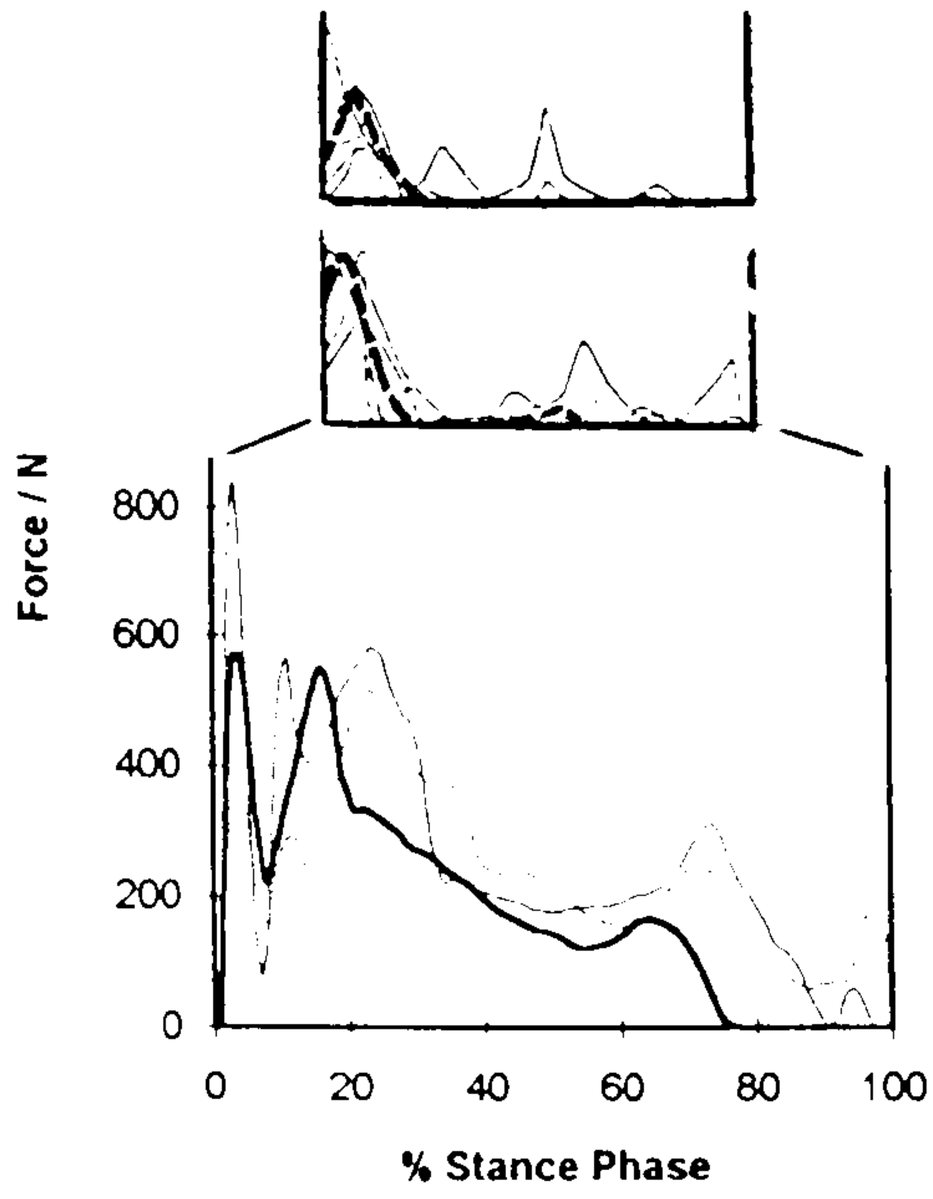

(g) Gluteus maximus

Figure 6.7 continued. Muscle activity during the stance phase of gait.

For each muscle the top figure shows the EMG data of the University of California, Berkeley (1953) for normal speed gait and the middle one shows the EMG data for fast speed gait. The dotted line on the EMG curves represents the average curve for all subjects in the EMG study.

For each muscle the bottom figure shows the predicted muscle activity in the current study for subjects 'G', 'I' and 'E'.

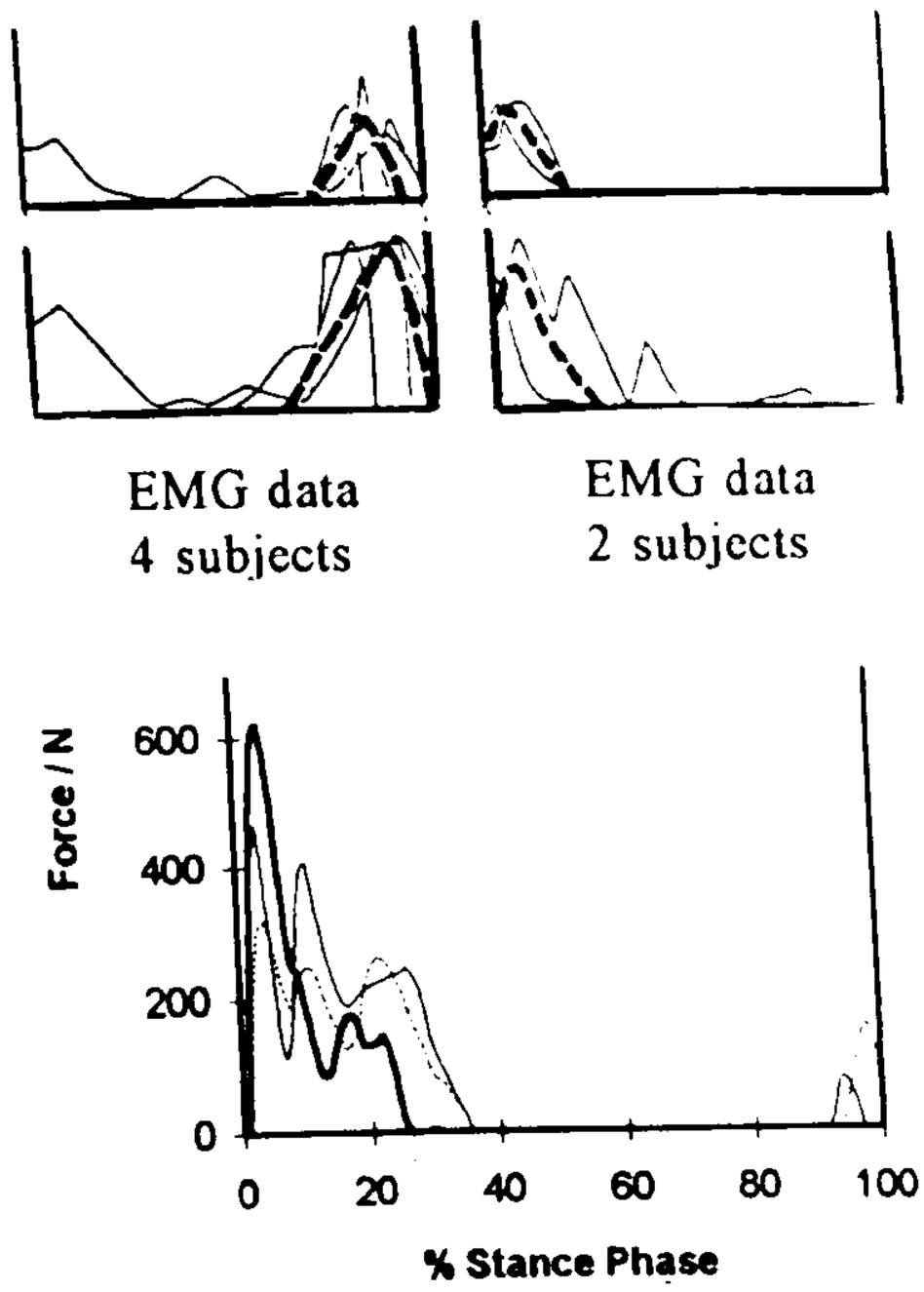

(h) Adductor magnus

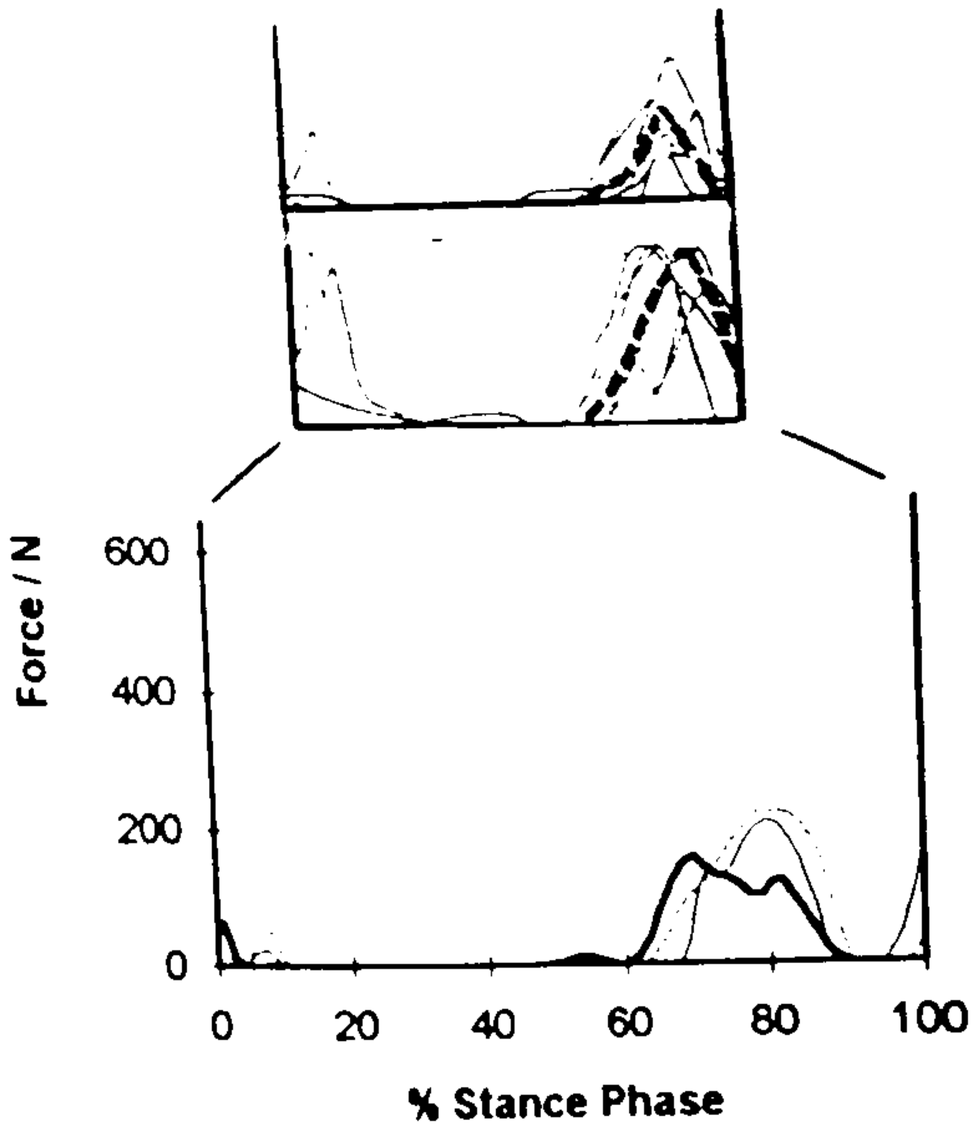

(i) Adductor longus

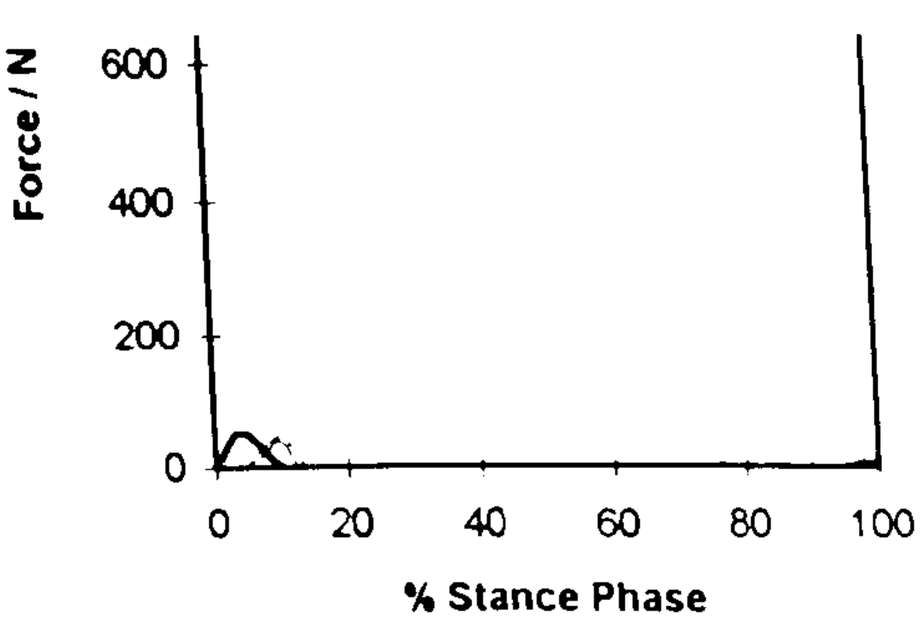

(j) Adductor brevis

Figure 6.7 continued. Muscle activity during the stance phase of gait. (h) Adductor magnus and (i) adductor longus activity. For each of these muscles the top figure shows the EMG data of the University of California, Berkeley (1953) for normal speed gait and the middle one shows the EMG data for fast speed gait. The dotted line on the EMG curves represents the average curve for all subjects in the EMG study. The bottom figure for each of these muscles shows the predicted activity in the current study for subjects 'G', 'I' and 'E'.

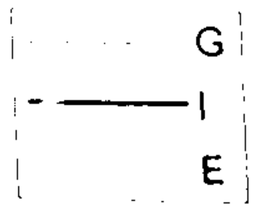

(j) Predicted activity in adductor brevis in the current study for subjects 'G', 'I' and 'E'.

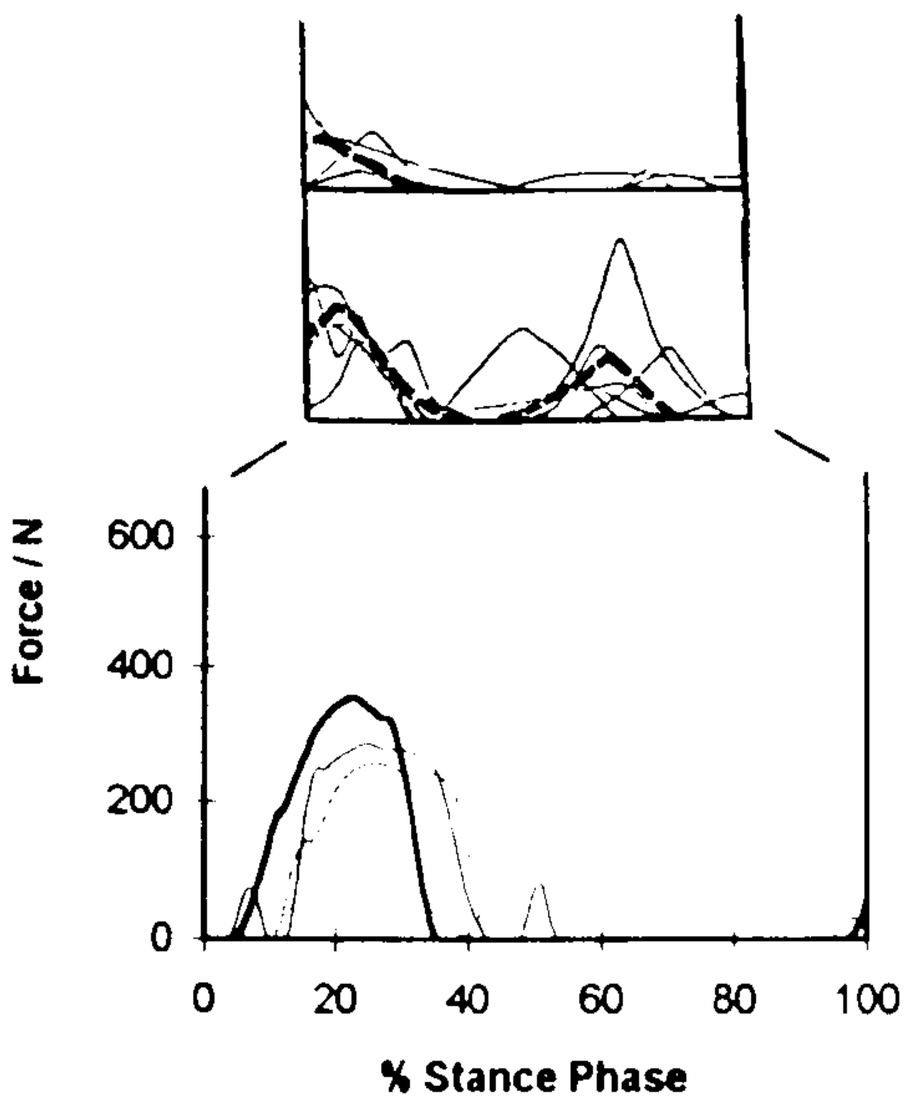

(k) Vastus medialis

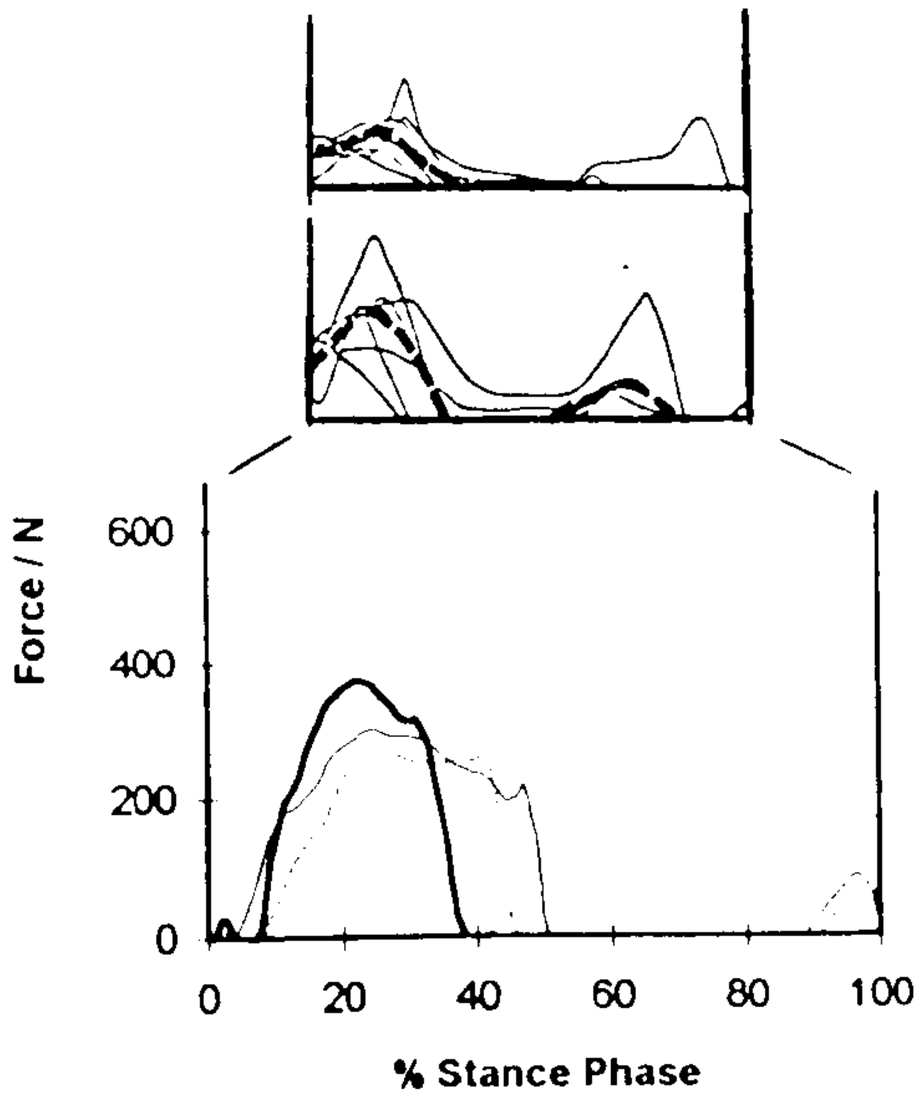

(l) Vastus lateralis

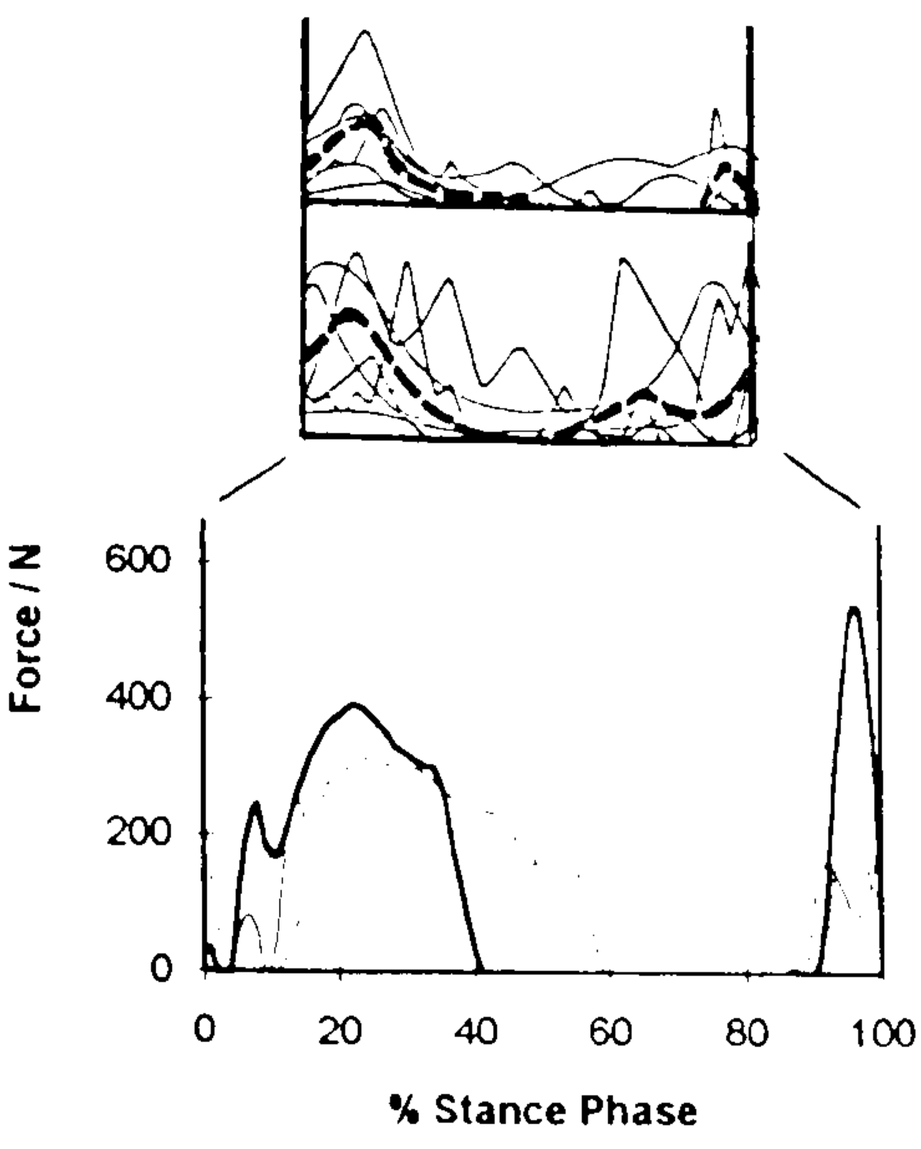

(m) Vastus intermedius

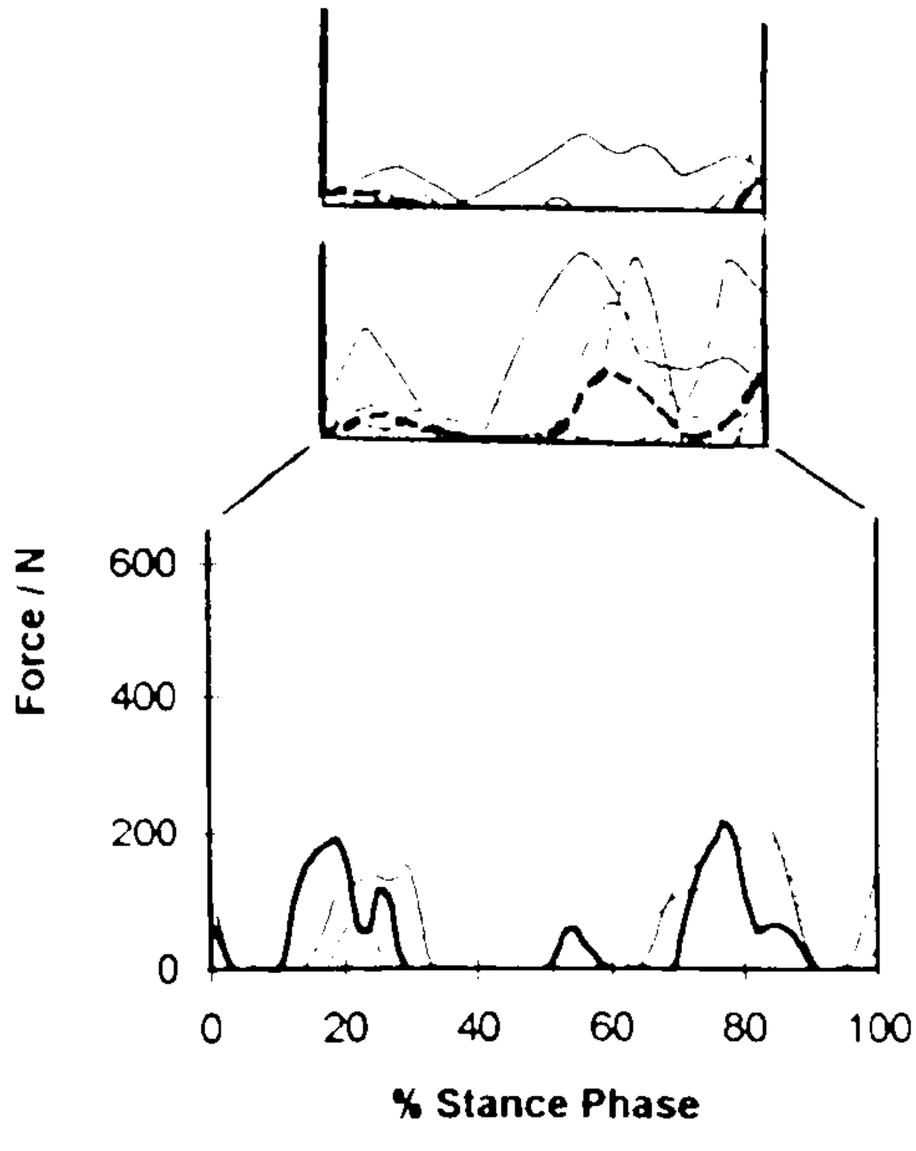

(n) Rectus femoris

Figure 6.7 continued. Muscle activity during the stance phase of gait.

For each muscle the top figure shows the EMG data of the University of California, Berkeley (1953) for normal speed gait and the middle one shows the EMG data for fast speed gait. The dotted line on the EMG curves represents the average curve for all subjects in the EMG study.

For each muscle the bottom figure shows the predicted muscle activity in the current study for subjects 'G', 'I' and 'E'.

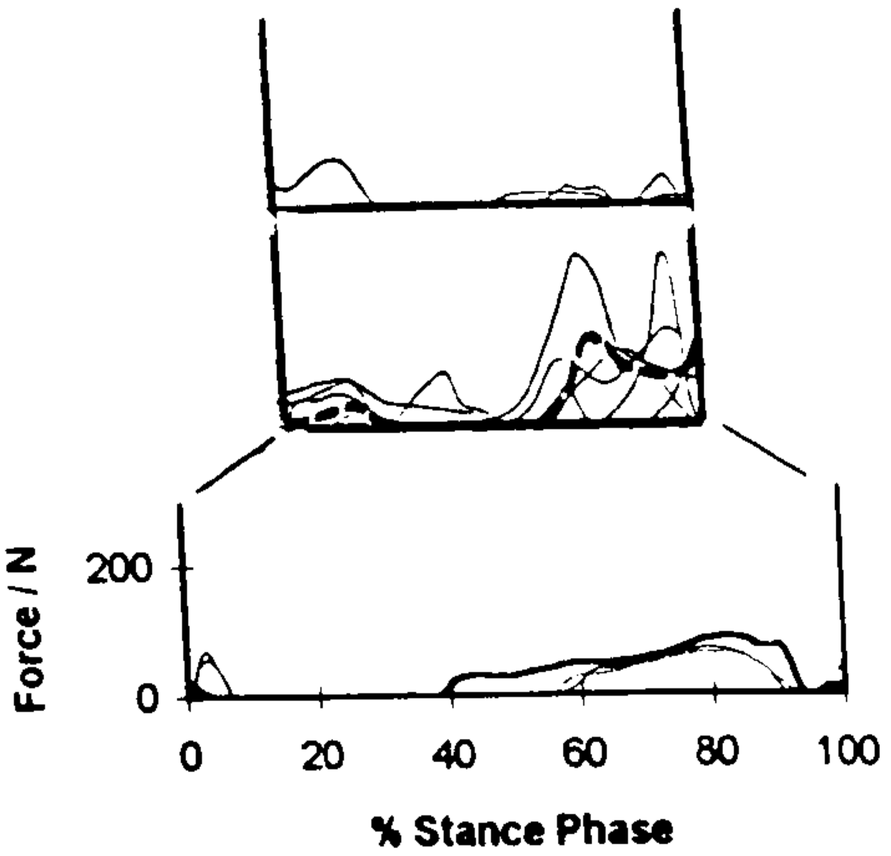

(o) Sartorius

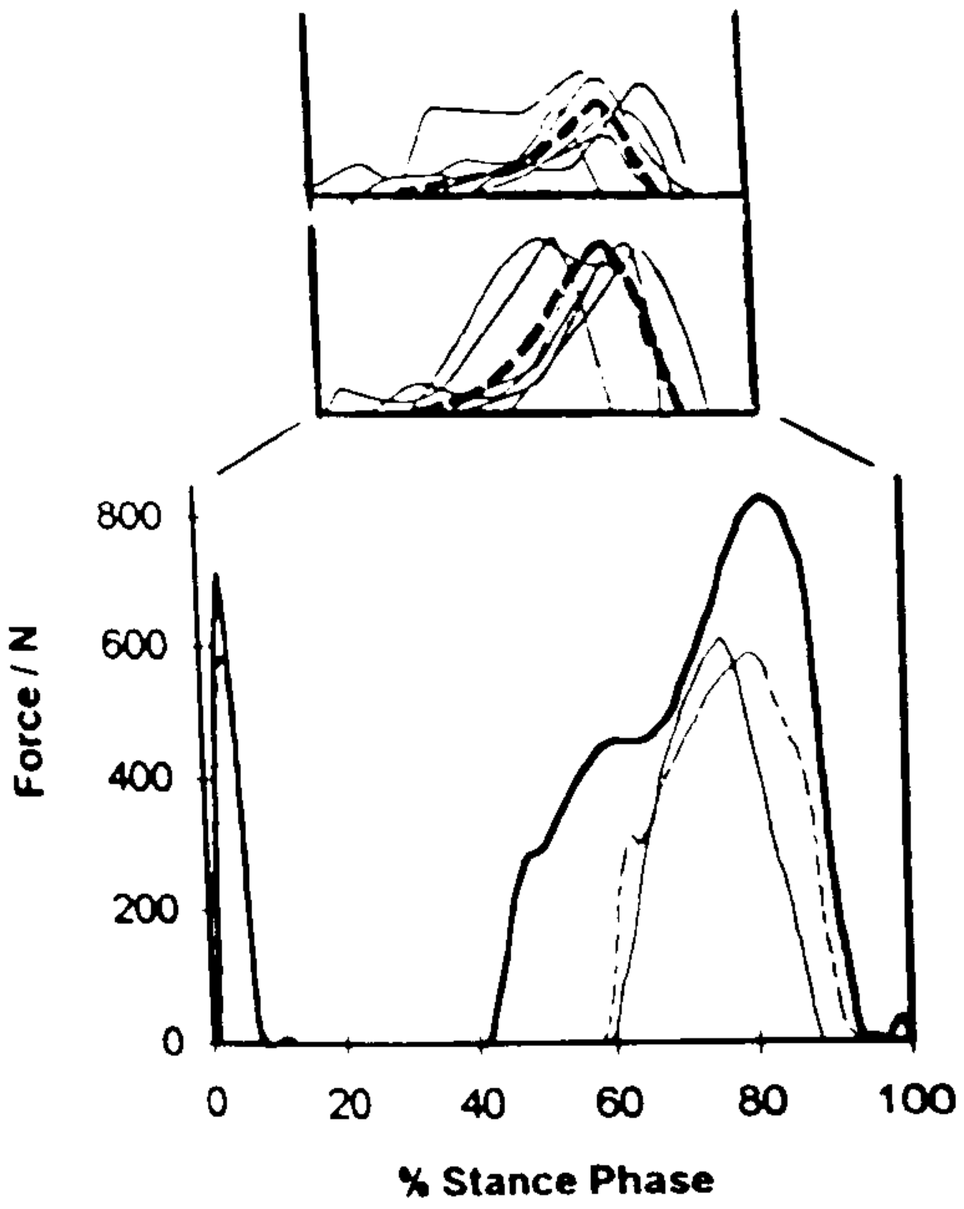

(p) Gastrocnemius

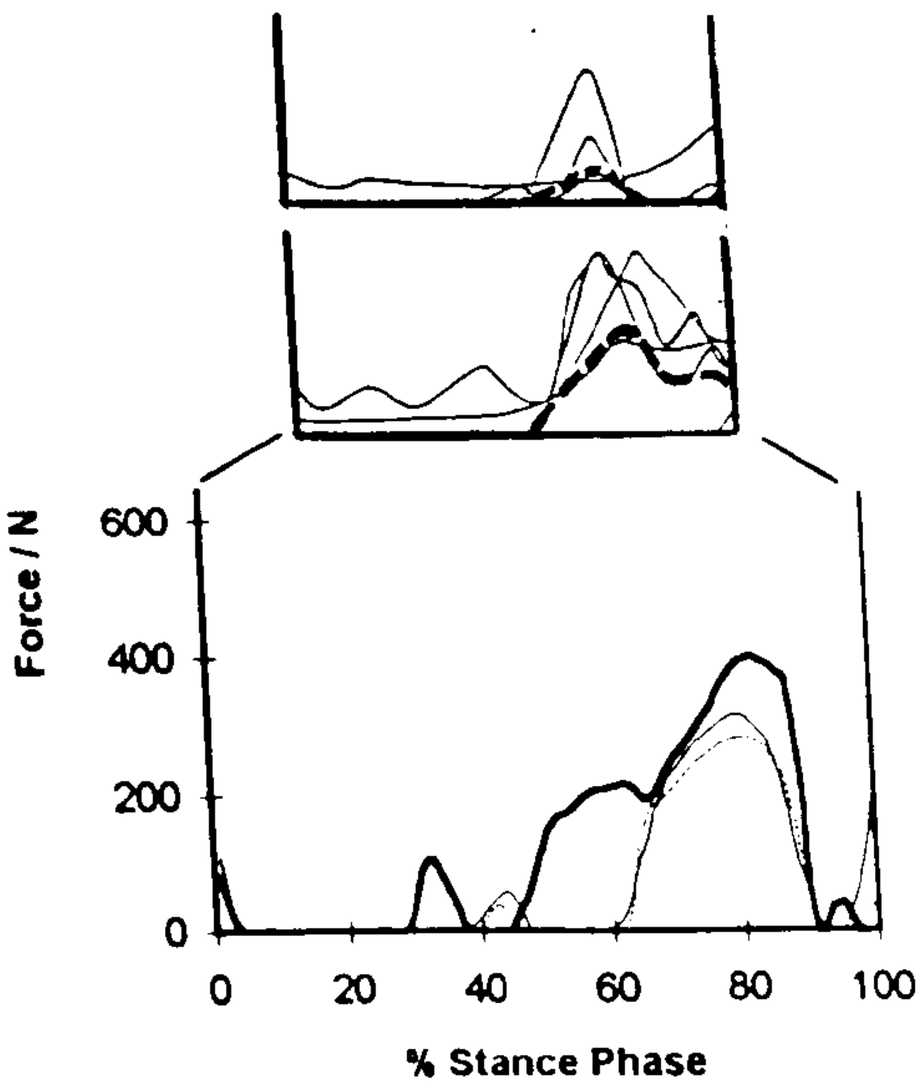

(q) Iliopsoas

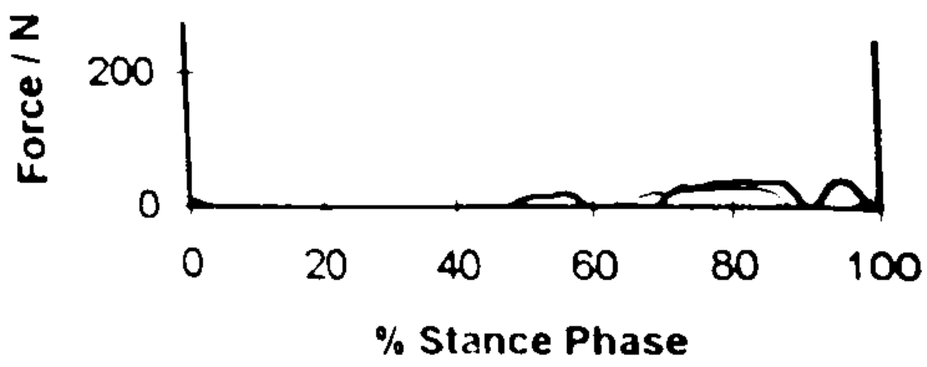

(r) Pectineus

Figure 6.7 continued. Muscle activity during the stance phase of gait.

(o) Sartorius and (p) gastrocnemius activity. For each of these muscles the top figure shows the EMG data of the University of California, Berkeley (1953) for normal speed gait and the middle one shows the EMG data for fast speed gait. The dotted line on the EMG curves represents the average curve for all subjects in the EMG study. The bottom figure for each of these muscles shows the predicted activity in the current study for subjects 'G', 'I' and 'E'.

(q) Iliopsoas activity. The layout of the figures is as for (o) and (p). EMG data is for iliacus and predicted activity in subjects 'G', 'I' and 'E' is for iliacus and psoas combined (i.e. iliopsoas).

(r) Predicted activity in pectineus in the current study for subjects 'G', 'I' and 'E'.

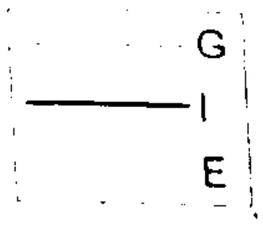

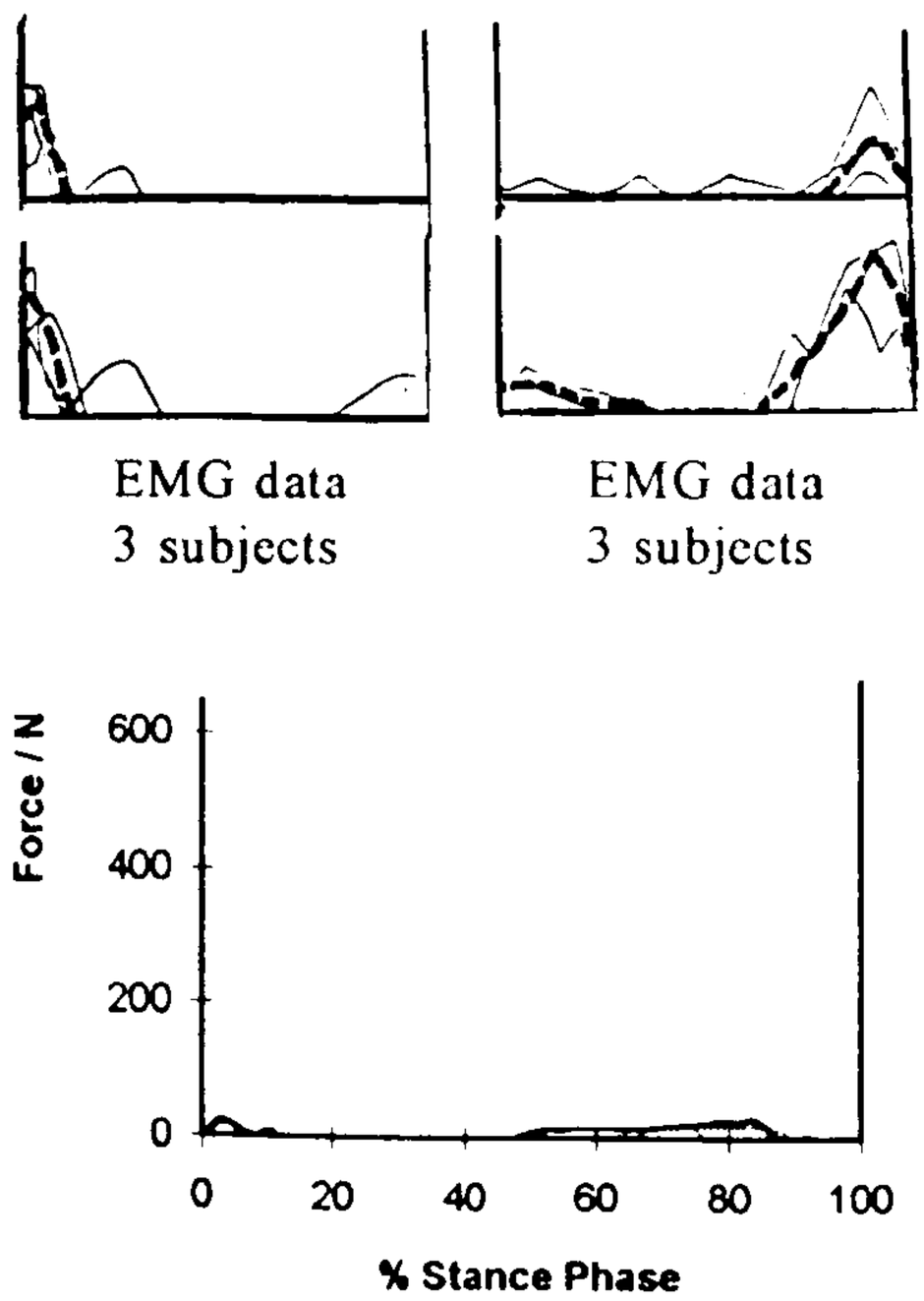

(s) Gracilis

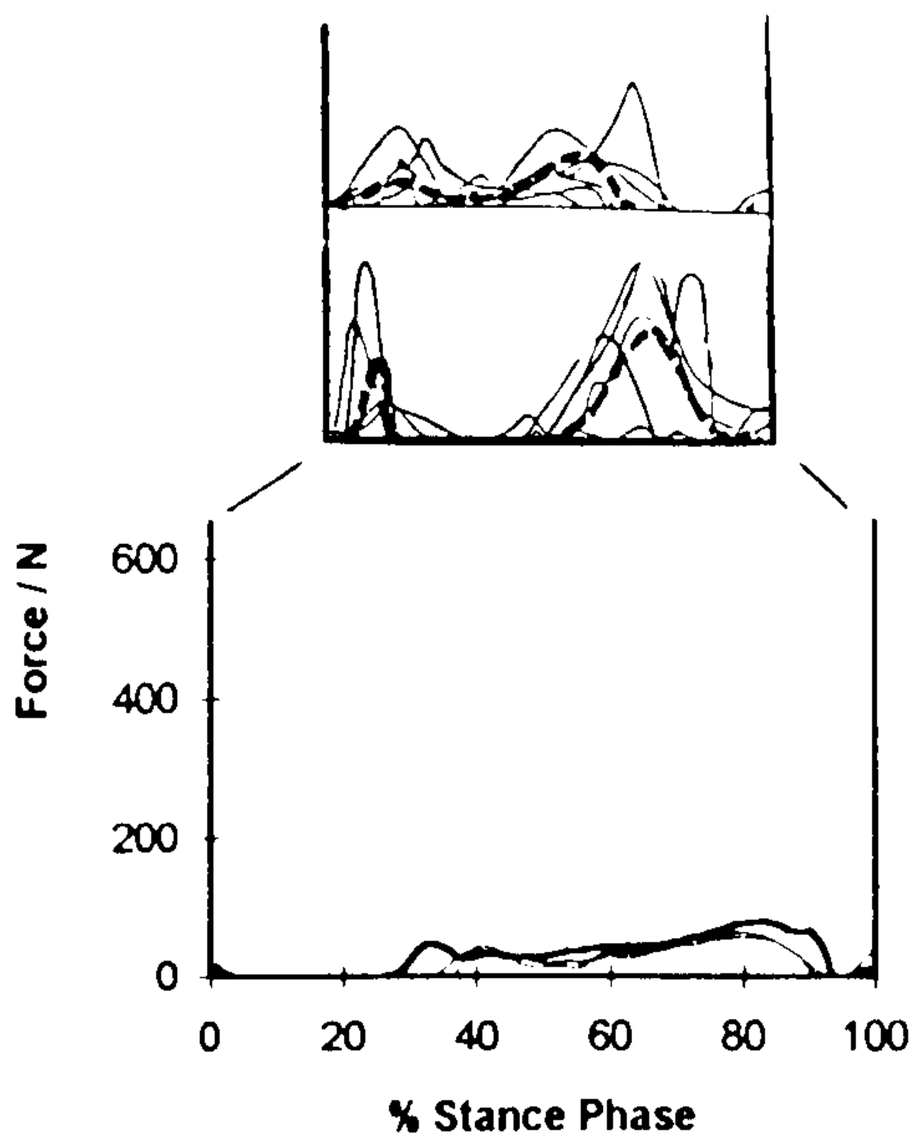

(t) Tensor fascia lata

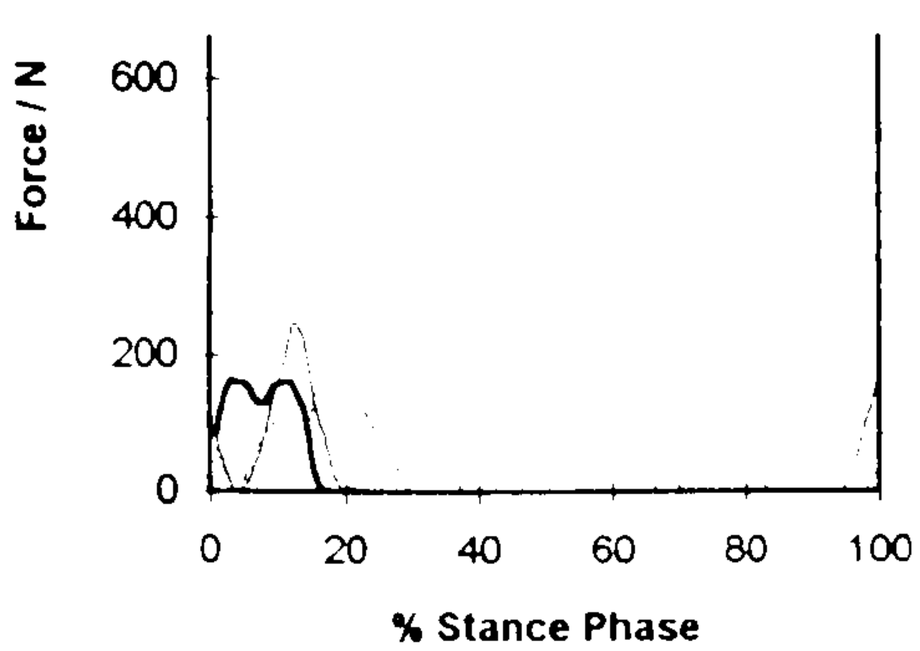

(u) External rotators

Figure 6.7 continued. Muscle activity during the stance phase of gait.

(s) Gracilis and (t) tensor fascia lata activity. For each of these muscles the top figure shows the EMG data of the University of California, Berkeley (1953) for normal speed gait and the middle one shows the EMG data for fast speed gait. The dotted line on the EMG curves represents the average curve for all subjects in the EMG study. The bottom figure for each of these muscles shows the predicted activity in the current study for subjects 'G', 'I' and 'E'.

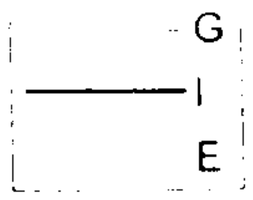

(u) Predicted activity in the external rotators (gemellus inferior, gemellus superior, obturator internus, piriformis, quadratus femoris and obturator externus) in the current study for subjects 'G', 'I' and 'E'.

(a) Sagittal plane hip joint moment ($Mz_{HC\ -\ F}$). A positive moment indicates an external moment tending to flex the hip joint and hip extensor muscle activity. A negative moment indicates an external moment tending to extend the hip joint and hip flexor muscle activity.

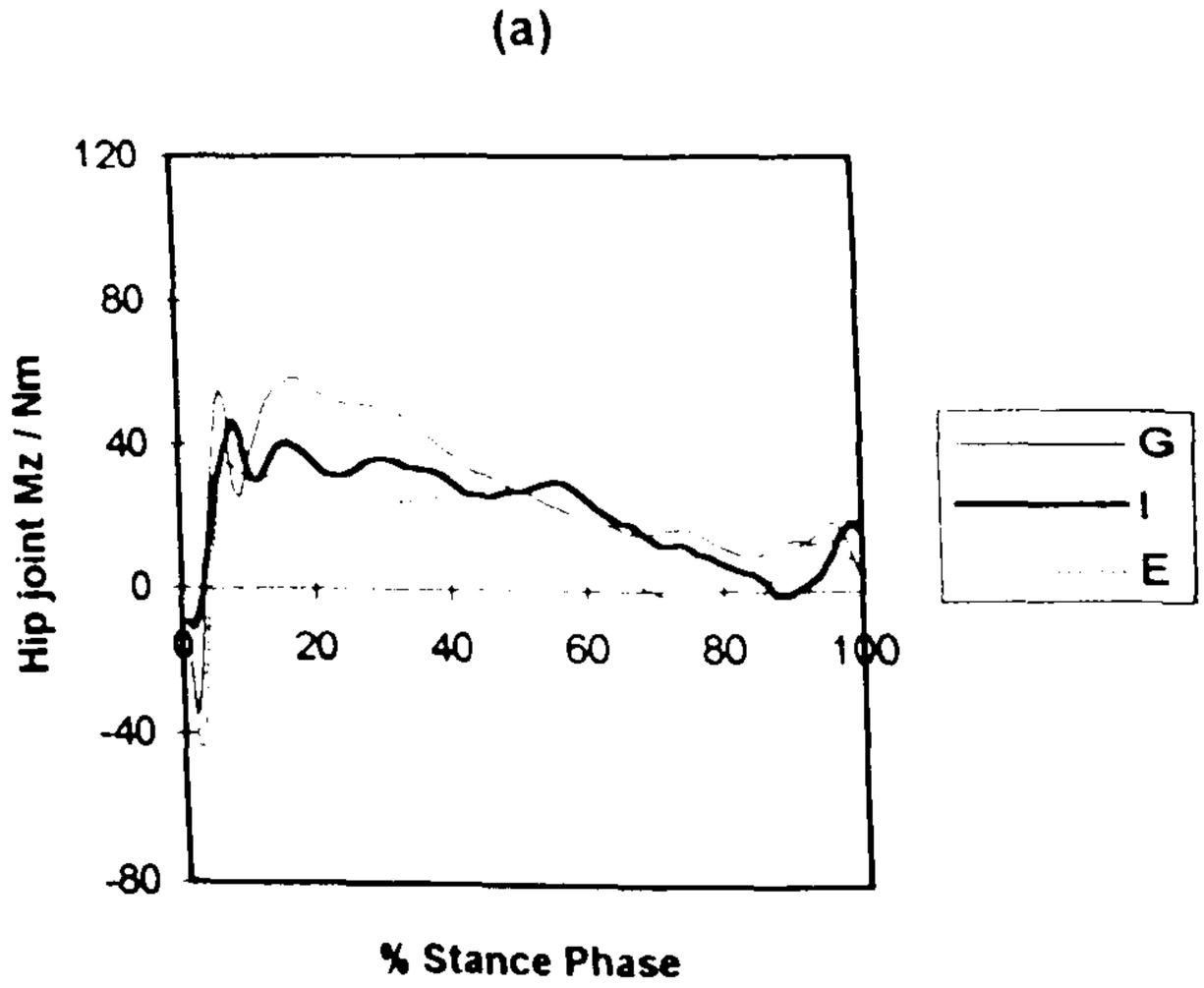

(b) Frontal plane hip joint moment ($Mx_{HC\ -\ r}$). A positive moment indicates an external moment tending to adduct the hip joint and hip abductor muscle activity. A negative moment indicates an external moment tending to abduct the hip joint and hip adductor muscle activity.

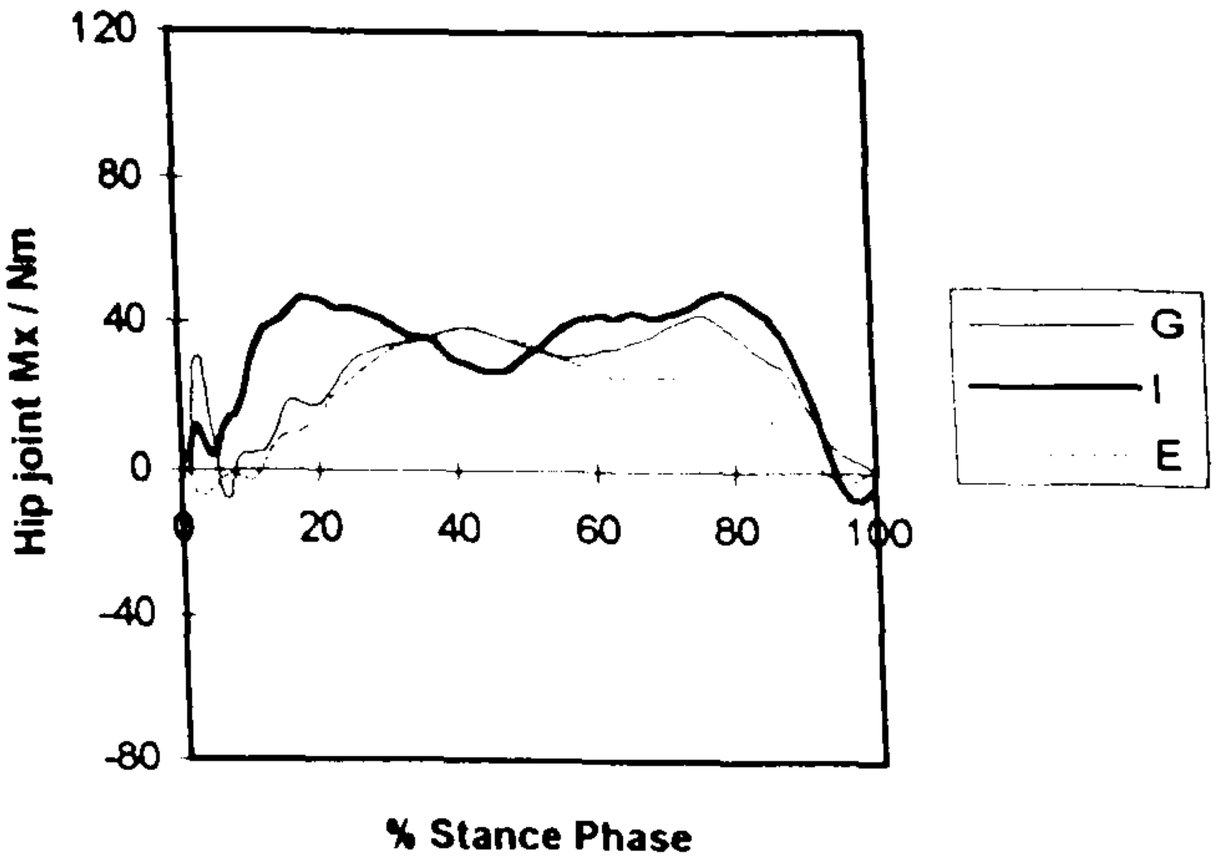

(c) Transverse plane hip joint moment ($My_{HC\ -\ F}$). A positive moment indicates an external moment tending to internally rotate the femur relative to the pelvis and hip external rotator muscle activity. A negative moment indicates an external moment tending to externally rotate the femur relative to the pelvis and hip internal rotator muscle activity.

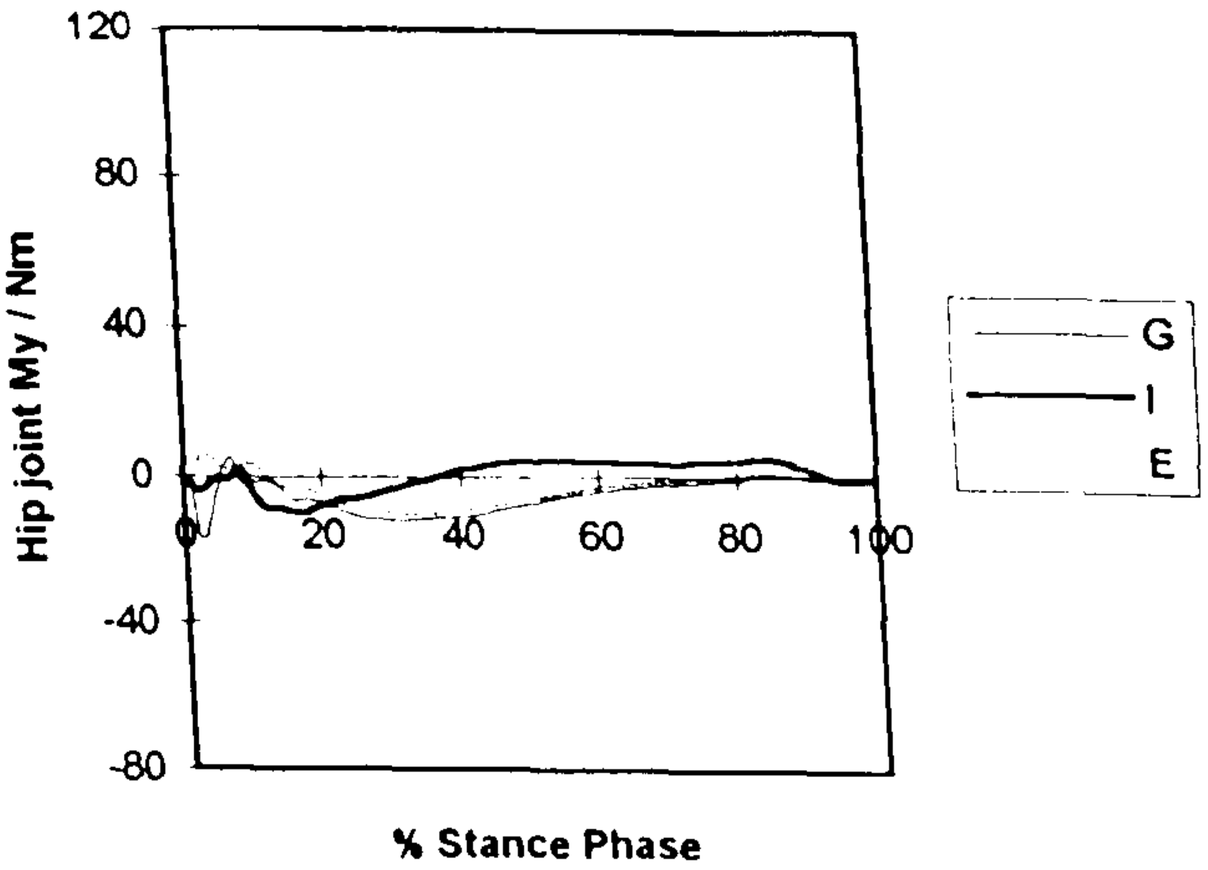

Figure 6.8 Hip joint moments measured in subjects 'G', 'I' and 'E' during the stance phase of stair ascent.

6.2 STAIR ASCENT

Having assessed the results of the model at the various stages of calculation for gait, it was considered important to examine the results when the model was applied to other activities. This section considers stair ascent and section 6.3 examines the activity of rising from a chair.

Each subject ascended the stairs at natural speed, resting their hands on the handrails. The subjects were instructed to use the handrails to aid ascent as much as required.

6.2.1 Joint Moments

In section 6.1.1 the patterns and values of joint moment for gait were examined and assessed in relation to those reported by other authors before going on to use them in the calculation of muscle forces. It was considered important in the development of the model to carry out the same process for the activity of stair ascent. The works chosen for comparison purposes are those of Andriacchi et al (1980) and McFadyen and Winter (1988). The study by Andriacchi et al included 10 men with a mean age of 28 years and an age range of 20 to 34 years. The staircase included three steps each of height 210mm and depth 255mm. One handrail was fitted to the staircase. McFadyen and Winter studied three normal males. The staircase of McFadyen and Winter consisted of 5 steps and no handrail. The step height was 220mm and the step depth was 280mm.

Hip joint

Figure 6.8a shows the sagittal plane component of hip joint moment throughout the stance phase of stair ascent. The external moment predominantly tends to flex the hip joint requiring hip extensor activity. In subject 'G', the tendency to flex continued throughout the entire stance phase whilst in 'I' and 'E' there was a small tendency to extend in late stance. Andriacchi et al (1980) presented a typical hip joint moment curve showing an external moment tending to flex the hip joint throughout the entire stance phase. The subjects of McFadyen and Winter (1988) exhibited an external moment tending to flex the hip joint in early stance followed by an external moment tending to extend later in stance.

The peak sagittal plane hip joint moment in subjects 'G', 'I' and 'E' occurred between heel strike and mid-stance. The mean peak in this moment was 46Nm which is considerably less than the 107.4Nm (S.D.±27.0) and 123.9Nm (S.D.±33.6) reported by Andriacchi et al with and without the aid of the handrail respectively. However, when normalized to body mass the mean peak was 0.71Nm/Kg which lies within the range of approximately 0.5-1Nm/kg as measured from the curves of McFadyen and Winter. The difference between the

Figure 6.9

Sagittal plane knee joint moment ($Mz_{KC\ .\ s}$) measured in subjects 'G', 'I' and 'E' during the stance phase of stair ascent. A positive moment indicates an external moment tending to extend the knee joint and knee flexor muscle activity. A negative moment indicates an external moment tending to flex the knee joint and knee extensor muscle activity.

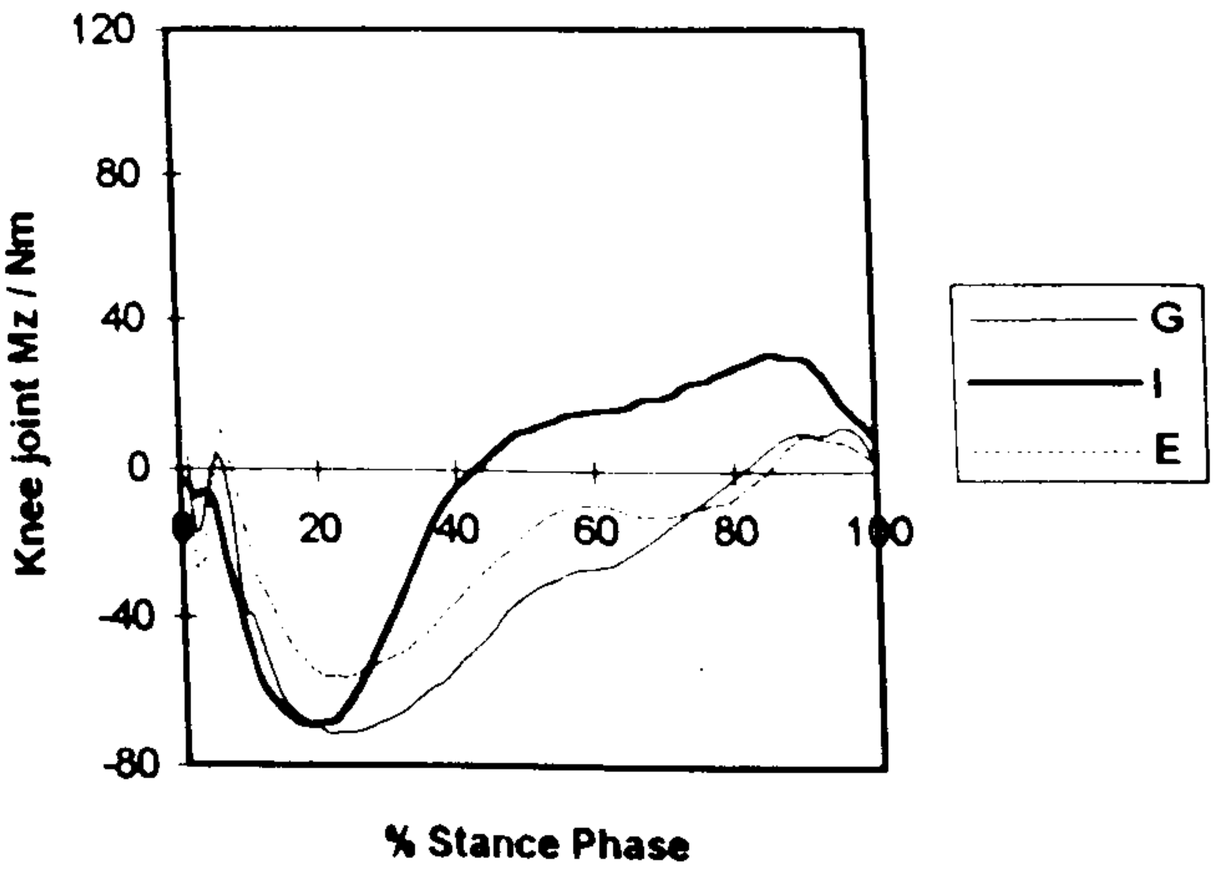

Figure 6.10

Sagittal plane ankle joint moment ($Mz_{AC\ .\ s}$) measured in subjects 'G', 'I' and 'E' during the stance phase of stair ascent. A positive moment indicates an external moment tending to dorsiflex the ankle joint and ankle plantarflexor muscle activity. A negative moment indicates an external moment tending to plantarflex the ankle joint and ankle dorsiflexor muscle activity.

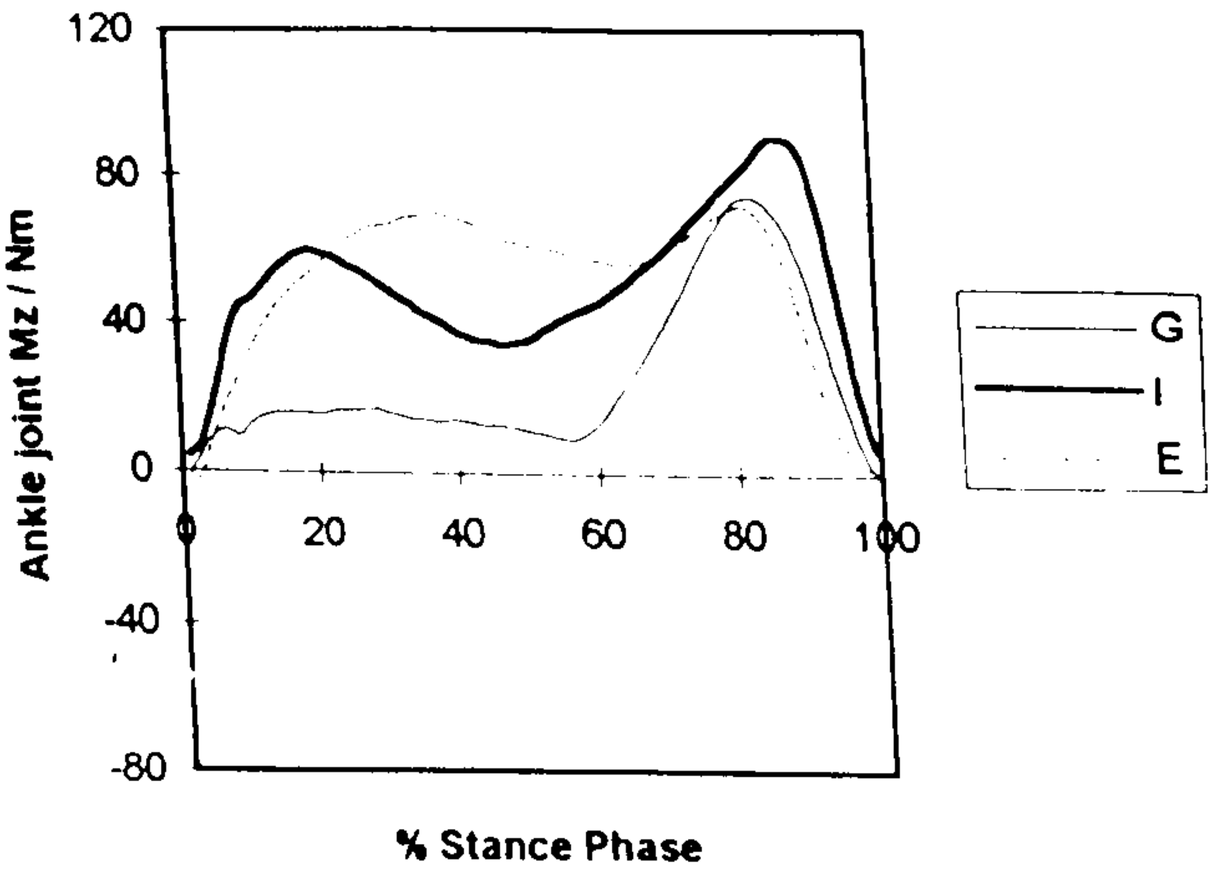

results of the current study and those of Andriacchi et al may stem from the fact that the hip joint moment can be highly variable in stair climbing. Indeed, McFadyen and Winter demonstrated in their study that each subject carried their upper body quite differently, resulting in major deviations in hip joint moment.

As can be seen from figure 6.8b, there was an external moment tending to adduct the hip joint throughout the stance phase of stair ascent requiring abductor activity. Andriacchi et al also presented a typical curve showing an external moment tending to adduct the hip joint throughout the majority of the stance phase. The mean peak value of this moment in 'G', 'I', and 'E' was 43Nm. That reported by Andriacchi et al was 36.5Nm (S.D.±20.3) when using the handrail and 37.0Nm (S.D.±18.7) without the use of the handrail. The mean peak of 'G', 'I' and 'E' lies within the range covered by the standard deviation of Andriacchi et al.

In the transverse plane, figure 6.8c shows a much smaller moment. The mean peak external moment tending to externally rotate the femur relative to the pelvis in subjects 'G', 'I' and 'E' was 11Nm and that tending to internally rotate was 2Nm..

Knee joint

Figure 6.9 shows the sagittal plane component of knee joint moment during the stance phase of stair ascent. The external moment tended to flex the knee following heel strike until mid-stance in subject 'I' and late stance in subjects 'G' and 'E'. Knee extensor activity was required throughout this time. The external moment then changed and tended to extend the knee joint, requiring knee flexor muscle activity. Andriacchi et al (1980) also presented a typical knee joint moment curve with an external moment tending to flex the knee until late stance followed by an external moment tending to extend the knee. The curves of McFadyen and Winter (1988) show a similar pattern.

The mean peak moment tending to flex the knee in subjects 'G', 'I' and 'E' was 66Nm When normalised to body mass this is 1Nm/kg. Andriacchi et al reported mean peak values of 52.4Nm (S.D.±14.1) and 54.2Nm (S.D.±17.2) with and without handrails respectively. Values between approximately 1.38 and 1.85Nm/kg were measured from the curves of McFadyen and Winter. The value found in this study lies between those of Andriacchi et al and McFadyen and Winter.

Ankle joint

Throughout the whole of the stance phase, the sagittal plane external moment at the ankle joint in subjects 'G', 'I' and 'E' tended to dorsiflex as show in figure 6.10. Plantarflexor activity was therefore required, the peak of activity occurring just before toe off. The typical curve presented by Andriacchi et al (1980) also exhibited an external moment tending to dorsiflex the ankle joint throughout the whole of the stance phase as did the curves of

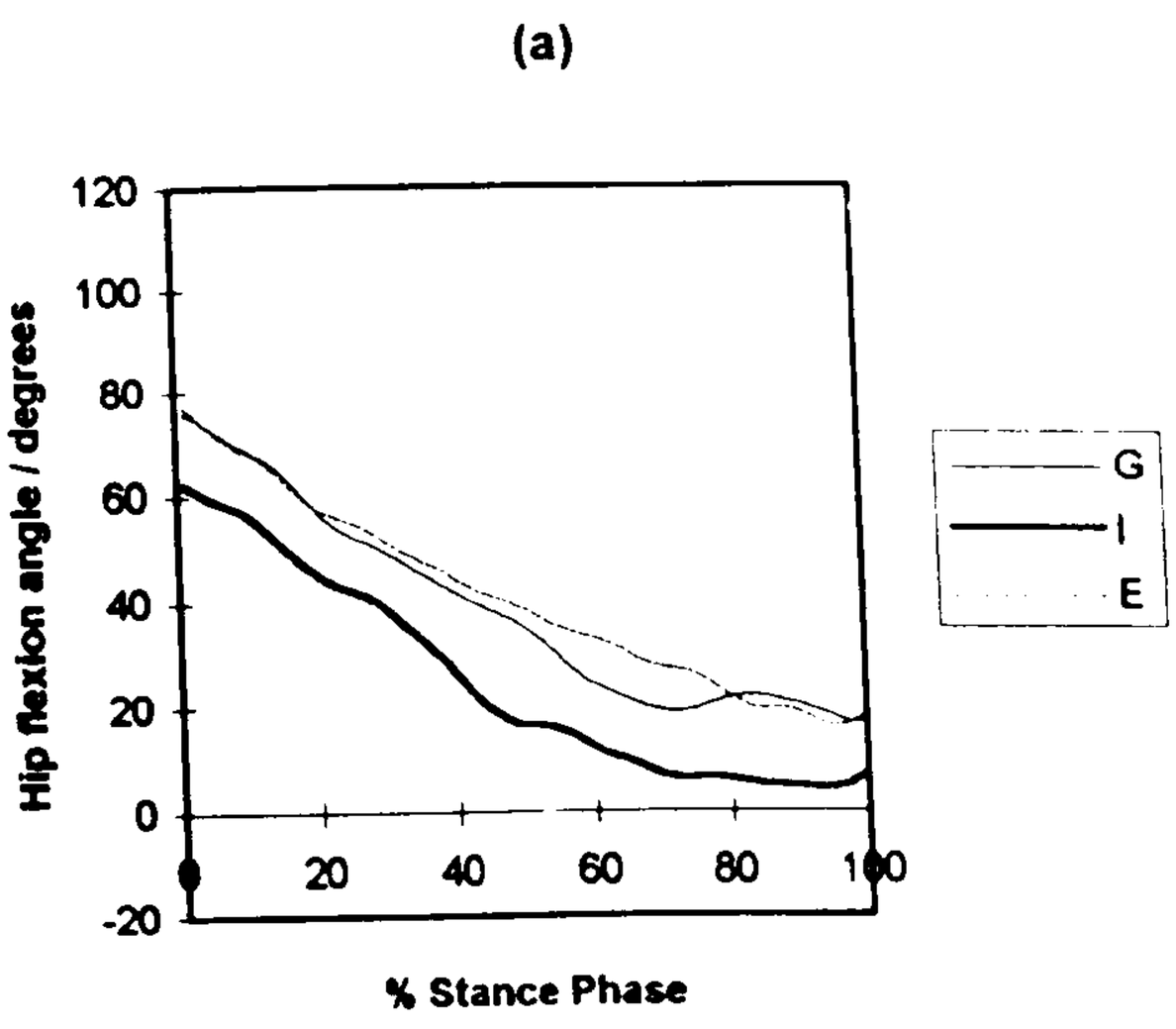

Figure 6.11 (a) Hip flexion and (b) knee flexion angles measured in subjects 'G', 'I' and 'E' during the stance phase of stair ascent.

McFadyen and Winter (1988).

The mean peak plantarflexor muscle moment in 'G', 'I' and 'E' was 79Nm. Andriacchi et al reported 108.6Nm (S.D.±44.0) and 101.8Nm (S.D.±38.0) with and without the use of handrails respectively. Hence the value calculated in the current study lies at the low end of the ranges covered by the standard deviations of Andriacchi et al. When normalized to body mass, the mean peak value in 'G', 'I' and 'E' was found to be 1.21Nm/kg which is just within the range of approximately 1.19-1.56Nm/kg as measured from the curves of McFadyen and Winter (1988). The differences between the values measured for subjects 'G', 'I' and 'E' and those reported by the other groups may be explained by variations in the style of stair climbing and the extent to which handrails were used.

6.2.2 Joint Angles

In section 6.1.2 the joint angles determined for the stance phase of gait were examined and assessed in relation to those reported by other authors. It was important to perform the same procedure for the activity of stair ascent.

Figure 6.11a shows the hip flexion angle throughout the stance phase of stair ascent. The angle was found to decrease in subjects 'G', 'I' and 'E' from a mean peak value of 72° to a mean minimum value of 12° giving a range of motion of 60°. McFadyen and Winter (1988) and Andriacchi et al (1980) also reported curves of decreasing hip flexion angle throughout the stance phase of stair ascent. The range of motion measured from the typical curve presented by McFadyen and Winter was 50°.

Knee flexion followed a similar pattern to hip flexion, decreasing in subjects 'G', 'I' and 'E' from a mean peak value of 73° to a mean minimum of 11° giving a range of 62°. McFadyen and Winter and Andriacchi et al also presented typical curves showing decreasing knee flexion angle. The range as measured from the typical curve of McFadyen and Winter was 64°.

6.2.3 Muscle Activity Patterns

In section 6.1.3 the predicted muscle activity patterns were examined for the stance phase of gait and compared to EMG measurements as part of the validation process. It is also important to test the validity of the results when the model is applied to other activities. This section therefore examines the patterns of predicted muscle activity for the stance phase of stair ascent and compares the patterns to EMG measurements. The same procedure is carried out in section 6.3.3 for rising from a chair. The EMG data used for comparison purposes for gait in section 6.1.3 was that from the University of California, Berkeley (1953). The Berkeley EMG study also included stair ascent and is therefore used in this section for comparison purposes.

The predicted muscle force curves for subjects 'G', 'I' and 'E' are presented with the EMG data from the University of California, Berkeley (1953) for the stance phase of stair ascent in figures 6.14a-u at the end of section 6.2. The muscle activity patterns predicted in the current study are considered first in the following discussion. They are then compared to the EMG data.

Predicted muscle activity patterns

The predicted activity follows patterns which may be expected from analysis of the joint moment curves in figures 6.8 to 6.10. As in gait, following heel strike, hip abductor activity was required throughout the whole of the stance phase. Significant activity was predicted in gluteus medius throughout the whole of stance providing the abductor activity (fid 6.14f). Gluteus minimus showed significant activity starting from 29-38% stance phase, also providing abductor activity (fig 6.14e).

In addition to abductor activity, hip and knee extensor activity were required throughout the first part of stance. This extensor activity was provided primarily by gluteus maximus and adductor magnus (fig 6.14g,h). Hamstring activity at this time was less than that in gait probably because the moment tending to flex the knee was greater in stair ascent than in gait and any activity in the hamstrings would be highly antagonistic at the knee joint at this time. The required knee extensor activity was provided by the vasti and rectus femoris, the activity in rectus femoris being antagonistic to the requirements at the hip at this time (fig 6.14k-n). The activity in rectus femoris and the vasti lasted longer in subjects 'G' and 'E' than 'I' since the knee moment changed from a tendency to flex to a tendency to extend much later in subjects 'G' and 'E'.

Later in stance, the moment combination at the hip and knee was more variable among subjects. Some activity was observed in adductor longus and iliopsoas in subjects 'I' and 'E' in late stance when the external moment tended to extend the hip or gave a very low tendency to flex (fig 6.14i.q). There was also some activity in the short head of biceps femoris and gastrocnemius in all subjects when the external knee moment changed from one tending to flex to a tendency to extend (fig 6.14d,p). With regard to the two joint muscles, rectus femoris exhibited some activity in subject 'E' when the external moment tended to extend the hip and flex the knee for a small period in late stance (6.14n). There was also a small amount of intermittent activity in the long two joint hamstrings, notably semimembranosus in subject 'I' when the external moment changed from a tendency to flex the knee to a tendency to extend and knee flexor activity was required (fig 6.14c).

Comparison of predicted muscle activity with EMG data

Having examined the patterns of muscle activity predicted in the current study, it was

important to compare these with EMG data as part of the validation process.

Consistency between the patterns of activity predicted in the current study and the EMG data reported by the University of California, Berkeley (1953) was exhibited in early and late stance. In early stance both hip and knee extensor activity were required and activity was shown in both studies in gluteus maximus, the vasti and rectus femoris (fig 6.14g,k,l,m,n). Activity was also predicted in adductor magnus in subjects 'G', 'I' and 'E' and measured in two subjects in the EMG study (fig 6.14h). Later in stance the predicted activity was more variable between subjects 'G', 'I' and 'E' as reflected in the joint moment patterns in figures 6.8 to 6.10. Hip flexor activity was displayed in adductor longus and iliopsoas in subjects 'I' and 'E' in late stance as was the case for the subjects in the EMG study (fig 6.14i,q). Activity was also shown in rectus femoris in subject 'E' in late stance as was the case for one subject in the EMG study (fig 6.14n). Knee flexor activity was displayed in late stance in both the EMG study and subjects 'G', 'I' and 'E' in semimembranosus, the short head of biceps femoris and gastrocnemius (fig 6.14c,d,p). Activity was also shown in both studies in late stance in sartorius (fig 6.14o). Abductor activity was required throughout the stance phase in both studies and supplied by gluteus minimus and gluteus medius (fig 6.14e,f).

Some differences were observed between the two studies in the activity patterns of semitendinosus, the gluteal muscles and tensor fascia lata (fig 6.14a,e,f,g,t). The activity of gluteus minimus started later in subjects 'G', 'I' and 'E' than in the EMG study and the activity in all of the gluteal muscles ended later in 'G', 'I' and 'E' than in the EMG study. Semitendinosus activity was predicted in mid and late stance in 'G', 'I' and 'E' whilst in the EMG study it was measured primarily in late stance. Tensor facia lata was predicted to be active only in late stance in subjects 'G', 'I' and 'E' but activity was also measured in early stance in the EMG study. There are two possible reasons for these differences. Firstly it is possible that the subjects climbed the stairs in such a way that the muscular requirements differed between the subjects in the two studies. Indeed, Joseph and Watson (1967) reported the end point of the activity of gluteus maximus to be variable in stair negotiation. Secondly it is possible that the theoretical model does not exactly predict the action of these muscles. The second explanation is most likely for tensor fascia lata since the model includes the action of this muscle at the hip joint but not at the knee joint.

As observed for gait, there were also some slight differences between the two studies with regard to the timing of muscle activity at the very start and end of the stance phase. At the start, the activity in gluteus maximus, adductor magnus, the vasti and rectus femoris started slightly later in subjects 'G', 'I' and 'E' than in the EMG study (fig 6.14g,h,k,l,m,n). As was the case for gait, this is likely to be due to the model not reflecting the true muscle

activity which occurs prior to heel strike in order to balance the inertial loading. At the very end of the stance phase there were slight differences between the two studies in the timing of the termination of activity in the short head of biceps femoris, gastrocnemius and iliopsoas (fig 6.14d,p,q). Although there were differences in timing at the start and end of the stance phase these were not of major concern since they were not the instants of peak hip joint force.

Overall, as was the case for gait, some differences were observed between the results of the current study and those of the EMG study. However, the majority of the muscles displayed patterns of activity which were consistent between the two studies.

6.2.4 Muscle Force Values

After studying the patterns of muscle activity, it was an important step in the development of the model to examine values of muscle force and assess them in relation to those reported in a selection of past studies before going on to use them in the calculation of joint force. In section 6.1.4 comparisons of muscle forces calculated during gait in subjects 'G', 'I' and 'E' were made to the works of Paul (1967), Morrison (1967), Poulson (1973) and Crowninshield et al (1978a). Paul (1967) did not study stair ascent and although Crowninshield et al (1978a) studied the activity, they did not present muscle forces. Hence the works used for stair ascent comparisons are Morrison (1967) and Poulson (1973). Morrison presented the results for two subjects and Poulson for five. Values quoted in this section from the work of Poulson were measured from the curves which he presented.

Starting with the hip extensors, a mean peak value of 1033N was predicted in gluteus maximus in early stance for subjects 'G', 'I' and 'E'. This lies within the range of 242-2826N predicted by Poulson and is equal to 67% of Poulson's mean peak value of 1546N. Adductor magnus also functioned as a hip extensor in early stance, the mean peak value of force predicted in subjects 'G', 'I' and 'E' being 508N. This lies at the lower end of the range of 290-1920N presented by Poulson and is equal to 40% of Poulson's mean peak of 1268N. Although the results for gluteus maximus and adductor magnus were observed to lie within the range of values presented by Poulson, the mean peak values were less than the mean peak values of Poulson. The difference between the values could be due to variations in the style of stair ascent between subjects in the two studies requiring different muscle activity levels. Indeed, McFadyen and Winter (1988) found the hip joint moment to be highly variable between subjects in stair ascent. Differences could also occur due to the differences in methodology used in the calculation of muscle force.

The quadriceps femoris group was predicted to be active in subjects 'G', 'I' and 'E' in early stance when the external moment tended to flex the knee joint. This group includes

the vasti and rectus femoris. A mean peak value of 1774N was predicted in the vasti which is 1.8 times the value of 990N predicted by Poulson and just outside his range of 326-1618N. As was the case for the hip extensors, this difference could be due to variations in the style of stair climbing and also due to differences in methodology used to calculate muscle forces.

Rectus femoris was predicted to be active with the vasti in early stance even though its action at the hip joint was antagonistic. Its activity was necessary in order that the external knee joint moment was balanced whilst muscle stresses were kept as low as possible. Adding the predicted force of 327N for rectus femoris to that of 1774N in the vasti gives a quadriceps force of 2101N. This is 1.1 times the value of 1931N predicted by Morrison.

Later in stance when the external moment tended to extend the knee, gastrocnemius became active in subjects 'G', 'I' and 'E', the mean peak force in this muscle being 325N. This value is only 19% of the mean peak value of 1675N predicted by Poulson and outwith his range of 853-2448N. It is much closer to the mean peak value of 352N reported by Morrison. Again, the difference between the value predicted in the current study and that reported by Poulson could be due to variation in the style of stair ascent between the subjects in the two studies. Such variation was observed between subjects 'G', 'I' and 'E', the peak moment tending to extend the knee joint being three times greater in 'I' than 'G' or 'E'. Differences could also occur due to the differences in the methodology used in the calculation of muscle force.

Peak activity in iliopsoas also occurred in late stance, the mean peak force in subjects 'G', 'I' and 'E' being 139N. This is only 23% of the value of 612N predicted by Poulson and also outwith his predicted range of 419-934N. Again, this difference could be due to variation in the style of stair climbing and also due to differences in methodology used in the calculation of muscle force.

Hamstring activity of approximately 378N was predicted in late stance in subjects 'G', 'I' and 'E' whilst Poulson predicted 354N.

Finally, hip abductor activity was predicted throughout the whole of stance in subjects 'G', 'I' and 'E' due to the action of gluteus medius, gluteus minimus and tensor fascia lata. Two peaks of activity were predicted, the first with a mean value of 822N and the second, 775N. The first peak of 822N is only 32% of the value of 2560N predicted by Poulson and also outwith his range of 1353-4106N. The second peak of 775N is equal to 76% of the value of 1015N predicted by Poulson and also outwith his range of 966-1715N. Again, these differences could be caused by variations in the style of stair ascent and also by differences in the methodology used in the calculation of muscle force.

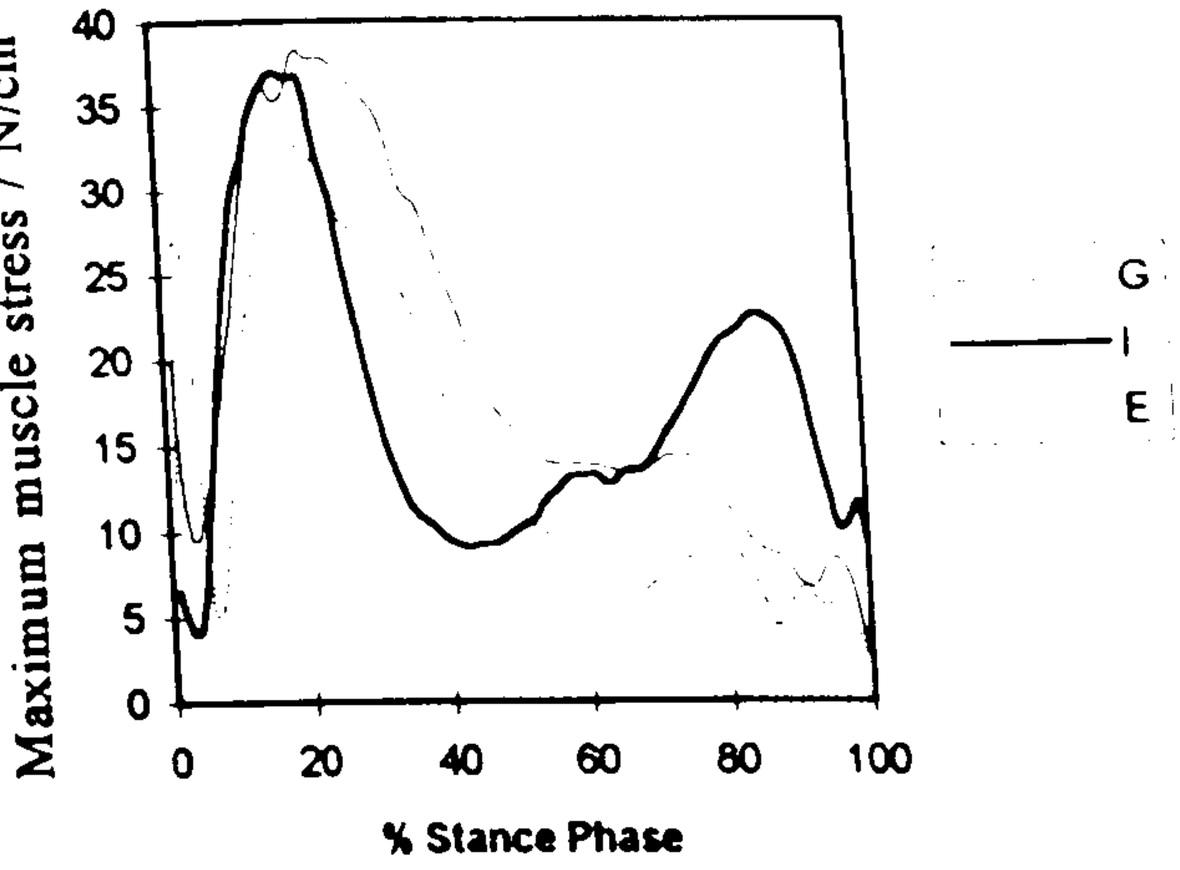

Figure 6.12 Maximum muscle stress calculated for subjects 'G', 'I' and 'E' during the stance phase of stair ascent.

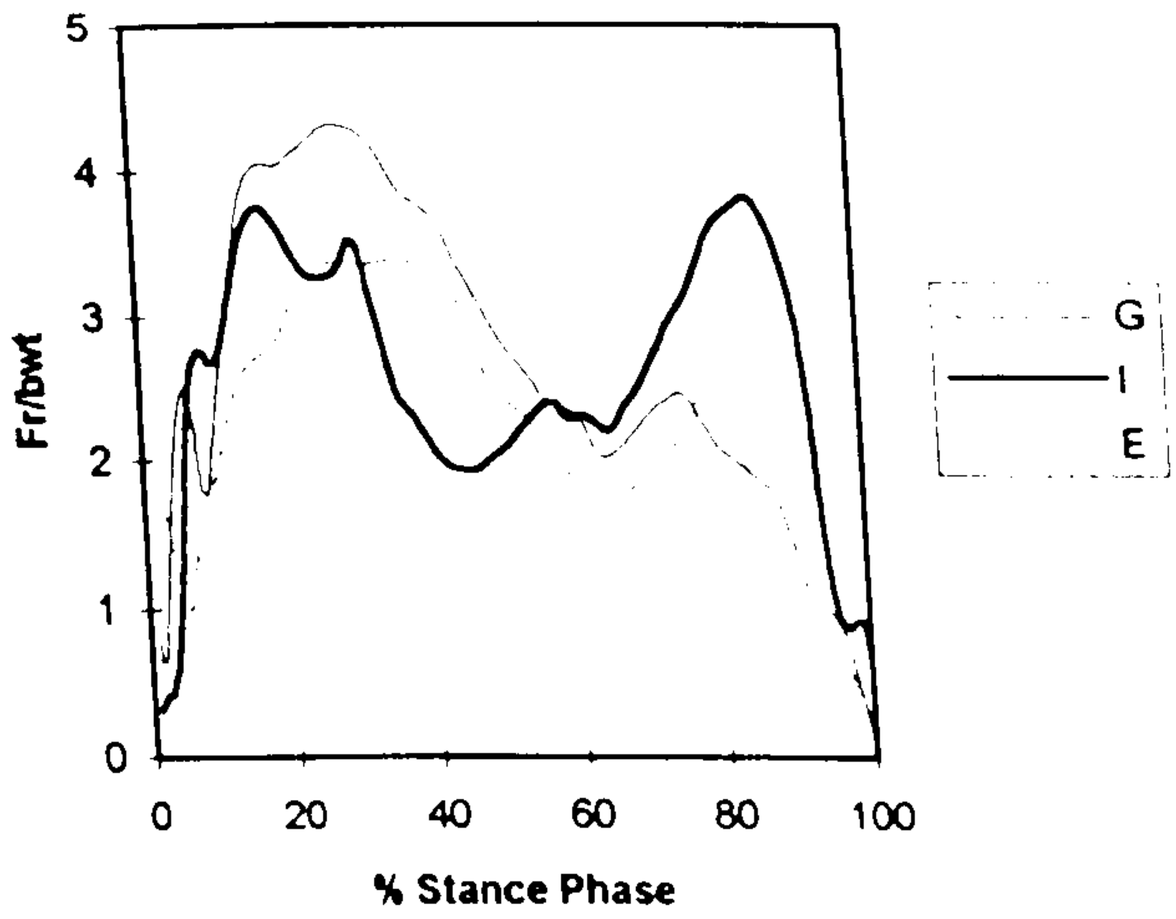

Figure 6.13 Resultant hip joint force, Fr, in terms of body weight calculated for subjects 'G', 'I' and 'E' during the stance phase of stair ascent.

6.2.5 Muscle Stress

Having considered muscle force, this section is concerned with muscle stress. In section 6.1.5 muscle stresses produced during the stance phase of gait were assessed as part of the validation process to ensure that they were physiologically reasonable. In order to further check the validity of the results, the muscle stresses produced in other activities must be assessed to ensure that they are physiologically reasonable. This section therefore assesses the maximum muscle stress in the stance phase of stair ascent whilst section 6.3.5 discusses the maximum muscle stress in rising from a chair.

Figure 6.12 shows the maximum muscle stress calculated for subjects 'G', 'I' and 'E' during the stance phase of stair ascent. The mean of the maximum muscle stresses exhibited by subjects 'G', 'I' and 'E' during stair ascent was 36N/cm^2 with a maximum value of 38.3 N/cm^2 occurring in subject 'G'. As was the case for gait, these values are well below the upper limit of the range of estimations of maximum achievable muscle stress. This range was quoted as 10-100N/cm^2 by Kaufman et al (1991).

6.2.6 Ankle Moment Balance

As described in section 6.1.6, the final stage in the model development was to check that ankle joint moment balance could be achieved since ankle joint moment equilibrium had not been included in the model. This was carried out for gait in section 6.1.6. It is also important to check that ankle joint moment equilibrium can be achieved in other activities. This section ensures that ankle joint equilibrium can be achieved during stair ascent and section 6.3.6 ensures that it can be achieved in rising from a chair. The maximum unbalanced ankle joint moment during stair ascent was 75Nm tending to dorsiflex the ankle in subject 'G' in late stance. It has already been shown in section 6.16 that a greater unbalanced moment of 83Nm can be balanced by the ankle joint plantarflexors not already included in the model whilst the muscle stress is maintained at a physiologically reasonable level. Hence if the assumptions made in the calculation in section 6.1.6 are made here, then it is possible to balance the smaller residual moment of 75Nm whilst maintaining the muscle stress at a physiologically reasonable level.

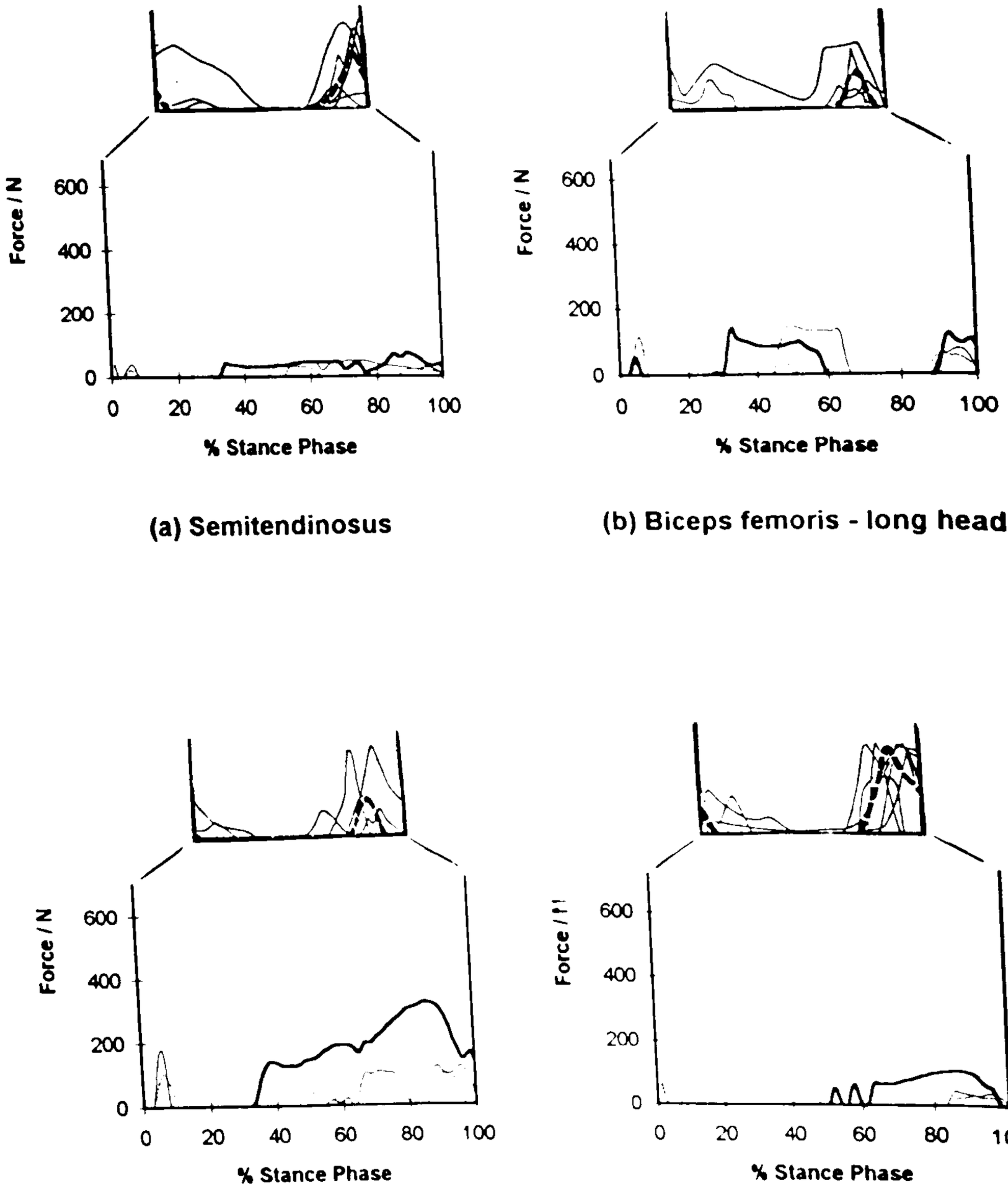

Figure 6.14 Muscle activity during the stance phase of stair ascent.

For each muscle the top figure shows the EMG data of the University of California, Berkeley (1953). The dotted line on the EMG curves represents the average curve for all subjects in the EMG study.

For each muscle the bottom figure shows the predicted muscle activity in the current study for subjects 'G', 'I' and 'E'.

G
I
E

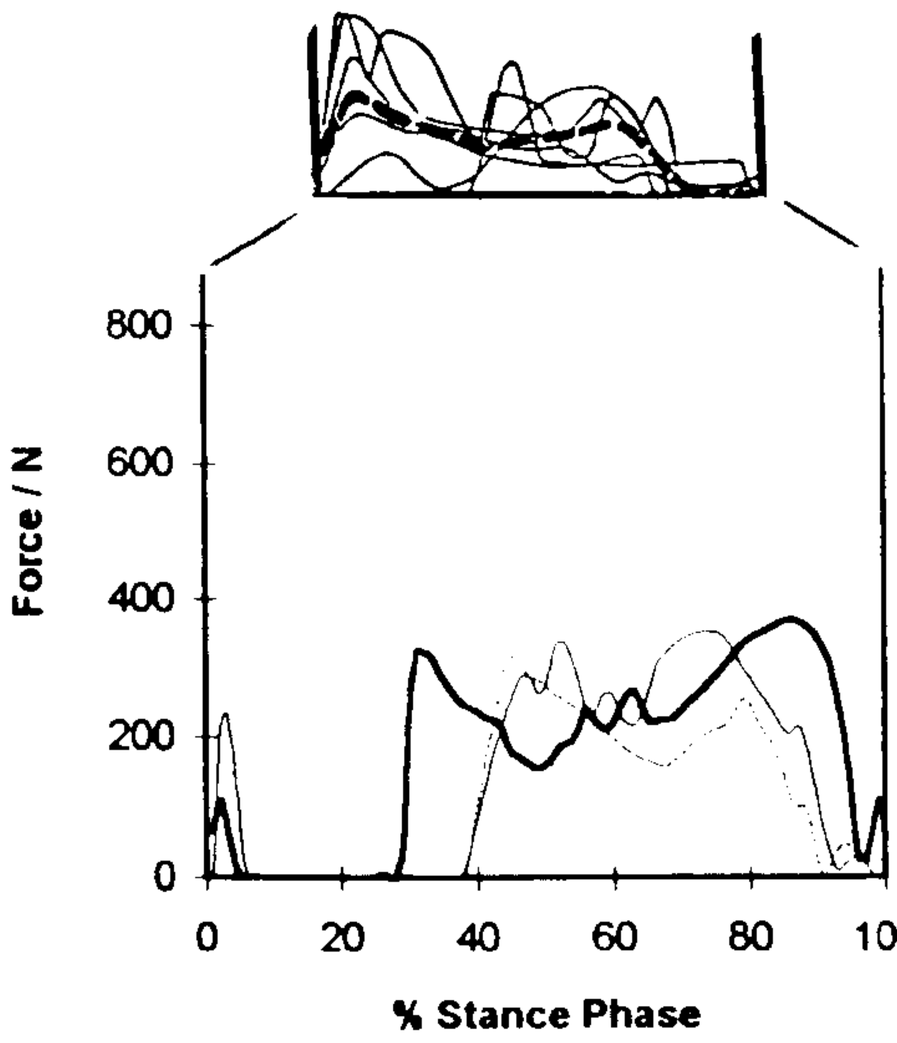

(e) Gluteus minimus

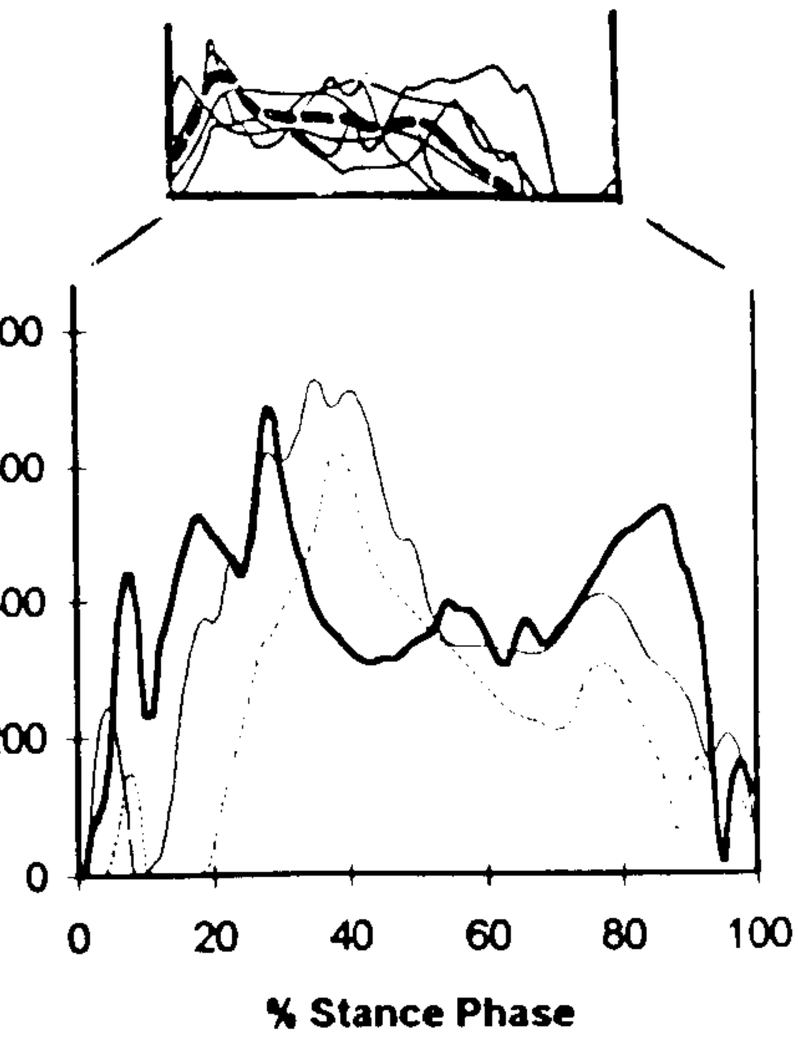

(f) Gluteus medius

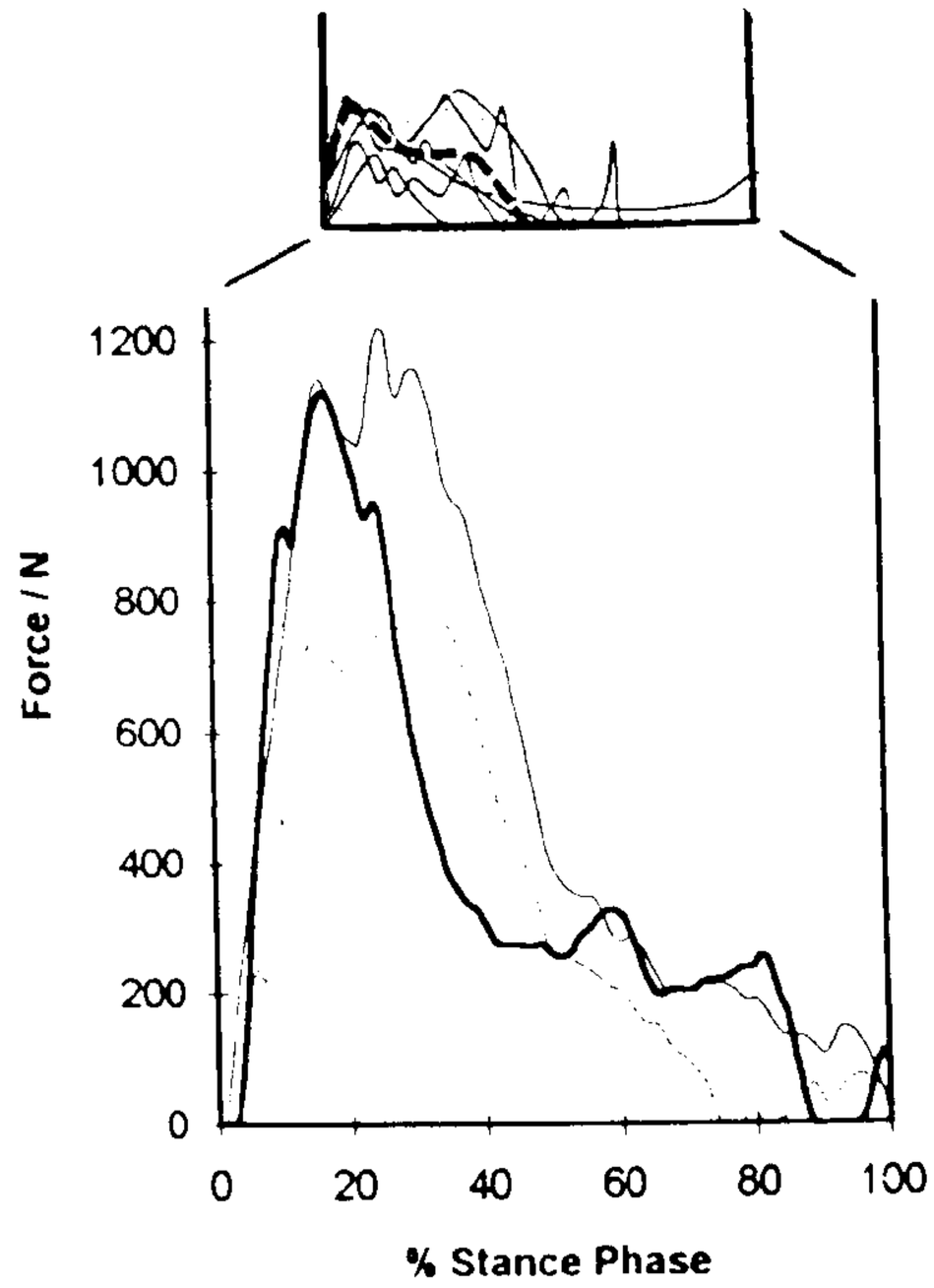

(g) Gluteus maximus

Figure 6.14 continued. Muscle activity during the stance phase of stair ascent.

For each muscle the top figure shows the EMG data of the University of California, Berkeley (1953). The dotted line on the EMG curves represents the average curve for all subjects in the EMG study.

For each muscle the bottom figure shows the predicted muscle activity in the current study for subjects 'G', 'I' and 'E'.

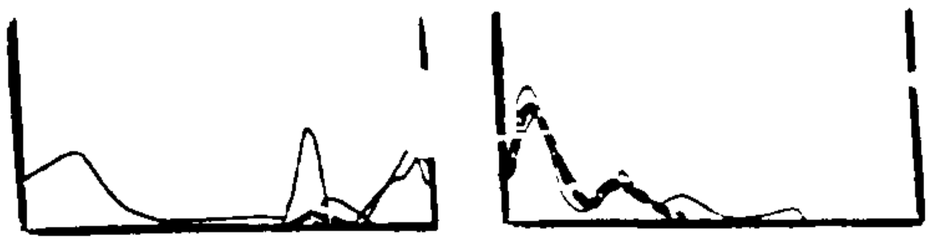

EMG data
4 subjects

EMG data
2 subjects

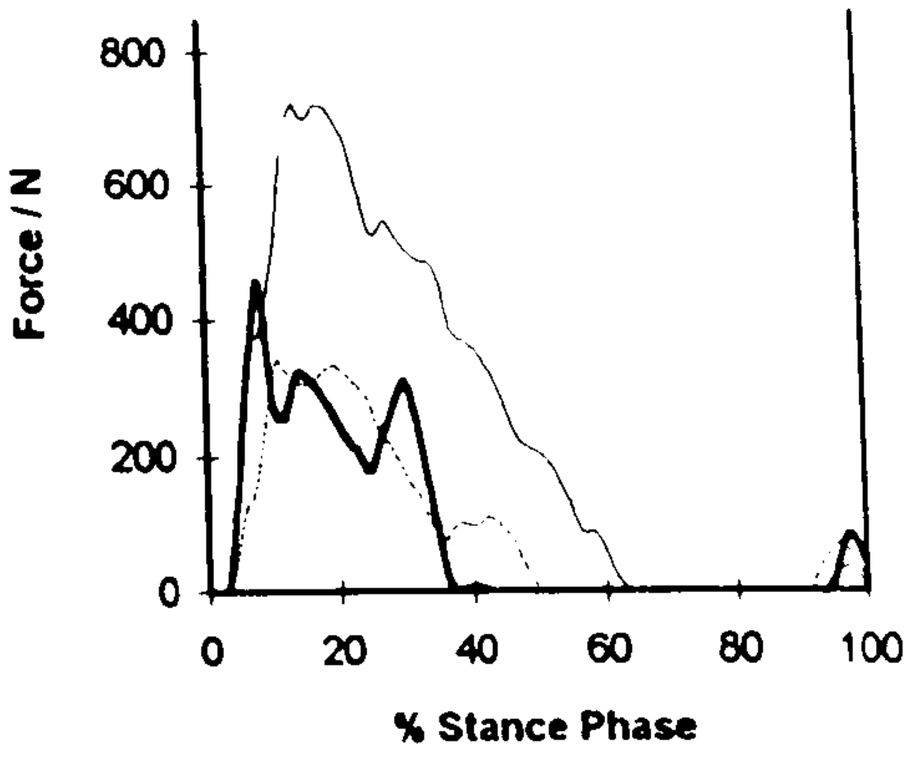

(h) Adductor magnus

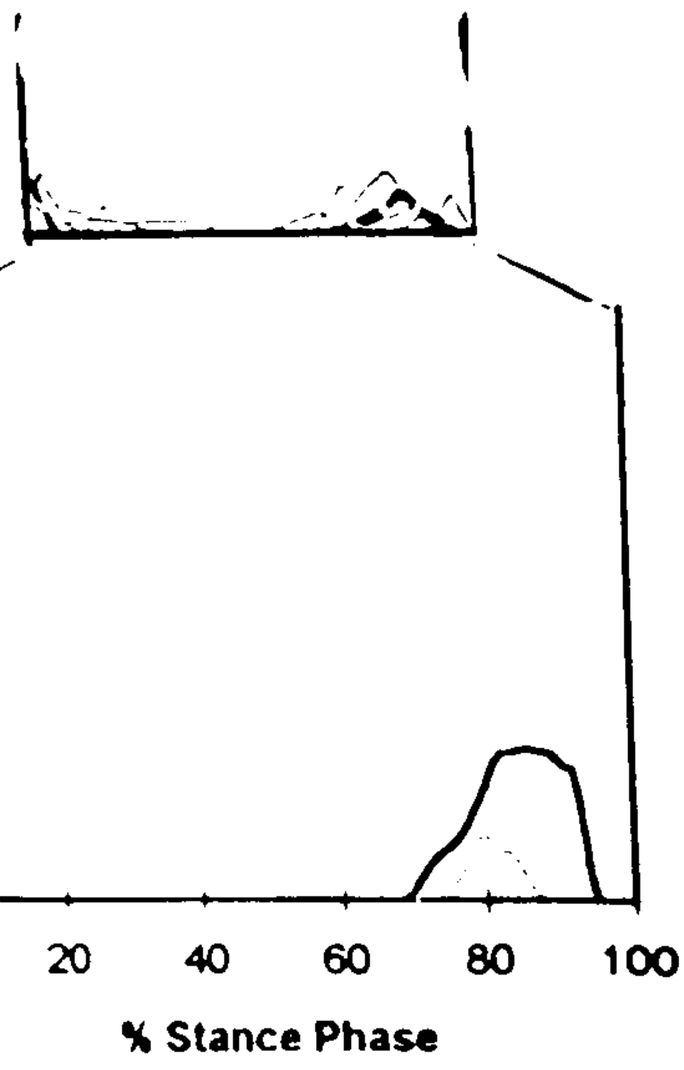

(i) Adductor longus

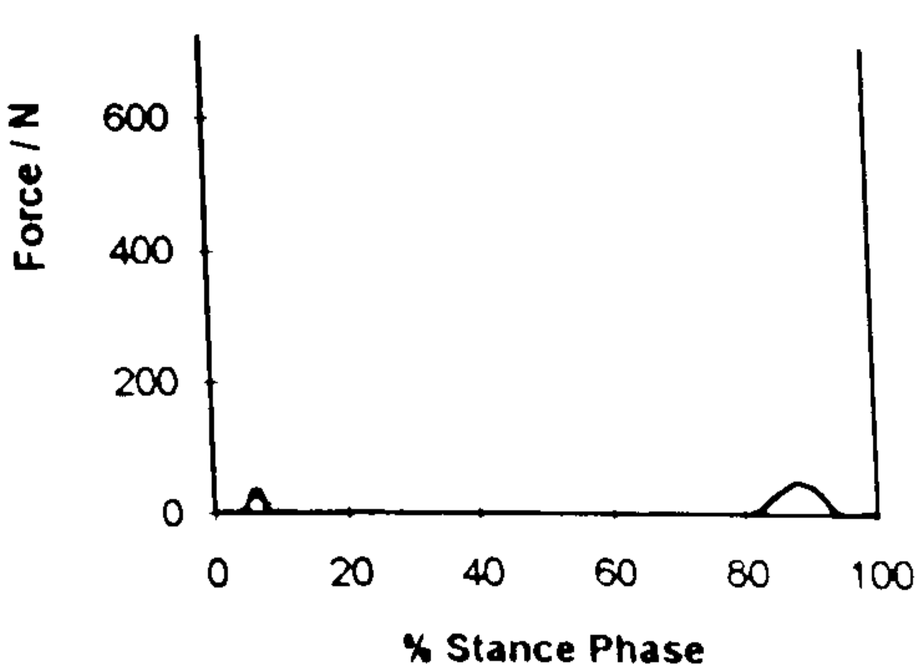

(j) Adductor brevis

Figure 5.14 continued. Muscle activity during the stance phase of stair ascent.

(h) Adductor magnus and (i) adductor longus activity. For each of these muscles the top figure shows the EMG data of the University of California, Berkeley (1953). The dotted line on the EMG curves represents the average curve for all subjects in the EMG study. The bottom figure for each of these muscles shows the predicted activity in the current study for subjects 'G', 'I' and 'E'

(j) Predicted activity in adductor brevis in the current study for subjects 'G', 'I' and 'E'

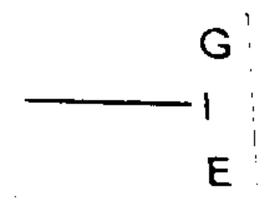

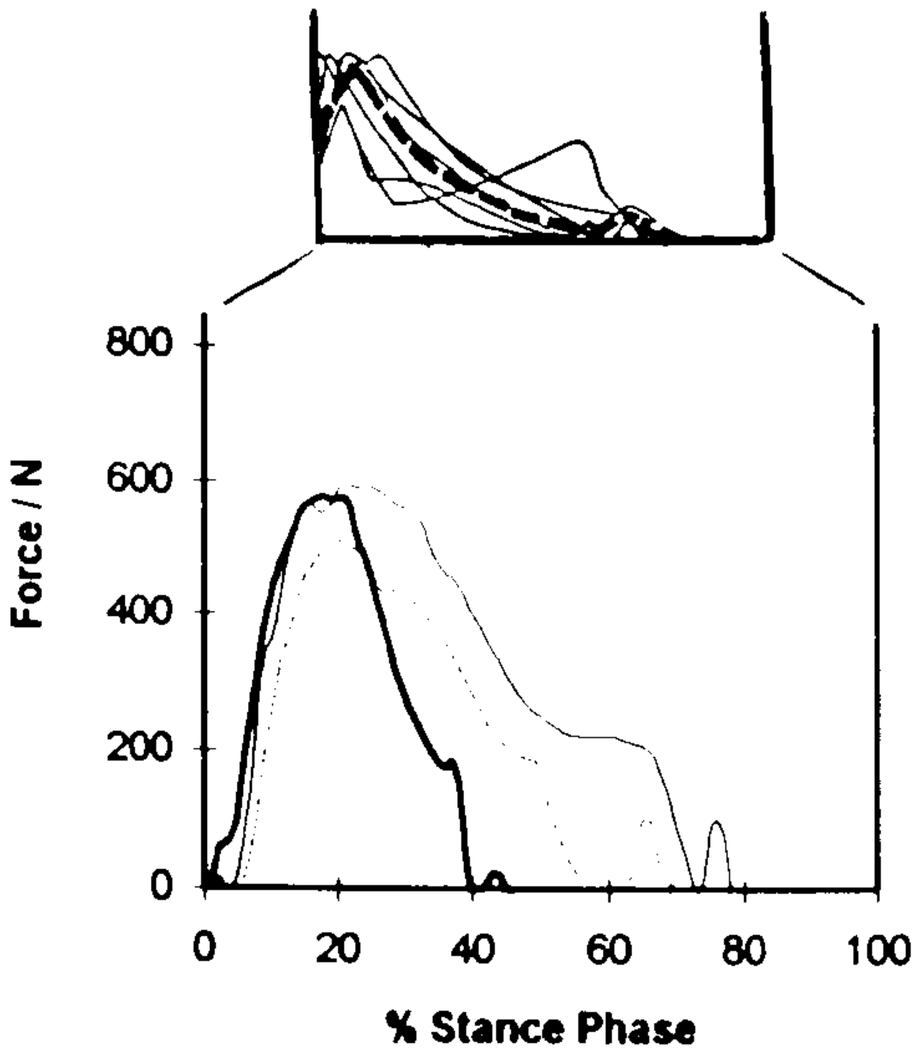

(k) Vastus medialis

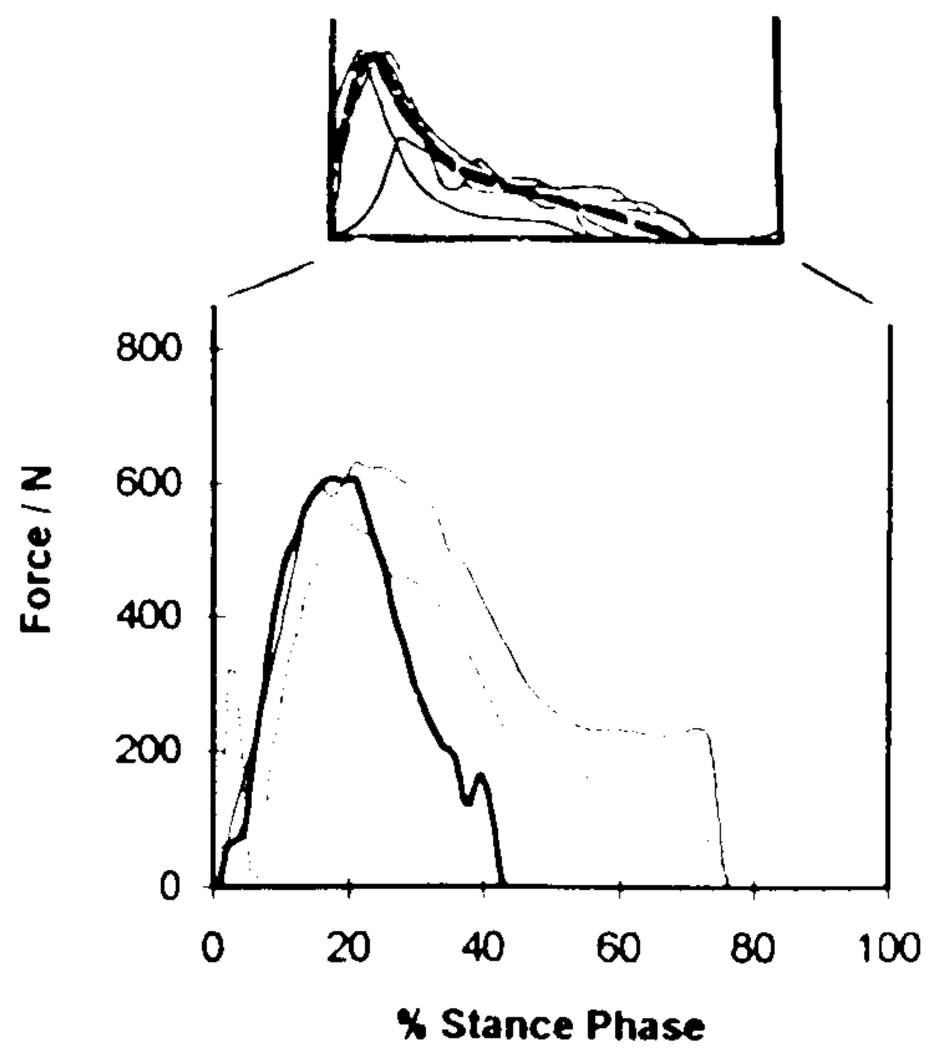

(l) Vastus lateralis

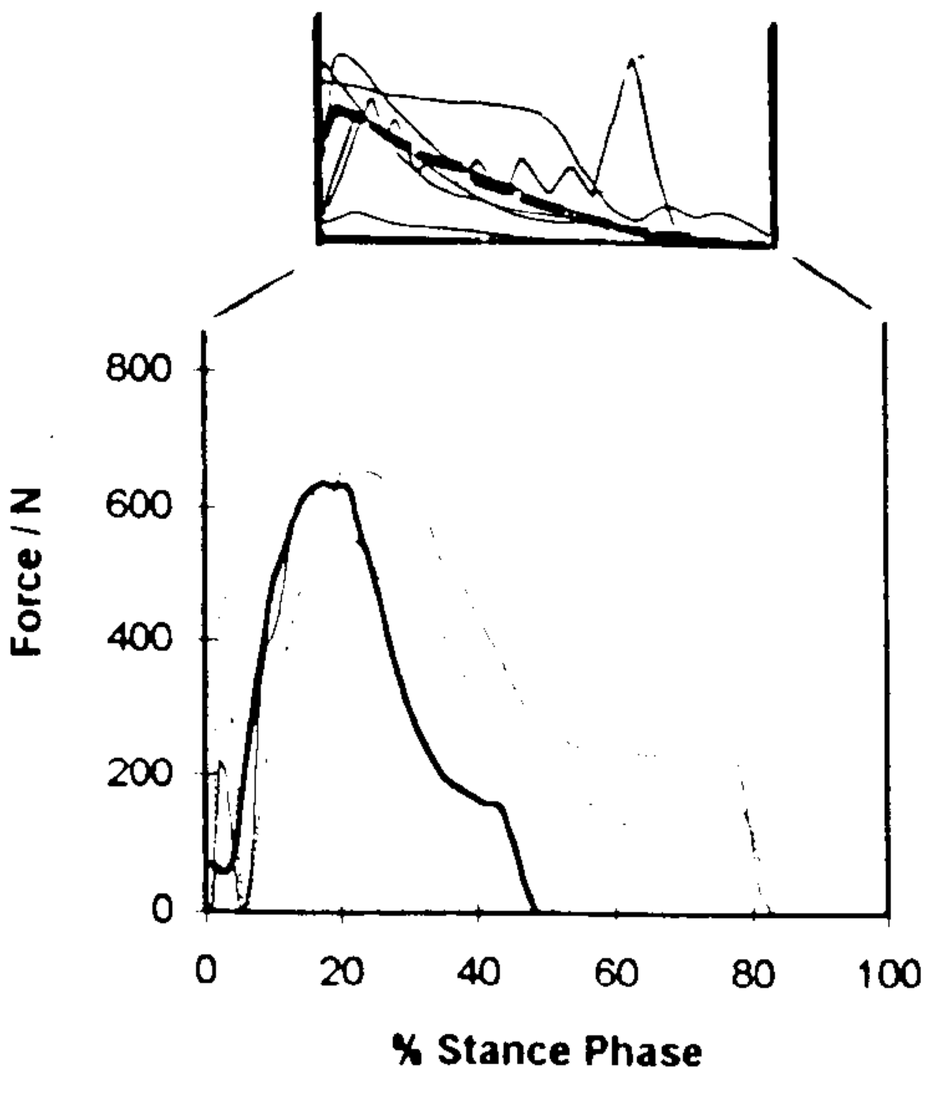

(m) Vastus intermedius

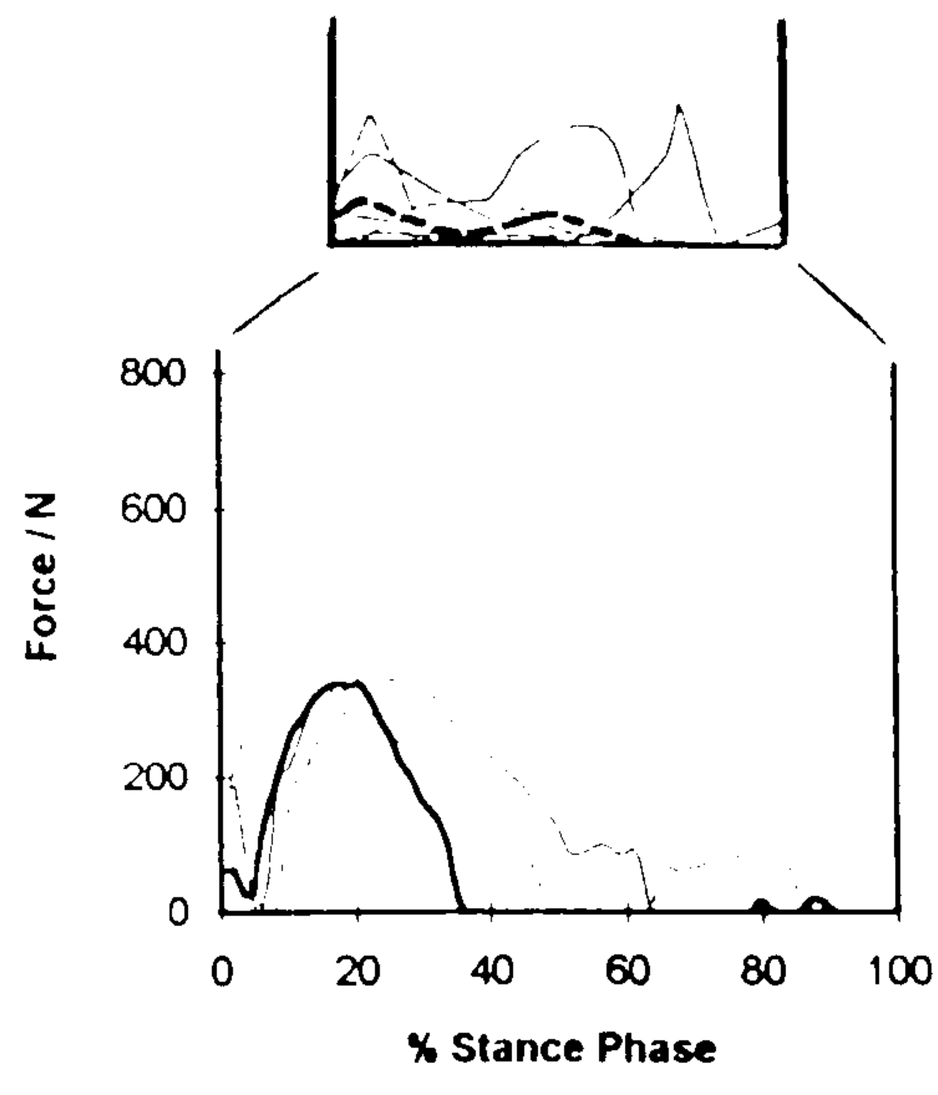

(n) Rectus femoris

Figure 6.14 continued. Muscle activity during the stance phase of stair ascent.

For each muscle the top figure shows the EMG data of the University of California, Berkeley (1953). The dotted line on the EMG curves represents the average curve for all subjects in the EMG study.

For each muscle the bottom figure shows the predicted muscle activity in the current study for subjects 'G', 'I' and 'E'.

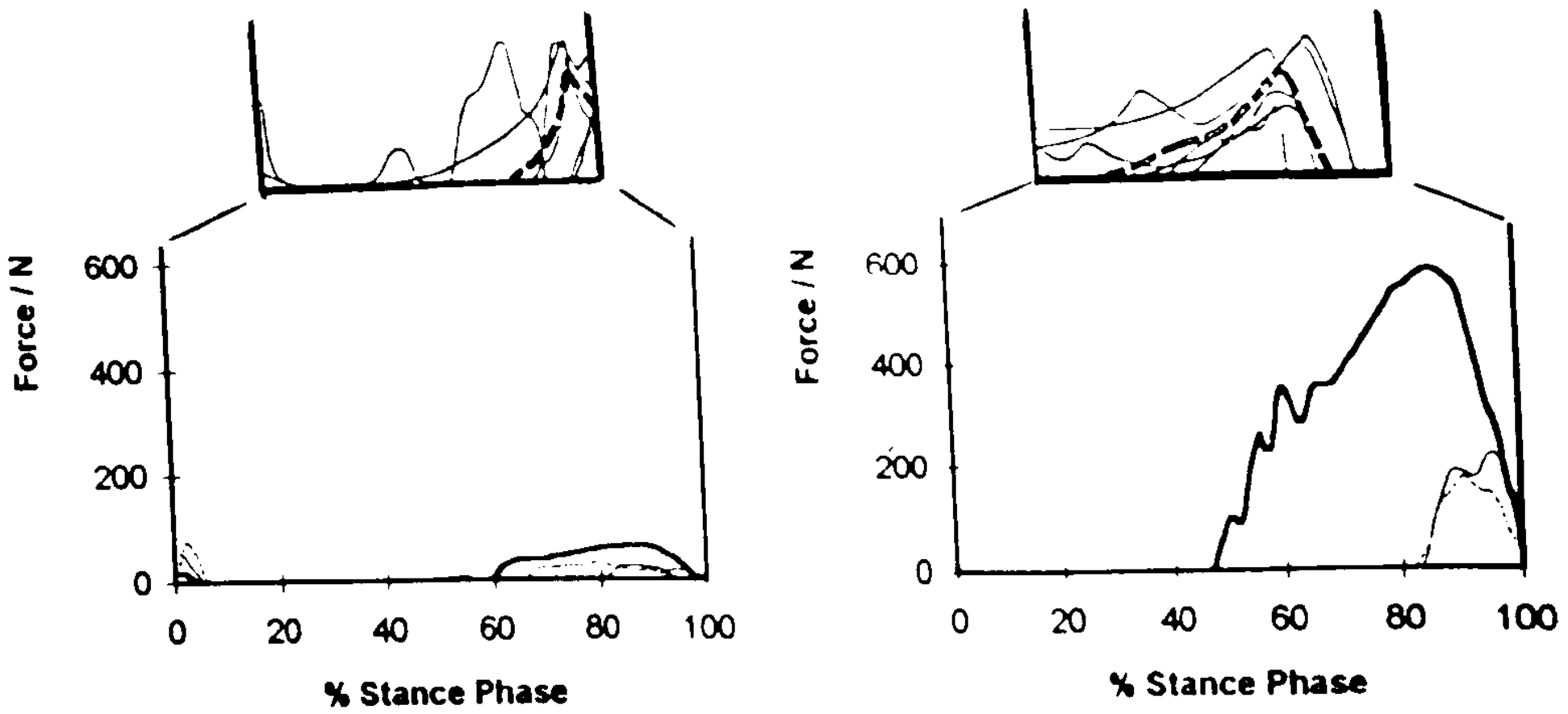

(o) Sartorius

(p) Gastrocnemius

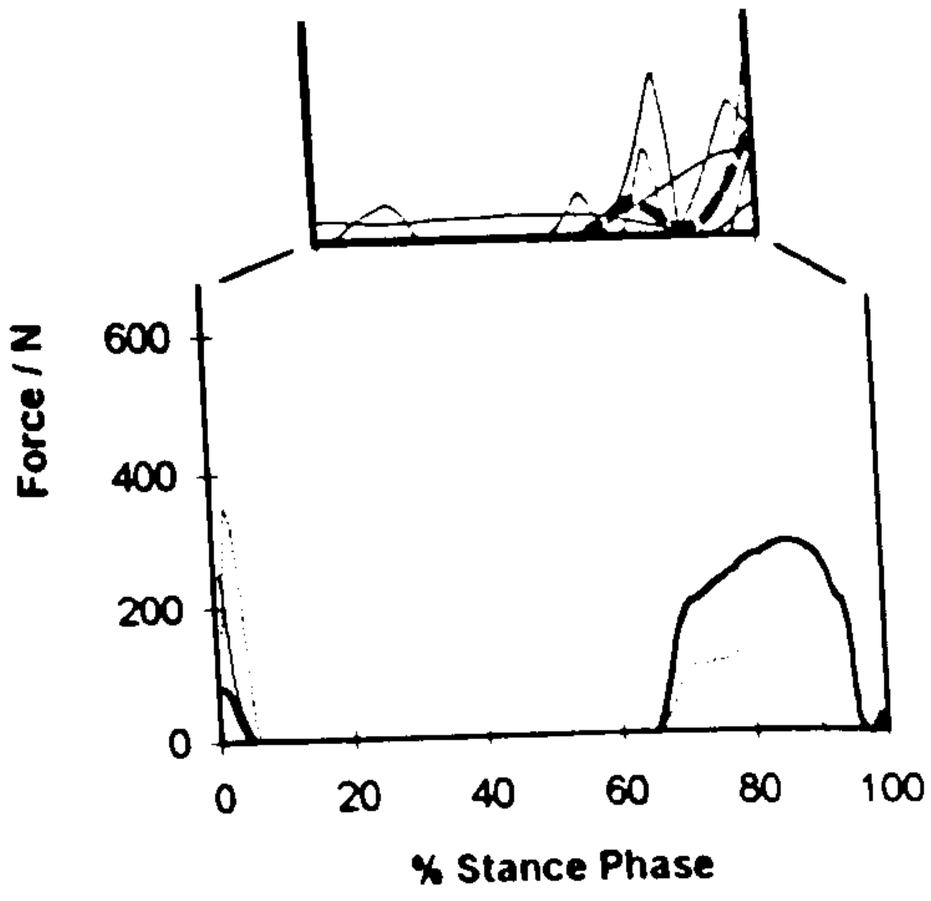

(q) Iliopsoas

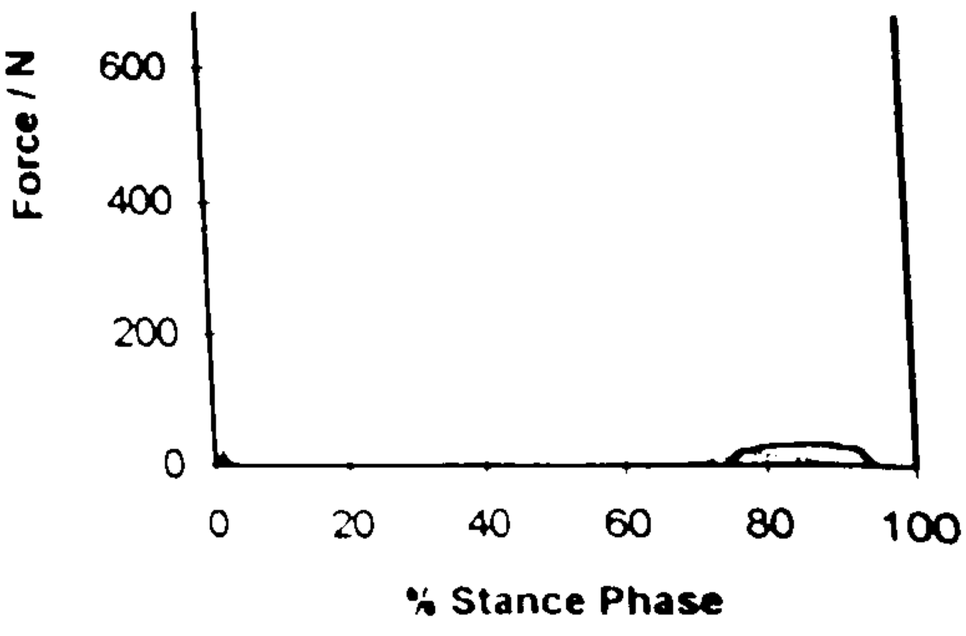

(r) Pectineus

Figure 6.14 continued. Muscle activity during the stance phase of stair ascent.

(o) Sartorius and (p) gastrocnemius activity. For each of these muscles the top figure shows the EMG data of the University of California, Berkeley (1953). The dotted line on the EMG curves represents the average curve for all subjects in the EMG study. The bottom figure for each of these muscles shows the predicted activity in the current study for subjects 'G', 'I' and 'E'.

(q) Iliopsoas activity. The layout of the figures is as for (o) and (p). EMG data is for iliacus and predicted activity in subjects 'G', 'I' and 'E' is for iliacus and psoas combined (i.e. iliopsoas).

(r) Predicted activity in pectineus in the current study for subjects 'G', 'I' and 'E'.

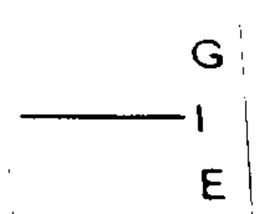

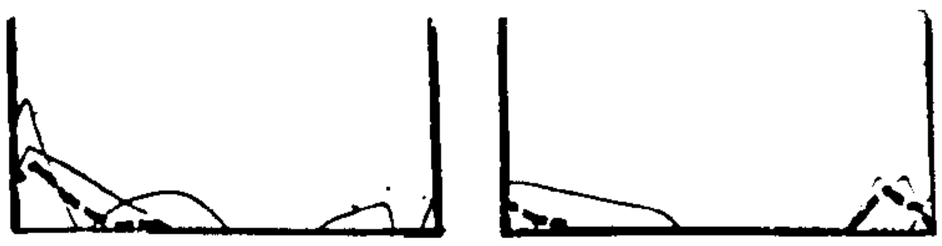

EMG data
3 subjects

EMG data
3 subjects

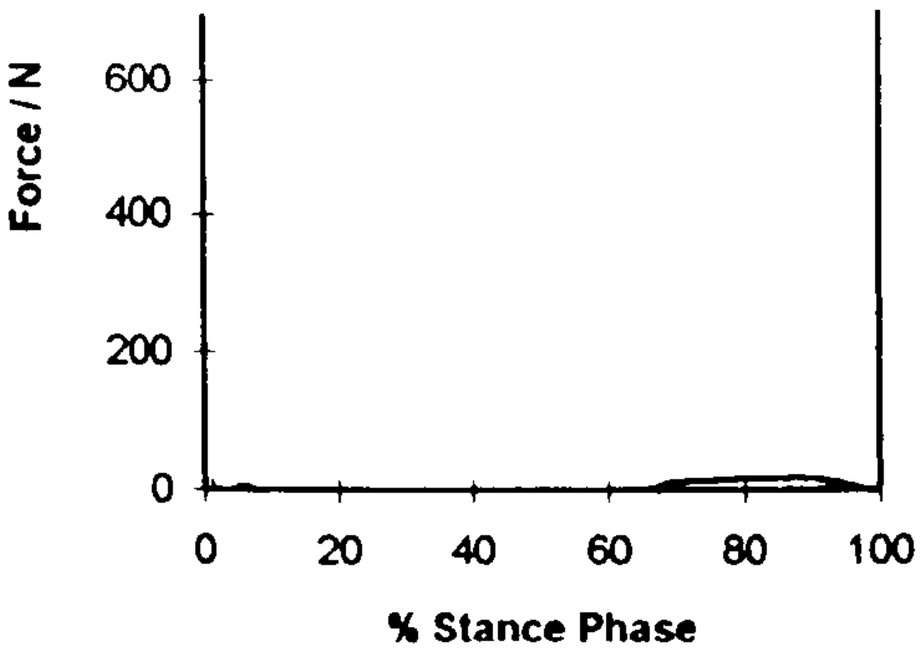

(s) Gracilis

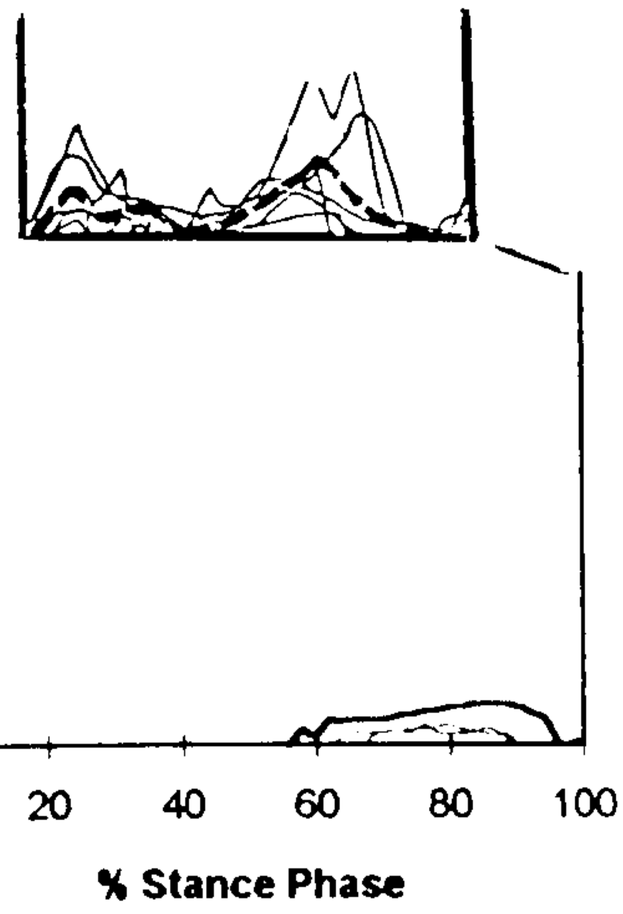

(t) Tensor fascia lata

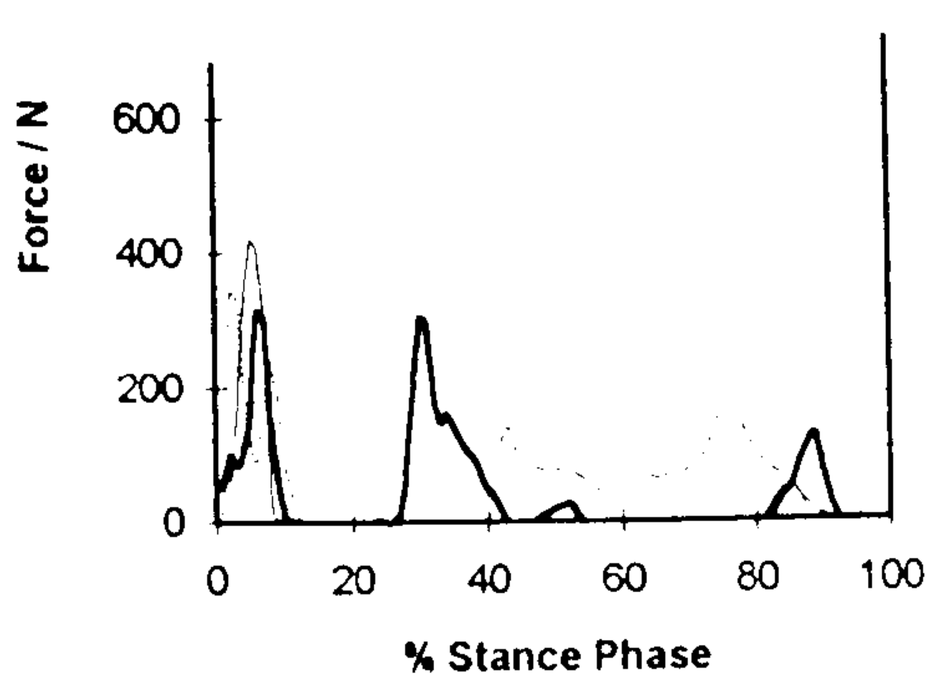

(u) External rotators

Figure 6.14 continued. Muscle activity during the stance phase of stair ascent.

(s) Gracilis and (t) tensor fascia lata activity. For each of these muscles the top figure shows the EMG data of the University of California, Berkeley (1953). The dotted line on the EMG curves represents the average curve for all subjects in the EMG study. The bottom figure for each of these muscles shows the predicted activity in the current study for subjects 'G', 'I' and 'E'.

(u) Predicted activity in the external rotators (gemellus inferior, gemellus superior, obturator internus, piriformis, quadratus femoris and obturator externus) in the current study for subjects 'G', 'I' and 'E'.

(a) Sagittal plane hip joint moment ($Mz_{HC\ .\ F}$). A positive moment indicates an external moment tending to flex the hip joint and hip extensor muscle activity. A negative moment indicates an external moment tending to extend the hip joint and hip flexor muscle activity.

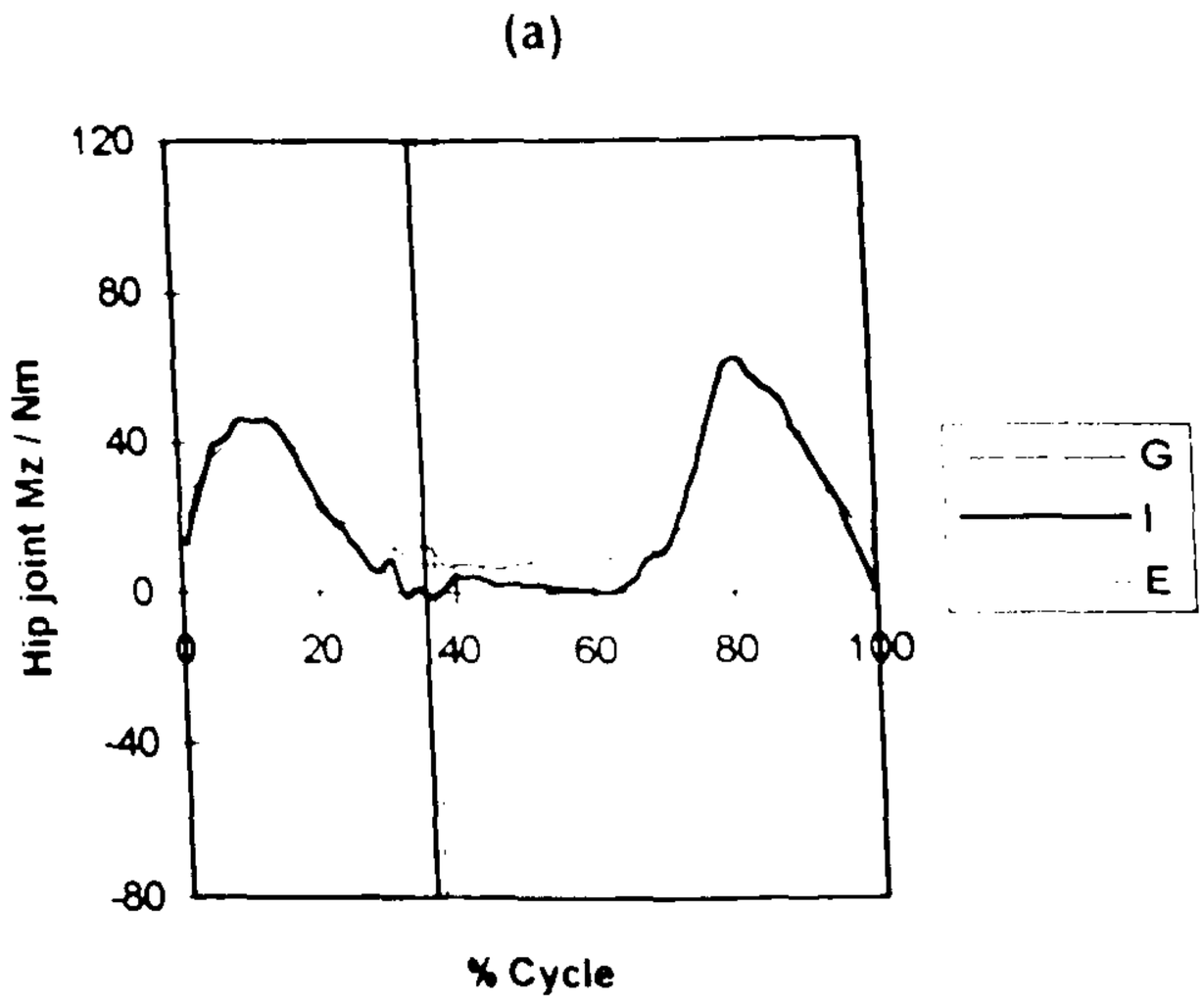

(b) Frontal plane hip joint moment ($Mx_{HC\ .\ F}$). A positive moment indicates an external moment tending to adduct the hip joint and hip abductor muscle activity. A negative moment indicates an external moment tending to abduct the hip joint and hip adductor muscle activity.

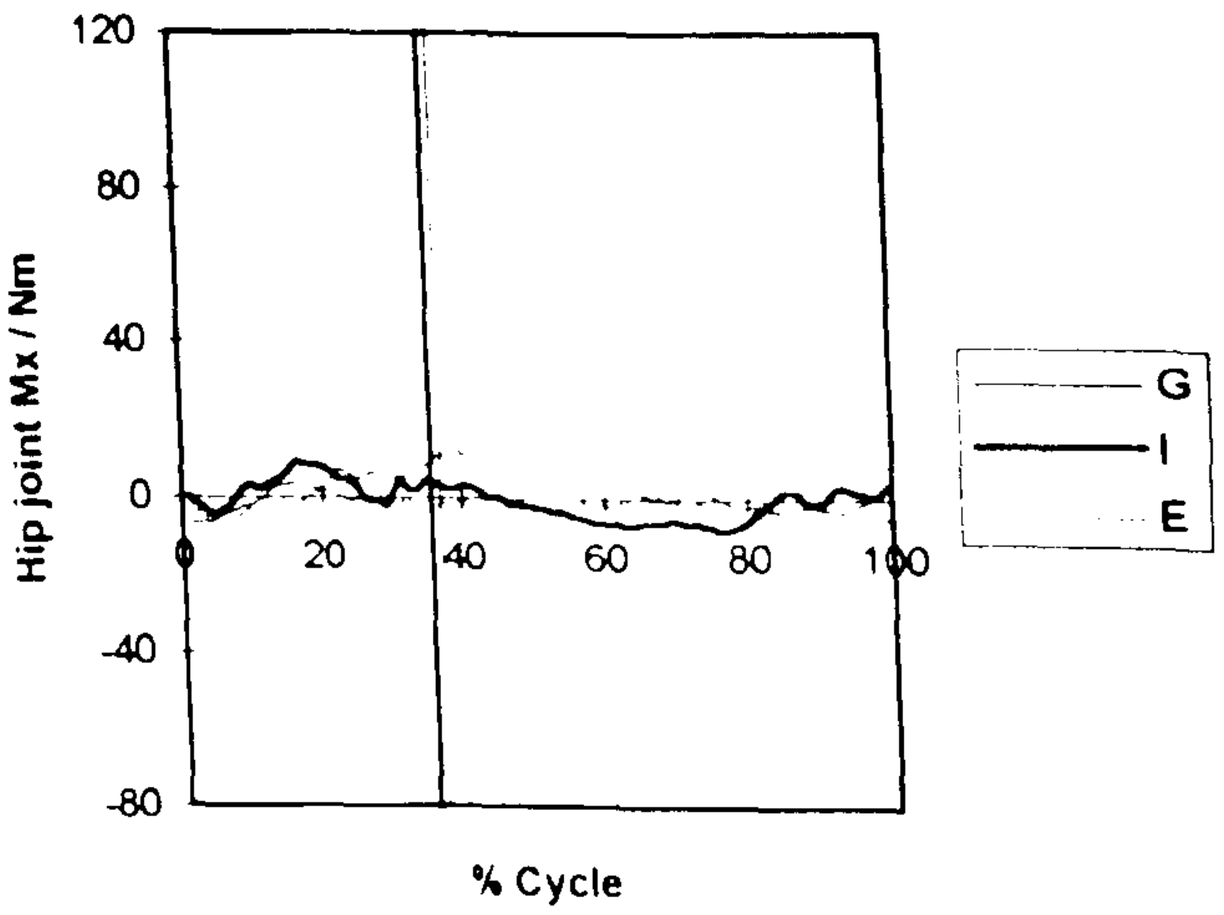

(c) Transverse plane hip joint moment ($My_{HC\ .\ F}$). A positive moment indicates an external moment tending to internally rotate the femur relative to the pelvis and hip external rotator muscle activity. A negative moment indicates an external moment tending to externally rotate the femur relative to the pelvis and hip internal rotator muscle activity.

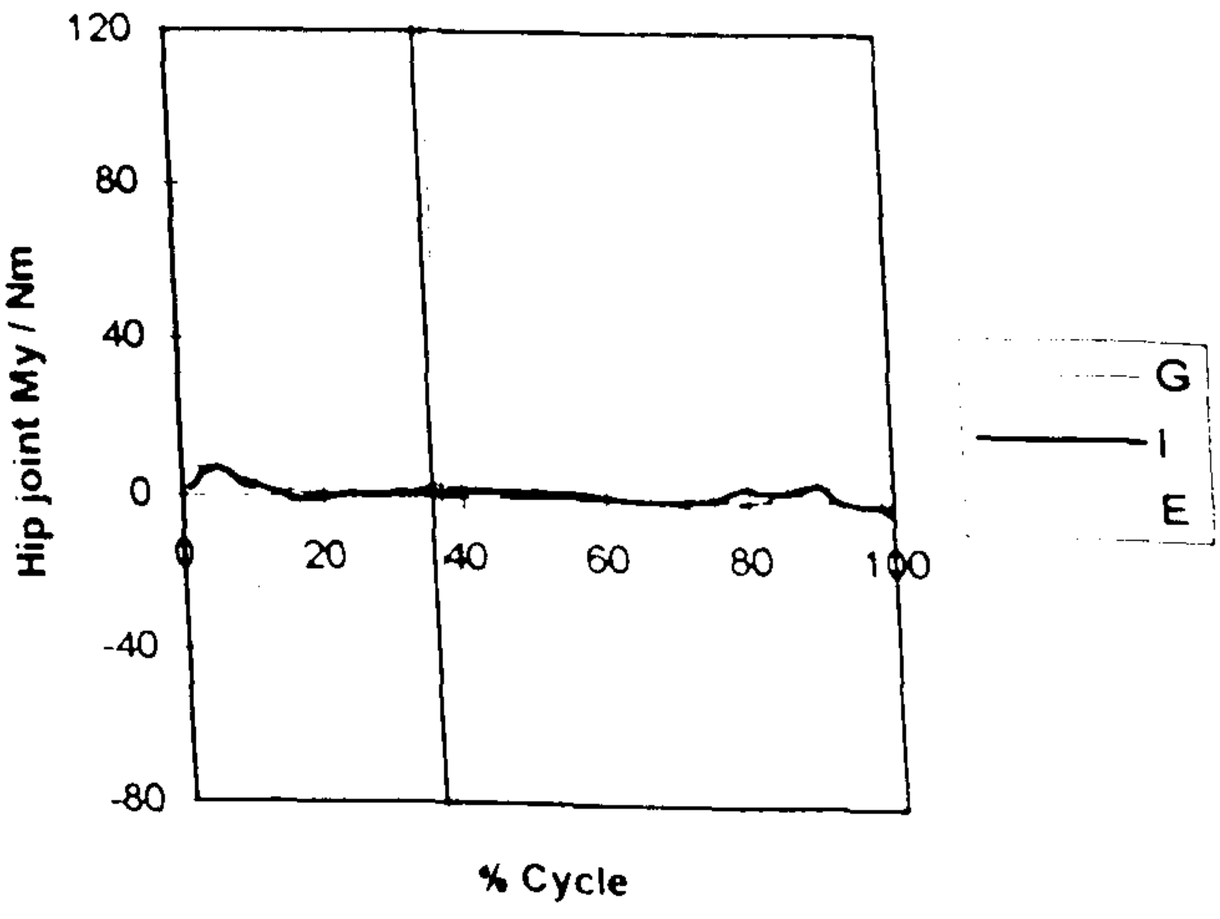

Figure 6.15 Hip joint moments measured in subjects 'G', 'I' and 'E' when rising from and sitting down onto a chair. The cycle starts when the subject loses contact with the seat and ends when the subject makes contact with the seat again. The vertical lines indicate the time at which each subject finished rising and was standing upright

6.3 RISING FROM A CHAIR

Having assessed the results of the model at the various stages of calculation for gait and stair ascent, the final activity to be examined is that of rising from a chair. Each subject rose from the chair at their natural speed. The subjects were instructed to use their hands on the edge of the chair to aid rising as required. The curves of joint moment, joint angle, muscle force, muscle stress and hip joint force shown in figures 6.15 to 6.21 include both rising from the chair and sitting down again. The vertical lines on each curve indicate the instant at which each subject finished rising and was fully upright. This section is concerned with the first part of each curve which presents the results for rising.

6.3.1 Joint Moments

In sections 6.1.1 and 6.1.2 the patterns and values of joint moment for gait and stair ascent were examined and assessed in relation to those reported by other authors before going on to use them in the calculation of muscle forces. It was important for the development of the model to perform the same process for the activity of rising from a chair.

The joint moments calculated for subjects 'G', 'I' and 'E' whilst rising from a chair are presented in figures 6.15 to 6.17. The external moment at the hip joint tends to flex the hip throughout all stages of rising. That at the knee joint tends to flex the knee until the late stages of rising when it changes to become a tendency to extend. The mean peak moment tending to flex the hip joint in subjects 'G', 'I' and 'E' was 49Nm. When normalized to body mass this is 0.76Nm/kg. That at the knee joint was 41Nm which is equivalent to 0.63Nm/kg.

There have been many studies concerned with the biomechanics of rising from a chair with a variety of results as different methods of rising were investigated. Pai and Rogers (1991) looked into the effects of speed of rising on joint moments. Fleckenstein et al (1988) evaluated the effect of limited knee flexion range on peak hip joint moments during rising. Rodosky et al (1989) examined the influence of chair height on hip and knee joint moments and Wretenberg et al (1993) looked at the effect of armrests and the different ways of using them on hip and knee joint moments. Doorenbosch et al (1994) compared the hip and knee joint moments in two strategies of rising. In one, subjects were instructed to rise naturally (NSTS) and in the other they were told to rise with full flexion of the trunk (FSTS). A sample of the results of these studies is given in table 6.2. As can be seen from table 6.2, the mean peak values of moment tending to flex the hip and knee joints in subjects 'G', 'I' and 'E' lie within the wide range of values reported by other authors.

As can be seen from figures 6.15b and 6.15c the values of the moments at the hip joint in the frontal and transverse planes were much lower than those in the sagittal plane.

Figure 6.16

Sagittal plane knee joint moment ($Mz_{KC\ .\ S}$) measured in subjects 'G', 'I' and 'E' when rising from and sitting down onto a chair. The cycle starts when the subject loses contact with the seat and ends when the subject makes contact with the seat again. A positive moment indicates an external moment tending to extend the knee joint and knee flexor muscle activity. A negative moment indicates an external moment tending to flex the knee joint and knee extensor muscle activity.

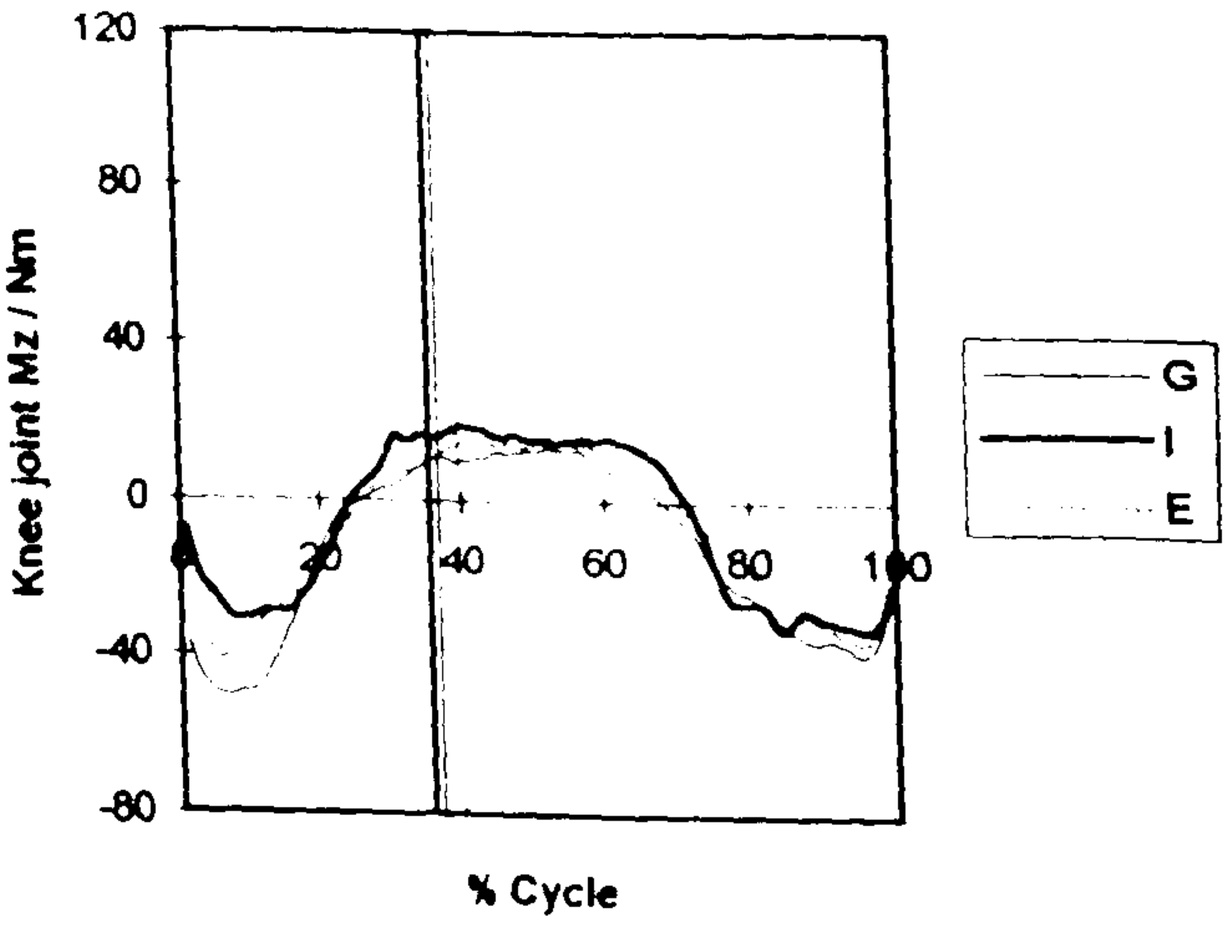

Figure 6.17

Sagittal plane ankle joint moment ($Mz_{AC\ .\ S}$) measured in subjects 'G', 'I' and 'E' when rising from and sitting down onto a chair. The cycle starts when the subject loses contact with the seat and ends when the subject makes contact with the seat again. A positive moment indicates an external moment tending to dorsiflex the ankle joint and ankle plantarflexor muscle activity. A negative moment indicates an external moment tending to plantarflex the ankle joint and ankle dorsiflexor muscle activity.

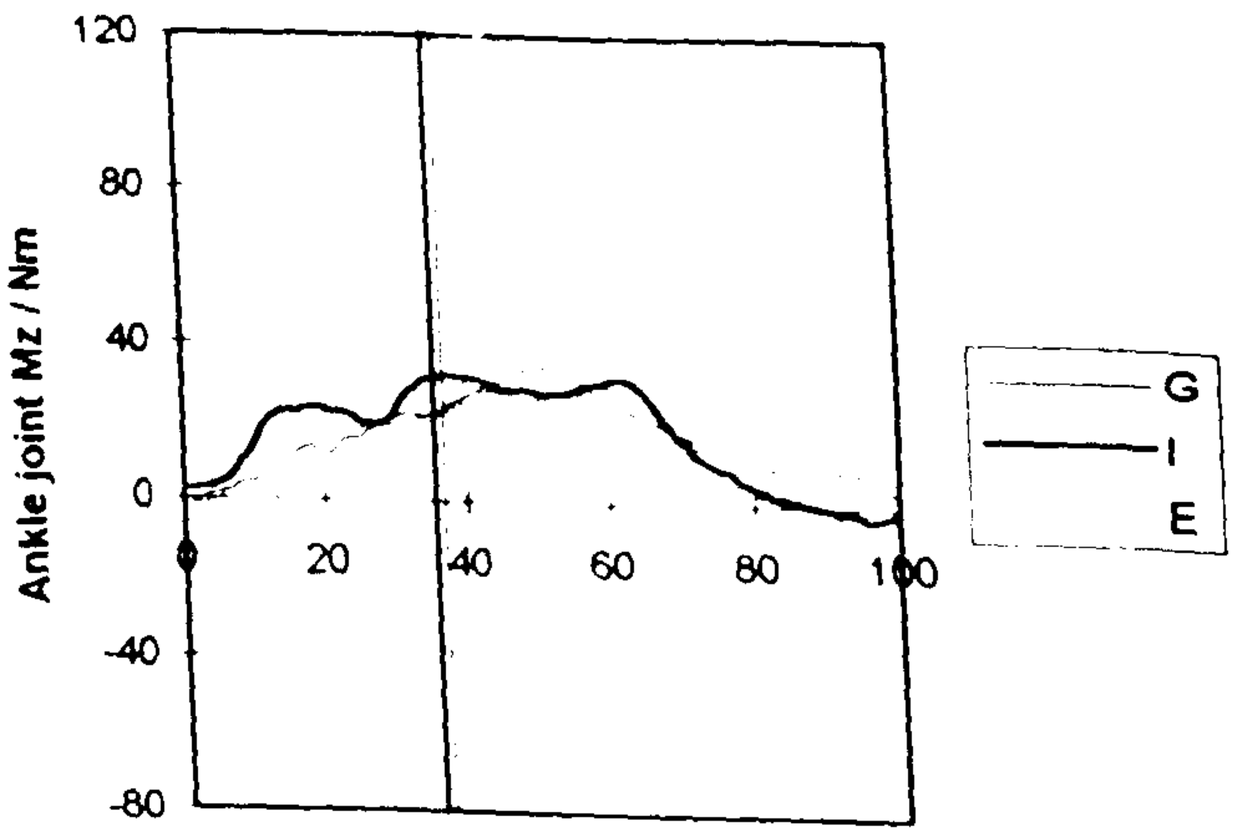

The vertical lines in figures 6.16 and 6.17 indicate the time at which each subject finished rising and was standing upright.

Author, subject and test details	External moment tending to flex the hip joint	External moment tending to flex the knee joint
Pai and Rogers (1991) (1) (2) 4 males 4 females Age : 26-38 yrs Seat height : 450mm Natural speed rise	38Nm	72Nm
Fleckenstein et al (1988) (1) 5 males 5 females Age : 25.4 yrs (S.D.±4.0) Seat height : 440mm Initial knee flexion angle : 105° Initial knee flexion angle : 75°	 71Nm 127Nm	 144Nm 157Nm
Wretenberg et al (1993) 10 males Age : 20-32 yrs Seat height : set to knee height Armrests not used Armrests used. Armrests were situated high and hands were placed to the rear of the armrests. Double the usual force was applied to the armrests.	 39Nm 17Nm	 83Nm 28Nm
Doorenbosch et al (1994) (3) 3 males 6 females Age : 27±3.5 yrs Natural sit-to stand transfer Sit-to-stand transfer with full flexion of the trunk	 0.62Nm/kg 0.81Nm/kg	 0.81Nm/kg 0.59Nm/kg

Table 6.2 Hip and knee joint moments during rising

Notes
(1) Combined results were reported for 2 limbs. The results in the table are for one limb assuming symmetry.
(2) The results in the table were measured from graphs presented by the author.
(3) Moments presented are normalized to body mass.

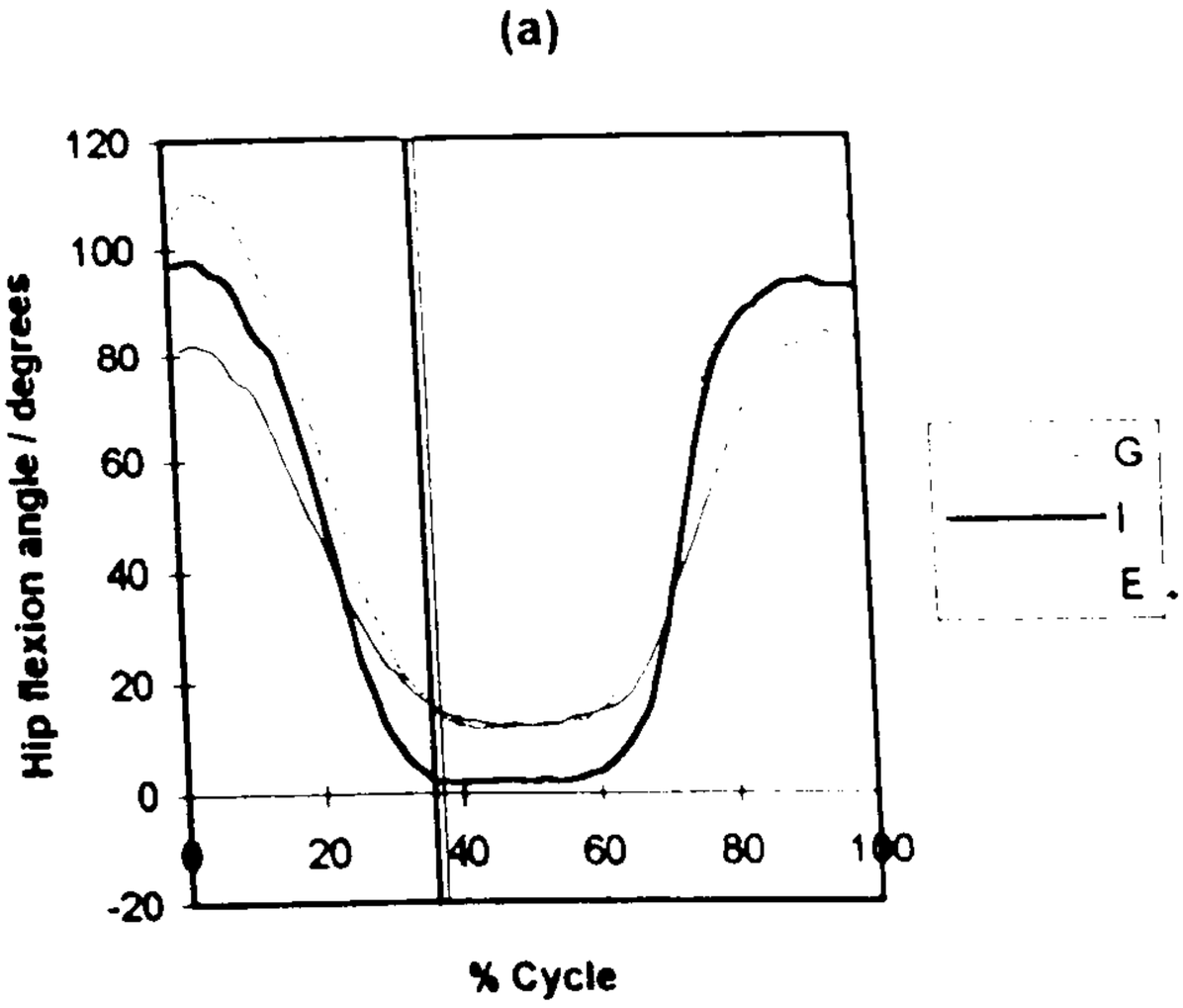

Figure 6.18 (a) Hip flexion and (b) knee flexion angles measured in subjects 'G', 'I' and 'E' when rising from and sitting down onto a chair. The cycle starts when the subject loses contact with the seat and ends when the subject makes contact with the seat again. The vertical lines indicate the time at which each subject finished rising and was standing upright.

6.3.2 Joint Angles

In sections 6.1.2 and 6.2.2 the joint angles determined for the stance phases of gait and stair ascent were examined and assessed in relation to those reported by other authors. It was important to perform the same procedure for the activity of rising from a chair.

Hip and knee flexion angles measured for subjects 'G', 'I' and 'E' whilst rising are presented in figure 6.18. The mean peak hip flexion angle was 97°. Doorenbosch et al (1994) reported a mean peak value of 93.4° (S.D.±8.4) whilst rising naturally. The value of 97° measured in the current study falls within the range covered by the standard deviation of Doorenbosch et al.

The mean peak knee flexion angle in subjects 'G', 'I' and 'E' was 83°. This occurred at the start of rising. There have been a range of initial knee flexion angles reported in the literature. Rodosky et al (1989) studied 10 normal subjects with a mean age of 25.5 years and an age range of 20-35 years. They reported the mean peak knee flexion angle to change from 110° at a chair height set as 65% of the knee height to 75° at a chair height of 115% of the knee height.

6.3.3 Muscle Activity Patterns

In sections 6.1.3 and 6.2.3 the predicted muscle patterns were examined for the stance phases of gait and stair ascent and compared to EMG measurements as part of the validation process. To further check the validity of the results it was necessary to perform the same process for the activity of rising from a chair. There have been a number of studies recording and analysing EMG patterns during rising from a chair (Kelley et al (1976), Naumann et al (1982), Wheeler et al (1985) and Doorenbosch et al (1994)). From these studies, that of Doorenbosch et al (1994) has been chosen for comparison purposes as this study measured the activity of the greatest number of muscles. Nine subjects with a mean age of 27±3.5 years took part in the study. The subject group included 6 females and 3 males. Surface electrodes were used to record activity in the following muscles: gluteus maximus, the long head of biceps femoris, semitendinosus, rectus femoris, vastus medialis, vastus lateralis, the medial head of gastrocnemius, soleus and tibialis anterior.

The predicted muscle force curves for subjects 'G', 'I' and 'E' whilst rising from a chair are presented with the EMG data of Doorenbosch et al (1994) in figures 6.21a-w at the end of section 6.3. The following discussion considers the patterns of muscle activity predicted in the current study first and then compares them to the EMG data.

Predicted muscle activity patterns

The predicted patterns of muscle activity are in accordance with what may be expected from the joint moment curves in figures 6.15 to 6.17.

Both hip and knee extensor muscle activity were required until the late stages of rising. Gluteus maximus was predicted to be active providing a significant component of hip extensor activity (fig 6.21h). Adductor magnus was also active and with the hip in such a flexed position, its action would be to aid gluteus maximus as a hip extensor (6.21i). Lower activity was predicted in subjects 'I' and 'E' in the long head of biceps femoris, providing some additional hip extensor activity (fig 6.21b). However, this was antagonistic to the extensor requirements at the knee joint. Knee extensor requirements were satisfied by the vasti group and rectus femoris although rectus femoris activity was antagonistic to the requirements of the hip joint (fig 6.21l,m,n,p).

It was also observed that the activity in the external rotators was significantly greater than it had been in gait or stair ascent (fig 6.21w). This group includes the gemelli, obturator internus, obturator externus, piriformis and quadratus femoris. Activity was greatest in piriformis, obturator internus and quadratus femoris. With the hip in a highly flexed position during rising, the lines of action of piriformis and obturator internus were such that they were acting as hip abductors and contributing to the abduction/adduction moment balance. Quadratus femoris was active as a hip extensor.

In the later stages of rising, the external moment at the knee joint changed from a tendency to flex to a tendency to extend. Knee flexor activity was then required in addition to hip extensor activity. Activity in the hamstrings therefore increased at this time providing hip extensor and knee flexor action (fig 6.21a-d). Gastrocnemius also became active, providing knee flexor action (fig 6.21t,u).

Comparison of predicted muscle activity with EMG data

Having examined the predicted muscle activity patterns, it was important to compare these with EMG data as part of the validation process.

The predicted activity in gluteus maximus in 'G', 'I' and 'E' was consistent with that measured in the EMG study (fig 6.21h). Consistency was also exhibited by the vasti and rectus femoris although activity in these muscles ended earlier in 'G', 'I' and 'E' than in the EMG study (fig 6.21l-p). The activity terminated in subjects 'G', 'I' and 'E' when the external joi.. moment changed from a tendency to flex the knee joint to a tendency to extend as shown in figure 6.16.

In measuring hamstring activity Doorenbosch et al (1994) placed electrodes over the long head of biceps femoris and over semitendinosus. The combined activity predicted in these muscles was consistent with the EMG data for subjects 'I' and 'E' but not for 'G'. Very little activity was predicted in the long head of biceps femoris for subject 'G' (fig 6.21a,b).

Finally, the most marked difference between the EMG results and the results for

subjects 'G', 'I' and 'E' was observed for the medial head of gastrocnemius (fig 6.21t). Activity was only predicted in 'G', 'I' and 'E' in the late stages of rising when the external moment at the knee joint changed from a tendency to flex to a tendency to extend as shown in figure 6.16. However, activity was measured throughout all stages of rising in the EMG study. One explanation is that gastrocnemius was not actually active in subjects 'G', 'I' or 'E' in the early stages of rising. Secondly, the theoretical model may not reflect the real situation exactly. With regard to this second option, gastrocnemius was only included as a variable in the model when there was a tendency to dorsiflex the ankle. This was the case in rising and hence it was possible for gastrocnemius to be active. However, the external moment at the knee joint exhibited a tendency to flex the knee joint throughout most of the time of rising, requiring knee joint extensor muscle action and eliminating the need for gastrocnemius. The model assumed that ankle moment balance would be achieved by the other ankle plantarflexors, notably soleus. Section 6.3.5 shows that this is physiologically possible with regards muscle stress. Thus although the results of the model are explainable, the difference in gastrocnemius activity between the current study and the EMG study may stem from the fact that ankle joint moment balance was not included in the model.

Overall, as was the case for gait and stair ascent, there were some differences in patterns of muscle activity between the current study and the EMG study. However, the majority of the muscles exhibited patterns which were consistent between the two studies.

6.3.4 Muscle Force Values

Having studied the patterns of muscle activity, it was important for the development of the model to examine values of muscle force and assess them in relation to those reported in a selection of past studies before going on to use them in the calculation of joint force. This was carried out in sections 6.1.4 and 6.2.4 for the stance phases of gait and stair ascent. This section performs the same procedure for the activity of rising from a chair.

Although there have been many studies measuring joint moments and angles whilst rising from a chair, there do not appear to have been many in which the magnitudes of muscle forces were calculated. The work used for comparison is that of Ellis et al (1984). Ellis et al included 9 males and 11 females in their study with a mean age of 27.5 years and presented the patterns and values of forces in the quadriceps femoris, hamstrings and gastrocnemius. A simplified 2D model of the lower limb was developed and the muscles were grouped in order to distribute the intersegmental joint moments among the muscles. EMG recordings were used to indicate which muscles were active.

Although the results of 'G', 'I' and 'E' can be compared with those of Ellis et al (1984), the information obtained is of limited use since the comparison is being made to a single

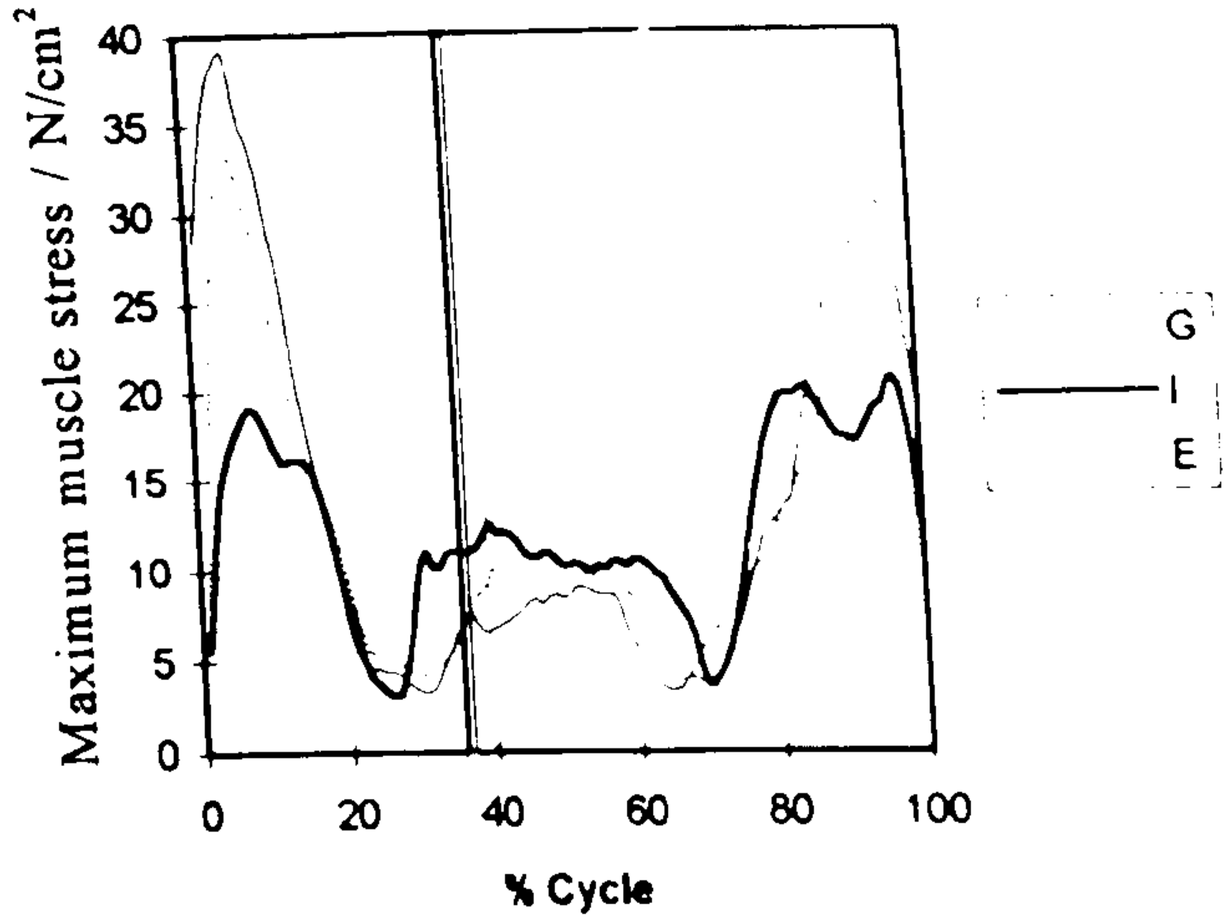

Figure 6.19 Maximum muscle stress calculated for subjects 'G', 'I' and 'E' when rising from and sitting down onto a chair. The cycle starts when the subject loses contact with the seat and ends when the subject makes contact with the seat again. The vertical lines indicate the time at which each subject finished rising and was standing upright.

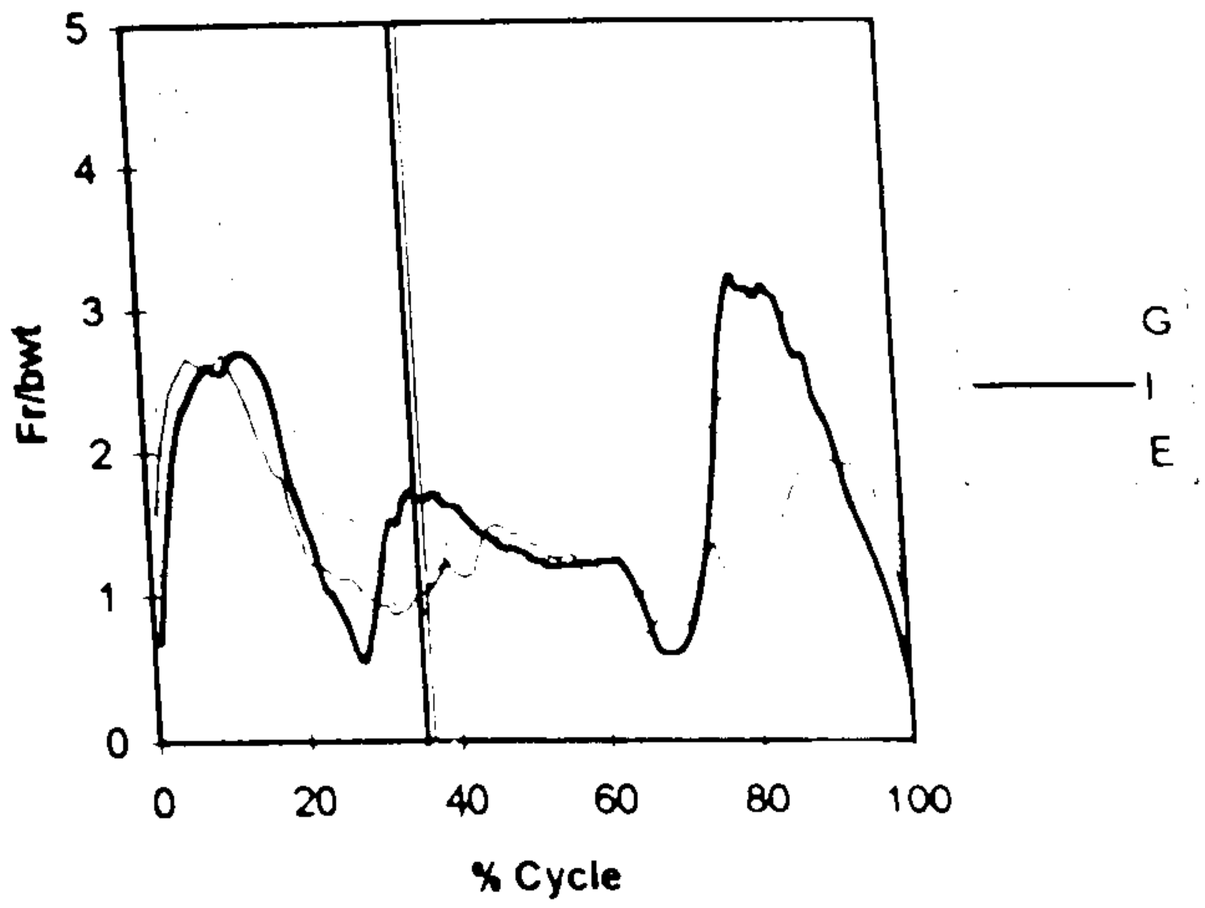

Figure 6.20 Resultant hip joint force, Fr, in terms of body weight calculated for subjects 'G', 'I' and 'E' when rising from and sitting down onto a chair. The cycle starts when the subject loses contact with the seat and ends when the subject makes contact with the seat again. The vertical lines indicate the time at which each subject finished rising and was standing upright.

study. The values quoted for Ellis et al in this section were measured from the curve presented by Ellis et al as being representative of all of the results.

The mean peak force predicted in quadriceps femoris in 'G', 'I' and 'E' was 1787N. That calculated by Ellis et al was 2269N. The mean peak hamstring force in 'G', 'I' and 'E' was 123N whilst that predicted by Ellis et al was 577N. A mean peak force of 237N was predicted in gastrocnemius in subjects 'G', 'I' and 'E' whilst that reported by Ellis et al was 76N.

The differences between the values predicted in the current study and those predicted by Ellis et al could be due to differences between the methodology used in the two studies in the calculation of muscle force. Differences could also occur due to variation in the style of rising requiring different levels of muscle activity. For example, some subjects may apply more force through their hands than others, resulting in lower intersegmental joint moments. Table 6.2 illustrates the high variation in joint moments reported in the literature for rising from a chair using different techniques. There was such variation between the three subjects, 'G', 'I' and 'E'. When the subjects were considered separately, the quadriceps force in 'G' alone was 2289N which is almost identical to the value of 2269N presented by Ellis et al.

6.3.5 Muscle Stress

Having considered muscle force, this section is concerned with muscle stress. In sections 6.1.5 and 6.2.5 the muscle stresses produced during the stance phases of gait and stair ascent were assessed as part of the validation process to ensure that they were physiologically reasonable. In order to further check the validity of the results, the maximum muscle stress produced in the activity of rising from a chair is assessed in this section.

Figure 6.19 shows the maximum muscle stress calculated in subjects 'G', 'I' and 'E' when rising from a chair. The mean of the maximum muscle stresses exhibited by subjects 'G', 'I' and 'E' whilst rising from a chair was 30.5N/cm^2 with a maximum value of 39.1N/cm^2 occurring in subject 'G'. These values are well below the upper limit of the range of estimations of maximum achievable muscle stress quoted as 10-100 N/cm^2 by Kaufman et al (1991).

6.3.6 Ankle moment balance

As described in section 6.1.6, the final stage in the model development was to check that ankle joint moment balance could be achieved since ankle joint moment equilibrium was not included in the model. This was carried out for gait in section 6.1.6 and for stair ascent in section 6.2.6. It is performed for the activity of rising from a chair in this section. The maximum unbalanced ankle joint moment during rising from a chair was 24Nm tending to dorsiflex the ankle joint in subject 'I'. This is much less than the unbalanced moment of

83Nm calculated in subject 'G' during gait. Section 6.1.6 showed that this residual moment of 83Nm could be balanced by ankle joint plantarflexors not already included in the model whilst maintaining the muscle stress within physiologically reasonable limits. Hence if similar assumptions to those in section 6.1.6 are made here, it is possible to balance the smaller residual moment of 24Nm whilst maintaining a physiologically reasonable muscle stress.

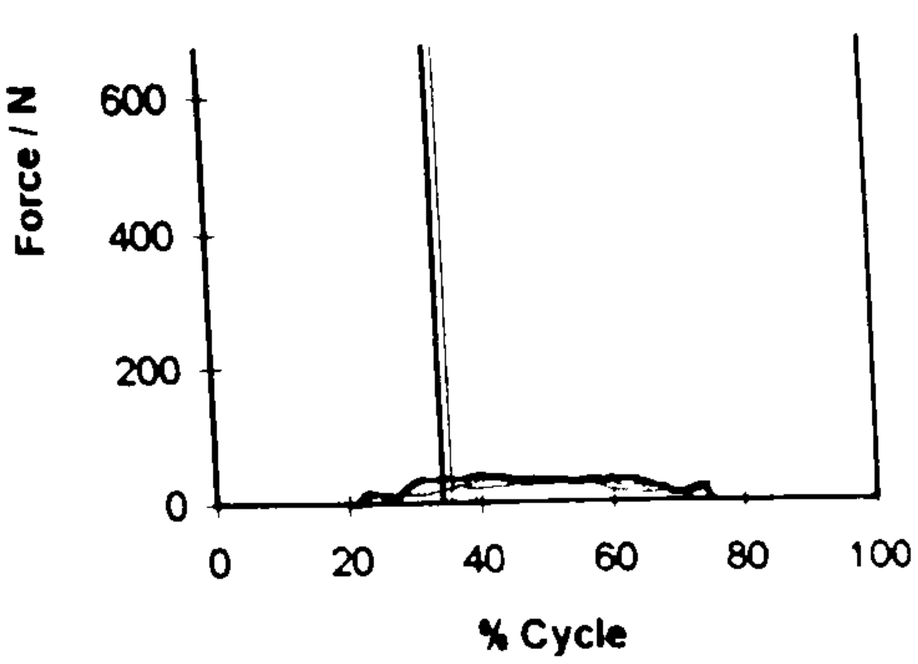

(a) Semitendinosus

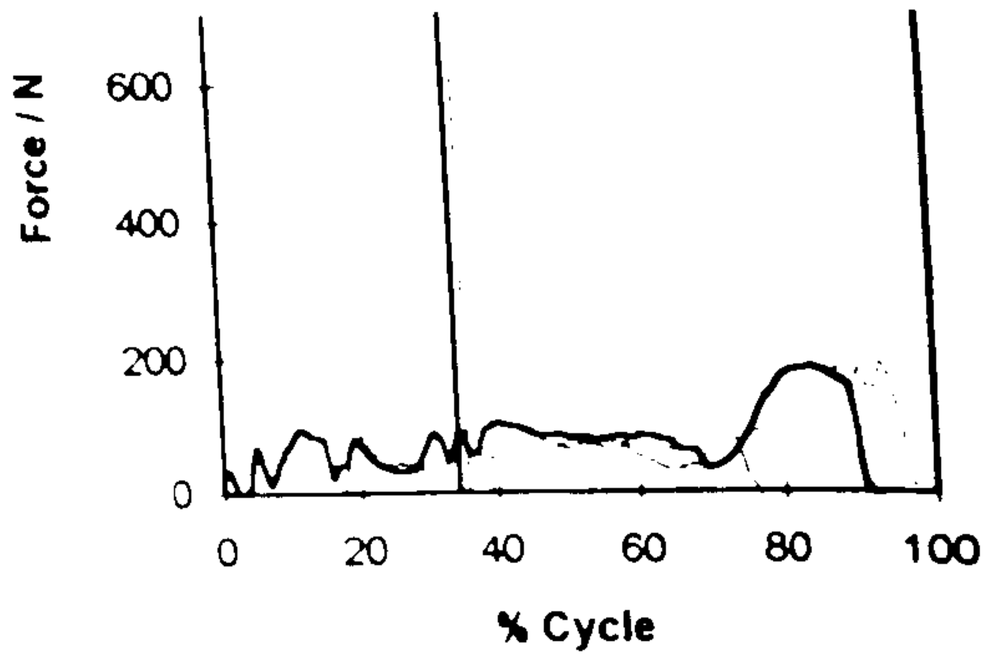

(b) Biceps femoris - long head

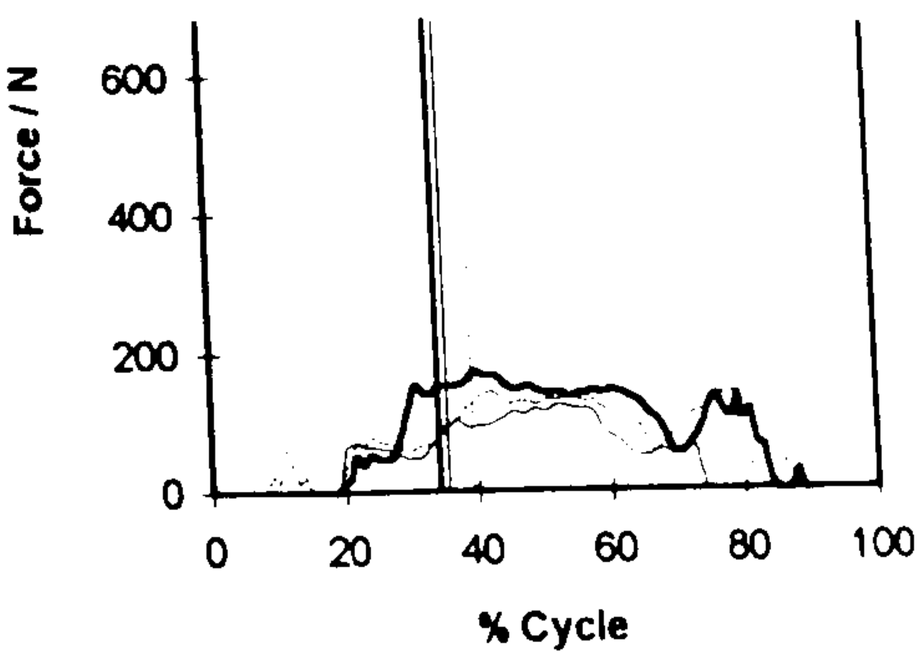

(c) Semimembranosus

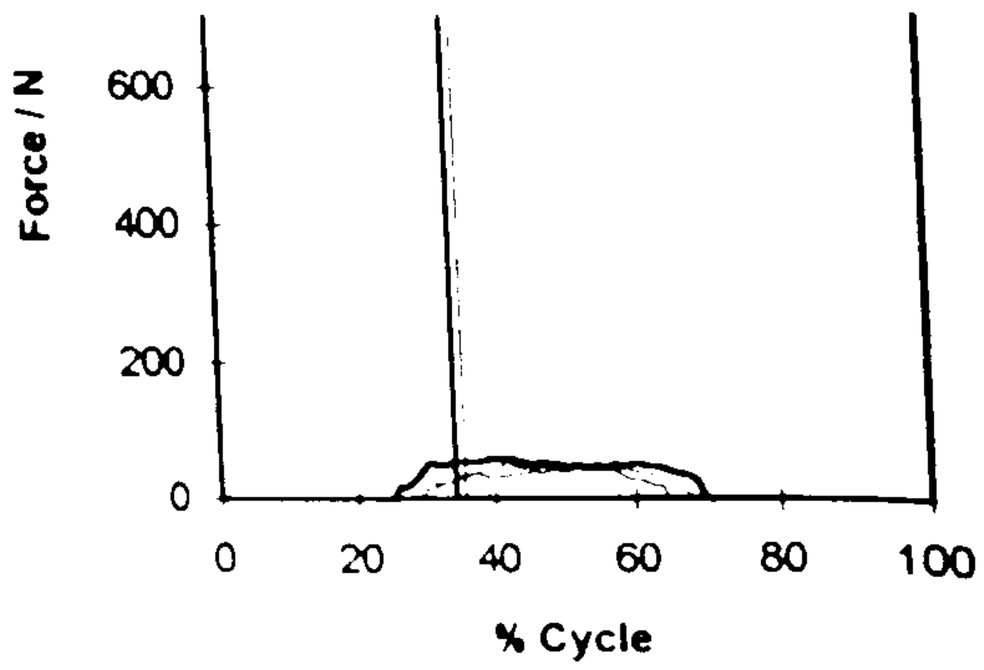

(d) Biceps femoris - short head

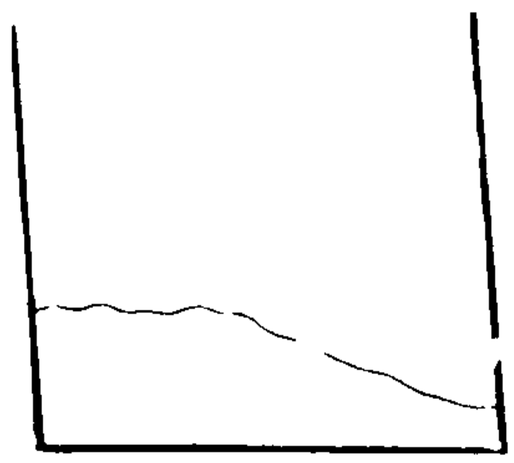

(e) EMG data

Figure 6.21. Muscle activity when rising from and sitting down onto a chair.

(a)(b)(c)(d) Hamstring activity predicted in the current study for subjects 'G', 'I' and 'E'. The cycle starts when the subject loses contact with the seat and ends when the subject makes contact with the seat again. The vertical lines in each figure indicate the time at which each subject finished rising and was standing upright.

G
I
E

(e) The mean curve of EMG data recorded in the hamstrings by Doorenbosch et al (1994) for rising from a chair. The curve starts when the subjects lose contact with the seat and ends when the subjects are standing fully upright

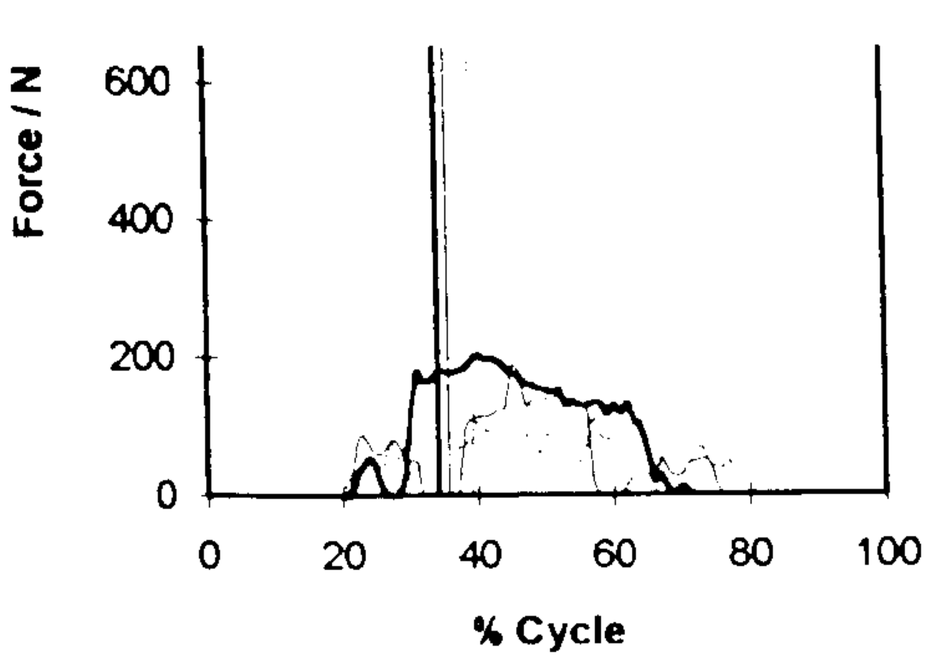

(f) Gluteus minimus

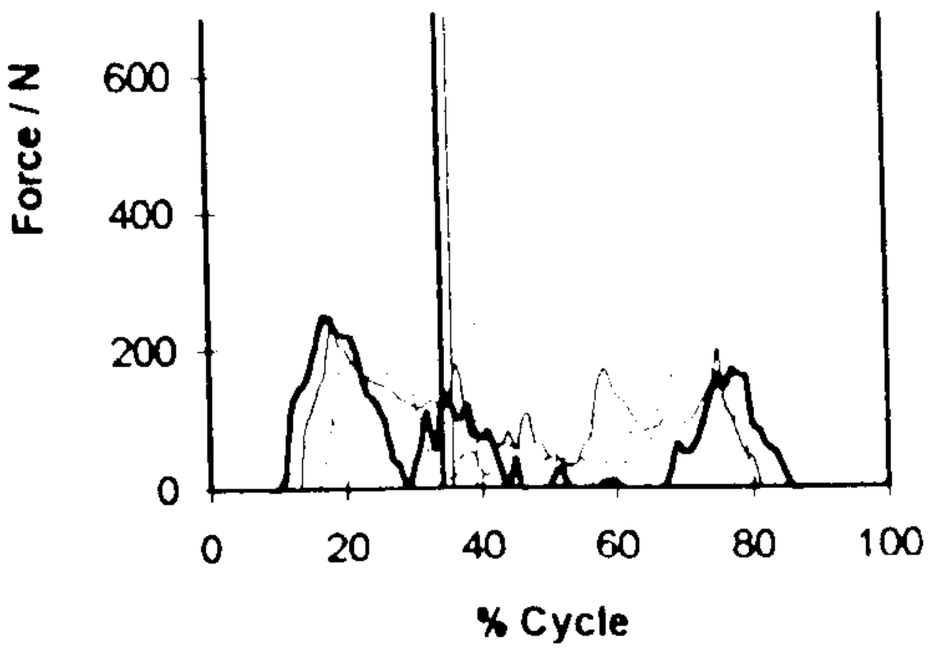

(g) Gluteus medius

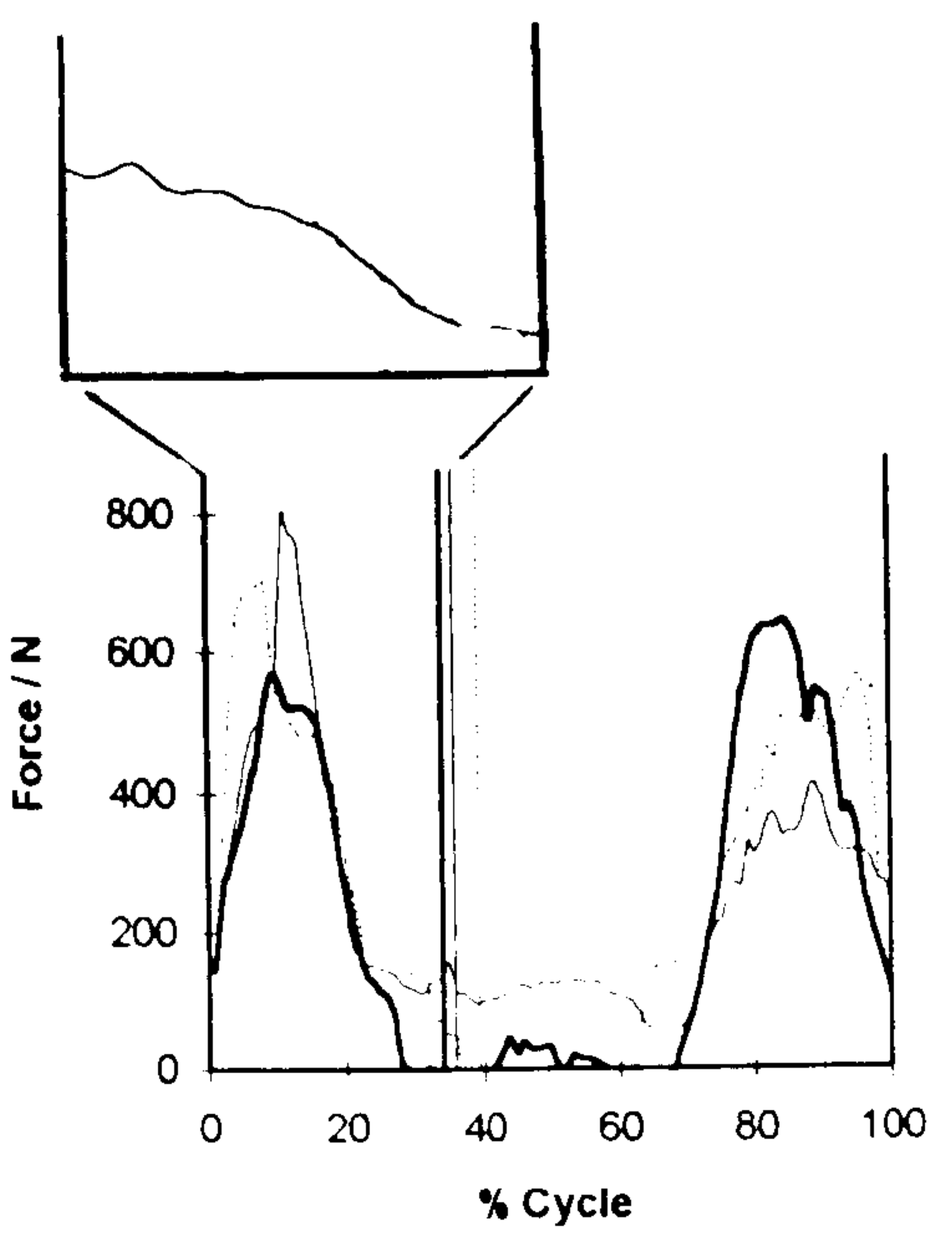

(h) Gluteus maximus

Figure 6.21 continued. Muscle activity when rising from and sitting down onto a chair.

(f) Gluteus minimus and (g) gluteus medius activity predicted in the current study for subjects 'G', 'I' and 'E'. The cycle starts when the subject loses contact with the seat and ends when the subject makes contact with the seat again. The vertical lines in each figure indicate the time at which each subject finished rising and was standing upright.

(h) Gluteus maximus activity. The top figure shows the mean curve of EMG data recorded by Doorenbosch et al (1994) for rising from a chair. The curve starts when the subjects lose contact with the seat and ends when the subjects are standing fully upright. The bottom figure shows the activity predicted in the current study for subjects 'G', 'I' and 'E'.

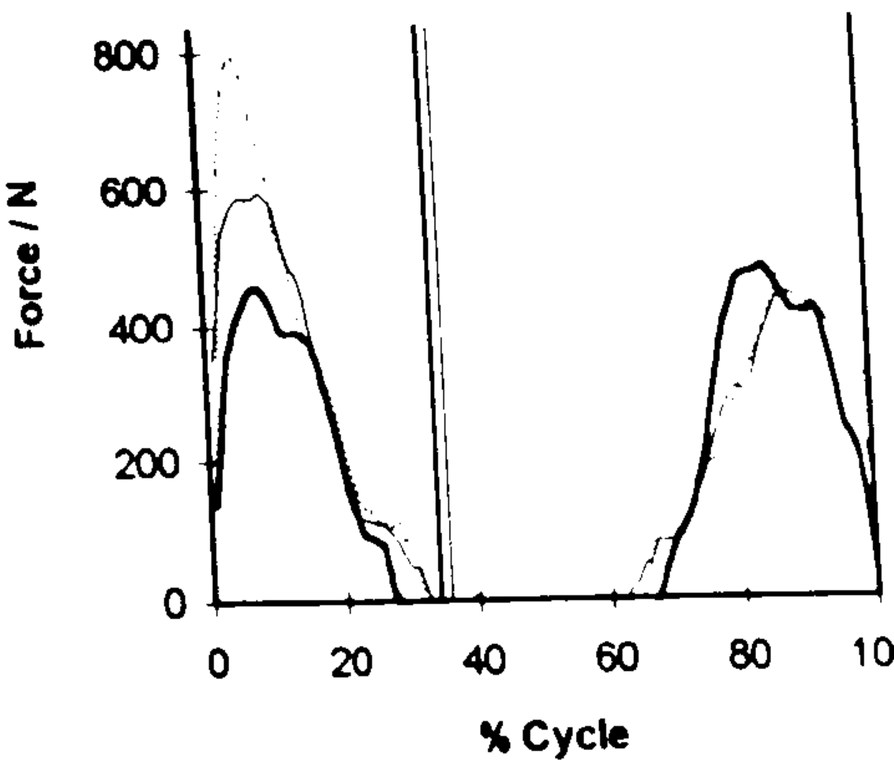

(i) Adductor magnus

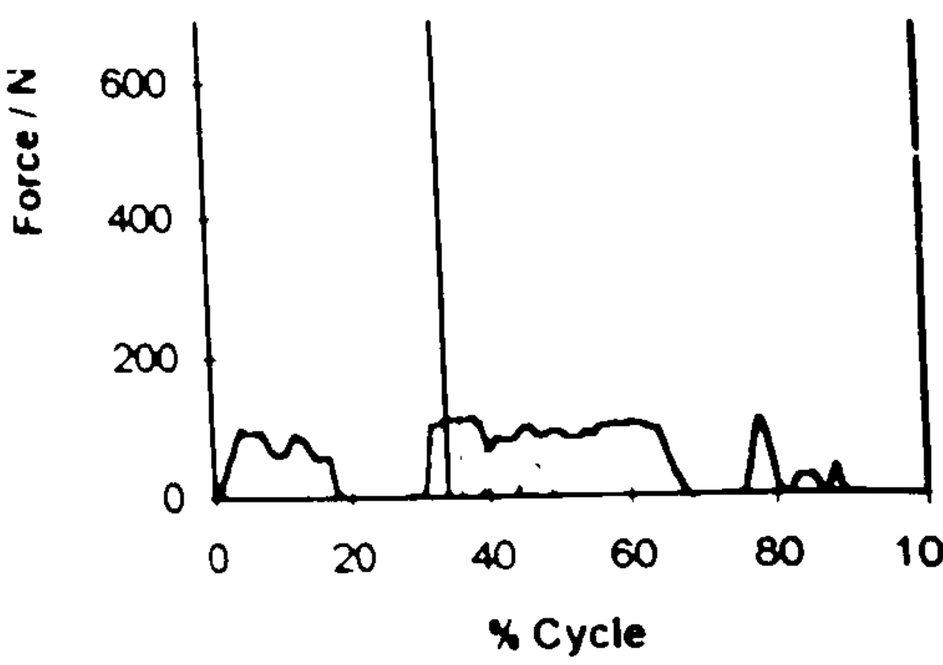

(j) Adductor longus

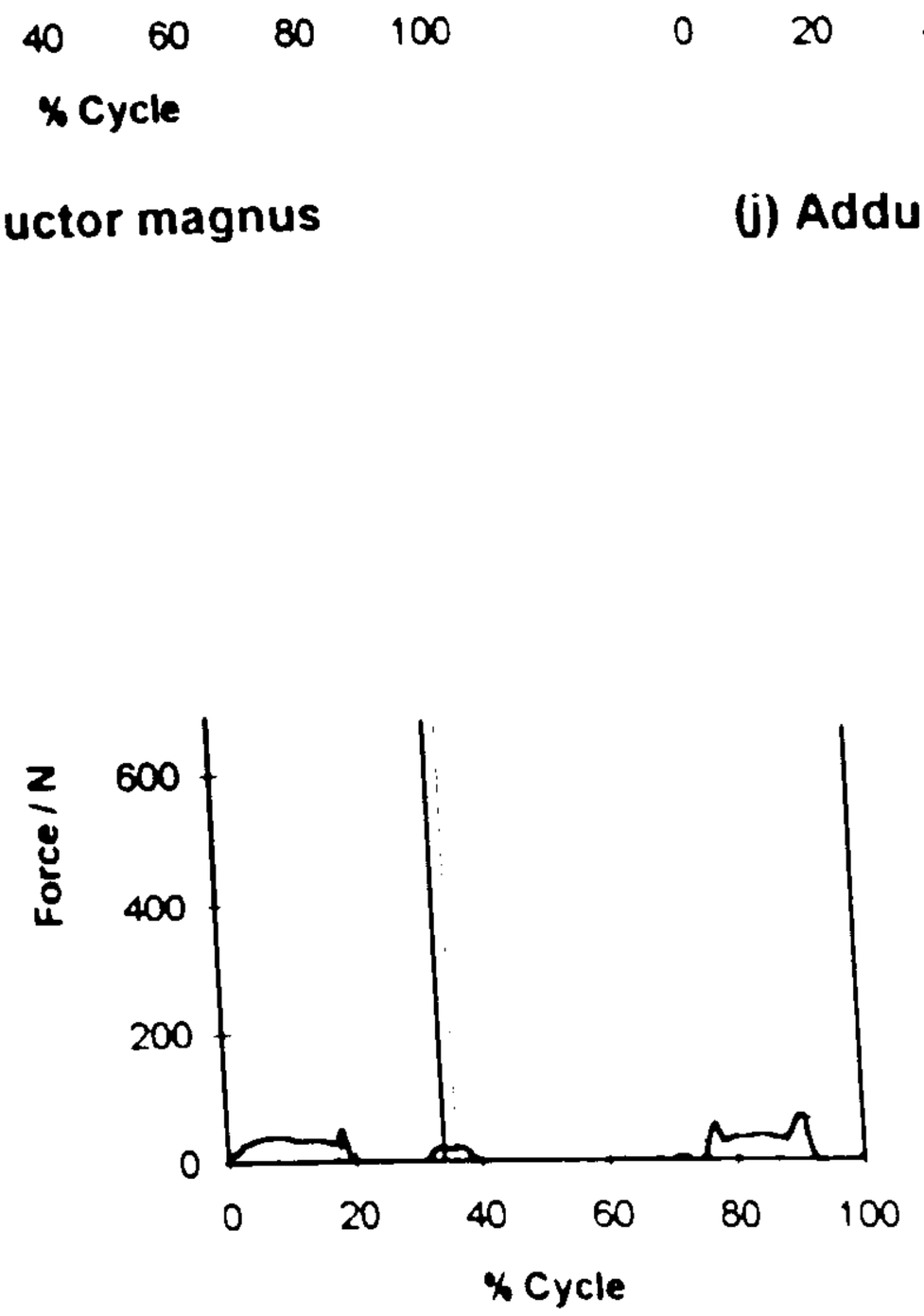

(k) Adductor brevis

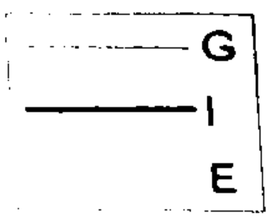

Figure 6.21 continued. Muscle activity when rising from and sitting down onto a chair.

For each muscle the figure shows the activity predicted in the current study for subjects 'G', 'I' and 'E'. The cycle starts when the subject loses contact with the seat and ends when the subject makes contact with the seat again. The vertical lines in each figure indicate the time at which each subject finished rising and was standing upright.

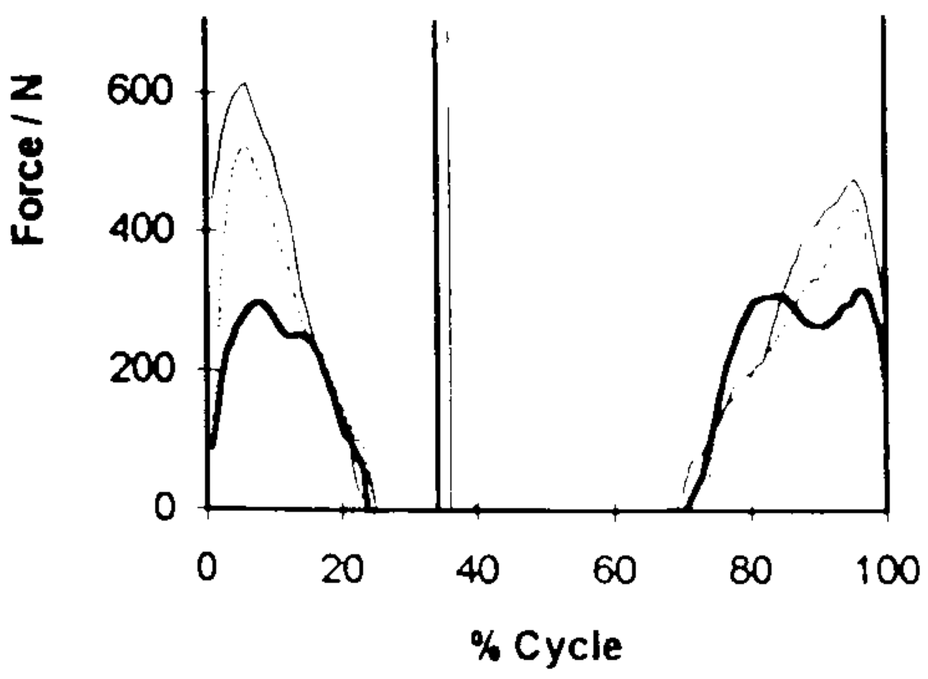

(l) Vastus medialis

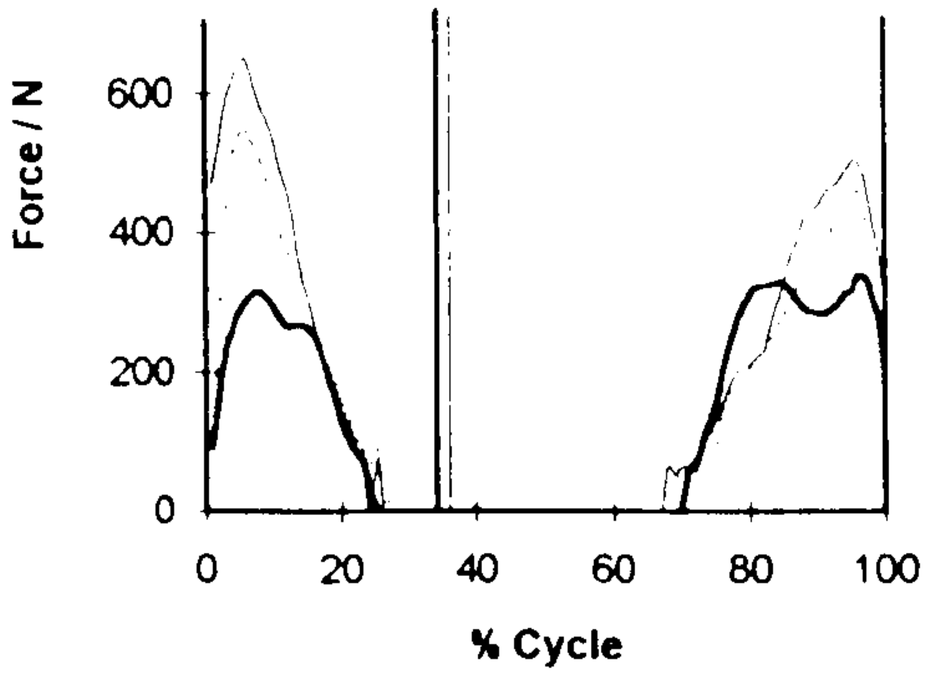

(m) Vastus lateralis

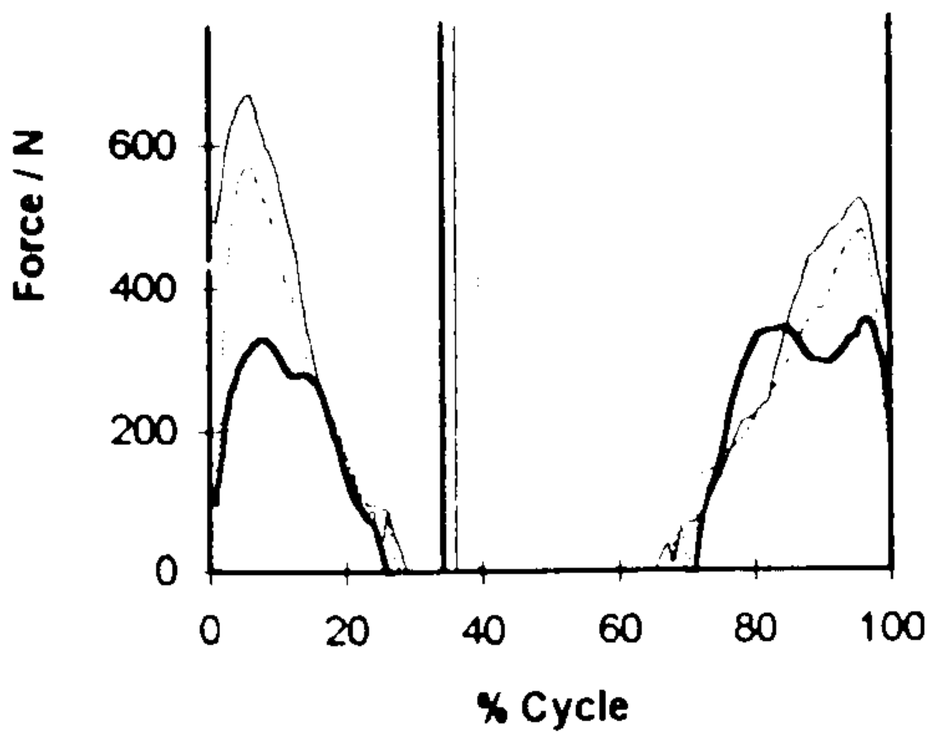

(n) Vastus intermedius

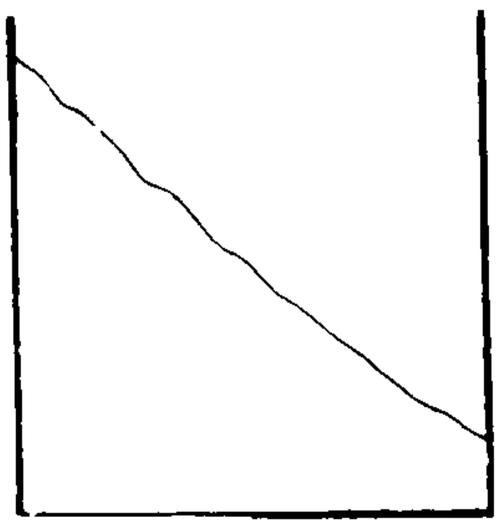

(o) EMG data

Figure 6.21 continued. Muscle activity when rising from and sitting down onto a chair.

(l)(m)(n) Vasti activity predicted in the current study for subjects 'G', 'I' and 'E'. The cycle starts when the subject loses contact with the seat and ends when the subject makes contact with the seat again. The vertical lines in each figure indicate the time at which each subject finished rising and was standing upright.

(o) The mean curve of EMG data recorded in the vasti by Doorenbosch et al (1994) for rising from a chair. The curve starts when the subjects lose contact with the seat and ends when the subjects are standing fully upright.

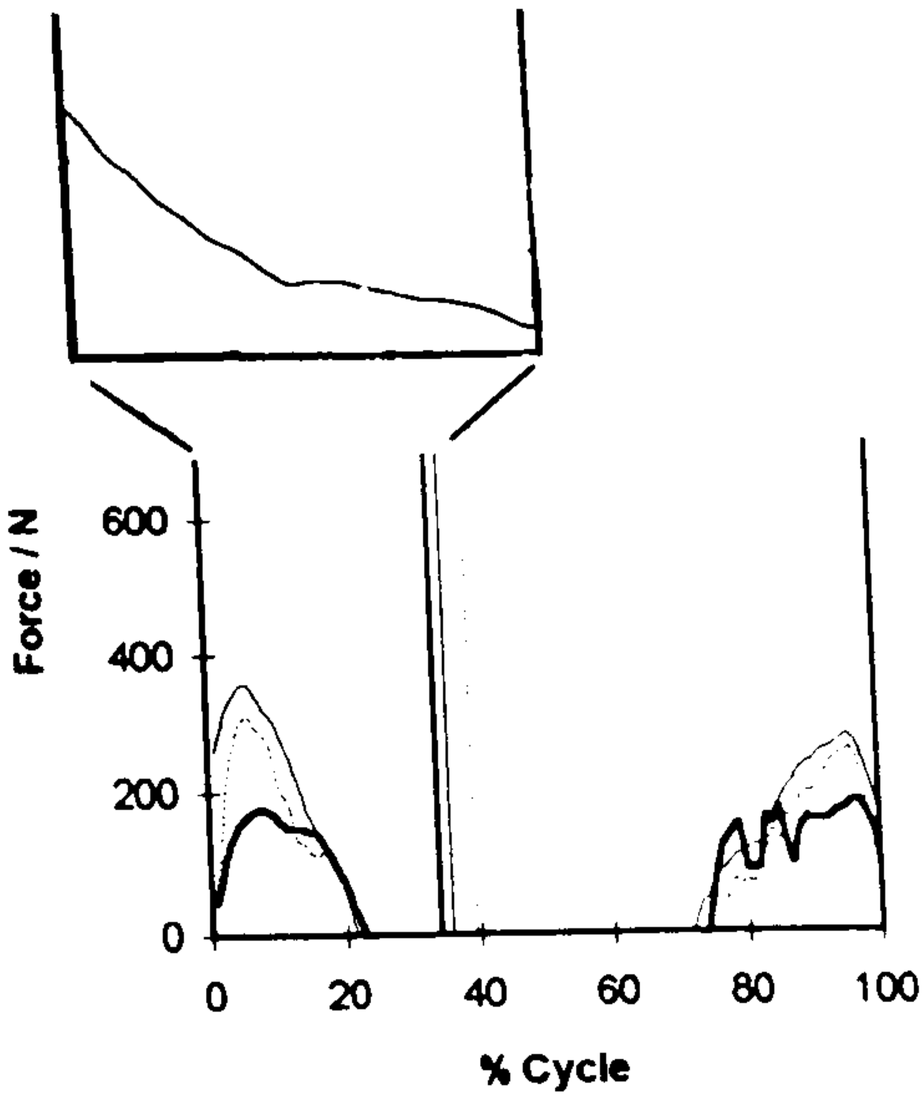

(p) Rectus femoris

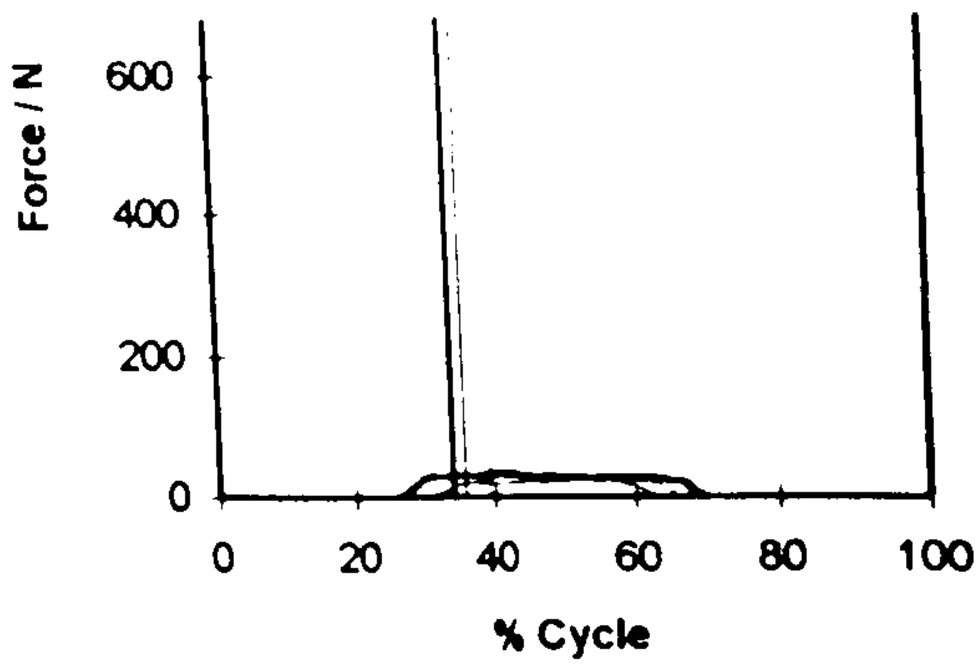

(q) Sartorius

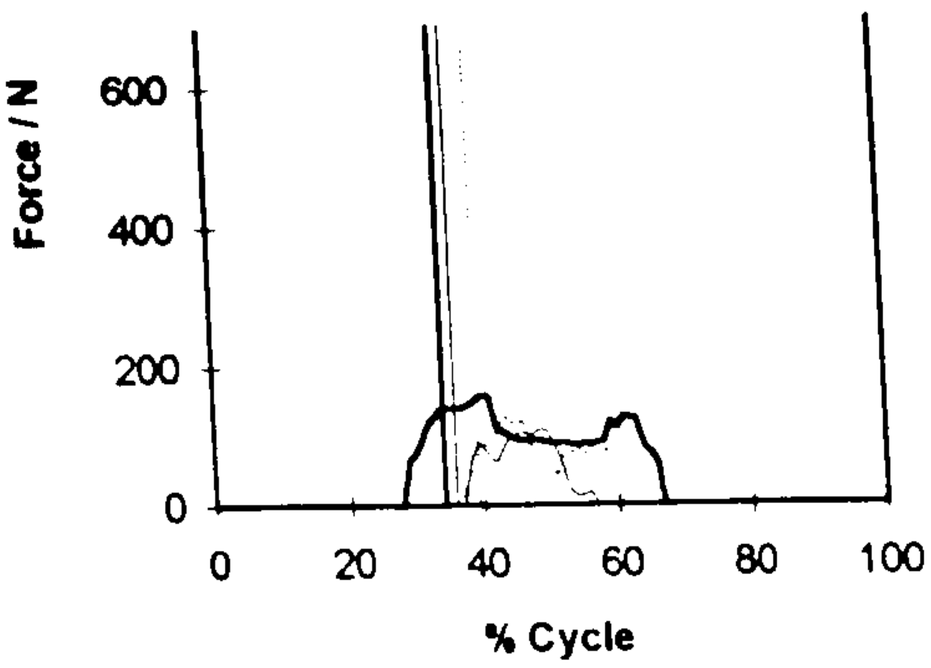

(r) iliopsoas

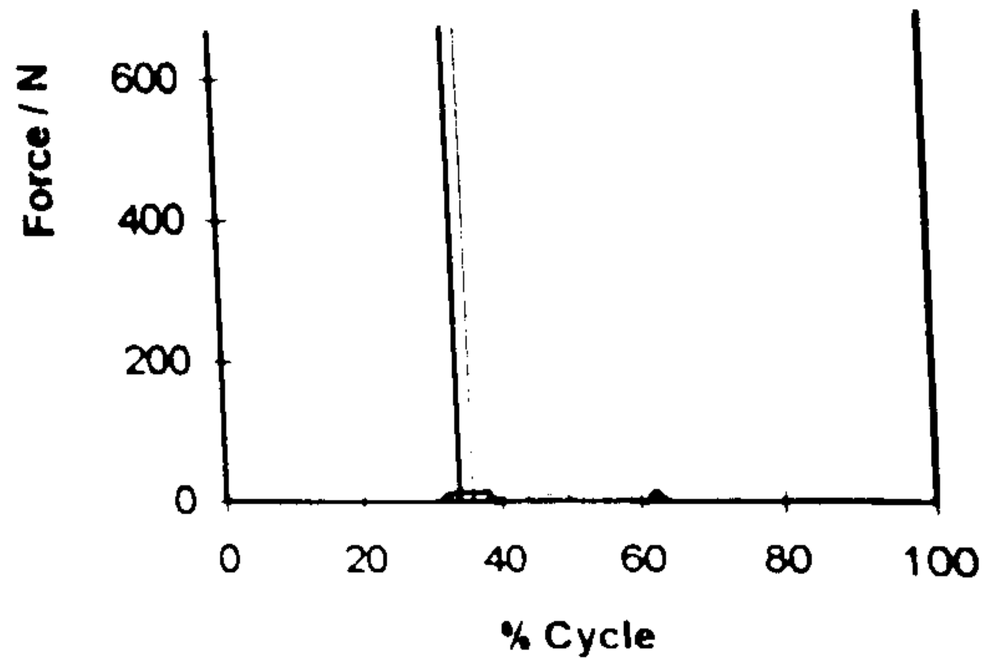

(s) Pectineus

Figure 6.21 continued. Muscle activity when rising from and sitting down onto a chair.

(p) Rectus femoris activity. The top figure shows the mean curve of EMG data recorded by Doorenbosch et al (1994) for rising from a chair. The curve starts when the subjects lose contact with the seat and ends when the subjects are standing fully upright. The bottom figure shows the activity predicted in the current study for subjects 'G', 'I' and 'E'. The cycle starts when the subject loses contact with the seat and ends when the subject makes contact with the seat again. The vertical lines indicate the time at which each subject finished rising and was standing upright.

(q) Sartorius, (r) iliopsoas and (s) pectineus activity predicted in the current study for subjects 'G', 'I' and 'E'.

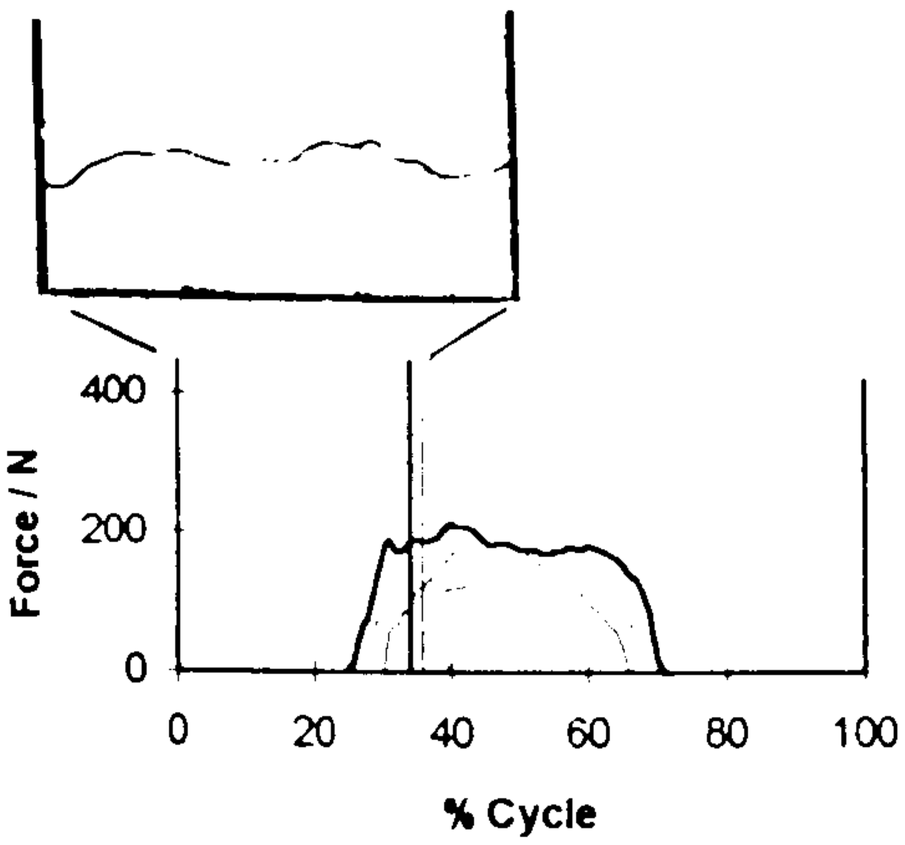

(t) Gastrocnemius - medial head

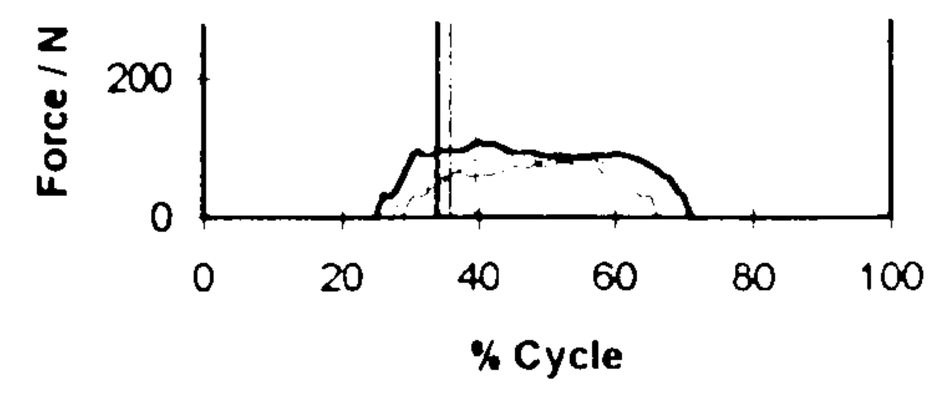

(u) Gastrocnemius - lateral head

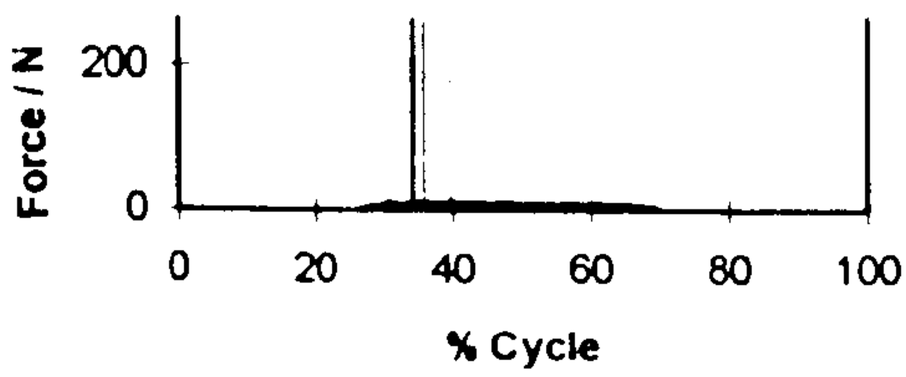

(v) Gracilis

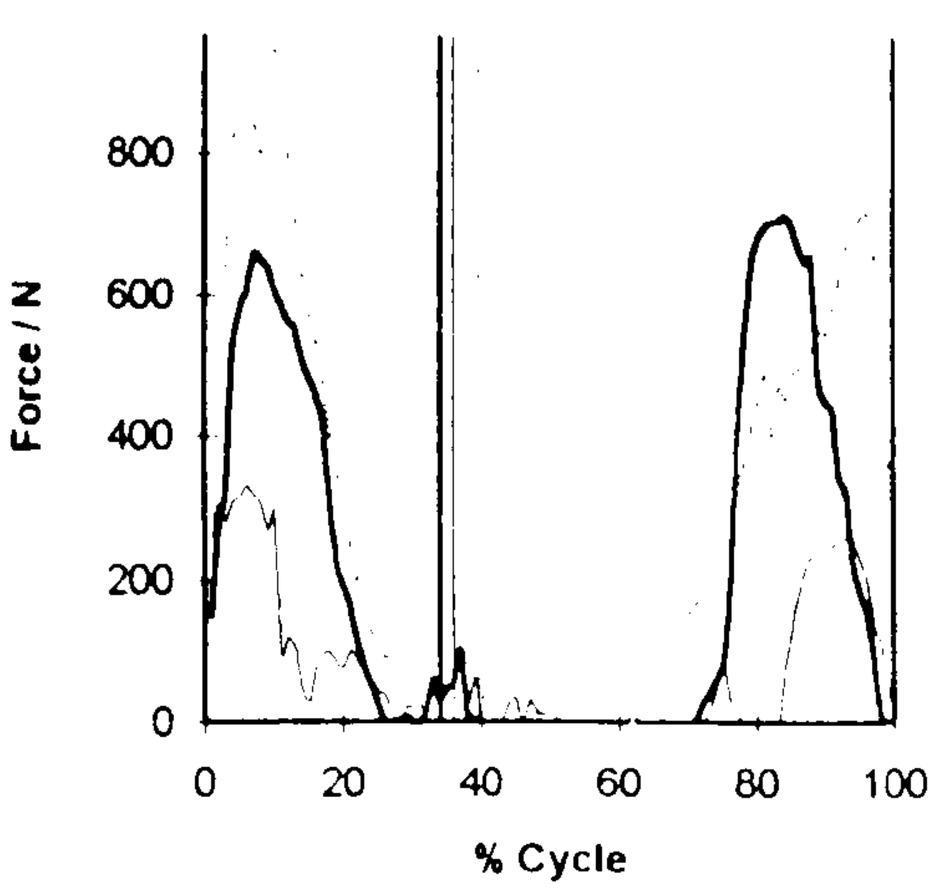

(w) External rotators

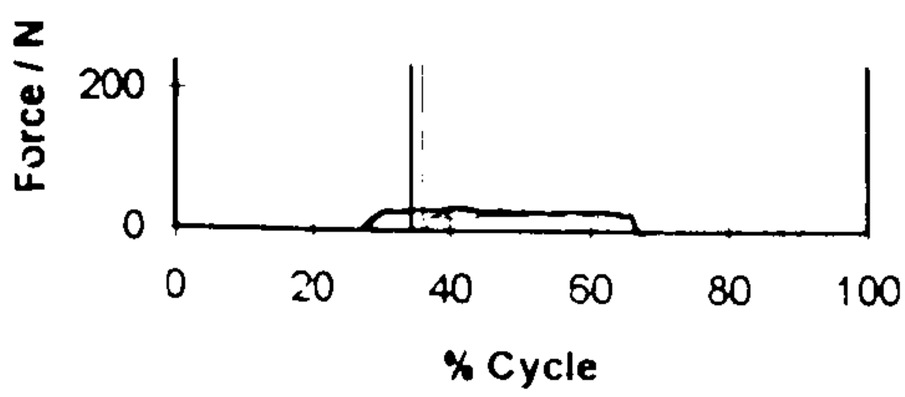

(x) Tensor fascia lata

Figure 6.21 continued. Muscle activity when rising from and sitting down onto a chair.

(t) Gastrocnemius (medial head) activity. The top figure shows the mean curve of EMG data recorded by Doorenbosch et al (1994) for rising from a chair. The curve starts when the subjects lose contact with the seat and ends when the subjects are standing fully upright. The bottom figure shows the activity predicted in the current study for subjects 'G', 'I' and 'E'. The cycle starts when the subject loses contact with the seat and ends when the subject makes contact with the seat again. The vertical lines indicate the time at which each subject finished rising and was standing upright.

(u) Gastrocnemius (lateral head), (v) gracilis, (w) external rotators (gemellus inferior, gemellus superior, obturator internus, piriformis, quadratus femoris and obturator externus) and (x) tensor facia lata activity predicted in the current study for subjects 'G', 'I' and 'E'.

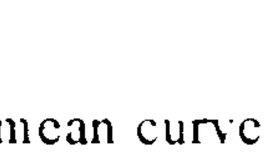

6.4 SUMMARY OF THE INTERMEDIATE RESULTS AND DISCUSSION

The results of the intermediate stages in the calculation of joint force have been assessed in this chapter as part of the model development process. Joint moments, joint angles and muscle forces have been examined for three normal subjects in the activities of gait, stair ascent and rising from a chair. The patterns of joint moments and angles were found to be consistent with those reported by other authors. The values of joint moments and angles were also found to be within the range reported by other authors. Some differences were observed in the values of muscle force predicted in the current study and those predicted by other authors. These were considered to be primarily due to differences between the styles in which subjects performed the activities and also due to differences in methods used in calculation.

The validity of the results predicted by the model has also been assessed. The patterns of muscle activity predicted in three normal subjects whilst performing the activities of gait, stair ascent and rising from a chair were compared with published EMG data. As detailed in sections 6.1.3, 6.2.3 and 6.3.3 there were some differences in muscle activity patterns between the current study and the EMG studies. However, the predicted activity patterns in the majority of the muscles were consistent with the EMG data. Maximum muscle stress was also assessed as part of the validation process since muscle stresses must not be physiologically unreasonable. All muscle stresses calculated for the three subjects whilst performing the three activities were found to be physiologically reasonable.

Having established that the model gave valid results for muscle activity in three subjects in the activities of gait, stair ascent and rising from a chair, it was considered that the model could be applied with confidence to the other subjects and the other activities. The other activities included the walking turn and getting into and out of the bath and car. The final stage in the calculation could then be performed in order to calculate hip joint forces using these muscle forces. The resulting hip joint forces are presented in chapter 7 and discussed in chapter 8.

CHAPTER 7. FINAL RESULTS

This chapter presents the final results in preparation for discussion in chapter 8. Details of the subjects and activities performed are given first, followed by the resulting hip joint forces. A sensitivity analysis was carried out to assess the accuracy of the results and the results of this analysis are also presented.

7.1 SUBJECT DETAILS AND ACTIVITIES PERFORMED

Details of the 16 patients and the control group of 10 normal subjects involved in the study are given in tables 7.1 and 7.2 at the end of this chapter. Three groups of results were produced for each activity. Group 1 was produced from the normal subjects. This contains a maximum of 20 sets of results consisting of 10 from the right hip and 10 from the left.

Two groups were produced from the patients. One was for the prosthetic hips and one for the non prosthetic hips. Group 2 includes the prosthetic hips and contains a maximum of 19 sets of results. This is made up of results from the prosthetic side of the 16 patients, 3 of whom had bilateral hip replacements. These are subjects 'N', 'P' and 'Y'. The left hip of subject 'P' and the right hip of subject 'N' are included in this group although they were not tested within the specified post-operative test period. This would have involved the subjects undergoing further testing and they had already given a substantial amount of time to the project. Group 3 is made up of the results for the non prosthetic hips of the patients and contains a maximum of 13 sets of results.

Not all of the subjects were capable of performing all of the activities and the use of the force platforms in the methodology restricted the amount of testing possible as was described in chapter 5. Also, some data were rejected for technical reasons including gaps in the marker trajectories. In the activities of gait, turning, ascent, descent and rising from a chair, both hips of each subject were tested. In each car and bath activity, only one side was tested. For example, in all car activity tests the passenger side of the car was used and the left hip was always the one tested in 'outside' tests and the right hip was always that tested on 'inside' tests.

Details of the activities for which results were obtained for each subject are given in appendix E of which table 7.3 is a summary. Table 7.3 is presented at the end of this chapter and gives the number of hips in each group for which results were obtained for each activity. Abbreviations used for each activity in the table and throughout the rest of the results and discussion are as follows:

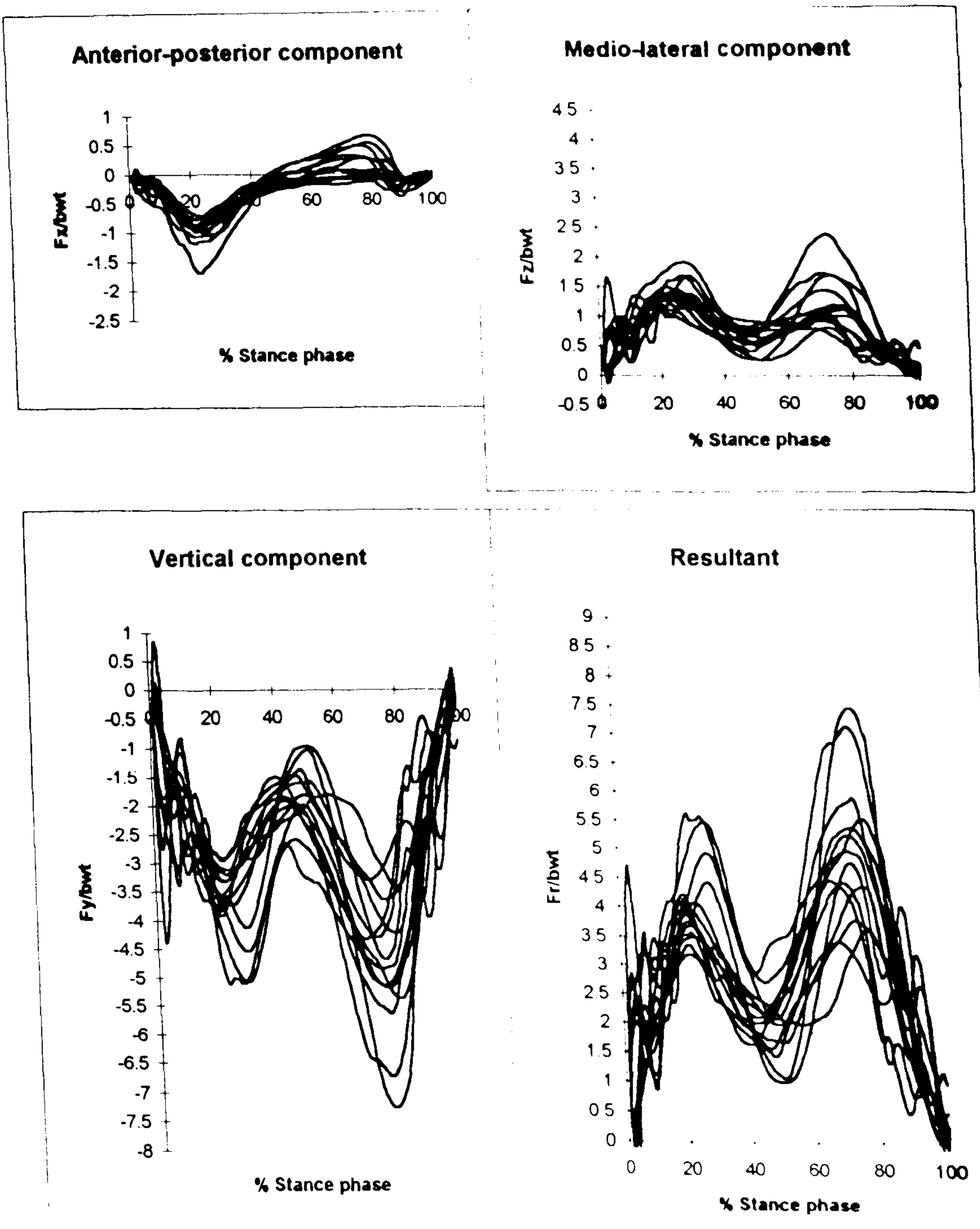

Figure 7.1 Group 1 - Normal subjects. Components of hip joint force, Fx, Fy, Fz and resultant hip joint force, Fr, in terms of body weight during the stance phase of gait. See figure 7.2 for sign convention.

turn: Walk with a 90° change in the direction of progression

asc: Stair ascent

des: Stair descent

rise: Rising from a chair

con: Car entry. The outside hip (i.e the left hip) was tested as the subject entered the car.

cox: Car exit. The outside hip (i.e the left hip) was tested as the subject exited from the car.

cin: Car entry. The inside hip (i.e. the right hip) was tested as the subject entered the car.

cix: Car exit. The inside hip (i.e the right hip) was tested as the subject exited from the car.

bon: Bath entry. The outside hip (i.e. that corresponding to the last foot to leave the ground) was tested as the subject entered the bath.

box: Bath exit. The outside hip (i.e. that corresponding to the first foot to make contact with the ground) was tested as the subject exited from the bath.

bin: Bath entry. The inside hip (i.e. that corresponding to the first foot to make contact with the bath floor) was tested as the subject entered the bath.

bix: Bath exit. The inside hip (i.e. that corresponding to the last foot to leave the bath floor) was tested as the subject exited from the bath.

7.2 HIP JOINT FORCE CURVES

Curves of the three orthogonal components of hip joint force, Fx, Fy, Fz and also the resultant hip joint force, Fr, all normalized to body weight were plotted for each hip for the time period of interest of each activity. These periods were described in chapter 5. That for gait is the stance phase. An example of one of these sets of curves is given in figure 7.1. This shows the three components of hip joint force and the resultant hip joint force for group 1, the normal subjects, throughout the stance phase of gait.

All forces presented are those acting **on** the femoral head, or in the case of the patients, **on** the head of the prosthesis. The sign convention of the results is illustrated in figure 7.2. For a right hip, the convention for the force components is in accordance with the right femur coordinate system. Fx is the component acting along the anterior-posterior (A-P) femoral axis, X_F. A positive Fx indicates an anteriorly directed force and a negative Fx, a posteriorly directed force. Fy is the component acting along the superior-inferior (S-I) or vertical femoral axis, Y_F. A positive Fy denotes a superiorly directed force whilst a negative Fy denotes an inferiorly directed force, coming from above. Finally, Fz acts along the femoral

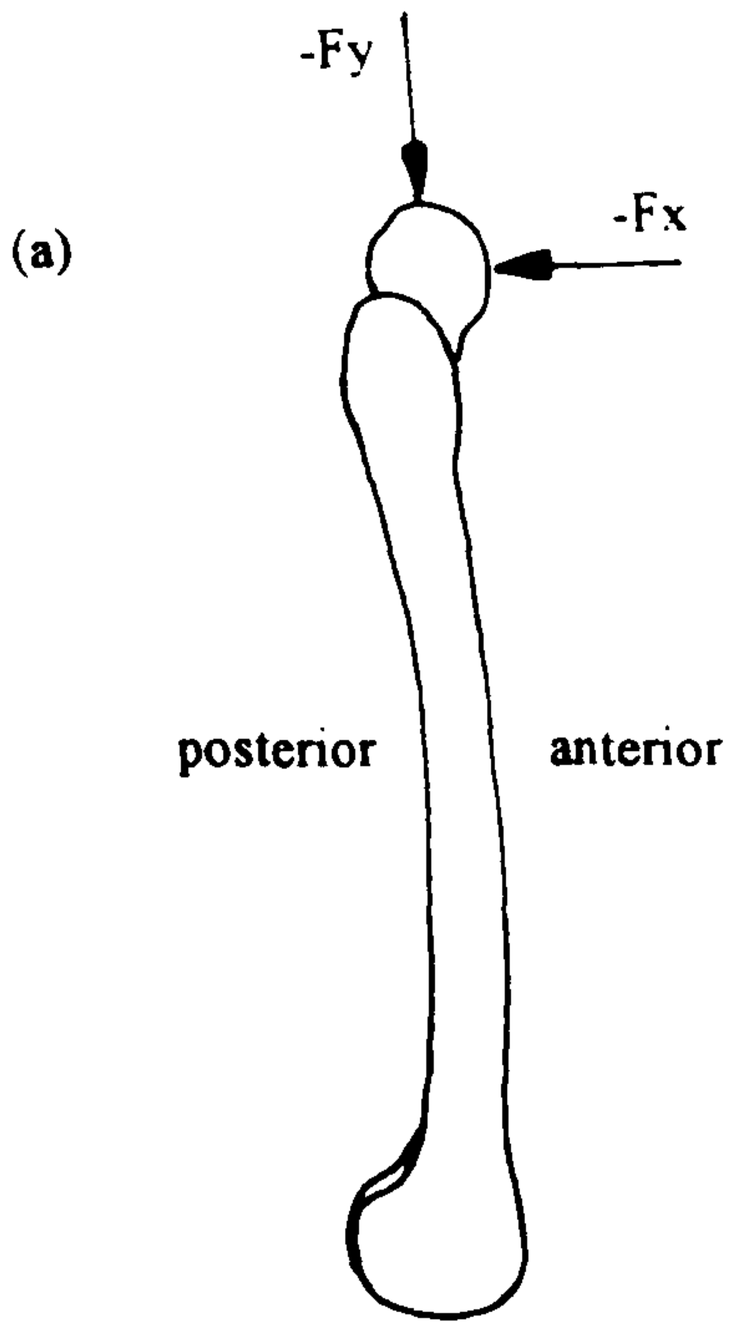

(a) Sagittal view of the femur. A negative Fy indicates an inferiorly directed joint force. A negative Fx indicates a posteriorly directed joint force.

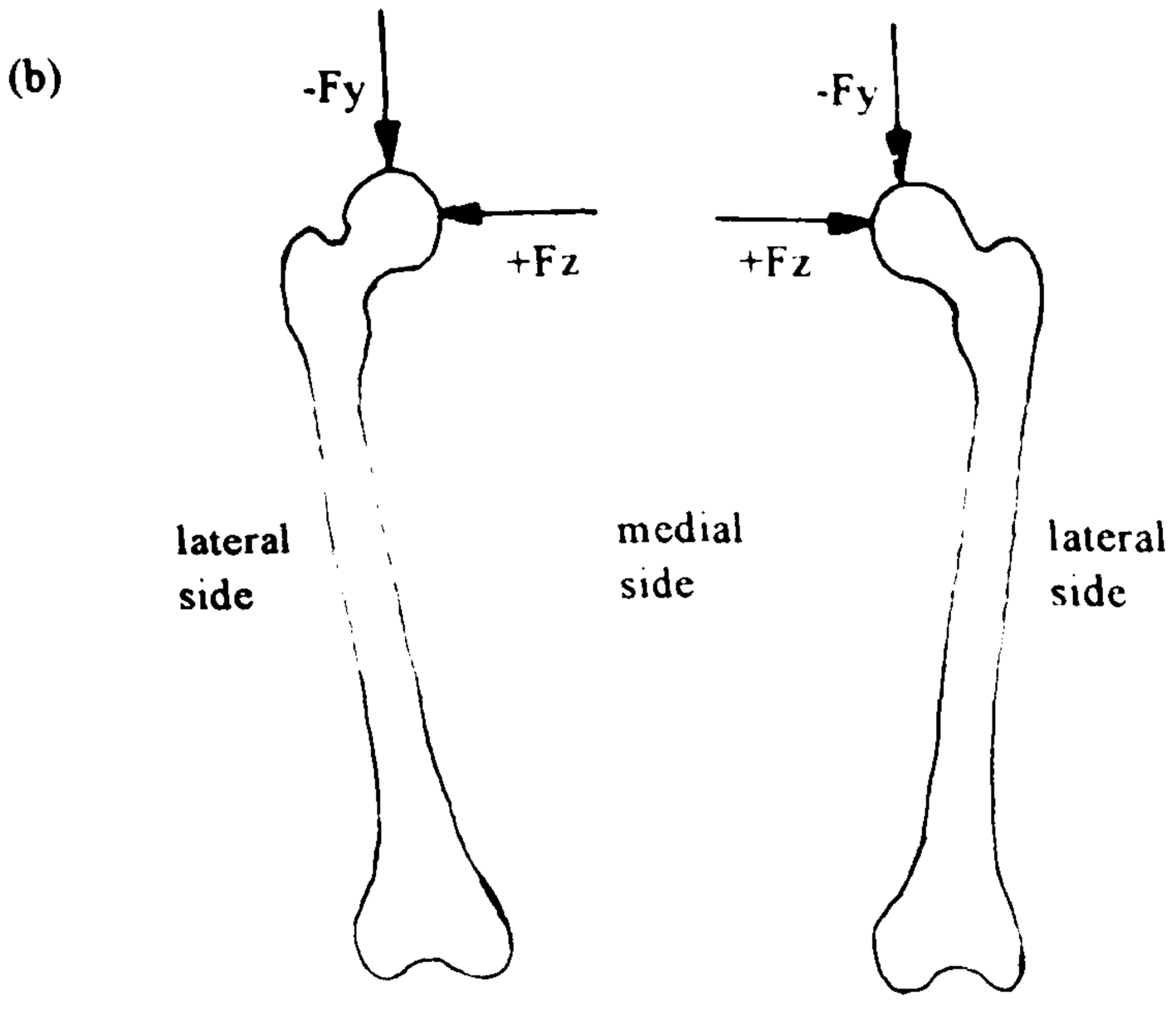

Posterior views of (b) the left femur and (c) the right femur. A positive Fz indicates a laterally directed joint force.

Figure 7.2 Sign convention of force components, Fx, Fy and Fz.

medio-lateral (M-L) axis. A positive Fz denotes a laterally directed force, coming from the medial side and a negative Fz, a medially directed force coming from the lateral side.

The system is the same for the left hip. Although the coordinate system of the left femur is right handed, the M-L component, Fz has been multiplied by -1 before presentation. Hence a positive Fz denotes a laterally directed force coming from the medial side.

The curves for the remaining activities for groups 1 and 2 are given in appendix F. Group 3, that consisting of the non prosthetic hips of patients has not been included in the curves since these results are not the main focus of the discussion. The majority of the curves produced are the averages of the curves for three trials. Sometimes the peaks in the curves of the three trials did not line up and in these cases typical trial curves were plotted. However, in obtaining values from the curves as described in the next section, all three curves were analyzed.

7.3 PEAK VALUES OF HIP JOINT FORCE

Having plotted the curves of hip joint force, peak values were obtained from the curves for each subject for each activity.

The curves of the stance phases of gait, stair ascent and descent generally exhibited two peaks as has been observed in previous studies (Paul, 1967, Poulson, 1973, Bergmann et al, 1995). Values at the two peaks were obtained for these activities allowing comparison with the work of other authors. Values at two peaks were also obtained for the walking with a turn. Occasionally, curves for these activities were not two peaked and hence only single peaks were obtained and included with the results for the first or second peak as appropriate. For the remaining activities of the car and bath, single peak values were obtained from each curve.

It was considered important to present peak values for the individual components of joint force, Fx, Fy and Fz for each activity in terms of body weight. These values will be useful in the design and testing of hip prostheses. Hence the peaks in these components were extracted from the curves. In general the peaks in the components for one trial of an activity for an individual subject occurred at the same time or were very close. This was generally the case for the activities of gait, stair negotiation, turning and rising from a chair. Sometimes the peaks in the three components did not occur simultaneously, particularly in the car and bath activities. In these cases, the peaks in two of the components usually occurred at the same time or were very close and the value of the third component at that time was similar to its peak value. Hence it was possible to calculate the peak resultant joint

(a)

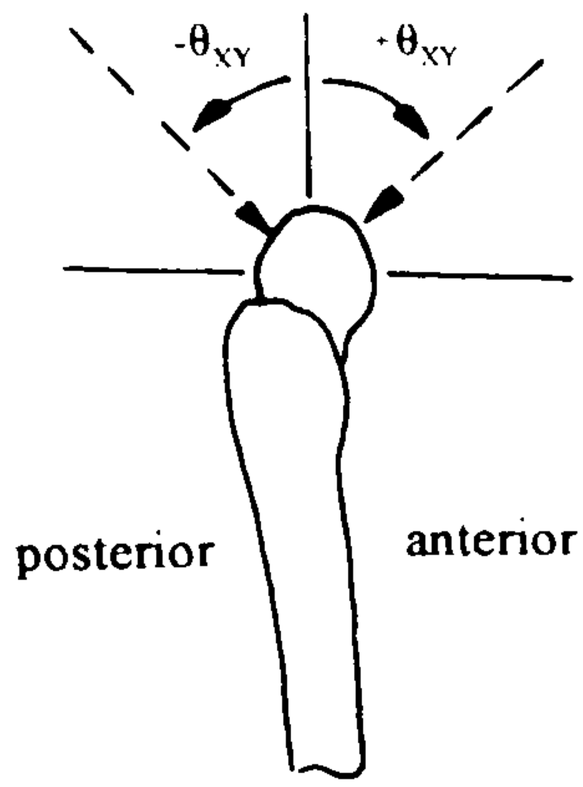

(a) Sagittal view of the proximal part of the femur. A positive θ_{XY} indicates a posteriorly and inferiorly directed joint force. A negative θ_{XY} indicates an anteriorly and inferiorly directed joint force.

(b)

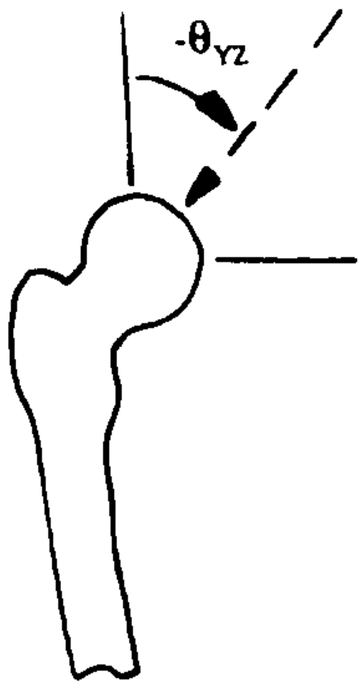

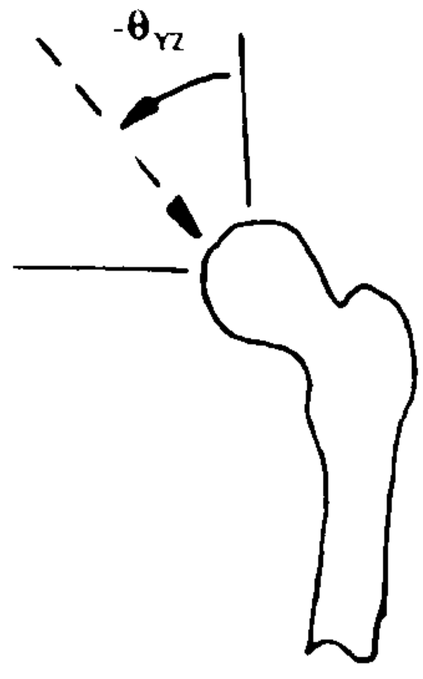

(c)

Posterior views of the proximal part of (b) the left femur and (c) the right femur. A negative θ_{YZ} indicates an inferiorly and laterally directed joint force.

(d)

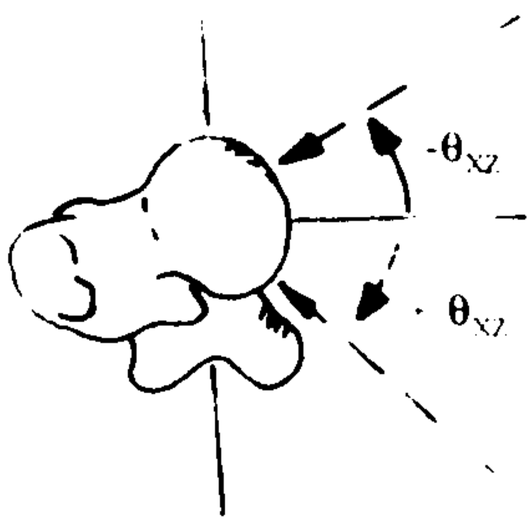

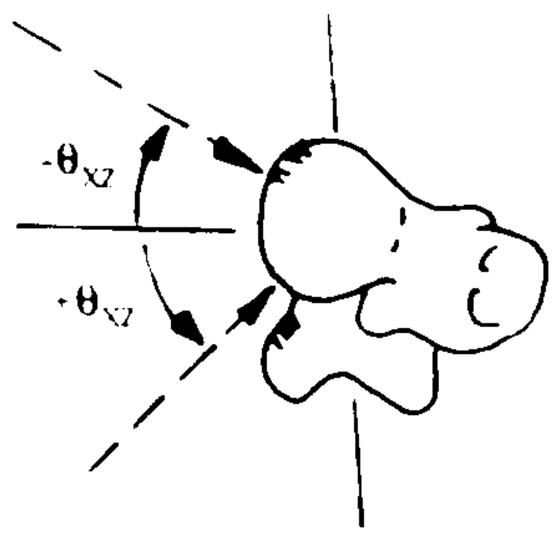

(e)

Coronal views of (d) the left femur and (e) the right femur. A negative θ_{XZ} indicates a posteriorly and laterally directed joint force. A positive θ_{XZ} indicates an anteriorly and laterally directed joint force.

Figure 7.3 Sign convention for θ_{XY}, θ_{YZ} and θ_{XZ}

force from the peak load component values with little error.

An estimate of the error resulting from the determination of the resultant peak value from the peak values of the components rather than selecting the value from the resultant force curve was obtained by examining the results of one subject, 'L', who performed all of the activities. The mean difference in peak resultant force obtained by the two methods across all of the activities was 0.03 times body weight. The maximum difference was 0.34 times body weight which occurred for the left hip on car entry. This is equivalent to 4% of the value of peak resultant force for the left hip on car entry as determined from the resultant force curve. Hence the method of calculation of peak resultant force from peaks in the load components was considered to be sufficiently accurate.

The direction of the peak resultant joint force was also calculated using the peak values of the components. This was expressed as three projected angles as illustrated in figure 7.3. The direction of the resultant projected onto the sagittal plane and measured relative to the femoral longitudinal axis, Y_F, is the angle θ_{XY}. That projected onto the frontal plane and also measured relative to the femoral longitudinal axis, Y_F, is the angle θ_{YZ}. Finally, θ_{XZ} is the direction projected onto the coronal plane and measured relative to the femoral medio-lateral axis, Z_F.

An estimate of the errors in calculating θ_{XY}, θ_{YZ} and θ_{XZ} from the peak values of the components of hip joint force was made using the results of subject 'L'. The results from this method were compared with the values of these angles at the instant of peak resultant hip joint force as determined from the resultant force curve. The mean difference in θ_{XY} between the two methods across all of the activities was 0.5°. A maximum difference of 1.7° was calculated for the outside hip on getting out of the bath. The mean difference in θ_{YZ} was 0.7° and the maximum difference was 4.4°. This was calculated for the inside hip when getting out of the bath. Finally, the mean difference in θ_{XZ} was 1° and the maximum, 4.4°. This was also calculated for the inside hip on getting out of the bath.

Having obtained peak values of Fx, Fy, Fz and Fr in terms of body weight and corresponding values of θ_{XY}, θ_{YZ} and θ_{XZ} for each subject for each activity, the mean peak values were calculated for each activity within each group. Appendix G shows the mean results with maxima, minima and standard deviations for group 1, the normal subjects, group 2, the prosthetic hips of the patients and group 3, the non prosthetic hips of patients. Standard deviations are not given in some cases due to the low number of results in that situation.

The results for subject 'Z' during stair negotiation are reported separately since this subject took the steps one at a time whilst the others climbed cyclically. Similarly, the

results for subject 'Y' for turning are reported separately since this subject turned right by twisting on the right foot and left by twisting on the left. This is opposite to the others who turned right by propulsion from the left foot and left by propulsion from the right.

For the activities of gait, stair negotiation and turning, the values for two peaks are presented. Mean greatest peak values were also calculated for Fr and Fx in terms of body weight for later discussion. These were determined using the greatest peak force for each subject, be it the first or second peak.

The results presented in appendix G are shown graphically for groups 1 and 2 in figures 7.4 to 7.11 at the end of this chapter. The results for subject 'Z' during stair negotiation and for subject 'Y' during the walking turn are not included in these figures. Also, group 3 is not included since this is not the main focus of the discussion. Figure 7.4 shows the mean peak resultant hip joint force in terms of body weight for group 1 for each activity in order of increasing magnitude. Figures 7.5 to 7.7 give the mean values of θ_{XY}, θ_{YZ} and θ_{XZ} for each activity in the same order as that presented in figure 7.4. Presentation of the results in this form allows the value of a parameter for one activity to be readily compared with that for another activity. Figures 7.8 to 7.11 show the results for group 2 in a similar format to that used for group 1.

7.4 SENSITIVITY ANALYSIS

In developing the model used to calculate hip joint forces, certain assumptions had to be made. It is the aim of this section to assess the effects of inaccuracies in these assumptions on the values of hip joint force calculated. An overall estimate of the accuracy of the results can then be made.

Each of the sources of variability is discussed in turn. The effects of each have been quantified by perturbing the parameter concerned and then examining the percentage change in each of the two peaks of resultant hip joint force during the stance phase of gait. The right hip of subject 'G' was used in the assessment. The maximum changes are discussed in this section but the results for all of the perturbations are given in appendix H.

With regard to marker placement, the points most difficult to locate by palpation are the anterior superior iliac spines (ASIS), greater trochanters and femoral epicondyles. It was estimated that these points could be located with an accuracy of ±15mm which takes into account errors in location by palpation, errors in the assessment of soft tissue thickness and Vicon measurement system errors. Markers on these points were used in static tests. They were located with respect to technical markers during these tests and then removed for

dynamic tests. Hence the effects of inaccuracies in bony point location on the final values of hip joint force were assessed by perturbing the static test data. The coordinates of each of the critical markers were moved in turn by ±15mm along each of the laboratory coordinate axes. The percentage changes in the two peaks of resultant hip joint force during the stance phase of gait were then assessed. The maximum change was a reduction of 19.9% and this occurred when the greater trochanter marker was moved by -15mm in the X coordinate direction (table H5). This may be expected since the greater trochanter marker was used to locate the hip joint centre in the anterior-posterior direction. The next greatest change was a reduction of 11.5% which occurred when the medial epicondyle marker was perturbed by -15mm in the X coordinate direction (table H3).

The second source of inaccuracy was that of skin movement and marker wobble relative to the underlying bone. Technical markers were used to reduce this problem but some errors could still occur. The technical markers for which there would be greatest skin movement relative to the underlying bone are the right and left iliac crest markers and the front and lateral thigh markers. It was estimated that the location of these markers relative to the underlying bone would not change by more than 10mm between the static and dynamic tests. The value of 10mm includes the effects of skin movement relative to underlying bone, marker wobble and Vicon system errors. In order to quantify the effects of marker movement relative to underlying bone, the gait data were perturbed. The coordinates of each of the 4 most critical markers were moved in turn by ±10mm along each of the laboratory coordinate axes. The maximum change in resultant hip joint force was an increase of 11.8% which occurred when the right iliac crest marker was perturbed by +10mm in the X coordinate direction (table H6).

The third source of inaccuracy considered was that in locating the hip joint centre. The method of Bell et al (1990) was used to predict the location of the hip joint centre. Bell et al assessed the accuracy of this method in 7 male adults and found it to predict the hip joint centre to within 11mm of the true location. Due to the differences in pelvic geometry between males and females, the inaccuracy in hip joint centre location could be slightly greater than 11mm for female subjects. In order to assess the effects of inaccurate hip joint centre location in terms of hip joint force, the coordinates of the hip joint centre were perturbed by ±11mm along each of the pelvic coordinate axes. The maximum change in the resultant hip joint force during the stance phase of gait was found to be a reduction of 15.4% which occurred for a perturbation of -15mm along the pelvic X coordinate axis (table H10).

Several anthropometric measurements were required to be made on each subject for input to the model. Those prone to greatest error include the distance between the anterior

superior iliac spines (inter ASIS distance) and the other measurements used to determine the pelvic and femoral muscle data scaling factors.

A measurement of inter ASIS distance was made using vernier callipers. This dimension was used for scaling muscle data in the +Z and -Z pelvic coordinate directions and in determining the hip joint centre location. It was estimated that the measurement obtained by the use of callipers was within ±15mm of the true value so the measurement was perturbed by this amount. The maximum change in resultant hip joint force during the stance phase of gait was an increase of 4.7% which occurred when the dimension was increased by 15mm (table H12).

The measurement used to scale the muscle data in the +X and -X pelvic coordinate directions was the distance between the frontal plane of the pelvis and the midpoint between the posterior superior iliac spines (midPSIS). This was determined using the measurement chair described in section 4.3.2. This measurement could be obtained to within ±15mm of the true value and was perturbed by this amount. The maximum change in resultant hip joint force during the stance phase of gait was an increase of 7.5% which occurred when the distance was reduced by 15mm (table H13).

The dimension used to determine the factor used for scaling muscle data in the +Y and -Y pelvic coordinate directions was the vertical distance between the ischial tuberosity and the iliac crest. This was determined by palpation and the use of vernier callipers. It was estimated that this distance could be measured to within ±15mm of the true value so it was perturbed by this amount. The maximum change in resultant hip joint force during the stance phase of gait was an increase of 2.6% which occurred when the distance was increased by 15mm (table H14).

The dimension used to determine the factor used for scaling the muscle data in the +Z and -Z femoral coordinate directions for all muscles except gastrocnemius was the lateral distance between the femoral head centre and the most lateral point on the greater trochanter. This dimension was determined using the inter ASIS distance, the medio-lateral distance between the hip joint centre and the ASIS as described by Bell et al (1990) and also the distance between the greater trochanters as measured with the subject standing in the anatomical position. It was estimated that this dimension could be determined to within ±15mm of its true value so it was perturbed by this amount. The maximum change in resultant hip joint force during the stance phase of gait was an increase of 8.8% which occurred when the dimension was reduced by 15mm (table H15).

The distance between the femoral epicondyles was used to scale muscle data in the +X and -X femoral coordinate directions and this was measured using callipers. The accuracy

to which this factor could be determined was estimated to be ±10mm and it was perturbed by this amount. The maximum change in resultant hip joint force during the stance phase of gait was a decrease of 3.4% which occurred when the factor was reduced by 10mm (table H16).

The pelvic coordinate system of Brand et al (1982) used to present muscle origin coordinates was taken to be the same as the anatomical pelvic coordinate system of the current study if a rotation of 10° was made about the medio-lateral pelvic axis. This axis is coincident in both systems. The value of 10° was the mean of measurements made on 6 pelvises. The range of measurements was between 5° and 15°. The angle was therefore perturbed by 5° and the maximum change in the resultant hip joint force during the stance phase of gait was an increase of 3.1% (table H11). This occurred when the angle was reduced by 5°.

Finally, the dimension assumed to have greatest effect on hip joint force from muscle wrapping calculations is the radius of the hip sphere. This was taken to be 25mm from cadaveric measurement and measurement of the musculoskeletal model. Morrey (1991) quoted a range of diameters from 35mm to 58mm and the radius used in the model was therefore perturbed to be 17.5mm and then 29mm. The maximum change in resultant hip joint force produced during the stance phase of gait was an increase of 6% which occurred when the hip sphere radius was reduced to 17.5mm (table H17).

This completes the quantification of errors due to sources assumed to have the greatest effects on hip joint force. There are other sources of error but these were estimated to be secondary to those already quantified. For example, there will be some error in muscle origin and insertion coordinates due to differences in musculoskeletal geometry between subjects but these are reduced by scaling. Also, the moment arms at the knee joint were assumed to be the same for all subjects but they will vary between subjects. Effects of these on hip joint force will be via the action of the two joint muscles.

Finally, the same method of calculation was used for the normal subjects and the post-operative hip replacement subjects. The joint centre location of the prosthetic hips of patients may change relative to that prior to disease in the pre-operative joint. The radius of the hip sphere can also change. There may also be changes in the hip joint muscle moment arms due to changes in femoral neck length and anteversion angle after surgery. The greatest error will occur due to the change in hip joint centre location relative to the femur. These changes could not be quantified since X rays taken in a standardised manner were not available.

In order to produce an estimation of the overall accuracy of the joint forces calculated the maximum percentage errors quoted above were summed. It is unlikely that all of the

inaccuracies will occur together and even if they did the effect of one may be counteractive to that of another. However, in order to give a worst case scenario, the maximum values were summed to give a total of 83.2%. If the maximum changes are considered as the quoted increases and decreases then the overall accuracy is an increase of only 5.8%. These methods of determining the overall accuracy are very simple. A full analysis of the interaction of the various perturbations would involve an extensive numerical study and is outwith the aims of this thesis.

Subject	Sex	Age / years	Height / m	Mass / kg
D	M	62	1.70	70.0
E	F	58	1.65	58.0
F	F	64	1.54	64.0
G	M	62	1.61	67.0
H	F	61	1.53	64.0
I	F	65	1.62	71.5
J	F	60	1.57	60.5
L	M	68	1.77	73.0
M	F	65	1.52	47.0
R	M	68	1.69	70.0

Table 7.1 Details of normal subjects

Subject	Sex	Age / years	Height / m	Mass / kg
A	F	77	1.63	70.0
B	F	74	1.61	78.5
C	F	64	1.52	67.5
K	M	74	1.66	65.0
N	M	70	1.66	90.0
O	M	72	1.80	81.0
P	M	73	1.66	69.5
Q	F	80	1.55	63.0
S	M	71	1.60	63.0
T	F	77	1.59	64.5
U	F	80	1.64	75.5
V	M	73	1.74	80.5
W	F	58	1.68	88.4
X	F	66	1.56	63.0
Y	M	60	1.81	83.0
Z	F	67	1.67	65.3

Table 7.2 Details of patients

Subject	Prosthetic hip	Non prosthetic hip	Prosthesis type	Time of test / months post op.
A	R	L	Howse	24.5
B	L	R	Howse	23.5
C	R	L	Howse	25.0
K	R	L	Howse	14.0
N	R L		Charnley Charnley	R - 74.0 L - 14.0
O	R	L	Howse	14.0
P	R L		Howse Howse	R - 14.5 L - 10.0
Q	R	L	Charnley	14.0
S	L	R	Howse	15.0
T	R	L	Charnley	13.0
U	L	R	Charnley	13.0
V	L	R	Charnley	13.0
W	R	L	Howse	13.0
X	R	L	Howse	15.0
Y	R L		Charnley Charnley	R - 13.0 L - 13.0
Z	R	L	Howse	22.0

Table 7.2 continued. Details of patients

Activity	Group1. Hips of normal subjects	Group 2. Prosthetic hips of patients	Group 3. Non prosthetic hips of patients
gait	15	19	12
turn	18	16	8
asc	20	18	12
des	20	17	12
rise	20	17	13
con	9	2	2
cox	10	5	6
cin	8	2	0
cix	8	1	0
bon	10	5	4
box	10	6	3
bin	8	4	4
bix	10	4	3

Table 7.3 Number of hips tested in each activity. For a description of each activity code see section 7.1.

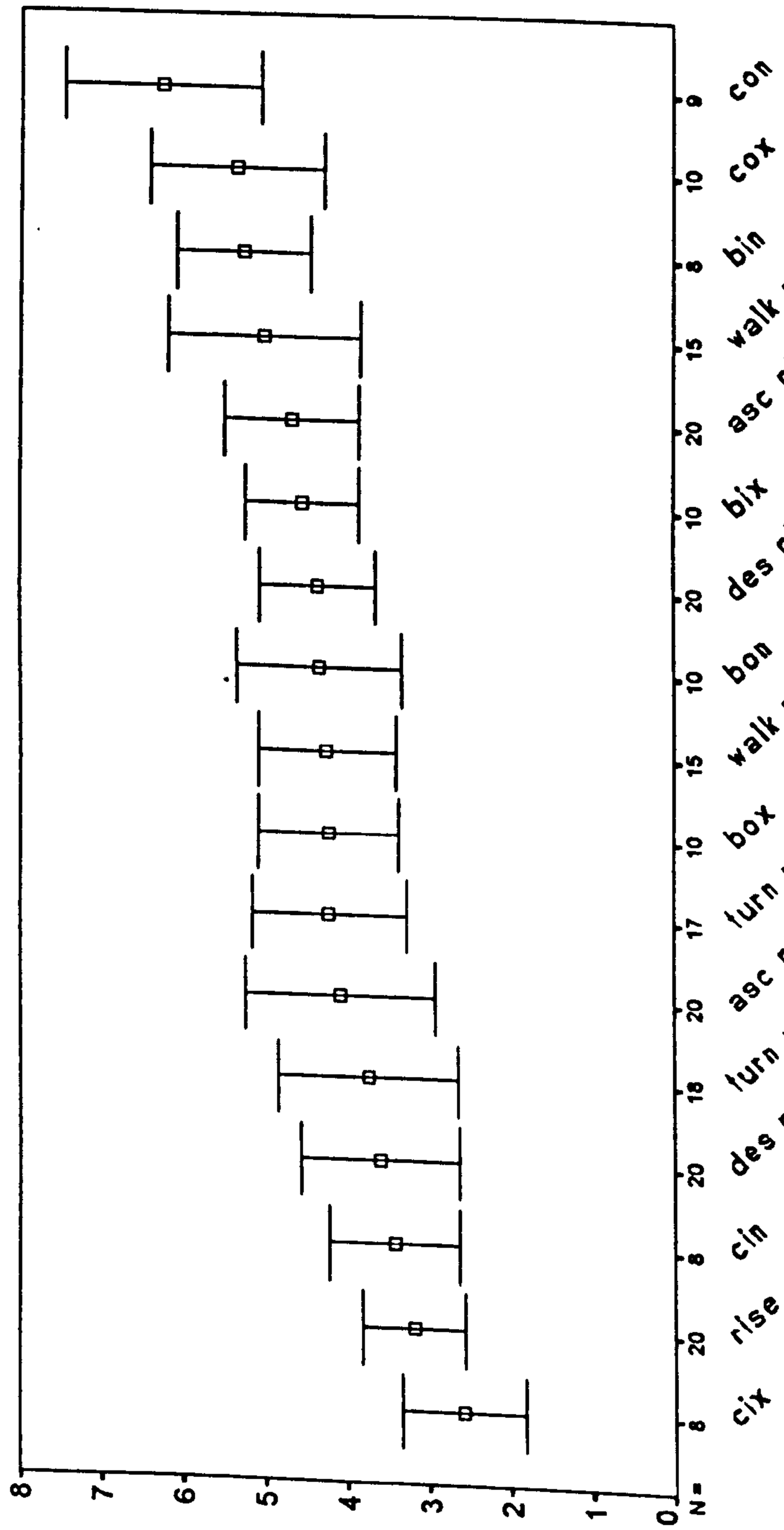

Figure 7.4 Group 1 - Hips of normal subjects. Mean peak values of resultant joint force, Fr, in terms of body weight (± 1 S.D.). For a description of each activity code see section 7.1.

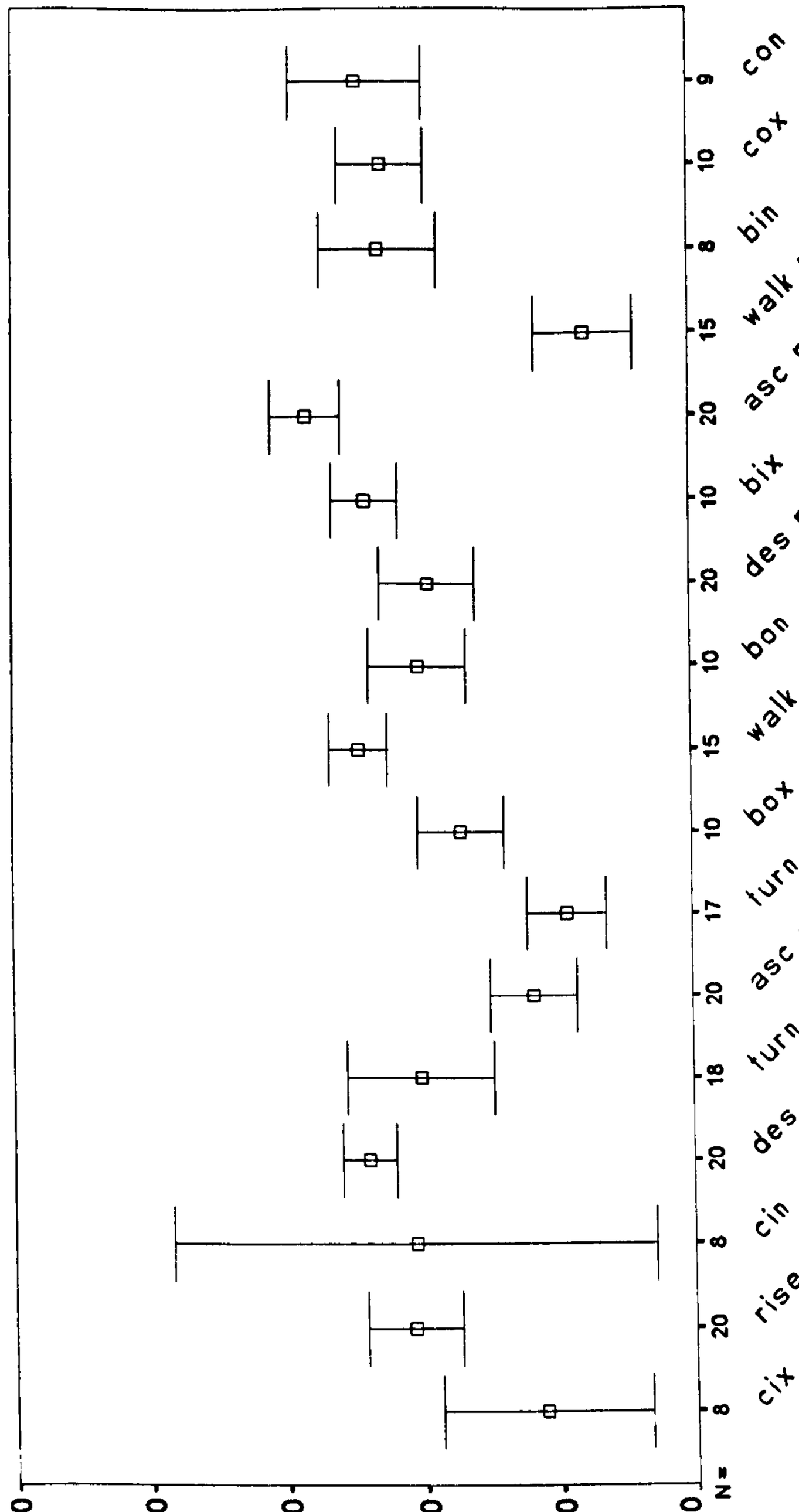

Figure 7.5 Group 1 - Hips of normal subjects. Mean values of θ_{xy} (± 1 S.D.). For sign convention see figure 7.3. For a description of each activity code see section 7.1.

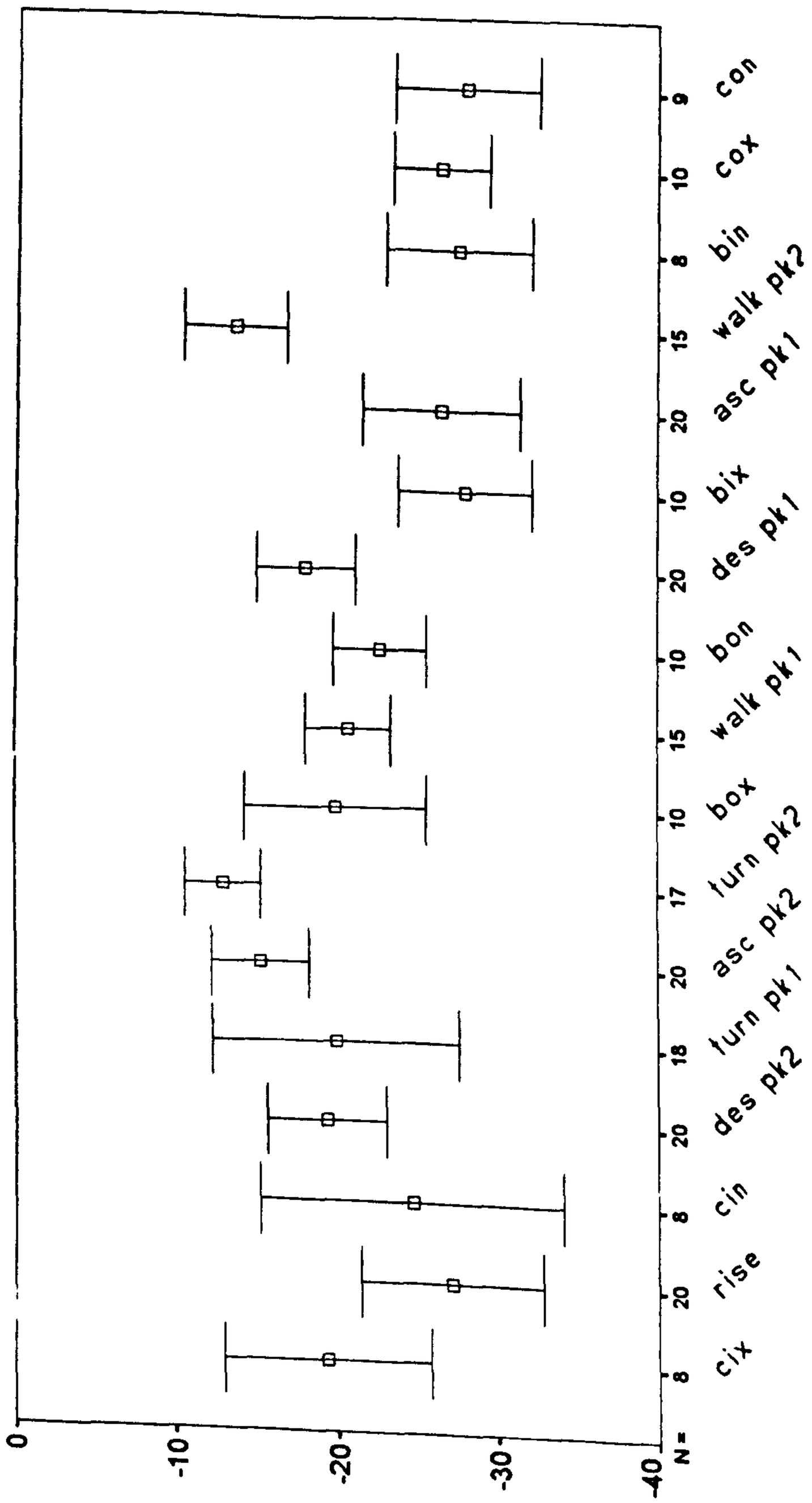

Figure 7.6 Group 1 - Hips of normal subjects. Mean values of θ_{yz} (± 1 S.D.). For sign convention see figure 7.3. For a description of each activity code see section 7.1.

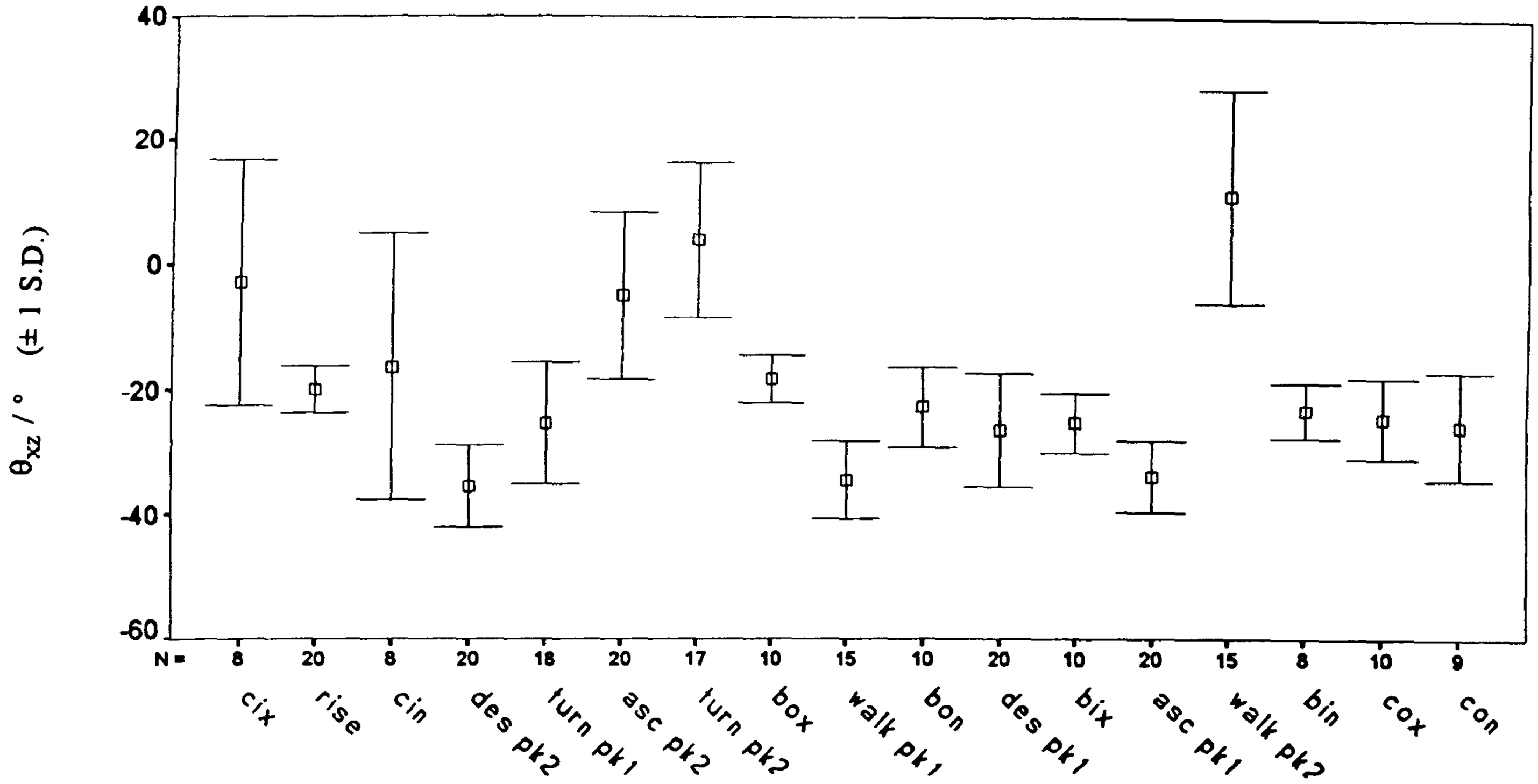

Figure 7.7 Group 1 - Hips of normal subjects. Mean values of θ_{xz} (± 1 S.D.). For sign convention see figure 7.3. For a description of each activity code see section 7.1.

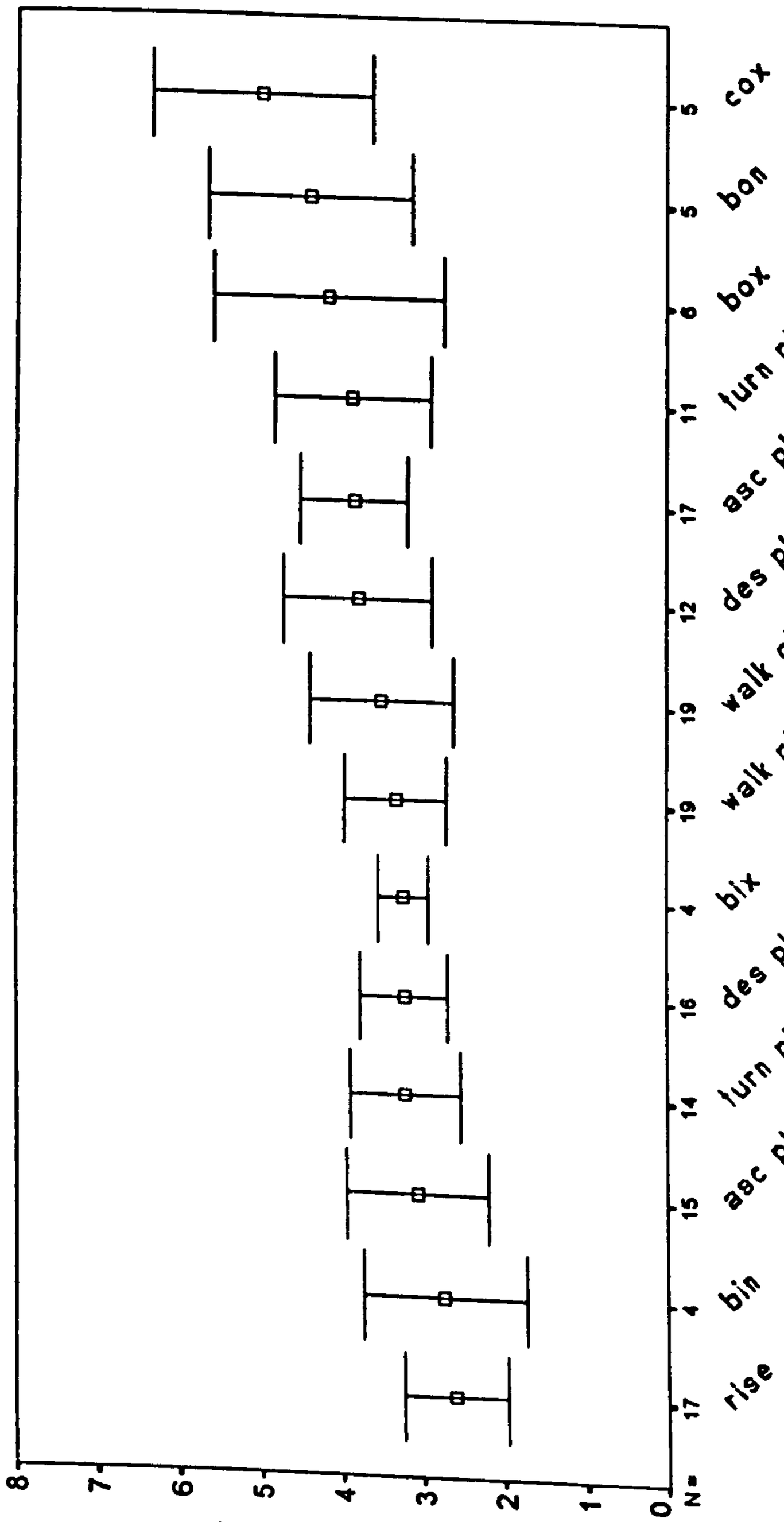

Figure 7.8 Group 2 - Prosthetic hips of patients. Mean peak values of resultant joint force, Fr, in terms of body weight (± 1 S.D.). For a description of each activity code see section 7.1.

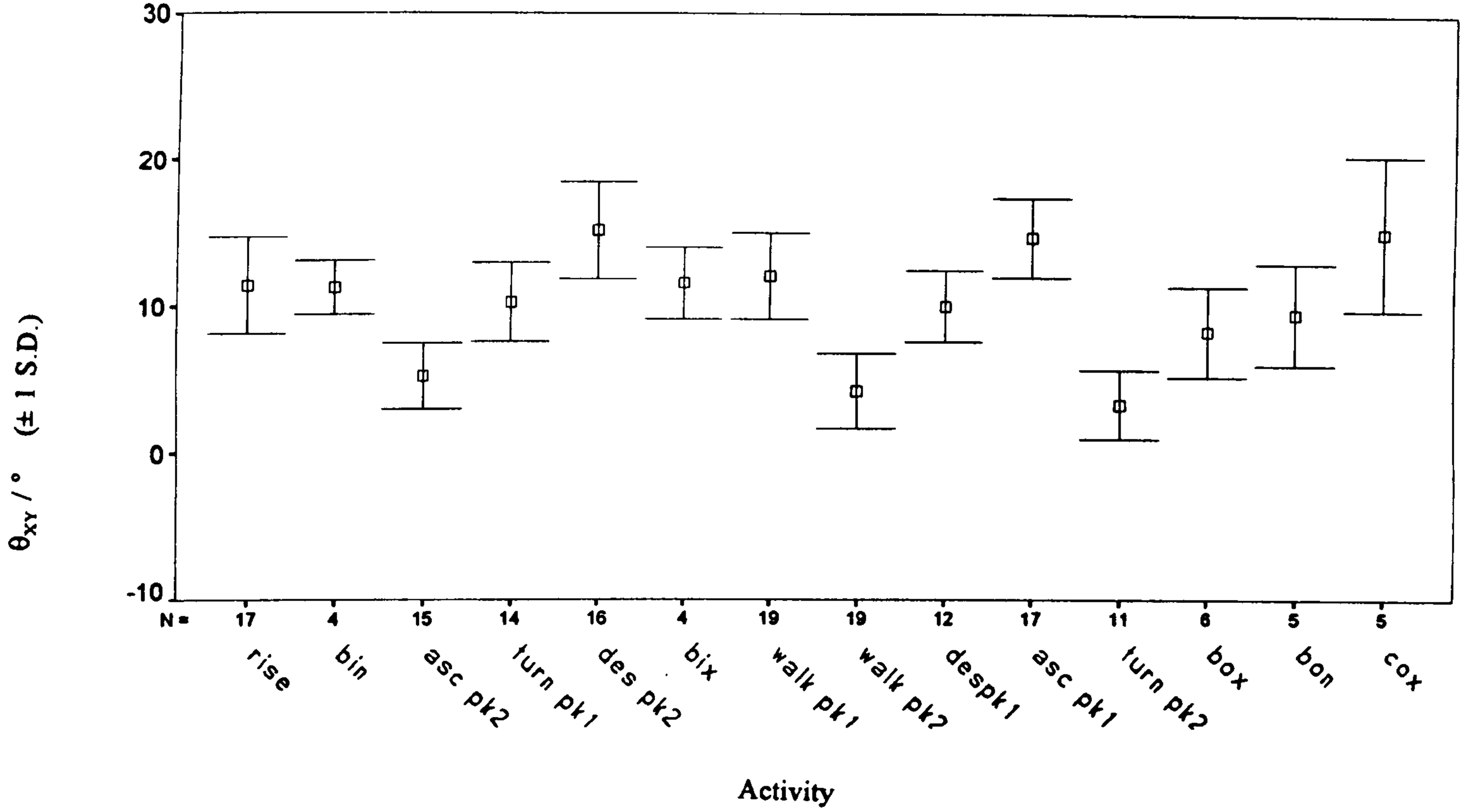

Figure 7.9 Group 2 - Prosthetic hips of patients. Mean values of θ_{XY} (± 1 S.D.). For sign convention see figure 7.3. For a description of each activity code see section 7.1.

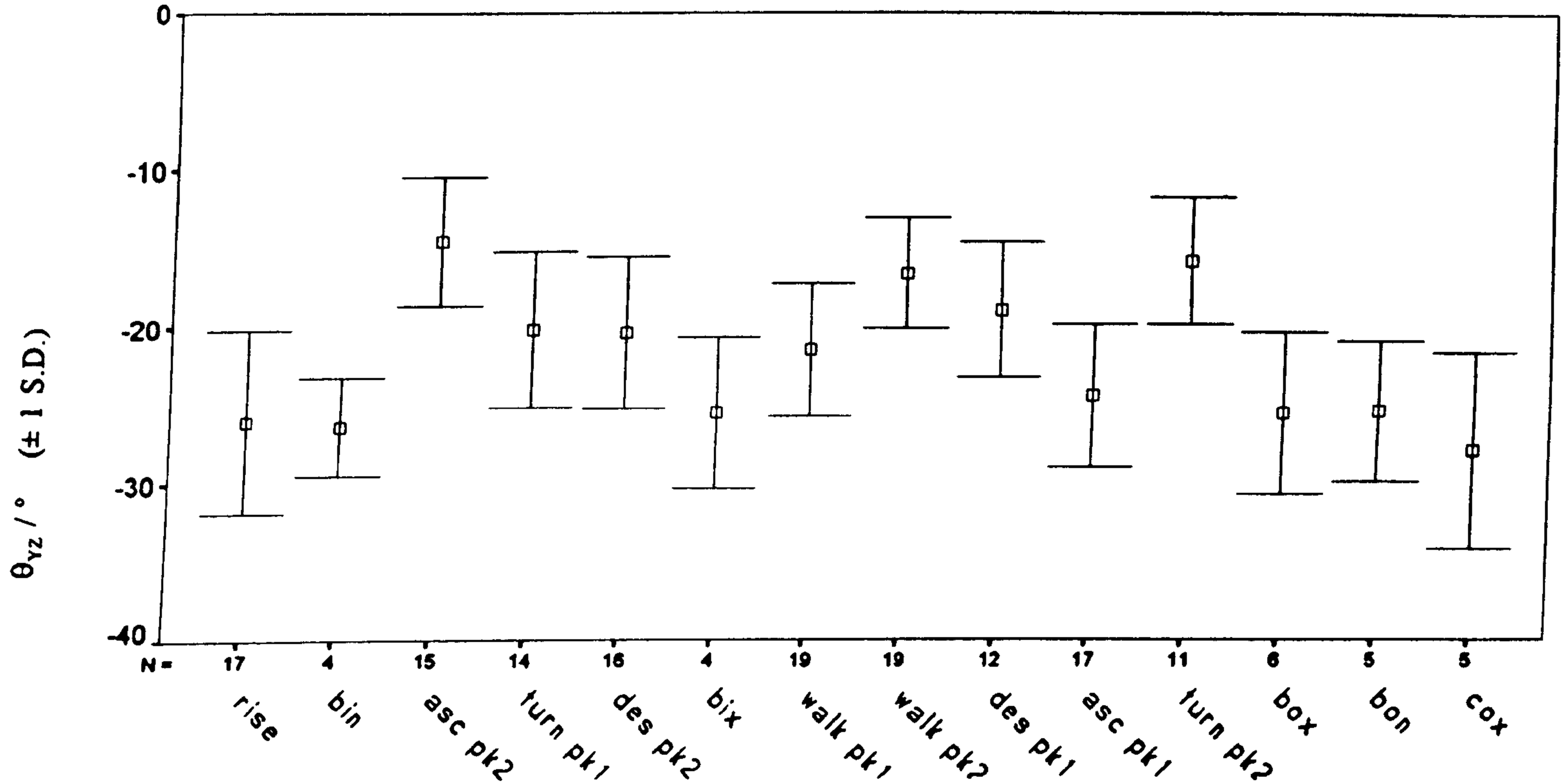

Figure 7.10 Group 2 - Prosthetic hips of patients. Mean values of θ_{YZ} (± 1 S.D.). For sign convention see figure 7.3. For a description of each activity code see section 7.1.

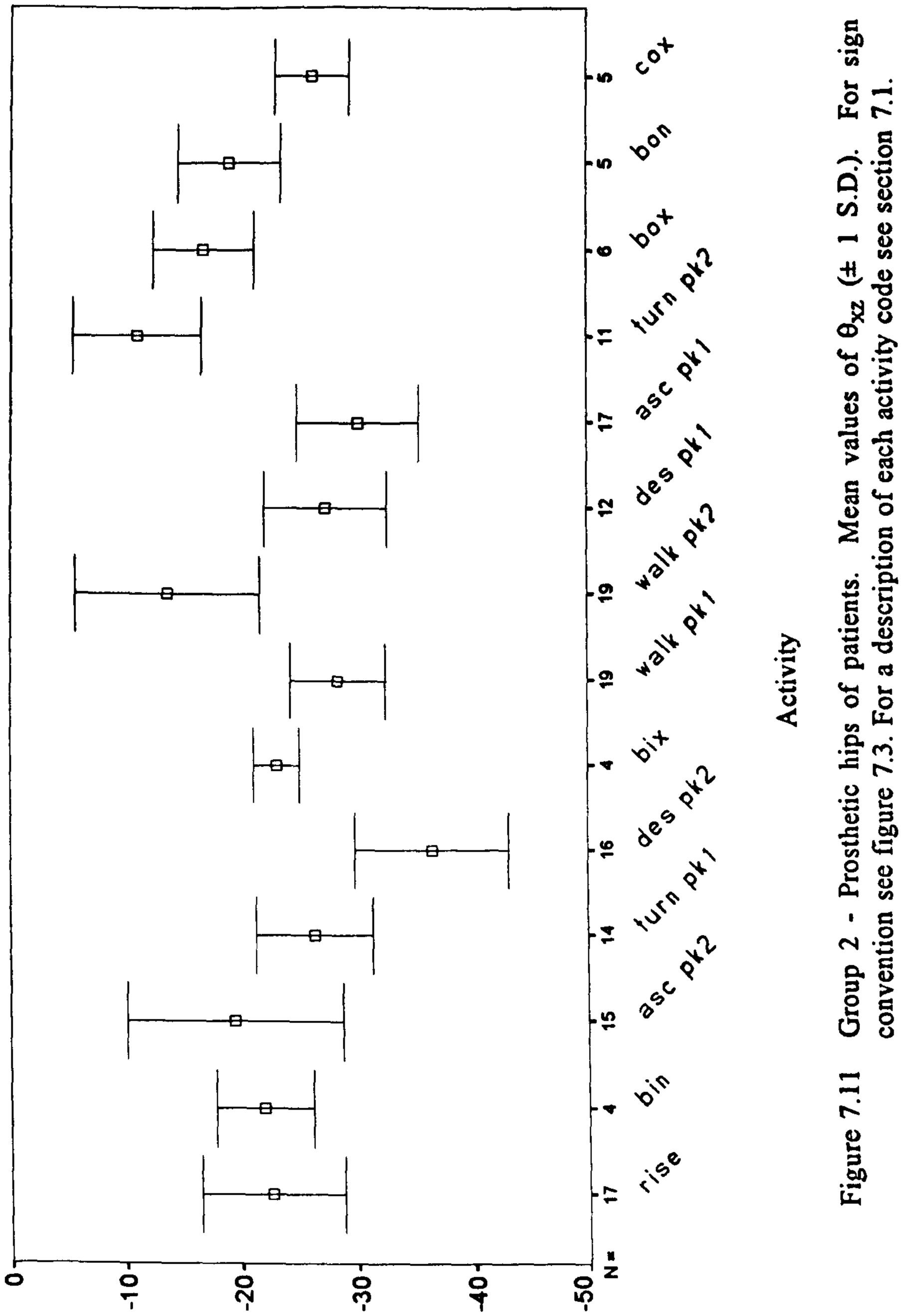

Figure 7.11 Group 2 - Prosthetic hips of patients. Mean values of θ_{xz} (± 1 S.D.). For sign convention see figure 7.3. For a description of each activity code see section 7.1.

CHAPTER 8. DISCUSSION OF FINAL RESULTS

The results presented in chapter 7 are discussed in this chapter. The results for gait, stair negotiation and rising from a chair are compared with those of other authors. The remaining activities have not to the author's knowledge been studied before and the second section of the discussion includes these activities.

8.1 COMPARISON WITH PUBLISHED WORK

It was considered important to assess the results of the current study in relation to those presented by other authors. The first part of this section discusses the results for group 2, the prosthetic hips of the patients and the second considers the results for group 1, the hips of the normal subjects.

8.1.1 Prosthetic Hips of Patients

There have been several studies performed to measure or calculate the forces at the prosthetic hip joint as various activities are performed. To the author's knowledge, the current study includes the greatest number of patients performing the greatest number of activities.

The first direct 'in vivo' measurements of hip joint force were made by Rydell (1966). Prostheses with strain gauges were implanted into two patients. The first case was a 51 year old male who sustained a fracture of the right femur in a motor accident. The second case was a 56 year old female who had fallen from a table and fractured her left femoral neck. In both cases, approximately 6 months after the implantation, the leads to the strain gauges were accessed and the forces measured during a ranges of activities including gait and stair negotiation.

Following Rydell, English and Kilvington (1979) implanted a strain gauged axial load femoral prosthesis into a 59 year old female and measured the joint force during gait up to 42 days post-operatively.

More recently, 'in vivo' hip joint forces were recorded using telemeterised strain gauged prostheses by a group from the Case Western Reserve University (CWRU), Cleveland (Davy et al, 1988, Kotzar et al, 1991). The first subject was a 67 year old female whose instrumented prosthesis was used to revise a right hemiarthroplasty. She also had a left hip replacement. The second subject was a 72 year old male with osteoarthritis. In both cases, gait data were obtained in the early post-operative period. Activities included gait, stair

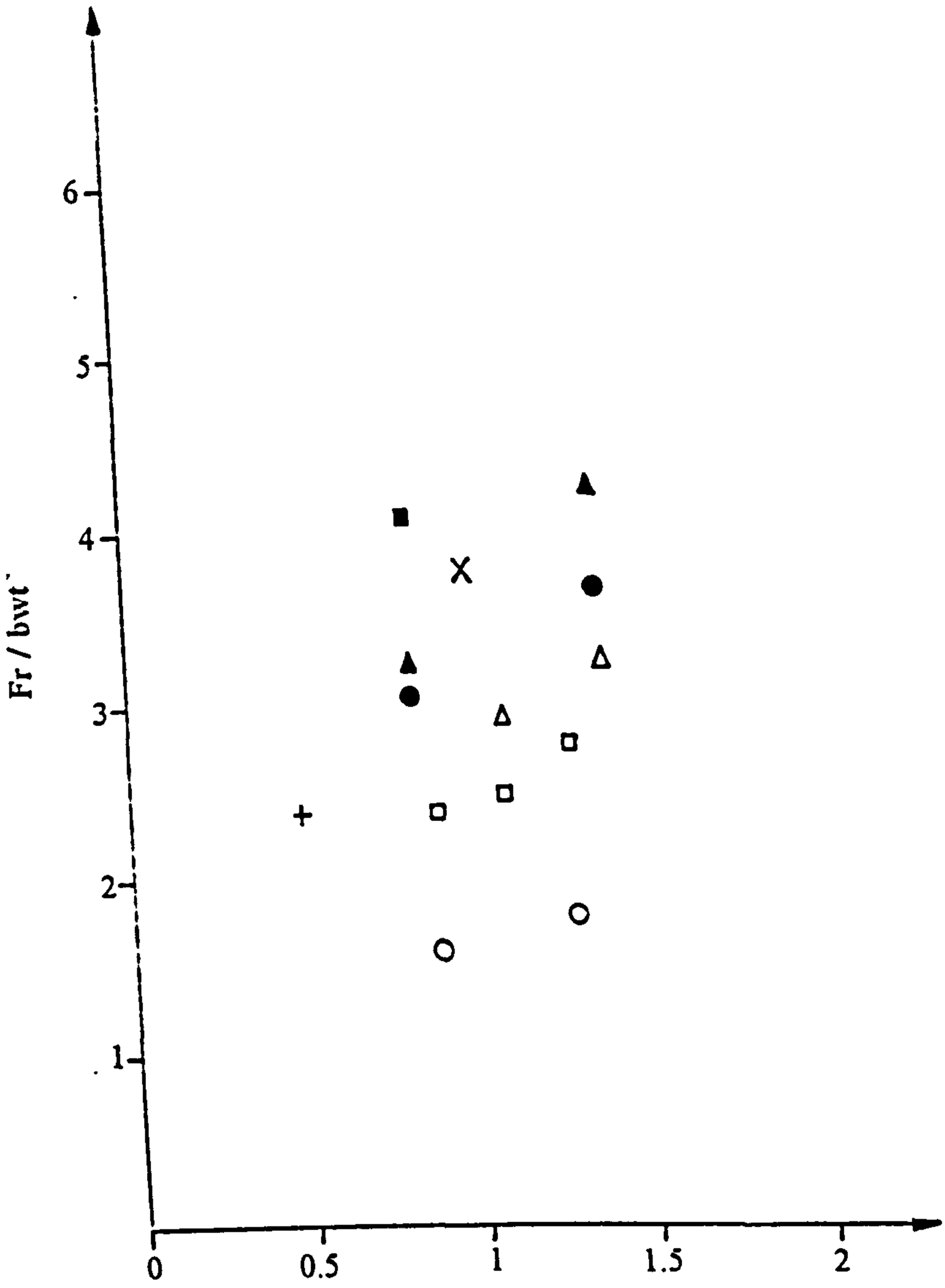

Figure 8.1 The variation of peak resultant hip joint force, Fr, in terms of body weight with gait speed for post-operative hip replacement patients. The values plotted are presented in table 8.1. Where two peaks are presented in table 8.1, the maximum is used in this figure.

× Current study
○ Rydell (1966) - Case 1
△ Rydell (1966) - Case 2
\+ CWRU Kotzar et al (1991) - Subject 1
□ CWRU Kotzar et al (1991) - Subject 2
● Bergmann et al (1993) - EBL
▲ Bergmann et al (1993) - EBR
■ Bergmann et al (1993) - JB

climbing and rising from a chair.

The final study involving direct measurement to be included in this section is that carried out by a group from the orthopaedic hospital of the Free University of Berlin (Bergmann et al, 1993, 1995). Bergmann's group have studied two subjects. The first, an 82 year old male with severe arthritis, received instrumented prostheses in both right and left hips. This patient had been an active swimmer and sky diver all his life and was in excellent physical condition. The second subject was a 69 year female with unilateral idiopathic femoral head necrosis. She received an instrumented implant in the right hip. This patient also suffered from cerebellar atrophy and axonal polyneuropathy in the right leg. She was chosen because her clinical symptoms were predicted to cause increased joint forces. Activities studied in both subjects included gait and stair negotiation. In the male subject, data were recorded up to 30 months after the operation and in the female subject, up to 18 months post-operatively.

Investigations which have calculated hip joint forces during gait in post-operative hip replacement subjects include Paul and McGrouther (1975) and Brown et al (1984). Paul and McGrouther calculated the forces for three patients with Charnley hip prostheses at 6 months after surgery. Brown et al determined the forces for 8 subjects with Charnley prostheses and 6 with CAD Muller prostheses 12 months after surgery. The values quoted for Brown et al in this section were obtained by measurement of the curves which they presented.

In the following sections, the results observed in the current study are assessed in relation to those from the foregoing research groups. Each of the activities of gait, stair negotiation and rising from a chair is discussed in turn. The magnitude of the resultant hip joint force is discussed first and then the direction of the joint force vector.

Gait - Resultant hip joint force

The mean speed of gait recorded for the patients was 1.01m/s with a standard deviation, S.D. of ±0.21m/s. As can be seen from appendix F (fig F2), the resultant hip joint force exhibited two peaks during the stance phase of gait. The mean value for the first peak was 3.33 times body weight (S.D.±0.63) and the second, 3.5 times body weight (S.D.±0.88). In 10 cases, the first peak was greater than the second and in 9 cases, the second peak was greater than the first. A mean greatest peak value of 3.79 times body weight (S.D.±0.79) was calculated using the greatest peak for each subject, be it the first or the second. Figure 8.1 shows this value in relation to those reported by other authors on a graph of peak resultant hip joint force versus speed.

It can be seen from figure 8.1 that within each study, the peak resultant hip joint force increases with gait speed. However, for a given speed, the values vary among authors. This

Author, subject, speed	Post op. time	Resultant hip joint force in terms of body weight, Fr/bwt		
		Peak 1	Peak 2	Greatest peak
Rydell (1) Case 1 0.9m/s 1.3m/s Case 2 1.1m/s 1.4m/s	6 months	1.51 (±0.13) 1.80 (±0.29) 2.95 (±0.16) 3.27 (±0.32)	1.59 (±0.11) 1.76 (±0.18) 2.23 (±0.12) 2.55 (±0.19)	
CWRU (2) Subject 1 0.5m/s (parallel bars) Subject 2 0.9m/s 1.1m/s 1.3m/s	31 days 58 days			2.4 (±0.1) 2.4 (±0.1) 2.5 (±0.3) 2.8 (±0.2)
Bergmann et al (3) EBL 0.83m/s 1.39m/s EBR 0.83m/s 1.39m/s JB 0.83m/s	30 months 8 months			3.07 (3.30) 3.69 (3.94) 3.24 (3.52) 4.29 (4.71) 4.09 (4.64)
Paul & McGrouther (4)	up to 6 months			2.5-4
Brown et al (5) Muller Charnley	12 months	4.04 (±0.33) 2.63 (±0.39)	4.82 (±0.31) 3.33 (±0.53)	

Table 8.1 Resultant hip joint forces during gait as recorded in post-operative hip replacement patients.
(1) From Rydell (1966). Average values (± standard deviation)
(2) From Kotzar et al (1991). Average values (± standard deviation)
(3) From Bergmann et al (1993). Median values given with maximums.
(4) From Paul & McGrouther (1975)
(5) From Brown et al (1984). Average values (± 2 standard errors)

illustrates that the resultant joint force is not simply related to speed but must also be determined by other factors. Such factors can include post-operative measurement time, other clinical disorders, stride length and cadence, all of which are inter-related. It is therefore difficult to compare across studies.

However, it can be seen from figure 8.1 that the mean peak resultant joint force calculated in the current study is most consistent with the values reported by Bergmann's group. It is greater than all of the values reported by the group from CWRU and Rydell even though some of the values of Rydell and the group from CWRU were recorded at speeds which were greater than the mean speed measured in the current study. These differences could be due to the longer post-operative measurement time of the current study as compared to those of Rydell and the group from CWRU. Rowe (1990) found the level of activity to increase after the operation for about the first 12 months and then reach a stable level. This would explain why the mean peak value for the current study is most consistent with those reported by Bergmann's group.

The following discussion makes detailed comparisons to the results of other authors presented in table 8.1 and figure 8.1. The results of Brown et al and Paul and McGrouther are included in addition to those of Rydell, the group from CWRU and Bergmann et al The two individual peaks in the resultant hip joint force calculated during the stance phase of gait are considered first, followed by a discussion of the mean greatest peak value.

Rydell and Brown et al reported values for each of the two peaks. It is most conclusive to compare to Rydell's second subject than the first. This is because the first subject exhibited an abnormal gait pattern, the vertical component of the ground reaction force showing irregularities. Rydell suggested that this could have been due to slackness in the joint. The first peak of 3.33 times body weight (S.D.±0.63) measured at 1.01m/s in the current study is greater than the value of 2.95 times body weight (S.D.±0.16) measured in Rydell's second subject at a comparable speed of 1.1m/s. It is less than the peak value of 4.04 times body weight (2S.E.±0.33) recorded by Brown et al at an unspecified speed. However, in both comparisons, the ranges covered by the standard deviations and standard errors overlap. The mean peak value reported by Rydell may be slightly less than that in the present study due to a shorter post-operative measurement time.

The second peak of 3.5 times body weight (S.D.±0.88) also lies between the value of 2.23 times body weight (S.D.±0.12) measured in Rydell's second subject at 1.1m/s and the maximum peak of 4.82 times body weight (2S.E.±0.31) reported by Brown et al at an unspecified speed. Again, the mean peak value reported by Rydell may be slightly less than that in the present study due to a shorter post-operative measurement time.

Author, subject,	Post op. time	Resultant hip joint force in terms of body weight, Fr/bwt		
		Peak 1	Peak 2	Greatest peak
Rydell (1) Case 1 Case 2	6 months	1.54 (±0.13)	1.30 (±0.14)	3.38 (±0.18)
CWRU (2) Subject 1 (bannister) Subject 2 (free)	31 days 58 days			2.3 (±0.2) 2.6 (±0.1)
Bergmann et al (3) EBL EBR JB	14-33 months 27-30 months 8 months			3.45 3.56 5.52

Table 8.2 Resultant hip joint forces during stair ascent as recorded in post-operative hip replacement patients.
(1) From Rydell (1966). Average values (± standard deviation)
(2) From Kotzar et al (1991). Average values (± standard deviation)
(3) From Bergmann et al (1995). Median values given.

Bergmann's group, the group from CWRU and Paul and McGrouther all reported single values describing the greatest peak in the resultant joint force curve. The mean greatest peak value of 3.79 times body weight (S.D.±0.79) calculated at a gait speed of 1.01m/s in the current study is consistent with the results for the right hip of Bergmann's first subject, EBR. It lies between the values of 3.24 and 4.29 times body weight measured in EBR at 0.83m/s and 1.39m/s respectively. However, it is greater than the results of 2.4 and 2.5 times body weight reported at 0.9m/s and 1.1m/s by the group from CWRU. These values may be low due to the comparatively early post-operative time at which they were measured. The value of 3.79 times body weight (S.D.±0.79) recorded in the current study also lies within the range of 2.5-4 times body weight reported by Paul and McGrouther at an unspecified speed.

Stair ascent - Resultant hip joint force

As in gait, the resultant hip joint force exhibited two peaks during the stance phase of stair ascent. This can be observed from appendix F (fig F6). The first peak was almost always greater than the second. The mean value of the first was 3.84 times body weight (S.D.±0.66) and the second, 3.06 times body weight (S.D.±0.88). A mean greatest peak value of 3.98 times body weight (S.D.±0.6) was calculated using the greatest peak for each subject, be it the first or the second. As can be seen from table 8.2, this value lies within the range of values reported by other authors.

Rydell, the group from CWRU and Bergmann's group studied stair ascent and their values are presented in table 8.2. Bergmann's group and the group from CWRU presented two peaked curves. Rydell observed two peaks for his first subject, the first always being greater than the second. He observed only one peak in the second subject who climbed the stairs at a greater speed.

The mean greatest peak value of 3.98 times body weight (S.D.±0.6) recorded in the current study lies between the value of 3.38 times body weight measured by Rydell in his second subject and the maximum of 5.52 times body weight reported by Bergmann's group. Bergmann's group measured this maximum value in subject JB. The large difference between the value calculated in the current study and that measured in subject JB is likely to be due to the previously mentioned clinical symptoms of subject JB resulting in increased joint forces. The value of 3.98 times body weight (S.D.±0.6) recorded in the current study is more consistent with the values of 3.45 and 3.56 times body weight recorded by Bergmann's group for their other subject. It is greater than the values of 2.3 and 2.6 times body weight reported by the group from CWRU. This is likely to be due to the longer post-operative measurement time in the current study as compared to that used by the group from CWRU.

Author, subject,	Post op. time	Resultant hip joint force in terms of body weight, Fr/bwt		
		Peak 1	Peak 2	Greatest peak
Rydell (1) Case 1 Case 2	6 months	1.29 (±0.11) 2.77 (±0.41)	1.59 (±0.18) 2.83 (±0.31)	
Bergmann et al (2) EBL EBR JB	 14-30 months 27-30 months 8 months			 3.94 3.90 5.09

Table 8.3 Resultant hip joint forces during stair descent as recorded in post-operative hip replacement patients.
(1) From Rydell (1966). Average values (± standard deviation)
(2) From Bergmann et al (1995). Median values given.

Author, subject	Post op. time	Peak resultant hip joint force in terms of body weight, Fr/bwt
CWRU (1) Subject 1 (with arm support) Subject 2 (free)	 31 days 58 days	 1.2 1.23

Table 8.4 Resultant hip joint forces during rising from a chair as recorded in post-operative hip replacement patients.
(1) From Kotzar et al (1991).

Stair descent - Resultant hip joint force

Again, two peaks were exhibited in the resultant hip joint force curve for the stance phase of stair descent. This is illustrated in appendix F (fig F8). The mean value for the first peak was 3.79 times body weight (S.D.±0.92) and for the second, 3.22 times body weight (S.D.±0.54). In 9 cases the first peak was greater than the second whilst in 10 cases the second was greater than the first. A mean greatest peak value of 3.67 times body weight (S.D.±0.78) was calculated using the greatest peak for each subject, be it the first or the second. This value lies within the range of values reported by other authors as presented in table 8.3.

Table 8.3 shows the peak values recorded by Rydell and Bergmann's group. These researchers also reported two peaked curves. The mean peak value of 3.67 times body weight (S.D.±0.78) reported in the current study lies between that of 2.83 times body weight measured in Rydell's second subject and the maximum of 5.09 times body weight reported by Bergmann' group. As was the case in stair ascent, this maximum value was recorded for subject JB. Again, the large difference between the value calculated in the current study and that measured in subject JB is likely to be due to the fact that subject JB suffered from clinical symptoms resulting in increased joint force. The value of 3.67 times body weight (S.D.±0.78) calculated in the current study is closer to those of 3.94 and 3.90 times body weight recorded by Bergmann's group in their other subject.

Rising from a chair - Resultant hip joint force

The mean peak resultant hip joint force during rising was 2.6 times body weight (S.D.±0.64). Of the studies used for comparison, that of the group from CWRU was the only one to report resultant hip joint forces during rising from a chair. The chair height was 445mm, similar to that used in the current study. As shown in table 8.4, the peak forces recorded were 1.2 times body weight for the first subject with the use of arms and 1.23 times body weight for the second subject who did not use arms.

Although the value in the current study is greater than those reported by the group from CWRU, the trend in values when compared to other activities is similar. The values reported by the CWRU group for gait (2.4-2.8 times body weight) and stair ascent (2.3-2.6 times body weight) were close to each other. This was also the case for the current study where 3.79 times body weight was calculated for gait and 3.98 times body weight for stair ascent. The reduction in force for rising from a chair as compared to gait and stair ascent was similar in both studies.

Thus in all of the activities the forces reported by the group from CWRU were lower than those of the current study. This may be due to the fact that the post-operative time at

which the results were recorded was up to 58 days whilst that in the current study was between 13 and 25 months with the exception of the right hip of subject 'N' and the left hip of subject 'P'.

Direction of the resultant hip joint force vector

It is difficult to make comparisons concerning the direction of the resultant hip joint force vector since different groups report results with respect to different coordinate systems. For example, Rydell and the group from CWRU expressed forces in terms of a prosthesis based coordinate system whilst Bergmann's group and Brown et al gave results in terms of a femoral based coordinate system. The coordinate system used in the current study was femoral based. It is consistent with that used by Brown et al but not with that used by Bergmann's group. If quantitative comparisons were to be made then many assumptions regarding the geometry of the system would have to be made. Hence it was decided to make qualitative rather than quantitative comparisons.

During the stance phase of all activities the joint force vector was directed primarily from above, from the anterior side and from the medial side. This is reflected in the values of θ_{XY} θ_{YZ} and θ_{XZ} shown in figures 7.9-7.11 for the current study. During gait, Rydell also reported the head of the prosthesis to be mainly subjected to a force from above, ventrally and medially throughout stance. Davy et al (1988) from CWRU reported a similar anterior superior contact region to that of Rydell. The curves of Bergmann et al (1993) show the joint force vector to act from above and from the medial and anterior sides in early stance and then from the posterior side later in stance. The curves of Brown et al show a similar pattern. Thus there was some difference in late stance between the results of the current study and those of Bergmann's group and Brown et al. It is possible that there was variation in the hip extension angle between the subjects in the different studies which would explain such differences.

With regard to the other activities, the main difference in direction of the hip joint force vector as compared to that in gait has been reported for the stance phase of stair ascent. The group from CWRU reported a greater anterior inclination of the force vector in their first subject in stair ascent as compared to gait. Bergmann's group also reported a greater anterior inclination of force vector as reflected by an increase in angle T where

T= arctan (A-P force component / M-L force component).

The results of the current study show a very slight increase in anterior inclination as compared to gait. This is reflected in the values of θ_{XY} and θ_{XZ} shown in figures 7.9 and 7.11. The degree of anterior inclination is not as marked as that reported by the other authors. It is possible that there were differences in styles of stair climbing and the use of

handrails between the different studies which may account for some differences in the results.

8.1.2 Hips of Normal Subjects

In the previous section the results for the prosthetic hips of the patients were assessed in relation to those reported by other authors. It was important to perform the same procedure for the hips of the normal subjects

Whilst it is possible to measure hip joint forces directly in patients with hip replacements using telemeterised prostheses, the only method available to determine such forces in normal hips is that of calculation. There have been a number of studies in the past investigating the hip joint force in normal subjects and a selection of these are used in this section for comparison purposes. These are Paul (1967), Poulson (1973), Crowninshield et al (1978a,1978b), Rohrle et al (1984), and Brown et al (1984). As will be seen, these authors have used a variety of methods of calculation and made a range of assumptions. The ages of the subjects assessed has also varied widely and this may affect the style in which an activity is performed. It may be expected that younger subjects will perform activities with more vigour than older ones. Having said this, some older subjects may be more active than some younger ones. Hence, comparisons are made in this section but there will be some differences between the results of the different studies due to the variation in the calculation methods, assumptions made and subject studied. It should be noted here that the work of Paul (1967), Poulson (1973) and Crowninshield et al (1978a) has already been the subject of comparison in chapter 6 in the assessment of muscle forces.

The first study to determine hip joint force by calculation was performed by Paul (1967). He performed a total of 18 laboratory tests on 12 subjects between the ages of 18.5 and 36.9 years. Using the information obtained along with anthropometric data, Paul calculated joint moments throughout the gait cycle. In order to simplify the problem of distributing joint moments between muscles he split the major muscles crossing the hip joint into 6 groups. He chose the combination of muscles which would be active to balance the moments and then calculated muscle and joint forces. For each test he produced an upper and a lower bound curve since the long or the short flexors could act to balance the external flexion/extension moments.

Poulson (1973) extended the work of Paul to include the knee as well as the hip in the analysis. He grouped the major hip and knee muscles into 9 groups and then determined the combination of muscles which would be active to balance the moments. His analysis procedure produced a set of solutions from which he chose that giving the minimum value for the sum of force actions of all of the muscles. Poulson presented the results of 46 tests performed on males between the ages of 23 and 31 years. He studied walking at slow and

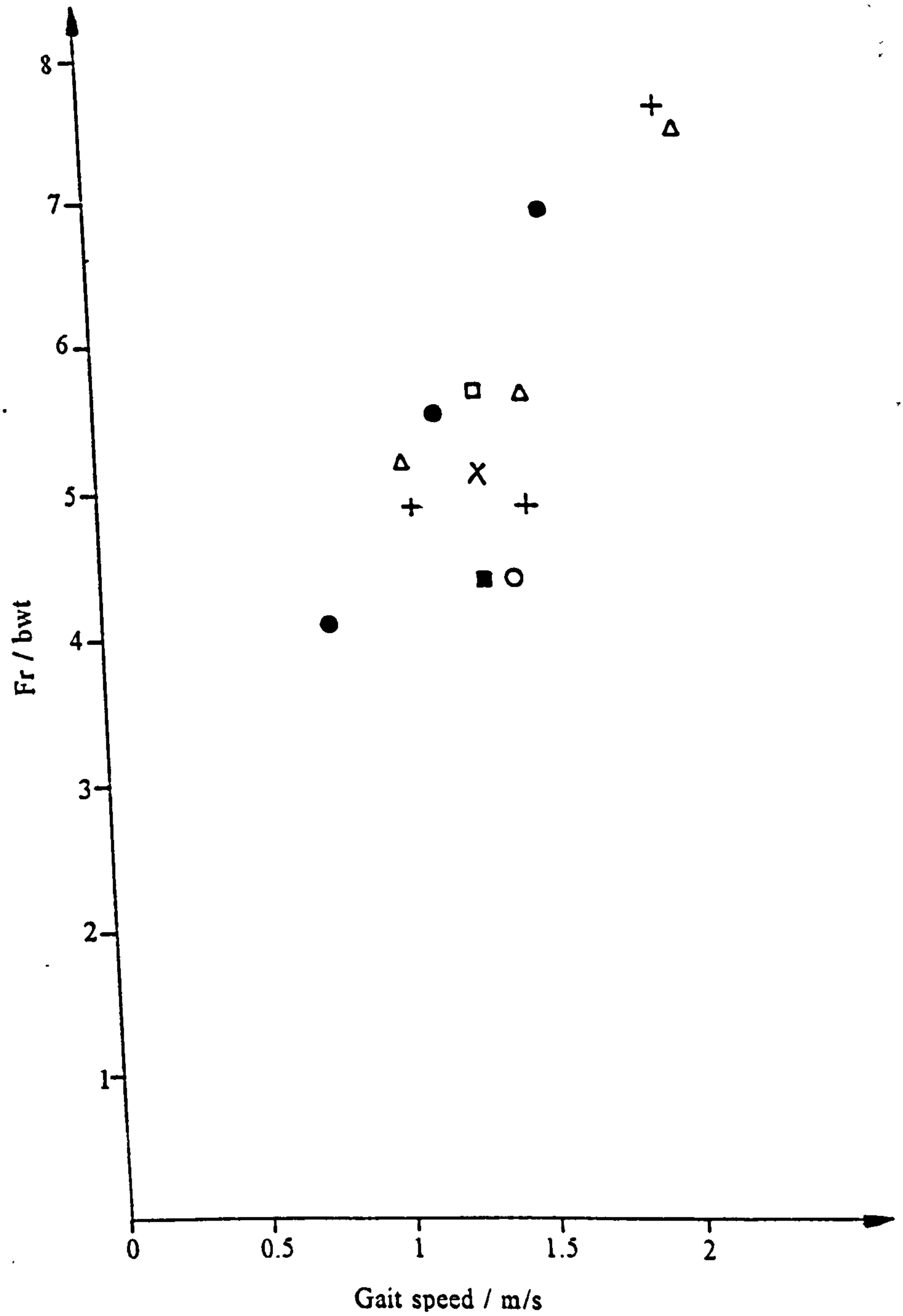

Figure 8.2 The variation of peak resultant hip joint force, Fr, in terms of body weight with gait speed for normal subjects. The values plotted are presented in table 8.5. Where two peaks are presented in table 8.2, the maximum is used in this figure.

× Current study
○ Paul (1967)
△ Poulson (1973)
+ Paul (1976)
□ Crowninshield et al (1978b) - young persons
■ Crowninshield et al (1978b) - old persons
● Rohrle et al (1984)

fast speeds in addition to normal speed. He also investigated ramp and stair negotiation.

The methods of Paul (1967), Morrison (1967) and Poulson (1973) were used by Paul (1976) in an examination of the effects of gait speed on hip joint force. Thirty-six tests were analyzed.

Crowninshield et al (1978a) used an optimization technique to determine joint forces during gait, stair climbing and rising from a chair. Twenty-seven musculotendinous units were included at the hip and the knee and ankle anatomy were modelled as far as was necessary to include the major effects of the two joint muscles. The cost function minimized was the sum of the individual values of muscle force divided by their physiological cross sectional areas, i.e the sum of the individual muscle stresses. Additional constraints were imposed on the solutions so that the stress in each muscle was less than a critical value.

The method of Crowninshield et al (1978a) was further used to investigate the effects of gait velocity and age on hip kinematics and kinetics (Crowninshield et al, 1978b). Two groups of subjects were studied. The first was a group of 11 subjects with a mean age of 24 and an age range of 22 to 30. The second included 15 subjects aged between 60 and 80 and with a mean age of 71.

Rohrle et (1984) also used an optimization technique to determine forces during gait. This model was comprised on 42 muscles and included three degrees of freedom at the hip, one degree at the knee and two degrees at the ankle. The cost function minimized was the sum of the muscle forces. Twenty-two subjects between the ages of 23 and 42 were studied.

Brown et al (1984) used the method of Paul and Poulson (1974) to determine joint forces in 11 normal subjects during gait. Fourteen patients were also studied as discussed in section 8.1.1.

In the following sections the results of the current study are assessed in relation to those from the foregoing research groups. Values quoted for Brown et al (1984) and Crowninshield et al (1978a,1978b) were measured from the curves which these authors presented. The format is the same as that of the previous section. Gait, stair negotiation and rising from a chair are discussed in turn. The magnitude of resultant hip joint force is discussed first, followed by the direction of the hip joint force vector.

Gait - Resultant hip joint force

The mean gait speed of the normal subjects was 1.33m/s (S.D.±0.15). As was the case for the patients, the resultant hip joint force exhibited two peaks during the stance phase of gait. This is illustrated in appendix F (fig F1). The mean value for the first peak was 4.25 times body weight (S.D.±0.84) and for the second, 5.01 times body weight (S.D.±1.17). In 10 cases, the second peak was greater than the first and in 5, the first was greater than the

Author, subject, speed	Resultant hip joint force in terms of body weight, Fr/bwt		
	Peak 1	Peak 2	Greatest peak
Paul (1) 1.46m/s (range 1.04-2.08)	3.22 (1.74-5.61)	4.41 (2.01-9.23)	
Poulson (2) 1.07m/s 1.49m/s 2.06m/s			5.19 5.66 7.47
Paul (3) 1.1m/s 1.48m/s 2.01m/s			4.9 4.9 7.6
Crowninshield et al (4) Young persons 1.33m/s Old persons 1.33m/s			5.68 (±1.45) 4.41 (±1.16)
Rohrle et al (5) 0.8m/s 1.2m/s 1.6m/s	 2.9 4.3 5.7	 4.1 5.5 6.9	
Brown et al (6)	3.42 (±0.53)	4.43 (±0.59)	

Table 8.5 Resultant hip joint forces during gait as recorded in normal subjects.
(1) From Paul (1967). Average values with range.
(2) From Poulson (1973).
(3) From Paul (1976).
(4) From Crowninshield et al (1978b) Average values (± 95% confidence interval)
(5) From Rohrle et al (1984)
(6) From Brown et al (1984). Average values (± 2 standard errors)

second. A mean greatest peak value of 5.16 times body weight (S.D.±1.11) was calculated using the greatest peak for each subject, be it the first or the second. Figure 8.2 presents this value in relation to those reported by other authors in a graph of peak resultant hip joint force versus gait speed.

It can be seen from figure 8.2 that where values are presented by an author for more than one speed, joint force increases with speed in all cases except Paul (1976). Paul (1976) only reported such an increase at higher speeds. However, for a given speed there is variation among the values reported by the different authors. This illustrates that other factors in addition to gait speed influence the joint force. Such factors include age, cadence and stride length, all of which are inter-related. The effects of age can be observed from the points plotted for Crowninshield et al (1978b) which show a reduction in joint force for an increase in age for a given speed. Variation can also occur due to the differences in methods used to calculate hip joint force. It is therefore difficult to compare across studies.

However, from figure 8.2 it can be seen that the mean peak value calculated in the current study is generally greater than or close to the values reported by other authors at lower speeds than that in the current study and less than those reported at higher speeds. There are some exceptions to this which are discussed in more detail later in this section. It can also be observed that the value calculated in the current study lies between those reported by Crowninshield et al (1978b) for young and old persons at the speed measured in the current study. This is consistent with what would be expected since the mean age of the subjects in the current study is less than that of the old persons and greater than that of the young persons.

Detailed comparisons to the results of other authors are made in the following discussion. These results are shown in table 8.5 as well as figure 8.2. The two individual peaks calculated during the stance phase of gait are considered first, followed by discussion of the mean greatest peak value.

The two individual peaks can be compared with the results of Paul (1967), Rohrle et al (1984) and Brown et al (1984). The value of 4.25 times body weight (S.D.±0.84) calculated at 1.33m/s in the current study would be expected to lie between the values reported by Rohrle et al at 1.2m/s and 1.6m/s. Rohrle et al reported 4.3 and 5.7 times body weight at these speeds. The value in the current study is slightly below these but the range covered by the standard deviation overlaps the lowest value. It is greater than that of 3.42 times body weight (2S.E.±0.53) reported by Brown et al at an unspecified speed but the ranges covered by the standard errors of Brown et al and the standard deviation of the current study overlap. The value of 4.25 times body weight (S.D.±0.84) calculated at 1.33m/s in the

Author	Peak resultant hip joint force in terms of body weight, Fr/bwt
Poulson (1)	7.21
Crowninshield et al (2)	Approximately 7-8

Table 8.6 Resultant hip joint forces during stair ascent as recorded in normal subjects
(1) From Poulson (1973)
(2) From Crowninshield et al (1978a)

Author	Peak resultant hip joint force in terms of body weight, Fr/bwt
Poulson (1)	7.06
Crowninshield et al (2)	Approximately 3-4

Table 8.7 Resultant hip joint forces during stair descent as recorded in normal subjects
(1) From Poulson (1973)
(2) From Crowninshield et al (1978a)

current study would be expected to be less than that reported by Paul for a mean speed of 1.46m/s. This is not the case since Paul reported 3.22 times body weight

The difference between the results of the current study and those of other authors for comparable gait speeds may be due to differences in age of the subjects resulting in variations in gait style. This is likely to be the case where the results of the current study are less than those reported by other authors who studied younger subjects. Differences may also be caused by variation in the calculation methods used in the different studies.

When comparing the values for the second peak similar observations to those for the first peak are made. The mean peak value of 5.01 times body weight (S.D.±1.17) was greater than the value of 4.43 times body weight (2S.E.±0.59) reported by Brown et al but the ranges covered by the standard errors of Brown et al and the standard deviation in the current study overlap. It lies below the values of 5.5 and 6.9 times body weight reported at 1.2m/s and 1.6m/s by Rohrle et al but as before, the range covered by the standard deviation overlaps the lowest value. It is greater than the value of 4.41 times body weight reported by Paul for a gait speed of 1.46m/s. The possible reasons for the differences between the results of the current study and those of other authors are the same as those discussed for the first peak.

The mean greatest peak value of 5.16 times body weight (S.D.±1.11) can be compared with those presented by Poulson (1973), Paul (1976) and Crowninshield et al (1978b). It would be expected that the value calculated in the current study at 1.33m/s would lie between the values determined at 1.1m/s and 1.5m/s by both Poulson and Paul. This is the case if the results of Poulson and Paul are combined together. The current study value of 5.16 times body weight (S.D.±1.11) lies between the value of 4.9 times body weight recorded by Paul at 1.1m/s and the value of 5.66 times body weight recorded by Poulson at 1.5m/s. At a speed of 1.33m/s, hip joint force values of approximately 4.41 and 5.68 times body weight were determined for old and young subjects from the curves presented by Crowninshield et al. The current study value of 5.16 times body weight (S.D.±1.11) lies between these values. This may be expected since the mean age of the normal subjects in the current study is 63 which is less than that of the older group of Crowninshield et al but greater than that of their younger group.

Stair ascent - Resultant hip joint force

As in the stance phase of gait, two peaks were observed in the resultant hip joint force during the stance phase of stair ascent as shown in appendix F (fig F5). The mean value of the first peak was 4.67 times body weight (S.D.±0.81) and the second, 4.08 times body weight (S.D.±1.15). A mean greatest peak value of 4.89 times body weight (S.D.±0.82) was

calculated using the greatest peak for each subject, be it the first or the second.

These values are much lower than those of 7.21 times body weight and around 7-8 times body weight reported by Poulson (1973) and Crowninshield et al (1978a) as shown in table 8.6. Whilst Poulson and Crowninshield et al reported increases in the mean peak as compared to normal speed gait, the value of 4.89 times body weight (S.D.±0.82) measured for stair ascent was slightly less than that of 5.16 times body weight (S.D.±1.11) measured for gait in the current study. This trend is similar to some of the results reported by the studies using instrumented prostheses. The peak resultant hip joint force measured by Bergmann et al (1995) in subject EB during stair ascent was between the values measured during gait at 0.83m/s and 1.39m/s. The group from CWRU reported similar forces in stair climbing and gait. The variation between the results of the different studies may be due to variation in styles of ascent and the use of handrails. Variation may also be due to the differences between the calculation methods used in the different studies.

Stair descent -Resultant hip joint force

Again, two peaks were exhibited in the resultant hip joint force during the stance phase of stair descent as shown in appendix F (fig F7). The mean value of the first peak was 4.36 times body weight (S.D.±0.71) and the second, 3.59 times body weight (S.D.±0.96). A mean greatest peak value of 4.49 times body weight (S.D.±0.74) was calculated using the greatest peak for each subject, be it the first or the second. This value lies between the value of 7.06 times body weight reported by Poulson (1973) and that of approximately 3-4 times body weight reported by Crowninshield et al (1978a) as shown in table 8.7. As was the case in stair ascent, variation in values of peak resultant in descent may be due to variation in style and the use of handrails. Variation may also be caused by the differences between the calculation methods used in the different studies.

Rising from a chair - Resultant hip joint force

The mean peak value of resultant hip joint force during rising from a chair was 3.19 times body weight (S.D.±0.63). This is consistent with that of approximately 3-4 times body weight presented by Crowninshield et al (1978a).

Direction of the resultant hip joint force vector

It is possible to make some quantitative as well as qualitative comparisons for the direction of the resultant hip joint force vector in normal subjects since some of the coordinate systems in which hip joint forces were calculated are coincident across the studies.

During the stance phase of gait, the resultant hip joint force vector was observed to generally come from above and from the medial side in the current study. In early stance, the vector was directed posteriorly and in late stance, in 10 cases the vector was directed

anteriorly and in 5, it continued to act in a posterior direction.

Considering the deviation of the joint force vector from the vertical projected onto the frontal plane, the mean value of θ_{YZ} was -20.8° (S.D.±2.6) at the instant of the first peak in the resultant and -13.7° (S.D.±3.2) at the instant of the second peak. Similar values of -21° and -12.5° were reported by Paul (1976). Lower values of -14.7° (2S.E.±6.3) and -9.8° (2S.E.±5.3) were presented by Brown et al (1984). However, the range covered by the standard deviation in the current study and the standard errors in the study of Brown et al overlap.

In the sagittal plane, the deviation of the resultant joint force from the vertical was given by θ_{XY}. The mean values of θ_{XY} at the instant of the first peak in the resultant joint force was 14.5° (S.D.±2.1). Paul (1976) reported 12° and Brown et al, 9.8° (S.D.±3.5) for the first peak. At the second peak, the value in the current study was -2.3° (S.D.±3.7). That reported by Paul (1976) was -7° and that by Brown et al, -6.3° (S.D.±3). It is likely that there were differences in the magnitude of hip extension between the studies which would account for the differences in the second peak.

With regard to the other activities, Crowninshield et al (1978a) gave components of hip joint force for stair negotiation and rising from a chair. The data are presented in terms of the pelvic coordinate system, making comparison difficult. However, in subjects with hip replacements, the literature presents the main difference between gait and other activities to be the marked anterior inclination of the hip joint force vector during the stance phase of stair ascent. This was described in section 8.1.1. It seems reasonable to believe that a similar occurrence may be expected in normal hips. This was not reflected in the results of the current study as can be seen from the values of θ_{XY} and θ_{XZ} in figures 7.5 and 7.7. It is possible that the styles of ascent and the use of handrails differed between the studies, resulting in different degrees of anterior inclination of the force vector.

8.2 HIP JOINT FORCE AND ACTIVITY

Having discussed the results for the activities of gait, stair negotiation and rising from a chair in relation to those presented by other authors, this section is concerned additionally with the car and bath activities and the walking turn.

Since the first total hip replacements were performed there have been extensive advances in the design of components and materials used. There have also been improvements in the surgical techniques. These advances should have continued to increase the long term success rate of hip joint replacements. However, there is still a high incidence

of loosening of the components which is a major source of concern in the orthopaedic community. There have been a number of theories proposed concerning the mechanism by which loosening occurs. These may be split simplistically into mechanical or biological actions or a combination of both.

With regard to the mechanical action, failure may occur at the interfaces between the bone, the component and the cement if used. Such failure may occur due to the stresses resulting from the imposed mechanical loads. Mjoberg (1994) proposed that if initial fixation of the prosthesis is insufficient then secondary factors which may influence the time to loosening will include the degree of stress imposed during activity.

With regard to biological action, the concern relates to the biological response to particulate foreign material produced by wear. Wear may occur at the bearing surface between the acetabular and femoral components or due to micromotion at the interfaces between the component, the bone, and the cement if used. The primary implant materials used are cobalt and titanium based alloys, polymethylmethacrylate (PMMA) bone cement and ultra high molecular weight polyethylene. These materials show biocompatibility in bulk but particles of these materials are suspected to have a role in bone resorption and implant loosening. Osteolysis which occurs is thought to be due to an inflammatory response to the particulate matter. Phagocytosis of the particles by macrophages and foreign body giant cells appears to be the initial response to the particulate matter. The presence of the intracellular particles is then associated with the release of cytokines and other mediators of inflammation. These factors initiate bone resorption by osteoclasts.

The loading imposed on the prosthetic hip and its fixation mechanisms may be one of the many factors influencing the loosening of the prosthesis. So far the loading has been determined for the common daily activities of gait, stair negotiation and rising from a chair as described in section 8.1. However, it may be that the loading caused by other daily activities such as getting into and out of the bath and car is more detrimental. This section therefore aims to analyze the hip joint loading during these other activities in addition to those during gait, stair negotiation and rising from a chair. To this end, the results for the prosthetic hips of the patients (group 2) will be discussed. Those for the hips of the normal subjects (group 1) are also considered. Finally, as a separate item, the results for the non prosthetic hips of the patients (group 3) are analyzed with those of the prosthetic hips (group 2) in order to identify any off-loading of the prosthetic side onto the non prosthetic side. Abbreviations used for the activities in the following discussion are as follows:

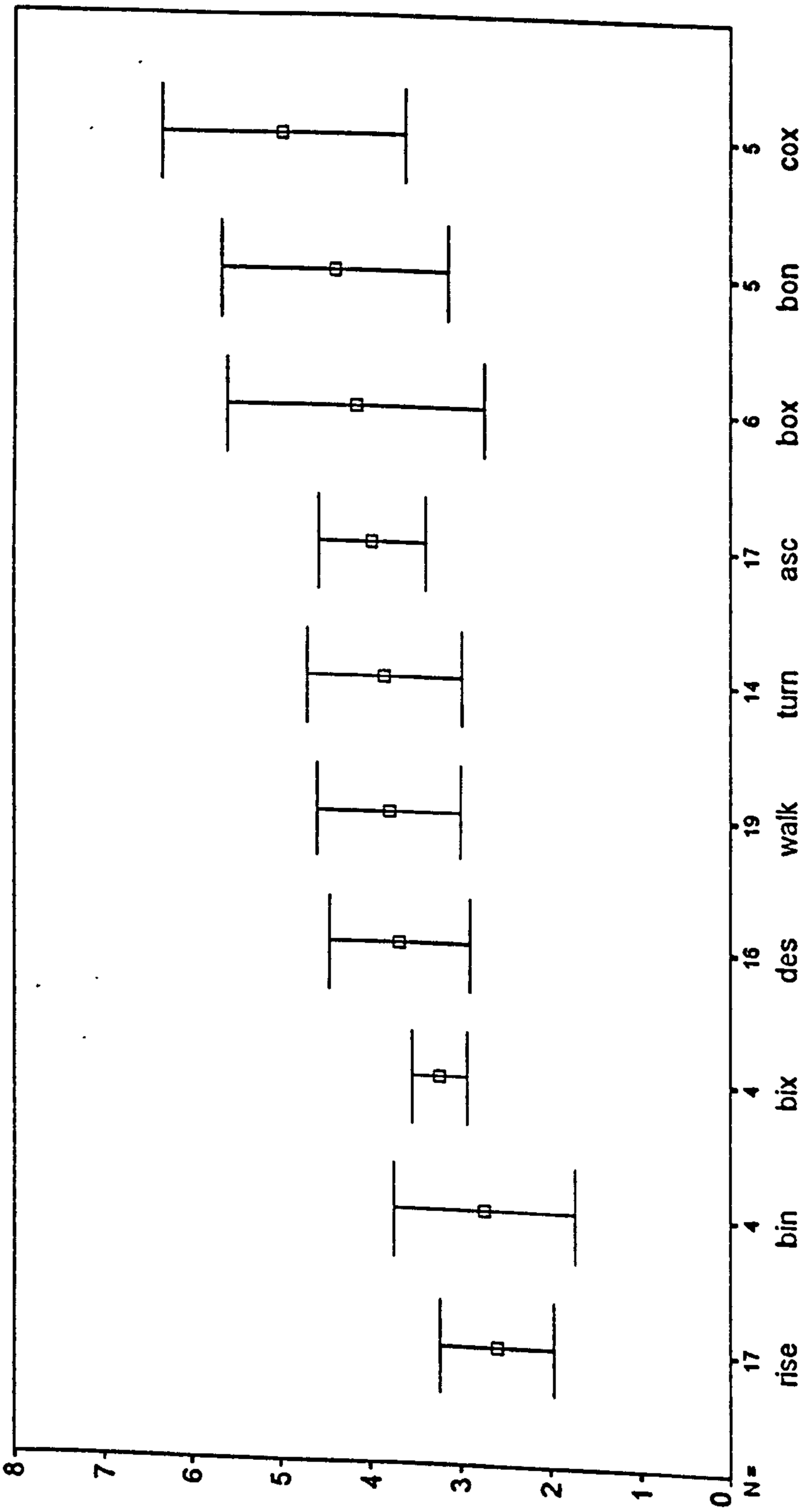

Figure 8.3 Group 2 - Prosthetic hips of patients. Mean peak values of resultant joint force, Fr, in terms of body weight (± 1 S.D.). For a description of each activity code see section 7.1.

turn: Walk with a 90° change in the direction of progression

asc: Stair ascent

des: Stair descent

rise: Rising from a chair

con: Car entry. The outside hip (i.e the left hip) was tested as the subject entered the car.

cox: Car exit. The outside hip (i.e the left hip) was tested as the subject exited from the car.

cin: Car entry. The inside hip (i.e. the right hip) was tested as the subject entered the car.

cix: Car exit. The inside hip (i.e the right hip) was tested as the subject exited from the car.

bon: Bath entry. The outside hip (i.e. that corresponding to the last foot to leave the ground) was tested as the subject entered the bath.

box: Bath exit. The outside hip (i.e. that corresponding to the first foot to make contact with the ground) was tested as the subject exited from the bath.

bin: Bath entry. The inside hip (i.e. that corresponding to the first foot to make contact with the bath floor) was tested as the subject entered the bath.

bix: Bath exit. The inside hip (i.e. that corresponding to the last foot to leave the bath floor) was tested as the subject exited from the bath.

8.2.1 Resultant Hip Joint Force

In this section the resultant hip joint force during the various activities is discussed first for group 2, the prosthetic hips of the patients and then for group 1, the hips of the normal subjects. The values in both groups are then compared and discussed together.

Group 2 - The prosthetic hips of the patients

The mean peak values of resultant hip joint force in terms of body weight, Fr/bwt, are plotted for the various activities for group 2, the prosthetic hips of the patients, in figure 8.3.

Figure 8.3 illustrates that the three activity tests resulting in the greatest mean peak values of Fr/bwt were, in order of increasing magnitude, the outside hip test performed during bath exit (box), that performed during bath entry (bon) and that carried out during car exit (cox). Those resulting in the lowest values were, in order of reducing magnitude, the inside hip test performed during bath exit (bix), that performed during bath entry (bin) and rising from a chair.

Statistical analysis was performed to identify whether the difference in mean peak values of Fr/bwt between the various activities and gait were statistically significant. Results were not obtained for all prosthetic hips in all activities. Paired T tests were therefore carried out,

Activity	P value	Number of hips included
turn	0.879	14
asc	0.476	17
des	0.431	16
rise	0	17
cox	0.187	5
bon	0.569	5
box	0.612	6
bin	0.164	4
bix	0.053	4

Table 8.8 Group 2 - Prosthetic hips of patients. Results of paired T tests comparing peak values of Fr/bwt in the various activities with those during gait. For a description of each activity code see section 7.1.

comparing the results for the hips within each activity with the results for the same hips during gait. The resulting P values are given in table 8.8.

At the 5% significance level, the only statistically significant difference observed was for rising from a chair which produced a lower mean peak value of Fr/bwt than that during gait. The greatest mean peak values of Fr/bwt were calculated at the outside hip in the car and bath activities (box, bon and cox). However, the differences between these values and those of gait were not statistically significant at the 5% level. This is probably due to the high variation in the value of Fr/bwt over a relatively low number of subjects. Although not statistically significant, these activities should not be disregarded as there will be some patients with values of Fr/bwt at the higher end of the standard deviation bars shown for these activities in figure 8.3.

Group 1 - The hips of the normal subjects

Figure 8.4 shows the mean peak resultant hip joint force in terms of body weight, Fr/bwt, for the various activities for the hips of the normal subjects, group 1. The values at the inside hip on car entry and exit (cin and cix) and also the outside hip on car entry (con) are included. Although it was not possible to obtain a sufficient number of results for the patients in these activities, enough were obtained for the normal subjects to make inclusion of them here feasible.

Figure 8.4 shows that the three activity tests resulting in the greatest mean peak values of Fr/bwt were, in order of increasing magnitude, the inside hip test carried out during bath entry (bin), the outside hip test performed during car exit (cox) and that performed during car entry (con). Those producing the lowest values were, in order of reducing magnitude, the inside hip test performed during car entry (cin), rising from a chair and the inside hip test carried out during car exit (cix).

Paired T tests were carried out to compare the results for the hips in group 1 for the various activities with the results for the same hips during gait. P values are given in table 8.9. At the 5% significance level, the value of Fr/bwt at the inside hip when getting out of the car (cix) was statistically significantly different to that in gait There were also statistically significant differences for rising from a chair and the walking turn. All of these activities produced lower mean peak values of Fr/bwt than gait. The highest mean peak value of Fr/bwt observed was that at the outside hip on getting into the car (con). Although the result for this activity was not statistically significantly different to that for gait at the 5% level, this activity should not be disregarded as there will still be some subjects with values of Fr/bwt at the higher end of the standard deviation bar shown for this activity in figure 8.4.

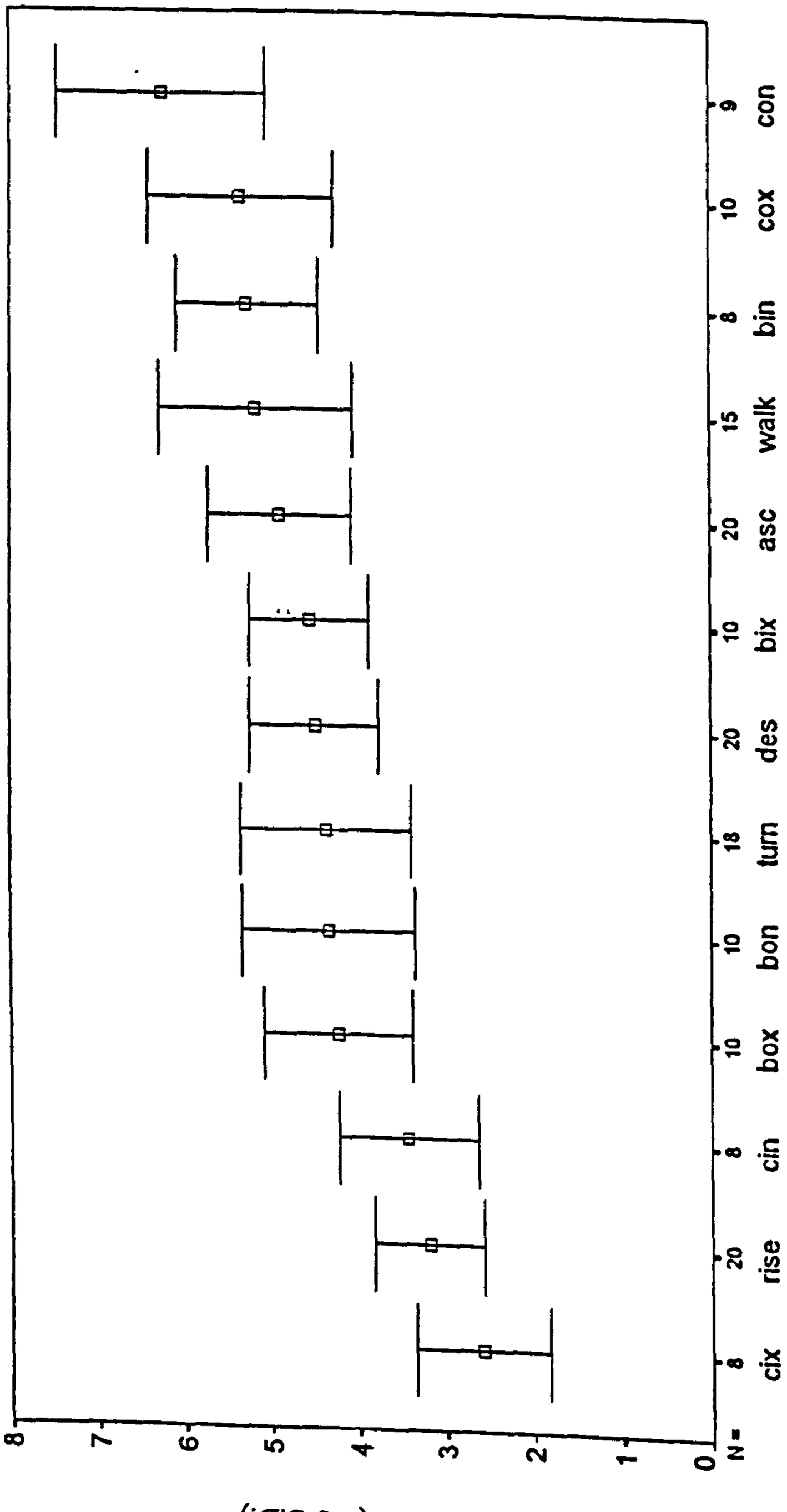

Figure 8.4 Group 1 - Hips of normal subjects. Mean peak values of resultant joint force, Fr, in terms of body weight (± 1 S.D.). For a description of each activity code see section 7.1.

Activity	P value	Number of hips included
turn	0	15
asc	0.455	15
des	0.008	15
rise	0	15
con	0.012	7
cox	0.291	7
cin	0.108	6
cix	0.001	7
bon	0.646	7
box	0.212	7
bin	0.722	7
bix	0.203	8

Table 8.9 Group 1 - Hips of normal subjects. Results of paired T tests comparing peak values of Fr/bwt in the various activities with those during gait. For a description of each activity code see section 7.1.

Activity	Group 2 - Mean peak Fr/bwt (± 1 S.D.)	Group 1 - Mean peak Fr/bwt (± 1 S.D.)	Percentage difference
gait	3.79 (±0.79)	5.16 (±1.11)	36
turn	3.84 (±0.86)	4.36 (±0.98)	14
asc	3.98 (±0.60)	4.89 (±0.82)	23
des	3.67 (±0.78)	4.49 (±0.74)	22
rise	2.60 (±0.64)	3.19 (±0.63)	23
cox	4.98 (±1.37)	5.33 (±1.07)	7
bon	4.39 (±1.26)	4.33 (±0.99)	-1
box	4.16 (±1.43)	4.22 (±0.86)	1
bin	2.73 (±1.01)	5.26 (±0.82)	93
bix	3.23 (±0.31)	4.54 (±0.68)	41

Table 8.10 Percentage difference in mean peak values of Fr/bwt between groups 1 and 2 in the activities common to both groups. For a description of each activity code see section 7.1

Comparison of the results for groups 1 and 2

Table 8.10 compares the mean peak values of Fr/bwt for groups 1 and 2 in the activities performed by both groups. A positive percentage difference indicates an increase in the mean peak value of Fr/bwt for the hips of the normal subjects as compared to that for the prosthetic hips of the patients. The values were greater at the hips of the normal subjects than at the prosthetic hips of the patients in the majority of the activities.

However, the values were similar for both groups at the outside hip on getting into and out of the bath (bon and box), the differences being 1% in each case. The standard deviation was greater for the prosthetic hips. Within each group there were variations in the activity style. For example, some subjects leant forwards, supporting themselves with their hands on the bath sides when getting into and out of the bath whilst some remained upright. On getting into the bath, some took a step onto the outside leg before bringing the inside leg over the bath side. In these cases the step was included in the test period. Others moved towards the bath and then, starting from a stationary position beside the bath, lifted the inside leg into the bath, followed by the outside leg. This style did not therefore include a step in the test period. On getting out of the bath some remained parallel to the bath and ended the activity standing beside it. Others twisted round as they got out and stepped away from the bath. Hence there were many styles observed and after splitting the subjects into categories of style, the number in each category was too low to perform any statistical analysis and draw firm conclusions as to the style producing the greatest and lowest peak values of Fr/bwt. However, from observation of the results, there was no particular style resulting in a consistently high or consistently low peak value of Fr/bwt.

There was also only a small difference of 7% between the two groups in mean peak values of Fr/bwt at the outside hip on getting out of the car (cox). Although the values were similar, the two groups performed the activity in quite different styles.

All of the patients twisted round on the seat, swinging both legs out of the car before standing up and moving away from the car. This is how they are taught to perform the activity by physiotherapists in the early post-operative period. Only one of the normal subjects performed the activity in this way. The rest moved the left leg out of the car first and took weight on this limb as they brought the right leg out and then moved away from the car. This style was carried out in two different ways. Four subjects twisted round as they got out, so that they faced towards the back of the car as they moved away from it. The remaining five did not twist round but moved out backwards. From observation of the results one style did not produce a consistently greater value of Fr/bwt than the other.

It would be expected that swinging the legs out before standing up would produce lower

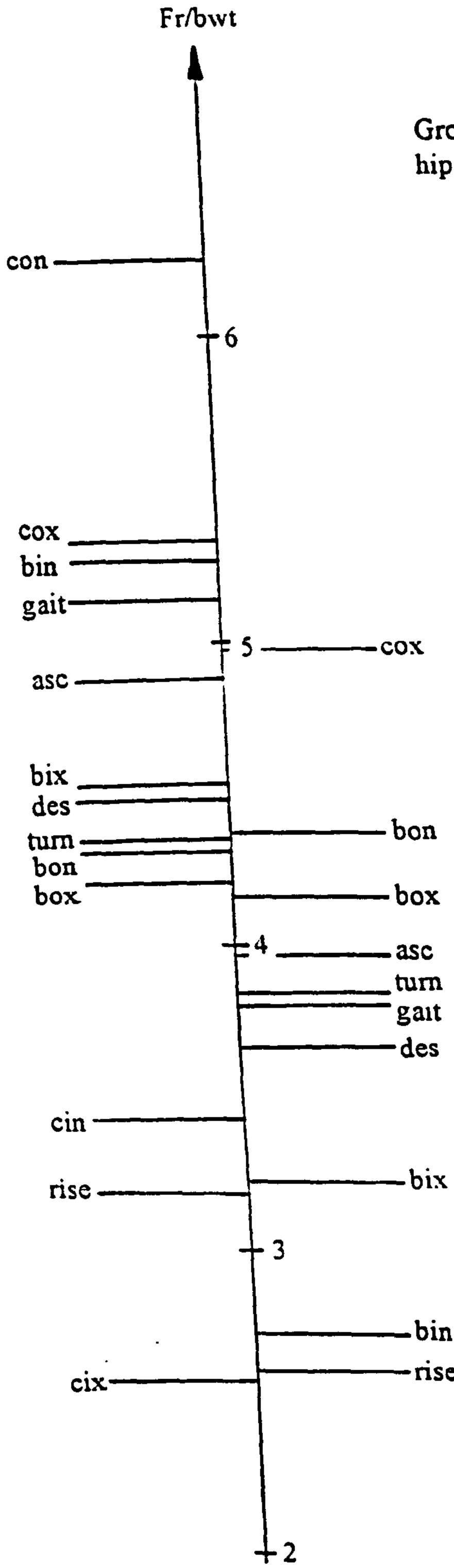

Figure 8.5 Groups 1 and 2. A comparison of mean peak values of resultant hip joint force in terms of body weight, Fr/bwt. For a description of each activity code see section 7.1.

mean peak values of Fr/bwt than the other styles since in this style the body weight should be distributed between the two limbs. However, this was not reflected in the results, the mean peak value for the activity at the prosthetic hips being similar to that at the hips of the normal subjects. It is possible that although the patients swung both legs out before standing up, they did not always distribute the weight evenly between the two limbs. Those at the higher end of the standard deviation band may have loaded the outside hip more highly than the inside one as they got up and moved diagonally away from the car. Those at the lower end may have distributed the weight more evenly, resulting in a value of Fr/bwt closer to that in rising from a chair.

In all of the other activities there were marked increases in the mean peak value of Fr/bwt in the hips of the normal subjects (group 1) as compared to the prosthetic hips of the patients (group 2). An increase of 36% was apparent for gait, probably partly due to the increase in speed from a mean value of 1.01m/s in group 2 to 1.33m/s in group 1. Mean peak values of Fr/bwt during rising from a chair, turning, and going up and down stairs increased by between 14 and 23% for the hips of the normal subjects as compared to the prosthetic hips of the patients.

Finally, the largest increases in the mean peak value of Fr/bwt at the hips of the normal subjects as compared to prosthetic hips of the patients were observed for the inside hip on getting into and out of the bath (bin and bix). A 41% increase was observed in getting out of the bath and a 93% increase in getting into the bath. The main difference between the two groups in terms of the style of the activity was that all of the normal subjects sat down in the bath whilst the majority of the patients did not.

On closer examination of the curves of Fr/bwt for the inside hips of the normal subjects when getting into the bath, peaks were observed in two places. The first was after the subjects had put the inside foot into the bath and were weight bearing on this as they brought the outside foot in. The second was in the early stages of sitting down. At this point it is possible that the weight was not yet evenly distributed between the two limbs. It may be expected that Fr/bwt would be high at the very end of the activity when the subjects were close to sitting down. However at this stage in the activity the hands could have been taking a substantial amount of weight on the bath sides and the weight could have been more evenly distributed between the two limbs.

On examination of the curves for the inside hips of the normal subjects when getting out of the bath, the peaks were observed predominantly at the late stages of knee extension. At this point the subjects would have been at the late stages of rising and at the same time pushing off from the inside foot to get out of the bath.

Figure 8.5 compares the results for the two groups when the activities are placed in order of increasing magnitude of mean peak Fr/bwt. The value calculated for rising from a chair is at the low end in both groups whilst that calculated at the outside hip when getting out of the car (cox) is at the high end in both groups. That at the outside hip during bath entry and exit (bon and box) is at the low end for the hips of the normal subjects but at the high end for the prosthetic hips of the patients. However, the mean peak values of Fr/bwt at the outside hip during bath entry and exit (bon and box) are similar as has already been discussed. The values calculated at the inside hip during bath entry and exit (bin and bix) are at the low end for the prosthetic hips of the patients but towards the high end for the hips of the normal subjects. There are a large differences in the mean peak values of Fr/bwt between the two groups for these activities as has already been discussed.

High resultant hip joint forces are undesirable as they may be related to failure of joint prostheses. In combination with direction, they will be related to mechanical failure. They may also be related to wear at the various surfaces. It is recognised that many factors including material, sliding velocity, lubrication and surface finish as well as load will affect wear. However, load is certainly one factor to be considered. It is possible that failures due to loosening could be reduced by reductions in resultant joint force.

The most critical activity appears to be the car activity. The greatest mean peak value of Fr/bwt of all the activities was produced at the outside hip during this activity in both subject groups. As previously discussed, the two groups got out of the car by two quite different styles but produced similar high resultant joint forces. It was concluded that even though the patients swung both legs out before standing up, those with higher joint force may not have been distributing the weight evenly between the two limbs, and were loading the outside limb more highly than the inside one as they got up and moved away. There may therefore be a need to emphasise the importance of taking the activity slowly and concentrating on an even distribution of load between the two feet as they stand up before moving away.

In the normal subject group, the highest mean peak value of Fr/bwt of all activities was that calculated at the outside hip when getting into the car (con). All of the subjects took a step onto the outside leg and whilst supporting their weight on this leg, moved the inside leg into the car. They then sat down and brought the outside leg in. Hence all of the weight was taken on the outside limb for the majority of the activity whilst the hip and knee were both considerably flexed. Such a style should be avoided if values of Fr/bwt are to be reduced. The majority of the patients did avoid this style and entered the car by sitting down on the seat and then swinging their legs into the car. The hip joint forces could not be

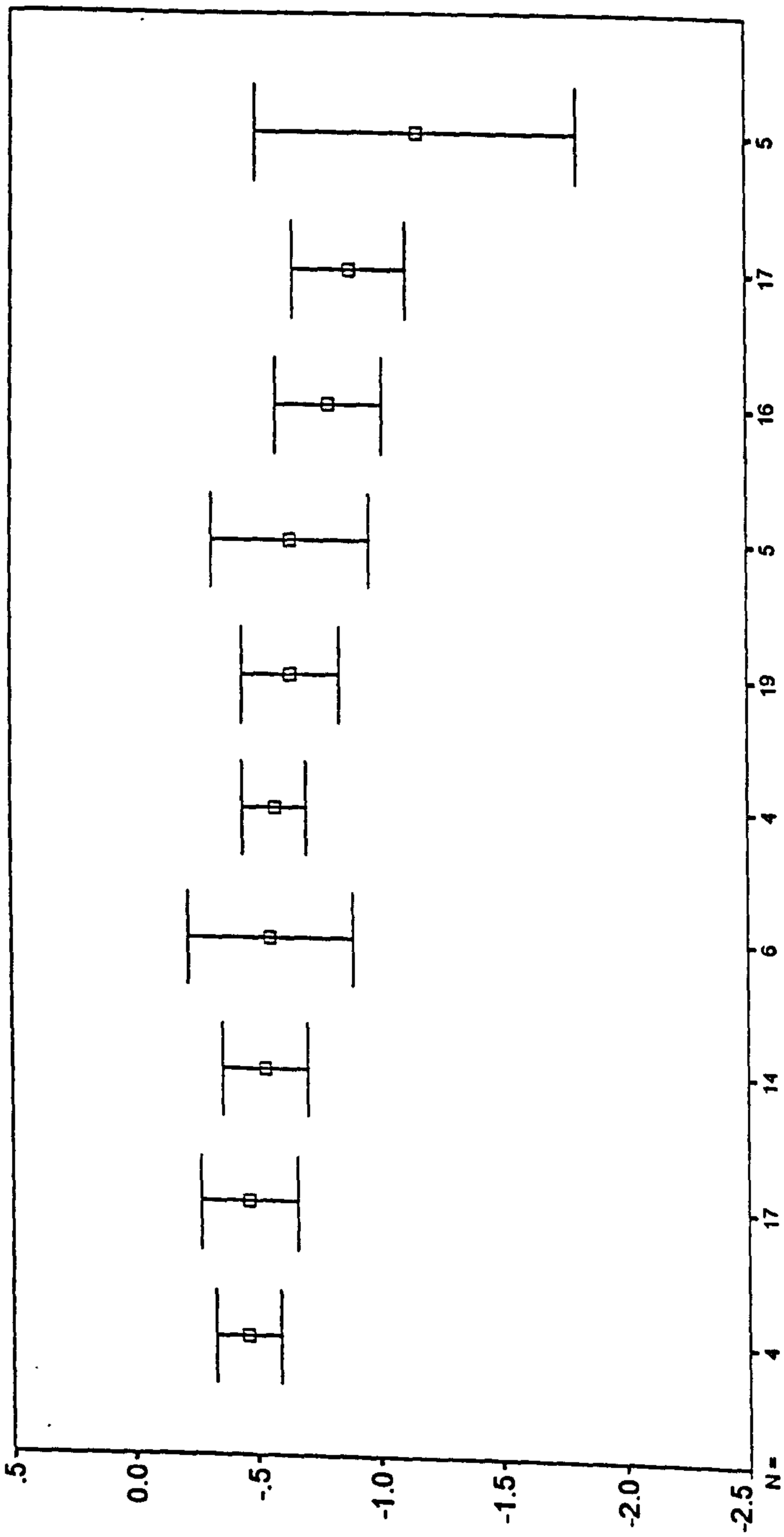

Figure 8.6 Group 2 - Prosthetic hips of patients. Mean peak values of the anterior-posterior component of joint force, Fx, in terms of body weight (± 1 S.D.). For a description of each activity code see section 7.1.

determined in these situations due to the limitations of the ground reaction force measuring methodology. However, as long as the load is evenly distributed between the two limbs, it is likely that this style will result in lower values of Fr/bwt than the style adopted by the normal subject group. Further investigation would be required to confirm this.

Finally, all of the normal subjects sat down in the bath whilst the majority of the patients did not sit down. The mean peak values of Fr/bwt calculated at the inside hip on getting into and out of the bath (bin and bix) were much greater for the hips of the normal subjects than for the prosthetic hips of the patients. Patients should therefore continue in the style they appear to be taking, that is not sitting down in the bath and only using it for a shower.

8.2.2 The Anterior-Posterior Component of Hip Joint Force

Although the resultant joint force is important, the components of the joint force must also be considered. This section therefore considers the anterior-posterior (A-P) component of joint force, Fx, and its contribution to the torsional moment imposed about the stem of the femoral component. This torsional moment may well be an important factor influencing the loosening of the femoral component. It will influence the micromotion and wear at the interfaces between the component, the bone, and the cement if used. It will influence the stresses at these surfaces, enhancing the mechanical loosening process. Indeed, it has been suggested that the role which torsional moments plays for the loosening of hip prostheses may be underestimated (Berme and Paul, 1979, Bergmann et al, 1995).

The components of hip joint force in the anterior-posterior and medio-lateral directions will both influence the torsional moment about the stem. The influence of each will depend on the geometry of the prosthesis and its orientation relative to the femur. Such parameters will vary greatly between subjects but the majority of the torsional moment will be due to the A-P force component, Fx. Hence this component is considered in this section. It is considered first for the prosthetic hips of the patients (group 2) and then for the hips of the normal subjects (group 1). The results for both groups are then discussed together.

Group 2 - The prosthetic hips of the patients

Figure 8.6 shows the mean peak value of Fx in terms of body weight (Fx/bwt) for each activity for the prosthetic hips of the patients. All of the mean peak values of Fx/bwt shown in figure 8.6 are negative indicating a posteriorly directed joint force.

Figure 8.6 shows that the three activity tests with the greatest mean peak magnitudes of Fx/bwt were, in order of increasing magnitude, stair descent, stair ascent and the outside hip test performed during car exit (cox). Those producing the lowest magnitudes were, in order of reducing magnitude, the walking turn, rising from a chair and the inside hip test

Activity	P value	Number of hips included
turn	0	14
asc	0	17
des	0.002	16
rise	0.006	17
cox	0.221	5
bon	0.413	5
box	0.401	6
bin	0.086	4
bix	0.300	4

Table 8.11 Group 2 - Prosthetic hips of patients. Results of paired T tests comparing peak values of Fx/bwt in the various activities with those during gait. For a description of each activity code see section 7.1.

carried out during bath entry (bin).

Paired T tests comparing the results for the prosthetic hips within an activity with those for the same hips during gait were performed and the resulting P values are given in table 8.11. At the 5% significance level, rising from a chair and the walking turn were found to produce statistically significantly lower magnitudes of Fx/bwt than those during gait. Ascent and descent produced statistically significantly greater magnitudes. The three greatest mean peak magnitudes of Fx/bwt were those for stair descent and ascent and that at the outside hip on car exit (cox), that at the outside hip on car exit being the greatest of all. The result for this activity was not statistically significantly different to that for gait. This was probably due to the high variation in the value of Fx/bwt over a relatively low number of subjects. However, this activity should still be considered as there will be some subjects with high magnitudes of Fx/bwt as indicated by the standard deviation bar for this activity in figure 8.6.

Group 1 - The hips of the normal subjects

Figure 8.7 shows the mean peak values of Fx/bwt during the various activities for the hips of the normal subjects. All of the mean peak values of Fx/bwt presented in figure 8.7 are negative indicating a posteriorly directed joint force.

Figure 8.7 illustrates that the three activity tests resulting in the greatest mean peak magnitudes of Fx/bwt were, in order of increasing magnitude, the inside hip test performed during bath entry (bin), stair ascent and the outside hip test performed during car entry (con). Those producing the lowest magnitudes were, in order of reducing magnitude, the inside hip test performed during car entry, the outside hip test carried out during bath exit (box) and the inside hip test carried out during car exit (cix).

Paired T tests were performed to compare the results for the hips of the normal subjects for each activity with the results for the same hips during gait. P values are given in table 8.12. At the 5% significance level, rising from a chair and the walking turn produced statistically significantly lower peak magnitudes of Fx/bwt than gait. The peak magnitude incurred by the inside hip during car exit (cix) was also significantly lower. The only statistically significantly greater magnitude was that for stair ascent. The highest mean peak magnitude of Fx/bwt was that calculated at the outside hip when getting into the car (con). Although the result for this activity was not statistically significantly different to that for gait, probably due to the high standard deviation, there will be some subjects with high magnitudes of Fx/bwt as indicated by the standard deviation bar for this activity in figure 8.7. Hence the activity should not be ignored.

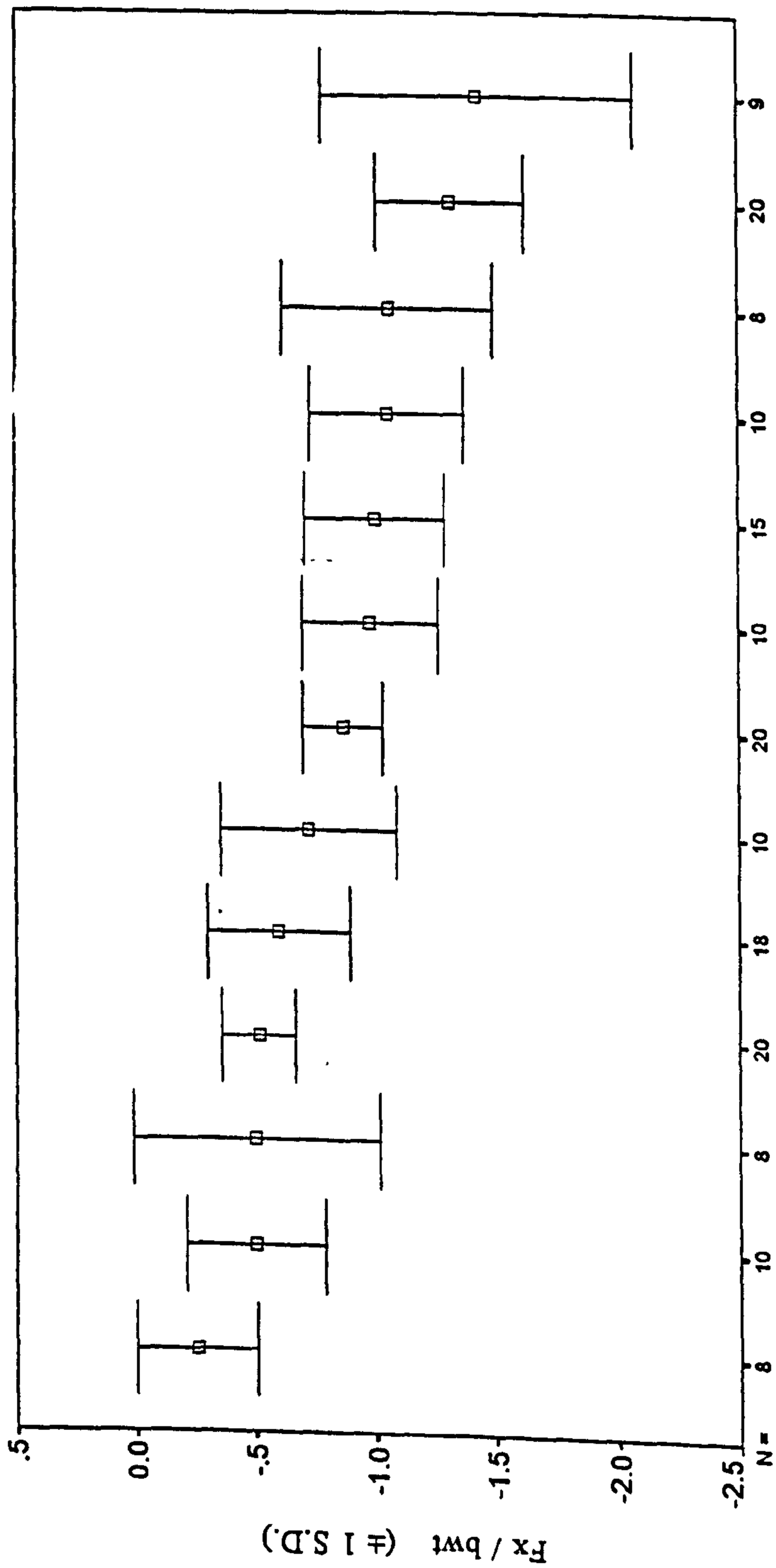

Figure 8.7 *Group 1 - Hips of normal subjects. Mean peak values of the anterior-posterior component of joint force, Fx, in terms of body weight (± 1 S.D.). For a description of each activity code see section 7.1.*

Activity	P value	Number of hips included
turn	0	15
asc	0.001	15
des	0.239	15
rise	0.000	15
con	0.105	7
cox	0.459	7
cin	0.131	6
cix	0.005	7
bon	0.167	7
box	0.013	7
bin	0.437	7
bix	0.604	8

Table 8.12 Group 1 - Hips of normal subjects. Results of paired T tests comparing peak values of Fx/bwt in the various activities with those during gait. For a description of each activity code see section 7.1.

Activity	Group 2 - Mean peak Fx/bwt (± 1 S.D.)	Group 1 - Mean peak Fx/bwt (± 1 S.D.)	Percentage difference
gait	-0.65 (±0.20)	-1.00 (±0.29)	54
turn	-0.54 (±0.17)	-0.60 (±0.29)	11
asc	-0.89 (±0.23)	-1.32 (±0.31)	48
des	-0.81 (±0.22)	-0.87 (±0.17)	7
rise	-0.47 (±0.20)	-0.52 (±0.15)	11
cox	-1.17 (±0.65)	-1.06 (±0.32)	-9
bon	-0.65 (±0.32)	-0.73 (±0.36)	12
box	-0.56 (±0.34)	-0.50 (±0.29)	-11
bin	-0.46 (±0.13)	-1.06 (±0.44)	130
bix	-0.58 (±0.13)	-0.98 (±0.28)	69

Table 8.13 Percentage difference in mean peak values of Fx/bwt between groups 1 and 2 in the activities common to both groups. For a description of each activity code see section 7.1.

Comparison of the results for groups 1 and 2

Table 8.13 compares the mean peak values of Fx/bwt for groups 1 and 2 in the activities for which results were obtained for both groups. A positive percentage difference indicates an increase in the mean peak magnitude of Fx/bwt for the hips of the normal subjects as compared to that for the prosthetic hips of the patients. In the majority of the activities, the mean peak magnitudes were similar for the two groups or those for the hips of the normal subjects were greater.

Similar values occurred at the outside hip on getting into and out of the bath (bon and box), the differences being 12% and 11%. This was also the case for the resultant joint force as discussed in section 8.2.1. As discussed, there was variation within each group in the style in which the activity was performed. The number of subjects performing each style was too low to perform statistical analysis and produce a correlation between style and the resulting value of Fx/bwt. However, from observation of the results there was no particular style which produced a consistently high or low value.

There was also little difference (9%) in the mean peak values of Fx/bwt at the outside hip when getting out of the car (cox) although the range covered by the standard deviation was greater for the prosthetic hips of the patients than that for the hips of the normal subjects. Similar observations were made for the resultant hip joint force in section 8.2.1 and a similar conclusion may be drawn. That is, although the majority of the patients swung both legs out before getting up, those with greater magnitudes of Fx/bwt at their prosthetic hip may have been distributing their weight unevenly between the two limbs, overloading the outside hip as they got up and moved away. Hence the mean peak value of Fx/bwt was similar to that of the hips of the normal subjects who moved the outside leg out first and supported their weight on this leg as they brought the inside leg out.

There was a marked increase of 54% in the mean peak magnitude of Fx/bwt during gait for the hips of the normal subjects as compared to that for the prosthetic hips of the patients. This is probably partly due to the fact that the normal subjects walked at a mean speed of 1.33m/s which is greater than the mean speed of 1.01m/s measured for the patients. A similar increase of 48% was observed for the hips of the normal subjects as compared to the prosthetic hips of the patients during stair ascent. Small changes of between 7% and 11% were observed for descent, rising from a chair and the walking turn.

As was the case for the resultant joint force, the greatest differences in mean peak magnitudes of Fx/bwt between the two groups were observed at the inside hip when getting into and out of the bath (bin and bix). There was a 130% increase on entry and a 69% increase on exit for the hips of the normal subjects as compared to the prosthetic hips of the

Group 1 - hips of normal subjects

Group 2 - prosthetic hips of patients

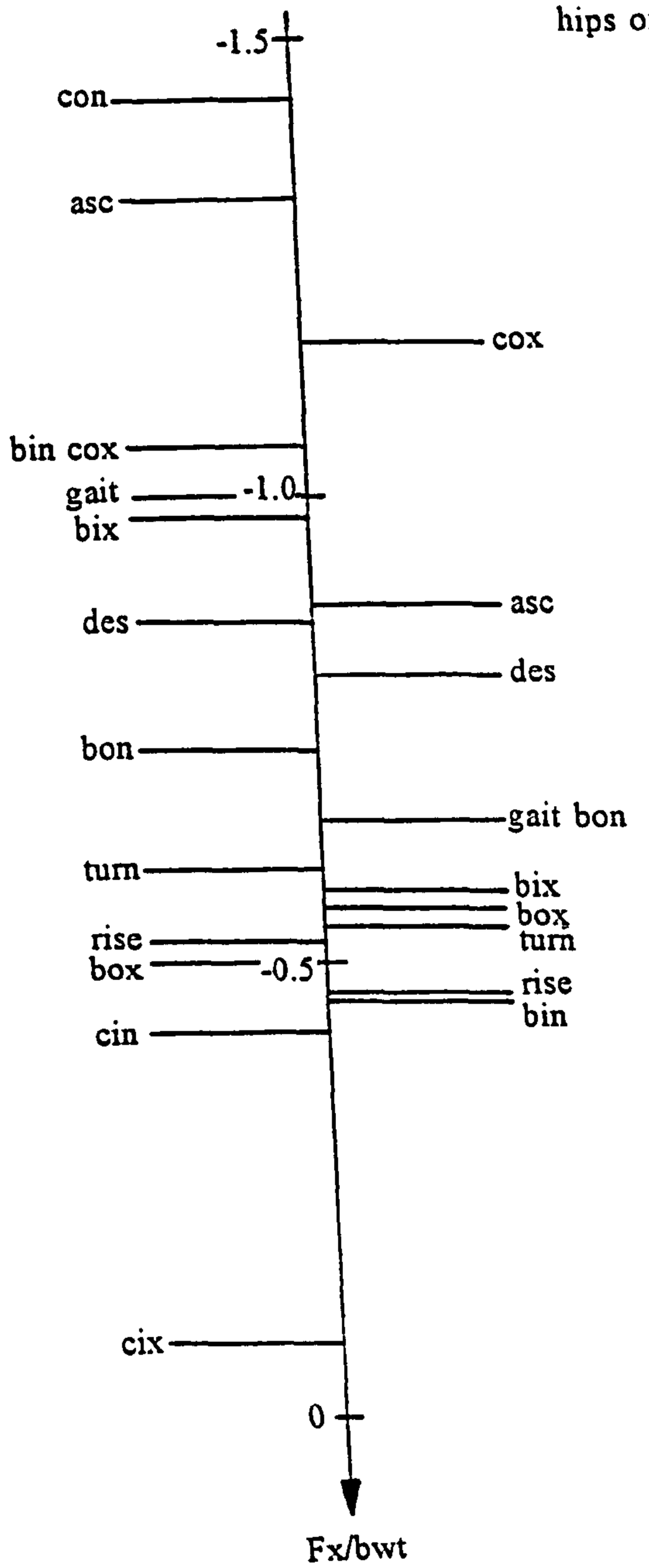

Figure 8.8 Groups 1 and 2. A comparison of mean peak values of the anterior-posterior component of hip joint force in terms of body weight, Fx/bwt. All values of Fx/bwt shown in this figure are negative, indicating a posteriorly directed joint. For a description of each activity code see section 7.1.

patients. As discussed in section 8.2.1, the normal subjects sat down in the bath whilst the majority of the patients did not.

On examination of the curves of Fx/bwt for the inside hips of the normal subjects when getting into the bath, the peak magnitude was found to occur predominantly in the early stages of sitting down. At this point, it is possible that the weight was not yet evenly distributed between the two limbs. The curves for getting out of the bath showed the peaks to be predominantly at the late stages of knee extension. At this point the subjects would be at the late stages of rising and at the same time pushing off from the inside foot to get out of the bath.

Figure 8.8 shows the activities for the two groups in order of increasing magnitude of mean peak Fx/bwt. In both groups rising from a chair is at the low end of the scale whilst stair ascent and the results for the outside hip test performed during car exit (cox) are at the top end. The mean peak magnitude calculated at the inside hip during bath entry (bin) is near the top of the scale for the hips of the normal subjects but near the bottom for the prosthetic hips of the patients This is due to the fact that the normal subjects sat down in the bath whilst the majority of the patients did not as has already been discussed. The mean peak magnitude determined at the inside hip on bath exit (bix) is also nearer to the top end of the scale for the hips of the normal subjects than for the prosthetic hips of the patients for similar reasons.

These mean peak magnitudes of Fx/bwt are very important with regard to the torsional moment imposed on the prosthesis. The most critical activities appear to be stair ascent and getting into and out of the car. The highest mean peak magnitude of Fx/bwt calculated for the prosthetic hips of the patients was that for the outside hip on getting out of the car (cox) and the second highest was that during stair ascent. The highest magnitude determined for the hips of the normal subjects was that at the outside hip during car entry (con) and the second highest was that during stair ascent.

An approximate calculation of the torsional moment incurred during these critical activities was made assuming a horizontal distance of 0.045m between the long axis of the femur and the centre of the prosthetic head. The anteversion angle was taken to be 15° (Norkin and Levangie, 1992). Since the moment due to the posteriorly directed Fx is opposed by that due to the laterally directed Fz, both components were included in the calculation. Torsional moments are expressed in %bwt.m but multiplication by body weight and division by 100 gives the results in Nm. Values were calculated for the prosthetic hips of the patients for the two activities with the highest magnitudes of Fx/bwt and also for gait. Hence that at the outside hip during car exit (cox) was 2.47%bwt.m (S.D.±1.74), that during

stair ascent was 2.13%bwt.m (S.D.±0.71) and that during gait, 1.47%bwt.m (S.D.±0.59). These values will be affected by the geometry of the prosthesis and its orientation with respect to the femur. For example, if an anteversion angle of 0° is assumed instead of 15° then the torsional moment is purely due to Fx, the lever arm for Fz being zero. Values then increase to 5.25%bwt.m (S.D.±2.94) at the outside hip during car exit (cox), 4.01% bwt.m (S.D.±1.04) during stair ascent and 2.92%bwt.m (S.D.±0.90) during gait.

Bergmann et al (1995) reported that the literature suggests a range of approximately 1-5 %Bwt.m for the torsional strength of implant fixation. They found the torsional moments to be within or to exceed this range as is the case in the current study. This implies that the prostheses should already be loose which is not necessarily the case in vivo. Bergmann et al suggested the discrepancy could be explained in part by permanent remodelling of the natural bone. Despite these discrepancies, it is likely that the torsional moments acting in these activities are close to the fixation strength of the implant.

The simple analysis used to calculate the torsional moment does not take into account the full 3D geometry and joint force configuration which results in a torsional moment which varies along the length of the stem. Such complex analysis would require accurate knowledge of the orientation of the prosthesis with respect to the femur in all three directions. However, the simple analysis does illustrate that the torsional moment will be affected by the orientation of the prosthesis with respect to the femur. It will additionally be affected by the geometry of the prosthesis. The value of Fx and hence the torsional moment can also be affected by the style in which an activity is performed.

There were no obvious differences among the majority of the patients with regard to the style in which they climbed the stairs. Most went up cyclically. Only one patient, 'Z', took the steps one at a time. Her results were not included in the calculation of mean peak values. During ascent, this subject exhibited a peak value of Fx/bwt of -0.49 at her prosthetic hip. The magnitude of this value is less than that of the mean peak value of -0.89 (S.D.±0.23) exhibited by the prosthetic hips of the other subjects and outwith the range covered by the standard deviation. This suggests that going upstairs one at a time as recommended in the early post-operative period by physiotherapists, may reduce torsional moments imposed on the prosthesis. However, firm conclusions cannot be drawn from this as only one subject performed the activity in this style.

With regard to getting out of the car, the same conclusions as those made for the resultant joint force may be made here. That is, it may be that even though the patients swung both legs out before standing up, those with higher magnitudes of Fx/bwt were not distributing the weight evenly between the two limbs, and were loading the outside limb

more highly than the inside one as they got up and moved away. There may therefore be a need to emphasise the importance of taking the activity slowly, concentrating on an even distribution of load between the two feet when standing up before moving away.

Also, with regard to getting into the car, the same conclusions as those drawn for the resultant joint force may be drawn here. The greatest mean peak magnitude of Fx/bwt during any activity in groups 1 and 2 was calculated for the outside hips of the normal subjects when getting into the car (con). If the calculation of torsional moment is made using the results for the normal subjects for the outside hip on car entry, the value obtained is 2.99%bwt.m (S.D.±2.54) assuming an anteversion angle of 15° and 6.43%Bwt.m (S.D.±2.89) assuming an anteversion angle of 0°. As described previously, these subjects got into the car by stepping onto the outside leg and whilst supporting their weight on this leg, they moved the inside leg into the car. They then sat down and brought the outside leg in. Hence all of the weight was taken on the outside limb for the majority of the activity whilst the hip and knee were both considerably flexed. It may be inferred from this that if the patients were to perform the activity in the same style as the normal subjects, then they may be imposing dangerously high torsional moments on their hips. They should therefore avoid this style. The majority of the patients did avoid this style, sitting down on the seat before bringing their legs into the car.

Finally, similar conclusions to those drawn from the resultant hip joint force analysis may be drawn for the inside hip when getting into and out of the bath. All of the normal subjects sat down in the bath but the majority of the patients did not. The mean peak magnitudes of Fx/bwt calculated at the inside hip when getting into and out of the bath (bin and bix) were much greater for the hips of the normal subjects than for the prosthetic hips of the patients. In order to reduce torsional moments, patients should continue in the style they appear to be taking, that is not sitting down in the bath, but only using it for a shower.

8.2.3 Off-loading of the Prosthetic hip onto the Non Prosthetic hip

Having looked at the results for groups 1 and 2, the results for group 3, the non prosthetic hips of patients are now discussed. These results are important since patients may be off-loading the prosthetic hip and overloading the non prosthetic hip. Even though they may feel no pain in the prosthetic hip, they may be wary of using it too much. Alternatively, in the pre-operative period they may have adopted ways of performing activities which allowed off-loading and thereby reduced the pain. These ways of performing activities can become habits and continue post-operatively. Whatever the reason, if patients off-load the prosthetic hip and put too much load on the non prosthetic hip, this can initiate or further

Activity	Group 2 - Prosthetic hips of patients. Mean peak Fr/bwt (± 1 S.D.)	Group 3 - Non prosthetic hips of patients. Mean peak Fr/bwt (± 1 S.D.)
gait	3.79 (±0.79)	4.69 (±0.97)
asc	3.98 (±0.60)	4.39 (±0.83)
des	3.67 (±0.78)	3.80 (±0.61)
rise	2.60 (±0.64)	3.55 (±0.97)

Table 8.14 Groups 2 and 3. Mean peak values of Fr/bwt. See section 7.1 for a description of each activity code.

Activity	P value	Number of hips included
gait	0.002	12
asc	0.076	11
des	0.325	11
rise	0.004	13

Table 8.15 Results of paired T tests comparing peak values of Fr/bwt at the prosthetic hip with those at the non prosthetic hip of patients. See section 7.1 for a description of each activity code.

problems at the non prosthetic hip. It may accelerate degeneration if the hip already shows signs of arthritis. Relieving the limb with the prosthetic hip will also reduce muscle strength in that limb, augmenting detrimental effects at the non prosthetic hip.

Hence in this section the loads on the non prosthetic hip are compared with those on the prosthetic hip for the activities involving symmetry. These are gait, rising from a chair and going up and down stairs.

The mean peak values of resultant hip joint force in terms of body weight, Fr/bwt, for these activities are shown in table 8.14. The values for the non prosthetic side are all greater than those for the prosthetic side. Paired T tests were performed in order to compare the results for the non prosthetic side with those for the prosthetic side in the same patients. The resulting P values are given in table 8.15. At the 5% significance level, the peak values of Fr/bwt were significantly greater at the non prosthetic side than the prosthetic side in the activities of gait and rising from a chair with P values of 0.002 and 0.004 respectively. The activity of ascending stairs was very close to being significant at the 5% level with a P value of 0.076. Descent did not produce a significantly greater value, the P value being 0.325. This may be because descent is a less controllable activity than the others and the subjects found it more difficult to adopt a style in which they could off-load the prosthetic hip. Alternatively they may not feel the need to off-load the prosthetic hip. If so, one would expect the hip joint forces to be very low in descent. However, this is not the case. The values incurred in rising from a chair were lower than those in descent but rising from a chair produced a statistically significant difference between the non prosthetic and prosthetic sides.

Overall, in some activities, notably gait, stair ascent and rising from a chair the patients were off-loading the prosthetic hip, increasing the loading on the non prosthetic hip. Although this may be advantageous for the prosthetic hip, it can initiate or accelerate degeneration at the non prosthetic hip, increasing the chances of another hip replacement.

CHAPTER 9. CONCLUSIONS AND RECOMMENDATIONS FOR FURTHER WORK

9.1 CONCLUSIONS

Hip joint forces have been calculated in three dimensions for 16 post-operative hip replacement patients and 10 age-matched normal subjects during various activities of daily living. The results will be useful for the design and testing of prostheses provided that the variability in the results is taken into account.

9.1.1 Validity of the Results

The validity of the results was assessed by comparing the predicted muscle activity patterns with published EMG data for the activities of gait, stair ascent and rising from a chair. The results for three normal subjects were examined and it was found that the activity patterns predicted for the majority of the muscles were consistent with the EMG data. The maximum muscle stress values calculated were found to be physiologically reasonable, further indicating that the results were not invalid.

The mean peak resultant hip joint force calculated during the stance phase of gait for the prosthetic hips of the patients was 3.79 times body weight (S.D±0.79). The mean speed of gait was 1.01m/s (S.D±0.21). The mean peak value of resultant joint force is consistent with those measured by Bergmann et al (1993) in patients with instrumented hip prostheses. This consistency provides further evidence for the validity of the results. The value is greater than those measured by Rydell (1966) and Kotzar et al (1991) even though some of the values of Rydell and Kotzar et al were recorded at speeds less than those in the current study. This is probably due to the longer post-operative time of the current study as compared to that of Rydell and Kotzar et al and other subject specific factors which were detailed in section 8.1.1.

9.1.2 Resultant hip joint force

The maximum resultant joint force predicted for both the prosthetic hips of the patients and the hips of the normal subjects was that for the car activity. High levels of resultant joint forces are undesirable as they may be related to failure of the prosthesis. Changing the manner in which an activity is carried out can reduce the resultant joint force.

The maximum mean peak resultant joint force calculated for the prosthetic hips of the patients was 4.98 times body weight (S.D.±1.37). This was for the left hip when getting out of the passenger side of a right hand drive car (activity code : cox). The difference between

this value and that during the same activity for the hips of the normal subjects was only 7% although the two groups performed the activity in different manners. All of the patients twisted round on the seat, swinging both legs out of the car before standing up and moving away. This is how they are taught to get out of a car in the early post-operative period. The majority of the normal subjects moved the left leg out of the car first and supported their weight on this limb as they brought the right leg out and moved away from the car. It would be expected that swinging both legs out before standing up would result in lower resultant joint forces than the other style since the body weight would be evenly distributed between the two limbs. This was not the case. Those patients with higher joint forces may not have been distributing the weight evenly between the two limbs and were thereby loading the left limb more heavily than the right one as they got up and moved away. There may therefore be a need for physiotherapists to emphasise the importance of taking the activity slowly in an attempt to attain a more even distribution of load between the two limbs.

The maximum mean peak resultant hip joint force determined for the normal subjects was 6.25 times body weight (S.D.±1.21). This was calculated at the left hip when getting into the passenger side of a right hand drive car (activity code : con). All of the normal subjects took a step onto the left leg and whilst supporting their weight on this leg, placed the right leg into the car. They then sat down and brought the left leg into the car. Such a style should be avoided by patients in order to protect their hip. The majority of the patients did avoid this style, sitting down on the seat and then swinging their legs into the car as they are taught in the early post-operative period.

The maximum increase in mean peak resultant joint force for the hips of the normal subjects as compared to that for the prosthetic hips of the patients was calculated for the inside hip when getting into and out of the bath (activity codes : bin and bix). The inside hip is that which corresponds to the first foot to touch the bath floor on entry and the last to leave it on exit. A 93% increase was observed on getting into the bath and a 41% increase on getting out of the bath. The main difference between the two groups in terms of activity style was that all of the normal subjects sat down in the bath onto the low bath stool (height : 145mm) whilst the majority of the patients did not. The majority of the patients stepped over the bath side in order to use a shower fitted in the bath. If possible, in order to reduce resultant hip joint force, patients should avoid sitting down in the bath and only use it for a shower as did the majority of those participating in the study. However, patients are often encouraged to soak in the bath to relieve arthritis at other joints. Sitting down in the bath may be advantageous for relieving arthritis in other joints but will increase the resultant joint force at the prosthetic hip.

9.1.3 Torsional Moment about the Stem of the Femoral Component

The torsional moment imposed about the stem of the prosthesis during the various activities was also assessed. The majority of the torsional moment is due to the component of hip joint force in the anterior-posterior direction, Fx. The maximum mean peak magnitude of this component in terms of body weight, Fx/bwt, calculated for the prosthetic hips of the patients was that at the left hip when getting out of the passenger side of a right hand drive car (activity code : cox). That for the hips of the normal subjects was for the left hip when getting into the passenger side of a right hand drive car (activity code : con). The second greatest mean peak magnitude in both subject groups was that during stair ascent.

Simple analysis using the components of hip joint force in the anterior-posterior and medio-lateral directions was used to estimate the torsional moments for the prosthetic hips of the patients. An accurate calculation of torsional moment would include full 3D geometry and joint force configuration requiring accurate knowledge of the orientation of the prosthesis with respect to the femur in all three directions. In the absence of all of this information, simple analysis was used to assess the torsional moments in the current study in the two activities with greatest magnitudes of Fx/bwt in addition to gait. Torsional moments during gait, stair ascent and at left hip during car exit were then found to be within or exceed the range of 1-5%bwt.m. This was quoted by Bergmann et al (1995) as the range reported in the literature for the torsional strength of implant fixation. This implies that the prostheses should already be loose 'in vivo' which is not necessarily the case. This discrepancy is likely to be due to the difference between the 'in vivo' and 'in vitro' situations including the permanent remodelling of natural bone in the 'in vivo' situation. Despite this discrepancy it seems justified to conclude that the torsional moment during some daily activities probably comes close to the torsional fixation limit of the implant.

Torsional moment depends strongly on the geometry of the prosthesis and on its orientation with respect to the femur. Simple analysis was performed changing the anteversion angle but using the same values for the force components. Reducing the anteversion angle produced an increase in torsional moment which suggests that the anteversion angle should not be reduced during the hip replacement operation. However, since a change in anteversion angle will result in changes in the calculated components of joint force, further analysis is required to confirm this.

A reduction in torsional moment can also be achieved through reducing the magnitude of anterior-posterior force component by altering the style in which an activity is carried out. During stair ascent one subject climbed the stairs one at a time, resulting in a reduced magnitude of Fx/bwt in comparison to the other subjects who climbed the stairs cyclically.

Further tests would be required to confirm that climbing the stairs one at a time always results in lower magnitudes of Fx/bwt than climbing cyclically.

The maximum mean peak magnitude of Fx/bwt for the prosthetic hips of the patients was calculated for the left hip when getting out of the passenger side of a right hand drive car (activity code : cox). This was only 9% different to that for the hips of the normal subjects during the same activity although both groups performed the activity in different styles. Similar observations were made for the mean peak resultant hip joint force in this activity in section 9.1.2 and similar conclusions may be drawn. In order to reduce torsional moments, patients should continue twisting on the seat and swinging both legs out of the car before standing up but they should take the activity slowly in an attempt to attain a more even distribution of weight between the two limbs.

The maximum mean peak magnitude of Fx/bwt for the hips of the normal subjects was calculated at the left hip when getting into the passenger side of a right hand drive car (activity code : con). This was also the case for the mean peak resultant joint force and similar conclusions to those in section 9.1.2 may be drawn. In order to reduce torsional moments, patients should avoid the style exhibited by most of the normal subjects. The majority of the normal subjects stepped onto the left leg and whilst supporting the weight on this leg moved the right leg into the car. They then sat down and brought the left leg into the car. The majority of the patients did avoid this style, sitting down onto the seat and then swinging both legs into the car.

As was the case for the mean peak resultant hip joint force in section 9.1.2, the maximum increase in Fx/bwt for the hips of the normal subjects as compared to the prosthetic hips of the patients was for the inside hip during bath entry and exit (activity codes : bin and bix). There was a 130% increase during entry and a 69% increase during exit. Most normal subjects sat down onto the bath stool of height 145mm whilst most patients stood in the bath. If possible, in order to reduce torsional moments, patients should avoid sitting down in the bath and only use it for a shower. Although soaking in the bath is encouraged to relieve arthritis at other joints, the action of sitting down in the bath will increase the torsional moment imposed about the prosthetic stem.

9.1.4 Off-loading of the Prosthetic hip onto the Non Prosthetic hip

Comparison of the results for the prosthetic and non prosthetic hips of the patients during the activities involving symmetry revealed that the loading on the non prosthetic hip was greater than that on the prosthetic hip when walking, going upstairs and when rising from a chair. Although advantageous for the prosthetic hip, this may initiate or accelerate degeneration at the non prosthetic hip, increasing the chances of a second hip replacement.

9.2 RECOMMENDATIONS FOR FURTHER WORK

The results were validated by comparing the predicted muscle activity patterns with published EMG data and ensuring that the maximum muscle stress was maintained within physiologically reasonable limits. Results for the prosthetic hips of the patients were also compared with published data measured for patients with instrumented hip prostheses. Of the activities studied in the current project, published data was only available for gait, stair negotiation and rising from a chair. It would be interesting to calculate the hip joint forces for a subject with an instrumented prosthesis as they performed the car, bath and walking turn activities in addition to gait, stair negotiation and rising from a chair. The calculated results could then be compared directly to the results measured in the same patient.

In the current study each subject performed the activity in their usual natural style and some styles were found to produce lower hip joint forces than others. It would be useful to investigate further the effects of style, taking one subject and asking them to perform each activity in a number of different styles.

A simple approach was taken in the calculation of torsional moment in the current study but it would be interesting to further investigate the torsional moment, including the full 3D geometry and joint force configuration. Effects of changes in the geometry of the prosthesis and its orientation with respect to the femur on torsional moment could then be accurately assessed.

The current study has concentrated on the loading incurred during various daily activities. Although this is important with regard to failure of prostheses, the frequency with which the patient performs the activity is also important. For example, the maximum mean peak resultant hip joint forces and torsional moments were calculated for the car activity but the frequency with which the activity is carried out will be far less than the frequency of the gait cycle. Further analysis is required to combine data on frequency of the activity with that on loading.

Finally, Bergmann et al (1993) measured the hip joint forces which occurred when their patients accidentally stumbled. Unfortunately, no data could be acquired in the current study to compare to that of Bergmann et al. However, this is an important area for further work since implant failure may be related to such occasional unintended high loads.

REFERENCES

Andriacchi TP, Andersson GBJ, Fermier RW, Stern D and Galante JO (1980), A study of lower-limb mechanics during stair-climbing. **J. Bone Joint Surg. [Am] 62, 749-757.**

Andriacchi TP, Galante GO and Fermier RW (1982), The influence of total knee-replacement design on walking and stair-climbing. **J. Bone Joint Surg. [Am] 64, 1328-1335.**

Andriacchi TP and Strickland AB (1983), Gait analysis as a tool to assess joint kinetics. **Proc. of NATO Advanced Study Institute Biomechanics of Normal and Pathological Articulating Joints,** pp83-102. Lisbon, Portugal.

Apkarian J, Naumann S and Cairns B (1989), A three-dimensional kinematic and dynamic model of the lower limb. **J. Biomech. 22, 143-155.**

Bean JC, Chaffin DB and Schultz AB (1988), Biomechanical model calculation of muscle contraction forces: A double linear programming method. **J. Biomech. 21, 59-66.**

Bell AL, Brand RA and Pederson DR (1989), Prediction of hip joint centre location from external landmarks. **Hum. Mov. Sci. 8, 3-16.**

Bell AL, Pederson RD and Brand RA (1990), A comparison of the accuracy of several hip center location prediction methods. **J. Biomech. 23, 617-621.**

Bergmann G, Graichen F and Rohlmann A (1993), Hip joint loading during walking and running, measured in two patients. **J. Biomech. 26, 969-990.**

Bergmann G, Graichen F and Rohlmann A (1995), Is staircase walking a risk for the fixation of hip implants. **J. Biomech. 28, 535-553.**

Berme N and Paul JP (1979), Load actions transmitted by implants. **J. Biomed. Eng. 1, 268-272.**

Brand RA, Crowninshield RD, Wittstock CE, Pederson DR, Clark CR and Van Kricken FM (1982), A model of lower extremity muscular anatomy. **J. Biomech. Eng. 104, 304-310.**

Brand RA, Pederson DR, Davy DT, Kotzar GM, Heiple KG, Goldberg VM (1994), Comparison of hip force calculations and measurements in the same patient. **J. Arthroplasty 9, 45-51.**

Brown TRM, Nicol AC and Paul JP (1984), Comparison of loads transmitted by Charnley and CAD Muller total hip arthroplasties. **Proc. Conf. Engineering and Clinical Aspects of Endoprosthetic Fixation,** pp 63-68. Inst. Mech. Eng. London.

Cappozzo A (1984), Gait analysis methodology. **Hum. Mov. Sci. 3, 27-50**

Cholewicki J and McGill SM (1994), EMG assisted optimization: A hybrid approach for estimating muscle forces in an intermediate biomechanical model. **J. Biomech. 27, 1287-1289.**

Crowninshield RD (1978), Use of optimization techniques to predict muscle forces. **J. Biomech. Eng. 100, 88-92.**

Crowninshield RD and Brand RA (1981), A physiologically based criterion of muscle force prediction in locomotion. **J. Biomech. 14**, 793-801.

Crowninshield RD, Brand RA and Johnston RC (1978b), The effects of walking velocity and age on hip kinematics and kinetics. **Clin. Orthop. Rel. Res. 132**, 140-144.

Crowninshield RD, Johnston RC, Andrews JG and Brand RA (1978a), A biomechanical investigation of the human hip. **J. Biomech. 11**, 75-85.

Davis RB, Ounpuu S, Tyburski D and Gage JR (1991), A gait analysis data collection and reduction technique. **Hum. Mov. Sci. 10**, 575-587.

Davy DT, Kotzar GM, Brown RH, Heiple KG, Goldberg VM, Heiple KG (Jr.), Berilla J and Burstein AH (1988), Telemetric force measurements across the hip after total arthroplasty. **J. Bone Joint Surg. [Am] 70**, 45-50.

Delp SL, Loan JP, Hoy MG, Zajac FE, Topp EL and Rosen JM (1990), An interactive graphics-based model of the lower extremity to study orthopaedic surgical procedures. **IEEE Trans. Biomed. Eng. 37**, 757-767.

Dempster WT (1955) Space requirements of the seated operator. **WADC Technical Report No. 55-159**, Wright Patterson Air Force Base, Dayton, Ohio.

Doorenbosch CAM, Harlaar J, Roebroeck ME and Lankhorst GJ (1994), Two strategies of transferring from sit-to-stand; the activation of monoarticular and biarticular muscles. **J. Biomech. 27**, 1299-1307.

Dostal WF and Andrews JG (1981), A three-dimensional biomechanical model of hip musculature. **J. Biomech. 14**, 803-812.

Drillis R and Contini R (1966) Body Segment Parameters. **Technical report No. 1166.03**, School of Engineering and Science, New York University.

Ellis MI, Seedhom BB and Wright V (1984), Forces in the knee joint whilst rising from a seated position. **J. Biomed. Eng. 6**, 113-120.

English TA and Kilvington M (1979) In vivo records of hip loads using a femoral implant with telemetric output (A preliminary report). **J. Biomed. Eng. 1**, 111-115.

Fleckenstein SJ, Lee Kirby R and MacLeod DA (1988), Effect of limited knee-flexion range on peak hip moments of force while transferring from sitting to standing. **J. Biomech. 21**, 915-918.

Friederich JA and Brand RA (1990), Muscle fiber architecture in the human lower limb. **J. Biomech. 23**, 91-95.

Gaudin AJ and Jones KC (1989), **Human Anatomy and Physiology**. Harcourt Brace Jovanovich, Inc, San Diego.

Goh JCH (1982), **Biomechanical Evaluation of Prosthetic Feet**, PhD Thesis, University of Strathclyde, Glasgow.

Grood ES and Suntay WJ (1983), A joint coordinate system for the clinical description of three-dimensional motions: Application to the knee. **J. Biomech. Eng. 105**, 136-144.

Hardt DE (1978), Determining muscle forces in the leg during normal human walking - An application and evaluation of optimization methods. **J. Biomech. Eng. 100**, 72-78.

Huntington LJ, Kendall JP and Tietjens BR (1979), A method of measuring from photographic records the movements of the knee joint during walking. **Eng. in Med. 8**, 143-148.

Ishai GA (1975), **Whole Body Gait Kinetics**. PhD Thesis, University of Strathclyde, Glasgow.

Jensen RH and Davy DT (1975), An investigation of muscle lines of action about the hip: A centroid line approach vs the straight line approach. **J Biomech. 8**, 103-110.

Johnston RC, Brand RA and Crowninshield RD (1979), Reconstruction of the hip. **J. Bone Joint Surg. [Am] 61**, 639-652.

Kadaba MP, Ramakrishnan HK and Wootten ME (1990), Measurement of lower extremity kinematics during level walking. **J. Orthop. Res. 8**, 383-392.

Kaufman KR, An KN, Litchy WJ and Chao EYS (1991), Physiological prediction of muscle forces-I. Theoretical formulation. **Neuroscience 40**, 781-792.

Kotzar GM, Davy DT, Goldberg VM, Heiple KG, Berilla J, Heiple KG (Jr.), Brown RH and Burstein AH (1991), Telemeterized in vivo hip joint force data: A report on two patients after total hip surgery. **J. Orthop. Res. 9**, 621-633.

Kelley DL, Dainis A and Wood GK (1976), Mechanics and muscular dynamics of rising from a seated position. In **Biomechanics V-B**, ed. Komi PV, pp 127-134. University Park Press, Baltimore.

McFadyen BJ and Winter DA (1988), An integrated biomechanical analysis of normal stair ascent and descent. **J. Biomech. 21**, 733-744.

Mjoeberg (1994), Theories of wear and loosening in hip prostheses. **Acta Orthop. Scand. 65**, 361-371.

Morrey BF (1991), **Joint Replacement Arthroplasty**, Churchill Livingstone, New York.

Morrison JB (1967), **The forces transmitted by the human knee joint during activity**. PhD thesis, University of Strathclyde, Glasgow.

Naumann S, Ziv I and Rang MC (1982), Biomechanics of standing up-from a chair. In **Human Locomotion II: Proc. of the Second Biannual Conf. of the Canadian Soc. for Biomechanics**, pp 78-69. Ottawa, Canada.

Nordin M and Frankel VH (1989), **Basic Biomechanics of the Musculoskeletal System**, Lea and Febiger, Pennsylvania.

Norkin CC and Levangie PK (1992), **Joint Structure and Function. A comprehensive Analysis**. F.A. Davis Company, Philadelphia.

Pai YC and Rogers MW (1991), Speed variation and resultant joint torques during sit-to-stand. **Arch. Phys. Med. Rehabil. 72**, 881-885.

Palastanga N, Field D and Soames R (1994), **Anatomy and Human Movement. Structure and Function**. Butterworth-Heinemann, Oxford.

Patriarco AG, Mann RW, Simon SR and Mansour JM (1981), An evaluation of the optimization models in the prediction of muscle forces during human gait. **J. Biomech. 14**, 513-525.

Paul JP (1967), **Forces at the human hip joint**. PhD thesis, University of Glasgow, Glasgow.

Paul JP (1976), Approaches to design. Force actions transmitted by joints in the human body. **Proc. Royal Soc. London B. 192**, 163-172.

Paul JP and McGrouther DA (1975), Forces transmitted at the hip and knee joint of normal and disabled persons during a range of activities. **Acta Orthop. Belg. 41 [Suppl 1]**, 78-88.

Paul JP and Poulson J (1974), The analysis of forces transmitted by joints in the human body. **Proc. Fifth International Conference on Experimental Stress Analysis, Udine, Italy.**

Pedotti A, Krishnan VV and Stark L (1978), Optimization of muscle force sequencing in human locomotion. **Math. Biosci. 38**, 57-76.

Penrod DD, Davy DT and Singh DP (1974), An optimization approach to tendon force analysis. **J. Biomech. 7**, 123-129.

Perry J, Enwemera CS and Gronley JF (1988), The stability of surface markers during knee flexion. **Orthop. Trans. 12**, 453-454.

Pierrynowski MR and Morrison JB (1985a), A Physiological model for the evaluation of muscular forces in human locomotion: Theoretical aspects. **Math. Biosci. 75**, 69-101.

Pierrynowski MR and Morrison JB (1985b), Estimating the muscle forces generated in the human lower extremity when walking: A physiological solution. **Math. Biosci. 75**, 43-68.

Poulson J (1973), **Biomechanics of the leg**. PhD thesis, University of Strathclyde, Glasgow.

Press WH, Flannery BP, Teukolsky SA and Vetterling WT (1989), **Numerical Recipes in Pascal. The Art of Scientific Computing**. Cambridge University Press, Cambridge.

Procter P (1980), **Ankle joint biomechanics**. PhD thesis, University of Strathclyde, Glasgow.

Rodosky MW, Andriacchi TP and Andersson GBJ (1989), The influence of chair height on lower limb mechanics during rising. **J. Orthop. Res. 7**, 266-271.

Rohrle H, Scholten R, Sigolotto C and Sollbach W (1984), Joint forces in the human pelvis-leg skeleton during walking. **J. Biomech. 17**, 409-424.

Rowe PJ (1990), **The evaluation of the functional ability of total hip replacement patients**. PhD thesis, University of Strathclyde, Glasgow.

Runciman JR and Nicol AC (1994), Modelling muscle and joint forces at the glenohumeral joint : Overview of a current study. **Proc IMechE (part H) 208, 97-102.**

Rydell NW (1966), Forces acting on the femoral head-prosthesis. A study on strain gauge supplied prostheses in living persons. **Acta Orthop. Scand. [Suppl. 88].**

Seireg A and Arvikar RJ (1973), A mathematical model for evaluation of forces in lower extremities of the musculo-skeletal system. **J. Biomech. 6, 313-326.**

Seireg A and Arvikar RJ (1975), The prediction of muscular load sharing and joint forces in the lower extremities during walking. **J Biomech. 8, 89-102.**

Small CF, Bryant JT and Pichora DR (1992), Rationalization of kinematic descriptors for three-dimensional hand and finger motion. **J. Biomed. Eng. 14, 133-141.**

Snell RS (1981), **Clinical Anatomy for Medical Students**. Little, Brown and Company, Boston.

Spoor CW and Van Leeuwen JL (1992), Knee muscle moment arms from MRI and from tendon travel. **J. Biomech. 25, 201-206.**

Spoor CW, Van Leeuwen JL, De Windt FHJ and Huson A (1989), A model study of muscle forces and joint-force direction in normal and dysplastic neonatal hips. **J. Biomech. 22, 873-884.**

Spoor CW, Van Leeuwen JL, Meskers CGM, Titulaer AF and Huson A (1990), Estimation of instantaneous moment arms of lower-leg muscles. **J. Biomech. 23, 1247-1259.**

Stewart CJ (1995) **Swing phase and its control in the trans-femoral amputee.** PhD thesis, University of Strathclyde, Glasgow.

Tylkowski CM, Simon SR and Mansour JM (1982), Internal rotation gait in spastic cerebral palsy, in **Proc. of the 10th Open Scientific Meeting of the Hip Society**. ed Nelson JP, pp 89-125. Mosby, St Louis.

University of California, Berkeley (1953), The pattern of muscular activity in the lower extremity during walking. **Prosthetic Devices Research Project, Inst. of Engineering Research. Series II, Issue 25.**

Watson WA, Philipson T and Oates PJ (1969), **Numerical Analysis - the Mathematics of Computing 2**. Edward Arnold, London, pp 62-63.

Wheeler J, Woodward C, Ucovich RL, Perry J and Walker JM (1985), Rising from a chair. Influence of age and chair design. **Phys. Ther. 65, 22-26.**

Winter (1984), Kinematic and kinetic patterns in human gait: Variability and compensating effects. **Hum. Mov. Sci. 3, 51-76.**

Wretenberg P, Lindberg F and Arborelius UP (1993), Effect of armrests and different ways of using them on hip and knee load during rising. **Clin. Biomech. 8, 95-101.**

This file contains video data only.
Header, then Data for markers 1 to n, for each Video Frame in turn.

30 = Number of frames
29 = Number of markers

1	1	275	899	470	1.4	0011100
1	2	268	892	215	1.1	0001110
1	3	183	956	516	2.0	0001110
1	4	172	943	159	1.3	0011100
1	5	162	833	524	1.2	0011001

Frame number

Marker number

X Y Z

Marker locations presented with respect to the laboratory coordinate system.

Figure A1 The beginning of a video data file. This illustrates the format required by program HIPR. The file continues for frame one with coordinate data for marker 6 and then 7 and so on until 29. Data is then given for frame 2, and then 3 and so on until data is given for all frames.

APPENDIX A

The first section of this appendix contains details of the computer programs developed to calculate joint angles, joint moments, muscle forces and joint forces and then normalize the data to make the time periods of interest in each activity 100%.

The second section explains the theory of the approach taken in the normalization procedure.

A.1 COMPUTER PROGRAMS

The computer programs used to calculate joint moments, joint angles, muscle forces and joint forces and then normalize the output data were written in Turbo Pascal. They were developed on a Viglen 486DX PC with DOS version 5.0. The compiled versions are presented on a high density floppy disk inside the back cover of this thesis. Program HIPR calculates the moments, angles and forces for the right limb and program NORMX performs the normalization procedure. The following sections describe how each program is used.

A.1.1 Program HIPR

This program should only be used with data files produced in the gait laboratory of the Bioengineering Unit of Strathclyde University. The format for the input and output data are described in the following sections.

Input Data Required

Marker coordinate data generated by the Vicon system are required for both the static trial and the dynamic trial to be analyzed. Figure A1 illustrates the format in which these video files must be supplied. Following the header which consists of eight lines, coordinate data are given for each marker for frame one. The data are then given for frame two and so on. All video files must have a name with the extension '.VID'. Table A1 describes the marker numbering system. For right limb analysis, coordinate data are required for markers 1,2,3,4,5,7,8,10,12,14,16,18,20,26, and 28 in the static trial and for markers 3,4,7,12,14,18,20 and 28 in the dynamic trial. It should be noted that the dynamic trial video data should be filtered before being input into the program in order to reduce the noise in the output. Filtering programs are not included in this thesis since the filtering procedure carried out in the current study was performed on a mainframe system. For details of the filtering method used see Stewart (1995).

Force platform analogue data for the dynamic trial must also be supplied. Figure A2 illustrates the required format for this data. Following a header consisting of eleven lines, analogue data are given for frame one, then frame two and so on. For each frame the first eight values of data are for force platform 'A', the next six are for force platform 'B' and the next 'six' for force platform 'C'. The final value is that for the seat switch. All force platform analogue data files must be given a name with the extension '.ANA'.

At least ten frames of data are required for the static trial. Also, at least ten frames of data are required before and after the time period of interest in the dynamic trial. For example, if the stance phase of gait is being analyzed then the data sampling must be started at least ten frames (0.2 seconds if sampling at 50Hz) before the foot strikes the force platform. It must be terminated at least ten frames after the foot leaves the force platform.

The program is run by typing HIPR when in the A:\ directory. A series of prompts are then given indicating what input data is required. A theoretical example is assumed in order to illustrate the format required for the answers to the prompts. In this example, it is assumed that the input data is in a directory named C:\INPUT and it is required that the output data be put into an output directory named C:\OUTPUT. The video data file for the static trial is assumed to be STAT.VID. The video and force platform analogue data files for the dynamic trial are assumed to be DYN.VID and DYN.ANA respectively.

Marker number	Marker location
1	Right anterior superior iliac spine
2	Left anterior superior iliac spine
3	Right iliac crest (anterior)
4	Left iliac crest (anterior)
5	Right greater trochanter
6	Left greater trochanter
7	Midpoint between posterior superior iliac spines
8	Right femoral lateral epicondyle
9	Left femoral lateral epicondyle
10	Right femoral medial epicondyle
11	Left femoral medial epicondyle
12	Front of the right thigh
13	Front of the left thigh
14	Lateral side of the right thigh
15	Lateral side of the left thigh
16	Right fibula head
17	Left fibula head
18	Right tibial tuberosity
19	Left tibial tuberosity
20	Front of the right shank
21	Front of the left shank
26	Right medial malleolus
27	Left medial malleolus
28	Right lateral malleolus
29	Left lateral malleolus

Table A1 Marker numbering system. For further details of marker locations see figure 4.1.

This file contains analogue data only.

The format of this file is header followed by:
Frame no., Sample No., Chan 1 .....Chan n, for each Video Frame in turn.

30 = Number of frames
8 = Number of analogue channels.
1 = Analogue/video frame rate

1 1 2042 2043 2045 2045 2035 2045 2046 2043
2 1 2042 2043 2045 2045 2035 2045 2046 2043
3 1 2042 2043 2045 2045 2035 2045 2046 2043
4 1 2042 2043 2045 2045 2035 2045 2046 2043
5 1 2042 2043 2045 2045 2035 2045 2046 2043

Frame number

Channel values

Figure A2 The beginning of a force platform analogue data file. This illustrates the format required by program HIPR. In the file illustrated, only force platform 'A' is being sampled. The file continues with data for frames 6, then 7 and so on until data is given for all frames.

The prompts are as follows:

Prompt 1 : Directory in which to put the output ?
Example answer : C:\OUTPUT\
Prompt 2 : M-L distance between the tibial condyles ?
Prompt 3 : M-L distance between the medial tibial condyle and fibula head ?
Prompt 4 : M-L distance between the malleoli ?
Prompt 5 : Distance between the tibial plateau and tibial tuberosity ?
Prompt 6 : Soft tissue thickness over the anterior superior iliac spine ?
Prompt 7 : Soft tissue thickness over the greater trochanter ?
Prompt 8 : Soft tissue thickness over the midpoint between the posterior superior iliac spines ?
Prompt 9 : Body mass in kg ?
Prompt 10 : Distance between the skin surface and the centre of each marker ?
Prompt 11 : Distance between the right and left anterior superior iliac spines ?
Prompt 12 : A-P distance between the pelvic frontal plane and the midpoint between the posterior superior iliac spines ?
Prompt 13 : Vertical distance between the iliac crest and the ischial tuberosity ?
Prompt 14 : Distance between the medial and lateral femoral epicondyles ?
Prompt 15 : M-L distance between the hip joint centre and the most lateral point on the greater trochanter ?
Prompt 16 : Distance between the tibial condyles ?
Prompt 17 : Static trial to be analyzed ? (Do not include the extension)
Example Answer : C:\INPUT\STAT
Prompt 18 : Directory of trial to be analyzed ?
Example answer : C:\INPUT\
Prompt 19 : Name of dynamic trial to be analyzed ? (Do not include the extension)
Example answer : DYN
Prompt 20 : Which force platform is used ? Type 1 for A, 2 for B or 3 for C

The responses to prompts 2, 3 and 4 should be the results of the measurements made using callipers and no adjustments should be made for soft tissue thickness. Those to prompts 12, 14, 15 and 16 should be the dimensions between the appropriate bony points and corrections should be made for soft tissue thickness. Unless otherwise stated, all dimensions should be in mm.

As the program runs, the number of the frame being processed at a particular time is displayed on the screen.

Output files produced

Intermediate files used in the processing of the data are produced in the A:\WORK directory. These should be ignored.

A flag file is produced in the output directory indicating whether the processing was successful or not. The first part of the stem name of the flag file is the same as the stem name of the dynamic trial. The letters 'RG' are then added. The extension is '.FLG'. For the example described above, the file name would be DYNRG.FLG. This file will be empty if the calculations for every frame were performed successfully. However, if the calculations were not successful then a message will appear in this file describing the problem along with the frame number at which the problem occurred. The output data should only be used if the frame number concerned is outwith the time period of interest

The output data files are put into the directory requested and have extensions '.PRN'. The first part of the stem name of each file is the same as the stem name of the dynamic trial. Extra letters are then added indicating the output data contained. For the example described above, the files would be as follows:

DYNRA.PRN This file contains joint angle data
DYNRM.PRN This file contains joint moment data
DYNRH.PRN This file contains hip joint force data
DYNRX.PRN This file contains muscle force data

The first column of each of these files contains the frame number.

For each frame number, the joint angle file presents a row of six values of joint angle expressed in degrees. Reading from left to right, the order of joint angles is as follows: Knee flexion, knee abduction, knee external rotation, hip flexion, hip abduction and hip external rotation.

For each frame number, the joint moment file presents a row of nine values of joint moment expressed in Nm. Reading from left to right, knee joint moments are presented first, then hip joint moments and then ankle joint moments. The order of joint moments is as follows: $Mx_{KC\text{-}S}$, $My_{KC\text{-}S}$, $Mz_{KC\text{-}S}$, $Mx_{HC\text{-}F}$, $My_{HC\text{-}F}$, $Mz_{HC\text{-}F}$, $Mx_{AC\text{-}S}$, $My_{AC\text{-}S}$ and $Mz_{AC\text{-}S}$. For a description of each moment see figures 6.1 to 6.3.

For each frame number, the muscle force file presents a row of muscle force values in Newtons. Reading from left to right, the order is as follows: Adductor brevis (S), adductor brevis (I), adductor longus, adductor magnus (1), adductor magnus (2), adductor magnus (3), gluteus maximus (1), gluteus maximus (2), gluteus maximus (3), gluteus medius (1), gluteus medius (2), gluteus medius (3), gluteus minimus (1), gluteus minimus (2), gluteus minimus (3), iliacus, psoas, gemellus inferior, obturator externus, obturator internus, pectineus, piriformis, quadratus femoris, gemellus superior, biceps femoris (long head), gracilis, rectus femoris, sartorius, semimembranosus, semitendinosus, tensor fascia lata, biceps femoris (short head), gastrocnemius (medial head), gastrocnemius (lateral head), vastus intermedius, vastus lateralis and vastus medialis. The maximum muscle stress is then presented in N/cm^2.

For each frame number, the hip joint force file presents a row of four values. The first three values are the components of hip joint force and the fourth value is the resultant hip joint force. All are expressed in Newtons. Reading from left to right, the order is as follows: Fx, Fy, Fz and Fr. See figure 7.2 for a description of the sign convention used .

It should be noted that if the optimization procedure was unsuccessful (i.e. the objective function was unbounded or no solution satisfied the constraints) then all values for the particular frame concerned are set to 11111 in the hip joint force and muscle force files. If this occurs for more than three consecutive frames then program NORMX should not be run. If it occurs for one, two or three consecutive frames then program NORMX will interpolate as necessary.

A.1.2 Program NORMX

Program NORMX normalizes the data generated from HIPR. A description of the theory of the normalization procedure is given in section A.2. The input files to NORMX are the output files from HIPR. In the example described in section A.1.1 these are DYNRA.PRN, DYNRM.PRN, DYNRH.PRN, DYNRX.PRN. The normalization program is run by typing NORMX when in the A:\ directory. A series of prompts are given as shown below. Answers are presented for the example described previously in order to illustrate the required format.

Prompt 1 : Directory of files to be normalized ?
Example answer : C:\OUTPUT\
Prompt 2 : Stem name of files to be normalized ?
Example answer : DYNR
Prompt 3 : Number of frames in the trial ?
Prompt 4 : Frame at which to start normalization ?
Prompt 5 : Frame at which to end normalization ?

Prompt 6 : Body mass in kg ?

The output files are placed in the same directory as the input files and each has an extension '.PRN'. The first part of the stem name of each output file is the same as that of the input files. Extra letters are then added indicating the output data contained. This naming system is illustrated below using the example described previously.

DYNRAN.PRN	This file contains normalized joint angle data
DYNRMN.PRN	This file contains normalized joint moment data
DYNRKN..PRN	This file contains normalized hip joint force data
DYNRZN.PRN	This file contains normalized muscle force data

The format of these output files is the similar to that of the input files but where the first column of the input files contained frame numbers, that of the output file contains the numbers 1 to 100. Also, each row in the hip joint force file now contains eight values instead of four. The first three values are the components of hip joint force and the fourth value is the resultant hip joint force. All are expressed in Newtons. The second four values are the components and resultant hip joint force expressed in terms of body weight. Reading from left to right, the order is as follows: Fx, Fy, Fz, Fr, Fx/bwt, Fy/bwt, Fz/bwt and Fr/bwt. See figure 7.2 for a description of the sign convention used .

Two extra files with stem names ending in K and Z are also produced. In the example above these would be DYNRK.PRN and DYNRZ.PRN. These are intermediate files produced in the data processing and should be deleted.

A.2 THEORY OF THE NORMALIZATION PROCEDURE

The time periods of interest of each activity for each subject lasted for different lengths of time according to how fast the subject performed the activity. The measurement system sampled data at a rate of 50 frames per second and hence each trial period could last for any number of frames. In order to compare the results of a parameter for different subjects for an activity, the results had to be normalized so that each period of interest contained the same number of values. This number was set to 100 so that time instants within the period could be expressed as a percentage of the total period.

Values of the parameter were therefore calculated at intervals of 1% between 1% and 100% from the values at each frame within the normalization period. In order to do this a Lagrangian interpolation approach was taken as presented by Watson et al (1969). The general approach was applied to the normalization procedure as follows.

Let FRB be the frame number at the start of the time period of interest and FRE be the frame number at the end of this period. Also, let the parameter to be normalized be S. The values of S at 1% and 100% are equal to the values at FRB and FRE respectively giving

$$S_{1\%} = S_{FRB}$$
$$S_{100\%} = S_{FRE}$$

The next stage was to calculate the values of $S_{C\%}$ for C = 2 to 99. For each value of C, a point F was denoted as the point corresponding to C% which lay between FRB and FRE. This was calculated as

$$F = \left[\frac{C-1}{99} * (FRE-FRB)\right] + 1$$

Rounding F to the nearest whole number gave the nearest frame to F. The rounded value

was denoted as FR. In order to calculate the value of the parameter at F and therefore also at C%, a fourth order polynomial was evaluated using the values of S at FR, the 2 frames before FR and the 2 frames after FR. Lagrangian coefficients were calculated as follows:

$$L(0) = \frac{(F-(FR-1)) * (F-FR) * (F-(FR+1)) * (F-(FR+2))}{(-1) * (-2) * (-3) * (-4)}$$

$$L(1) = \frac{(F-(FR-2)) * (F-FR) * (F-(FR+1)) * (F-(FR+2))}{(1) * (-1) * (-2) * (-3)}$$

$$L(2) = \frac{(F-(FR-2)) * (F-(FR-1)) * (F-(FR+1)) * (F-(FR+2))}{(2) * (1) * (-1) * (-2)}$$

$$L(3) = \frac{(F-(FR-2)) * ((F-FR-1)) * (F-FR) * (F-(FR+2))}{(3) * (2) * (1) * (-1)}$$

$$L(4) = \frac{(F-(FR-2)) * (F-(FR-1)) * (F-FR) * (F-(FR+1))}{(4) * (3) * (2) * (1)}$$

The value of S at F and therefore at C% was then

$$S_{C\%} = (L(0)*S_{FR-2}) + (L(1)*S_{FR-1}) + (L(2)*S_{FR}) + (L(3)*S_{FR+1}) + (L(4)*S_{FR+2})$$

APPENDIX B

This appendix presents the physiological cross sectional area (PCSA) data used in the model. All data except those for quadratus femoris were taken from Friederich and Brand (1990). Those for quadratus femoris were calculated as described in section 4.3.5.

Muscle	PCSA /cm²	Muscle	PCSA /cm²
Adductor brevis (1)	1.92	Obturator internus	9.30
Adductor brevis (2)	1.97	Pectineus	1.24
Adductor longus	9.75	Piriformis	9.16
Adductor magnus (1)	10.91	Quadratus femoris	9.16
Adductor magnus (2)	6.97	Gemellus superior	1.45
Adductor magnus (3)	5.93	Biceps femoris (Long)	9.12
Gluteus maximus (1)	14.59	Gracilis	0.79
Gluteus maximus (2)	9.60	Rectus femoris	9.20
Gluteus maximus (3)	8.10	Sartorius	2.68
Gluteus medius (1)	13.09	Semimembranosus	13.99
Gluteus medius (2)	10.43	Semitendinosus	3.12
Gluteus medius (3)	9.64	Tensor fascia lata	2.46
Gluteus minimus (1)	7.45	Biceps femoris (Short)	4.69
Gluteus minimus (2)	8.76	Gastrocnemius (Med)	17.04
Gluteus minimus (3)	7.97	Gastrocnemius (Lat)	8.60
Iliacus	8.82	Vastus intermedius	17.20
Psoas	3.70	Vastus lateralis	16.48
Inferior gemellus	1.51	Vastus medialis	15.60
Obturator externus	4.88		

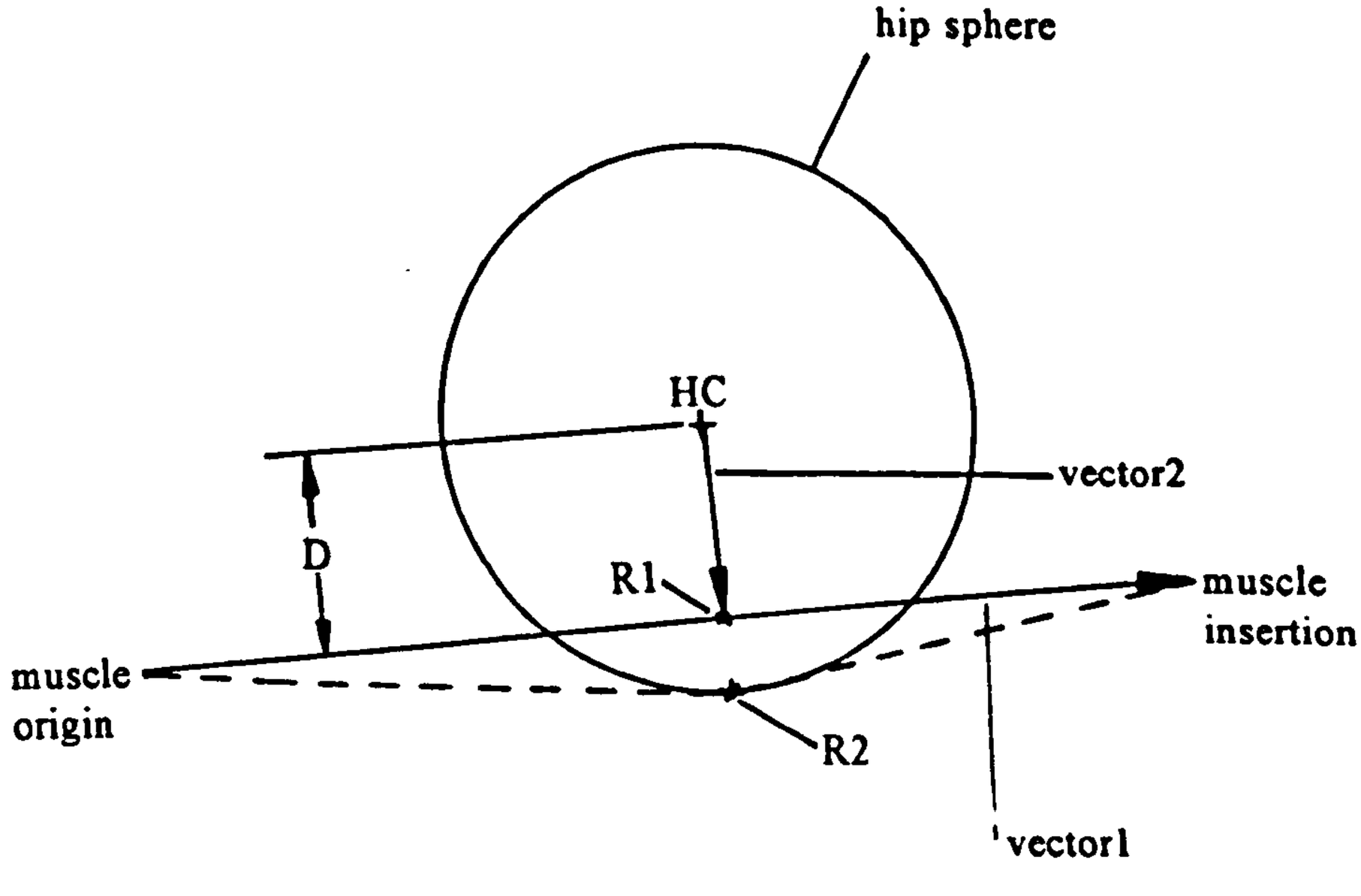

Figure C1 An illustration of the approach taken in making adjustments for the wrapping of muscles around the posterior surface of the hip joint. Point R2 is calculated and set up as an effective origin or insertion as appropriate.

APPENDIX C

This appendix contains details of the wrapping calculations performed. The wrapping around the back of the hip joint by obturator internus, piriformis, the gemelli and the lower part of gluteus minimus is considered first. This is followed by the details of the wrapping calculations performed for the middle and lower parts of gluteus maximus and then iliacus and psoas. All calculations presented are for the right side. The approach taken for the left side was the same as that for the right but some alterations were required to the calculations. These are not detailed here.

C.1 OBTURATOR INTERNUS, PIRIFORMIS, GEMELLI AND THE LOWER PART OF GLUTEUS MINIMUS

Constants used in the wrapping calculations for these muscles were as follows. The radius of the hip sphere (RHC) was assumed to be 25mm as determined from cadaveric measurement and measurement of the practical musculoskeletal model. The acetabulum was assumed to face 45° caudally and 15° anteriorly as quoted by Morrey (1991).

Steps in the calculation procedure for these muscles were as follows:

(a) The femoral insertion of the muscle concerned was calculated with respect to the pelvic coordinate system to give $(X,Y,Z)_{MUS\ IN\ -\ P}$. The muscle origin was already given with respect to the pelvic coordinate system as $(X,Y,Z)_{MUS\ OR\ -\ P}$. The origin of the pelvic coordinate system is at the hip joint centre, HC.

(b) The coordinates of point R1 in figure C1 were calculated as follows:

Let vector1 = $(X,Y,Z)_{MUS\ IN\ -\ P} - (X,Y,Z)_{MUS\ OR\ -\ P}$
and vector2 = $(X,Y,Z)_{R1\ -\ P}$

The point R1 was then located as $(X,Y,Z)_{R1\ -\ P} = (X,Y,Z)_{MUS\ OR\ -\ P} + \lambda$(vector 1) (C1)

Also, since vectors 1 and 2 are perpendicular to one another their dot product should be zero giving

$$(\text{vector1}).(\text{vector2}) = 0 \qquad (C2)$$

Solving equations C1 and C2 simultaneously gave λ and hence $(X,Y,Z)_{R1\ -\ P}$.

(c) The distance between the hip joint centre, HC and point R1 was calculated as D and compared with the radius of the hip sphere, RHC.

If D>RHC - The procedure was terminated since no wrapping occurred.
If D<RHC - Wrapping occurred and the calculation procedure continued to step (d).

(d) Further checks were performed to ensure that the muscle remained on the correct side of the hip joint centre. The wrapping point R2 was then calculated as follows:

Let vector3 be a unit vector relative to the pelvic coordinate system in the direction of vector2. Then

$$(X,Y,Z)_{R2\ .\ P} = \text{RHC(vector3)}$$

(e) The final stage was to determine whether wrapping point R2 was on the acetabular or

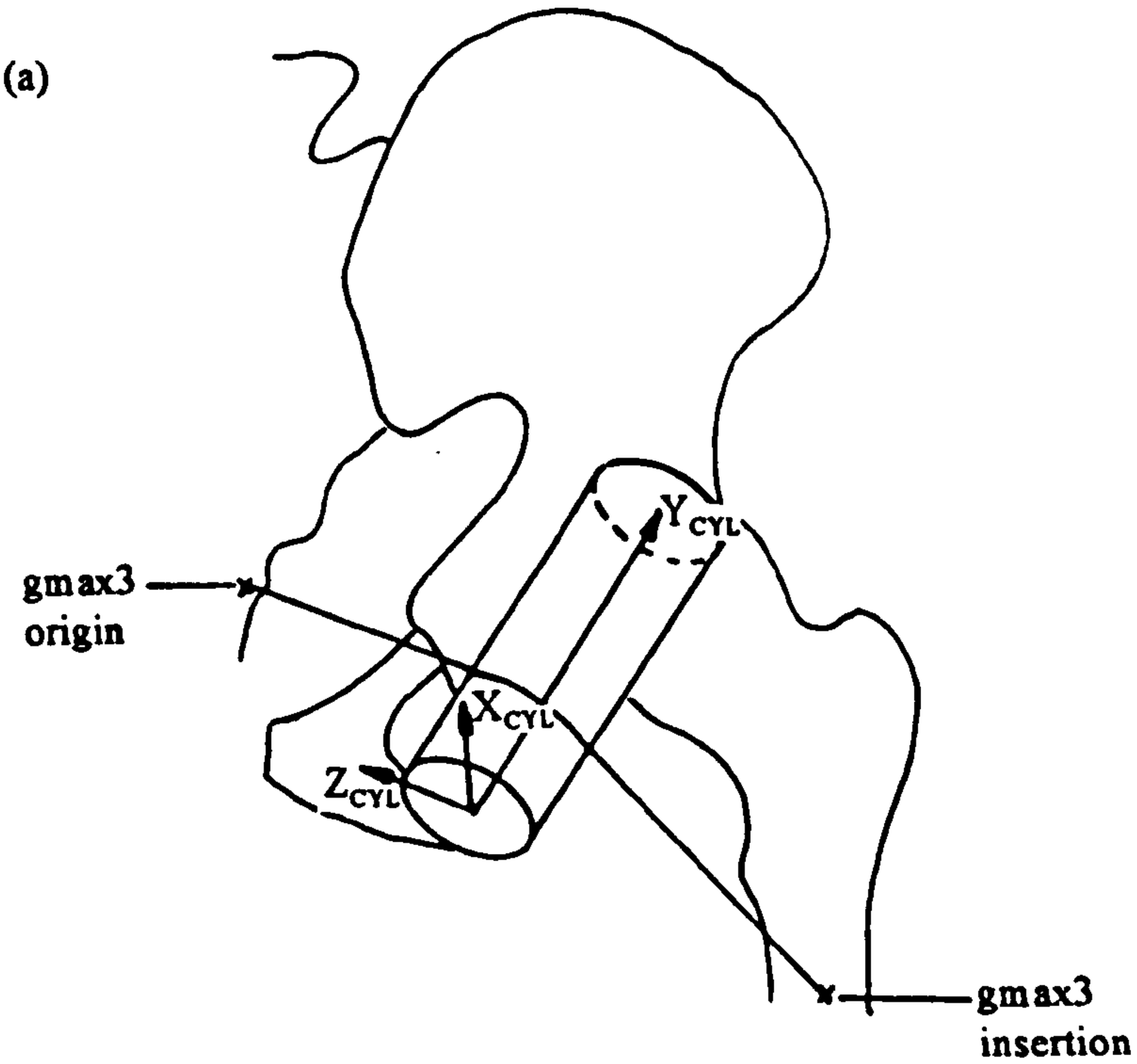

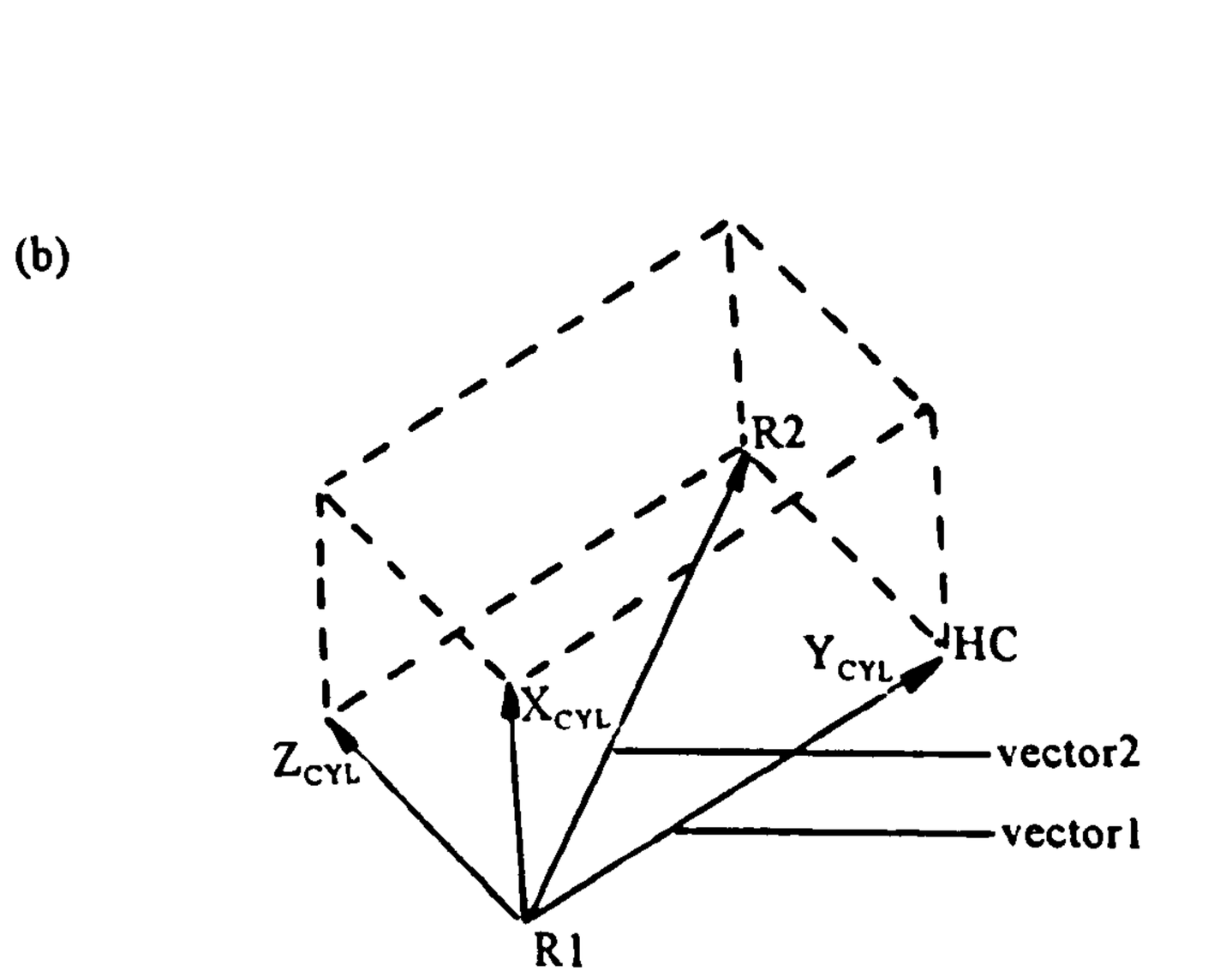

Figure C2 An illustration of the approach taken to set up the cylinder coordinate system used in the wrapping calculations of gmax3.

the femoral region of the hip sphere. ACVEC was set up as a unit vector relative to the pelvic coordinate system perpendicular to the plane of opening of the acetabulum, pointing away from the pelvis. Then

$$C = (ACVEC).(X,Y,Z)_{R2\,-\,P}$$

If C>0 - The angle between ACVEC and a vector running between HC and R2 was less than 90°. Hence R2 was on the femoral side. R2 was calculated with respect to the femoral coordinate system and set up as the effective insertion.

If C<0 - The angle between ACVEC and a vector running between the HC and R2 was greater than 90° and hence R2 was on the acetabular side. $(X,Y,Z)_{R2\,-\,P}$ was therefore set up as the effective origin.

C.2 THE LOWER ELEMENT OF GLUTEUS MAXIMUS (GMAX3)

The only constant used in the wrapping calculations of gmax3 was the radius of the cylinder used to model the region of the pelvis between the ischial tuberosity and the hip joint centre (RCYL). This was set as 20mm from examination of the practical musculoskeletal model.

Steps in the calculation procedure for this muscle element were as follows:

(a) The cylinder coordinate system shown in figure C2 was set up in two stages. Points used include the hip joint centre (HC), the origin of the long head of biceps femoris located on the ischial tuberosity (R1) and the origin of adductor longus located on the front of the body of the pubis (R2). Points R1 and R2 were already given with respect to the pelvic coordinate system as $(X,Y,Z)_{R1\,-\,P}$ and $(X,Y,Z)_{R2\,-\,P}$. The origin of the pelvic system was at HC. Vectors 1 and 2 were set up as shown in figure C2b as

$$\text{vector1} = -(X,Y,Z)_{R1\,-\,P}$$
$$\text{vector2} = (X,Y,Z)_{R2\,-\,P} - (X,Y,Z)_{R1\text{-}P}$$

The first approximation was set up with origin at R1 as follows:

Y_{CYL} : Between HC and R1. i.e. vector1
X_{CYL} : Perpendicular to a plane containing HC, R1 and R2 pointing into the pelvis i.e vector1 x vector2.
Z_{CYL} : $X_{CYL} \times Y_{CYL}$

with unit vectors I_{CYL}, J_{CYL}, K_{CYL} relative to the pelvic coordinate system. These unit vectors were used to set up the direction cosine matrix $[B_{CYL\,-\,P}]$ relating the cylinder and pelvic coordinate systems.

In the second approximation for the cylinder coordinate system, a point R3 was located with respect to the first approximation system as follows:

$$X_{R3\,-\,CYL} = 0$$
$$Y_{R3\,-\,CYL} = 0$$
$$Z_{R3\,-\,CYL} = RCYL$$

where RCYL is the radius of the cylinder. Point R3 was calculated with respect to the pelvic coordinate system and the second approximation for the coordinate system was set up in the

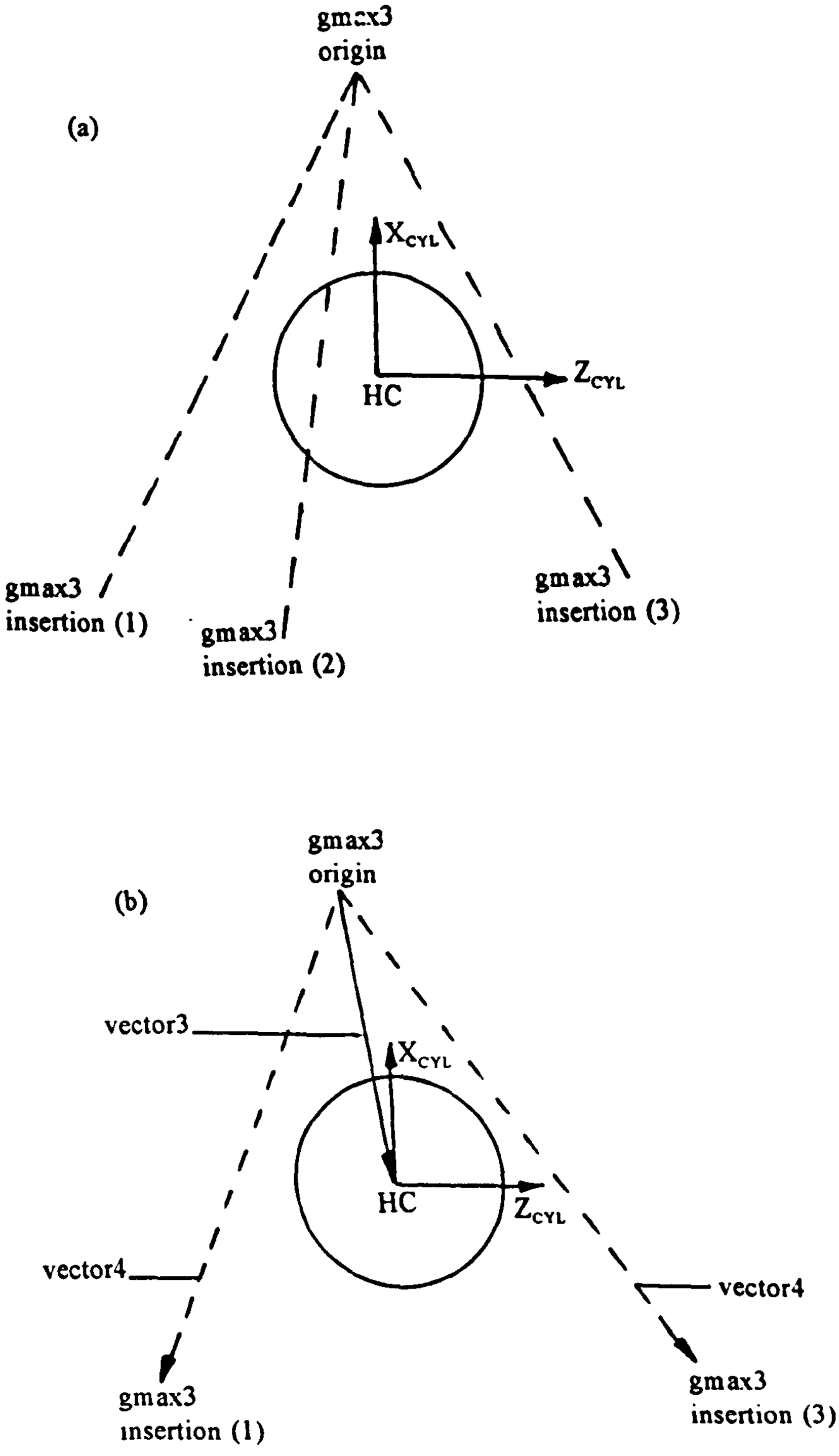

Figure C3 Diagrams used in checking for wrapping of gmax3 around the cylinder. See text in section C.2 steps (d) and (e) for explanation.

same way as the first, replacing R1 with R3. This was used in the subsequent calculations.

(b) The origin and insertion of gmax3 were calculated with respect to the cylinder coordinate system as $(X,Y,Z)_{GMAX3\ OR\ -\ CYL}$ and $(X,Y,Z)_{GMAX3\ IN\ -\ CYL}$.

(c) Checks were performed to ensure that the origin lay outside the cylinder as follows

$$A = [\ (X_{GMAX3\ OR\ -\ CYL})^2 + (Z_{GMAX3\ OR\ -\ CYL})^2\ ]^{1/2}$$

If A<RCYL - The origin lay inside the cylinder. An error message was produced and the processing terminated.
If A>RCYL - The origin lay outside the cylinder and the calculation continued.

Similar checks were performed for the insertion.

(d) Wrapping of gmax3 around the cylinder was checked for by viewing the cylinder end on along the cylinder Y axis as shown in figure C3a. This view onto the XZ plane forms a circle. The line of action of gmax3 with respect to the circle was examined. Three situations were possible as illustrated in figure C3a.

(1) This would occur in hip extension. There was no intersection between the line of action of gmax3 and the circle and no wrapping occurred.
(2) This would occur with increasing hip flexion. There was intersection between the line of action of gmax3 and the circle and wrapping occurred.
(3) This would occur with even greater hip flexion. There was no intersection between the line of action of gmax3 and the circle but there was wrapping.

The correct situation had to be determined. Firstly, intersection between the line of action of gmax3 and the circle was checked for. This would distinguish situation (2) from situations (1) and (3). This was performed as follows.

The equation of the line of action of gmax3 can be set up in the XZ plane as

$$X = MZ+D \qquad (C3)$$

where (X,Z) is a point on the line and M and D are given by

$$M = (X_{GMAX3\ OR\ -\ CYL} - X_{GMAX3\ IN\ -\ CYL})/(Z_{GMAX3\ OR\ -\ CYL} - Z_{GMAX3\ IN\ -\ CYL})$$
$$D = (X_{GMAX3\ OR\ -\ CYL}) - M(Z_{GMAX3\ OR\ -\ CYL})$$

The equation of the circle is as follows

$$(X - X_{HC\ -\ CYL})^2 + (Z - Z_{HC\ -\ CYL})^2 = RCYL^2 \qquad (C4)$$

where RCYL is the radius of the cylinder and hence the radius of the circle. $(X,Z)_{HC\ -\ CYL}$ is the centre of the circle and (X,Z) is a point on the circle.

Solving equations C3 and C4 simultaneously gave a quadratic equation of the form

$$AZ^2 + BZ + C$$

where $A = (1+M^2)$
$B = (2MD - 2Z_{HC\ -\ CYL} - 2X_{HC\ -\ CYL}M)$

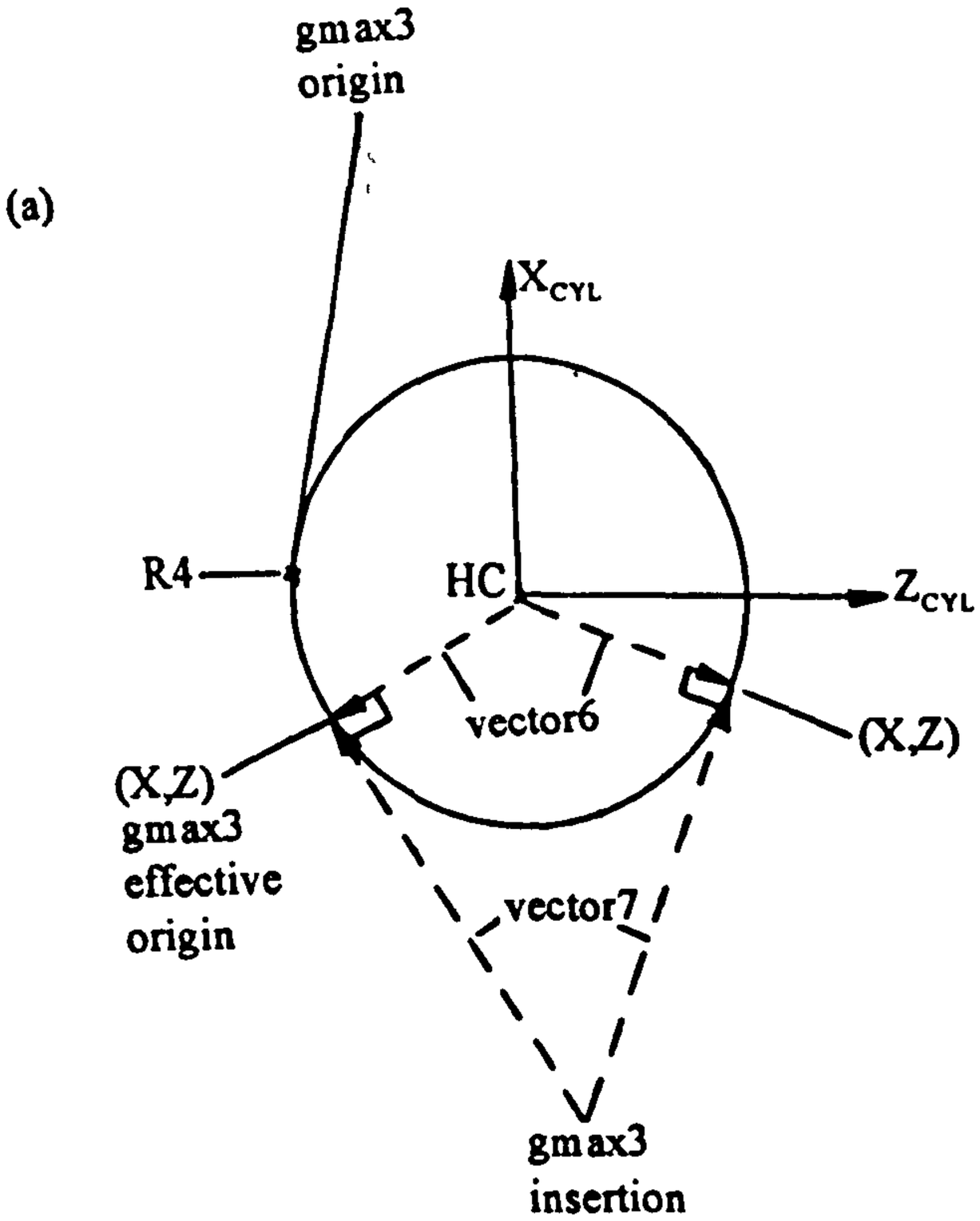

Figure C4 Diagrams used in the calculation of the effective origin of gmax3. See text in section C.2 steps (f) and (g) for explanation.

$$C = D^2 - 2DX_{HC\,.\,CYL} + (Z_{HC\,.\,CYL})^2 + (X_{HC\,.\,CYL})^2 - RCYL^2$$

In this case $X_{HC\text{-}CYL} = Z_{HC\text{-}CYL} = 0$. The general solution to the quadratic equation is then

$$Z = [\, -B \pm (B^2 - 4AC)^{1/2} \,] / 2A$$

If $(B^2 - 4AC) > 0$ - The line of action of gmax3 intersected the circle. Wrapping occurred. The calculation was continued from step (f).

If $(B^2 - 4AC) < 0$ - There was no intersection. Step (e) was required to distinguish between situations (1) and (3) and thereby check for wrapping.

(e) In order to distinguish between situations (1) and (3) vectors 3 and 4 were set up as illustrated in figure C3b.

$$\text{vector3} = -(X,Z)_{GMAX3\ OR\,-\,CYL}$$
$$\text{vector4} = (X,Z)_{GMAX3\ IN\,-\,CYL} - (X,Z)_{GMAX3\ OR\,-\,CYL}$$

$$\text{vector5} = \text{vector3} \times \text{vector4}$$

Examination of the component of vector5 in the direction of Y_{CYL} (vector5[Y_{CYL}]) revealed whether or not wrapping occurred.

If vector5[Y_{CYL}] >0 - Situation (3) occurred. There was wrapping and the calculation continued with step (f).

If vector5[Y_{CYL}] <0 - Situation (1) occurred. There was no wrapping and the calculation was terminated.

(f) Having established that wrapping was occurring the next step was to determine the coordinates of the effective origin for gmax3 in the XZ cylinder plane, $(X,Z)_{GMAX3\ EFFO\,-\,CYL}$. This point was that at which a straight line passing through the insertion of gmax3 made a tangent with the circle. Two points, both labelled as (X,Z) in figure C4a satisfy these criteria. The coordinates of these were calculated as follows and then the correct one selected.

The equation of the circle is as follows

$$(X - X_{HC\,.\,CYL})^2 + (Z - Z_{HC\,.\,CYL})^2 = RCYL^2 \qquad (C5)$$

where RCYL is the radius of the cylinder and hence the radius of the circle. $(X,Z)_{HC\,.\,CYL}$ is the centre of the circle and (X,Z) is a point on the circle.

Vectors 6 and 7 were set up as shown in figure C4a as

$$\text{vector6} = (X,Z) - (X,Z)_{HC\,.\,CYL}$$
$$\text{vector7} = (X,Z) - (X,Z)_{GMAX3\ IN\,-\,CYL}$$

These vectors are perpendicular to each other and hence their dot product is zero

$$(\text{vector6}).(\text{vector7}) = 0 \qquad (C6)$$

$X_{HC\text{-}CYL} = Z_{HC\text{-}CYL} = 0$. Solving equations C5 and C6 simultaneously produced a quadratic equation with two solutions for (X,Z). The correct point had to be selected. Vector8 was set up using one of the solutions for (X,Z) as

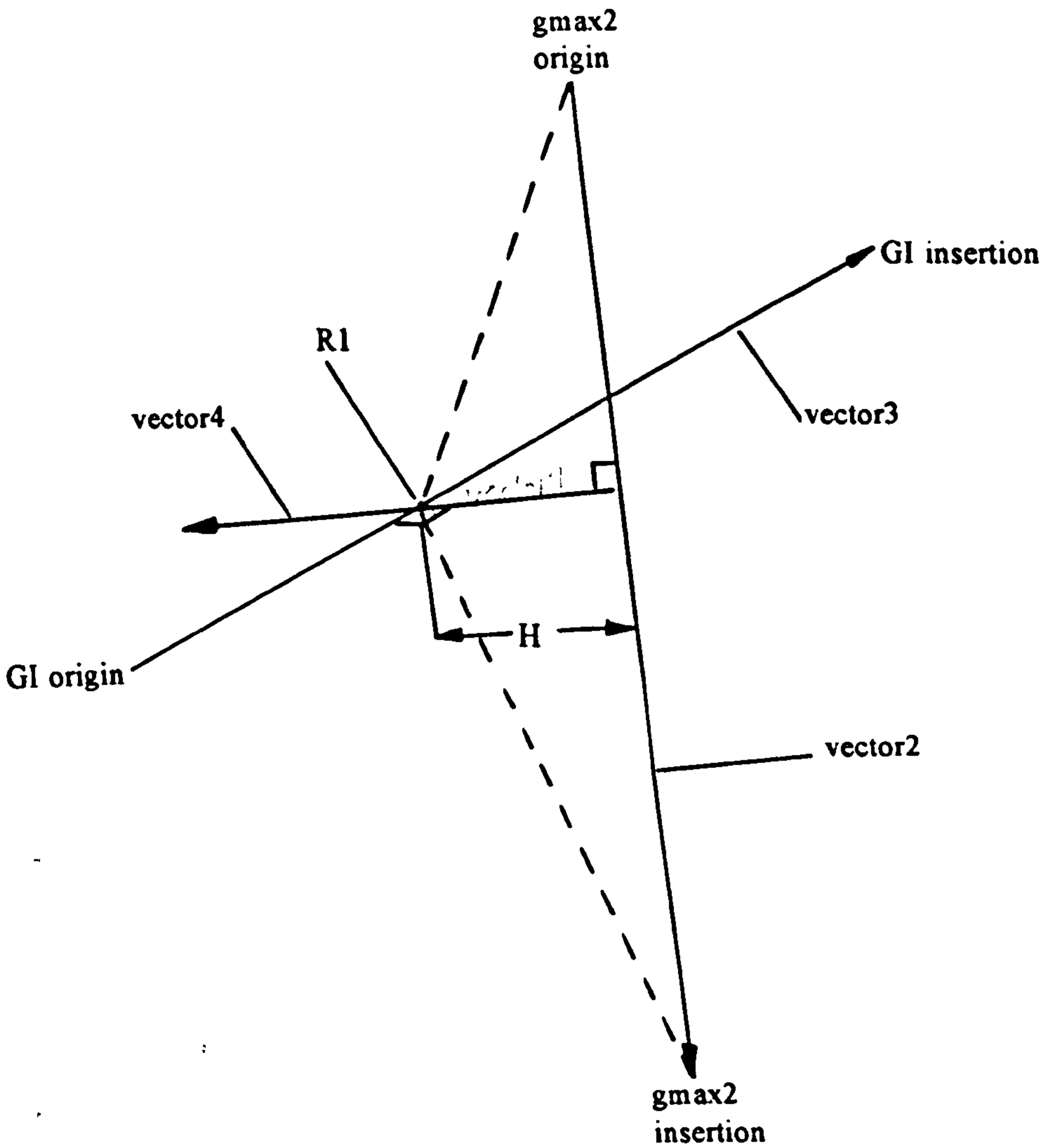

Figure C5 An illustration of the approach taken in making adjustments for the wrapping of the middle element of gluteus maximus, gmax2 around gemellus inferior, GI. Point R1 is calculated and set up as the effective origin.

$$\text{vector8} = (X,Z)_{\text{GMAX3 IN - CYL}} - (X,Z)_{\text{HC - CYL}}$$

Then vector9 = (vector6) x (vector8)

Examination of the component of vector9 in the direction of Y_{CYL} (vector9[Y_{CYL}]) revealed whether or not the correct solution for (X,Z) had been selected.

If vector9[Y_{CYL}] > 0 - The correct solution was chosen giving $(X,Z)_{\text{GMAX3 EFFO - CYL}}$
If vector9[Y_{CYL}] < 0 - The solution chosen was incorrect. The other solution for (X,Z) was set up as $(X,Z)_{\text{GMAX3 EFFO - CYL}}$

(g) Having obtained $(X,Z)_{\text{GMAX3 EFFO - CYL}}$ the next stage was to calculate $(Y)_{\text{GMAX3 EFFO - CYL}}$ In order to do this it was necessary to calculate the coordinates of point R4 shown in figure C4b. This is the point at which a straight line passing through the origin of gmax3 makes a tangent with the circle. The approach taken to calculate the coordinates of this point was similar to that adopted in the calculation of $(X,Z)_{\text{GMAX3 EFFO - CYL}}$. The wrapping angle ($\theta$) and wrapped length (G) as shown in figure C4b could then be calculated. Lengths H and I were also calculated. Assuming progression of the muscle to be constant in the direction of Y_{CYL}, $Y_{\text{GMAX3 EFFO - CYL}}$ could be determined as follows:

$$Y_{\text{GMAX3 EFFO - CYL}} = (Y)_{\text{GMAX3 OR - CYL}} + [\,((G+H)/(G+H+I))*(Y_{\text{GMAX3 IN - CYL}} - Y_{\text{GMAX3 OR - CYL}})]$$

Having obtained $(X,Y,Z)_{\text{GMAX3 EFFO - CYL}}$ the final stage was to calculate the coordinates of this point with respect to the pelvic coordinate system.

C.3 THE MIDDLE ELEMENT OF GLUTEUS MAXIMUS (GMAX2)

Steps in the calculation procedure for this muscle element were as follows:

(a) The femoral insertion of gmax2 was calculated with respect to the pelvic coordinate system as $(X,Y,Z)_{\text{GMAX2 IN - P}}$. The origin of gmax2 was already given with respect to the pelvic coordinate system as $(X,Y,Z)_{\text{GMAX2 OR - P}}$.

(b) From calculations described in section C.1 it was determined whether of not gemellus inferior (GI) wrapped around the back of the hip joint. If it did not then the calculation was continued as follows. If it did then alterations to the calculation were required as detailed in (note 1) at the end of this section.

If no wrapping of GI had occurred, gmax2 was assumed to wrap over GI somewhere along the length of GI between the origin and insertion of GI. The femoral insertion of GI was calculated with respect to the pelvic coordinate system as $(X,Y,Z)_{\text{GI IN - P.}}$ The origin of GI was already given with respect to the pelvic coordinate system as $(X,Y,Z)_{\text{GI OR - P.}}$

(d) Point R1 in figure C5 was then calculated. The location of R1 with respect to the pelvic coordinate system could be obtained by the following two equations:

$$(X,Y,Z)_{\text{R1 - P}} = (X,Y,Z)_{\text{GMAX2 OR - P}} + \lambda_1\,(\text{vector2}) + H(\text{vector5}) \qquad (C7)$$
$$(X,Y,Z)_{\text{R1 - P}} = (X,Y,Z)_{\text{GI OR - P}} + \lambda_2\,(\text{vector3}) \qquad (C8)$$

Where vector2 = $(X,Y,Z)_{\text{GMAX2 - IN P}} - (X,Y,Z)_{\text{GMAX2 OR - P}}$
vector3 = $(X,Y,Z)_{\text{GI- IN P}} - (X,Y,Z)_{\text{GI OR - P}}$
vector4 = vector2 x vector3
vector5 = A unit vector relative to the pelvic coordinate system in the direction of vector4.

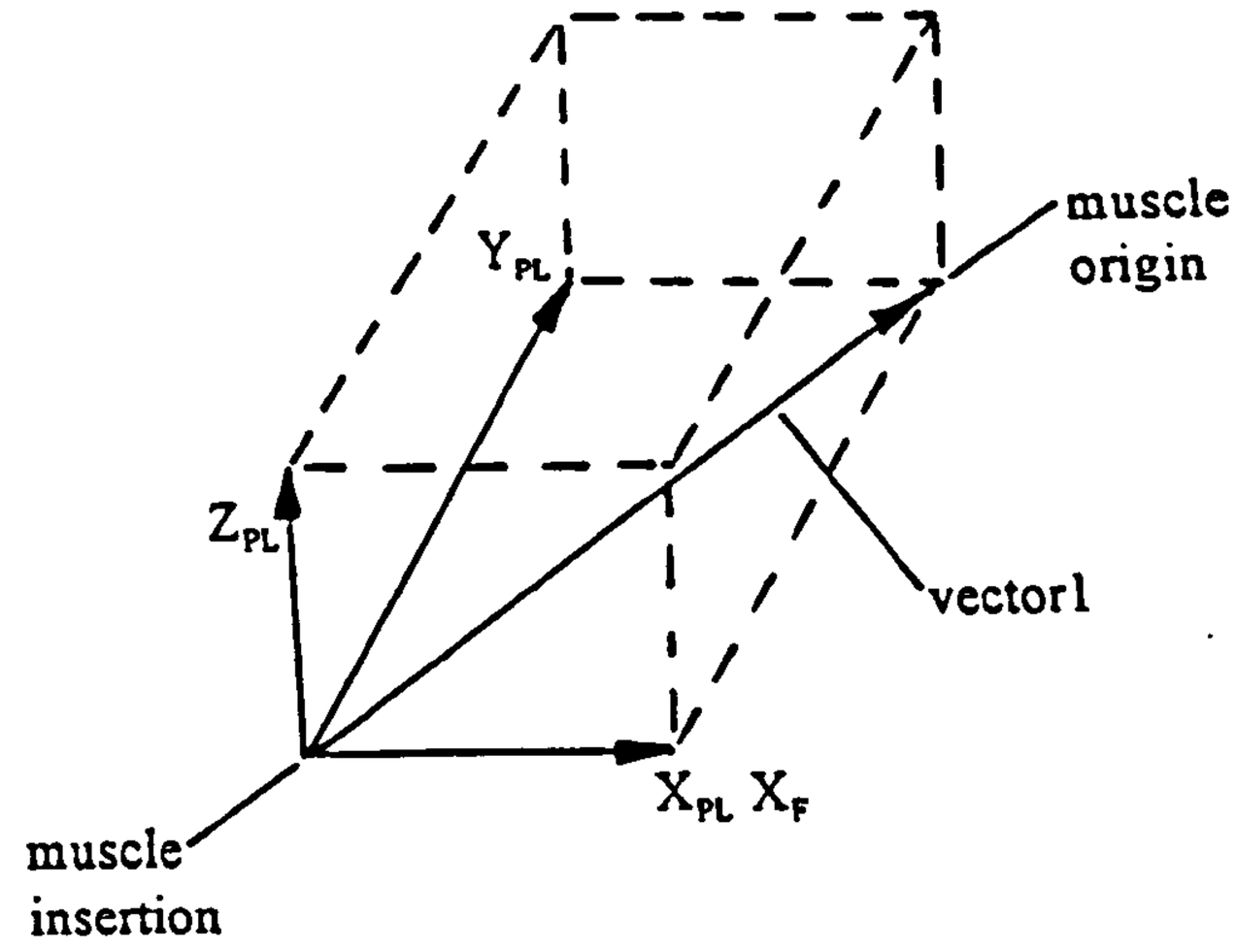

Figure C6 An illustration of the approach taken to set up the muscle plane coordinate system for iliacus and psoas.

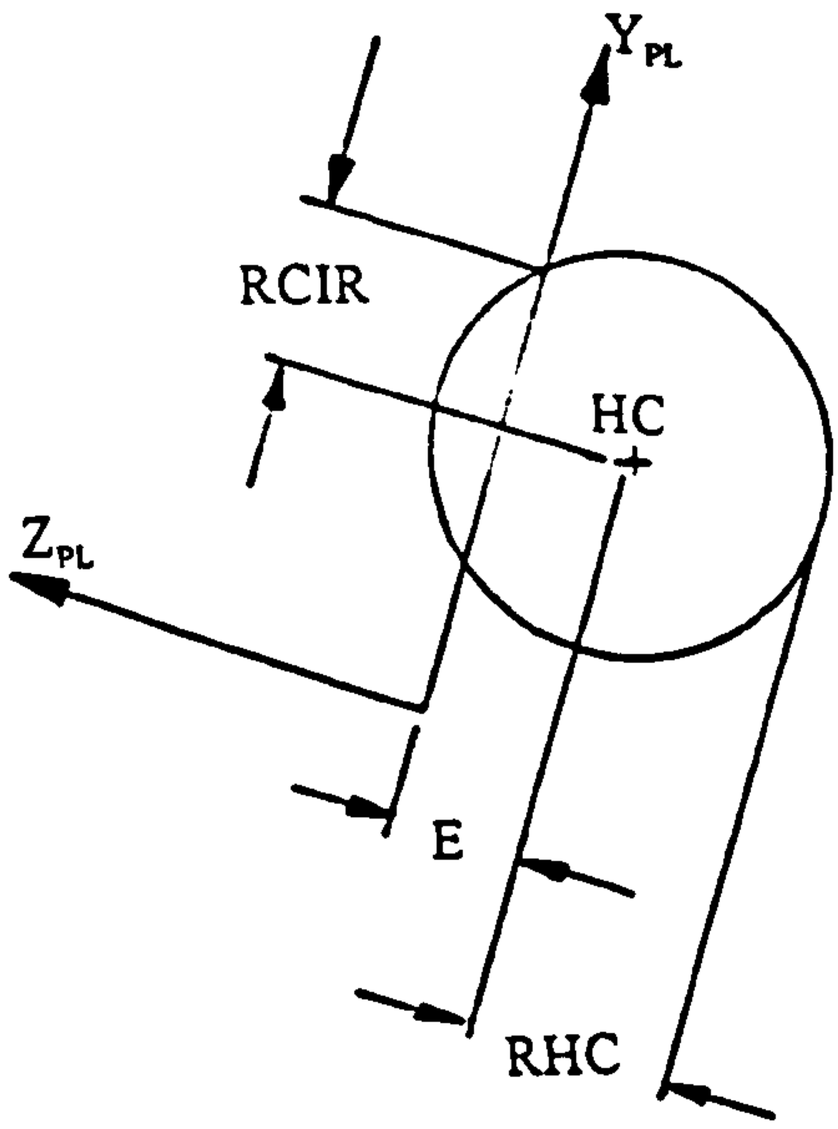

Figure C7 Diagram used in determining whether or not the muscle plane cuts the sphere. See text in section C.4 step (c) for explanation.

Solving equations C7 and C8 simultaneously allows calculation of λ_1 and λ_2 and also distance H.

Then vector1 = H(vector5)

Examination of the component of vector1 in the direction of X_p (vector1[X_p]) revealed whether or not interaction between gmax2 and GI had occurred or not.

If (vector1[X_p])>0 - No interaction occurred. The line of action of gmax2 lay posterior to that of GI. The procedure was terminated.

If (vector1[X_p])<0 - Interaction occurred. $(X,Y,Z)_{R1\,.\,P}$ was calculated from equation C7. This point was set up as the effective origin of gmax2.

Adjustments were made to the calculation procedure to allow for muscle thickness to ensure that the distance between the lines of action of the two muscles was at least half the thickness of GI plus half the thickness of gmax2 in the area of wrapping. A total thickness of 10mm was assumed as determined from cadaveric measurement.

(note 1)

If GI wrapped around the back of the hip joint then GI was considered as two straight lines. One was between the original origin of GI and the wrapped point and the other between the wrapped point and the original insertion of GI. The interaction point between gmax2 and GI could be on either of the lines. The correct situation was determined as follows. The origin of GI ($(X,Y,Z)_{GI\,OR\,.\,P}$) was replaced by the wrapping point of GI as ($(X,Y,Z)_{GI\,WP\,.\,P}$) in the above analysis and λ_2 was calculated.

If λ_2>0 - Interaction occurred on the line between the wrapped point of GI and the original insertion of GI. The analysis was continued.

If λ_2<0 - Interaction was on the line between the original origin of GI and the wrapping point. Hence ($(X,Y,Z)_{GI\,IN\,.\,P}$) was replaced with (($(X,Y,Z)_{GI\,WP\,.\,P}$) and the original analysis procedure was repeated.

C.4 ILIACUS AND PSOAS

Constants used in the wrapping calculations for iliacus and psoas were the radius of the hip sphere (RHC) and the angle of opening of the acetabulum. Values for these have already been given in section C.1.

Steps in the calculation procedure for these muscles were as follows:

(a) The origin of the muscle was calculated with respect to the femoral coordinate system giving $(X,Y,Z)_{MUS\,OR\,.\,F}$. The hip joint centre was also calculated with respect to the femoral coordinate system giving $(X,Y,Z)_{HC\,.\,F}$. The muscle insertion was already given with respect to the femoral coordinate system as $(X,Y,X)_{MUS\,IN\text{-}\,F}$.

(b) The muscle plane coordinate system was set up using vector1 as shown in figure C6 and given by

$$\text{vector1} = (X,Y,X)_{MUS\,OR\,.\,F} - (X,Y,X)_{MUS\,IN\,.\,F}$$

The muscle plane coordinate system was then set up with an origin at the muscle insertion as shown in figure C6 as

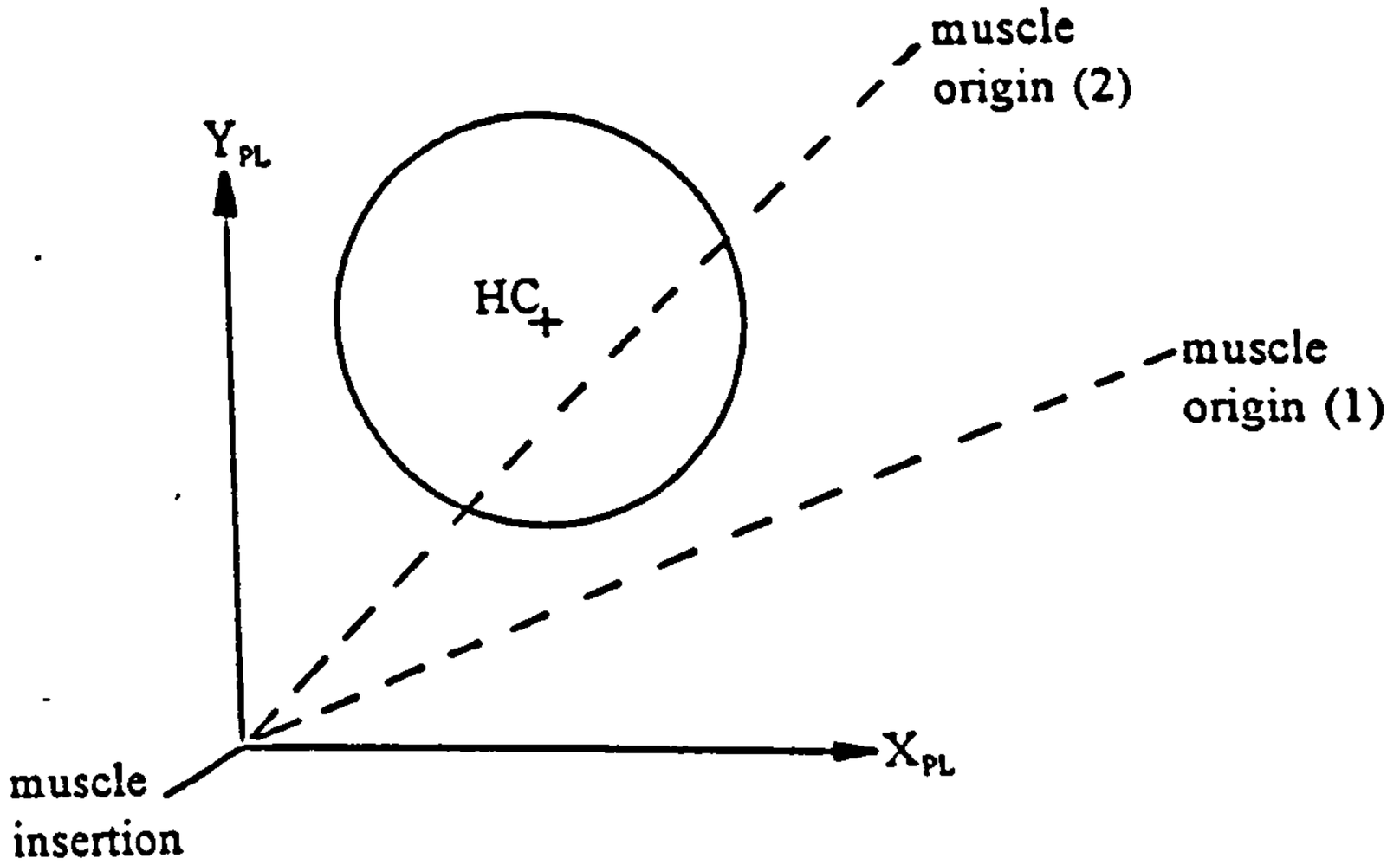

Figure C8 Diagram used in checking for wrapping on the muscle plane. See text in section C.4 step (d) for explanation.

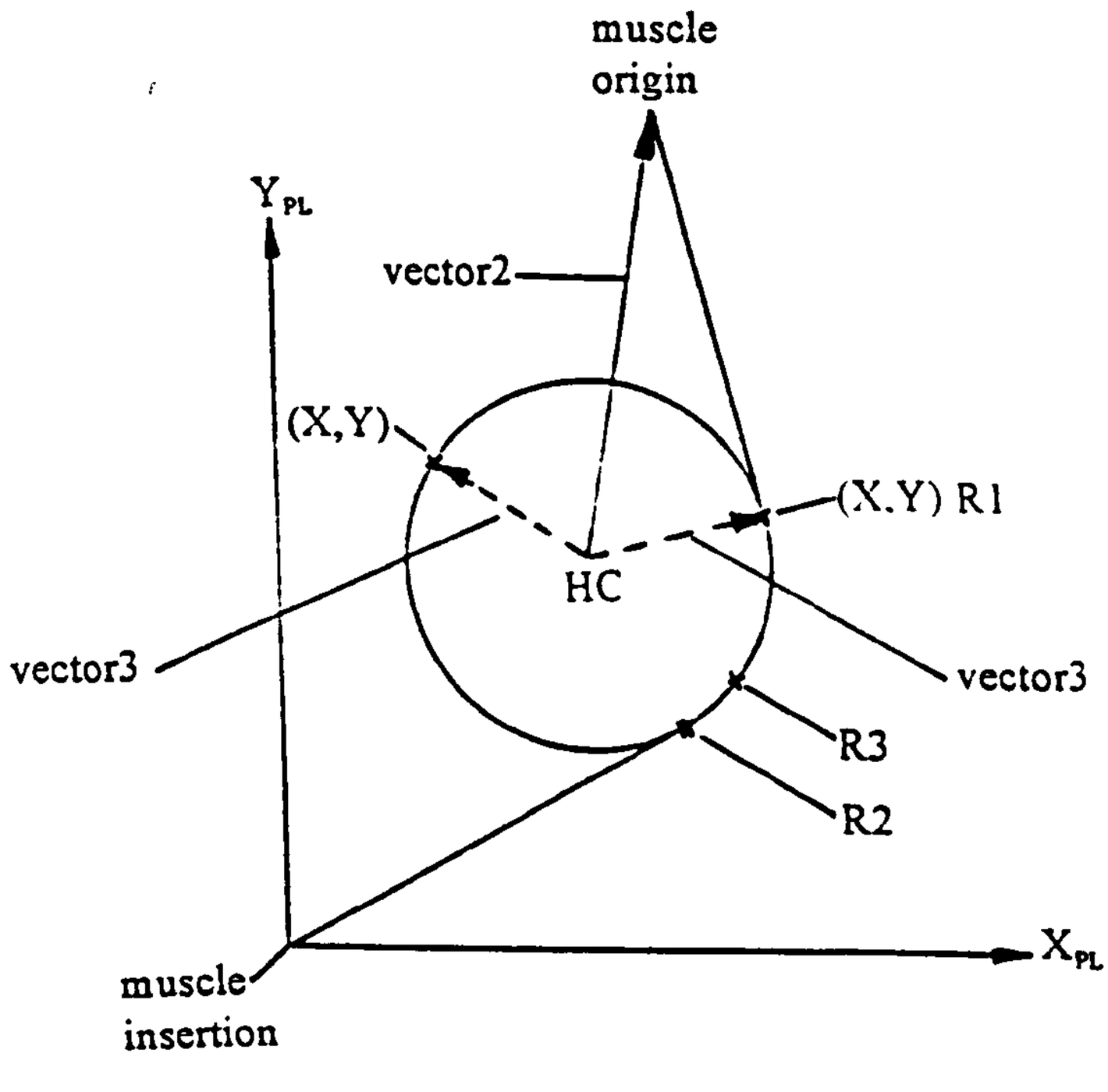

Figure C9 Diagram used in the calculation of wrapping points R1 and R2. See text in section C.4 step (e) for explanation.

X_{PL} : Parallel to X_F

Z_{PL} : Perpendicular to the muscle plane which contains X_{PL} and the muscle origin and insertion. i.e X_{PL} x vector 1

Y_{PL}: This lies in the muscle plane and is perpendicular to X_{PL} and Z_{PL}.

with unit vectors I_{PL}, J_{PL} and K_{PL} relative to the femoral coordinate system. These were used to set up the direction cosine matrix $[B_{PL-F}]$ relating the muscle plane and femoral coordinate systems.

(c) The coordinates of the hip joint centre were calculated with respect to the muscle plane coordinate system as $(X,Y,Z)_{HC\,-\,PL}$. A check for the plane cutting the hip sphere was then performed as follows by considering the magnitude of $Z_{HC\,-\,PL}$ as illustrated in figure C7. This was compared with the radius of the hip sphere, RHC.

$$E = |Z_{HC\,-\,PL}|$$

If E > RHC - The plane did not cut the sphere. The calculation was terminated.

If E < RHC - The plane cut the sphere. The radius of the circle formed by the intersection of the sphere and the plane was calculated as

$$RCIR = [\,(RHC)^2 - E^2\,]^{1/2}$$

and the wrapping calculations were continued.

(d) Further checks for wrapping were required on the muscle plane. Prior to these it was necessary to check that the muscle origin and insertion were outside the circle formed by the intersection of the plane with the sphere. After calculation of the coordinates of the muscle origin with respect to the muscle plane coordinate system giving $(X,Y)_{MUS\ OR\ -\ PL}$ the check was performed for the origin as follows:

$$B = [\,(X_{MUS\ OR\ PL} - X_{HC\,-\,PL})^2 + (Y_{MUS\ OR\ PL} - Y_{HC\,-\,PL})^2\,]^{1/2}$$

If B < RCIR - The muscle origin was inside the circle. The calculation was terminated and an error message produced.

If B > RCIR - The muscle origin was outside the circle and the wrapping calculation was continued.

A similar calculation was performed for the insertion. If both origin and insertion were outside the circle, wrapping around this circle on the muscle plane was checked for. Two situations could occur as illustrated in figure C8.

(1) - This would occur with increasing hip flexion. There was no intersection between the line of action of the muscle and the circle and no wrapping.

(2) This would occur with increasing hip extension. There was intersection between the line of action of the muscle and the circle and wrapping occurred.

The correct situation was determined by performing a check similar to that used in step (d) in section C.2 when assessing the wrapping situation for gmax3. If wrapping occurred then the calculation continued with step (e).

(e) The next step was to calculate the muscle plane coordinates of point R1 shown in figure

C9. This was the point at which a straight line passing through the muscle origin made a tangent with the circle. Two points, both shown as (X,Y) in figure C9 satisfied these criteria. Both of these were calculated using a procedure similar to that used in step (f) in section C.2 in the wrapping of gmax3. In order to chose the correct one, vector2 was set up as shown in figure C9 as

$$\text{vector2} = (X,Y)_{\text{MUS OR - PL}} - (X,Y)_{\text{HC - PL}}$$

Vector3 was set up using one of the solutions as

$$\text{vector3} = (X,Y)_{\text{R1 - PL}} - (X,Y)_{\text{HC - PL}}$$

Then vector4 = (vector3) x (vector2)

Examination of the component of vector4 in the direction of Z_{PL} (vector4[Z_{PL}]) revealed whether or not the correct solution for (X,Y) had been selected.

If vector4[Z_{PL}] > 0 - The correct solution was chosen giving $(X,Y)_{R1 - PL}$
If vector4[Z_{PL}] < 0 - The solution chosen was incorrect. The other solution for (X,Y) was set up as $(X,Y)_{R1 - PL}$.

Point R2, that at which a line straight line passing through the muscle insertion made a tangent to the circle was set up using a similar approach to that for R1.

$Z_{R1 - PL} = Z_{R2 - PL} = 0$. Hence calculation of $(X,Y,Z)_{R1 - PL}$ and $(X,Y,Z)_{R2 - PL}$ was complete.

(f) The final step was to determine which point to use as the wrapping point, R1 or R2. If all wrapping occurred on the femoral region of the sphere then an effective insertion was set up but if all of the wrapping was on the acetabular side then an effective origin was required. If some wrapping was on the femoral side and some on the acetabular side then an alternative approach was taken. The correct situation was established as follows:

ACVEC was set up as a unit vector relative to the pelvic coordinate system perpendicular to the plane of opening of the acetabulum, pointing away from the pelvis. Point R1 was calculated with respect to the pelvic coordinate system giving $(X,Y,Z)_{R1 - P}$. Then

$$C = (\text{ACVEC}).(X,Y,Z)_{R1 - P}$$

If C > 0 - The angle between ACVEC and a vector running between HC and R1 was less than 90^0. Hence R1 was on the femoral head. If this was the case, R2 would also be on the femoral head. Point R1 was calculated with respect to the femoral coordinate system and set up as the effective insertion of the muscle.

If C < 0 - The calculation continued. Point R2 was calculated with respect to the pelvic coordinate system giving $(X,Y,Z)_{R2 - P}$. Then the calculation continued as follows

$$D = (\text{ACVEC}).(X,Y,Z)_{R2 - P}$$

If D < 0 - The angle between ACVEC and a vector running between the HC and R2 was greater than 90° and hence R2 was on the acetabulum. R1 was also on the acetabulum. $(X,Y,Z)_{R2 - P}$ was therefore set up as the effective origin.

If $C < 0$ and $D > 0$ then R1 was on the acetabular side and R2 on the femoral side. The equation of the line of intersection between the muscle plane and the plane of opening of the acetabulum was determined. The intersection points of this line with the circle formed by the intersection of the muscle plane with the sphere were calculated. That lying between R1 and R2 was chosen to give wrapping on the correct side of the hip sphere and determined as point R3 in figure C9. The corrected line of action of the muscle was then set up as a tangent to point R3.

APPENDIX D

This appendix presents the questionnaires completed for each subject prior to testing. That for the post-operative hip replacement patients is presented first, followed by that for the normal subjects.

D.1 PATIENT QUESTIONNAIRE

Name .....

1 Apart from your hip replacement, do you have any history of lower limb, upper limb or back injury/problem/disability? If so, please give details.

2 How are you at the moment? Are you experiencing any pain at any time? If so, please give details.

3 Are you able to take regular exercise - i.e. walk to the shops etc? If so, what do you do and approximately how often?

4 Do you use any walking aids? If so, what do you use? Do you use them all of the time or only at certain times eg when outside the house? Please give details.

5 a)Can you comfortably stand up from and sit down onto a chair that does not have arms - eg a dining room/kitchen chair?

b)Do you normally use your hands when standing up from a chair that does not have arms - eg a dining room/kitchen chair? If so, where do you place them?

c)Do you normally use your hands when sitting down onto a chair that does not have arms - eg a dining room/kitchen chair? If so, where do you place them?

6 a)Approximately how often do you use stairs - in your house if it has them, in other buildings, and outside?

b)Do you have stairs in your house? If so, on which side of the stairs is there a handrail/bannister - left or right as seen on diagram? Do the stairs have any spirals/unusual features?

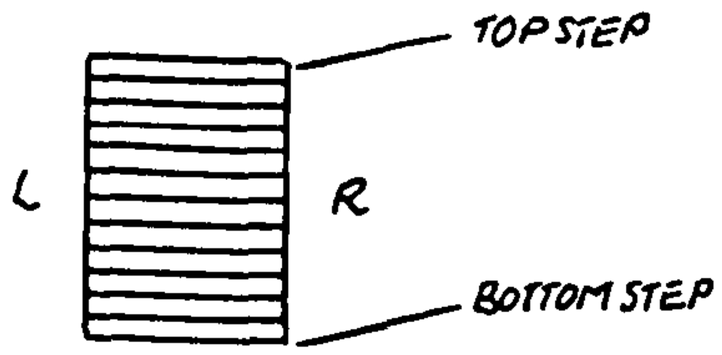

7 a)Do you ascend stairs cyclically (i.e. with only one foot on one step at any one time) or do you take one step at a time (i.e place one foot on a step and then bring the other foot up beside it onto the same step)

b)When ascending straight stairs (i.e. those without spirals) do you normally start ascent with a specific leg? If so, which one? Would it be comfortable to start with the other leg?

c)When ascending straight stairs do you normally hold the handrail/bannister?

8 a)Do you descend stairs cyclically (i.e. with only one foot on one step at any one time) or do you take one step at a time (i.e place one foot on a step and then bring the other foot down beside it onto the same step)

b)When descending straight stairs (i.e. those without spirals) do you normally start descent with a specific leg? If so, which one? Would it be comfortable to start with the other leg?

c)When descending straight stairs do you normally hold the handrail/bannister?

9 Approximately how often do you use a car as a passenger and as a driver?

10 a)How do you get into the passenger side of a car? Please state where you put each hand and each leg as you enter the car and the sequence of these hand and leg movements.

b) How do you get out of the passenger side of a car? Please state where you put each hand and each leg as you get out of the car and the sequence of these hand and leg movements.

11 Can you get into and out of a bath comfortably and without difficulty?

If the answer to question 11 is yes then please answer the following

12 Do you have a bath in your house?

13 Approximately how often do you use a bath?

14 Does the bath that you normally use have any aids? i.e. handles, a stool etc? If so what does it have?

15 a)From which side do you normally get into and out of the bath - left or right as seen on the diagram?

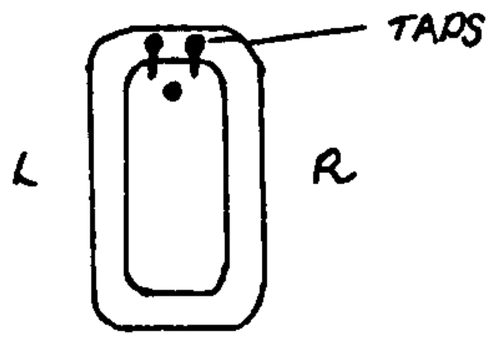

b)Do you normally face the taps or have your back to the taps when sitting in the bath?

16 a)How do you normally get into the bath? Please state where you put each hand and each leg as you enter the bath and the sequence of these hand and leg movements.

b)How do you normally get out of the bath? Please state where you put each hand and each leg as you get out of the bath and the sequence of these hand and leg movements.

D.2 NORMAL SUBJECT QUESTIONNAIRE

Name .....

1 How is your general fitness? Do you take regular exercise, walk to the shops etc? If so approximately how often?

2 a) Do you normally use your hands when standing up from a chair that does not have arms - eg a dining room/kitchen chair? If so, where do you place them?

b) Do you normally use your hands when sitting down onto a chair that does not have arms - eg a dining room/kitchen chair? If so, where do you place them?

3 a) Do you have stairs in your house? If so, on which side of the stairs is there a handrail/bannister - left or right as seen on diagram? Do the stairs have any spirals/unusual features?

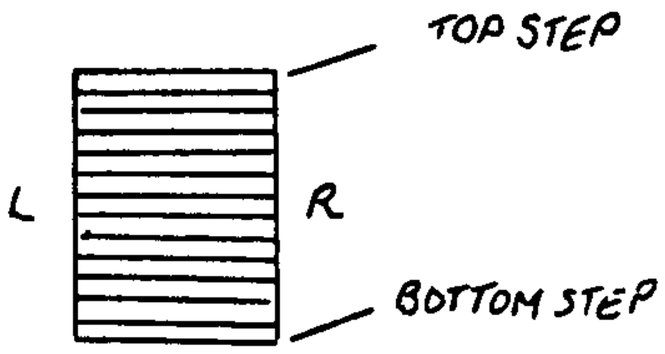

b) Approximately how often do you use stairs - in your house if it has them, in other buildings, and outside?

4 a) When ascending straight stairs (i.e. those without spirals) do you normally start ascent with a specific leg? If so, which one? Would it be comfortable to start with the other leg?

b) When ascending straight stairs do you normally hold the handrail/bannister?

5 a)When descending straight stairs (i.e. those without spirals) do you normally start descent with a specific leg? If so, which one? Would it be comfortable to start with the other leg?

b)When descending straight stairs do you normally hold the handrail/bannister?

6 Approximately how often do you use a car as a passenger and as a driver?

7 a)How do you normally get into the passenger side of a car? Please state where you put each hand and each leg as you enter the car and the sequence of these hand and leg movements.

b) How do you normally get out of the passenger side of a car? Please state where you put each hand and each leg as you get out of the car and the sequence of these hand and leg movements.

8 Do you have a bath in your house?

9 Approximately how often do you use a bath?

10 Can you get into and out of a bath comfortably and without difficulty?

If the answer to question 10 is yes then please answer questions 11 - 13.

11 Does the bath that you normally use have any aids? i.e. handles, a stool etc? If so what does it have?

12 a) From which side do you normally get into and out of the bath - left or right as seen on the diagram?

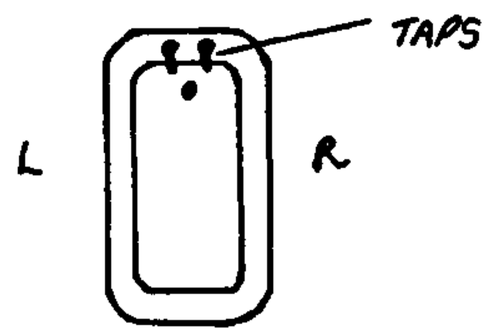

b) Do you normally face the taps or have your back to the taps when sitting in the bath?

13 a) How do you normally get into the bath? Please state where you put each hand and each leg as you enter the bath and the sequence of these hand and leg movements.

b) How do you normally get out of the bath? Please state where you put each hand and each leg as you get out of the bath and the sequence of these hand and leg movements.

APPENDIX E

This appendix describes which activities each subject performed. Details for the normal subjects (group 1), the prosthetic hips of the patients (group 2) and the non prosthetic hips of the patients (group 3) are presented.

Subject hip	Gait speed / m/s	turn	asc	des	rise
DR	✓ 1.58	✓	✓	✓	✓
DL	✓ 1.58	✓	✓	✓	✓
ER	✓ 1.22	✓	✓	✓	✓
EL	✓ 1.22	✓	✓	✓	✓
FR	✓ 1.29	✓	✓	✓	✓
FL	✓ 1.29	✓	✓	✓	✓
GR	✓ 1.14	✓	✓	✓	✓
GL	✓ 1.14	✓	✓	✓	✓
HR	✓ 1.52	✓	✓	✓	✓
HL	✓ 1.52	✓	✓	✓	✓
IR	✓ 1.27	✓	✓	✓	✓
IL		✓	✓	✓	✓
JR		✓	✓	✓	✓
JL		✓	✓	✓	✓
LR	✓ 1.23	✓	✓	✓	✓
LL	✓ 1.23	✓	✓	✓	✓
MR	✓ 1.37	✓	✓	✓	✓
ML	✓ 1.37	✓	✓	✓	✓
RR		✓	✓	✓	✓
RL		✓	✓	✓	✓
Total number of hips tested	15	18	20	20	20

Table E1 Activity details of group 1 - hips of normal subjects. A ✓ indicates that the activity was tested. R and L following the subject letter denote right and left hips. For a description of each activity code see section 7.1

Subject hip	con	cox	cin	cix	box	box	bin	bix
DR			✓				✓	✓
DL	✓	✓			✓	✓		
ER			✓	✓				✓
EL	✓	✓			✓	✓		
FR				✓	✓	✓		
FL	✓	✓					✓	✓
GR			✓	✓			✓	✓
GL	✓	✓			✓	✓		
HR			✓	✓			✓	✓
HL	✓	✓			✓	✓		
IR			✓	✓			✓	✓
IL		✓			✓	✓		
JR			✓	✓	✓	✓		
JL	✓	✓						✓
LR			✓	✓			✓	✓
LL	✓	✓			✓	✓		
MR				✓			✓	✓
ML	✓	✓			✓	✓		
RR			✓				✓	✓
RL	✓	✓			✓	✓		
Total number of hips tested	9	10	8	8	10	10	8	10

Table E1 continued.

Activity details of group 1 - hips of normal subjects. A ✓ indicates that the activity was tested. R and L following the subject letter denote right and left hips. For a description of each activity code see section 7.1

Subject hip	Gait speed / m/s	turn	asc	des	rise
AR	✓ 0.77		✓	✓	✓
BL	✓ 1.00	✓	✓	✓	✓
CR	✓ 0.96	✓	✓	✓	✓
KR	✓ 0.69		✓	✓	✓
NR	✓ 1.01	✓	✓		✓
NL	✓ 1.01	✓			✓
OR	✓ 1.09	✓	✓	✓	✓
PR	✓ 1.07	✓	✓	✓	✓
PL	✓ 1.07	✓	✓	✓	✓
QR	✓ 0.83		✓	✓	✓
SL	✓ 1.05	✓	✓	✓	✓
TR	✓ 1.01	✓	✓	✓	✓
UL	✓ 0.83	✓	✓	✓	✓
VL	✓ 0.89	✓	✓	✓	✓
WR	✓ 1.01	✓	✓	✓	✓
XR	✓ 1.30	✓	✓	✓	✓
YR	✓ 1.59	✓	✓	✓	
YL	✓ 1.59	✓	✓	✓	
ZR	✓ 1.03	✓	✓	✓	✓
Total number of hips tested	19	16	18	17	17

Table E2 Activity details of group 2 - prosthetic hips of patients. A ✓ indicates that the activity was tested. R and L following the subject letter denote right and left hips. For a description of each activity code see section 7.1

Subject hip	con	cox	cin	cix	bon	box	bin	bix
AR			✓	✓				
BL					✓			✓
CR								✓
KR								
NR								
NL		✓						
OR							✓	
PR							✓	✓
PL		✓				✓		
QR			✓		✓	✓		
SL	✓	✓						
TR							✓	
UL								
VL		✓			✓	✓		
WR					✓			
XR						✓	✓	
YR						✓		
YL	✓	✓						✓
ZR					✓	✓		
Total number of hips tested	2	5	2	1	5	6	4	4

Table E2 continued.

Activity details of group 2 - prosthetic hips of patients. A ✓ indicates that the activity was tested. R and L following the subject letter denote right and left hips. For a description of each activity code see section 7.1

Subject hip	Gait speed / m/s	turn	asc	des	rise
AL	✓ 0.77		✓	✓	✓
BR	✓ 1.00		✓		✓
CL	✓ 0.96		✓	✓	✓
KL			✓	✓	✓
OL	✓ 1.09	✓		✓	✓
QL	✓ 0.83		✓	✓	✓
SR	✓ 1.05	✓	✓	✓	✓
TL	✓ 1.01	✓	✓	✓	✓
UR	✓ 0.83	✓	✓	✓	✓
VR	✓ 0.89	✓	✓	✓	✓
WL	✓ 1.01	✓	✓	✓	✓
XL	✓ 1.30	✓	✓	✓	✓
ZL	✓ 1.03	✓	✓	✓	✓
Total number of hips tested	12	8	12	12	13

Table E3 Activity details of group 3 - non prosthetic hips of patients. A ✓ indicates that the activity was tested. R and L following the subject letter denote right and left hips. For a description of each activity code see section 7.1

Subject hip	con	cox	cin	cix	bon	box	bin	bix
AL	✓							
BR								
CL		✓				✓		
KL								
OL		✓			✓			
QL	✓						✓	✓
SR					✓	✓		
TL		✓			✓	✓		
UR								
VR							✓	✓
WL		✓					✓	
XL		✓			✓			
ZL		✓					✓	✓
Total number of hips tested	2	6	0	0	4	3	4	3

Table E3 continued.

Activity details of group 3 - non prosthetic hips of patients. A ✓ indicates that the activity was tested. R and L following the subject letter denote right and left hips. For a description of each activity code see section 7.1

APPENDIX F

This appendix presents the curves of the three orthogonal components of hip joint force, Fx, Fy, Fz and also the resultant hip joint force, Fr, all normalized to body weight for the time period of interest of each activity. These periods are described in section 5.2 . The periods are all labelled as stance phase in the curves presented in this appendix since in each period, the body weight was supported by the limb under test.

Curves are presented for all of the activities for hips of the normal subjects (group 1). The curves for three of the activities are not included for the prosthetic hips of the patients (group 2) due to the low number of patients performing these activities. The three activity tests not included are the 'inside' hip tests during car entry and exit and the 'outside' hip test during car entry.

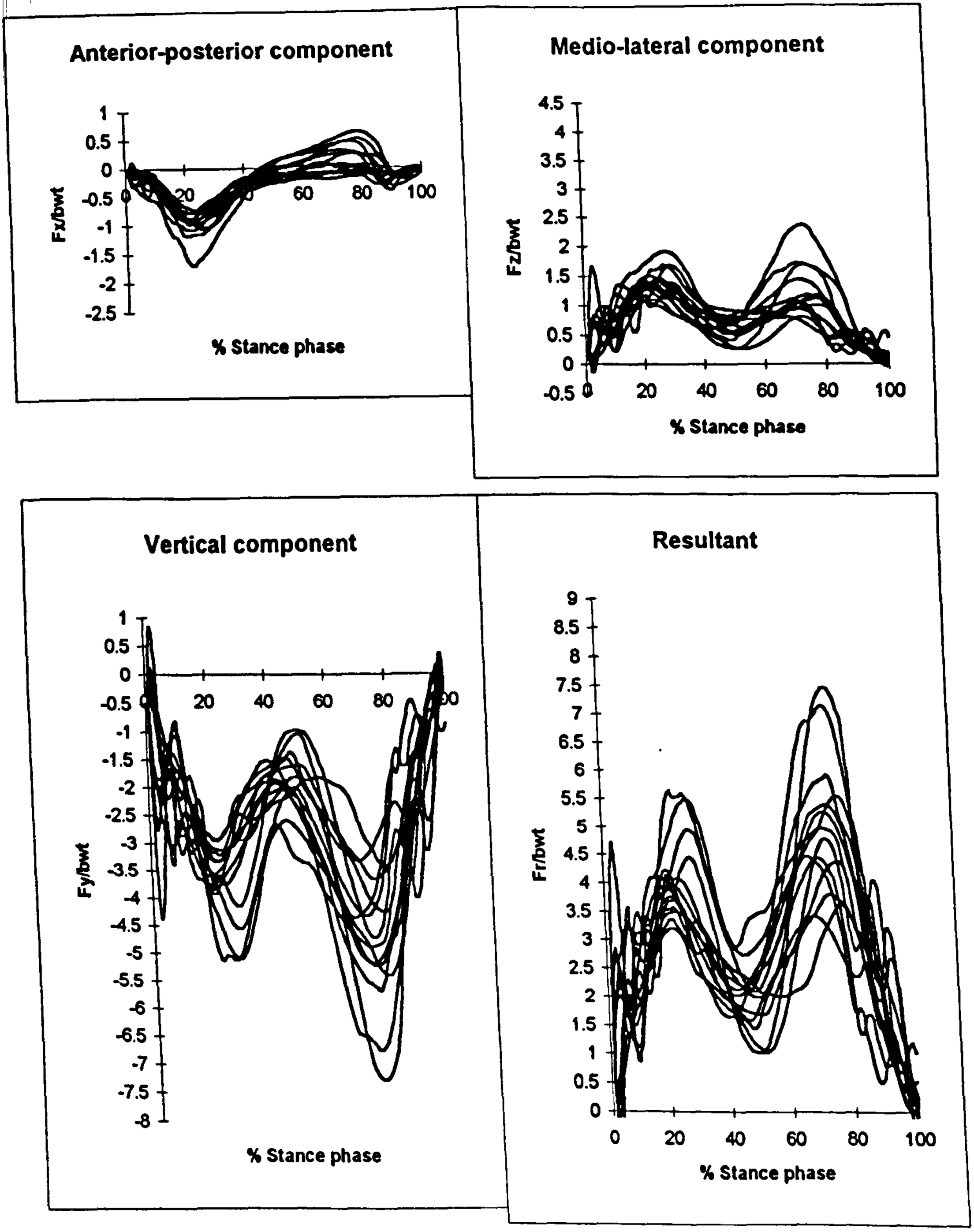

Figure F1 Group 1 - Hips of normal subjects. Components of hip joint force, Fx, Fy, Fz and resultant hip joint force, Fr, in terms of body weight during the stance phase of gait. See figure 7.2 for the sign convention used for force components.

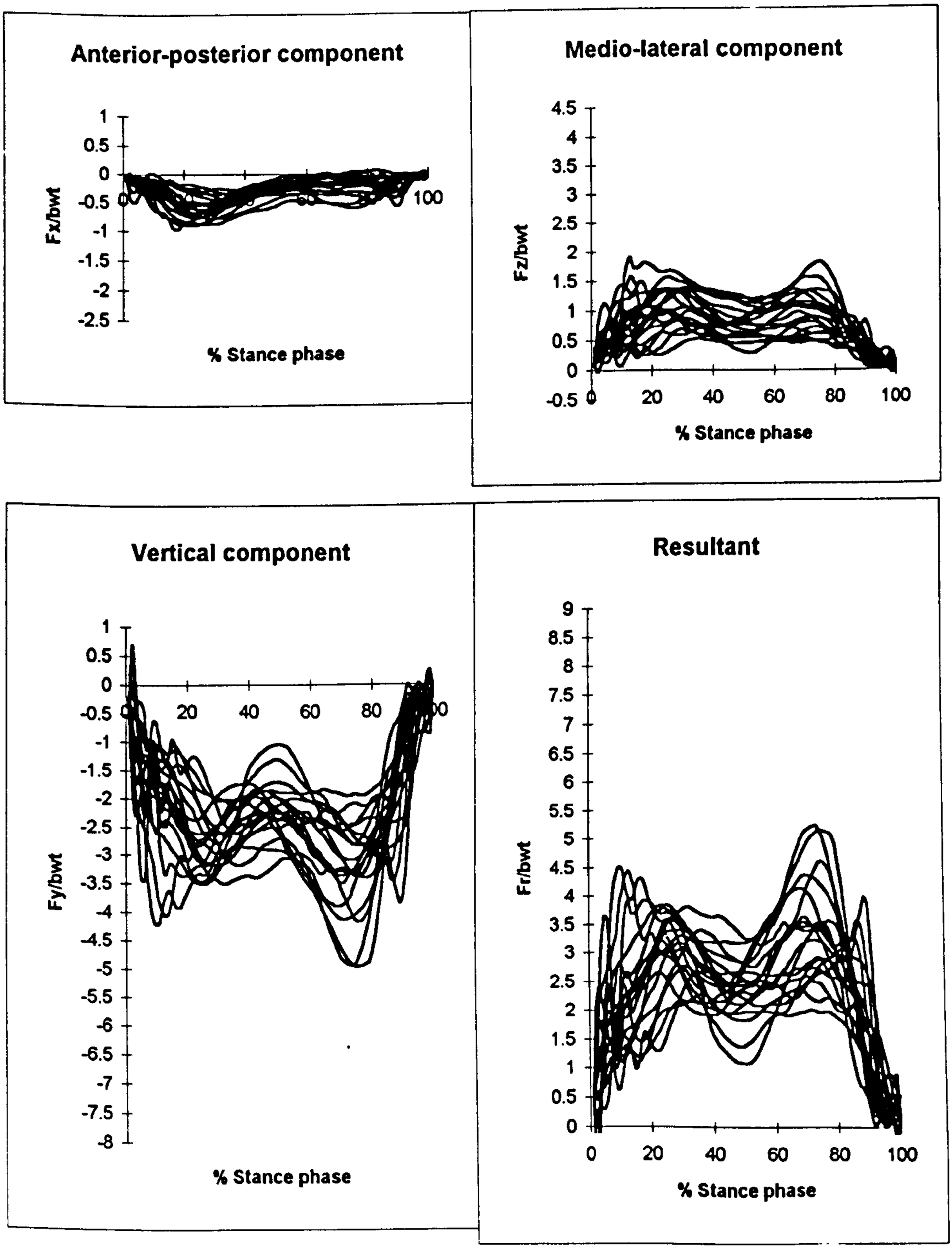

Figure F2 Group 2 - Prosthetic hips of patients. Components of hip joint force, Fx, Fy, Fz and resultant hip joint force, Fr, in terms of body weight during the stance phase of gait. See figure 7.2 for the sign convention used for force components.

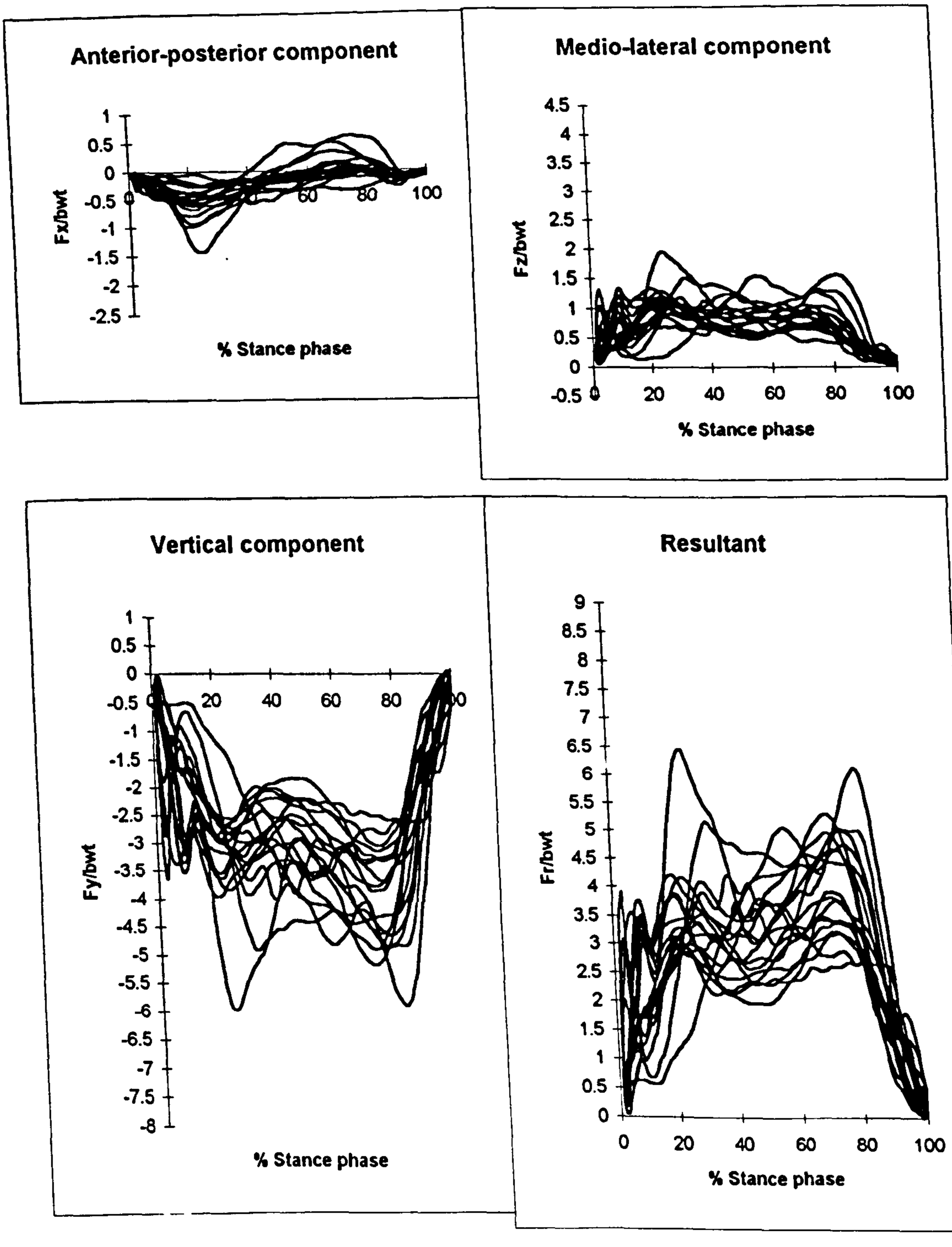

Figure F3 Group 1 - Hips of normal subjects. Components of hip joint force, Fx, Fy, Fz and resultant hip joint force, Fr, in terms of body weight determined for the walking turn activity. See section 5.2 for further description of this activity. See figure 7.2 for the sign convention used for force components.

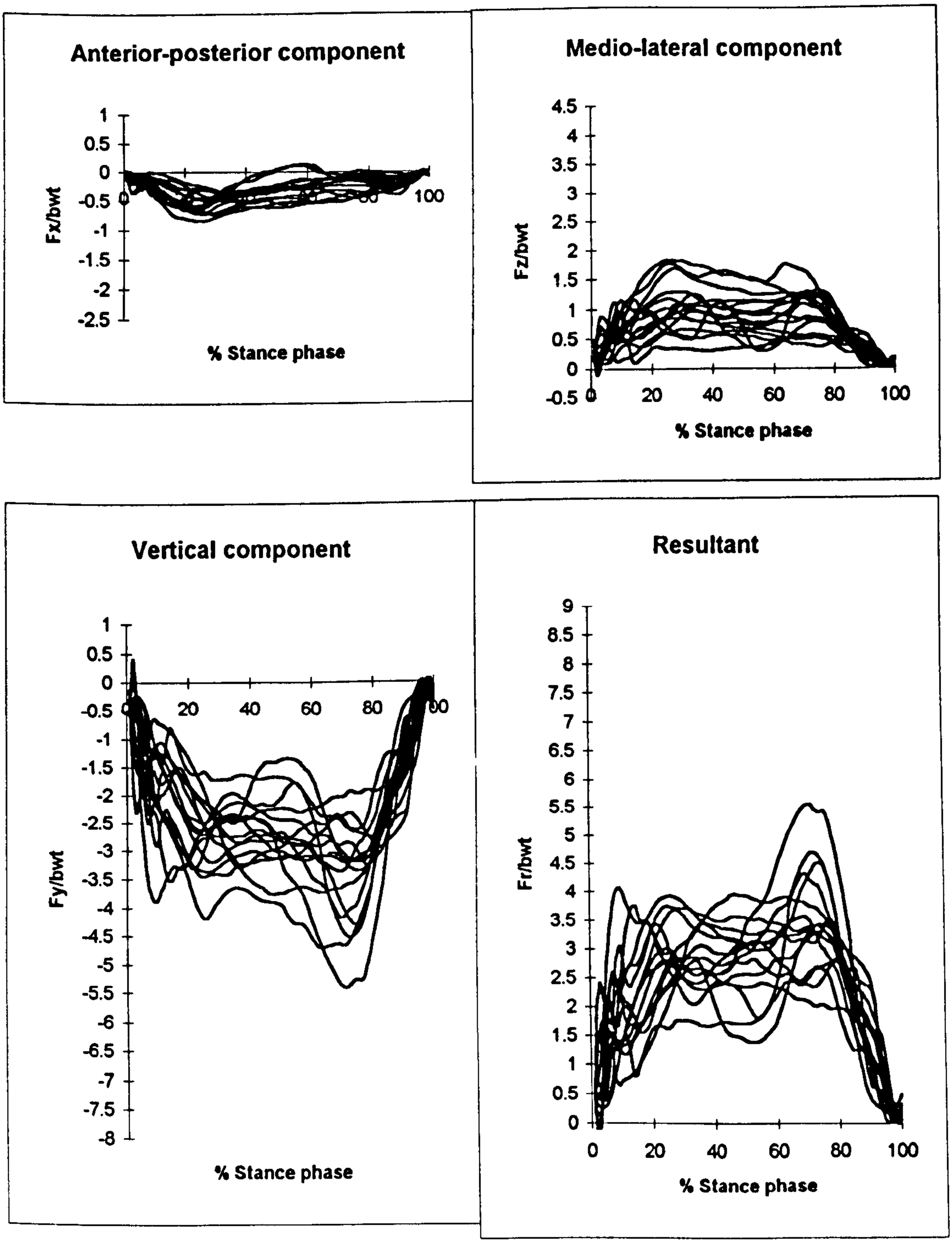

Figure F4 Group 2 - Prosthetic hips of patients. Components of hip joint force, Fx, Fy, Fz and resultant hip joint force, Fr, in terms of body weight determined for the walking turn activity. See section 5.2 for further description of this activity. See figure 7.2 for the sign convention used for force components.

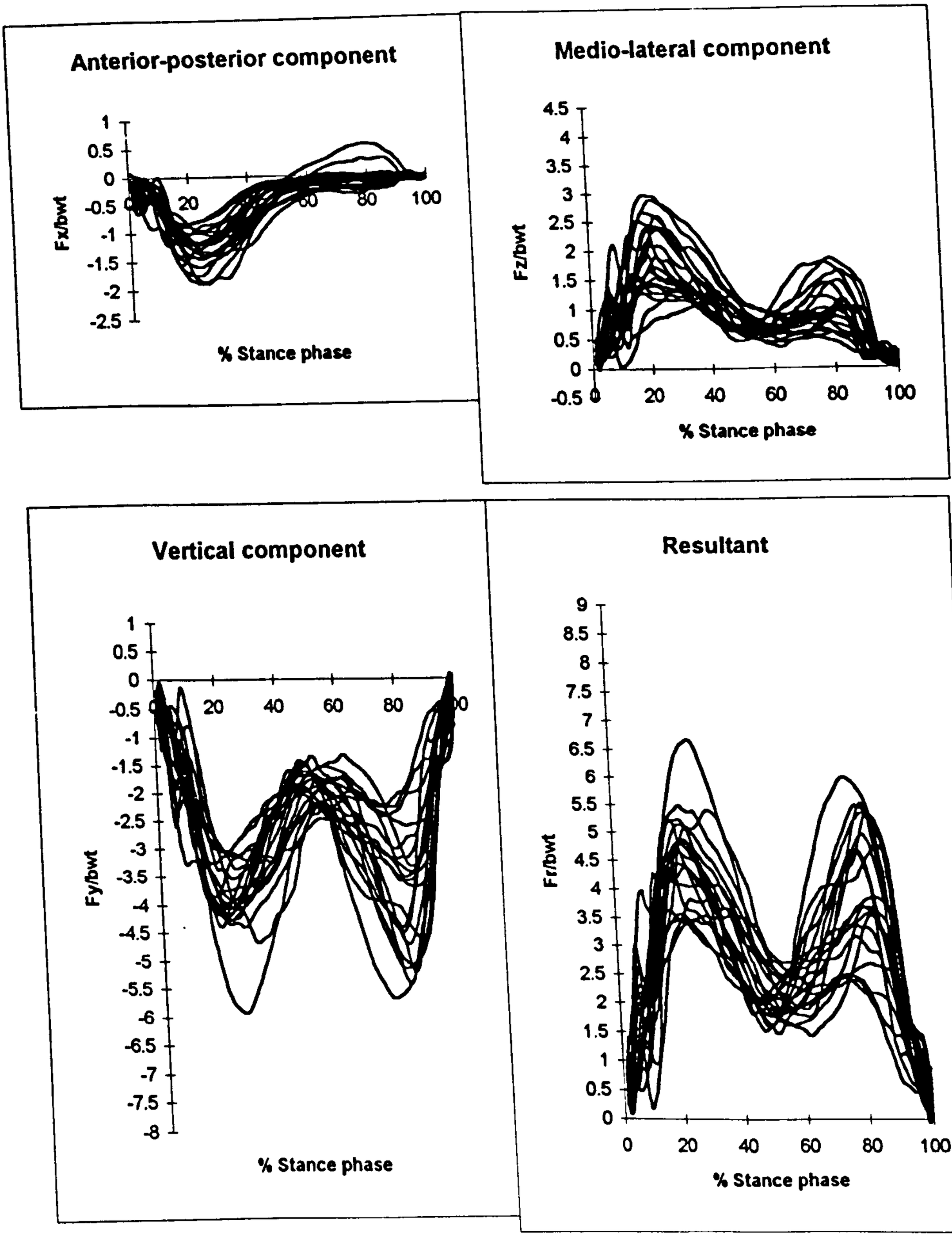

Figure F5 Group 1 - Hips of normal subjects. Components of hip joint force, Fx, Fy, Fz and resultant hip joint force, Fr, in terms of body weight during the stance phase of stair ascent. See figure 7.2 for the sign convention used for force components.

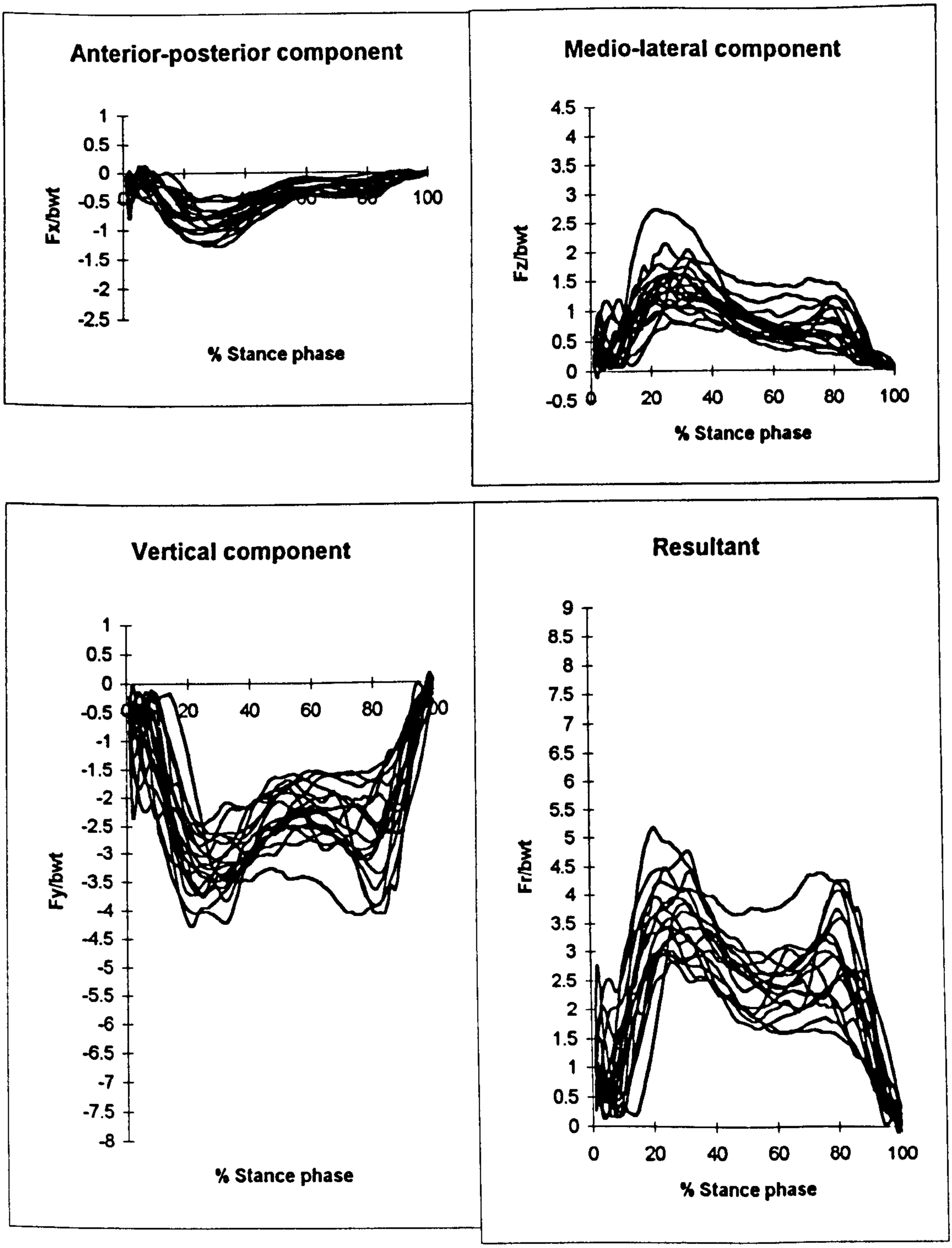

Figure F6 Group 2 - Prosthetic hips of patients. Components of hip joint force, Fx, Fy, Fz and resultant hip joint force, Fr, in terms of body weight during the stance phase of stair ascent. See figure 7.2 for the sign convention used for force components.

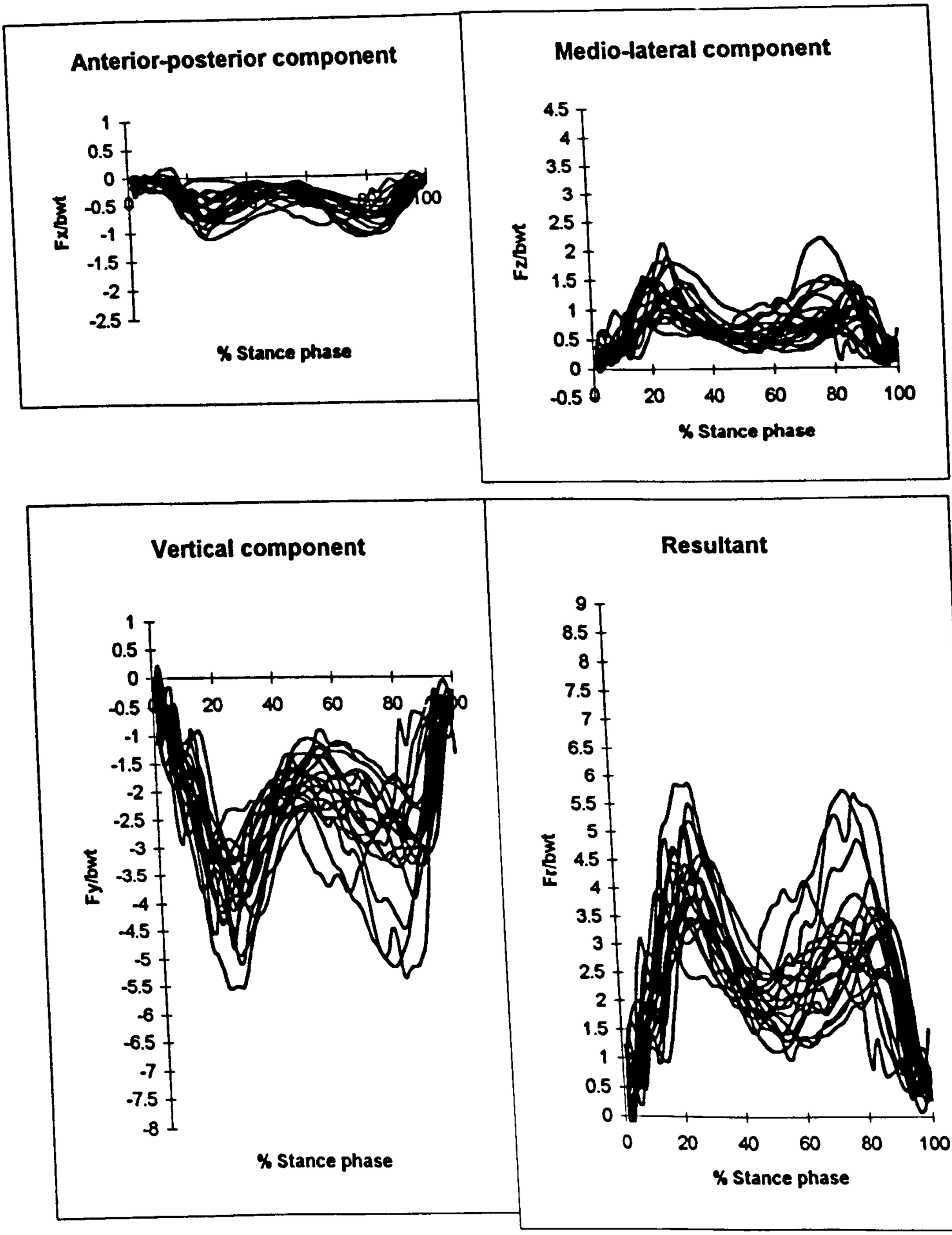

Figure F7 Group 1 - Hips of normal subjects. Components of hip joint force, Fx, Fy, Fz and resultant hip joint force, Fr, in terms of body weight during the stance phase of stair descent. See figure 7.2 for the sign convention used for force components.

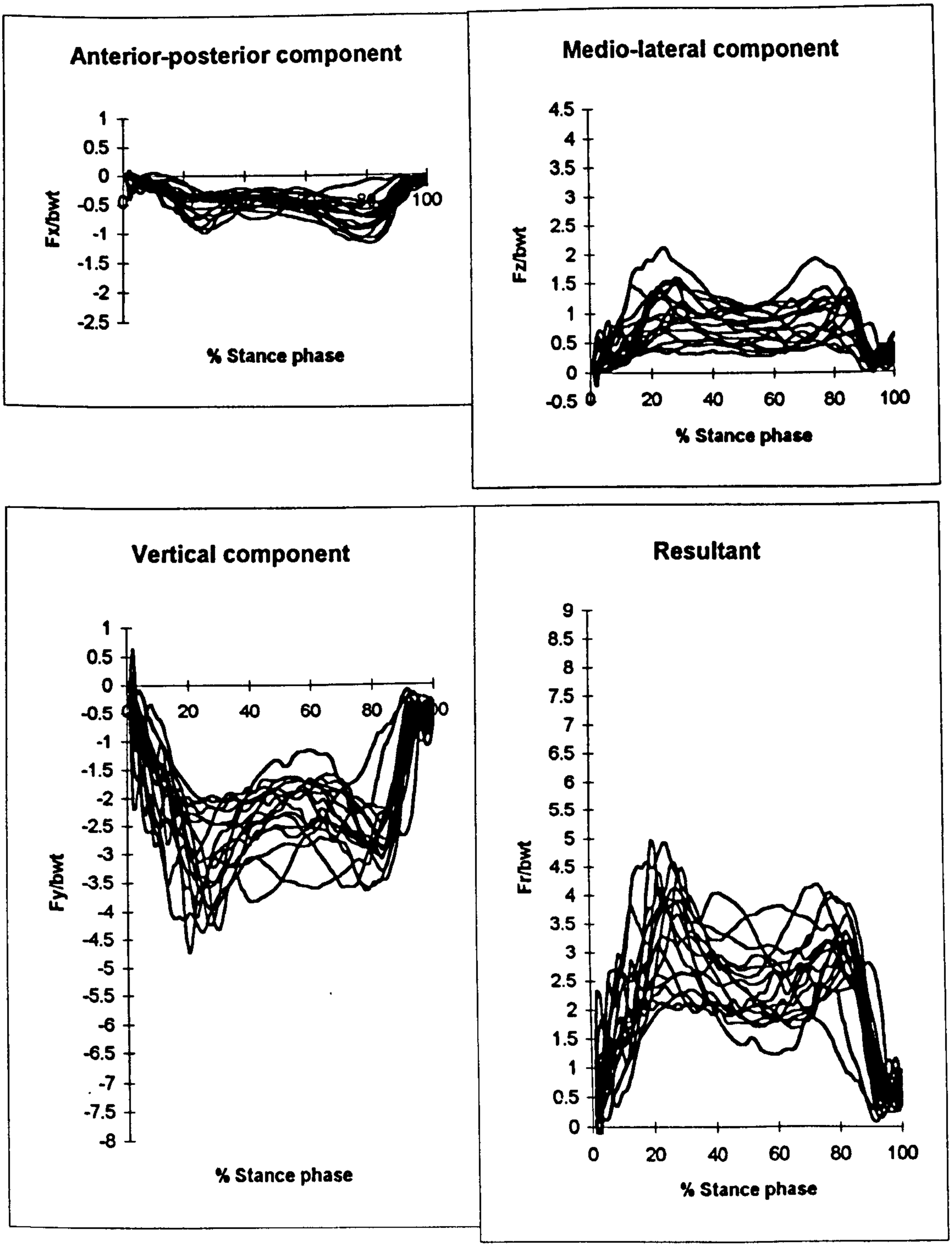

Figure F8 Group 2 - Prosthetic hips of patients. Components of hip joint force, Fx, Fy, Fz and resultant hip joint force, Fr, in terms of body weight during the stance phase of stair descent. See figure 7.2 for the sign convention used for force components.

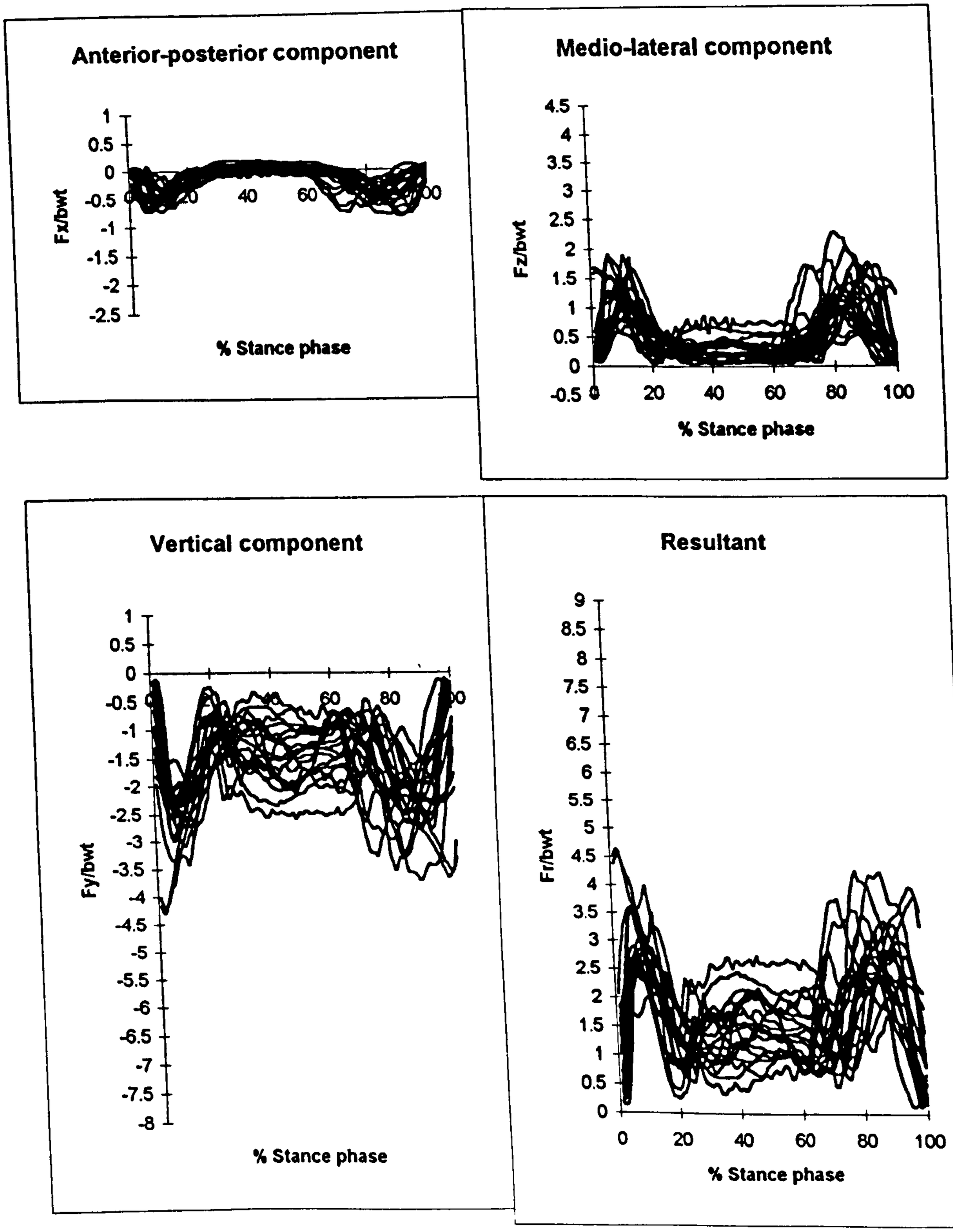

Figure F9 Group 1 - Hips of normal subjects. Components of hip joint force, Fx, Fy, Fz and resultant hip joint force, Fr, in terms of body weight determined for rising from and then sitting down onto a chair. See section 5.2 for further description of this activity. See figure 7.2 for the sign convention used for force components.

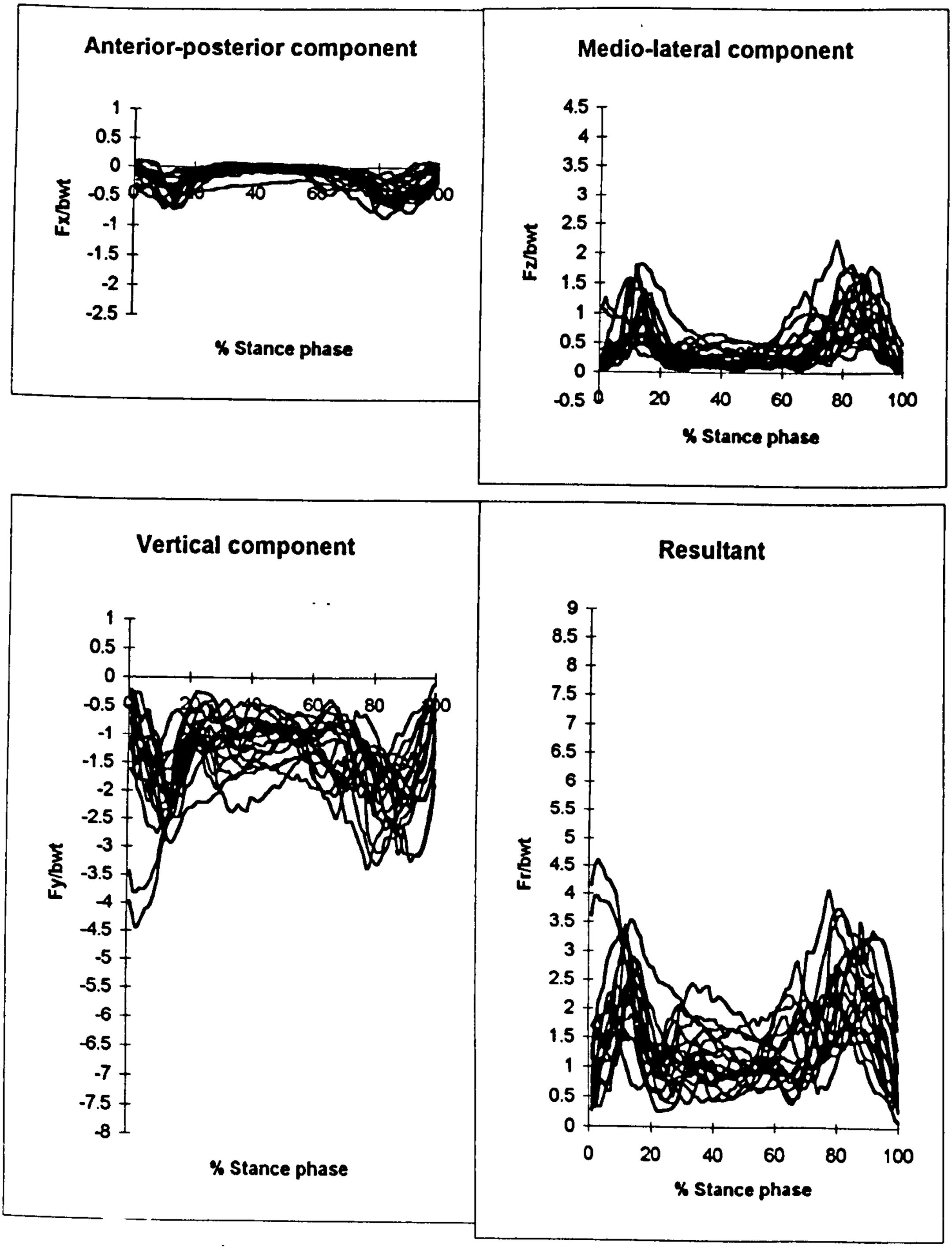

Figure F10 Group 2 - Prosthetic hips of patients. Components of hip joint force, Fx, Fy, Fz and resultant hip joint force, Fr, in terms of body weight determined for rising from and then sitting down onto a chair. See section 5.2 for further description of this activity. See figure 7.2 for the sign convention used for force components.

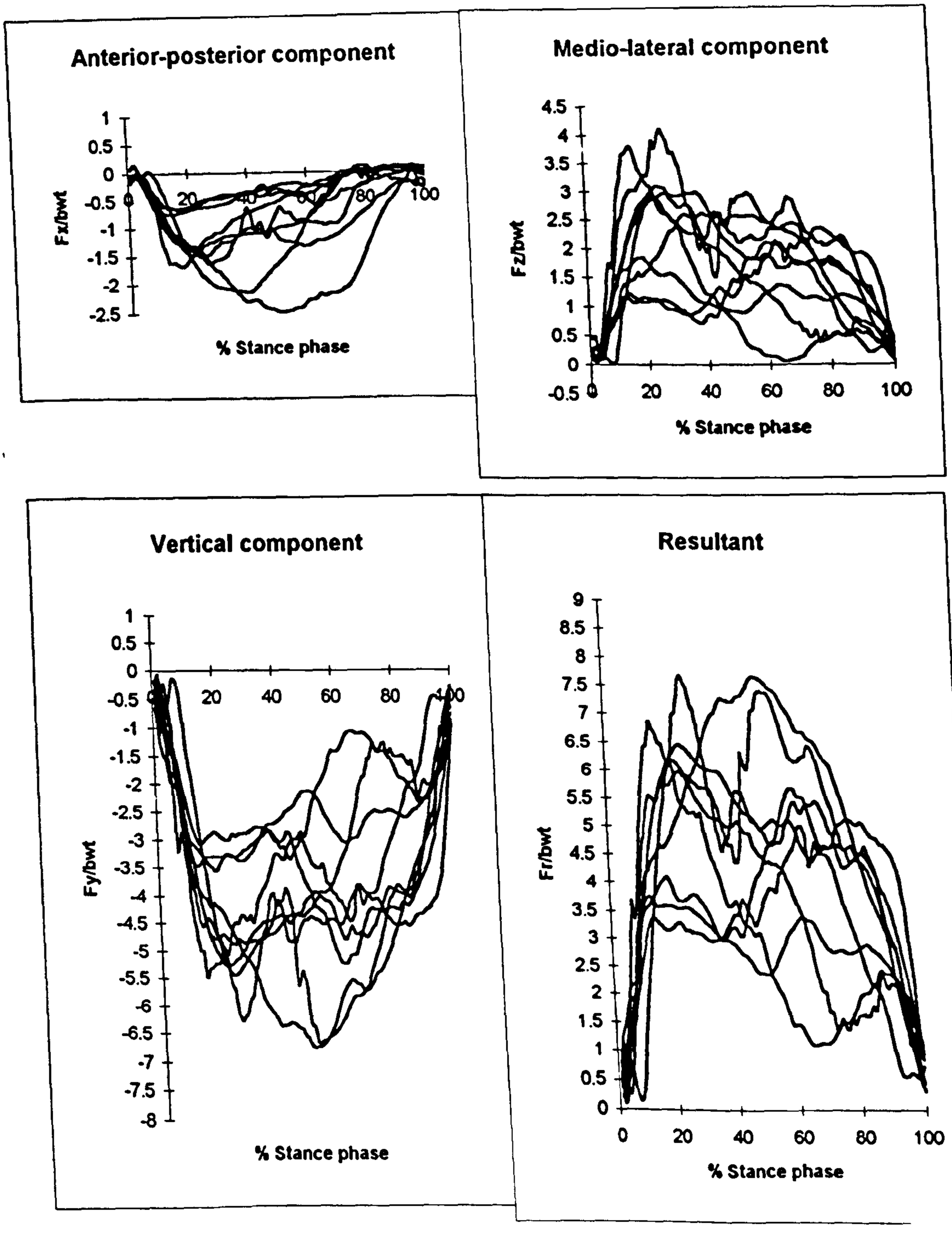

Figure F11 Group 1 - Hips of normal subjects. Components of hip joint force, Fx, Fy, Fz and resultant hip joint force, Fr, in terms of body weight determined for the outside hip on getting into the car (con). See section 5.2 for further description of this activity. See figure 7.2 for the sign convention used for force components.

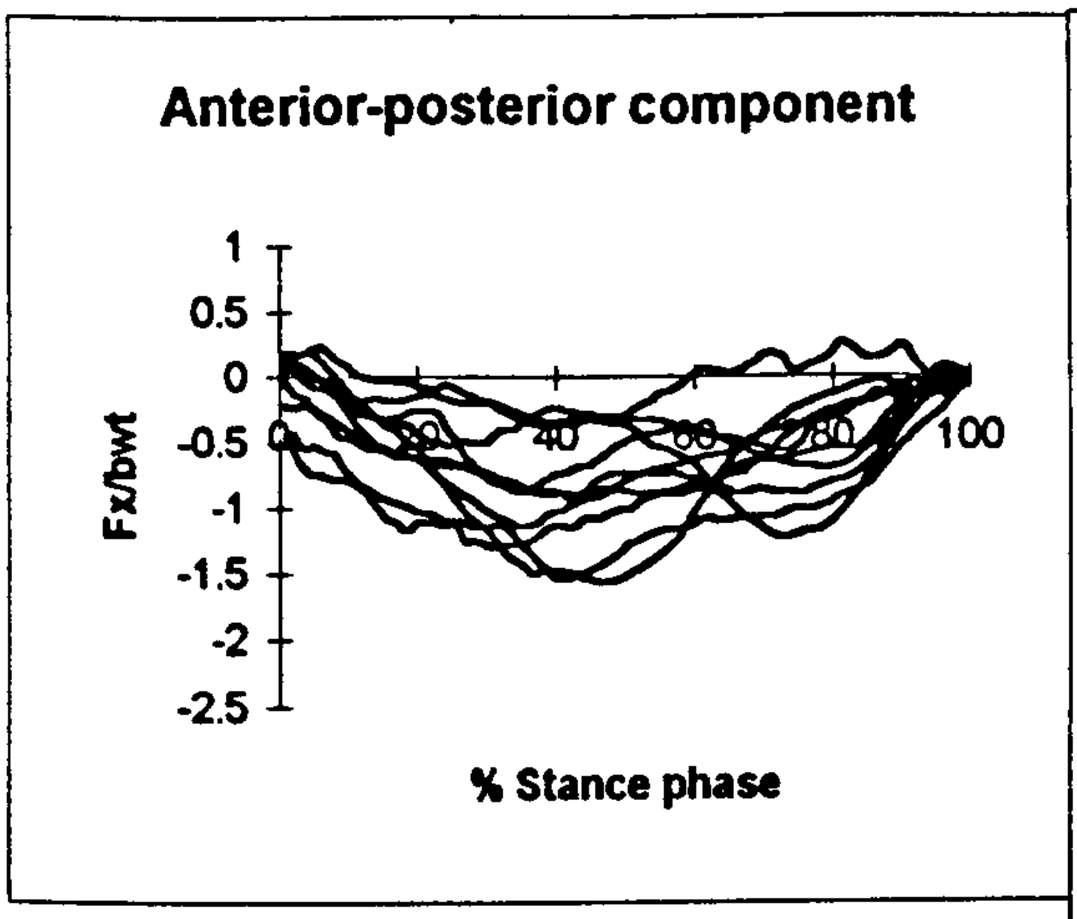

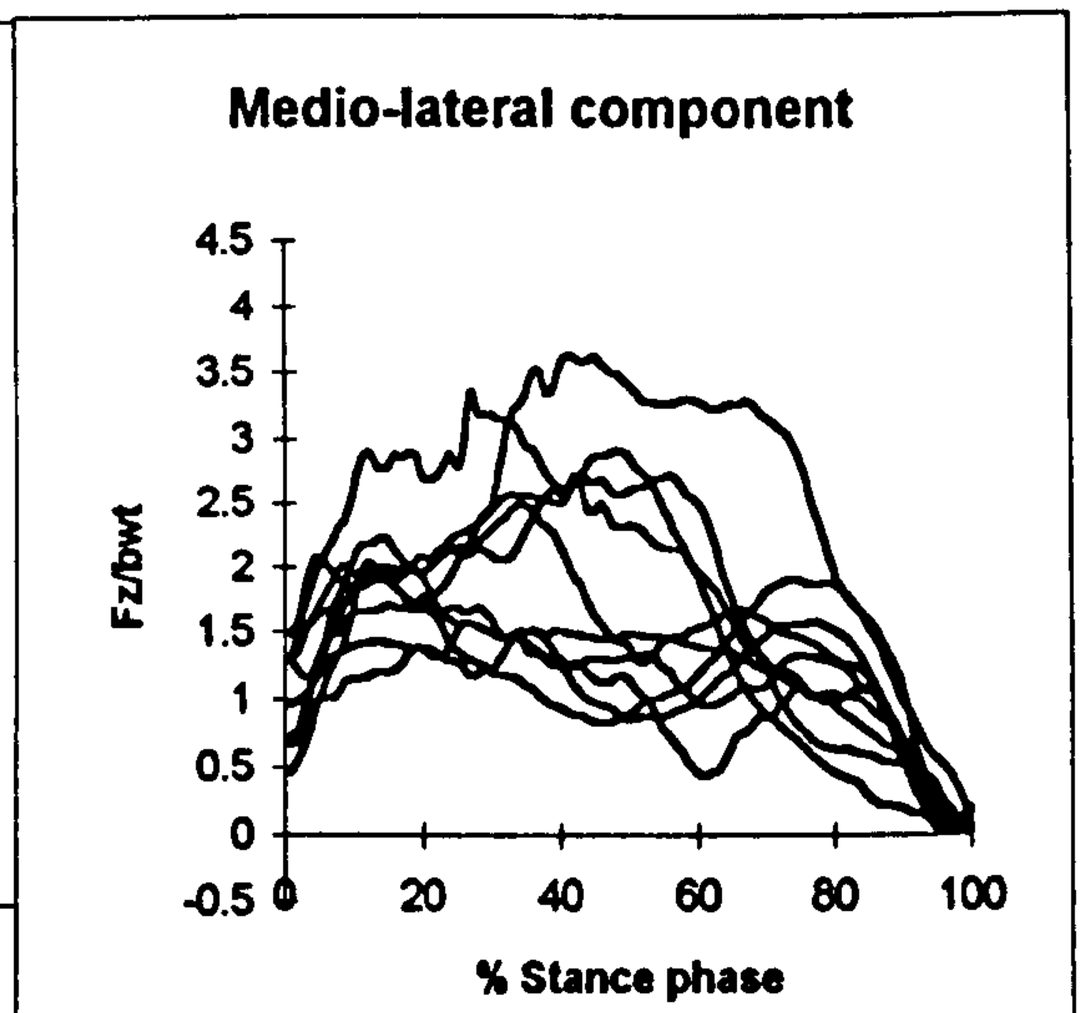

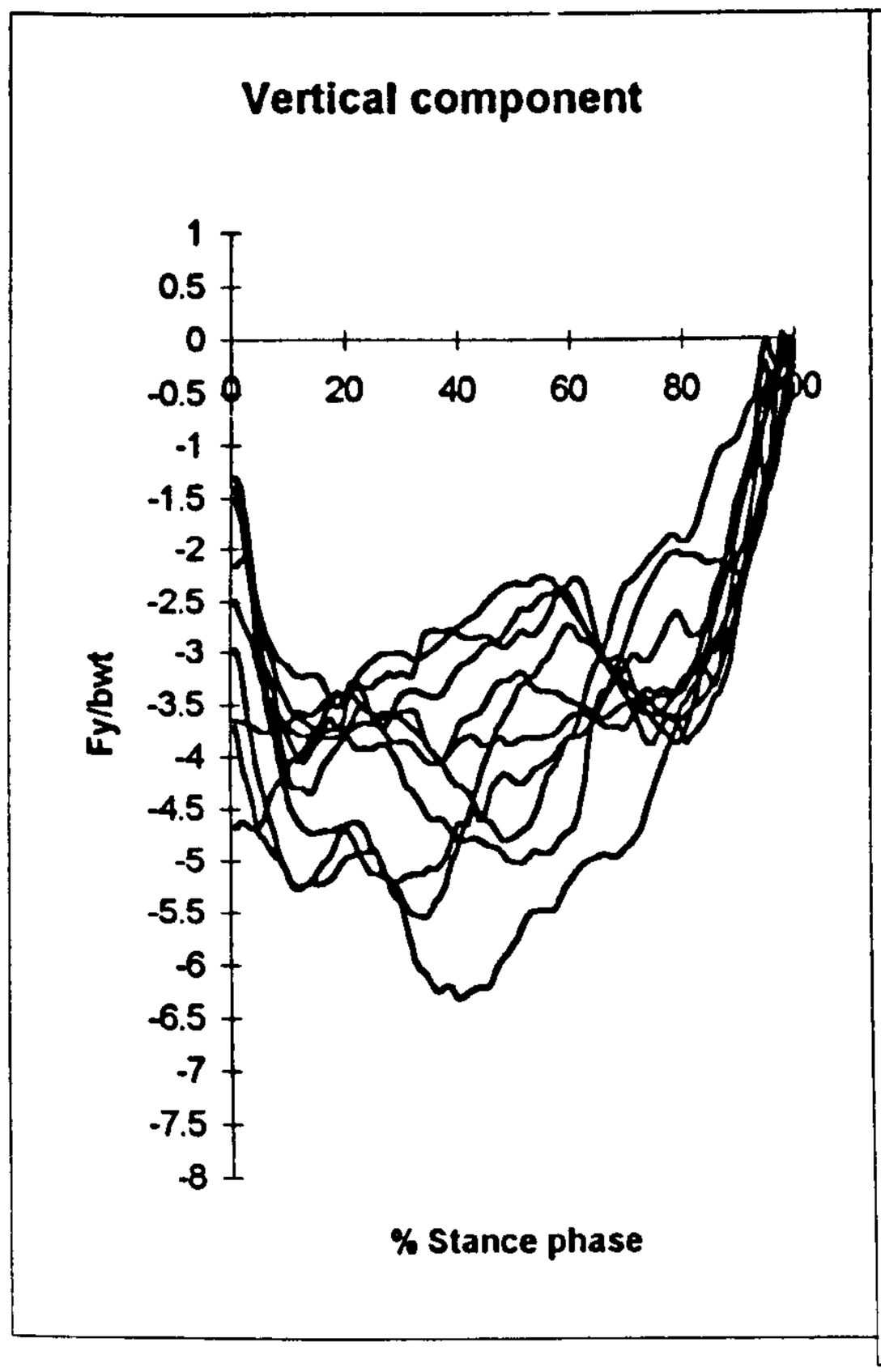

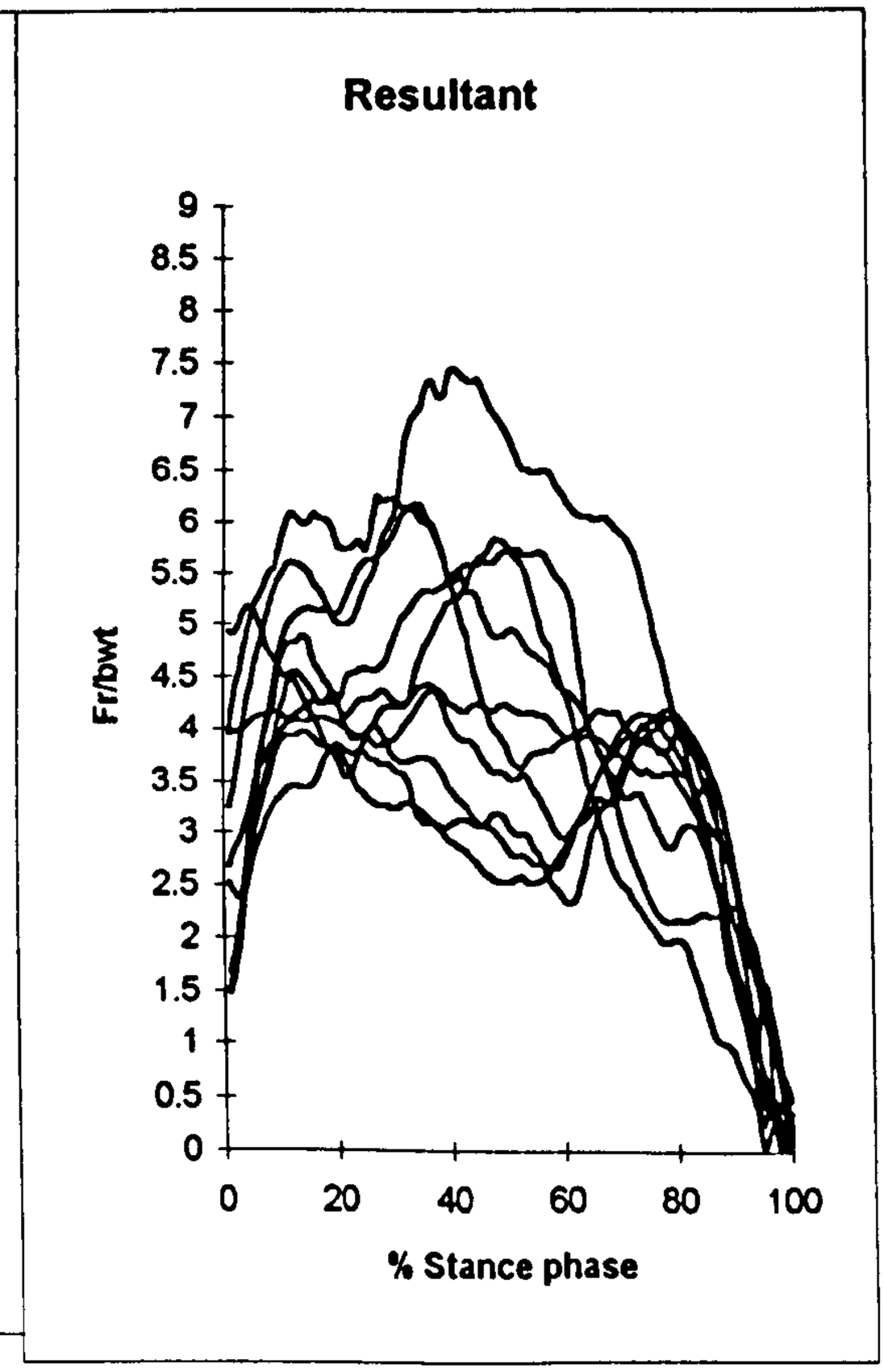

Figure F12 Group 1 - Hips of normal subjects. Components of hip joint force, Fx, Fy, Fz and resultant hip joint force, Fr, in terms of body weight determined for the outside hip on getting out of the car (cox). See section 5.2 for further description of this activity. See figure 7.2 for the sign convention used for force components.

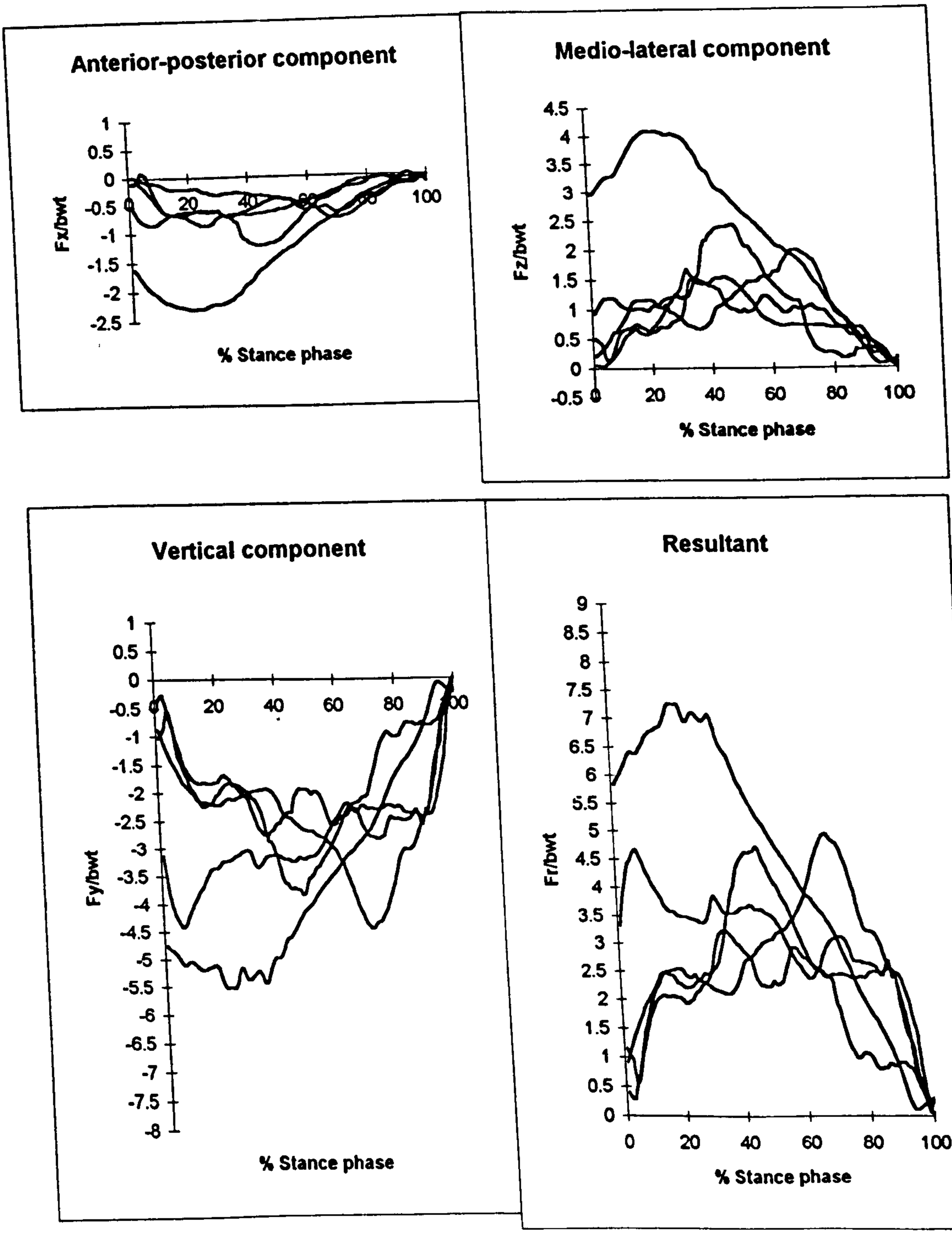

Figure F13 Group 2 - Prosthetic hips of patients. Components of hip joint force, Fx, Fy, Fz and resultant hip joint force, Fr, in terms of body weight determined for the outside hip on getting out of the car (cox). See section 5.2 for further description of this activity. See figure 7.2 for the sign convention used for force components.

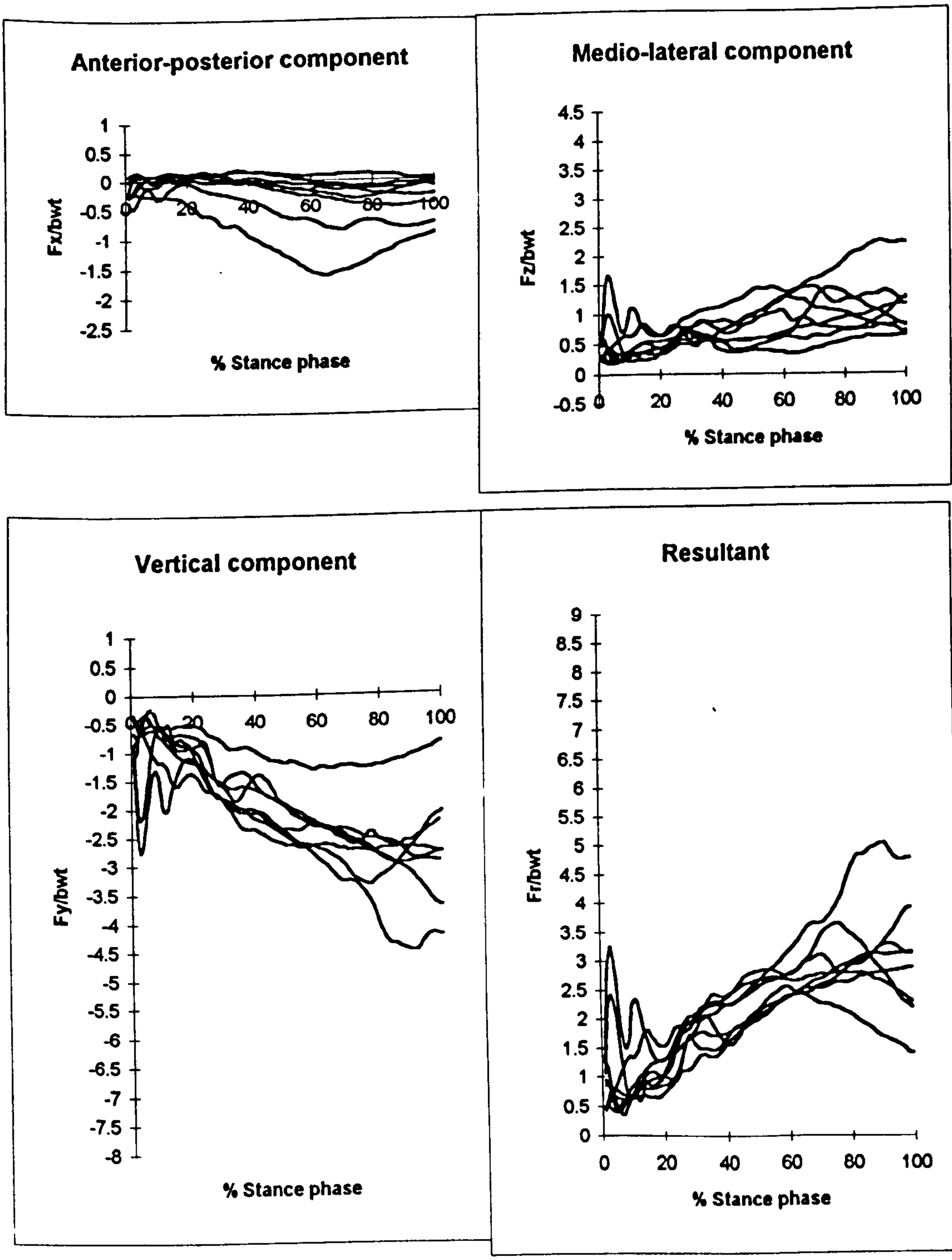

Figure F14 Group 1 - Hips of normal subjects. Components of hip joint force, Fx, Fy, Fz and resultant hip joint force, Fr, in terms of body weight determined for the inside hip on getting into the car (cin). See section 5.2 for further description of this activity. See figure 7.2 for the sign convention used for force components.

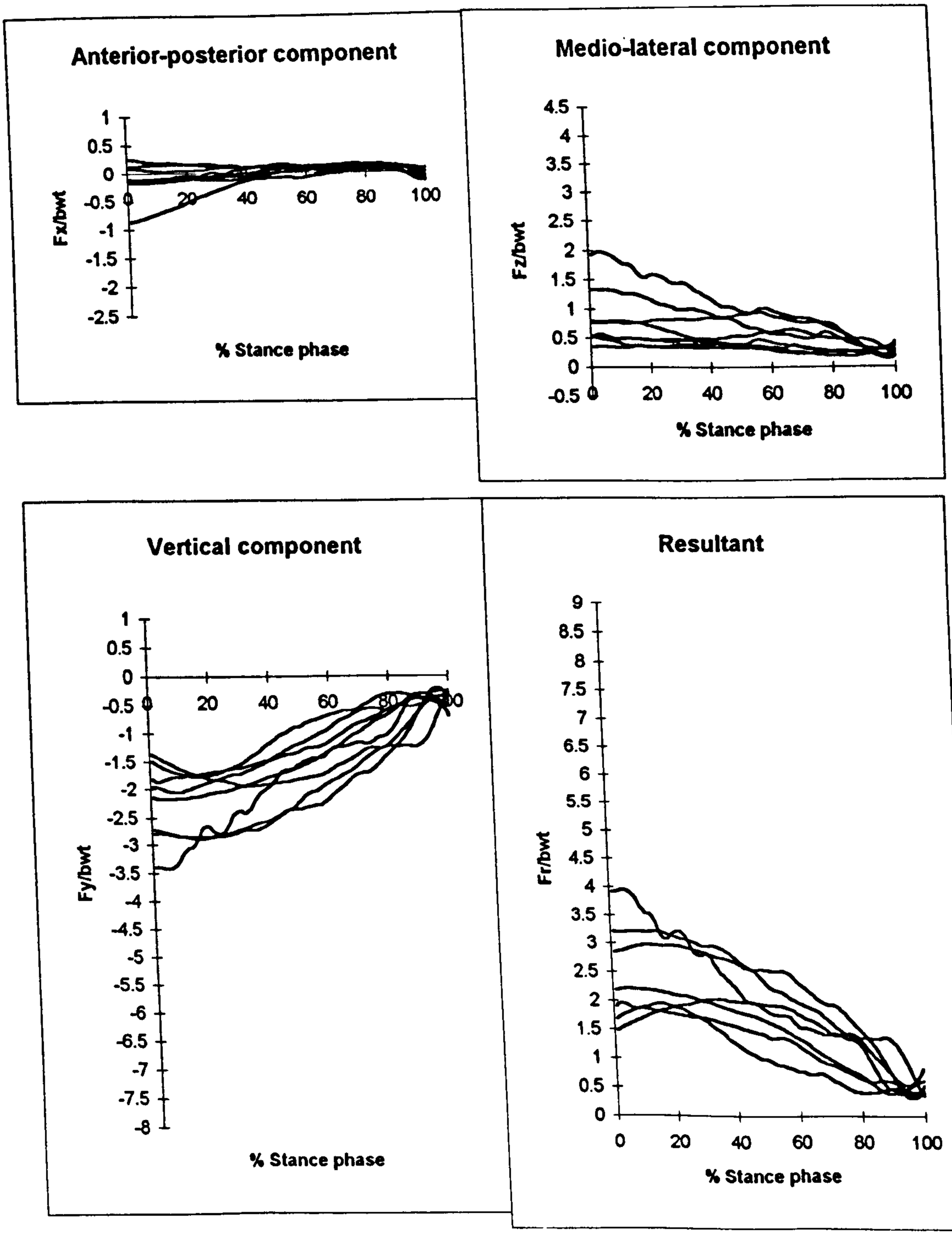

Figure F15 Group 1 - Hips of normal subjects. Components of hip joint force, Fx, Fy, Fz and resultant hip joint force, Fr, in terms of body weight determined for the inside hip on getting out of the car (cix). See section 5.2 for further description of this activity. See figure 7.2 for the sign convention used for force components.

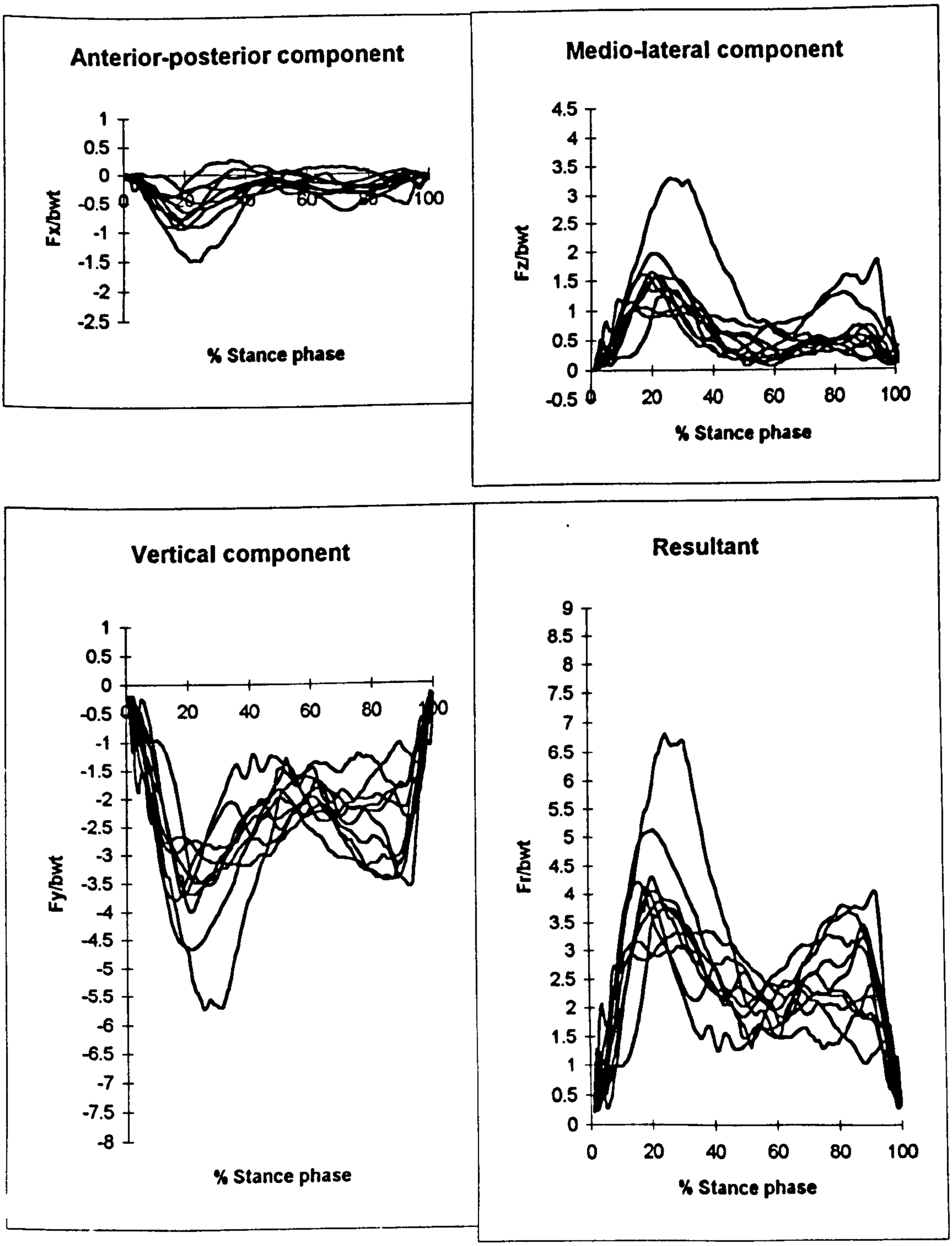

Figure F16 Group 1 - Hips of normal subjects. Components of hip joint force, Fx, Fy, Fz and resultant hip joint force, Fr, in terms of body weight determined for the outside hip on getting into the bath (bon). See section 5.2 for further description of this activity. See figure 7.2 for the sign convention used for force components.

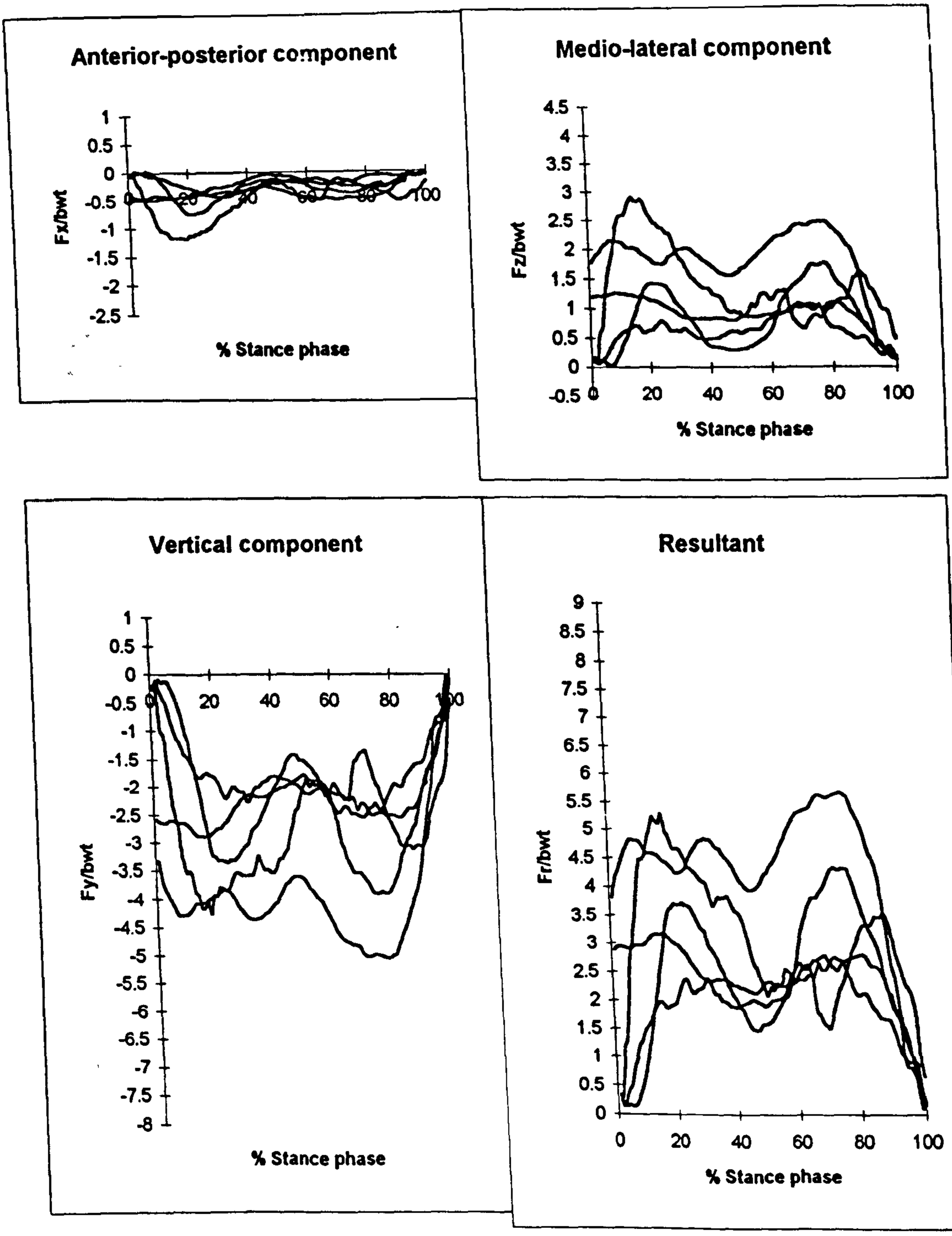

Figure F17 Group 2 - Prosthetic hips of patients. Components of hip joint force, Fx, Fy, Fz and resultant hip joint force, Fr, in terms of body weight determined for the outside hip on getting into the bath (bon). See section 5.2 for further description of this activity. See figure 7.2 for the sign convention used for force components.

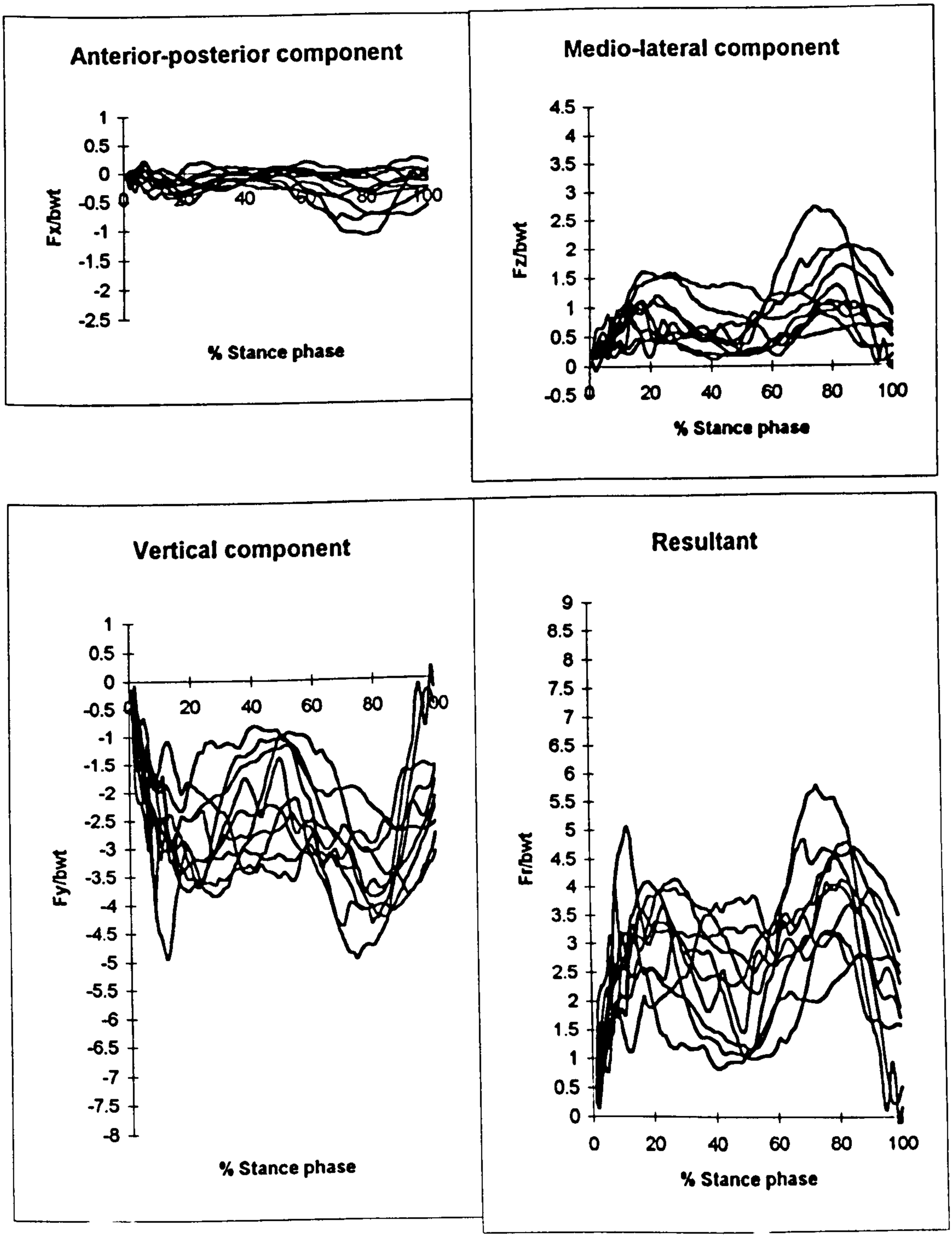

Figure F18 Group 1 - Hips of normal subjects. Components of hip joint force, Fx, Fy, Fz and resultant hip joint force, Fr, in terms of body weight determined for the outside hip on getting out of the bath (box). See section 5.2 for further description of this activity. See figure 7.2 for the sign convention used for force components.

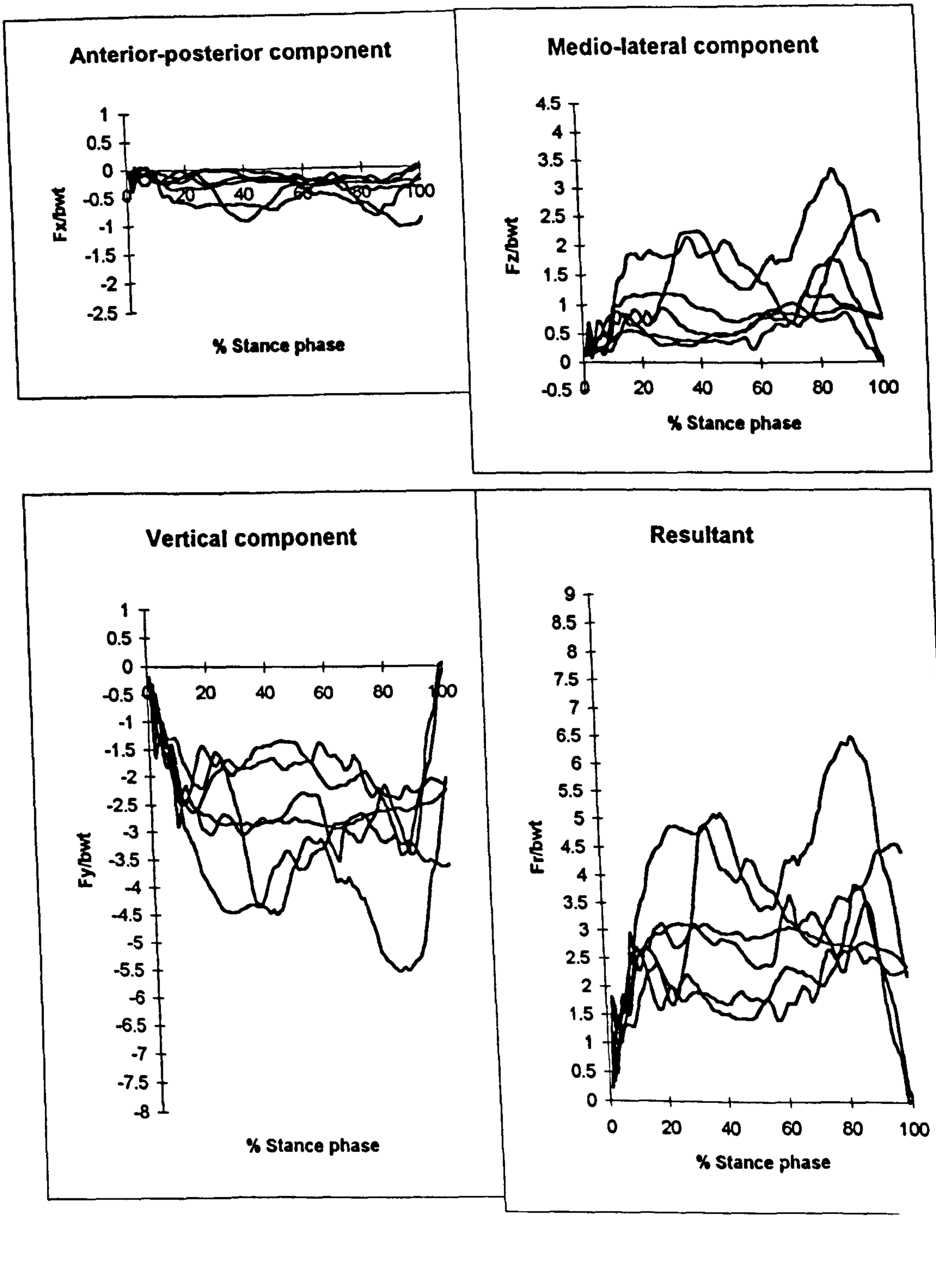

Figure F19 Group 2 - Prosthetic hips of patients. Components of hip joint force, Fx, Fy, Fz and resultant hip joint force, Fr, in terms of body weight determined for the outside hip on getting out of the bath (box). See section 5.2 for further description of this activity. See figure 7.2 for the sign convention used for force components.

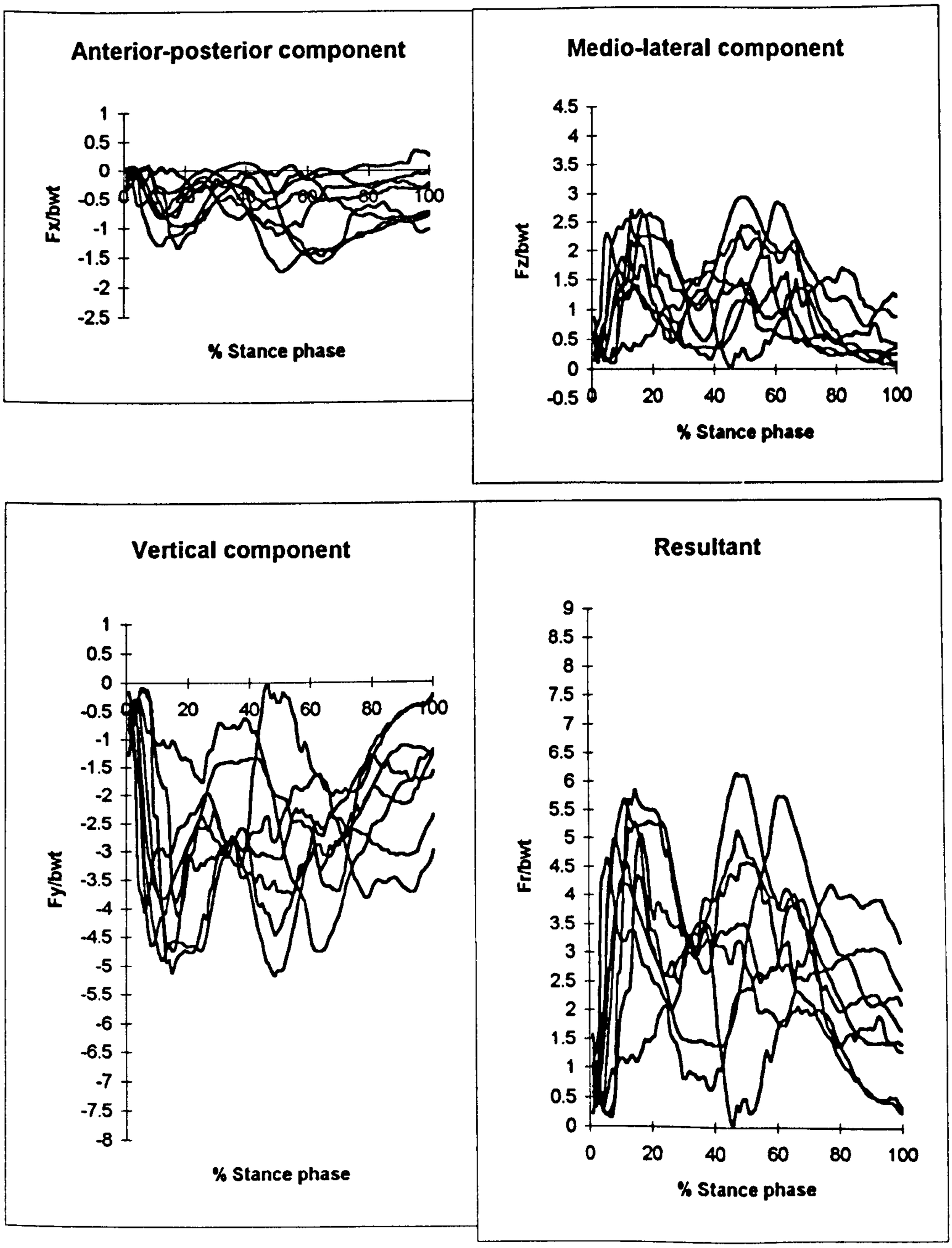

Figure F20 Group 1 - Hips of normal subjects. Components of hip joint force, Fx, Fy, Fz and resultant hip joint force, Fr, in terms of body weight determined for the inside hip on getting into the bath (bin). See section 5.2 for further description of this activity. See figure 7.2 for the sign convention used for force components.

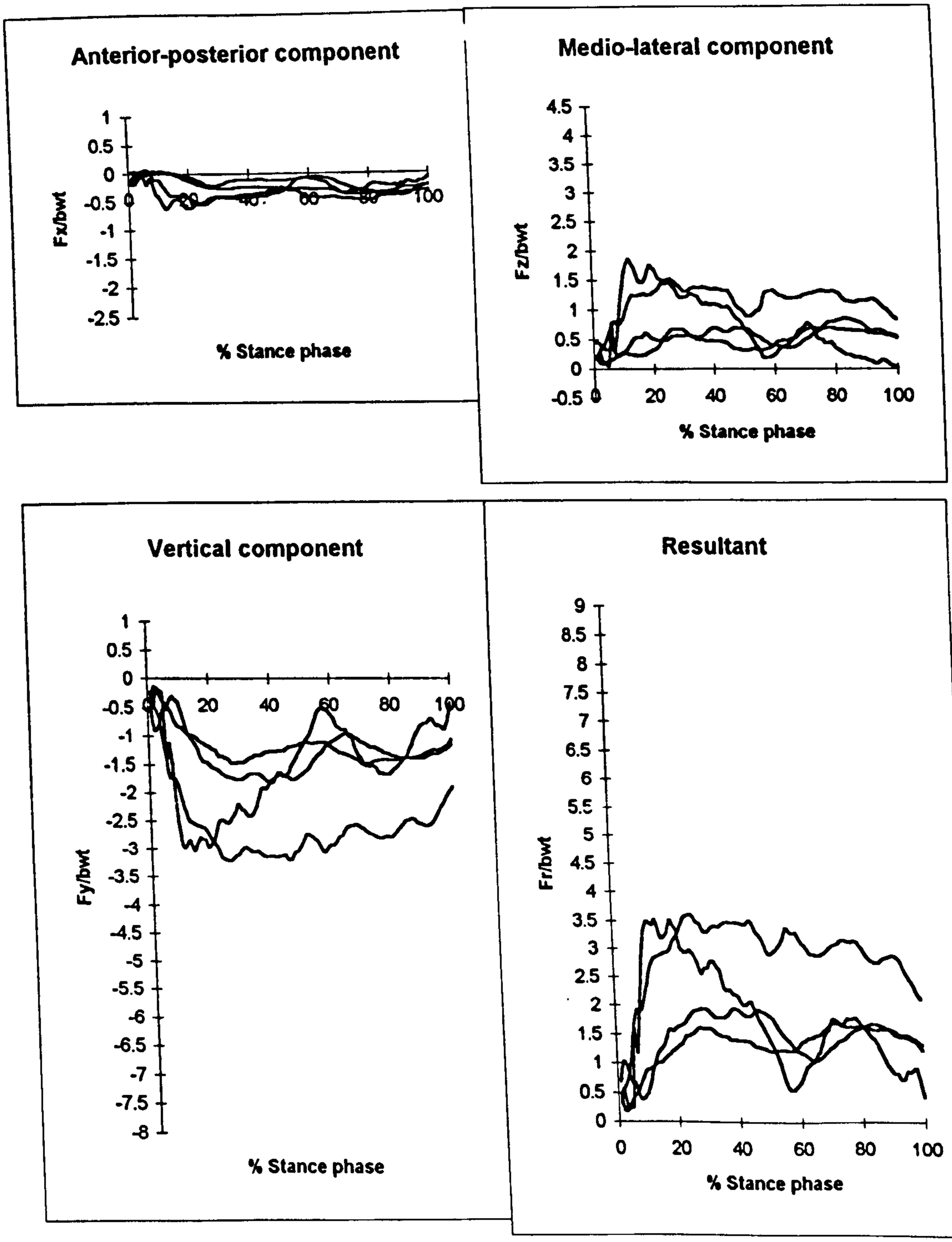

Figure F21 Group 2 - Prosthetic hips of patients. Components of hip joint force, Fx, Fy, Fz and resultant hip joint force, Fr, in terms of body weight determined for the inside hip on getting into the bath (bin). See section 5.2 for further description of this activity. See figure 7.2 for the sign convention used for force components.

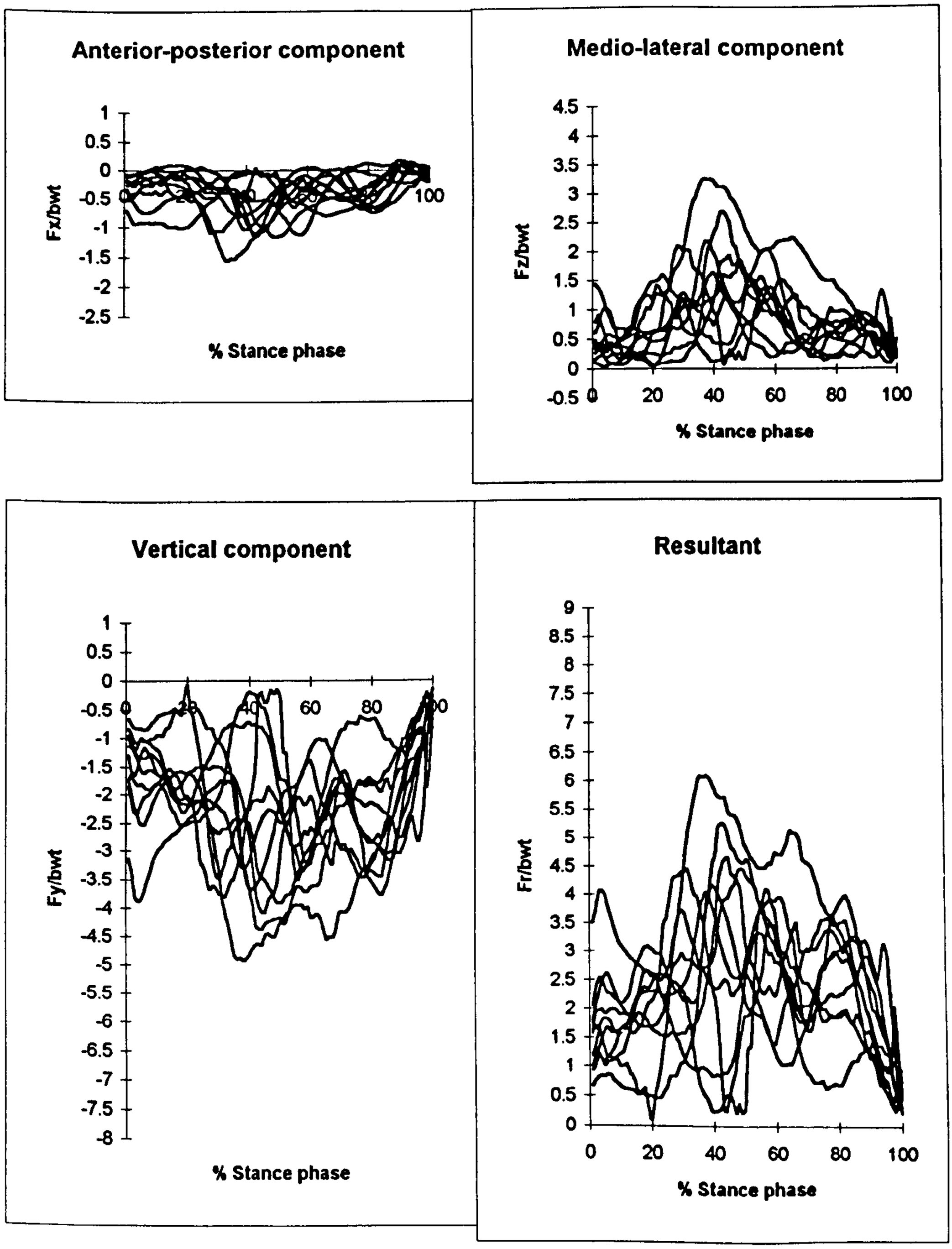

Figure F22 Group 1 - Hips of normal subjects. Components of hip joint force, Fx, Fy, Fz and resultant hip joint force, Fr, in terms of body weight determined for the inside hip on getting out of the bath (bix). See section 5.2 for further description of this activity. See figure 7.2 for the sign convention used for force components.

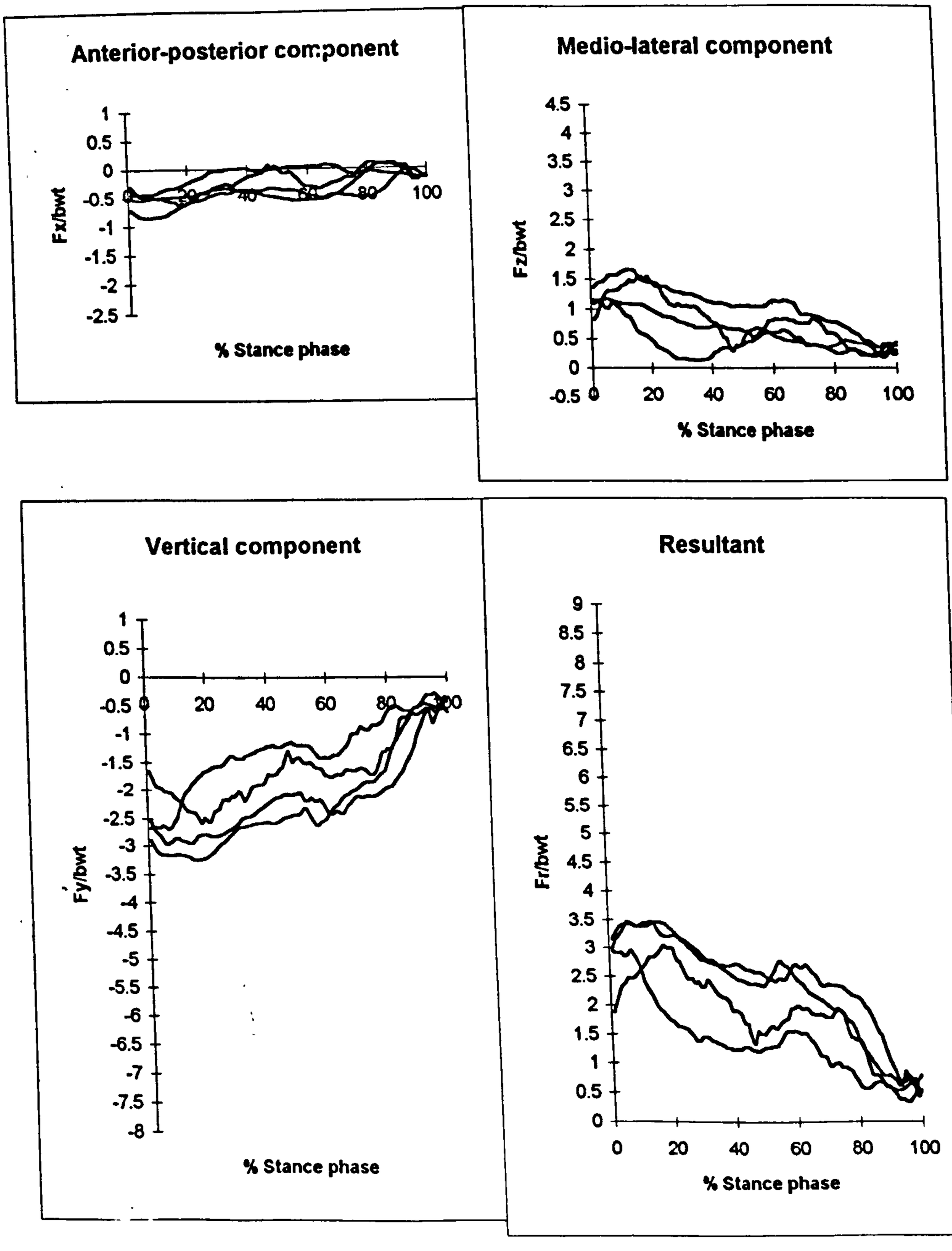

Figure F23 Group 2 - Prosthetic hips of patients. Components of hip joint force, Fx, Fy, Fz and resultant hip joint force, Fr, in terms of body weight determined for the inside hip on getting out of the bath (bix). See section 5.2 for further description of this activity. See figure 7.2 for the sign convention used for force components.

APPENDIX G

This appendix presents the mean peak values of the components of hip joint force, Fx, Fy, Fz and the resultant hip joint force, Fr, in terms of body weight for the activities tested. Values of θ_{XY}, θ_{YZ} and θ_{XZ} describing the direction of the peak resultant hip joint force are also given. For a description of the activity codes see section 7.1. For the sign convention of Fx, Fy and Fz see figure 7.2. For conventions for θ_{XY}, θ_{YZ} and θ_{XZ} see figure 7.3. The values for the normal subjects (group 1) are presented in section G.1. These are followed by those for the prosthetic hips of the patients (group 2) in section G.2 and those for the non prosthetic hips of the patients (group 3) in section G.3.

G.1 GROUP 1 - HIPS OF NORMAL SUBJECTS

	Fx/bwt	Fy/bwt	Fz/bwt	Fr/bwt	θ_{XY} / °	θ_{YZ} / °	θ_{XZ} / °
Mean	-1.00	-3.86	1.44	4.25	14.5	-20.8	-34.4
Min	-1.70	-5.20	1.10	3.19	11.5	-25.3	-46.8
Max	-0.71	-2.91	1.92	5.68	18.3	-16.6	-27.6
S.D.	0.29	0.79	0.22	0.84	2.1	2.6	6.3

Group 1. Gait - peak 1. N = 15

	Fx/bwt	Fy/bwt	Fz/bwt	Fr/bwt	θ_{XY} / °	θ_{YZ} / °	θ_{XZ} / °
Mean	0.19	-4.85	1.19	5.01	-2.3	-13.7	11.1
Min	-0.19	-7.27	0.61	3.42	-10.1	-19.4	-6.6
Max	0.78	-3.33	2.38	7.47	1.8	-8.0	51.8
S.D.	0.30	1.12	0.45	1.17	3.7	3.2	17.2

Group 1. Gait - peak 2. N = 15

	Fx/bwt	Fr/bwt
Mean	-1.00	5.16
Min	-0.71	3.60
Max	-1.70	7.47
S.D.	0.29	1.11

Group 1. Gait - greatest peak. N = 15

	Fx/bwt	Fy/bwt	Fz/bwt	Fr/bwt	θ_{XY} / °	θ_{YZ} / °	θ_{XZ} / °
Mean	-0.57	-3.48	1.17	3.74	10.1	-20.0	-25.4
Min	-1.44	-5.98	0.75	1.42	3.1	-47.7	-44.0
Max	-0.26	-0.91	1.94	6.44	25.4	-11.6	-9.8
S.D.	0.31	1.09	0.28	1.09	5.4	7.6	9.9

Group 1. Turn - peak 1. N = 18

	Fx/bwt	Fy/bwt	Fz/bwt	Fr/bwt	θ_{XY} / °	θ_{YZ} / °	θ_{XZ} / °
Mean	0.07	-4.09	0.94	4.21	-0.8	-13.0	3.9
Min	-0.35	-5.91	0.65	2.71	-7.7	-16.6	-15.6
Max	0.60	-2.61	1.56	6.11	4.2	-9.1	29.5
S.D.	0.23	0.91	0.25	0.93	2.9	2.3	12.3

Group 1. Turn - peak 2. N = 17

	Fx/bwt	Fr/bwt
Mean	-0.60	4.36
Min	-0.27	2.83
Max	-1.44	6.44
S.D.	0.29	0.98

Group 1. Turn - greatest Peak. N = 18

	Fx/bwt	Fy/bwt	Fz/bwt	Fr/bwt	θ_{XY} / °	θ_{YZ} / °	θ_{XZ} / °
Mean	-1.32	-3.98	2.01	4.67	18.2	-26.5	-33.8
Min	-1.89	-5.93	1.18	3.48	14.2	-35.3	-49.4
Max	-0.83	-3.05	2.96	6.66	22.5	-19.3	-25.5
S.D.	0.31	0.66	0.56	0.81	2.6	4.9	5.8

Group 1. Asc - peak 1. N = 20

	Fx/bwt	Fy/bwt	Fz/bwt	Fr/bwt	θ_{XY} /°	θ_{YZ} / °	θ_{XZ} / °
Mean	-0.11	-3.92	1.08	4.08	1.7	-15.3	-5.0
Min	-0.33	-5.69	0.51	2.39	-8.6	-19.7	-22.1
Max	0.55	-2.27	1.85	5.97	6.2	-9.0	42.2
S.D.	0.20	1.11	0.39	1.15	3.2	3.0	13.3

Group 1. Asc - peak 2. N = 20

	Fx/bwt	Fr/bwt
Mean	-1.32	4.89
Min	-0.83	3.60
Max	-1.89	6.66
S.D.	0.31	0.82

Group 1. Asc - greatest peak. N = 20

	Fx/bwt	Fy/bwt	Fz/bwt	Fr/bwt	θ_{XY} /°	θ_{YZ} / °	θ_{XZ} / °
Mean	-0.67	-4.07	1.35	4.36	9.4	-18.1	-26.4
Min	-1.11	-5.51	0.88	3.45	2.2	-25.0	-39.0
Max	-0.14	-3.20	2.12	5.84	15.3	-14.3	-7.8
S.D.	0.25	0.65	0.36	0.71	3.5	3.0	9.1

Group 1. Des - peak 1. N = 20

	Fx/bwt	Fy/bwt	Fz/bwt	Fr/bwt	θ_{XY} /°	θ_{YZ} / °	θ_{XZ} / °
Mean	-0.80	-3.30	1.16	3.59	13.9	-19.4	-35.5
Min	-1.11	-5.39	0.54	2.13	11.2	-24.6	-54.8
Max	-0.46	-1.96	2.20	5.73	17.7	-12.2	-26.7
S.D.	0.18	0.90	0.37	0.96	2.0	3.7	6.6

Group 1. Des - peak 2. N = 20

	Fx/bwt	Fr/bwt
Mean	-0.87	4.49
Min	-0.49	3.45
Max	-1.11	5.84
S.D.	0.17	0.74

Group 1. Des - greatest peak. N = 20

	Fx/bwt	Fy/bwt	Fz/bwt	Fr/bwt	θ_{XY} /°	θ_{YZ} /°	θ_{XZ} /°
Mean	-0.52	-2.79	1.41	3.19	10.7	-27.1	-19.9
Min	-0.73	-4.30	0.72	2.31	3.6	-33.5	-28.1
Max	-0.19	-1.98	1.88	4.65	17.3	-13.2	-10.0
S.D.	0.15	0.62	0.33	0.63	3.4	5.7	3.7

Group 1. Rise N = 20

	Fx/bwt	Fy/bwt	Fz/bwt	Fr/bwt	θ_{XY} /°	θ_{YZ} /°	θ_{XZ} /°
Mean	-1.43	-5.33	2.86	6.25	14.5	-28.1	-25.7
Min	-2.47	-6.76	1.84	4.08	8.1	-34.7	-43.4
Max	-0.65	-3.58	4.09	8.00	21.3	-21.2	-15.6
S.D.	0.64	0.98	0.74	1.21	4.8	4.5	8.7

Group 1. Con N = 9

	Fx/bwt	Fy/bwt	Fz/bwt	Fr/bwt	θ_{XY} /°	θ_{YZ} /°	θ_{XZ} /°
Mean	-1.06	-4.66	2.35	5.33	12.7	-26.5	-24.5
Min	-1.55	-6.31	1.52	4.19	7.8	-30.0	-37.9
Max	-0.55	-3.68	3.63	7.44	18.3	-20.6	-15.2
S.D.	0.32	0.87	0.65	1.07	3.1	3.0	6.5

Group 1. Cox N = 10

	Fx/bwt	Fy/bwt	Fz/bwt	Fr/bwt	θ_{XY} /°	θ_{YZ} /°	θ_{XZ} /°
Mean	-0.42	-3.02	1.33	3.43	10.6	-24.7	-16.4
Min	-1.63	-4.49	0.63	2.46	-3.0	-45.0	-51.3
Max	0.18	-1.30	2.28	5.04	51.3	-13.0	8.2
S.D.	0.59	0.92	0.47	0.80	17.7	9.4	21.3

Group 1. Cin N = 8

	Fx/bwt	Fy/bwt	Fz/bwt	Fr/bwt	θ_{XY} /°	θ_{YZ} /°	θ_{XZ} /°
Mean	-0.08	-2.38	0.89	2.57	1.1	-19.4	-2.9
Min	-0.87	-3.43	0.37	1.95	-7.4	-30.0	-33.5
Max	0.25	-1.79	1.98	3.96	16.8	-9.6	23.1
S.D.	0.36	0.60	0.53	0.76	7.7	6.4	19.6

Group 1. Cix N = 8

	Fx/bwt	Fy/bwt	Fz/bwt	Fr/bwt	θ_{XY} /°	θ_{YZ} /°	θ_{XZ} /°
Mean	-0.73	-3.91	1.68	4.33	10.2	-22.7	-22.7
Min	-1.50	-5.73	1.09	3.17	4.8	-29.9	-33.1
Max	-0.30	-2.95	3.30	6.78	14.7	-20.2	-12.8
S.D.	0.36	0.77	0.62	0.99	3.6	2.9	6.4

Group 1. Bon N = 10

	Fx/bwt	Fy/bwt	Fz/bwt	Fr/bwt	θ_{XY} /°	θ_{YZ} /°	θ_{XZ} /°
Mean	-0.50	-3.90	1.46	4.22	7.1	-20.0	-18.2
Min	-1.11	-4.97	0.68	2.81	3.4	-28.8	-22.6
Max	-0.21	-2.71	2.74	5.79	12.6	-12.8	-10.7
S.D.	0.29	0.69	0.62	0.86	3.2	5.6	3.9

Group 1. Box N = 10

	Fx/bwt	Fy/bwt	Fz/bwt	Fr/bwt	θ_{XY} / °	θ_{YZ} / °	θ_{XZ} / °
Mean	-1.06	-4.53	2.40	5.26	12.9	-27.6	-23.2
Min	-1.75	-5.17	1.31	3.74	8.1	-35.1	-30.6
Max	-0.49	-3.48	3.07	6.20	18.7	-20.6	-18.9
S.D.	0.44	0.60	0.61	0.82	4.3	4.5	4.4

Group 1. Bin N = 8

	Fx/bwt	Fy/bwt	Fz/bwt	Fr/bwt	θ_{XY} / °	θ_{YZ} / °	θ_{XZ} / °
Mean	-0.98	-3.90	2.09	4.54	13.9	-28.0	-25.2
Min	-1.57	-4.93	1.43	3.73	10.7	-33.4	-33.2
Max	-0.62	-3.21	3.26	6.11	17.6	-20.2	-18.9
S.D.	0.28	0.50	0.52	0.68	2.4	4.2	4.8

Group 1. Bix N = 10

G.2 GROUP 2 - PROSTHETIC HIPS OF PATIENTS

	Fx/bwt	Fy/bwt	Fz/bwt	Fr/bwt	θ_{XY} / °	θ_{YZ} / °	θ_{XZ} / °
Mean	-0.65	-3.02	1.20	3.33	12.0	-21.5	-28.4
Min	-0.97	-4.08	0.53	2.17	7.4	-28.3	-38.1
Max	-0.32	-2.03	1.82	4.47	17.9	-11.4	-20.6
S.D.	0.20	0.56	0.34	0.63	2.9	4.2	4.1

Group 2. Gait - peak 1. N = 19

	Fx/bwt	Fy/bwt	Fz/bwt	Fr/bwt	θ_{XY} / °	θ_{YZ} / °	θ_{XZ} / °
Mean	-0.25	-3.34	1.01	3.50	4.3	-16.6	-13.7
Min	-0.61	-4.98	0.52	2.01	-0.3	-24.7	-29.2
Max	0.03	-1.94	1.83	5.21	8.8	-11.2	1.1
S.D.	0.17	0.83	0.36	0.88	2.5	3.5	8.0

Group 2. Gait - peak 2. N = 19

	Fx/bwt	Fr/bwt
Mean	-0.65	3.79
Min	-0.32	2.17
Max	-0.97	5.21
S.D.	0.20	0.79

Group 2. Gait - greatest peak. N = 19

	Fx/bwt	Fy/bwt	Fz/bwt	Fr/bwt	θ_{XY} / °	θ_{YZ} / °	θ_{XZ} / °
Mean	-0.54	-2.95	1.11	3.21	10.3	-20.2	-26.4
Min	-0.85	-4.19	0.37	1.77	6.7	-28.6	-33.8
Max	-0.21	-1.72	1.83	4.60	14.4	-12.1	-17.8
S.D.	0.18	0.59	0.42	0.68	2.7	5.0	5.0

Group 2. Turn - peak 1. N = 14

	Fx/bwt	Fy/bwt	Fz/bwt	Fr/bwt	θ_{XY} / °	θ_{YZ} / °	θ_{XZ} / °
Mean	-0.22	-3.70	1.07	3.86	3.3	-15.8	-11.0
Min	-0.55	-5.41	0.44	2.66	1.0	-21.7	-18.7
Max	-0.05	-2.60	1.77	5.57	7.3	-8.9	-5.3
S.D.	0.17	0.92	0.41	0.98	2.3	4.0	5.6

Group 2. Turn - peak 2. N = 11

	Fx/bwt	Fr/bwt
Mean	-0.54	3.84
Min	-0.21	2.66
Max	-0.85	5.57
S.D.	0.17	0.86

Group 2. Turn - greatest peak. N = 14

	Fx/bwt	Fy/bwt	Fz/bwt	Fr/bwt	θ_{XY} / °	θ_{YZ} / °	θ_{XZ} / °
YR pk1	-0.51	-3.88	1.16	4.08	7.5	-16.6	-23.7
YR pk2	-0.06	-3.35	0.80	3.44	1.0	-13.4	-4.3
YL pk1	-0.67	-3.53	1.17	3.78	10.7	-18.3	-29.8
YL pk2	-0.14	-4.18	1.11	4.33	1.9	-14.9	-7.2

Subject Y. Turn. YR is the right hip of subject 'Y' and YL is the left hip.

	Fx/bwt	Fy/bwt	Fz/bwt	Fr/bwt	θ_{XY} / °	θ_{YZ} / °	θ_{XZ} / °
Mean	-0.89	-3.38	1.56	3.84	14.7	-24.4	-30.1
Min	-1.28	-4.28	0.85	3.01	9.9	-32.6	-43.9
Max	-0.48	-2.48	2.73	5.21	18.4	-16.8	-22.2
S.D.	0.23	0.53	0.46	0.66	2.7	4.6	5.2

Group 2. Asc peak 1. N = 17

	Fx/bwt	Fy/bwt	Fz/bwt	Fr/bwt	θ_{XY} / °	θ_{YZ} / °	θ_{XZ} / °
Mean	-0.27	-2.93	0.80	3.06	5.2	-14.5	-19.5
Min	-0.46	-4.09	0.28	1.66	0.5	-22.1	-42.1
Max	-0.02	-1.60	1.53	4.39	8.5	-7.3	-3.6
S.D.	0.13	0.82	0.39	0.88	2.2	4.1	9.3

Group 2. Asc - peak 2. N = 15

	Fx/bwt	Fr/bwt
Mean	-0.89	3.98
Min	-0.48	3.02
Max	-1.27	5.21
S.D.	0.23	0.60

Group 2. Asc - greatest peak. N = 17

	Fx/bwt	Fy/bwt	Fz/bwt	Fr/bwt	θ_{XY} / °	θ_{YZ} / °	θ_{XZ} / °
ZR pk1	-0.49	-3.17	1.22	3.43	8.8	-21.0	-21.9
ZR pk2	-0.36	-2.69	0.62	2.78	7.6	-13.0	-30.1

Subject Z. Asc. ZR is the right hip of subject 'Z'.

	Fx/bwt	Fy/bwt	Fz/bwt	Fr/bwt	θ_{XY} / °	θ_{YZ} / °	θ_{XZ} / °
Mean	-0.63	-3.51	1.25	3.79	10.0	-18.9	-27.4
Min	-0.98	-4.72	0.47	2.10	6.2	-25.9	-35.7
Max	-0.34	-2.02	2.12	5.05	14.7	-13.1	-20.4
S.D.	0.24	0.81	0.48	0.92	2.4	4.3	5.2

Group 2. Des - peak 1. N = 12

	Fx/bwt	Fy/bwt	Fz/bwt	Fr/bwt	θ_{XY} / °	θ_{YZ} / °	θ_{XZ} / °
Mean	-0.79	-2.91	1.10	3.22	15.2	-20.4	-36.4
Min	-1.18	-3.64	0.49	2.44	10.2	-29.9	-49.4
Max	-0.49	-2.19	1.92	4.22	23.3	-9.6	-27.7
S.D.	0.21	0.46	0.35	0.54	3.3	4.9	6.6

Group 2. Des - peak 2. N = 16

	Fx/bwt	Fr/bwt
Mean	-0.81	3.67
Min	-0.49	2.53
Max	-1.18	5.05
S.D.	0.22	0.78

Group 2. Des - greatest peak. N = 16

	Fx/bwt	Fy/bwt	Fz/bwt	Fr/bwt	θ_{XY} / °	θ_{YZ} / °	θ_{XZ} / °
ZR pk1	-0.74	-3.82	1.10	4.04	11.0	-16.1	-33.9

Subject Z. Des. ZR is the right hip of subject 'Z'.

	Fx/bwt	Fy/bwt	Fz/bwt	Fr/bwt	θ_{XY} / °	θ_{YZ} / °	θ_{XZ} / °
Mean	-0.47	-2.27	1.14	2.60	11.4	-26.0	-22.7
Min	-0.74	-3.05	0.54	1.54	4.9	-32.3	-35.5
Max	-0.18	-1.37	1.84	3.64	16.6	-12.9	-11.8
S.D.	0.20	0.49	0.45	0.64	3.3	5.8	6.2

Group 2. Rise N = 17

	Fx/bwt	Fy/bwt	Fz/bwt	Fr/bwt	θ_{XY} / °	θ_{YZ} / °	θ_{XZ} / °
Mean	-0.72	-3.54	1.53	3.93	11.2	-23.6	-24.5
Min	-0.96	-4.06	1.41	3.37	9.0	-25.1	-30.3
Max	-0.48	-3.02	1.65	4.49	13.4	-22.1	-18.6

Group 2. Con N = 2

	Fx/bwt	Fy/bwt	Fz/bwt	Fr/bwt	θ_{XY} / °	θ_{YZ} / °	θ_{XZ} / °
Mean	-1.17	-4.22	.2.30	4.98	15.0	-27.9	-26.2
Min	-2.31	-5.52	1.58	3.63	9.6	-36.5	-29.5
Max	-0.76	-3.17	4.08	7.25	22.7	-20.7	-20.9
S.D.	0.65	0.92	1.02	1.37	5.3	6.3	3.2

Group 2. Cox N = 5

	Fx/bwt	Fy/bwt	Fz/bwt	Fr/bwt	θ_{XY} / °	θ_{YZ} / °	θ_{XZ} / °
Mean	-0.22	-1.62	0.83	1.86	7.6	-26.4	-16.5
Min	-0.23	-1.64	0.50	1.69	7.1	-35.4	-21.7
Max	-0.20	-1.61	1.17	2.03	8.0	-17.4	-11.3

Group 2. Cin N = 2

	Fx/bwt	Fy/bwt	Fz/bwt	Fr/bwt	θ_{XY} / °	θ_{YZ} / °	θ_{XZ} / °
AR	-0.32	-1.51	1.24	1.98	11.9	-39.2	-14.5

Group 2. Cix N = 1. AR is the right hip of subject 'A'.

	Fx/bwt	Fy/bwt	Fz/bwt	Fr/bwt	θ_{XY} /°	θ_{YZ} / °	θ_{XZ} / °
Mean	-0.65	-3.89	1.90	4.39	9.5	-25.4	-19.1
Min	-1.18	-5.08	1.09	2.92	5.6	-33.0	-22.3
Max	-0.37	-2.68	2.87	5.67	14.9	-22.0	-11.4
S.D.	0.32	1.04	0.76	1.26	3.5	4.5	4.5

Group 2. Bon N = 5

	Fx/bwt	Fy/bwt	Fz/bwt	Fr/bwt	θ_{XY} /°	θ_{YZ} / °	θ_{XZ} / °
Mean	-0.56	-3.67	1.84	4.16	8.3	-25.5	-16.8
Min	-1.06	-5.52	1.02	2.92	4.9	-30.9	-22.3
Max	-0.29	-2.64	3.30	6.49	13.3	-16.7	-9.4
S.D.	0.34	1.12	0.92	1.43	3.1	5.2	4.4

Group 2. Box N = 6

	Fx/bwt	Fy/bwt	Fz/bwt	Fr/bwt	θ_{XY} /°	θ_{YZ} / °	θ_{XZ} / °
Mean	-0.46	-2.40	1.21	2.73	11.3	-26.4	-22.0
Min	-0.61	-3.22	0.70	1.71	9.6	-31.0	-27.9
Max	-0.33	-1.52	1.84	3.62	13.8	-24.2	-18.3
S.D.	0.13	0.87	0.53	1.01	1.8	3.1	4.2

Group 2. Bin N = 4

	Fx/bwt	Fy/bwt	Fz/bwt	Fr/bwt	θ_{XY} /°	θ_{YZ} / °	θ_{XZ} / °
Mean	-0.58	-2.86	1.36	3.23	11.6	-25.5	-23.2
Min	-0.76	-3.25	1.15	2.95	9.4	-29.7	-25.2
Max	-0.44	-2.54	1.67	3.50	14.3	-19.8	-21.1
S.D.	0.13	0.32	0.25	0.31	2.4	4.8	2.0

Group 2. Bix N = 4

G.3 GROUP 3 - NON PROSTHETIC HIPS OF PATIENTS

	Fx/bwt	Fy/bwt	Fz/bwt	Fr/bwt	θ_{XY} / °	θ_{YZ} / °	θ_{XZ} / °
Mean	-0.62	-3.24	1.28	3.55	10.8	-21.4	-26.2
Min	-0.88	-4.04	0.79	2.59	7.8	-29.1	-34.6
Max	-0.38	-2.39	1.98	4.35	14.5	-16.6	-17.5
S.D.	0.16	0.58	0.36	0.65	2.2	4.0	5.1

Group 3. Gait - peak 1. N = 12

	Fx/bwt	Fy/bwt	Fz/bwt	Fr/bwt	θ_{XY} / °	θ_{YZ} / °	θ_{XZ} / °
Mean	0.09	-4.34	1.10	4.49	-0.7	-14.1	3.5
Min	-0.37	-6.16	0.61	2.95	-5.1	-19.3	-21.8
Max	0.50	-2.89	2.04	6.40	6.5	-10.2	23.9
S.D.	0.25	1.11	0.40	1.16	3.4	3.0	13.9

Group 3. Gait - peak 2. N = 12

	Fr/bwt
Mean	4.69
Min	3.60
Max	6.40
S.D.	0.97

Group 3. Gait - greatest peak. N = 12

	Fx/bwt	Fy/bwt	Fz/bwt	Fr/bwt	θ_{XY} / °	θ_{YZ} / °	θ_{XZ} / °
Mean	-0.48	-3.26	1.07	3.47	8.3	-18.1	-23.7
Min	-0.74	-4.30	0.65	2.42	4.4	-22.2	-28.9
Max	-0.24	-2.27	1.40	4.51	12.4	-13.0	-14.0
S.D.	0.18	0.64	0.28	0.68	2.8	3.1	4.8

Group 3. Turn - peak 1. N = 8

	Fx/bwt	Fy/bwt	Fz/bwt	Fr/bwt	θ_{XY} / °	θ_{YZ} / °	θ_{XZ} / °
Mean	0.00	-3.99	1.02	4.13	0.4	-14.4	1.3
Min	-0.39	-4.73	0.68	3.38	-2.5	-23.1	-21.6
Max	0.20	-3.24	1.44	4.87	6.7	-10.2	13.5
S.D.	0.26	0.68	0.27	0.66	4.1	4.2	13.8

Group 3. Turn - peak 2. N = 7

	Fr/bwt
Mean	4.18
Min	3.42
Max	4.87
S.D.	0.56

Group 3. Turn - greatest peak. N = 8

	Fx/bwt	Fy/bwt	Fz/bwt	Fr/bwt	θ_{XY} / °	θ_{YZ} / °	θ_{XZ} / °
Mean	-1.22	-3.55	2.11	4.34	19.3	-30.8	-30.7
Min	-2.00	-5.00	1.40	3.18	14.9	-38.5	-39.6
Max	-0.96	-2.27	3.29	6.13	31.9	-19.2	-21.3
S.D.	0.31	0.76	0.60	0.87	4.7	6.3	6.4

Group 3. Asc - peak 1. N = 11

	Fx/bwt	Fy/bwt	Fz/bwt	Fr/bwt	θ_{XY} / °	θ_{YZ} / °	θ_{XZ} / °
Mean	-0.26	-3.30	0.92	3.44	4.6	-15.6	-16.3
Min	-0.46	-4.12	0.60	2.53	0.5	-22.8	-24.1
Max	-0.04	-2.44	1.51	4.20	8.0	-10.5	-2.0
S.D.	0.12	0.58	0.25	0.60	2.0	3.2	6.7

Group 3. Asc - peak 2. N = 10

	Fr/bwt
Mean	4.39
Min	3.18
Max	6.13
S.D.	0.83

Group 3. Asc - greatest Peak. N = 11

	Fx/bwt	Fy/bwt	Fz/bwt	Fr/bwt	θ_{XY} / °	θ_{YZ} / °	θ_{XZ} / °
ZL pk1	-1.41	-3.92	2.31	4.76	19.8	-30.5	-31.4

Subject Z. Asc. ZL is the left hip of subject 'Z'

	Fx/bwt	Fy/bwt	Fz/bwt	Fr/bwt	θ_{XY} / °	θ_{YZ} / °	θ_{XZ} / °
Mean	-0.55	-3.34	1.17	3.59	9.5	-19.1	-24.9
Min	-1.04	-4.90	0.69	2.48	5.0	-26.6	-35.9
Max	-0.27	-2.36	1.89	5.17	16.4	-14.6	-15.4
S.D.	0.25	0.69	0.35	0.74	4.2	3.7	6.8

Group 3. Des - peak 1. N = 10

	Fx/bwt	Fy/bwt	Fz/bwt	Fr/bwt	θ_{XY} / °	θ_{YZ} / °	θ_{XZ} / °
Mean	-0.85	-3.10	1.12	3.42	15.1	-19.9	-37.2
Min	-1.36	-3.63	0.75	2.34	11.1	-27.0	-50.6
Max	-0.56	-2.06	1.52	4.03	20.5	-14.1	-26.2
S.D.	0.24	0.50	0.30	0.55	2.6	4.4	6.9

Group 3. Des - peak 2. N = 11

	Fr/bwt
Mean	3.80
Min	2.92
Max	5.17
S.D.	0.61

Group 3. Des - greatest Peak. N = 11

	Fx/bwt	Fy/bwt	Fz/bwt	Fr/bwt	θ_{XY} / °	θ_{YZ} / °	θ_{XZ} / °
ZL pk1	-0.53	-3.19	0.88	3.35	9.4	-15.4	-31.1
ZL pk2	-0.68	-2.37	0.96	2.65	16.0	-22.1	-35.3

Subject Z. Des. ZL is the left hip of subject 'Z'

	Fx/bwt	Fy/bwt	Fz/bwt	Fr/bwt	θ_{XY} / °	θ_{YZ} / °	θ_{XZ} / °
Mean	-0.73	-3.00	1.73	3.55	14.0	-30.0	-23.9
Min	-1.07	-4.73	0.78	2.16	10.6	-36.7	-42.7
Max	-0.49	-1.73	2.59	5.49	22.6	-16.8	-17.7
S.D.	0.17	0.86	0.51	0.97	3.1	4.6	7.3

Group 3. Rise N = 13

	Fx/bwt	Fy/bwt	Fz/bwt	Fr/bwt	θ_{XY} / °	θ_{YZ} / °	θ_{XZ} / °
Mean	-0.59	-2.81	1.25	3.17	11.9	-23.9	-23.9
Min	-0.85	-2.94	0.87	3.08	6.3	-31.2	-27.5
Max	-0.32	-2.68	1.63	3.25	17.5	-16.5	-20.4

Group 3. Con N = 2

	Fx/bwt	Fy/bwt	Fz/bwt	Fr/bwt	θ_{XY} / °	θ_{YZ} / °	θ_{XZ} / °
Mean	-1.12	-4.65	2.76	5.54	13.6	-30.6	-22.0
Min	-1.53	-5.72	1.81	4.80	8.9	-34.8	-28.5
Max	-0.69	-3.91	3.49	6.55	18.8	-22.3	-17.3
S.D.	0.30	0.63	0.57	0.74	3.7	4.8	3.8

Group 3. Cox N = 6

	Fx/bwt	Fy/bwt	Fz/bwt	Fr/bwt	θ_{XY} / °	θ_{YZ} / °	θ_{XZ} / °
Mean	-0.65	-3.83	1.97	4.36	9.7	-27.0	-18.6
Min	-0.83	-4.51	1.57	3.72	8.0	-29.1	-22.8
Max	-0.52	-3.27	2.51	5.22	11.7	-25.0	-15.1
S.D.	0.13	0.61	0.45	0.75	1.7	1.8	3.2

Group 3. Bon N = 4

	Fx/bwt	Fy/bwt	Fz/bwt	Fr/bwt	θ_{XY} / °	θ_{YZ} / °	θ_{XZ} / °
Mean	-0.45	-3.90	1.88	4.38	4.4	-24.9	-7.4
Min	-1.26	-5.84	1.11	3.07	-5.1	-27.8	-22.3
Max	0.25	-2.86	3.07	6.72	12.2	-21.2	12.9
S.D.	0.76	1.68	1.05	2.03	8.8	3.3	18.2

Group 3. Box N = 3

	Fx/bwt	Fy/bwt	Fz/bwt	Fr/bwt	θ_{XY} / °	θ_{YZ} / °	θ_{XZ} / °
Mean	-1.33	-4.35	2.82	5.37	16.7	-32.7	-24.9
Min	-1.98	-5.08	1.88	3.92	11.5	-38.9	-32.6
Max	-0.89	-3.33	3.42	6.27	21.3	-29.5	-18.5
S.D.	0.51	0.77	0.66	1.01	4.4	4.2	5.9

Group 3. Bin N = 4

	Fx/bwt	Fy/bwt	Fz/bwt	Fr/bwt	θ_{XY} / °	θ_{YZ} / °	θ_{XZ} / °
Mean	-1.36	-4.74	2.81	5.68	15.2	-30.4	-24.5
Min	-2.21	-5.93	1.76	3.66	12.0	-32.0	-30.8
Max	-0.67	-3.14	3.70	7.33	20.4	-29.3	-20.7
S.D.	0.78	1.44	0.98	1.86	4.6	1.4	5.5

Group 3. Bix N = 3

APPENDIX H

This appendix contains the results of the sensitivity analysis described in section 7.4. The percentage changes in resultant hip joint force are given for the two peaks in the stance phase of gait for each perturbation. A positive percentage change indicates an increase in joint force following the perturbation and a negative change indicates a decrease. The right hip of subject 'G' was used in assessment.

Perturbation relative to laboratory coordinate system / mm	Percentage change in resultant hip joint force	
	Peak 1	Peak 2
X : +15	4.6	0.6
X : -15	-3.5	1.6
Y : +15	0.6	5.0
Y : -15	5.2	-3.9
Z : +15	2.1	5.8
Z : -15	-1.7	-4.6

Table H1 Perturbation of the right anterior superior iliac spine (RASIS) marker.

Perturbation relative to laboratory coordinate system / mm	Percentage change in resultant hip joint force	
	Peak 1	Peak 2
X : +15	-3.8	1.0
X : -15	4.0	0.0
Y : +15	0.9	-4.8
Y : -15	-1.1	4.7
Z : +15	2.7	6.0
Z : -15	-1.3	-5.3

Table H2 Perturbation of the left anterior superior iliac spine (LASIS) marker.

Perturbation relative to laboratory coordinate system / mm	Percentage change in resultant hip joint force	
	Peak 1	Peak 2
X : +15	-3.7	11.3
X : -15	5.6	-11.5
Y : +15	1.0	0.2
Y : -15	-0.3	0.9
Z : +15	-0.9	4.0
Z : -15	0.7	-2.6

Table H3 Perturbation of the medial epicondyle marker.

Perturbation relative to laboratory coordinate system / mm	Percentage change in resultant hip joint force	
	Peak 1	Peak 2
X : +15	4.7	-11.3
X : -15	-2.2	9.5
Y : +15	0.2	1.3
Y : -15	0.1	-0.8
Z : +15	0.8	-1.7
Z : -15	-0.5	2.7

Table H4 Perturbation of the lateral epicondyle marker.

Perturbation relative to laboratory coordinate system / mm	Percentage change in resultant hip joint force	
	Peak 1	Peak 2
X : +15	-8.9	14.1
X : -15	9.9	-19.9
Y : +15	-1.8	4.4
Y : -15	-1.8	4.3
Z : +15	0.6	-0.1
Z : -15	0.3	0.6

Table H5 Perturbation of the greater trochanter marker.

Perturbation relative to laboratory coordinate system / mm	Percentage change in resultant hip joint force	
	Peak 1	Peak 2
X : +10	-4.3	11.8
X : -10	4.7	-10.7
Y : +10	-0.9	8.4
Y : -10	4.7	-5.8
Z : +10	3.6	6.9
Z : -10	-1.7	-7.3

Table H6 Perturbation of the right iliac crest marker.

Perturbation relative to laboratory coordinate system / mm	Percentage change in resultant hip joint force	
	Peak 1	Peak 2
X : +10	-0.9	1.5
X : -10	-1.7	-7.3
Y : +10	1.0	-1.4
Y : -10	-2.8	3.3
Z : +10	2.6	-3.9
Z : -10	0.5	0.1

Table H7 Perturbation of the left iliac crest marker.

Perturbation relative to laboratory coordinate system / mm	Percentage change in resultant hip joint force	
	Peak 1	Peak 2
X : +10	-0.1	0.7
X : -10	-1.8	8.5
Y : +10	2.8	-7.3
Y : -10	-1.7	1.1
Z : +10	2.1	-0.4
Z : -10	-2.9	8.5

Table H8 Perturbation of the front thigh marker.

Perturbation relative to laboratory coordinate system / mm	Percentage change in resultant hip joint force	
	Peak 1	Peak 2
X : +10	3.7	-8.2
X : -10	1.8	-7.1
Y : +10	-0.5	7.8
Y : -10	1.1	-0.1
Z : +10	-0.7	1.0
Z : -10	3.8	-8.0

Table H9 Perturbation of the lateral thigh marker.

Perturbation relative to pelvic coordinate system / mm	Percentage change in resultant hip joint force	
	Peak 1	Peak 2
X : +11	-7.0	11.4
X : -11	7.6	-15.4
Y : +11	-3.0	2.6
Y : -11	2.7	-2.3
Z : +11	2.5	8.7
Z : -11	-2.0	-9.2

Table H10 Perturbation of the hip joint centre location.

Perturbation / °	Percentage change in resultant hip joint force	
	Peak 1	Peak 2
+5	1.2	0.2
-5	1.3	3.1

Table H11 Perturbation of the angle (θ) used in conversions between the pelvic coordinate system of Brand et al (1982) and that used in the current study.

Perturbation / mm	Percentage change in resultant hip joint force	
	Peak 1	Peak 2
+15	3.0	4.7
-15	-2.6	-3.7

Table H12 Perturbation of the distance between the anterior superior iliac spines (inter ASIS distance).

Perturbation / mm	Percentage change in resultant hip joint force	
	Peak 1	Peak 2
+15	-1.1	-5.1
-15	2.2	7.5

Table H13 Perturbation of the pelvic X scaling factor.

Perturbation / mm	Percentage change in resultant hip joint force	
	Peak 1	Peak 2
+15	-1.2	2.6
-15	2.5	-0.6

Table H14 Perturbation of the pelvic Y scaling factor.

Perturbation / mm	Percentage change in resultant hip joint force	
	Peak 1	Peak 2
+15	-2.3	-6.1
-15	5.1	8.8

Table H15 Perturbation of the femoral Z scaling factor used for all muscles except gastrocnemius.

Perturbation / mm	Percentage change in resultant hip joint force	
	Peak 1	Peak 2
+10	-0.9	2.6
-10	1.7	-3.4

Table H16 Perturbation of the femoral X scaling factor.

Hip sphere radius / mm	Percentage change in resultant hip joint force	
	Peak 1	Peak 2
17.5	0.0	6.0
29.0	0.0	-2.6

Table H17 Perturbation of hip sphere radius.

APPENDIX I

This appendix presents the muscle origin and insertion coordinate data of Brand et al (1982).

	Muscle	X / m	Y / m	Z / m
1	Adductor brevis (S)	0.0312	-0.0373	-0.0611
2	Adductor brevis (I)	0.0326	-0.0371	-0.0613
3	Adductor longus	0.0490	-0.0316	-0.0610
4	Adductor magnus (1)	-0.0117	-0.0552	-0.0486
5	Adductor magnus (2)	-0.0120	-0.0552	-0.0485
6	Adductor magnus (3)	-0.0120	-0.0551	-0.0486
7	Gluteus maximus (1)	-0.0338	0.1288	-0.0275
8	Gluteus maximus (2)	-0.0652	0.0842	-0.0429
9	Gluteus maximus (3)	-0.0747	0.0127	-0.0709
10	Gluteus medius (1)	0.0168	0.0905	0.0356
11	Gluteus medius (2)	-0.0239	0.1090	0.0054
12	Gluteus medius (3)	-0.0546	0.0721	-0.0257
13	Gluteus minimus (1)	0.0236	0.0611	0.0305
14	Gluteus minimus (2)	-0.0084	0.0648	0.0130
15	Gluteus minimus (3)	-0.0293	0.0423	-0.0053
16	Iliacus	0.0199	0.0493	0.0025
17	Psoas	0.0315	0.0111	-0.0102
18	Gemellus inferior	-0.0426	-0.0165	-0.0095
19	Obturator externus	0.0057	-0.0280	-0.0415

Table I1 Actual X, Y and Z muscle origin coordinates. Pelvic coordinates are in the pelvic reference frame.

1 Adductor brevis (S) - S denotes superior part.
2 Adductor brevis (I) - I denotes inferior part.

Muscle	X / m	Y / m	Z / m
20 Obturator internus	-0.0488	-0.0091	-0.0135
21 Pectineus	0.0318	-0.0096	-0.0299
22 Piriformis	-0.0559	0.0562	-0.0404
23 Quadratus femoris	-0.0319	-0.0479	-0.0231
24 Gemellus superior	-0.0435	0.0009	-0.0201
25 Biceps femoris (L)	-0.0414	-0.0474	-0.0146
26 Gracilis	0.0303	-0.0441	-0.0691
27 Rectus femoris	0.0326	0.0323	0.0174
28 Sartorius	0.0488	0.0649	0.0438
29 Semimembranosus	-0.0382	-0.0448	-0.0143
30 Semitendinosus	-0.0457	-0.0446	-0.0125
31 Tensor fascia lata	0.0327	0.0882	0.0547
32 Biceps femoris (S)	-0.0007	0.1784	0.0144
33 Gastrocnemius (M)	-0.0204	0.0077	-0.0157
34 Gastrocnemius (L)	-0.0198	0.0048	0.0226
35 Vastus intermedius	0.0232	0.2067	0.0176
36 Vastus lateralis	0.0010	0.2127	0.0365
37 Vastus medialis	0.0043	0.1880	0.0088

Table I1 continued. Actual X, Y and Z muscle origin coordinates. Pelvic coordinates are in the pelvic reference frame and femoral coordinates are in the femoral reference frame.

25 Biceps femoris (L) - L denotes long head.
32 Biceps femoris (S) - S denotes short head.
33 Gastrocnemius (M) - M denotes medial head.
34 Gastrocnemius (L) - L denotes lateral head.

	Muscle	X / m	Y / m	Z / m
1	Adductor brevis (S)	-0.0082	0.2828	0.0215
2	Adductor brevis (I)	-0.0112	0.2534	0.0211
3	Adductor longus	-0.0031	0.1924	0.0134
4	Adductor magnus (1)	-0.0122	0.2758	0.0290
5	Adductor magnus (2)	-0.0036	0.1740	0.0163
6	Adductor magnus (3)	-0.0064	0.0166	-0.0297
7	Gluteus maximus (1)	-0.0158	0.4055	0.0350
8	Gluteus maximus (2)	-0.0158	0.3609	0.0350
9	Gluteus maximus (3)	-0.0158	0.2894	0.0350
10	Gluteus medius (1)	-0.0195	0.3899	0.0598
11	Gluteus medius (2)	-0.0197	0.3902	0.0597
12	Gluteus medius (3)	-0.0195	0.3901	0.0596
13	Gluteus minimus (1)	-0.0073	0.3810	0.0572
14	Gluteus minimus (2)	-0.0072	0.3810	0.0571
15	Gluteus minimus (3)	-0.0073	0.3810	0.0572
16	Iliacus	-0.0179	0.3350	0.0116
17	Psoas	-0.0180	0.3352	0.0116
18	Gemellus inferior	-0.0113	0.3949	0.0448
19	Obturator externus	-0.0242	0.3821	0.0415

Table I2 Actual X, Y and Z muscle insertion coordinates. Femoral coordinates are in the femoral reference frame.

1 Adductor brevis (S) - S denotes superior part.
2 Adductor brevis (I) - I denotes inferior part.

Muscle	X / m	Y / m	Z / m
20 Obturator internus	-0.0113	0.3947	0.0446
21 Pectineus	-0.0109	0.3146	0.0248
22 Piriformis	-0.0132	0.3983	0.0484
23 Quadratus femoris	-0.0164	0.3446	0.0329
24 Gemellus superior	-0.0113	0.3947	0.0445
25 Biceps femoris (L)	-0.0383	0.3321	0.0431
26 Gracilis	-0.0586	0.3426	-0.0095
27 Rectus femoris	0.0041	0.4084	-0.0006
28 Sartorius	-0.0515	0.3478	-0.0205
29 Semimembranosus	-0.0564	0.3297	-0.0072
30 Semitendinosus	-0.0542	0.3369	-0.0058
31 Tensor fascia lata	-0.0099	0.3504	0.0292
32 Biceps femoris (S)	-0.0384	0.3323	0.0433
33 Gastrocnemius (M)	-0.0368	-0.0429	0.0028
34 Gastrocnemius (L)	-0.0369	-0.0430	0.0028
35 Vastus intermedius	-0.0018	0.4110	0.0006
36 Vastus lateralis	0.0089	0.4050	0.0151
37 Vastus medialis	-0.0079	0.3996	-0.0137

Table I2 continued. Actual X, Y and Z muscle insertion coordinates. Femoral coordinates are in the femoral reference frame and tibial and patellar coordinates are in the tibial reference frame.

25 Biceps femoris (L) - L denotes long head.
32 Biceps femoris (S) - S denotes short head.
33 Gastrocnemius (M) - M denotes medial head.
34 Gastrocnemius (L) - L denotes lateral head.

	Muscle	X	Y	Z
1	Adductor brevis (S)	0.4611	-0.1927	-0.7865
2	Adductor brevis (I)	0.4822	-0.1917	-0.7882
3	Adductor longus	0.7266	-0.1629	-0.7862
4	Adductor magnus (1)	-0.1810	-0.2785	-0.6454
5	Adductor magnus (2)	-0.1856	-0.2784	-0.6434
6	Adductor magnus (3)	-0.1850	-0.2776	-0.6447
7	Gluteus maximus (1)	-0.4892	0.6544	-0.3505
8	Gluteus maximus (2)	-0.9664	0.4315	-0.5495
9	Gluteus maximus (3)	-1.0937	0.0682	-0.9122
10	Gluteus medius (1)	0.2462	0.4556	1.0205
11	Gluteus medius (2)	-0.3523	0.5470	0.2392
12	Gluteus medius (3)	-0.8096	0.3584	-0.3306
13	Gluteus minimus (1)	0.3508	0.3079	0.8956
14	Gluteus minimus (2)	-0.1228	0.3265	0.3571
15	Gluteus minimus (3)	-0.4348	0.2092	-0.0657
16	Iliacus	0.3022	0.2350	0.1228
17	Psoas	0.4675	0.0567	-0.1279
18	Gemellus inferior	-0.6331	-0.0811	-0.1172
19	Obturator externus	0.0821	-0.1419	-0.5320

Table I3 Scaled X, Y and Z muscle origin coordinates. Pelvic coordinates are in the pelvic reference frame.

1 Adductor brevis (S) - S denotes superior part.
2 Adductor brevis (I) - I denotes inferior part.

Muscle	X	Y	Z
20 Obturator internus	-0.7265	-0.0444	-0.1603
21 Pectineus	0.4725	-0.0501	-0.3798
22 Piriformis	-0.8331	0.2902	-0.4803
23 Quadratus femoris	-0.4774	-0.2364	-0.2910
24 Gemellus superior	-0.6465	0.0043	-0.2423
25 Biceps femoris (L)	-0.6206	-0.2370	-0.1888
26 Gracilis	0.4481	-0.2262	-0.8847
27 Rectus femoris	0.4852	0.1638	0.4944
28 Sartorius	0.7252	0.3231	1.0923
29 Semimembranosus	-0.5668	-0.2246	-0.1614
30 Semitendinosus	-0.6844	-0.2235	-0.1595
31 Tensor fascia lata	0.4819	0.4429	1.3515
32 Biceps femoris (S)	-0.0086	0.4563	0.2832
33 Gastrocnemius (M)	-0.2635	0.0186	-0.1920
34 Gastrocnemius (L)	-0.2475	0.0116	0.2887
35 Vastus intermedius	0.2888	0.5253	0.3578
36 Vastus lateralis	0.0148	0.5392	0.6861
37 Vastus medialis	0.0483	0.4779	0.1730

Table I3 continued. Scaled X, Y and Z muscle origin coordinates. Pelvic coordinates are in the pelvic reference frame and femoral coordinates are in the femoral reference frame.

25 Biceps femoris (L) - L denotes long head.
32 Biceps femoris (S) - S denotes short head.
33 Gastrocnemius (M) - M denotes medial head.
34 Gastrocnemius (L) - L denotes lateral head.

	Muscle	X	Y	Z
1	Adductor brevis (S)	-0.1126	0.7174	0.4125
2	Adductor brevis (I)	-0.1451	0.6477	0.4068
3	Adductor longus	-0.0407	0.4858	0.2591
4	Adductor magnus (1)	-0.1542	0.6961	0.5411
5	Adductor magnus (2)	-0.0463	0.4351	0.3034
6	Adductor magnus (3)	-0.0768	0.0419	-0.5723
7	Gluteus maximus (1)	-0.2023	1.0407	0.7167
8	Gluteus maximus (2)	-0.2023	0.9262	0.7167
9	Gluteus maximus (3)	-0.2023	0.7427	0.7167
10	Gluteus medius (1)	-0.2329	0.9971	1.0869
11	Gluteus medius (2)	-0.2336	0.9977	1.0857
12	Gluteus medius (3)	-0.2325	0.9976	1.0846
13	Gluteus minimus (1)	-0.0853	0.9658	1.0814
14	Gluteus minimus (2)	-0.0842	0.9658	1.0801
15	Gluteus minimus (3)	-0.0851	0.9659	1.0818
16	Iliacus	-0.2200	0.8544	0.2070
17	Psoas	-0.2207	0.8548	0.2061
18	Gemellus inferior	-0.1298	0.9975	0.8385
19	Obturator externus	-0.2963	0.9662	0.7647

Table I4 Scaled X, Y and Z muscle insertion coordinates. Femoral coordinates are in the femoral reference frame.

1 Adductor brevis (S) - S denotes superior part.
2 Adductor brevis (I) - I denotes inferior part.

Muscle	X	Y	Z
20 Obturator internus	-0.1307	0.9969	0.8348
21 Pectineus	-0.1501	0.7985	0.4674
22 Piriformis	-0.1829	1.0039	0.9366
23 Quadratus femoris	-0.2205	0.8766	0.6147
24 Gemellus superior	-0.1304	0.9971	0.8321
25 Biceps femoris (L)	-0.5884	1.0742	0.6863
26 Gracilis	-0.9692	1.0923	-0.1333
27 Rectus femoris	0.0591	1.3037	-0.0084
28 Sartorius	-0.8524	1.1075	-0.3240
29 Semimembranosus	-0.9018	1.0521	-0.0886
30 Semitendinosus	-0.9478	1.0917	-0.0682
31 Tensor fascia lata	-0.1578	1.1039	0.4869
32 Biceps femoris (S)	-0.5897	1.0746	0.6888
33 Gastrocnemius (M)	-0.5649	-0.1371	0.0603
34 Gastrocnemius (L)	-0.5667	-0.1372	0.0594
35 Vastus intermedius	-0.0339	1.3120	0.0085
36 Vastus lateralis	0.1375	1.2927	0.2423
37 Vastus medialis	-0.1321	1.2751	-0.2238

Table I4 continued. Scaled X, Y and Z muscle insertion coordinates. Femoral coordinates are in the femoral reference frame and tibial and patellar coordinates are in the tibial reference frame.

25 Biceps femoris (L) - L denotes long head.
32 Biceps femoris (S) - S denotes short head.
33 Gastrocnemius (M) - M denotes medial head.
34 Gastrocnemius (L) - L denotes lateral head.